IDENTIFICATION OF MICROPOLLUTANTS IN ERGENE RIVER AND THEIR BIOTRANSFORMATION POTENTIAL UNDER ANAEROBIC CONDITIONS

by

SeyedMehdi Emadian

B.S. in Chemical Engineering, Sharif University of Technology, 2007

M.S. in Environmental Technology, Boğaziçi University, 2015

Submitted to the Institute of Environmental Sciences in partial fulfillment of

the requirement for the degree of

Doctor of Philosophy

in

Environmental Technology

Boğaziçi University

2019

ACKNOWLEDGEMENTS

Firstly, I would like to sincerely thank my PhD advisor Assist. Prof. Ulaş Tezel for his guidance, support and encouragement. His passion for science and extensive knowledge about the field uplift me. Also his being reachable at any time needed was a great chance for me. I also extend my appreciation to the members of my thesis committee, Prof. Nadim Copty, Prof. Burak Demirel, Prof. Ahmet Karagündüz and Assist. Prof. Recep Kaya Göktaş for allocating their time to evaluate this work.

I would like to show my special appreciation to my parents and my sister who support me. Their supports always encouraged me to keep on each step of my life especially in my academic life. I would like to thank Melis Temel with her incredible support specially during the difficult times of this period.

I would like to thank my lab mates Sevda Avcı, Emre Karakaya, Fahry Koray Sakarya, Feride Öyku Sefiloğlu, Zeynep Demiray, Elifcan Çalışkan, Ezgi Uysal, Arca Yılmaz, Duygu Özçelik, Derya gelgör, Dila Hocaoğlu Özgecan Eken, Begüm Sepetçi, Emren Borhan, Siamak Vajdi, Sina Ahamdvash Aghbash, Sina Zare Pakzad, Aidin Sheykhi, Samad Kazemi, Elif Irmak Erdem and other friends for their help in laboratory and friendship. I would also like to appreciate the staff of the Institute of Environmental Sciences at Bogazici University for their help.

I would like to specially thank Fılız Yilmaz, the technician at the Institute of Environmental Sciences who helped me a lot during my analysis.

This research was partially supported by The Scientific and Technological Research Council of Turkey (TUBITAK 115Y064).

ABSTRACT

IDENTIFICATION OF MICROPOLLUTANTS IN ERGENE RIVER AND THEIR BIOTRANSFORMATION POTENTIAL UNDER ANAEROBIC CONDITIONS

Ergene River spans Thrace from northeast to southwest and joins to Maritsa River, then falls to Aegean Sea at Turkey-Greece border. The river suffers pollution from different sources such as industrial and urban discharges, runoff from agricultural and animal farms. In this study, 222 micropollutants which are listed as contaminants of emerging concern or priority substances, 18 heavy metals and 13 conventional water pollution parameters were measured in 300 samples taken from 75 points on Ergene River at four seasons in the years of 2017-2018. Moreover, major source of micropollutants as well as pollutant fingerprint of major pollution source zones in the watershed were identified. Among the most important conventional parameters, COD, varied between 17 to 1660 mg/L during the year. The highest COD values were observed next to the Evrensekiz OIZ as well as Büyükkarıştıran OIZ consist of different industries such as textiles, dyes, food and chemical industries. Arsenic, aluminum, zinc, copper, lead and chromium concentrations reached to 1.0, 83.9, 33.6, 14.6 and 7.1 mg/L next to the OIZs, respectively. 131, 135, 96 and 103 organic micropollutants were detected in at least one point during summer, fall, winter and spring sampling, respectively. Concentration of micropollutants ranged from 10 ng/L to 330 mg/L. The micropollutants embraced a wide spectrum of chemicals originated from various industrial, agricultural and domestic activities. Benzotriazoles, hexa(methoxymethyl) melamine (HMMM), tris (2-butoxyethyl) phosphate (TBEP) and benzalkonium chlorides (BACs) were the most frequently detected chemicals as well as the ones with the highest concentration. OIZs located next to the Çorlu and Ergene Creeks as well as Büyükkarıştıran OIZ were the main sources of those pollutants. For instance, HMMM was mainly originated from the textile industries located in Büyükkarıştıran OIZ. In addition, biotransformation potential of the aforementioned micropollutants which are mainly discharged from textile and metal industries into the river, at the simulated water-sediment system was tested under anaerobic and sulfate reducing conditions. Benzotriazoles and TBEP were degraded partially whereas no biodegradation was determined for HMMM and BACs. The outcomes of this study can be used to understand the fate of dominant contaminants in the river sediment and develop future pollution mitigation strategies for Ergene River.

ÖZET

ERGENE NEHRİ'NDEKİ MİKROKİRLETİCİLERİN VE ANAEROBİK KOŞULLAR ALTINDAKİ BİYODÖNÜŞÜM POTANSİYELLERİNİN BELİRLENMESİ

Ergene Nehri, kuzeydoğu-güneybatı yönünde Trakya boyunca akarak, Türkiye-Yunanistan sınırında Ege Denizi'ne dökülmeden önce Meriç Nehri ile birleşir. Nehir, endüstriyel ve kentsel deşarjlar, tarım ve hayvan çiftliklerinden gelen akış gibi farklı kaynaklar tarafından kirletilmektedir. Bu çalışmada, 2017-2018 yılları arasında dört mevsimde Ergene Nehri üzerindeki 75 noktadan alınan 300 örnekte, 'ortaya çıkan maddeler' veya 'öncelikli maddeler' şeklinde sınıflandırılan 222 adet mikrokirletici madde, 18 adet ağır metal ve 13 adet konvansiyonel su kirliliği parametresi ölçülmüştür. Ayrıca, havzadaki başlıca kirlilik kaynak bölgelerinin kirletici parmak izlerinin yanı sıra, başlıca kirletici kaynakları da tespit edilmiştir. En önemli konvansiyonel parametreler arasında olan KOİ, yıl boyunca 17 ila 1660 mg/L arasında değişmiştir. En yüksek KOİ değerleri, Evrensekiz OSB'nin yanı sıra tekstil, boya, gıda ve kimya endüstrisi gibi farklı endüstrilerden oluşan Büyükkarıştıran OSB'nin yakınlarında gözlenmiştir. Arsenik, alüminyum, çinko, bakır, kurşun ve krom konsantrasyonlarının sırasıyla 1.0, 83.9, 33.6, 14.6 ve 7.1 mg/L ye ulaştığı belirlenmiştir. Yaz, sonbahar, kış ve ilkbahar aylarında alınan nehir suyu örneklerinde en az bir noktada sırasıyla 131, 135, 96 ve 103 adet organik mikrokirletici madde tespit edilmiştir. Mikrokirleticilerin konsantrasyonu, 10 ng /L ila 330 mg/L arasında değişmektedir. Mikrokirleticiler, çeşitli endüstriyel, tarımsal ve evsel faaliyetlerden kaynaklanan geniş bir kimyasal yelpazesini kapsamaktadır. Benzotriazoller, heksa(metoksimetil)melamin (HMMM), tris(2-butoksietil) fosfat (TBEF) ve benzalkonyum klorürler (BAK'lar), en yüksek konsantrasyona sahip olanların yanı sıra en sık saptanan kimyasallardır. Çorlu ve Ergene Dereleri'nin yakınında bulunan OSB'lerin yanı sıra, Büyükkarıştıran OSB'nin de bu kirleticilerin ana kaynakları arasında olduğu belirlenmiştir. Ek olarak, yukarıda bahsedilen esas olarak tekstil ve metal endüstrilerinden nehre deşarj edilen bu mikrokirleticilerin biyodönüşüm potansiyeli, simule edilmiş su sediment sisteminde anaerobik ve sülfat indirgeyici koşullar altında test edilmiştir. Benzotriazoller ve TBEF kısmen parçalanmış, HMMM ve BAK'lar için ise biyolojik bozunma tespit edilmemiştir. Bu çalışmanın sonuçları, nehir sedimentindeki baskın kirleticilerin akıbetini anlamak ve Ergene Nehri'deki kirliliği azaltma stratejilerini geliştirmek amacıyla kullanılabilir.

TABLE OF CONTENTS

ACKNOWLEDGEMENTS iii
ABSTRACT iv
ÖZET v
TABLE OF CONTENTS vi
LIST OF FIGURES x
LIST OF TABLES xxiv
LIST OF SYMBOLS AND ABBREVIATIONS xxvii
1. INTRODUCTION 1
2. LITRATURE REVIEW 3
2.1. Micropollutants 3
2.1.1. Pharmaceuticals and Personal Care Products (PPCPs) 4
2.1.2. Surfactants 7
2.1.3. Industrial Chemicals 8
2.1.4. Pesticides 11
2.1.5. Natural Chemicals 11
2.2. Prioritization of Micropollutants and Current Legislations 12
2.2.1. Priority Substances (PSs) and Contaminants of Emerging Concerns (CECs) 12
2.2.2. Prioritization of Pollutants 13
2.2.3. European Commission Water Frame Directive on PSs 14
2.2.4. The Watch List of European Commisson and Norman Network 17
2.3. Instrumental Methods to Measure Micropollutants 18
2.4. Occurrence of Micropollutants in Surface Water 23
2.4.1. Pharmaceuticals and Personal Care Products (PPCPs) 24
2.4.1.1. Pharmaceutically active compounds (PhACs). 24
2.4.1.2. Personal care products (PCPs). 25
2.4.2. Surfactants 27
2.4.3. Industrial Chemicals 28
2.4.3.1. Flame retardants. 28
2.4.3.2. Plasticizers 29
2.4.3.3. Other important industrial chemicals. 30
2.4.4. Pesticides 32
2.4.5. Natural Pollutants 33

2.5. Fate of Micropollutants in Surface Water 33
2.5.1. Volatilization and Atmospheric Deposition....34
2.5.2. Sorption and Desorption 34
2.5.3. Hydrolysis....35
2.5.4. Photodegradation 35
2.5.5. Biodegradation....36
2.6. Ergene Watershed and Its Pollution 43
2.6.1. Urban and Domestic Sectors....45
2.6.2. Industrial Sector....48
2.6.3. Agricultural Sector....51
3. EVALUATION OF POLLUTION AND IDENTIFICATION OF POLLUTION SOURCES AND THEIR FINGERPRINT POLLUTANTS IN ERGENE RIVER....54
3.1. Introduction 54
3.2. Materials and Methods 58
3.2.1. Study Area and Sampling Points 58
3.2.2. Sampling and Sample Preparation....63
3.2.3. Measurement of Conventional Parameters 64
3.2.3.1. pH....64
3.2.3.2. Temperature. 64
3.2.3.3. Color....64
3.2.3.4. Chemical oxygen demand. 65
3.2.3.5. Total organic carbon. 65
3.2.3.6. Ammonia. 66
3.2.3.7. Anions. 66
3.2.3.8. Heavy metals. 66
3.2.3.9. Schematic analysis of the data. 67
3.2.4. Measurement of The Selected Micropollutants 68
3.2.4.1. Identification and quantification of the selected micropollutants. 68
3.2.4.2. Schematic and statistical analysis. 69
3.2.5. Non-targeted Analysis of Water Samples....70
3.3. Results and Discussions 71
3.3.1. Conventional Water Quality Parameters....71
3.3.1.1. pH. 77
3.3.1.2. Temperature. 81
3.3.1.3. Color....85

3.3.1.4. COD. 92
3.3.1.5. Ions. 96
3.3.1.6. Heavy metals. 113
3.3.2. Targeted Identification and Quantification of Micropollutants 118
3.3.2.1. Targeted analysis of the micropollutants in the Ergene River. 118
3.3.2.2. Pharmaceuticals 127
3.3.2.3. Personal Care Products (PCPs). 132
3.3.2.3. Surfactants. 139
3.3.2.4. Industrial chemicals 144
3.3.2.5. Pesticides. 165
3.3.2.6. Natural Chemicals. The presence of three 173
3.3.3. Important Micropollutants Sources and Their Fingerprint Pollutants 176
3.3.4. Non-targeted Analysis of Micropollutants in The Ergene River 219
4. BIOTRANSFORMATION OF MICROPOLLUTANTS UNDER ANAEROBIC AND SULFATE REDUCING CONDITIONS 230
4.1. Introduction 230
4.2. Materials and Methods 232
4.2.1. Chemicals and Solutions 232
4.2.2. Sediment and Water Samples Collection 232
4.2.3. Characterization of The Sediment Samples 239
4.2.3.1. Total and volatile solids (TS and VS). 239
4.2.3.2. Sediment particle size classification. 239
4.2.3.3. Micropollutants content. 240
4.2.4. Extraction of Micropollutants from Sediment Samples 240
4.2.5. Biotransformation of Selected Micropollutants under Anaerobic and Sulfate Reducing Conditions at Water-Sediment System 240
4.2.5.1. Biotransformation potential of the selected micropollutants under anerobic and sulfate-reducing conditions using synthetic chemicals mix (SET 1). 241
4.2.5.2. Biotransformation potential of the selected micropollutants under anaerobic and sulfate-reducing conditions using associated water (SET 2). 242
4.2.5.3. Total gas, pH, sulfate and selected micropollutants analysis. 243
4.3. Results and Discussions 244
4.3.1. Characterization of The Sediments 244
4.3.2. Optimizing the Extraction of Micropollutants from The Sediment Samples 248

4.3.3. Biotransformation of Selected Micropollutants under Anaerobic and Sulfate Reducing Conditions at Water-Sediment System....251
4.3.2.1. pH....251
4.3.2.2. Total gas production....252
4.3.2.3. Sulfate....253
4.3.2.4. Micropollutants....254
5. CONCLUSION....268
REFERENCES....271
APPENDIX A....309
APPENDIX B....339
APPENDIX C....357
APPENDIX D....363
APPENDIX E....393

LIST OF FIGURES

Figure 2.1. Main physico(bio)chemical processes of micropollutants in aquatic environments. 34

Figure 2.2 SRB using sulfate as electron acceptor and organic molecule as electron donor (Madigan et al., 2008). 41

Figure 2.3. Catabolism of different organic compounds by SRB (Rabus et al., 2015). (1) benzene; (2) toluene or ethylbenzene; (3) o-, m- or p-xylene; (4) phenol; (5) benzoate; (6) o-, m- or p-hydroxybenzoate; (7) phenylalanine or phenylacetate; (8) vanillate; (9) benzoyl CoA; (10) naphthalene; (11) 2-methylnaphthalene; (12) indole; (13) ethane or longer chained n alkanes; (14) ethanol or longer chained alcohols; (15) acetaldehyde or longer chained aldehydes; (16) acetate or longer chained carboxylic acids; (17) 1-propanol; (18) 1-propanal; (19) propionate; (20) propionyl-CoA; (21) lactate; (22) pyruvate; (23) methylmalonyl-CoA; (24) acetyl-CoA; (25) methyl-THP (THP: tetrahydropterin); (26) methylene-THP; (27) formyl-THP; (28) formate.....42

Figure 2.4 Scheme of heavy metals precipitation under sulfate-reducing conditions (Jiang and Fan, 2008).....43

Figure 2.5. Ergene Watershed geographical location. 44

Figure 2.6. Urban areas in Ergene Watershed.....45

Figure 2.7. Distribution of industrial facilities in Ergene Watershed (purple: OIZ, Blue: single industry).....48

Figure 2.8. Locations of OIZs in Ergene Watershed.....49

Figure 2.9. Distribution of agricultural land in Ergene Watershed.....52

Figure 3.1. Map of Ergene river, its tributaries and the sampling points along the river and the industries. 59

Figure 3.2. Sampling points located on main river. 60

Figure 3.3. Industrial, transition and agricultural zones in the Ergene Watershed. 63

Figure 3.4. Calibration curves prepared for (A) high-range and (B) low-range COD measurements. 65

Figure 3.5. Box plots to show the seasonal measurements of the conventional parameters. 68

Figure 3.6. Optimum workflow for targeted and non-targeted analysis of chemicals in aqueous matrix.....69

Figure 3.7. Box plots to show the concentration range of the selected micropollutants. 70

Figure 3.8. A simple illustration of "industrial zone". 74

Figure 3.9. A simple illustration of "transition zone". 75

Figure 3.10. A simple illustration of "agricultural zone". 76

Figure 3.11. Seasonal profile of pH in (A) main stream and (B) tributary samples taken from the industrial zone. 78

Figure 3.12. Seasonal profile of pH in (A) main stream and (B) tributary samples taken from the transition zone. 79

Figure 3.13. Seasonal profile of pH in (A) main steam and (B) tributary samples taken from the agricultural zone. 80

Figure 3.14. Location of sampling points t3-1 and t7-1 with lowest pH values. 81

Figure 3.15. Seasonal profile of temperature in (A) main stream and (B) tributary samples taken from industrial zone. 83

Figure 3.16. Seasonal profile of temperature in (A) main stream and (B) tributary samples taken from transition zone. 84

Figure 3.17. Seasonal profile of temperature in (A) main stream and (B) tributary samples taken from agricultural zone. 85

Figure 3.18. Seasonal profile of color in (A) main stream and (B) tributary samples taken from industrial zone. 87

Figure 3.19. ec6 and t1-1 sampling points next to the Ergene 1 and Büyükkarıştıran OIZs with highest color values. 88

Figure 3.20. Seasonal profile of color in (A) main stream and (B) tributary samples taken from transition zone. 89

Figure 3.21. Seasonal profile of color in (A) main stream and (B) tributaries sampling points of agricultural zone. 90

Figure 3.22. Seasonal color values of the main contributors of color pollution in Ergene River. 91

Figure 3.23. Seasonal profile of COD in (A) main stream and (B) tributary samples taken from *industrial zone*. 93

Figure 3.24. Seasonal profile of COD in (A) main stream and (B) tributary samples taken from transition zone. 94

Figure 3.25. Seasonal profile of COD in (A) main stream and (B) tributary samples taken from agricultural zone. 95

Figure 3.26. Seasonal profile of NH_3-N in (A) main stream and (B) tributary samples taken from industrial zone. 97

Figure 3.27. Seasonal profile of NH_3-N in (A) main stream and (B) tributary samples taken from transition zone. 98

Figure 3.28. Seasonal profile of NH_3-N in (A) main stream and (B) tributary samples taken from agricultural zone. 99

Figure 3.29. Seasonal profile of phosphate in (A) main stream and (B) tributary samples taken from industrial zone. 102

Figure 3.30. Seasonal profile of phosphate in (A) main stream and (B) tributary samples taken from transition zone. 103

Figure 3.31. Seasonal profile of phosphate in (A) main river and (B) tributary samples taken from agricultural zone. 104

Figure 3.32. Seasonal profile of sulfate in (A) main stream and (B) tributary samples taken from industrial zone. 106

Figure 3.33. Seasonal profile of sulfate in (A) main stream and (B) tributary samples taken from transition zone. 107

Figure 3.34. Seasonal profile of sulfate in (A) main stream and (B) tributary samples taken from agricultural zone. 108

Figure 3.35. Seasonal profile of chloride in (A) main stream and (B) tributary samples taken from industrial zone. 110

Figure 3.36. Seasonal profile of chloride in (A) main stream and (B) tributary samples taken from transition zone. 111

Figure 3.37. Seasonal profile of chloride in (A) main stream and (B) tributary samples taken from agricultural zone. 112

Figure 3.38. Seasonal aluminum concentration profile in Ergene River. 114

Figure 3.39. Location of sampling points t1-1 and t1-2 next to Büyükkarıştıran OIZ and presence of an aluminum industry between those two points. 116

Figure 3.40. Location of sampling points cc9 and cc10 with high chromium concentration. 117

Figure 3.41. Number of specific and shared micropollutants detected in all seasons. The numbers represent the numbers of shared micropollutants in those seasons.....119

Figure 3.42. Seasonal frequency of detection of micropollutants in 75 sampling points on Ergene watershed. 120

Figure 3.43. Location of OIZs and sampling points on Çorlu Creek.....120

Figure 3.44. Location of other important OIZs and sampling points at which high number of micropollutants detected. 121

Figure 3.45. Heatmap of ofloxacin clustered by spatial-temporal concentration (µg/L) profiles in (A) industrial, (B) transition and (C) agricultural zones.....128

Figure 3.46. Seasonal profile of ofloxacin concentration in Ergene watershed, location of sampling point t2-3 next to a pharmaceutical facility in industrial zone with the highest ofloxacin concentration.....129

Figure 3.47. Location of sampling point t4 in transition zone and t12-3 in agricultural zone.....130

Figure 3.48. Heatmap of acetaminophen clustered by spatial-temporal concentration (µg/L) profiles in (A) industrial, (B) transition and (C) agricultural zones.....131

Figure 3.49. Location of sampling points t1-1 and t11-2 at which the highest acetaminophen concentration was detected. 132

Figure 3.50. Heatmap of methyldihydrojasmonate clustered by spatial-temporal concentration (µg/L) profiles in (A) industrial, (B) transition and (C) agricultural zones. 133

Figure 3.51. Concentration profile of galaxolide and methyldihydrojasmonate in Ergene River in fall, distribution of cosmetic and food facilities in industrial zone.....134

Figure 3.52. Heatmap of oxybenzone clustered by spatial-temporal concentration (µg/L) profiles in (A) industrial, (B) transition and (C) agricultural zones. 135

Figure 3.53. Seasonal profile of oxybenzone concentration in Ergene River. 136

Figure 3.54.. Location of sampling point t16 and t9. 137

Figure 3.55. Heatmap of methyl paraben clustered by spatial-temporal concentration (µg/L) profile in industrial zone. 138

Figure 3.56. Concentration profile of methyl paraben in Ergene River in fall, Location of sampling point t9 at which high methyl paraben concentration was detected. 139

Figure 3.57. Heatmap of BDDDA clustered by spatial-temporal concentration (µg/L) profiles in (A) industrial, (B) transition and (C) agricultural zones. 140

Figure 3.58. Seasonal BDDDA concentration profiles in Ergene River and its tributaries. 141

Figure 3.59. Location of sampling point t1-2 in industrial zone and t8-1 in transition zone. 142

Figure 3.60. Heatmap of nonylphenol diethoxylate clustered by spatial-temporal concentration (µg/L) profiles in (A) industrial, (B) transition and (C) agricultural zones. 143

Figure 3.61. Heatmap of TBEP clustered by spatial-temporal concentration (µg/L) profiles in (A) industrial, (B) transition and (C) agricultural zones. 145

Figure 3.62. Seasonal concentration profiles of TBEP in the Ergene River. 146

Figure 3.63. Sampling point cc9 representing high BDE-153 concentration during summer and spring samplings. 147

Figure 3.64. Heatmap of DEHP clustered by spatial-temporal concentration (µg/L) profiles in (A) industrial, (B) transition and (C) agricultural zones. 148

Figure 3.65. Profile of DEHP concentration in summer, Location of sampling points next to cities having high DEHP concentration. 149

Figure 3.66. Heatmap of PCBs clustered by spatial-temporal concentration (µg/L) profiles in (A) industrial, (B) transition and (C) agricultural zones. 150

Figure 3.67. Concentration profile of PCBs in summer and fall, location of OIZs in the Ergene Watershed. 151

Figure 3.68. Heatmap of (A) benzo[a]pyrene (B) anthracene clustered by spatial-temporal concentration (µg/L) profiles in industrial zone. 152

Figure 3.69. Concentration profile of anthracene in summer and fall, location of sampling point t3-1 next to the Evrensekiz OIZ in industrial zone. 153

Figure 3.70. Heatmap of (A) 1,3-dinitropyrene, (B) 1,6-dinitropyrene and (C) 1,8-dinitropyrene clustered by spatial-temporal concentration (µg/L) profiles in industrial zone. 154

Figure 3.71. Heatmap of 1,2,3-B clustered by spatial-temporal concentration (µg/L) profiles in (A) industrial, (B) transition and (C) agricultural zones. 156

Figure 3.72. Seasonal distribution of 1,2,3-B in Ergene watershed, OIZs in Ergene creek and Çorlu creek and Büyükkarıştıran OIZ and Evrensekiz OIZ responsible for benzotriazoles discharges. 157

Figure 3.73. Heatmap of HMMM clustered by spatial-temporal concentration (µg/L) profiles in (A) industrial, (B) transition and (C) agricultural zones. 159

Figure 3.74. Seasonal concentration profile of HMMM in Ergene River, location of the main sources of HMMM next to Velimeşe OIZ (sampling points cc7 and cc8) and Büyükkarıştıran OIZ (sampling points t1-1 and t1-2). 160

Figure 3.75. Seasonal HMMM concentration (mg/L) in sampling points located next to the three main contributors of HMMM contamination. 161

Figure 3.76. Heatmap of (A) 3-chloroaniline (B) 4-chloroaniline clustered by spatial-temporal concentration (µg/L) profiles in industrial zone. 162

Figure 3.77. Concentration profiles 3-chloroaniline and 4-chloroanailine in the Ergene River in summer and winter. 163

Figure 3.78. Heatmap of (A) 2-mercapto-benzothiazole and (B) benzothiazole clustered by spatial-temporal concentration (µg/L) profiles in industrial zone. 164

Figure 3.79. Location of sampling point cc2 at which high concentration of benzothiazoles was detected. 165

Figure 3.80. Heatmap of acetamiprid clustered by spatial-temporal concentration (µg/L) profile in industrial zone. 166

Figure 3.81. Seasonal concentration profiles of acetamiprid, Location of sampling point cc5 next to agricultural fields and Veliköy OIZ. 167

Figure 3.82. Heatmap of diuron clustered by spatial-temporal concentration (µg/L) profiles in (A) industrial, (B) transition and (C) agricultural zones. 168

Figure 3.83. Location of sampling points t15 and t16 in agricultural zone. 169

Figure 3.84. Heatmap of carbendazim clustered by spatial-temporal concentration (µg/L) profiles in (A) industrial, (B) transition and (C) agricultural zones. 170

Figure 3.85. Concentration profile of carbendazim in the Ergene River in summer and spring. ...171

Figure 3.86. Location of sampling point cc10 in industrial zone and t17 in agricultural zone. 171

Figure 3.87. Heatmap of N,N-diethyl-m-toluamide clustered by spatial-temporal concentration (µg/L) profiles in (A) industrial, (B) transition and (C) agricultural zones. 172

Figure 3.88. Concentration profiles of DEET in the Ergene River in summer and fall, Location of sampling point t6 and t9 in transition zone. 173

Figure 3.89. Heatmap of microcystin-RR clustered by spatial-temporal concentration (µg/L) profile in industrial zone. 174

Figure 3.90. Concentration profiles of microcystin-RR in Ergene River in summer and fall. 175

Figure 3.91. Location of sampling points cc8 and t2-3 in industrial zone. 175

Figure 3.92. Sampling point cc8 next to an algal bloom and with the highest microcystin-LR concentration. 176

Figure 3.93. Heatmap of micropollutants clustered by spatial z-score normalized concentration profiles in all samples taken in summer. The color of each cell represents the z-score value calculated for a pollutant at a sampling point. 179

Figure 3.94. Heatmap of micropollutants clustered by spatial z-score normalized concentration profiles in all samples taken in fall. The color of each cell represents the z-score value calculated for a pollutant at a sampling point. 180

Figure 3.95. Heatmap of micropollutants clustered by spatial z-score normalized concentration profiles in all samples taken in winter. The color of each cell represents the z-score value calculated for a pollutant at a sampling point. 181

Figure 3.96. Heatmap of micropollutants clustered by spatial z-score normalized concentration profiles in all samples taken in spring. The color of each cell represents the z-score value calculated for a pollutant at a sampling point. 182

Figure 3.97. Heatmap of micropollutants clustered by spatial z-score normalized concentration profiles in the samples taken from the main stream in summer. The color of each cell represents the z-score value calculated for a pollutant at a sampling point. 184

Figure 3.98. Heatmap of micropollutants clustered by spatial z-score normalized concentration profiles in the samples taken from the main stream in fall. The color of each cell represents the z-score value calculated for a pollutant at a sampling point. 185

Figure 3.99. Heatmap of micropollutants clustered by spatial z-score normalized concentration profiles in the samples taken from the main stream in winter. The color of each cell represents the z-score value calculated for a pollutant at a sampling point. 186

Figure 3.100. Heatmap of micropollutants clustered by spatial z-score normalized concentration profiles in the samples taken from the main stream in spring. The color of each cell represents the z-score value calculated for a pollutant at a sampling point.....187

Figure 3.101. Heatmap of micropollutants clustered by spatial z-score normalized load profiles in the samples taken from the junction sampling points of all tributaries and the main stream in summer. The color of each cell represents the z-score value calculated for a pollutant at a sampling point. 189

Figure 3.102. Heatmap of micropollutants clustered by spatial z-score normalized load profiles in the samples taken from the junction sampling points of all tributaries and the main stream in fall. The color of each cell represents the z-score value calculated for a pollutant at a sampling point. 190

Figure 3.103. Heatmap of micropollutants clustered by spatial z-score normalized load profiles in the samples taken from the junction sampling points of all tributaries and the main stream in winter. The color of each cell represents the z-score value calculated for a pollutant at a sampling point. 191

Figure 3.104. Heatmap of micropollutants clustered by spatial z-score normalized load profiles in the samples taken from the junction sampling points of all tributaries and the main stream in spring. The color of each cell represents the z-score value calculated for a pollutant at a sampling point. 192

Figure 3.105. Heatmap of micropollutants clustered by spatial z-score normalized concentration profiles in all samples taken from the transition zone in fall. The color of each cell represents the z-score value calculated for a pollutant at a sampling point.....194

Figure 3.106. Heatmap of micropollutants clustered by spatial z-score normalized concentration profiles in all samples taken from the agricultural zone in fall. The color of each cell represents the z-score value calculated for a pollutant at a sampling point.....195

Figure 3.107. Heatmap of micropollutants clustered by spatial z-score normalized concentration profiles in all samples taken from the transition zone in spring. The color of each cell represents the z-score value calculated for a pollutant at a sampling point.....196

Figure 3.108. Heatmap of micropollutants clustered by spatial z-score normalized concentration profiles in all samples taken from the agricultural zone in spring. The color of each cell represents the z-score value calculated for a pollutant at a sampling point.....197

Figure 3.109. Heatmap of micropollutants clustered by spatial z-score normalized concentration profiles in the samples taken from the Çorlu Creek in summer. The color of each cell represents the z-score value calculated for a pollutant at a sampling point.....199

Figure 3.110. Heatmap of micropollutants clustered by spatial z-score normalized concentration profiles in the samples taken from the Çorlu Creek in fall. The color of each cell represents the z-score value calculated for a pollutant at a sampling point.....200

Figure 3.111. Heatmap of micropollutants clustered by spatial z-score normalized concentration profiles in the samples taken from the Çorlu Creek in winter. The color of each cell represents the z-score value calculated for a pollutant at a sampling point.....201

Figure 3.112. Heatmap of micropollutants clustered by spatial z-score normalized concentration profiles in the samples taken from the Çorlu Creek in spring. The color of each cell represents the z-score value calculated for a pollutant at a sampling point.....202

Figure 3.113. Heatmap of micropollutants clustered by spatial z-score normalized concentration profiles in the samples taken from the Ergene Creek in summer. The color of each cell represents the z-score value calculated for a pollutant at a sampling point.....203

Figure 3.114. Heatmap of micropollutants clustered by spatial z-score normalized concentration profiles in the samples taken from the Ergene Creek in fall. The color of each cell represents the z-score value calculated for a pollutant at a sampling point.....204

Figure 3.115. Heatmap of micropollutants clustered by spatial z-score normalized concentration profiles in the samples taken from the Ergene Creek in winter. The color of each cell represents the z-score value calculated for a pollutant at a sampling point.....205

Figure 3.116. Heatmap of micropollutants clustered by spatial z-score normalized concentration profiles in the samples taken from the Ergene Creek in spring. The color of each cell represents the z-score value calculated for a pollutant at a sampling point.....206

Figure 3.117. Zones of Pollution sources in the Ergene River. 207

Figure 3.118. Location of 24 sampling points selected for non-targeted analysis.....219

Figure 3.119. Comparison of the mass spectrum of water sample taken from cc11 with blank. ...220

Figure 3.120. MS^2 comparison of precursor ion 216.900 in the water sample taken from cc11 and detomidine carboxylic acid.....221

Figure 3.121. MS^2 spectra comparison of precursor ion 248.900 Da in the water sample taken from cc4 and difenzoquat. 222

Figure 3.122. MS^2 spectra comparison of precursor ion 288.900 Da in the water sample taken from cc4 and tetrazepam. 223

Figure 3.123. MS^2 spectra comparison of precursor ion 353.100 Da in the water sample taken from cc7 and 6β-hydroxyfluoxymestrone. 224

Figure 3.124. MS^2 spectra comparison of precursor ion 185.100 Da in the water sample taken from ec5 and Fuberidazole. 225

Figure 3.125. MS^2 spectra comparison of precursor ion 134.000 in the water sample taken from ec8 and 4-M-1H-B. 226

Figure 3.126. MS^2 spectra comparison of precursor ion 304.200 Da in the water sample taken from t2-3 and BDDDA.....227

Figure 3.127. MS^2 spectra comparison of precursor ion 370.100 Da in the water sample taken from t2-3 and prajmalium.....228

Figure 3.128. MS^2 spectra comparison of precursor ion 117.900 in the water sample taken from t3-1 and betaine. 229

Figure 4.1. Selected sampling points for testing the anaerobic biodegradation of pollutants under anaerobic and sulfate reducing conditions. 233

Figure 4.2. Sulfate concentration profile in 75 sampling points and the selected sampling points. 237

Figure 4.3. 40 mL amber glass vials used in setting up the reactors. 241

Figure 4.4. Flushing of 40 mL vials with helium to provide anaerobic conditions. 243

Figure 4.5. Detail profile of particle size distribution of sediments A) m2, B) ec8 and C) t1-1, D) t3-2 and E) m10. 247

Figure 4.6. Desorption profile of micropollutants from sediment from sampling point t1-1 by (A) water, (B) methanol, (C) methanol + acetonitrile (50:50), (D) acetonitrile + 50 mM phosphate buffer (60:40) and (E) silver nitrate solution + acetonitrile + ethyl acetate (20:30:50). 250

Figure 4.7. pH profiles in vials containing sediment from sampling point (A) t1-1 and (B) t3-2, along with (1) synthetic water and (2) associated water. 251

Figure 4.8. Total gas production (mL) profiles in vials containing sediment from sampling point (A) t1-1 and (B) t3-2, along with (1) synthetic water and (2) associated water. 252

Figure 4.9. Sulfate reduction profiles in vials containing sediment from sampling point (A) t1-1 and (B) t3-2, along with (1) synthetic water and (2) associated water. 254

Figure 4.10. Concentration reduction profile of (A) 4-M-1H-B, (B) 5-M-1H-B, (C) 5,6-D-1H-B and (D) 1,2,3-B in aqueous phase of the vials containing sediment t1-1 along with (1) synthetic water and (2) associated water. 256

Figure 4.11. Total mass reduction profile of (A) 4-M-1H-B, (B) 5-M-1H-B, (C) 5,6-D-1H-B and (D) 1,2,3-B in the vials containing sediment t1-1 along with (1) synthetic water and (2) associated water. 257

Figure 4.12. Concentration reduction profile of (A) 4-M-1H-B, (B) 5-M-1H-B, (C) 5,6-D-1H-B and (D) 1,2,3-B in aqueous phase of the vials containing sediment t3-2 along with (1) synthetic water and (2) associated water. 259

Figure 4.13. Total mass reduction profile of (A) 4-M-1H-B, (B) 5-M-1H-B, (C) 5,6-D-1H-B and (D) 1,2,3-B in the vials containing sediment t3-2 along with (1) synthetic water and (2) associated water. 260

Figure 4.14. Concentration reduction profile of (A) HMMM, (B) TBEP, (C) BDDDA and (D) BDTDA in aqueous phase of the vials containing sediment t1-1 along with (1) synthetic water and (2) associated water. 263

Figure 4.15. Total mass reduction profile of (A) HMMM, (B) TBEP, (C) BDDDA and (D) BDTDA in the vials containing sediment t1-1 along with (1) synthetic water and (2) associated water.....264

Figure 4.16. Concentration reduction profile of (A) HMMM, (B) TBEP, (C) BDDDA and (D) BDTDA in aqueous phase of the vials containing sediment t3-2 along with (1) synthetic water and (2) associated water. 265

Figure 4.17. Total mass reduction profile of (A) HMMM, (B) TBEP, (C) BDDDA and (D) BDTDA in the vials containing sediment t3-2 along with (1) synthetic water and (2) associated water 266

LIST OF TABLES

Table 2.1. List of PSs in directive 2013/39/EU along with their usage, adverse effects and concentration limits (Eurpean Commission, 2013, Sousa et al., 2018). 15

Table 2.2. Population distribution of the cities located in Ergene Watershed. 46

Table 2.3. Domestic WWTPs in Ergene Watershed, their activity status and type of treatment.....47

Table 2.4. Number of active industrial facilities in Ergene Watershed. 50

Table 2.5. Number of types of the industries recorded to have industrial discharges. 50

Table 2.6. Consumption of different groups of pesticides in provinces. 52

Table 3.1. Abbreviations used in naming the sampling points. 60

Table 3.2. Location and coordinates of sampling points.....61

Table 3.3. Location and coordinates of industries where individual samples were taken. 62

Table 3.4. Samples processing and analyses. 64

Table 3.5. Details of parameters for the measurements of heavy metals using ICP-OES instrument. 67

Table 3.6. LOD of the heavy metals measured using the developed method along with their EQS assigned by the Turkish Ministry of Forestry and Water. 67

Table 3.7. Summary of conventional pollution parameters measured along the Ergene River in four seasons. 72

Table 3.8. Maximum, minimum, mean and median concentrations of detected organic micropollutants. 122

Table 3.9. List of micropollutants with high concentration in sampling point cc7 in all season. ...208

Table 3.10. List of micropollutants with high concentration in sampling point ec6 in all season. .210

Table 3.11. List of micropollutants with high concentration in sampling point t1-1 in all season. 211

Table 3.12. List of micropollutants with high concentration in sampling point t3-1 in all season. 213

Table 3.13. List of micropollutants with high concentration in sampling point t4 during all season. 215

Table 3.14. Characterization of wastewater samples taken from four industries. 218

Table 4.1. List of chemicals detected during summer 2017 in selected sampling points for testing the anaerobic biodegradation of pollutants under sulfate-reducing and anerobic conditions. 234

Table 4.2. Selected chemicals for biotransformation assays. 238

Table 4.3. Maximum, minimum and mean concentration (µg/L) and frequency detection of the most detected micropollutants in the samples taken from the Ergene River in Summer 2017. 239

Table 4.4. Concentration of the analytes amended to the reactors in SET 1. 241

Table 4.5. Initial concentration of the analytes in associated water of the sediments t1-1 and t3-2. 242

Table 4.6. Components of reactors in detailed biotransformation assay. 243

Table 4.7. Characterization of sediment samples. 245

Table 4.8. Recovery (%) of the selected micropollutants from sediments taken from sampling points t1-1 and t3-2. 249

Table 4.9. Removal (%) of micropollutants in aqueous phase and their total biodegradation (%).267

LIST OF SYMBOLS AND ABBREVIATIONS

Symbol	Explanation	Unit
K_p	Sediment-water partitioning Coefficient	-
K_{ow}	Octanol-water partitioning Coefficient	-
$P_{i,x}$	Concentration of pollutant *i* at sampling point *x*	µg/L
$Z_{i,x}$	Z-score of pollutant *i* at sampling point *x*	-
μ_i	Mean concentration of pollutant *i*	µg/L
σ_i	Standard deviation of pollutant *i*	µg/L
$CONC_{Supernatant}$	Concentration of a pollutant in the supernatant	µg/L
$CONC_{REFs}$	Concentration of a pollutant in the reference	µg/L
$MASS_{Supernatant}$	Mass of a pollutant in the supernatant	µg
$MASS_{Pellet}$	Mass of a pollutant in the pellet	µg
$MASS_{REFs}$	Mass of a pollutant in the reference	µg

Abbreviation	Explanation
1,2,3-B	1,2,3-Benzotriazole
4-M-1H-B	4-Methyl-1H-Benzotriazole
4-MBC	3-(4-methyl benzylidene) camphor
5-M-1H-B	5-Methyl-1H-Benzotriazole
5,6-D-1H-B	5,6-Dimethyl-1H-Benzotriazole
AA-EQS	Annual Average Environmental Quality Standard
ADAF	Airplane Deicer and Anti-Freezing agent
Ag	Silver
Al	Aluminum

APCI	Atmospheric Pressure Chemical Ionization
ASTM	American Society for Testing and Materials
B	Boron
Ba	Barium
BDDDA	Benzyldimethyldodecylammonium
BDE	Brominated Diphenyl Ethers
BDTDA	Benzyldimethyltetradecylammonium
BP-3	Benzophenone-3
Br^-	Bromide
CAD	Nitrogen Gas
CAS	Chemical Abstract System
Cd	Cadmium
CE	Collision Energy
CECs	Contaminants of Emerging Concern
CFRs	Chlorinated Flame Retardants
CID	Collision Induced Dissociation
Cl^-	Chloride
Co	Cobalt
COD	Chemical Oxygen Demand
COMMPS	Combined Monitoring-based and Modeling-based Priority Setting Scheme
Cr	Chromium
Cu	Copper
CUR	Curtain gas flow
DC	Direct Current potential
DBP	Dibutyl phthalate
DEET	N,N-Diethyl-m-toluamide
DEHP	Di(2-ethylhexyl)phthalate
DEP	Diethyl Phthalate
DMP	Dimethyl Phthalate
DP	Declustering Potential
EC_{50}	50% Effective Concentration
EMS	Enhanced Mass Scanning
EP	Entrance Potential
EPI	Estimation Program Interface

EPI	Enhanced Product Ion
EQSs	Environmental Quality Standards
ESI	Electrospray Ionization
EU	European Union
F^-	Fluoride
FT-ICR	Fourier-Transform Ion Cyclotron Resonance
GC-MS	Gas Chromatography-Mass Spectrometry
GC-MS/MS	Gas Chromatography - Tandem Mass Spectrometry
HBCDs	Hexabromocyclododecanes
HMMM	Hexa(methoxymethyl)melamine
HPLC	High-Performance Liquid Chromatography
HPVC	High Production Volume Chemical
HRMS	High-Resolution Mass Spectrometry
IS	Ion Spray Voltage
IWM	Integrated Watershed Management
LC	Liquid Chromatography
LC_{50}	50% Lethal Concentration
LC-HRMS	Liquid Chromatography- High Resolution Mass Spectrometry
LC-MS	Liquid Chromatography-Mass Spectrometry
LC-MS/MS	Liquid Chromatography - Tandem Mass Spectrometry
LC-TOF-MS	Liquid Chromatography–Time of Flight Mass Spectrometry
LLE	Liquid-Liquid Extraction
LOD	Limit of Detection
LogP	Octanol/Water Partition Coefficient
LOQ	Limit of Quantitation
LTQ-FT	Linear Ion Trap Fourier Transfrom
(m/z)	mass-to-charge ratio
MAC-EQS	Maximum Allowable Environmental Quality Standard
MEC	Measured Environmental Concentration
MRM	Multiple Reaction Monitoring
MS	Mass Spectrometry
MSD	Mass Detector
Ni	Nickel
NH_3-N	Ammonia-Nitrogen
NO_2^-	Nitrite

NO_3^-	Nitrate
Non-SRB	Non Sulfate Reducing Bacteria
NP	Nonylphenol
NPEO	Nonylphenol Ethoxylate
OC	Octocrylene
OECD	Organization for Economic Co-operation and Development
OMC	Octyl 4-methylcinnamate
OP	Organophosphorus
PAHs	Polycyclic Aromatic Hydrocarbons
PBDEs	Polybrominated Diphenyl Ethers
PBT	Persistency, Bioaccumulation, Toxicity
PCBs	Poly Chlorinated Byphenyls
PCPs	Personal Care Products
PEC	Predicted Environmental Concentration
PFs	Perfluorinated Surfactants
PFOA	Perfluorooctanate
PFOS	Perfluoroocatane Sulfonate
PhACs	Pharmaceuticals
PNEC	Predicted No Effect Concentration
PO_4^{3-}	Phosphate
POCIS	Polar Organic Chemical Integrative Samplers
POPs	Persistent Organic Pollutants
PPCPs	Pharmaceuticals and Personal Care Products
Q1	Parent ion
Q3	Fragment ion
QACs	Quaternary Ammonium Compounds
QqQ	Triple-Quadrupole
R^2	Regression Coefficient
RC	Regenerated Cellulose
REACH	Registration, Evaluation, Authorization, and Restriction of Chemicals
RF	Radio Frequency potential
RT	Retention Time
SIM	Selected Ion Monitoring
Sn	Tin

SP	Sample Point
SPE	Solid-Phase Extraction
SRB	Sulfate Reducing Bacteria
STP	Sewage Treatment Plant
TBEP	Tris(2-butoxyethyl) phosphate
TCEP	Tris(2-chloroethyl) phosphate
TCMP	Tris(2-chloro-1-methyl) Phosphate
TCPP	Tris(1-chloro-2-propyl) Phosphate
TIC	Timed-Ion Selector
TOC	Total Organic Carbon
TOF	Time-of-Flight
TS	Total Solids
UPLC	Ultra-Performance Liquid Chromatography
UPLC-MS/MS	Ultra-Performance Liquid Chromatography - Tandem Mass Spectrometry
UV	Ultraviolet
UV-326	2-(3-t-butyl-2-hdroxy 5-methylphenyl) 5-chloro benzotriazole
UV-329	2-(2-hydroxy-5-octylphenyl) benzotriazole
V	Vanadium
VS	Volatile Solids
WFD	Water Framework Directive
WWTP	Waste Water Treatment Plant
Zn	Zinc

1. INTRODUCTION

Water is vital for every organism on earth. However, recently urbanization and industrialization pose a threat on fresh water resources. Improper discharge of industrial and domestic wastewater, use of agricultural chemicals and landfill leachates result in contamination of surface water specially in developing countries such as Turkey (Aldenberg and Jaworska, 2000).

Untreated or partially treated wastewater from municipalities and industrial facilities as well as agricultural run-off are the major sources of contaminants in the environment. Those contaminants are mainly associated with the products used in human activities, raw materials or product enhancers utilized in industrial process lines and pesticides used in agriculture. Those contaminants are generally present in the water at trace concentrations i.e. few ng/L to several µg/L so they are called micropollutants. Micropollutants frequently detected in water environment are hormones, pharmaceuticals, personal care products, corrosion inhibitors, combustion byproducts, flame retardants, fragrances, surfactants and pesticides (Luo et al., 2014). Some of these pollutants are known to pose high environmental risks (priority substances) while sufficient data for others (Contaminants of emerging concerns) is still missing.

A total 45 chemical substances or group of chemicals are listed as priority substances (PSs) in Directive 2013/39/EU (Eurpean Commission, 2013) are the pollutants that their concentration in water bodies should not exceed their Environmental Quality Standard (EQS). Monitoring of PSs in water bodies is essential due to their significant toxicity to human health and aquatic organisms. Unlike PSs, contaminants of emerging concern (CECs) are pollutants that the information regarding their toxicity and effects is not sufficient and worldwide monitoring data is required for further prioritization of these chemicals (Sousa et al., 2018).

Identification and quantification of micropollutants at low concentrations in complex environmental matrices require advanced instrumental methods. Hyphened instrumental methods such as gas chromatography-mass spectrometry (GC-MS) and liquid chromatography-mass spectrometry (LC-MS) are mainly utilized for this purpose (Robles-Molina et al., 2014). Measurement of micropollutants enhances understanding on contaminant-source relationships, also known as pollutant fingerprinting (Zheng et al., 2013), and may facilitate the identification of pollution sources affecting a water body and taking pollution mitigation actions.

In addition to identification of contaminants, assessment of their fate in a water body is crucial for evaluation of risk associated with those contaminants. There are four major mechanisms that can affect the fate of pollutants in a river: (1) volatilization; (2) sorption; (3) abiotic degradation e.g. hydrolysis and oxidation/reduction with metals and (4) biotic degradation. Understanding the role of those mechanisms on the overall fate and removal of contaminants in the water environment may promote the development of strategies for efficient remediation of water resources.

Ergene River is the most polluted river in Turkey. The watershed is occupied by crowded cities and villages, many industrial facilities as well as agricultural land and animal farms. The water originated from those sources contain micropollutants including PSs and CECs which result in very bad water quality of Ergene River. Further using the Ergene River water for the irrigation of different plants in the region causes soil pollution and transfer of pollutants to the agricultural products. This pollution cycle finally affects the human and other organisms in the Ergene Watershed (Kocaman et al., 2015). In this study, the occurrence and distribution of selected CECs and PSs along the Ergene River were evaluated. In addition, major micropollutants other than selected contaminants were identified. Major pollution sources in the watershed as well as their pollutant fingerprints were determined.

Many contaminants frequently detected in the Ergene River are non-biodegradable in the water phase. Given their relatively high hydrophobicity, it is assumed that they are accumulated in the sediment layer of the Ergene River. Current remediation progress on the Ergene River aims to divert polluted streams to Marmara Sea and let the river replenish itself naturally. However, fate of contaminants sorbed on the sediment and their role as source of pollution in the future are uncertain. Given that the sediment of Ergene River is anoxic; nitrate, sulfate and iron in the overlying water may serve as electron acceptor and facilitate the degradation of contaminant sorbed on the sediment. Therefore, biodegradation of frequently detected micropollutants in Ergene River was investigated under anaerobic and sulfate reducing conditions at the water-sediment interphase in this study. The outcomes of the study further improve the understanding of the aftermath of currently active pollution mitigation actions on Ergene River.

2. LITRATURE REVIEW

2.1. Micropollutants

Water is vital for every organism on earth. It is the most essential resource used for different applications in household, industry and agriculture. For instance, approximately 40% of food production in the world is accomplished by irrigation (Halder and Islam, 2015). Day by day, the water demand is increasing because of population growth and industrialization, while access to clean water is decreasing. It was estimated that 62.5% of the world population will encounter water stress by the year 2025. Besides, contamination with chemicals used in our daily life and during industrial production of consumer products decreases the current quality of fresh water sources. Although, wastewater treatment technologies were improved and environmental regulations get stricter, chemicals still find their ways to water bodies and cause pollution. Thus, monitoring the water bodies is crucial to provide a safe water for further usages such as irrigation and drinking water (Inyinbor Adejumoke et al., 2018, Sousa et al., 2018).

Water pollution is comprised of mainly two types of pollutants: macropollutants and micropollutants. Macropollutants include organics and nutrients. Exact structure and identity of chemicals that are classified under macropollutants are not known. Therefore, their quantity is presented with cumulative parameters such as chemical oxygen demand, total nitrogen and total phosphorus. The concentration of those parameters in water is generally at mg/L levels. Main impact of those pollutants on the environment is depletion of oxygen and algal blooms in the aquatic environment. On the other hand, micropollutants are substances with known molecular structure that are present in the environment at very low concentrations ranging from few ng/L to several µg/L (Kim and Zoh, 2016). In the last three decades, micropollutants gained a lot of attention due to their prospective impact on the environment, their high toxicity, endocrine disrupting, mutagenic, and carcinogenic effects as well as contribution to antibiotic resistance (Ruff et al., 2015, Schwarzenbach et al., 2006). Pharmaceutically active compounds and antibiotics, musks, preservatives, biocides, flame retardants, corrosion inhibitors, combustion byproducts, UV blockers and many other anthropogenically produced chemicals are examples to micropollutants that have been frequently detected in water (Luo et al., 2014). Micropollutants are generally released into the water environment through: (1) direct discharge from a pollution source; (2) discharge after insufficient treatment; (3) surface run-off; (4) subsurface percolation of solid waste leachate and (5) wet deposition. In addition,

many micropollutants are produce *in situ* as result of abiotic or biotic transformation of other chemicals.

In particular, the major source of micropollutants in the environment is industrial discharge. Different industries use approximately 300 million tons of synthetic chemicals which may end up in the aquatic environments as a result of uncontrolled, poorly or untreated wastewater discharges (Schwarzenbach et al., 2006). Although some advanced technologies such as granulated active carbon, nanofiltration, reverse osmosis membrane, etc. are able to remove these chemicals from wastewater to a certain extent, generally complete removal is not achieved. In addition to industrial wastewater, agricultural runoff which carries chemicals, mainly pesticides, used in the protection of crops is another major source of micropollutants. Annually, 140 million tons of agricultural chemicals are used worldwide, most of which are detected in surface water (Aldenberg and Jaworska, 2000, Eu, 2003, Tröger et al., 2018, Schwarzenbach et al., 2006). As a result of industrial, agricultural and domestic activity many different chemicals end up in the environment and threaten ecosystem and public health. Those chemicals can be grouped into pharmaceuticals and personal care products, surfactants, industrial chemicals, pesticides and natural pollutants (Luo et al., 2014).

2.1.1. Pharmaceuticals and Personal Care Products (PPCPs)

PPCPs are consumed by general public for cosmetic or health care purposes. They were classified as CECs since they are frequently detected in the environment at relatively high concentrations as well as they are persistent. The main sources of PPCPs include discharges from urban wastewater treatment plants, manufacturing facilities, hospitals as well as runoff from animal farms (Luo et al., 2014, Yang et al., 2017). As a result, PPCPs are very abundant in surface waters, sediments and soils (Gogoi et al., 2018).

PPCPs include a wide spectrum of chemicals. Chemicals classified as pharmaceuticals include antibiotics, analgesics, beta-blockers and therapeutic hormones (estriol, estradiol, estrone, etc.) (Tran et al., 2014, Tiwari et al., 2017). Antibiotics are a group of pharmaceuticals specifically designed for the treatment of microbial infections in human and animals. Clarithromycin, amoxicillin, azithromycin, ofloxacin, etc. are among the most frequently prescribed antibiotics. Since most of the antibiotics are resistant to biodegradation, they are not removed in conventional treatment systems which employ biological treatment, and released into the environment. Presence of antibiotics in the environment leads to exposure of microorganisms to those chemicals at very low concentrations and contributes to development and dissemination of antibiotic resistance. Resistance of microorganisms

to antibiotics is currently a major health problem which has strong ties with environmental pollution (Tiwari et al., 2017).

As another widely used group of pharmaceuticals, analgesic drugs are mainly consumed as painkillers and anti-inflammatory drugs. Acetaminophen (paracetamol), salicylic acid, ibuprofen, diclofenac, naproxen, etc. are analgesic drugs that are extensively consumed throughout the world since most of these drugs do not need any prescription. Hundreds tons of analgesic drug are annually used in developed countries (Ziylan and Ince, 2011). Certain amount of the drug is assimilated by the body whereas the rest is excreted. Given the fact that complete removal of these drugs in the conventional wastewater treatment plants cannot be achieved, now active ingredients of analgesic drugs are one of the most frequently detected micropollutants in surface water (Tiwari et al., 2017). Most of analgesic drugs showed either high chronic (naproxen) or acute (diclofenac and ibuprofen) toxicities. As a result, occurrence of analgesic drugs in surface water may disrupt the life of aquatic organisms (Ziylan and Ince, 2011).

Beta-blockers are pharmaceuticals that are consumed for treatment of cardiovascular diseases. Acebutolol, propranolol, nadolol, etc. are belonging to this group of pharmaceutically active compounds. Based on sales data in Europe, the UK has the highest numbers of consumers of beta-blockers while Finland has the lowest number. Atenolol and metoprolol are the active ingredient of 80% of total beta-blockers in Europe. Either themselves or their metabolites of the beta-blockers are excreted after use. For instance, 50% of atenolol is absorbed by the body whereas the rest is released via urine and feces. Beta-blockers subject to biotransformation in wastewater treatment plants. It was reported that 25-50% of sotalol, propranolol, metoprolol and atenolol were removed in a batch reactor. Despite of partial biotransformation, rest of those compounds in the wastewater is finally discharged into the environment (Alder et al., 2010). Beta-blockers are toxic and persistent chemicals. For instance, predicted no effect concentration (PNEC) of 0.73 and 7.9 µg/L was reported for propranolol and atenolol, respectively. Because of their high risk, presence of beta-blockers in water can deteriorate the quality of aquatic life (Kibbey et al., 2007, Gabet-Giraud et al., 2014).

Hormones are natural molecules present in humans and animals. Those molecules may be supplemented to individuals in case of hormonal deficiency or disorder. Both natural and therapeutic hormones are excreted from the body. For instance, a woman excrete 2-12 and 3-20 µg 17β-estradiol and estrone, respectively while the value is 5 µg of former for a man on daily basis (Belfroid et al., 1999, Tiwari et al., 2017, Raman et al., 2004). Some hormones used for therapeutic purposes such as ethynylestradiol are synthetic and mainly used for birth control and as substitute for estrogen in some

treatments. No matter they are natural or synthetic, hormones are excreted from human populations and are frequently detected in wastewater and surface water (Tiwari et al., 2017). Presence of hormones in surface waters negatively affect the aquatic life and human health because of endocrine disrupting properties of those chemicals (Aydin and Talinli, 2013).

As pharmaceuticals are used for therapeutic purposes, PCPs are consumed for personal hygiene, and cosmetics. PCPs include sunscreens, perfumes, shampoos and household cleaning products (Gogoi et al., 2018, Villa et al., 2012). Such products contain active ingredients like UV filters (drometrizole, homosalate, etc), fragrances (celestolide, phantolide, tonolide, etc) and disinfectants (triclosan, etc). Unlike pharmaceuticals, PCPs are used externally and thus no metabolization occurs in the human body. Therefore, they are easily carried to the environment with water applied to skin and surfaces at which those products applied (Villa et al., 2012, Lv et al., 2010).

Fragrances, which are the ingredients responsible of good odor in perfumes and other cosmetic and cleaning products, are consumed heavily as raw material in the industry manufacturing a wide spectrum of products (Sumner et al., 2010). Synthetic musks are the most popular fragrances. They include nitro, polycyclic and macrocyclic musks. Among them, polycyclic musks are categorized as high production volume chemicals (HPVC). Currently, galaxolide and tonalide are very highly demanded polycyclic musks with an annual consumption of 1473 and 358 tons per year, respectively. Their high demand and consumption rate as well as resistance to biodegradation make them one of the important CECs in surface water (Villa et al., 2012). Fragrances in surface waters have been reported to adversely affect different organs of fishes and mussels. Moreover, they may have potential contribution to breast cancer in human (Lee et al., 2014)

UV filters, which are another PCPs, are mainly used either in sunscreens to reduce the adverse impacts of sunlight on body of human or other consumer products made of textiles and plastics to protect them from photo-deterioration and discoloration. Dromatrizole, homosalate, benzophenone and their derivatives and 4-methylbenzylidenecamphor are active ingredients of UV filters. Annually, 10,000 tons of these compounds are produced. Consequently, they enter the water bodies, since their tendency for biodegradation is low compared to organic macropollutants in WWTP. Since many of them have endocrine-disrupting properties, they can endanger the life of aquatic organisms as well as human health (Jurado et al., 2014).

Antimicrobial agents and biocides such as triclosan and triclocarban, which are present in many PCPs e.g. toothpastes, soaps etc. are chemicals that are used to inhibit microorganisms and maintain

personal hygiene. Biocides used at homes released in to the environment by direct domestic discharge or after treatment of domestic wastewater. Given the fact that they have antimicrobial properties, they facilitate development and dissemination of antimicrobial resistance. Since antimicrobial and antibiotic resistance share quite a common mechanisms, currently many commercial biocides are under the objective of regulation makers which promotes their stringent monitoring in the environment (Giebultowicz et al., 2018). In addition, adverse effects of triclosan and triclocarban on immune and metabolic systems as well as hormone production mechanism of humans and animals have been reported in the literature. For instance, 0.07 mg/L of triclosan was reported to disrupt immune system in rats (Venkatesan et al., 2012).

Parabens, which are one of the essential ingredients of personal care products, are esters of p-hydroxybenzoic acid and include chemicals such as methylparaben, ethylparaben, propylparaben, butyl paraben and benzylparaben. They are extensively used as preservatives in cosmetic, pharmaceutical and food products. Their high consumption couples with resistance to biodegradation and they find their way to the aquatic environments. Parabens have carcinogenic and endocrine disrupting properties and that is why their presence in the environment arise concerns in public (Czarczynska-Goslinska et al., 2017, Galinaro et al., 2015).

2.1.2. Surfactants

Surfactants or surface-active agents are compounds that are widely used as disinfectant in different activities including household cleaning and food processing as well as manufacturing of textiles, electronics, paints, personal care products and pesticides. Linear alkyl sulfonates, alkylphenol ethoxylates, perflourinated surfactants (PFs) and quaternary ammonium compounds (QACs) are among the most well-known surfactants. After they are utilized during a manufacturing process or a product containing surfactants is consumed, they get into water. Due to their antimicrobial properties, many of the surfactants are non- or hardly biodegradable. As a result, surfactants are one of the most frequently detected chemicals in the environment. Moreover, many of the surfactants are extremely toxic to organisms or they contribute to antibiotic resistance due to their antimicrobial properties, whereas some, such as alkylphenol ethoxylates, are endocrine disruptors (Tezel and Pavlostathis, 2015, Hanif et al., 2012, Olkowska et al., 2014, Petrovic et al., 2002).

Alkylphenol ethoxylates (APEO) are a group of surfactants that are considered as important pollutants since they have endocrine-disrupting and estrogenic properties. It was reported that up to 65% of nonylphenol ethoxylates (NPEOs) entering the WWTPs are biotransformed to products such

as nonylphenol monoethoxylate (NP_1EO), nonylphenol diethoxylate (NP_2EO) and nonylphenol (NP) which are also endocrine disruptors (Petrovic et al., 2002).

Perfluorinated surfactants (PFs) such as perfluorooctanic acid (PFOA) and perfluorooctane sulfonate (PFOS) are widely used in different industrial processes specially textiles and paper production as well as they are ingredients of floor polishes and fire extinguishers because of their high thermal stability and high polarity. Due to their chemical stability, they are not biodegradable therefore PFs are not eliminated in WWTPs. As a result, they are widely distributed in the environment. Their presence in the environment can result in bioaccumulation and biomagnification in human body by entering the drinking water network as well as food chain (Skutlarek et al., 2006).

Quaternary ammonium compounds (QACs) are cationic surfactants that are mainly used in domestic, agricultural and industrial applications. They are among the HPVCs and their annual production was more than 1,000 tons in EU countries. About 75% of the QACs consumed are introduced into WWTPs through domestic wastewater every year and the rest is directly discharged into the water bodies. Their potential environmental impact is toxicity and contribution to antibiotic resistance due to their antimicrobial properties (Elersek et al., 2018, Tezel and Pavlostathis, 2015).

2.1.3. Industrial Chemicals

Industrial chemicals are mainly used as additives in manufacturing of various products where they introduce a specific feature to that product. Plasticizers, flame retardants, corrosion inhibitors and dielectric fluids are examples of industrial chemicals (Luo et al., 2014, Kim and Zoh, 2016).

Flame retardants are mainly used to prevent rapid ignition of flammable products when they are exposed to fire and avoid the emission of toxic gases in case a product burns. They are added to plastics, textiles, dyes and coatings as well as materials used in manufacturing of electrical equipment. Regarding their chemical structure, flame retardants mainly include organophosphorus (OPs) such as tris(2-chloroethyl-phosphate and tris(2-butoxyethyl) phosphate and halogenated chemicals including polychlorinated diphenyl ethers (PBDEs) (Segev et al., 2009, Bacaloni et al., 2007). Flame retardants are not bound to the polymers and therefore they are easily entering the surface water either via discharge of wastewater from manufacturing processes or leaching from the product itself. Many of flame retardants have high toxicity impacts on aquatic organisms when enter the surface water. For instance, PBDEs have high endocrine disrupting and bioaccumulation potentials (Cristale et al., 2013a, Aznar-Alemany et al., 2017).

Plasticizers are used to boost the durability and flexibility of products. They are used in production of furniture, building materials, PVC plastic and rubber and manufacturing of PCPs. different industries. Phthalate esters such as dimethyl phthalate (DMP), diethyl phthalate (DEP), dibutyl phthalate (DBP) and di-(2-ethylhexyl) phthalate (DEHP) are among the most popular plasticizer. Similar to flame retardants, plasticizers are not bound to the plastics and polymers. As a result, they are widely distributed in the environment. Phthalate esters were announced to have carcinogenic and endocrine disrupting properties on aquatic organisms and human health. That is why they are also categorized as PSs by European Commission and U.S. Environmental Protection Agency (EPA) (Fatoki et al., 2010, Edjere et al., 2016, Kovacevic et al., 2013, Aznar-Alemany et al., 2017).

Polychlorinated biphenyls (PCBs) are used as dielectric fluid in the production of electrical equipment, hydraulic oils in mining, plasticizers, flame retardants as well as production of inks, glues, resins and pesticides. Industrial wastewater discharges, runoff from lands, leaching from landfill and industrial disposal sites are potential sources of these chemicals. After releasing into the environment, PCBS are distributed in different environmental compartments (water, soil and atmosphere) because of low vapor pressure and water solubility as well as high octanol-water partitioning coefficient. In addition, although PCBs production has been forbidden since 1970, they are still illegally produced or desorbed from the soils and sediments and enters the surface water (Yang et al., 2009). In the environment, PCBs showed adverse impacts such as bioaccumulation, neurotoxicity and endocrine disrupting effects on living organisms. Because of their unavoidable effects, they are among the initial groups of persistent organic pollutants (POPs) listed in Stockholm Convention of POPs (Jing et al., 2018, Megahed et al., 2015, Gakuba et al., 2015).

Polycyclic aromatic hydrocarbons (PAHs) are important group of anthropogenic PSs that consist of two or more fused benzene rings. They are mainly generated in combustion processes. Exhaust of vehicles and industrial pyrolysis (paper industry), oil and refinery activities as well as oil spills and discharges are the main sources of PAHs. Anthracene, benzo[ghi]pyrene, dibenzo[a,h]anthracene and fluoranthene are examples to these chemicals. PAHs enters the surface water via industrial wastewater discharges and fumes (Gupta, 2018). In the environment, PAHs are reported to have carcinogenic, mutagenic and high toxicity effect on organisms. Thus their presence in the environment specially surface water can adversely influence the human health (Fernandez et al., 1997, Malik et al., 2011, Eisler, 1987, Manzetti, 2013).

Benzotriazoles (BTRs) are among the HPVCs and are used in various industrial productions due to their specific features. They have an annual production of 9,000 tons in USA. BTRs are used mainly as corrosion inhibitors, airplane deicers and anti-freezing agents (ADAF) and UV light stabilizers. They are also found in products such as dyes, detergents, and in the production of fungicides, herbicides and pharmaceuticals products. 1H-benzotriazole (1H-B), 1-hydroxy-benzotriazole (1-OH-B), 4-hydroxy-benzotriazole (4-OHB), 5-hydroxy-benzotriazole (5-OH-B), tolyltriazole (4-methyl-1H benzotriazole [4-M-1H-B] and 5-methyl-1H-benzotriazole [5-M-1H-B]), 5,6-dimethyl-1H-benzotriazole [5,6-D-1H-B], and 5-chloro-1Hbenzotriazole (5-Cl-1H-B) are belonging to this group of chemicals (Asimakopoulos et al., 2013). Incomplete treatment of BTRs in WWTPs, runoff of ADAF from the airports to the surface water or/and discharge into the municipal sewage system and emission from vehicles are the major sources of BTRs in surface waters. Carcinogenic and estrogenic as well as mutagenic potential effect are the potential environmental effects of BTRs when enter the environment (Asimakopoulos et al., 2013, Alotaibi et al., 2015, Van Leerdam et al., 2009, Shi et al., 2019, Kiss and Fries, 2009).

Beside the aforementioned industrial chemical groups, there are other chemicals that are used as the main ingredients in the manufacturing of different products such as dye, paints, rubbers, coatings, plastics, chemicals and etc. These chemicals include hexa(methoxymethyl) melamine (HMMM), anilines, benzothiazoles, etc.

HMMM is used as the main ingredient in the production of melamine nanoparticles, castings, production of coatings and plastics for coils, cans and automobiles. Due to its industrial usages, HMMM mainly enters the surface waters through WWTPs. Its extensive consumption lead to its high detection frequency in the environment. Information on effects of HMMM on human health and other organisms is still scarce, however, some studies reported the genotoxicity effects of HMMM on organisms (Dsikowitzky and Schwarzbauer, 2015).

Anilines are industrial chemicals that are mainly utilized in the production of dyes, pesticides and pharmaceutical drugs. 3-chloroaniline and 4-chloroaniline are the most important anilines. Anilines find their way to the surface water either through the industrial wastewaters or agricultural runoff where the transformation and metabolism of pesticides occurs (Hwang et al., 1987, Okumura et al., 1996). Anilines such as abovementioned chloroanilines in surface water pose potential genotoxicity and carcinogenic risks to human health and aquatic organisms (Bohencke et al., 2003).

Benzothiazoles such as are among the HPVCs and are mainly used as vulcanization accelerators in the production of rubber, preservative in leather production as well as antifreeze agent and corrosion inhibitors. 2-morpholinothiobenzothiazole and 2-mercaptobenzothiazole are the most popular benzothiazole derivatives. Benzothiazoles have been reported to be frequently detected in surface waters originated from industrial discharges as well as urban surface runoff. When enter the surface water, they show high acute toxicity to fish and other organisms (Avagyan et al., 2015, Kloepfer et al., 2005).

2.1.4. Pesticides

Pesticides are used to repel or destroy any kind of pests such as unwanted plants and animal organisms that disrupt the quality lives of the crops and livestock. They are also applied on food and agricultural products during transport and storage. Considering their mode of action, pesticides are categorized into insecticides including mainly organophosphate and organochlorinated ones (aldrin, dichlorovos), acaricides (dicofol), fungicides (pentachlorophenols, chlorothalonil), soil fumigants and nematicides (formaldehyde, ethylene dibromide), herbicides (atrazine, trifluralin), plant growth regulators (propham, chloropropham) and rodenticides (methyl bromide) (Dich et al., 1997).

Global concern toward pesticides has been increased because of high consumption and application of those chemicals. In 2007, 5.2 billion tons of pesticides have been consumed throughout the world (Glinski et al., 2018). Large-scale catchment studies on losses of pesticides into surface waters revealed that less than 2% of the applied pesticide eventually found its way to the surface water. Runoff from agricultural field and lands as non-point sources is the main source of pesticides in surface water. In addition, point sources such as the spill originated from filling or cleaning the spraying instrument as well as inappropriate disposal of empty containers are other important contributors to the presence of pesticides in surface water. High toxicity, bioaccumulation and carcinogenic effects are the major environmental and health effects of pesticides. As a result, due to their frequent detection and adverse health risks, European Commission considered several pesticides as PSs in monitoring programs (Holvoet et al., 2007, Dich et al., 1997, Herrero-Hernández et al., 2013).

2.1.5. Natural Chemicals

Microcystins are naturally generated chemicals that are produced by cyanobacteria. The high occurrence of these chemical substances in surface waters is contributed to increased eutrophication

as a result of anthropogenic activities. Different genera such as *Microcystis, Anabaena, Aphanizomenon* and etc. are capable of producing these chemicals. Microcystin LR, microcystin-RR and microcystin-YR are examples to microcystins. In surface water, microcystins bioaccumulate in aquatic animals such as fishes through food ingestion or absorption into the skin (Amé et al., 2010). They are reported to particularly target the liver in animals, while depending on the microcystin congeners and their structures, they may target other organs as well (Buratti and Testai, 2015). Beside bioaccumulation, microcystins have hepatotoxicity and neurotoxicity effects on human and other organisms. That is why they are listed as CECs. World Health Organization (WHO) assigned a maximum limit of 1 µg/L for those chemical substances in drinking waters (Diez-Quijada et al., 2019, Scoglio, 2018).

2.2. Prioritization of Micropollutants and Current Legislations

2.2.1. Priority Substances (PSs) and Contaminants of Emerging Concerns (CECs)

Thousands of chemicals known as pollutants enters the water environments via either direct discharge from different sources (point and/or diffuse) or from treatment plants because of poor removal efficiency. Therefore, pollutants monitoring according to strict regulations is essential to provide a safe water environment (Tousova et al., 2017). In 2000, European Commission established a water framework directive (WFD), requiring the members to monitor various parameters including chemicals and biological parameters (Directive 2000/60/EC), in order to achieve water with good chemical and ecological statue (European Commission, 2000). In 2013, Directive 2013/39/EC, the recent updated version of Directive 2000/60/EC and the other relative directives was introduced with the aim of monitoring 45 PSs along with their established Environmental Quality Standards (EQSs) (Eurpean Commission, 2013). PSs are pollutants that their concentration in water bodies should not exceed their EQS values, and thus their monitoring is essential due to their potential risks to human health and aquatic organisms. However, it should be noted that PSs are not the only substances that deteriorate the quality of water and the health of human and aquatic biota. Therefore, in addition to PSs, other pollutants, so-called contaminants of emerging concern (CECs) are needed to be identified and further be monitored. CECs are compounds that the information regarding their occurrence, fate, transport and toxicity is not sufficient and worldwide monitoring data is required for further prioritization of these chemicals. They encircle three groups of chemicals including (1) substances that are recently introduced into the environment, (2) known substances that present in the environment for a long time but their potential risks to aquatic environments have not been asserted yet, and (3) compounds that present in the environment but analytical methods to measure them have

recently been developed. CECs composed of different groups of chemicals including PCPPs, surfactants, industrial-derived substances, pesticides, algal toxins as well as their transformation products (Sousa et al., 2018, Tousova et al., 2017). While, researches and studies concerning the occurrence, fate and toxicity of pollutants in aquatic environments is rapidly improving, a holistic prioritization approach is needed to determine the most important CECs for further monitoring programs of water systems (James et al., 2015).

2.2.2. Prioritization of Pollutants

Several publications have proposed methods to prioritize CECs. The prioritization methods introduced in literature include risk-based, chemical properties-based or other processes. Risk-based prioritization identify CECs compounds with the highest potential adverse impacts by comparing measured environmental concentration (MEC) or predicted environmental concentration (PEC) with predicted no effect concentration (PNEC) or other toxicity measurements (to human or other animals) (James et al., 2015). Von Der Ohe and his colleagues evaluated the risks of 500 organic compounds in four river basins. In that study, the organic substances were classified into six groups based on the available data. Further, two indicators, frequency of exceedance and the extent of exceedance of PNEC, which are based on MEC and 95% of MEC (MEC_{95}) values in each river basin, were utilized and compared to the lowest acute-PNEC or chronic PNEC to prioritize the compounds in each group. The spatial exposure was assessed by determining the frequency of the sites with MEC values more than the lowest PNEC while the extent of exceedance of PNEC (MEC_{95}/lowest PNEC) was used to evaluate the risk level (Von Der Ohe et al., 2011).

Strempel and coworkers proposed a prioritization process based on chemical properties. They prioritize the chemicals by comparing the estimated data of persistence (P). bioaccumulation (B) and toxicity (T) (PBT) properties of 95,000 chemicals to the limits regulated by REACH (registration, evaluation, authorization and restriction of chemicals). The PBT properties of each chemical in this study was either attained from the literature or estimated using Estimation Program Interface (EPI) Suite™ software of EPA. BIOWIN3, BCFBAF and ECOSAR predictive programs were applied to calculate biodegradation potential, bioaccumulation and toxicity, respectively. The calculated P, B and T values were then summed to report a final score for each chemical (Strempel et al., 2012). In another study, PBT values were determined or estimated using Pollution Prevention Software of USEPA (PBT profiler) for persistency, Log K_{ow} for bioaccumulation and ECOSAR for toxicity. Further, a score was calculated based on each PBT parameter and summed to achieve a final ranking (Diamond et al., 2011).

Beside risk-based and chemical properties-based prioritization process, some authors used other methods to develop the most important CECs. Kumar and Xagoraraki, (2010) suggested a ranking algorithm for prioritization of 100 PCPPs and endocrine-disrupting compounds in surface waters as well as drinking water in USA. The algorithm was evolved based on four criteria including occurrence, treatment, ecological effects and human health effects. Further, the ranking of each chemical was determined based on each criterion and further the overall ranking score was calculated to select the most important chemicals (Kumar and Xagoraraki, 2010).

2.2.3. European Commission Water Frame Directive on PSs

Environmental water quality monitoring in Europe entered a new phase in 2000. European union has forced the member states to monitor different chemical and biological parameters to provide a safe water based on legislated water frame directive (WFD). Directive 2000/60/EC was defined for this purpose. This directive requires the PSs to be identified and further compared with the established EQSs (European Commission, 2000). The first list of PSs was published under directive 2455/2001/EC where 33 PSs were subjected to be monitored in European water bodies. The list of PSs was selected by using combined monitoring-based and modelling-based priority setting scheme (COMMPS) which considers the automated risk-based score with the subsequent expert judgement. COMMPS procedure include (1) selection of potential substances for the ranking process which were taken from official monitoring lists such as directive 76/464/EEC, OSPAR list of individual candidate compounds, HELCOM list of priority substances and etc, (2) Exposure scores determination which was calculated for organic substances in both aquatic environments and sediments considering the existed monitoring data as well as modelling data (Mackay I distribution model), (3) Effect scoring which was accomplished for organic substances in water phase and sediments by considering the toxicity (PNEC), bioaccumulation potential data and selected endpoints for indirect effects on human health (carcinogenic, mutagenic, etc), (4) Risk-based priority index calculated from multiplication of exposure score with effect score and (5) Processing the ranked list and combining with expert judgment by firstly screening the obtained list and removing the historic pollutants and secondly, by making recommendations to include or exclude the remained pollutants into the priority list (Klein, 1999). Seven years later, directive 2008/105/EC representing the first list of EQS values of 33 PSs and 8 certain pollutants was released. The EQSs were set as annual average value (AA-EQS) and maximum allowable concentration (MAC-EQS) derived from the chronic and acute toxicity data, respectively (European Commission, 2008). In 2013, the number of PSs to be monitored was increased to 45 which was published along with their EQSs under directive 2013/39/EU. PSs list

contains chemicals from different groups such as pesticides, flame retardants, surfactants, organic solvents and etc. (Table 2.1) (Eurpean Commission, 2013).

Table 2.1. List of PSs in directive 2013/39/EU along with their usage, adverse effects and concentration limits (Eurpean Commission, 2013, Sousa et al., 2018).

Chemical name	**Usage and Type**	**Adverse effects**	**AA-EQS (µg/L)**	**MAC-EQS (µg/L)**
Aclonifen	pesticide		0.12	0.12
Alachlor	pesticide		0.3	0.7
Atrazine	pesticide		0.6	2
Bifenox	pesticide		0.12	0.04
Chlorfenvinphos	pesticide		0.1	0.3
Chlorpyrifos	pesticide		0.03	0.1
Cybutryne	pesticide		0.0025	0.016
Cypermthrin	pesticide		0.00008	0.0006
Aldrin	pesticide	Carcinogenic and mutagenic, causing nervous-system diseases	∑=0.01	Not applicable
Dieldrin	pesticide			
Endrin	pesticide			
Isodrin	pesticide			
Dichlorvos	pesticide		0.0006	0.0007
DDT	pesticide		0.025	not applicable
Diuron	pesticide		0.2	1.8
Endosulfan	pesticide		0.005	0.01
Heptachlor and heptachlor epoxide	pesticide		0.0000002	0.0003
Hexachlorobenzene	pesticide		-	0.05
Hexachlorocyclohexane	pesticide		0.02	0.04
Isoproturon	pesticide		0.3	1
Quinoxyfen	pesticide		0.15	2.7
Pentachlorophenol	pesticide, disinfectant		0.4	1
Simazine	pesticide		1	4
Terbutryn	pesticide		0.065	0.34
Trifluralin	pesticide		0.03	not appicable
Cadmium and its compounds	Heavy metal	High toxicity, carcinogenic effects	0.08	0.45
Lead and its compounds	Heavy metal		1.2	14
Mercury and its compounds	Heavy metal			0.07
Nickel and its compounds	Heavy metal		4	34
Polybrominated diphenylethers (PBDEs)	Flame retardants	Endocrine disrupting and carcinogenic effects	-	0.14

Table 2.1. Continued.

Chemical name	Usage and Type	Adverse effects	AA-EQS (µg/L)	MAC-EQS (µg/L)
Hexabromocyclododecane (HBCDD)	Flame retardants		0.0016	0.05
1,2-dichloroethane	Organic solvent		10	not applicable
Benzene	Organic solvent		10	50
Carbon tetrachloride	Organic solvent		12	not applicable
Chloroalkenes	Organic solvent		0.4	1.4
Dichloromethane	Organic solvent	Carcinogenic, reproductive and developmental risks	20	not applicable
Hexachlorobutadiene	Organic solvent		-	0.6
Pentachlorobenzene	Organic solvent		0.007	not applicable
Tetrachloroethylene	Organic solvent		10	not applicable
Trichloroethylene	Organic solvent		10	not applicable
Trichloromethane	Organic solvent		2.5	not applicable
Trichlorobenzenes	Organic solvent		0.4	not applicable
Di(2-ethylhexyl) phthalate (DEHP)	Plasticizer	Endocrine disrupting and carcinogenic effects	1.3	not applicable
Nonylphenols	Surfactant		0.3	2
Octylphenols	Surfactant	Endocrine-disrupting, estrogenic effects	0.1	not applicable
Perfluorooctane sulfonic acid (PFOS)	Surfactant	High bioaccumulation and biomagnifiction in environment, toxic effects	0.0065	36
Anthracene	Combustion byproducts, PAH		0.1	0.1
Benzo(a)pyrene	Combustion byproducts, PAH		0.0017	0.27
Benzo(b)fluoranthene	Combustion byproducts, PAH	Toxic, carcinogenic, mutagenic, long life time in the environment	[a]	0.017
Benzo(k)fluoranthene	Combustion byproducts, PAH		[a]	0.017
Benzo(ghi)-perylene	Combustion byproducts, PAH		[a]	0.082
Indeno(1,2,3-cd)-pyrene	Combustion byproducts, PAH		[a]	not applicable

Table 2.1. Continued.

Chemical name	Usage and Type	Adverse effects	AA-EQS (µg/L)	MAC-EQS (µg/L)
Fluoranthene	Combustion byproducts, PAH		0.0063	0.12
Naphthalene	Combustion byproducts, PAH		2	130
Polychlorinated dibenzo-p-dioxins and dibenzofurans (PCDD/PCDS) and polychlorinated biphenyls (PCBs)	Dioxins, incineration products, metal industries	bioaccumulation, neurotoxicity and endocrine disrupting effects	not applicable	not applicable

[a] The AA-EQS values were corresponding to the concentration of benzo(a)pyrene.

[b] Insufficient data for AA-EQS of these substances.

2.2.4. The Watch List of European Commission and Norman Network

In addition to PSs listed in directive 2013/39/EU, European Commission published the first Watch List of ten groups of CECs (directive 495/2015/EU) to be monitored in European water bodies in 2015. The substances in Watch List are selected from the ones for which the existing data represent that they may pose a significant risk, however, the monitoring data to show their actual caused risk is still not sufficient. Thus, the monitoring data is needed for further prioritization of these substances (European Commission, 2015). The Watch List comprise of pharmaceuticals including diclofenac as analgesic drug, clarithromycin, azithromycin and erythromycin as macrolide antibiotics, 17β-ethinylestradiol, estrone and 17 β -estradiol as hormones. These pharmaceuticals gained a lot of attention due to their high persistency as well as evolving antimicrobial resistance in some microorganisms. 2,6-ditert-butyl-4-methylphenol (BHT) applied as antioxidant in food industries. Although BHT itself was not determined to pose a risk, its biodegradation product, 3,5-di-tert-butyl-4-hydroxybenzaldehyde was investigated to damage DNA in organisms. In addition to the abovementioned chemicals, 2-ethylhexyl-4-methoxymethoxycinnamate (EHMC), an UV filter which is mainly used as sunscreening agents as well as an ingredient in the production of paints, has a high persistency, bioaccumulation potential and endocrine-disrupting effects on organism. Watch List also include eight pesticides, acetamiprid, clothianidin, imidacloprid, methiocarb, oxadiazon, thiacloprid, thiamethoxam and triallate. These pesticides have high persistency, toxicity, bioaccumulation potential and cause carcinogenic and mutagenic effects (European Commission, 2015, Sousa et al., 2018).

NORMAN is the network of reference laboratories, research centers and related organization for monitoring of emerging substances which was developed in 2005. NORMAN was originally a three years project funded by European Commission with the objective of providing the recent topics of concerns and research requirements in order to prepare a platform for the identification and prioritization of CECs under the WFD. The network was commenced and developed by establishing an algorithm to determine the most effective techniques and methods to identify and prioritize the CECs as well as evaluating the availability of the data for the risk assessment of the CECs. After three-year project, NORMAN became a permanent network working on CECs. NORMAN network considers the behavior of an emerging substance not only in water environment but also in all environmental compartments. Currently, NORMAN list of CECs contains 1036 chemicals including PPCPs, flame retardants, biocides, pesticides and their biotransformation products. The number of chemicals in the is growing considering the fact that more than 100 million chemicals are registered to the Chemicals Abstracts Service (CAS). In addition, NORMAN established a CECs prioritization scheme in which the CECs are evaluated and categorized based on their monitoring data, analytical performance as well as toxicity information (Dulio and Slobodnik, 2009, Dulio et al., 2018, Norman, 2016).

Enhanced number of studies on chemicals in the Watch List of directive 495/2015/EU and CECs listed in NORMAN network provide comprehensive monitoring data of those chemicals in the environment. Further, introducing an appropriate and powerful prioritization method can lead to select the most important chemicals for further achievement of a water with high quality.

2.3. Instrumental Methods to Measure Micropollutants

Micropollutants are present in the environment at very low concentrations. Quantification of those chemicals at such a low concentration in complex environmental matrices is challenging. Therefore, a proper sampling methodology, sample preparation and analytical method are required to identify and quantify the micropollutants in surface water (Sánchez-Avila et al., 2009, Padhye et al., 2018).

The first step in the analysis and monitoring of micropollutants in surface water is to obtain a representative sample. The sampling is a significant step in environmental monitoring programs of water bodies since any small error can invalidate the analysis (Padhye et al., 2018). Sampling of a surface water is carried out by firstly selecting the sampling sites. The sampling sites should reflect the relative effects of both point and non-point source pressures. The frequency of sampling shall be

selected in a way that minimizes the effect of seasonal variation on the monitoring results. For instance, the sampling frequency for PSs is once per month while for other pollutants is once per three months. In addition, the method for sampling shall be in compliance with international standards (e.g. ISO) or other standards which verify to provide data with sufficient quality (European Commission, 2000).

Grab sampling or time-integrated sampling may be used in monitoring programs. Grab sampling as the most popular technique requires the sampling at one point and time. While time-integrated sampling such as passive sampling technique provide samples from a discrete point in a time period using a sampling device. Although time-integrated samplings provide temporal information about the contamination, they may be influenced by environmental factors such as water flow rate, temperature as well as biofilm creation on the surface of the sampling device (Sousa et al., 2018).

The sampling equipment shall be selected based on the type of the sampling. In addition, it should not interact with the pollutants of interest. For instance, for analysis of hydrophobic organic pollutants, glass or polytetrafluoroethylene (PTFE) plastics are recommended. While for metals, plastic containers are preferred. After collection and transporting of samples to the laboratory, they shall be stored at 1-5 ^{o}C in order to minimize the analysis errors (European Commission, 2009).

After sample collection and transport to the laboratory, samples are processed to get ready for instrumental analysis. Since micropollutants are present in the environment at very low concentrations, they have to be isolated from the matrix to reduce the interferences and also pre-concentrated to meet the detection limits of the chromatographic equipment. Liquid-liquid extraction (LLE) and solid-phase extraction (SPE) are among the most important extraction methods to isolate and concentrate micropollutants in the water samples. The former is used to extract a chemical from water with an organic solvent whereas the latter uses solid media to isolate the chemical from the water. Selection of the right solvent and solid media is critical in both methods and affects the recovery rate of the target chemical from the water matrix. Both methods are capable to concentrate the target chemical for over 10-100 times (Padhye et al., 2018, Bueno et al., 2012).

Micropollutants in processed samples are quantified using a sensitive analytical instrument. Gas chromatography (GC) or liquid chromatography (LC) coupled with mass spectrometer (MS) are two very common instrument systems for the analysis of micropollutants. Mass detector is the key element of the analytical system due to its high sensitivity which enables the quantification of micropollutants at very minute concentrations. Main components of an MS detector are: (1) ion source, (2) mass

analyzer and (3) detector. When a chemical substance is introduced to an MS, it is ionized positively or negatively in the ion source and further the ions are sorted based on their mass to charge ratio (m/z ratio) in the mass analyzer. At the end, the ions hit the detector and generate a signal for the ion of a chemical substance as a peak. There are various types of MS analyzers such as quadrupole, ion trap, time-of-flight (TOF), orbitrap and ion cyclotron. The type of the MS analyzer is selected according to the objective of the analysis For instance, if the objective is to accurately measure a target chemical at very low concentration then quadrupoles and ion trap are the MS detectors of choice. On the other hand, if identification of chemicals present in a complex sample is the objective, high resolution mass detectors such as orbitrap and TOF are preferred (Haag, 2016).

Quadrupole: Quadrupole analyzers are comprised of four parallel cylindrical rods from which the opposite ones are electrically connected. A radio frequency potential (RF) is applied and further a direct current potential (DC) is imposed over the RF. Depending on the applied RF and DC potentials, the ions with similar m/z ratio which also have stable oscillation routes, are passed to the detector and the rest are filtered out. Thus, ions with different m/z ration are scanned by changing the RF and DC potentials and be detected. Quadrupole MS analyzers are one of the most widely used analyzers since it is reliable, have compact design, durable and are economical effective. However, they have low mass range and resolution and therefore not suitable for detecting high mass molecules and identification of unknown chemical substances (Haag, 2016).

Ion trap: Ion trap analyzers consist of two hyperbolic endcap electrodes encountering each other and a ring electrode between them. Like quadrupole analyzers, a RF and DC is applied. However, in the case of ion trap analyzers, the ions are trapped and sorted according to their m/z within a voltage gradient between endcap electrodes. Ion trap analyzers have a relatively high sensitivity due to their ability to accumulate the ions. However, they have moderate resolving power which is a disadvantage of these analyzers (Haag, 2016).

TOF: These analyzers have two main components, (1) an acceleration grid and (2) a field free region flight tube. After the ions being ionized, they are accelerated by applying a pulsed electrical potential on acceleration grid. Further, the accelerated ions, considering their m/z ratio, move through the field free region and are separated. The heavier the ion, it takes longer time for it to pass through the field and hit the detector and produce signal. Considering their features, TOF analyzers can provide a broader mass range due to high ion transmission efficiencies and better resolution compared to other analyzers (Haag, 2016).

Fourier transform ion cyclotron resonance (FT-ICR): In FT-ICR analyzers, the generated ions firstly enter and trap in a Penning trap where a cyclotron frequency perpendicular to the magnetic field is applied. The ions are separated based on their m/z ratio which is depended on cyclotron frequency. However, in order to detect the ions by detector, they are excited into larger ions by a RF pulse, attain a higher cyclotron orbit and further be detected by the receiver plates. A Fourier transform converts the generated signal into a frequency spectrum. The most important advantage of FT-ICR analyzers is their high resolution and mass accuracy which is proportional to magnetic field. Therefore, the size of the magnets is major problem which may require a larger laboratory space. In addition, the high cost of helium as coolant for these big magnets is another drawback of these analyzers (Haag, 2016).

Orbitrap: These analyzers consist of two concave electrodes facing each other and a spindle electrode placed between them. In orbitrap analyzers, the introduced ions swirl due to an electric field applied between the concave electrodes and the inner spindle electrode and oscillate back and forth. Further, same as FT-ICR, Fourier transform is used in orbitrap analyzers to convert the detected oscillation signals to the frequency spectrum. Like FT-ICR, orbitrap analyzers also possess high resolving power which may use as substitute for FT-ICR analyzers considering that orbitrap analyzers require less space. However, in experiments where high acquisition rate is required, orbitrap analyzers may face problems when compared to TOF analyzers due to space-charge effects (Haag, 2016).

Tandem mass: Tandem mass analyzers comprised of at least two mass analyzers in series. In tandem mass analyzers. The first mass analyzer is utilized to select the ions and apply collision-induced dissociation (CID). Consequently, the produced ions in the first analyzer are analyzed by the second analyzer. Triple quadrupoles (QqQ), Q-TOF and TOF/TOF are among the most used tandem mass analyzers (Haag, 2016).

Triple quadrupoles mass spectrometers consist of three quadrupoles in series. The produced ions in ion source enter the first quadrupole (Q1) where the ions with m/z ratio of interest are scanned. Further, the selected ions are fragmented in the second quadrupole (Q2). The fragmented ions are then filtered through the last quadrupole (Q3) where they can be fixed or scanned. Using different scan modes can result in different analysis. One of the most important and useful scanning modes is multiple reaction monitoring (MRM) which is used to quantify chemicals in a mixture. In this mode, Q1 is fixed to a specific m/z ratio. Further, after association of the ions in Q2, the fragmentation ions attributed to a particular m/z ration will be selected in Q3. Therefore, MRM can determine the fragmentation ions of a specific chemical and that is why it is suitable to identify and quantify a compound with known mass in a mixture (Haag, 2016).

Q-TOF mass spectrometers consist of a quadrupole analyzer and a TOF analyzer following it. In addition, the CID occur in between the two aforementioned analyzers. The stream of ions inject into the quadrupole will be further introduced into the TOF analyzer as ion pocket using plates in between the two mass analyzers. Combination of quadrupole and TOF result in a tandem mass spectrometer with high mass accuracy, scan speed and resolution (Haag, 2016).

TOF/TOF mass spectrometers are the combination of two TOF analyzer with a collision chamber located between them. In these tandem spectrometers, the produced ions are accelerated in the first TOF analyzer. In this step, the ions with specific m/z ratio are separated with a timed-ion-selector (TIS) and further slow down. The selected ions are then fragmented. The fragment ions are re-accelerated and injected into the second TOF analyzer where their time-of-flight is detected. TOF/TOF tandem mass spectrometers are fast method for analyzing the samples in MS and MS^2 levels (Haag, 2016).

Hyphened techniques, gas chromatography-mass spectrometry (GC-MS) and liquid chromatography- mass spectrometry (LC-MS), are benchmarks for targeted identification and quantification of micropollutants in the environment (Robles-Molina et al., 2014). While GC-MS is mainly used mainly for volatile compounds, LC-MS is preferred for the analysis of polar and non-volatile pollutants such as PPCPs and their metabolites, surfactants, flame retardants, plasticizers and etc. In addition, LC-MS analysis requires less sample pretreatment compared to GC-MS (Sosa-Ferrera et al., 2012). Considering the features of different mass spectrometers, LC coupled with triple quadrupole mass spectrometer is a suitable instrument for determination of trace components of complex mixtures by high selectivity and sensitivity with multiple reaction monitoring (MRM). Research articles retrieved from Web of Science in 2012 showed that triple quadrupole mass spectrometer was the choice of mass analyzer used in 23% of the studies examined (Giger, 2009, Albergamo et al., 2018, Holcapek et al., 2012). Many studies have used LC-MS techniques to identify and quantify different groups of micropollutants including pharmaceutical drugs and hormones (Albergamo et al., 2018, Carpenter and Helbling, 2018, Kasprzyk-Hordern et al., 2008, Giebultowicz et al., 2018, Ma et al., 2016, Alder et al., 2010, Paiga et al., 2016), Musks and UV filters (Jurado et al., 2014), OPs, CFRs and PBDEs flame retardants and plasticizers (Kim and Kannan, 2018, Shi et al., 2016), nonylphenol and PFs surfactants (Skutlarek et al., 2006, Petrovic et al., 2002, Munoz et al., 2017) ,Pesticides (Papadakis et al., 2015, Ruff et al., 2015, Herrero-Hernández et al., 2013, Charalampous et al., 2015), PCBs (Moukas et al., 2014), PAHs (Lien et al., 2007, Lung and Liu, 2015) and benzotriazoles as corrosion inhibitors (Wang et al., 2016b).

Development of various LC-MS and/or LC-MS/MS methods have eased the identification and quantification of different group of known and popular chemicals. Targeted analysis that includes the identification and quantification of predetermined compound or group of compounds in a sample to meet the regulatory goals has been successful due to its good sensitivity and reliability. However, targeted monitoring ignores other pollutants (site-specific contaminants) with probable high concentrations or with high toxicity potentials such as metabolites and transformation byproducts. Non-targeted analysis as a novel approach has been evolved to broaden the identification of so-called unknown chemicals (Krauss et al., 2019). In particular, the combination of LC with high-resolution mass spectrometry (LC-HRMS) such as QTOF broaden the identification capability as well as the sensitivity of pollutant analysis via full scan acquisition. Developing of LC-HRMS instruments eased the screening of water samples in non-targeted analysis to achieve a wider spectrum of present chemicals substances in a water sample (Dom et al., 2018, Schlabach et al., 2013). As a result, combining the findings of both targeted and non-targeted analyses can give a comprehensive information about the present potential pollutants in surface waters.

2.4. Occurrence of Micropollutants in Surface Water

Presence of micropollutants in surface water passing across an area having cities, industrial zones and agricultural fields is inevitable (Goktas and Macleod, 2018). Factors affecting the spatiotemporal occurrence of micropollutants in surface water include geographical, geological and meteorological properties of the area; physical and chemical properties of water and water flowrate; consumption rate of the chemicals, their physicochemical properties as well as their biodegradation and photodegradation rates (Sousa et al., 2018). For instance, Moreno-Gonzalez et al. (2014) investigated the occurrence of pharmaceutical compounds in surface water in Campo de Cartagena in Spain. In that study, concentration of macrolide antibiotics including azithromycin and clarithromycin was very high at a sampling point close to the discharge point of a WWTP. The measured concentration was so far the highest concentration reported for macrolides in the literature. Authors suggested that the extreme concentration was due to very high consumption of those antibiotics in that region which coupled with poor treatment at WWTP as well as low flow rate of the water. In addition, they indicated that more than 60% decrease in concentration of the aforementioned antibiotics at the end of the river route may be related to their sorption onto sediment and/or photodegradation (Moreno-Gonzalez et al., 2014).

The studies on micropollutant monitoring in surface water are increasing day by day. Since 2012, 136 studies were conducted in different countries throughout the world on the occurrence of

micropollutants in surface waters among which China, Spain, Portugal and Greece are the pioneers. The studies mainly focused on the PSs listed in directive 2013/39/EU and CECs mentioned in the Watch List of directive 2015/495/EU. Among the PSs monitored, triazine pesticides (e.g. atrazine, simazine), organophosphorus pesticides (chlorpyrifos), phthalates (DEHP) and PAHs were the most studied ones. PAHs, DEHP and atrazine were the PSs with highest detected concentrations. For instance, highest PAHs concentration up to 59.6 µg/L was reported in Iran. Among the CECs, diclofenac, estrogens and macrolide antibiotics were the most reported and studied ones (Sousa et al., 2018).

2.4.1. Pharmaceuticals and Personal Care Products (PPCPs)

2.4.1.1. Pharmaceutically active compounds (PhACs). Antibiotics are frequently detected in surface waters. Antibiotics belonging to chloramphenicols, sulfanoamides, fluoroquinolones, tetracyclines and macrolides were measured in Yangtze Estuary in China at concentrations between 0.05 and 23.5 ng/L using LC-MS/MS (Yan et al., 2013). The same groups of antibiotics were also analyzed with a LC-MS/MS in water and sediment samples taken from Huangpu River in Shanghai where sulfonamides were the most abundant antibiotics with a concentration range between 34 and 859 ng/L (Chen and Zhou, 2014). Maximum concentrations up to 580.4, 3.1, 14.8, 3.2, 82.2 and 4.3 ng/L of sulfadimidine, sulfamethoxazole, sulfadiazine, sulfapyridine, doxycycline and ofloxacin were measured in a river water in Hong-Kong, respectively (Deng et al., 2016). In another study, 24 antibiotics at concentrations up to 2 µg/L, which was reported for sulfamethoxazole, were detected in the South Queensland Watershed in Australia using LC-MS/MS. In addition, the authors concluded that WWTP discharges were the main sources of the antibiotics in those surface waters (Watkinson et al., 2009). Azithromycin, which has the highest consumption rate among all of the other antibiotics in Spain since 2008, was measured at a concentration as high as 16.6 µg/L in various surface waters in Spain using an LC coupled with triple quadrupole-linear ion trap mass spectrometer (Moreno-Gonzalez et al., 2014).

Analgesic drugs are another widely used PhACs that are frequently detected in surface waters. A study on the occurrence of the pharmaceuticals in surface water on the northern Antarctic Peninsula region utilizing LC-MS/MS, showed that acetaminophen, diclofenac and ibuprofen were present in the river water at 48.74, 15.09 and 10.05 µg/L, respectively (Gonzalez-Alonso et al., 2017). In another research, 10 analgesic drugs were measured in the water samples taken from three lakes in Hanoi, Vietnam. Concentrations of the most frequently detected drugs, ibuprofen and carbamazepine, in those three lakes were 0.58, 0.95 and 1.1 µg/L, and 0.35, 0.53 and 0.67µg/L, respectively (Tran et al.,

2014). The concentration of diclofenac as analgesic drug listed in the Watch List of directive 2015/495/EU, was reported at a concentration up to 10.2 µg/L in surface waters of Africa (Gumbi et al., 2017).

Beta-blockers are PhACs used to combat cardiovascular illnesses. They are released into the environment after they are excreted from the human body (Alder et al., 2010). Atenolol and propranolol were measured using LC coupled with a triple quadrupole mass spectrometer in a study conducted on the surface water samples from Buyukcekmece Watershed in Turkey. The highest concentration of atenolol was detected in Ahlat creek at 122 ng/L. Highest propranolol concentration was 561 ng/L and measured in the samples taken from the Hamza River. In addition, atenolol was detected in every sampling point in the region suggested that it is a popular beta-blocker in Turkey (Aydin and Talinli, 2013). LC/Q-TOF-MS analysis of samples from water samples taken from South Platte River in Denver Metro area, wells and lakes showed average concentrations of 80, 237 and 53 ng/L for atenolol, metoprolol and propranolol, respectively (Ferrer and Thurman, 2012).

Hormones are substances that are abundant in the environment, however, their potential risks to aquatic organisms and human have not been considered seriously. Therefore, they gained a lot of attention in the last decade and included in the Watch List of directive 2015/495/EU due to their frequent occurrence in surface water and their endocrine disrupting potential (Velicu et al., 2007, Ma et al., 2016, Sousa et al., 2018). In a study on estrogen hormones in 21 streams in Eastern Pennsylvania, estrone was determined as the most dominant hormone at concentrations between 0.6 and 2.6 ng/L using GC-MS. In that study, estriol and ethinyl estradiol had the highest concentrations of 19.7 and 3.0 ng/L, respectively (Velicu et al., 2007). A study on quantification of hormones in Karun River in Ahvaz, Iran indicated that 17β-estradiol was detected in 69% of the samples at a mean concentration of 13.66 ng/L (Hassani et al., 2016). LC-MS analysis of the water samples taken from Santa Ana River showed that estrone and 17β-estradiol-3-sulfate were the most detected hormones at concentrations 0.24-6.37 ng/L and 0.49-9.25 ng/L, respectively (Ma et al., 2016).

2.4.1.2. Personal care products (PCPs). PCPs consist of chemicals such as fragrances, UV filters, biocides and preservatives that are frequently found in surface waters (Villa et al., 2012).

Fragrances are reported to be present in different environmental compartments including water, sediment as well as humans body (Villa et al., 2012). Several studies reported the presence of fragrances in surface waters and aquatic environments. In a study on Molgora River in Italy, concentration of galaxolide, tonalide and celestolide were determined using a GC-MS. Galaxolide

was the most abundant chemical at concentrations up to 1141 ng/L while the concentration ranges determined for tonalide and celestolide were 0.25-365 ng/L and 0.25-23.4 ng/L, respectively. In addition, all of those three fragrances had the elevated concentrations in suspended sediment as well, because of their high Log K_{oc} in that region. Discharge of the effluents from three STPs around the Molgora River were indicated as the major source of those fragrances (Villa et al., 2012). Sumner et al. (2010) measured the presence of different fragrances in Tamar Estuary in UK, utilizing a GC-MS. The maximum concentrations of 28 and 10 ng/L of galaxolide and tonalide were determined, respectively while the other musks including phantolide, celestolide, musk xylene , musk ambrette and musk ketone were not detected in that estuary (Sumner et al., 2010). Galaxolide was detected in more than 80% of the freshwater samples taken from Nakdong River in Korea at concentrations up to 2.0 µg/L. The fragrances quantification in that study was accomplished using a GC-MS. Other musks including musk ketone and tonalide were also present but at a lower detection frequency and concentration than galaxolide, suggested the high consumption of galaxolide in that region (Lee et al., 2014).

UV filters have large production volume and applications which is the main factor of their high detection in the surface waters considering that they are not completely removed in WWTPs (Jurado et al., 2014). LC-MS/MS and GC-MS analysis of the water samples from Glutt River in Switzerland revealed the contamination of this river with several UV filters including benzophenone-4> benzophenone-3> 3-(4-methyl)benzylidene-camphor > 2-ethyl-hexyl-4-trimethoxycinnamate. Benzophenone-4 was present at concentrations between 0.27 and 24.0 µg per polar organic chemical integrative samplers (POCIS) whereas maximum 0.1 µg/POCIS was recorded for the other most frequently detected UV filters. The study also found that the concentration of UV filters in water samples decreases as their lipophilicity increased (Fent et al., 2010). Analyzing the river water samples utilizing LC coupled with a Quatro micro triple quadrupole mass spectrometer found that benzophenone-4 was present at a concentration up to more than 100 ng/L. Compared to other PCPs analyzed, benzophenone-4 was the most frequently found PCP in the rivers Ely and Taff in UK (Kasprzyk-Hordern et al., 2008).

The occurrence of antimicrobial agents in surface waters have been well documented due to their frequent detection. Concentrations up to 8.72 µg/L for triclosan and up to 0.36 µg/L for triclocarban was reported in a river in Gauteng Province, South Africa, using LC-MS/MS at ESI ionization mode (Lehutso et al., 2017). In another study triclosan was detected at several sampling sites along the Vistula River in Poland at a maximum concentration of 144 ng/L measured by LC-MS/MS (Giebultowicz et al., 2018). One of the main users of triclosan are the hospitals. In this regard, a study

was conducted on the triclosan concentration in tropical rivers receiving the effluent of hospital wastewater treatment plant. The LC-MS/MS quantification of triclosan revealed concentrations between 3 and 68 ng/L in Jiaosu River and between 2.7 and 51 ng/L in Dian-Bao River in Southern Taiwan, indicated the contribution of hospital treatment plant effluent on the triclosan pollution in those rivers (Yang et al., 2015).

Parabens as preservatives in PPCP products are releasing into the surface water via mainly wastewater discharges (Czarczynska-Goslinska et al., 2017). Methyl paraben and propyl paraben were determined by LC-MS/MS at concentrations 2.2-17.3 ng/L and 9.2-12.0 ng/L in the waters of the Greater Pittsburgh area in USA, respectively (Renz et al., 2013). In another study on the waters of Greater Poland Voivodeship, up to 1.6 µg/L of methyl paraben was quantified by an LC coupled with Qtrap triple quadrupole tandem mass spectrometer (Czarczynska-Goslinska et al., 2017). In water samples taken from Mogi Guacu River in Brazil, the concentration of methyl paraben, ethyl paraben and propyl paraben were measured using HPLC instrument. Mean concentrations of 8.0, 5.8 and 13.1 µg/L of the aforementioned parabens were recorded, respectively (Galinaro et al., 2015).

2.4.2. Surfactants

Alkylphenol ethoxylates are a group of surfactants that are listed as important CECs. Petrovic et al. (2002) investigated the concentration of NPEO and NP in different sampling points on Mediterranean coast in Spain using LC-MS operating in ESI ionization mode. Concentration as high as 11 µg/L of NPEO was measured in the sampling point receives the effluent from an industrial plant. In addition, NP was detected in seawater samples of the region at concentrations between less than 0.15 and 4.1 µg/L (Petrovic et al., 2002). Cespedes et al. (2006) determined the concentration of nonylphenol monoehtoxylate (NP_1EO), nonylphenol diehtoxylate (NP_2EO), 4-tert-octylphenol, 4-nonylphenol and 4-heptylphenol along the Ter River in Spain using LC-MS. Among those compounds, $NP_{1+2}EO$ (NP_1EO+NP_2EO) was quantified in all of the river water samples at concentrations between 0.66 and 3.63 µg/L (Cespedes et al., 2006)

PFs are another group of important surfactants. Due to their extensive consumption and release into the environment as well as their adverse effects on human health, they were included in the last update of the PSs of WFD (2013/39/EU) (Skutlarek et al., 2006). A spatial occurrence study of various PFs compounds in Rhine River and its tributaries using a LC coupled with a triple-quadrupole mass analyzer found that the PFs concentration as high as 94 ng/L was present in Ruhr River as a tributary of the Rhine River. The PFs compounds studied had higher concentrations in the tributaries

than the Rhine river itself, suggesting the effect of dilution factor. For instance, the concentration of total PF compounds at the upper intersect of Ruhr River and its tributary (Moehne River) was 4,385 ng/L while the concentration in the point right after Ruhr River meets the Rhine river was as low as 41 ng/L (Skutlarek et al., 2006). Munoz et al. (2017) implementing their developed LC-MS/MS method, found a high frequency of 79% and 65% for perfluorooctane sulfonate (PFOS) and perfluorooctanate (PFOA) in surface water samples taken from several regions in France, respectively. Up to about 13.5 ng/L of PFOS was measured whereas the highest PFOA concentration was 15 ng/L. In addition, concentration of PFs in the groundwater samples taken from the same region was higher than surface waters (Munoz et al., 2017).

Quaternary ammonium compounds (QACs) are often present in the influent and effluent of STPs and WWTPs as well as surface waters (Elersek et al., 2018). Ding and Liao. (2001) reported different benzalkonium chloride in selected river water in Taiwan using GC-MS. The highest detected concentration was associated to C_{18}BDMA (C_{18}-benzyldimthylammoniumchloride) at concentrations between 15 and 55 µg/L (Ding and Liao, 2001). In another study, chemicals quantification by LC coupled with an ion trap mass spectrometer showed the presence of 1.22- 5.35 µg/L C_{12}BDMA and 2.38-36.6 µg/L C_{14}BDMA in WWTPs effluent and river downstream samples (Ferrer and Furlong, 2001).

2.4.3. Industrial Chemicals

Industrial chemicals are compounds that encircle a wide spectrum of anthropogenic substances consumed or produced during various industrial processes. Flame retardants, plasticizers, combustion byproducts and corrosion are categorized as industrial chemical substances (Luo et al., 2014).

2.4.3.1. Flame retardants. Organophosphorus and halogenated flame retardant are the most studied ones in the literature as they are present in the environment at high frequency and they pose risks to the human (Segev et al., 2009).

Many studies have reported the presence of OP flame retardants in surface waters. Regnery and Puttmann. (2010) monitored five OPs in different surface waters of Germany using GC-MS. Tris(2-chloroethyl) phosphate (TCEP), tris(2-chloro-1-methylethyl) phosphate (TCMP), tris(2- butoxyethyl) phosphate (TBEP), tri-iso-butyl phosphate (TiBP), and tri-n-butyl phosphate (TnBP) were measured at concentrations as high as 184, 379, 652, 82 and 83 ng/L, respectively (Regnery and Puttmann, 2010). In another study, LC-MS/MS quantification of OPs in water samples such as tap water, lake,

river and rainwater revealed that tris(1-chloro-2-propyl) phosphate (TCPP) was the most frequently detected OP. Concentration as high as of 329 ng/L in lake sample was recorded for that chemical. Moreover, TBEP was found at concentrations between 2.53 and 366 ng/L in the lake water and between 0.60 and 689 ng/L in the river water as well (Kim and Kannan, 2018). TCPP and TBEP were also quantified using GC-MS in a study on the water samples from the Elbe River in Germany. TCPP was present at concentrations between 40 and 250 ng/L while TBEP was found up to 80 ng/L (Bollmann et al., 2012). Based on the presented results and findings from other researches in the literature, TCPP and TBEP were determined as the most abundant OP flame retardants in the surface waters (Cristale et al., 2013a, Shi et al., 2016).

Beside OPs, chlorinated flame retardants (CFRs) and polybrominated diphenyl ethers (PBDEs) as halogenated flame retardants are found frequently in surface waters. Among the halogenated flame retardants, PBDEs are among the PSs listed in WFD because of their high potential risk to human and aquatic life (Aznar-Alemany et al., 2017). PBDEs in Asunle Stream in Nigeria were analyzed by a GC-MS/MS during 8 months and were measured at concentrations between 0.03 and 0.45 µg/L. In addition, PBDEs were found at high concentrations during the wet season compared to the rest of the year (Olutona et al., 2017). Wurl et al. (2006) reported a total PBDEs concentrations between 31.1 and 118.7 pg/L in dissolve phase and between 25.7 and 32.5 pg/L in suspended phase in seawater samples taken from Hong Kong utilizing GC-MS/MS (Wurl et al., 2006). In another study, a GC coupled to a quadrupole mass analyzer was implemented to quantify the BDE-209 as a PDBE in the River Aire in UK where its concentration ranged between 17 and 295 ng/L (Cristale et al., 2013b). Dechlorane plus (DP) is a CFR that was reported in several studies. Hoh et al. (2006) detected DP in sediments and atmosphere of Great Lakes region using GC-MS (Hoh et al., 2006). DP at a mean concentration of 1.8 ng/L was measured using a GC-MS in the water samples taken from the coastal regions in Northern China as well (Jia et al., 2011).

2.4.3.2. Plasticizers. Phthalate esters as the most widely used plasticizers are known to be easily discharge into the WWTP and further surface waters since they are physically bound to the products (Net et al., 2015). Fatoki et al. (2010) studied the occurrence of four phthalate esters including dimethyl phthalate (DMP), diethyl phthalate (DEP), dibutyl phthalate (DBP) and di-(2-ethylhexyl) phthalate (DEHP) in the surface waters in Venda, South Africa using GC. Among the studied phthalates, DBP and DEHP had the highest concentrations. Except DMP, the rest of phthalate esters have been detected frequently in the water samples at concentrations up to 10.17, 2.18 and 3.56 mg/L for DBP, DEHP and DEP, respectively (Fatoki et al., 2010). Concentrations between 52.5 and 4498 ng/L for DBP and between 128.9 and 6570.9 ng/L for DEHP were quantified with a GC-MS in the

water sources in Northeast China (Liu et al., 2013b). In another study on the surface waters in Delta State, Nigeria, DBP and DEHP were found at mean concentrations of 0.61 and 0.45 µg/L using a GC-MS, respectively, suggested to be the phthalate esters with the highest measured concentrations (Edjere et al., 2016).

2.4.3.3. Other important industrial chemicals. PCBs, PAHs, benzotriazoles and chemical substances used in the manufacturing industries are other important industrial chemicals. They are important as are extensively consumed and frequently present in surface waters.

PCBs were used mainly as dielectric insulating fluids in different industries. Their production was banned in 1970s, however they are still found in the surface waters because of their high persistency in the environment (Gakuba et al., 2015). Zhang et al. (2004) reported a concentration range between 31.58 and 344.9 ng/L of PCBs using GC in Tonghui River in China where PCB18, PCB31 and PCB52 were the most frequently detected ones (Zhang et al., 2004). In another study, seven PCBs at concentrations between 94 to 206 ng/L were determined using a GC instrument in water samples from the Soulou Stream in Northwestern Greece. The study suggested that the PCBs are originated from the effluents of two combustion plants emptied their effluents to the Soulou Stream (Katsoyiannis, 2006). The sum of concentration of eight PCB congeners in the water samples taken from Umgeni River in South Africa were analyzed with a GC coupled to a mass spectrometer. The PCB congeners were present at concentrations between 6.91 and 21.69 µg/L and among them, PCB180 was detected mostly (Gakuba et al., 2015). Megahed et al. (2015) also reported the PCB at concentrations between 14 and 20 µg/L in Nile river in Egypt quantified using a gas chromatography-electron capture detector (GC-ECD) (Megahed et al., 2015).

The presence of PAHs as PSs listed in WFD are investigated and reported extensively in surface waters. A study on 16 PAHs distribution in surface waters of Northern Greece using a HPLC with fluorescence detector revealed that naphthalene, phenanthrene and benzo[e]pyrene had the highest concentrations. They were found at 108-677, 30-70 and 15-78 ng/L, respectively (Manoli et al., 2000). Chen et al. (2004) measured the total PAHs at concentrations 0.989-9.663 µg/L and 132.7-7,343 ng/g, respectively, in surface water and sediment samples using HPLC. They concluded that the presence of PAHs in the surface waters may be originated from the absorbed PAHs on sediments and further desorption and transport into the water phase (Chen et al., 2004). Mean concentrations of 69, 72, 16, 71, 139, 16, 17, 20 and 25 ng/L of naphthalene, acenaphthylene, acenaphthene, fluorene, phenanthrene, fluoranthene, pyrene, benzo(b)fluoranthene and benzo(a)pyrene were quantified by GC-MS in the water environments of Egypt, respectively (Jahin et al., 2009). In Raba River in

Hungry, the mean concentration of total PAHs was 111 ng/L measured using a GC-MS. Among the target PAHs, phenanthrene and naphthalene were the most frequent ones while benzo[a]pyrene and dibenz[ah]anthracene had the major contribution to carcinogenic effects (Nagy et al., 2013). The same results for benzo[a]pyrene and dibenz[ah]anthracene were reported by Aziz et al. (2014) in a study on Soan River, in Pakistan as well (Aziz et al., 2014).

The occurrence of benzotriazoles (BTRs) as ubiquitous chemicals in surface waters is well documented in several review papers (Alotaibi et al., 2015, Shi et al., 2019, Careghini et al., 2015). Reemtsma et al. (2010) found concentrations between less than 0.05 and 0.5 µg/L and between 0.2 and 0.5 µg/L of 1,2,3-B and 4-M-1H-B in the Rhine and Elbe Rivers in Germany using LC-MS/MS, respectively (Reemtsma et al., 2010). In another study, 1,2,3-B and 5-M-1H-B in seven rivers in Switzerland were analyzed by LC coupled with a triple quadrupole mass spectrometer. The respective highest mean concentration of 2.68 and 0.47 µg/L in Glatt River was quantified and recorded (Giger et al., 2006). 1,2,3-B, 4-M-1H-B and 5-M-1H-B were present at concentrations 38-1,474 ng/L, 25-952 ng/L and 25-281 ng/L in Hengstbach and Hegbach rivers in Germany, quantified using a GC-MS. The main source of the studied BTRs were the release of dishwashing detergents via wastewater sewers into the rivers (Kiss and Fries, 2009). Van Leerdam et al. (2009) measured five different BTRs in ultra-pure, drinking water and surface waters using HPLC attached to a linear ion trap-Fourier Transform (LTQ-FT) orbitrap mass spectrometer. The concertation of BTRs in the surface water samples was between 0.01 and 0.2 µg/L (Van Leerdam et al., 2009).

HMMM, anilines and benzothiazoles are among the other important chemicals in industrial facilities which their occurrence in surface waters is inevitable. Analysis by GC-MS revealed that HMMM was present in about 50% of the samples at concentration as high as 880 ng/L in water samples taken from three rivers in Germany. In addition, the automotive wastewaters discharged into those rivers were the main sources of HMMM (Dsikowitzky and Schwarzbauer, 2015). HMMM was also identified using LC-MS/MS in surface water samples in Netherlands originated from industrial wastewater discharges (Bobeldijk et al., 2002).

The presence of anilines in aquatic environments have been reported in different studies in the literature. The average concertation of 3-chloroaniline in a raw water feeding a drinking water treatment plant was 2.1 ng/L that was measured using a GC-MS (Jurado-Sanchez et al., 2012). In another study, 3-chloroaniline and 4-chloroaniline were measured at 0.59 and 2.0 µg/L in a river water in Italy using LC coupled to a tandem mass spectrometer, respectively (Gosetti et al., 2010).

Because of their widely usage, benzothiazoles have been reported to be frequently detected in wastewaters as well as surface waters (Avagyan et al., 2015, Kloepfer et al., 2005). In surface waters of Netherlands, benzothiazole at a mean concentration of 0.01 µg/L was determined by an LC attached to a linear ion trap-Fourier Transform (LTQ-FT) orbitrap mass spectrometer (Van Leerdam et al., 2009). In another study, the concentration of 2-methylthiobenzothiazole in the effluent of two STPs was measure by an LC-MS. The concentrations were 1.25 and 6.18 µg/L. The STPs were receiving the discharges from close industries in the region suggested to be the major sources of benzothiazoles in the STPs effluents (Cespedes et al., 2006).

2.4.4. Pesticides

Occurrence of pesticides in surface waters was reported in different regions around the world. Compared to other chemicals, pesticides gain more attentions due to their toxicity, persistence and bioaccumulation potentials. That is why 29 pesticides are listed as PSs in the last update of WFD. In addition, eight pesticides are included for monitoring in the Watch List of directive 2015/495/EU. Among 91 studies on the occurrence of PSs in the aquatic environments, 58.1% were attributed to pesticides (Sousa et al., 2018, Eurpean Commission, 2013, European Commission, 2015). Esminger et al. (2013) studied the distribution of several urban pesticides which were present in urban surface waters. In that study, more than 5 pesticides were detected in 50% of the water samples from three different urban areas in USA. Among them, malathion, imidacloprid, bifenthrin and fipronil. were the most frequently detected insecticides (Esminger et al., 2013). Glinski et al. (2018) quantified the concentration of insecticides, herbicides, fungicides and other pesticides groups in surface water samples taken from South Georgia, USA using a 4D GC×GC-TOF instrument. Alachlor, atrazine, metalaxyl and metolachlor at concentrations 1.40, 1.65, 5.76 and 10.50 ng/L, respectively, were the pesticides with the highest concentrations (Glinski et al., 2018). Desethyl-terbuthylazine followed by terbuthylazine, metolachlor, procymidone and atrazine were determined as the most frequent pesticides during the analysis of the surface waters in Italian territory during the year 2005 and 2006 (Finizio et al., 2011). Out of 83 water samples taken from regions in Spain analyzed by a GC-MS, lindane, simazine and atrazine with the detection frequencies of 14.5%, 8.4% and 6.0%, respectively, were the most frequently measured pesticides (Planas et al., 1997). A study on the surface waters and groundwaters in a wine-growing area in Spain indicated the excessive contamination of the region by pesticides. In that study, 40 out of 58 pesticides were analyzed by an LC-MS, among which, terbuthylazine, pyrimethanil, ethofumesate, terbucanazole and fluometuron had the highest detection frequency (Herrero-Hernández et al., 2013). In another study, eleven pesticides were quantified in the surface water driven from the Lake Vistonis basin in Greece using LC-MS/MS and GC-MS/MS.

Fluometuron, chlorpyrifos and prometryn at maximum concentrations of 317.6, 0.419 and 0.483 µg/L, respectively, were the most frequently pesticides (Papadakis et al., 2015).

2.4.5. Natural Pollutants

Several studies have reported the occurrence of microcystins as naturally occurred pollutants in surface waters. Microcystin-YR and microcystin-LY in Egirdir Lake in Turkey were measured using an HPLC and were present at concentrations 2.9-13.5 µg/L and 4.0-6.6 µg/L, respectively (Gurbuz et al., 2016). The total concentration of microcystins in Lake Taihu in China reached the value of 0.96 µg/L (Sakai et al., 2013). In another study on the waters of Lake Chaohu in China, concentration as high as 3.73 µg/L for microcystin-RR and up to 3.58 µg/L for microcystin-YR were quantified using an HPLC during the fall samplings. On the other hand, microcystin-LR at a maximum concentration of 3.22 µg/L was present in the lake during summer (Shang et al., 2018).

2.5. Fate of Micropollutants in Surface Water

When chemicals are released in to a river, they undergo different physico(bio)chemical processes. These processes include physical transport, distribution of the pollutants between water, air and sediment (volatilization, atmospheric deposition, sorption and desorption) and biotic and abiotic transformations (hydrolysis, microbial degradation and photodegradation). Molecular structure and physicochemical properties of the chemicals as well as characteristics of the river and its environment, affect the extent of each process (Musolff et al., 2009). Studying those processes gives valuable information on the fate of micropollutants in the river environment (Figure 2.1) (Jaffe, 1991).

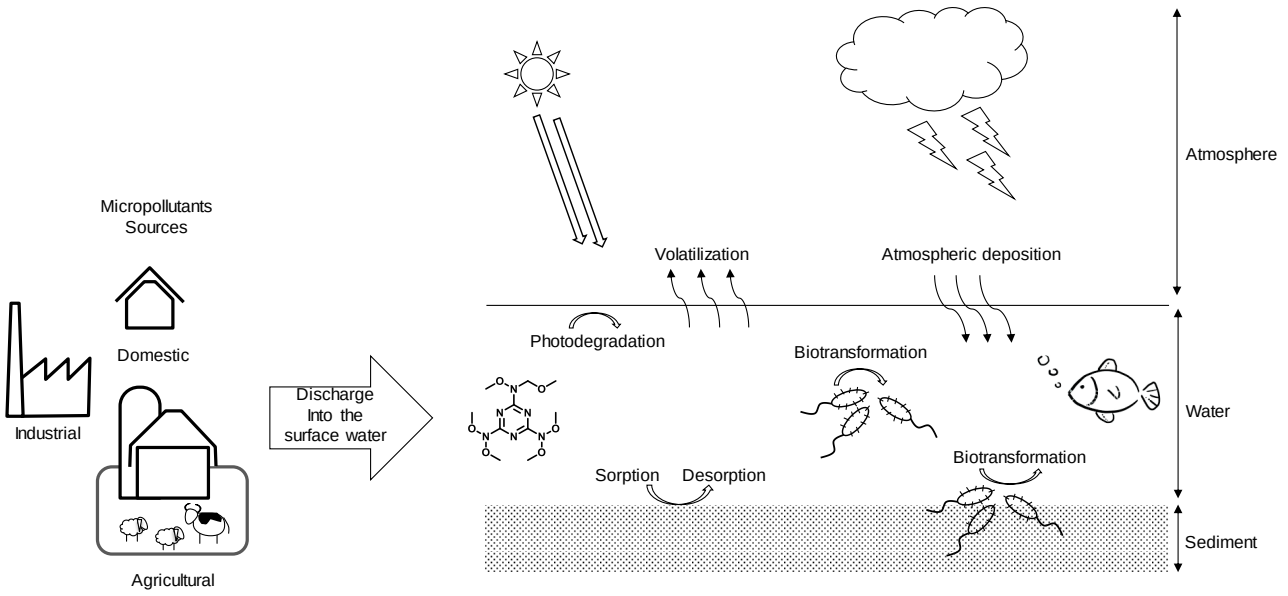

Figure 2.1. Main physico(bio)chemical processes of micropollutants in aquatic environments.

2.5.1. Volatilization and Atmospheric Deposition

Volatilization and atmospheric deposition of pollutants between river water and air are important processes affecting the fate of pollutants. Solubility and vapor pressure of the compounds as well as the weather conditions are important factors influencing these processes. Highly soluble chemicals with low vapor pressure tend to stay in water compared to the less soluble chemicals with high vapor pressure. Partitioning of a compound between air and water is governed by Henry's law constant (Jaffe, 1991, Schwarzenbach et al., 2003). If a chemical substance has a high Henry's Law constant (more than 0.001 Pa. m^3. mol^{-1}), it would have a high tendency to volatilize. As a result, we would not expect this chemical substance present in the river water or it would be detected at a very low concentration (Salgueiro-González et al., 2015). For instance, in a study on phthalate esters, DEHP with Henry's constant of 3.95 Pa. m^3. $mol^{-1}$was measured at a mean concentration of 8.01 ng/m^3 and 0.11 µg/L in the air and water samples, respectively. However, DMP with Henry's constant of 0.001 Pa. m^3. mol^{-1} was present at 0.74 ng/m^3 and 0.04 µg/L in air and water samples, respectively (Lee et al., 2019). Moreover, pollutants already transferred to the air can then enter the river water via precipitation (Wilkinson et al., 2017).

2.5.2. Sorption and Desorption

When considering the water-sediment environment in surface waters such as rivers, pollutant partitioning occurs depending on how much a chemical tends to stay in water or sediment. Sediment-water partitioning coefficient (K_p) which is the ratio of concentration of a chemical in sediment to its

concentration in water phase is a defined for this process. Solubility and polarity of the chemical as well as water flow rate and composition of the sediment are important factors in partitioning of a chemical between water and sediment phases. Hydrophilic compounds have high solubility and stay in water while hydrophobic pollutants tend to sorb on sediment. In addition, high flow rate of river water either decrease the extent of sorption or lead to the desorption of pollutants from the sediment into the water. For instance, the amount of nonylphenol and PAHs, which are hydrophobic compounds, in sediments were detected up to 21.5 and 10 times more than their amount in associated water, respectively (Jaffe, 1991, Wilkinson et al., 2017).

2.5.3. Hydrolysis

Hydrolysis is transformation of a chemical by reacting with water. At the end of the reaction, functional group(s) of the chemical substance is replaced with a hydroxyl group (OH) donated from water. Hydrolysis is an important abiotic transformation mechanism in water environments. Many chemicals such as pesticides and plasticizers can undergo hydrolysis when they enter the surface waters. For instance, malathion, hexachlorocyclopentadiene and 2-(thiocyanimethylthio)benzothiazole were reported to get hydrolyzed in the Fraser River, British Columbia (Carey, 1993). In other studies, carbaryl, malathion and diazinon were hydrolyzed in water depending on the pH and temperature of the water, while atrazine and simazine were stable (Starner et al., 1999). In addition, hydrolysis is mainly affected by the concentration of the chemical, pH, temperature and ion composition of water including metal oxides (Mabey and Mill, 1978).

2.5.4. Photodegradation

Photodegradation of organic pollutants in water occurs through both direct and indirect processes. Direct photodegradation includes the absorption of sunlight while the indirect transformation is resulted from the reaction of organic pollutants with species (e.g. humic substances) in water which are induced or excited by sunlight. Direct photodegradation mainly happens at the two meters depth of the water where sunlight percolates. On the other hand, organic pollutants that do not react directly with sunlight undergo photochemical degradation by reacting with radicals generated by absorption of solar radiation by chromophores. For instance, diclofenac is directly photodegraded to 1-(8-chlorocarbazolyl) acetic acid, while cimetidine prefers indirect transformation (Wilkinson et al., 2017). Ibuprofen was reported to be directly and indirectly transformed to 4-isobutylacetophenone (Ruggeri et al., 2013). Therefore, photodegradation of different pollutants depends mainly on their molecular structure such as presence of chromophoric groups in the

molecule, depth of river, turbidity, intensity of solar radiation, pH, as well as presence of photochromic species in the water (Wilkinson et al., 2017).

2.5.5. Biodegradation

Biodegradation is a transformation process where organic compounds are broken into smaller compounds by the action of microorganisms. Specific version of biotic transformation is mineralization in which complete biodegradation of a compound occurs. Microorganisms such as bacteria, fungi, yeast, algae and protozoa were reported to be involved in biodegradation processes of different compounds (Tahri et al., 2013).

Biodegradation of organic micropollutants occurs by microorganisms consume pollutants as primary, secondary or cometabolic substrates. Direct biodegradation is a mechanism where the organic chemical is used as primary substrate providing carbon and energy sources for microorganisms. For instance, benzalkonium chlorides (BACs) are biodegraded directly by bacteria under aerobic conditions. Another biodegradation mechanism may also carry out where microorganisms are using the organic pollutant as secondary substrate while using the primary substrate (usually at higher concentration to support the growth of microorganisms). In this case, the organic pollutants are removed with the primary substrates simultaneously. For instance, readily available organic matters serve as primary substrates while trace pollutants such as estrogens are removed as secondary substrates by microorganisms. Unlike direct and secondary biodegradation mechanisms, cometabolism is a biodegradation process where the organic pollutant does not have any impact on the growth (non-growth substrate or cometabolite) of the microorganisms. In fact, microorganisms use primary substrates as their carbon and energy sources and produce non-specific enzymes which are capable to biodegrade or biotransform the organic pollutants as cometabolite. For instance, trichloroethane (TCE) can be biodegraded cometabolically when the microorganisms use methanol as their primary substrate to produce the enzymes responsible for TCE biodegradation (Cecen, 2018).

As mentioned, biotransformation of the organic pollutants occurs by the enzymes produced by microorganisms (Livingstone, 1998). In addition to enzymes activity, environmental factors such as redox conditions, pH, temperature, available nutritions and chemicals concentration play important roles in biotransformation processes of pollutants by microorganisms (Wilkinson et al., 2017).

Microorganisms need energy for their growth. This energy is attained from oxidation-reduction reactions occurs in the environment in which transfer of electrons play the main role. During the oxidation-reduction reactions, a compound is reduced when accepting electrons (electron donor) while the other one is oxidized (electron acceptor). Terminal electron accepting process (TEAP) is defined when the last step of electron transfer is happening. In this process, the final electron acceptor, also called terminal electron acceptor (TEA), describes the nature of the system. Considering the redox potential, TEAs are placed in the order as $O_2 > NO_3^- > Mn(IV) > Fe(III) > SO_4^{2-} > CO_2$. Among the TEAs, oxygen lead to the highest energy production and its presence resulted in aerobic biodegradation while the least produced energy attributed to carbon dioxide as the TEA in methanogenic conditions. The reduction of other TEAs occur during anoxic conditions where microorganisms capable of reducing nitrate, manganese, iron and sulfate play the major role (Smith and Harris, 2007). TEAPs are mainly controlled by the distribution of aforementioned electron acceptors, concentration of electron donors as well as the diversity of the microbes responsible for each process (Mcmahon and Bruce, 1997) Therefore, TEAPs lead to the change in biogeochemical statue of the system, production of toxic and non-toxic compounds as a result of chemicals biodegradation as well as generation of different gases such as methane, hydrogen disulfide, etc. (Vincent et al., 2017).

In water-sediment environment, the oxidation-reduction reactions catalyzed by microorganisms through TEAPs, extensively affect the system dynamic as well as fate of organic and inorganic pollutants (Heimann et al., 2010). Sediments considering their biogeochemical properties carry microorganisms capable of using different organic compounds as their carbon source. These microorganisms depend on the distribution of TEAs, may result in various biodegradation processes. However, in sediments, dissolved oxygen level depletion can occur due to low circulation and flow of water in deep waters as well as high organic carbon loading which increases the oxygen consumption. Therefore, at deeper points from water-sediment interface where oxygen concentration is so low, the anaerobic condition is dominant. Moreover, microbial activities at this point via biodegradation of organic compounds using different TEAs (e.g. nitrate and sulfate) can lead to enhanced water quality by removing the organic pollutants as well as nutrients (Middleburg and Levin, 2009, Vincent et al., 2017, Freixa et al., 2016).

The fate of organic micropollutants gained a lot of attention when the adverse effects of those pollutants were investigated. Biodegradation or biotransformation of organic pollutants as one of the substantial processes occurring in the nature lead to total or partial transformation of those pollutants. Yet, many studies have studied the biodegradation of different groups of organic pollutants under

different redox condition. Liu et al. (2013) compared the biodegradation of three BTRs including benzotriazole (1,2,3-B), 5-methyl-1H-benzotriazole (5-M-1H-B) and 5-chloro-benzotriazole (CBT) under aerobic as well as nitrate, sulfate and Fe (III) reducing conditions using sediment and groundwater collected from an aquifer well in Australia during 77 days. In addition, anaerobic control was also considered without addition of any electron acceptor. The initial applied concentration of each BTR was 1000 µg/L. 1,2,3-B and 5-M-1H-B were mainly biodegraded under aerobic conditions by removal percentages of 72% and 84%, respectively. Under anaerobic conditions, the highest reduction in 1,2,3-B and 5-M-1H-B concentrations occurred under Fe (III) reducing followed by anaerobic control, nitrate reducing and sulfate reducing. CBT loss, on the other hand was mainly occurred under anaerobic conditions where the highest loss (89%) was attributed to nitrate reducing condition followed by Fe (III) reducing (75%), anaerobic control (71%) and sulfate reducing (61%). The high biodegradation of CBT under nitrate reducing conditions may resulted from the reductive dehalogenation of this compound (Liu et al., 2013c). The same BTRs in the previous study were subjected to 91 days biodegradation test under different redox conditions using activated sludge as inoculum to investigate their fate in WWTPs. The most 1,2,3-B and 5-M-1H-B losses (46% and 100%, respectively) were under aerobic condition and the least losses were under sulfate reducing and nitrate reducing, respectively. LC-MS/MS analysis showed that 5-M-1H-B was biotransformed to 1,2,3-B during the aerobic condition which is the reason of total removal of 5-M-1H-B under aerobic condition. CBT, showed removal percentages of 86%, 71%, 53%, 52% and 45% under Fe (III) reducing, anaerobic control, nitrate reducing, aerobic and sulfate reducing conditions, respectively (Liu et al., 2011b).

PhACs are ubiquitous compounds discharged into the environment since they are not completely removed in WWTPs. Therefore, their fate and biodegradation in the environment is important to understand their behavior. De Wilt et al. (2018) studied the biodegradation of six PhACs including metoprolol, propranolol, carbamazepine, caffeine, naproxen and ibuprofen by sediment of constructed wetland under aerobic condition for 6 weeks and under anoxic (nitrate and sulfate reducing) and anaerobic conditions for three months. Under aerobic condition, all of the six PhACs except carbamazepine and propranolol, showed high biodegradations ranges between 66 and 85%. carbamazepine and propranolol were 21 and 26% biodegraded in the presence of oxygen as TEA. However, under anoxic and anerobic conditions, only caffeine was biodegraded (46%) at the end of the incubation time. The removal of the other compounds under anoxic and anaerobic conditions were mainly due to abiotic processes including sorption (De Wilt et al., 2018). In another study, sulfadiazine from the sulfonamide group of antibiotics was subjected to biodegradation by soil samples under different redox conditions. Comparing the degradation rate of this antibiotic after 49

days incubation in sterile and non-sterile soils revealed that it was partially biodegraded under aerobic conditions, however, no significant biodegradation was observed under anoxic conditions (Yang et al., 2009)

Biodegradation of six UV filters including benzophenone-3 (BP-3), 3-(4-methylbenzylidene) camphor (4-MBC), octyl 4-methoxycinnamate (OMC), octocrylene (OC), 2-(3-t-butyl-2-hydroxy 5-methylphenyl)-5-chloro benzotriazole (UV-326), and 2-(2'-hydroxy-5'-octylphenyl)-benzotriazole (UV-329) by groundwater and sediment samples was investigated under different redox conditions during 77 days incubation test. The initial applied concentration was 1 µg/g sediment. All six UV filters show biodegradation under different redox conditions. BP-3, OMC and OC had half-lives of 5.3, 1.3 and 10.3 days under aerobic conditions, respectively. However, 4-MBC, UV-326 and UV-329 showed half-lives of 33, 52 and 34 days. The behavior of the studies UV filters under anoxic and anaerobic conditions revealed that addition of different TEAs may lead to faster biodegradation of the UV filters. For instance, BP-3 and OMC was biodegraded faster under anaerobic control and sulfate reducing conditions where BP-3 had respective half-lives of 1.5 and 2.2 days and OMC showed respective half-lives of 1.4 and 1.6 days. The shortest biodegradation half-lives of 4-MBC, OC, UV-326 and UV-329 occurred under anaerobic control (75 days), nitrate reducing (11.6 days), anaerobic control (72 days) and sulfate reducing (47 days) conditions, respectively. Moreover, based on the results, Fe (III) reducing condition was the less favorable redox condition for the biodegradation of the six UV filters except 4-MBC and UV-326 which had the longest half-lives under sulfate reducing conditions. Among the UV filters, OMC was the compounds which was completely biodegraded during 77 days incubation period. This study clarified that redox conditions as well as the chemical structure are the main factor in affecting the biodegradation of UV filters (Liu et al., 2013a).

Biodegradation of triclosan as one of the most widely used antimicrobial agents was studies under aerobic, anoxic (nitrate and sulfate reducing) and methanogenic conditions. Aerobic sludge effluent and anaerobic sludge spiked with 1 mg/L of triclosan were incubated to provide an enriched culture for aerobic and anaerobic test, respectively. 95.8% of triclosan (10 mg/L initial concentration) was biodegraded under aerobic condition in 5 days. However, under anoxic and anaerobic conditions, the highest biodegradation was achieved under methanogenic condition (acetate-added). In addition, triclosan showed its lowest biodegradation under sulfate reducing conditions (about 70%) which was due to probable inhibition by generated sulfide. In this study, the further isolated *Pseudomonas* sp. were responsible for the biodegradation of triclosan under aerobic condition (Gangadharan Puthiya Veetil et al., 2012).

As summarized in the abovementioned studies, many organic compounds released into the environment may undergo biotransformation under different conditions. Besides, biodegradation of organic pollutants under different redox potentials depends on the presence of the respective microorganisms as well as the availability of the electron acceptors (Ghattas et al., 2017). For instance, oxygen is mainly originated from the atmospheric oxygen and result in aerobic respiration of the organic pollutants. Atmospheric nitrogen, fertilizers sued in agriculture or manures can be the possible sources of nitrate in surface waters and lead to biotransformation of organic chemicals under nitrate reducing conditions by responsible microorganisms (Vrzel et al., 2016). Among the aforementioned electron acceptors, sulfate is extensively detected in the effluents of industrial sectors such as textile, food processing, petroleum refineries, solid waste processing, paper industry and etc. Thus, sulfate concentration is high in water bodies receiving the effluent from the aforementioned industrial facilities. As a result, sulfate reducing condition is dominant in those regions. In addition, discharges of these sulfate-containing wastewaters to the receiving water bodies can cause adverse effects to human and animal health such as losing consciousness, dyspnea, coma, coughing, confusion and other impairments. Biodegradation of organic pollutants under sulfate reducing condition provide an environment to remove both sulfate and organic pollutants from water bodies (Hussain et al., 2016).

Biodegradation of organic compounds under sulfate reducing condition is accomplished by sulfate reducing bacteria (SRBs). Sulfate reducing bacteria (SRBs) are anaerobes which use sulfate as an electron acceptor and reduce it to sulfide (Figure 2.2) (Han et al., 2017). Different studies have reported the anaerobic oxidation of the organic pollutants by SRB utilizing the organic pollutant as electron donor and sulfate as terminal electron acceptor. The complete mineralization of 0.1 mM of 2,3 and 4-chlorophenol and 2,4-dichlorophenol to CO_2 by sediment cultures was achieved during a period time of 120 to 220 days under sulfate reducing conditions. In addition, this study stated that the biodegradation of re-spiked chlorophenols after the first set was accomplished in 40 days which shows the enhanced biodegradation rate (Häggblom and Young, 1990). In another study, the endocrine disrupting estrogens such as 17-β-estradiol was biotransformed from 5 mg/L to 0.46 mg/L to estrone (Czajka and Londry, 2006). PAHs were also degraded under sulfate-reducing conditions. Phenanthrene and pyrene were biodegraded by SRB present in Mangrove sediments (Chang et al., 2008). Rockne and coworkers found that PAHs such as naphthalene, biphenyl and phenanthrene were mineralized to CO_2 by culture from soil contaminated with creosote under sulfate reducing condition (Rockne and Strand, 1998). Two studies showed that sulfate reducing cultures obtained from oilfield were able to remove sulfate while consuming alkene, alkane and aromatic hydrocarbons (such as BTEX) as electron donors (Chen and Taylor, 1997, Gieg et al., 2010).

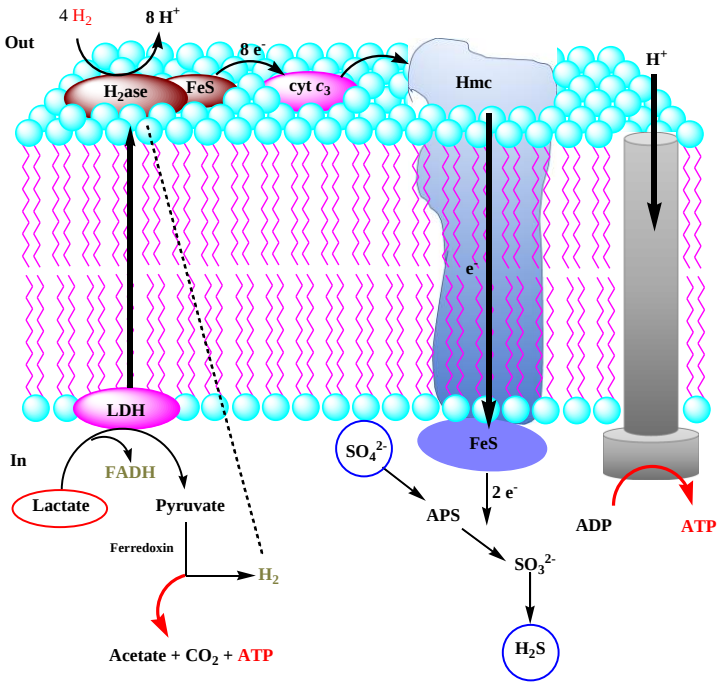

Figure 2.2 SRB using sulfate as electron acceptor and organic molecule as electron donor (Madigan et al., 2008).

Fluorene and phenanthrene were almost completely biotransformed to phenol within 21 days under sulfate-reducing condition at 30°C (Tsai et al., 2009). Antibiotics as emerging organic pollutants were also biodegradable under sulfate-reduction conditions. For instance, sulfamethoxazole, one of the most widely used antibiotics, was converted to phenylamine as the end product at a rate between 3.9 and 21.3 µg/L/d by SRB sludge. In addition, 5 different metabolites have been detected using LC-TOF-MS/MS during the biodegradation of sulfamethoxazole (Jia et al., 2017). In another study, Schmidt et al. (2017) showed that 10 µg/L of naproxen was completely biodegraded under anaerobic condition during 10 months when sulfate was provided as terminal electron acceptor (Schmidt et al., 2017). Methyl tert-butyl ether (MTBE) and methyl tert-amyl ether (TAME) were completely biotransformed under sulfate reducing condition to tert-butyl alcohol (TBA) and tert-amyl alcohol (TAA) by a sediment obtained from a contaminated estuarine sediment, within 167 days, respectively (Somsamak et al., 2001). The pathway of different organic compounds biotransfomred by SRB is shown in Figure *2.3*.

SRB are chemoorganotrophs including the species of *Desulfovibro*, *Desulfomicrobium*, *Desulfosarcina*, *Desulfobacter*, *Thermodesulfo-bacterium* and *Desulfotomaculum* (Han et al., 2017). *Desulfomonile tiedjei* strain DCB-1 was isolated from sewage sludge which was able to biodegrade halobenzoates while reducing sulfate as the terminal electron acceptor (Deweerd et al., 1990). Two novel SRB strains (oXyS1 and mXyS1) were isolated from enriched culture obtained from North Sea

oil tank in Wilhelmshaven, Germany, which were able to grow anaerobically on aromatic and nonaromatic hydrocarbons. oXyS1 utilized toluene, o-xylene, o-ethyltoluene, o-methylbenzyl alcohol, benzoate, o-methylbenzoate, benzylsuccinate while mXyS1 was capable of growth on toluene, m-xylene, m-ethyltoluene, m-isopropyltoluene, benzoate, m-methylbenzoate (Harms et al., 1999).

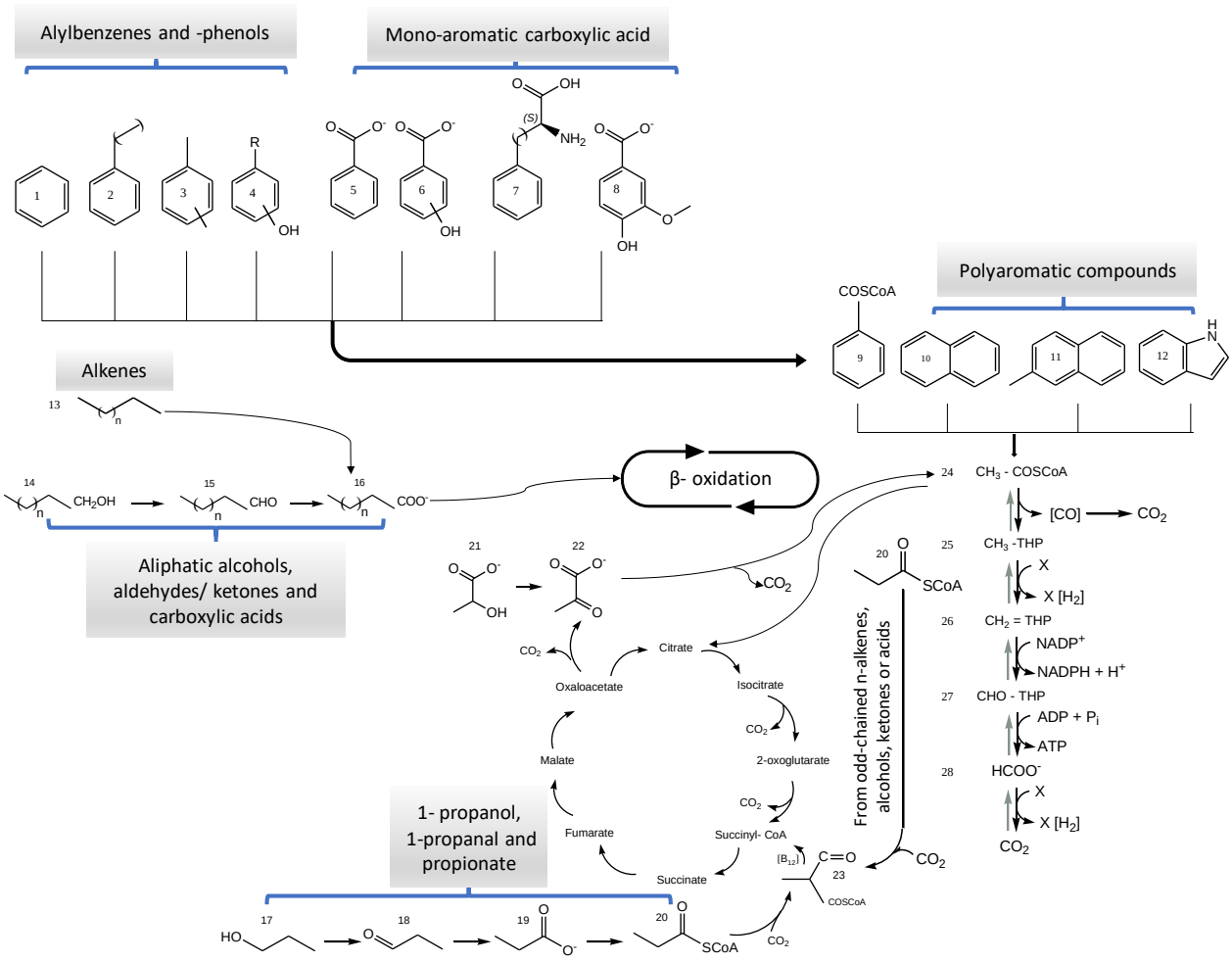

Figure 2.3. Catabolism of different organic compounds by SRB (Rabus et al., 2015). (1) benzene; (2) toluene or ethylbenzene; (3) o-, m- or p-xylene; (4) phenol; (5) benzoate; (6) o-, m- or p-hydroxybenzoate; (7) phenylalanine or phenylacetate; (8) vanillate; (9) benzoyl CoA; (10) naphthalene; (11) 2-methylnaphthalene; (12) indole; (13) ethane or longer chained n alkanes; (14) ethanol or longer chained alcohols; (15) acetaldehyde or longer chained aldehydes; (16) acetate or longer chained carboxylic acids; (17) 1-propanol; (18) 1-propanal; (19) propionate; (20) propionyl-CoA; (21) lactate; (22) pyruvate; (23) methylmalonyl-CoA; (24) acetyl-CoA; (25) methyl-THP (THP: tetrahydropterin); (26) methylene-THP; (27) formyl-THP; (28) formate.

It was reported that an anaerobic sulfate reducing bacterium (*Desulfotomaculum* strain OX39) oxidized o-xylene as substrate to CO_2 while reducing sulfate as the terminal electron acceptor to sulfide (Morasch et al., 2004).

In addition to organic pollutants, inorganic pollutants such as heavy metals can be also removed under sulfate reducing conditions. In this scenario, the SRB utilizes the organic compounds as energy and carbon source and produce H_2S during biosulfidogenic process. The generated H_2S will be then react with the dissolved metals in the water and precipitate them as their sulfide form (Figure 2.4) (Hussain et al., 2016; Hussain & Qazi, 2016; Jiang & Fan, 2008). SRB can play an important role in concomitant removal of heavy metals and sulfate. SRB culture originally obtained from DaQing water flooding was capable of removing 70% of total cadmium in soil (Hussain et al., 2016; Hussain & Qazi, 2016; Jiang & Fan, 2008). In another research, an upflow packed-bed bioreactor filled with SRB granules was used to remove heavy metals from acid mine drainage. About 99.9% of Fe, Cu, Cd and Zn (maximum influent concentrations of 436, 76, 58 and 118 mg/L, respectively) and 42.1-99.3% of Mn (maximum influent concentration of 79 mg/L) were removed from the water while 80.2% of sulfate was reduced during the process (M. Zhang & Wang, 2016).

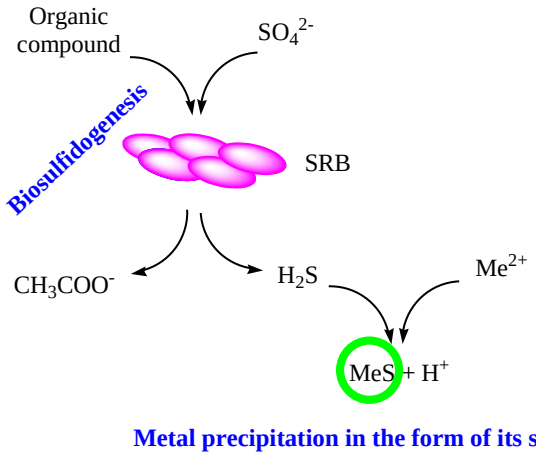

Figure 2.4 Scheme of heavy metals precipitation under sulfate-reducing conditions (Jiang and Fan, 2008).

2.6. Ergene Watershed and Its Pollution

Ergene Watershed is one of the major river basins in Turkey which is under the stress of heavy industrial and urban as well as agricultural pollutions. It has been subject of many academic and governmental studies aiming to identify and solve its serious environmental problems (Turkish Ministry of Enviornment and Forestry, 2008a, Turkish Ministry of Enviornment and Forestry, 2008b,

Hepsağ Güneş, 2009). Ergene Watershed is located in the northwestern of Turkey, where it is surrounded by Istanbul on the east, Greece and Bulgaria borders on the west and northeast and have shores to Black Sea on the north, Marmara Sea on the south and Aegean Sea on the southwest. With a total drainage basin area of 12,438 km^2, it spans 160 km from east to west and 140 km from north to south. In addition, the watershed consists of 78 rivers and 37 lakes. Ergene river along with its tributaries constitutes the most important surface water sources in Ergene Watershed. The length of the main river is 319 km. The provinces that comprise Ergene Watershed are Kırklareli in the north, Tekirdağ in the south and Edirne in the west (Figure 2.5).

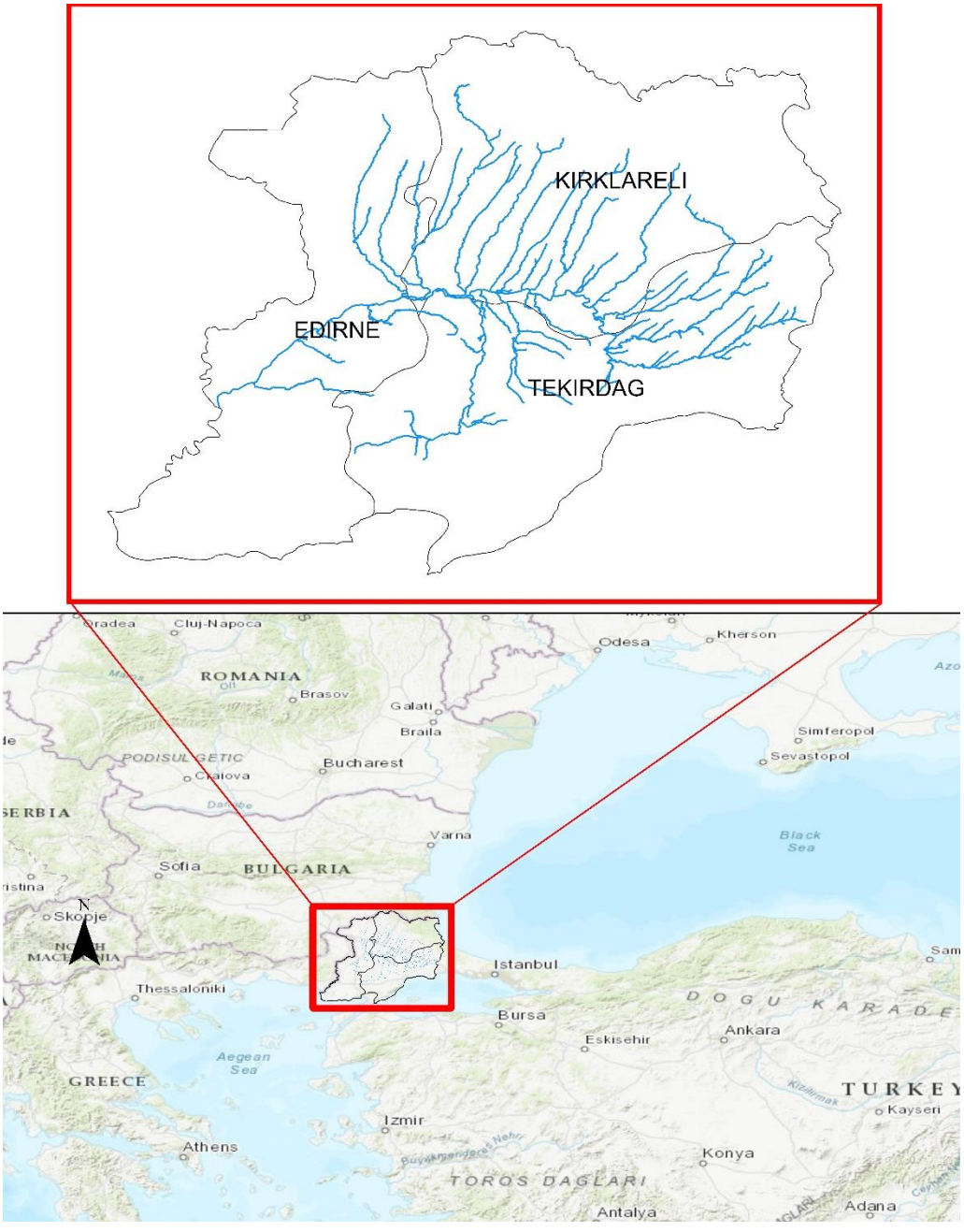

Figure 2.5. Ergene Watershed geographical location.

Having a fertile soil, the region is also home to different types of agricultural activities. Agricultural lands occupy 38% of total area of the watershed. Sunflower, rice, sugar beet and wheat are the main agricultural products of the region. For instance, approximately 55% of rice production of the country is carried out in this region. In addition, livestock farming is another major activities in Ergene Watershed (Turkish Ministry of Enviornment and Forestry, 2008b, Hepsağ Güneş, 2009). In addition to agricultural activities, Ergene Watershed is now a home of many industrial facilities such as metal, automotive, dye, plastics and etc. which started to locate in the region since 1980s (Turkish Ministry of Enviornment and Forestry, 2008b).

2.6.1. Urban and Domestic Sectors

Edirne, Kırklareli and Tekirdağ are the provinces located in Ergene Watershed. Edirne with 9 cities covers about 40% of Ergene Watershed region. Following Edirne, Kırklareli with 8 cities and Tekirdağ with 11 cities compose approximately 31% and 30% of the area of the Ergene Watershed (Figure 2.6). Based on the data, the population of residents in Ergene Watershed (28 cities) was 1,726,260 in 2016 (Table 2.2). Population of Tekirdağ constitutes 55% of total population in Ergene Watershed from which 26% and 14% are inhabiting in Çorlu and Çerkezköy cities, respectively (Iklim Su, 2016).

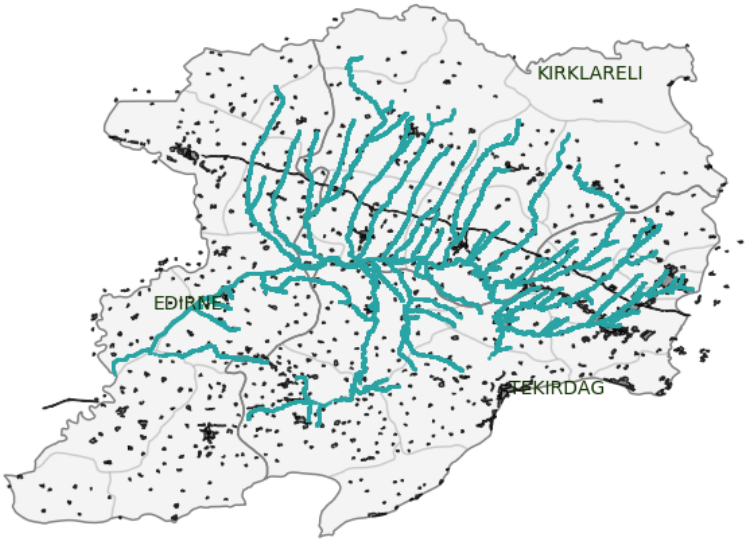

Figure 2.6. Urban areas in Ergene Watershed.

The population of Ergene Watershed region is increasing continuously due to rapid industrialization. Although agriculture is still a very important component of occupation in the region, urban population has significantly increased, specially in Tekirdağ (Table 2.2), due to rapid

industrialization while rural population decreased. With its fertile soil, lower Tekirdağ region has become the home of industrial facilities that use agricultural products as an input in their processes. For instance, industries that produce flour, dairy products, vegetable oils, fodder, etc. has proliferated in the region. In addition, because of the closeness of Ergene Watershed to Istanbul, the largest metropolis of Turkey, there has been a constant increase in working population especially in Tekirdağ. Textile, leather, metal and chemicals industries have migrated to the region as a result of governmental incentives and investment rebates for Lower Tekirdağ region in order to decentralize industries located in Istanbul.

Despite of increasing population in Ergene Watershed, only 2% of the urban area have WWTP. Table 2.3 summarized the type as well as activity status of WWTPs in different cities of three provinces of Ergene Watershed.

Table 2.2. Population distribution of the cities located in Ergene Watershed.

Province	**2009**	**2010**	**2011**	**2012**	**2013**	**2014**	**2015**	**2016**
Tekirdağ								
Merkez	170692	167704	173162	176848	179239	182522	187727	191864
Çerkezköy	154298	164220	177442	188712	113134	123119	133626	146319
Çorlu	243285	252974	264567	273362	225540	235630	245588	253551
Hayrabolu	35968	35242	35817	34478	33839	33488	32602	32158
Malkara	54658	54315	54771	54121	53293	53014	52663	52331
Marmara E.	21787	20950	21079	21469	22816	23476	23452	24043
Muratlı	26052	25944	26010	23341	26764	26821	26987	27561
Saray	46322	46351	46739	46999	47171	47522	48272	48834
Kapaklı	-	-	-	-	85898	92003	97700	105243
Ergene	-	-	-	-	56787	57613	58311	59641
Şarköy	30248	30409	30286	29991	29994	31524	30982	31330
Total	**783310**	**798109**	**829873**	**849321**	**874475**	**906732**	**937910**	**972875**
Kırklareli								
Merkez	86663	84085	87798	88956	89509	92514	95274	97626
Babaeski	50131	50041	51249	50559	49992	49121	47851	47950
Demirköy	8708	8578	8750	8782	8455	8566	8448	8464
Kofçaz	2879	2798	3001	2924	2702	2707	2644	2564
Lüleburgaz	131438	134073	136783	137872	138827	140236	142840	145263
Pehlivanköy	4634	4481	4308	4211	4140	3965	3790	3681
Pınarhisar	19813	19582	19699	19686	19035	18914	18704	18580
Vize	28913	29153	28611	28228	27899	27700	27422	27556
Total	**333179**	**332791**	**340199**	**341218**	**340559**	**343723**	**346973**	**351684**
Edirne								
Merkez	156155	152993	158929	162161	164048	165979	171386	173037
Enez	10816	10818	11066	10516	10497	11203	10580	10494

Table 2.2. Continued.

Province	2009	2010	2011	2012	2013	2014	2015	2016
Havsa	21186	20875	20477	20457	20248	19976	19380	19292
İpsala	30201	30112	29629	29770	29021	28915	28249	27822
Keşan	76606	77246	80010	79716	79889	80486	81054	80894
Lalapaşa	7708	7523	7706	7279	7194	7077	6979	6834
Meriç	16403	15970	15816	15365	14782	14509	14259	14028
Süloğlu	8027	7628	8415	8383	7870	7823	7457	7000
Uzunköprü	68361	67263	67268	66061	65033	64312	63193	62300
Total	**395463**	**390428**	**399316**	**399708**	**398582**	**400280**	**402537**	**401701**

Table 2.3. Domestic WWTPs in Ergene Watershed, their activity status and type of treatment.

Province	Activity status	Type
Tekirdağ		
Yenice	Active	Biological
Barbaros	Active	Biological
Marmara Ereğlisi	Active	Biological
Yeniçiftlik	Active	Biological
Sultanköy	Active	Biological
Şarköy	Active	Physical
Merkez-Doğu	Under construction	Advanced Biological
Merkez-Batı	Under construction	Advanced Biological
Hayrabolu	Under construction	Advanced Biological
Muratlı	Under construction	Advanced Biological
Çorlu	Under construction	Advanced Biological
Çerkezköy	Under construction	Advanced Biological
Saray	Under construction	Advanced Biological
Malkara	Under construction	Advanced Biological
Kırklareli		
Vize	Active	Advanced Biological
Merkez	Active	Advanced Biological
Lüleburgaz	Active	Biological
Pınarhisar	Under construction	Advanced Biological
Babaeski	Under construction	Advanced Biological
Edirne		
Uzunköprü	Active	Advanced Biological
Lalapaşa	Active	Biological
Süleoğlu	Active	Biological
Ipsala-Yenikarpuzlu	Active	Biological
Enez	Active	Biological
Enez-Büyükevren Köyü	Active	Biological
Sultan	Active	Natural Treatment

Table 2.3. Continued.

Province	Activity status	Type
Kurtbey	Active	Biological
Sultaniçe-Gülçavaş-Küçükevren	Active	Biological
Merkez	Under construction	Advanced Biological
Keşan+Yenimuhacir	Under construction	Advanced Biological

2.6.2. Industrial Sector

Rapid industrialization led to increased number of industrial facilities in Ergene Watershed. Currently 1303 industrial facilities and 17 organized industrial zones (OIZs) are located in the region (Figure 2.7). 82% of those facilities are located in Tekirdağ province and the rest are distributed in Kırklareli (10%) and Edirne (8%) provinces. 12 out of 17 OIZs are located in Tekirdağ province which shows the high density of industrial facilities in this region (Figure 2.8). In addition to OIZs, single industrial facilities which are not a member of any of the OIZs, are frequently found in the region (Table 2.4).

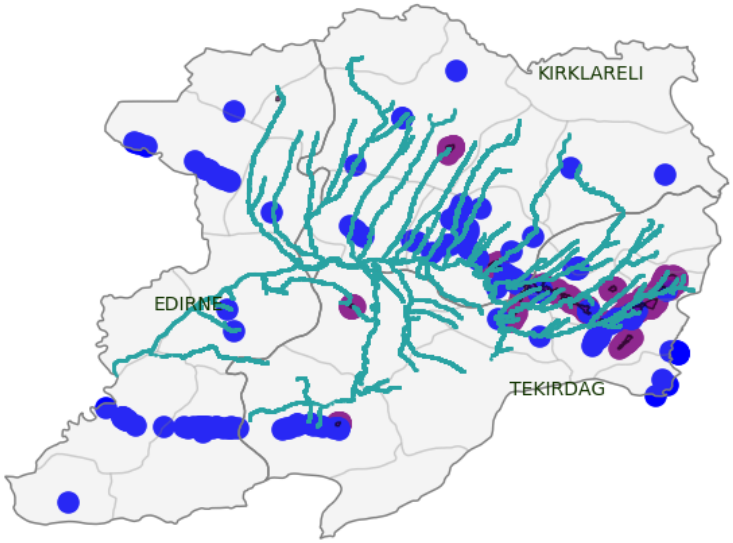

Figure 2.7. Distribution of industrial facilities in Ergene Watershed (purple: OIZ, Blue: single industry).

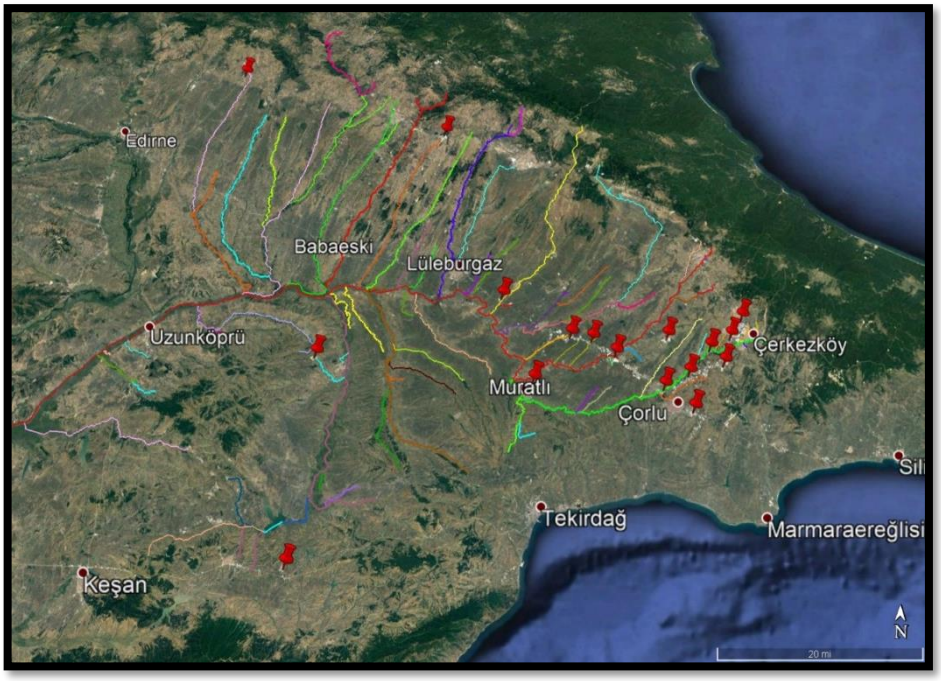

Figure 2.8. Locations of OIZs in Ergene Watershed.

The industrial facilities located in the watershed are occupied with different activities including mainly textiles, leather, dye, metals, chemicals production, paper and wood industries, food production and processing, etc. These industries include both the ones located in OIZs as well as single industries. Therefore, the industrial facilities located in OIZs either have their own discharge point or their wastewater is emptied into the OIZ's joint treatment plant. Out of 1303 industrial facilities located in the region, 676 facilities were recorded to have industrial discharges among which textile industries are the dominant sectors. As represented in Table 2.5, 35.9% of those facilities are textile industries and about 91% of them are located in Tekirdağ region specially in Velimeşe OIZ and Ergene-2 OIZ.

Tekirdağ region have the highest number of OIZs. Among them, Çerkezköy OIZ, Çorlu Leather OIZ, and Avrupa Serbest Bölgesi OIZ have active wastewater treatment facilities. On the other hand, Kırklareli consists of 3 OIZs from which Kırklareli OIZ was determined to have active wastewater treatment facility. There is one OIZ in Edirne province (Edirne OIZ) in which 4 facilities were reported to have their own wastewater treament facility. Apart from the industrial facilities in the OIZs of all provinces, single industries play an important role in the quality of the water of Ergene River by discharging their wastewater or wastewater effluents into the river.

Table 2.4. Number of active industrial facilities in Ergene Watershed.

Province-OIZ	Number of industrial facilities
Tekirdağ	
Avrupa Serbest Bölgesi	11
Çerkezköy OIZ	261
Çorlu leather OIZ	81
Ergene-1 OIZ	54
Ergene-2 OIZ	121
Hayrabolu OIZ	5
Kapaklı OIZ	6
Muratlı OIZ	21
Çorlu-1 OIZ	45
Velimeşe OIZ	191
Veliköy OIZ	36
Yalıboyu OIZ	7
Single industries	235
Total	**1074**
Kırklareli	
Kırklareli OIZ	44
Büyükkarıştıran OIZ	21
Evrensekiz OIZ	9
Single industries	54
Total	**128**
Edirne	
Edirne OIZ	5
Single industries	96
Total	**101**
Total (Ergene Watershed)	**1303**

Table 2.5. Number of types of the industries recorded to have industrial discharges.

Province-OIZ	Number of industrial facilities
Tekirdağ	
Leather	1
Wood	3
Mixed industries	14
Industrial-Domestic	140
Textile	221
Petroleum	2
Paper	13
Chemical production	48

Table 2.5. Continued.

Province-OIZ	Number of industrial facilities
Metal	40
Other industrial-domestic	2
Food	61
Brewery	8
Total	**553**
Kırklareli	
Glass	3
Textile	19
Chemical production	3
Metal	4
Mixed industrial	1
Water softening	1
Industrial-domestic	19
Food	19
Total	**69**
Edirne	
Textile	3
Paper	2
Metal	2
Industrial-domestic	6
Food	40
Brewery	1
Total	**54**

2.6.3. Agricultural Sector

Ergene Watershed is one of the main regions for agricultural activities because of its fertile soil (Figure 2.9). Wheat, corn, sunflower, clover, canola, barley, watermelon and rice are the main agricultural products of the region. Wheat is the major agricultural product of the region. 46%, 36% and 33% of total agricultural activities in Tekirdağ, Kırklareli and Edirne, is attributed to wheat production, respectively. 32% of total agricultural production in Kırklareli is associated to corn production while rice production constituting 20% of total agricultural production in Edirne.

The irrigation of agricultural lands in Ergene Watershed is performed mainly by river water or dams. Therefore, quality of these waters as well as their pollutant content are important factors to provide a safe water for irrigation. In addition, having high agricultural activity in the region leads to a consequence high pesticides consumption. Approximately 1,561,000 kg of pesticides was consumed in the region in 2016 out of which herbicides and fungicides with 57.5% and 35.7%

consumption percentages were the most widely used pesticides, respectively (Table 2.6). Epoxiconazole, fenpropimorph, imazamox, pendimethalin, pinoxaden, prochloraz, tebuconazole, benfluralin, pyraclostrobin, etc are the among the most widely used pesticides in the region.

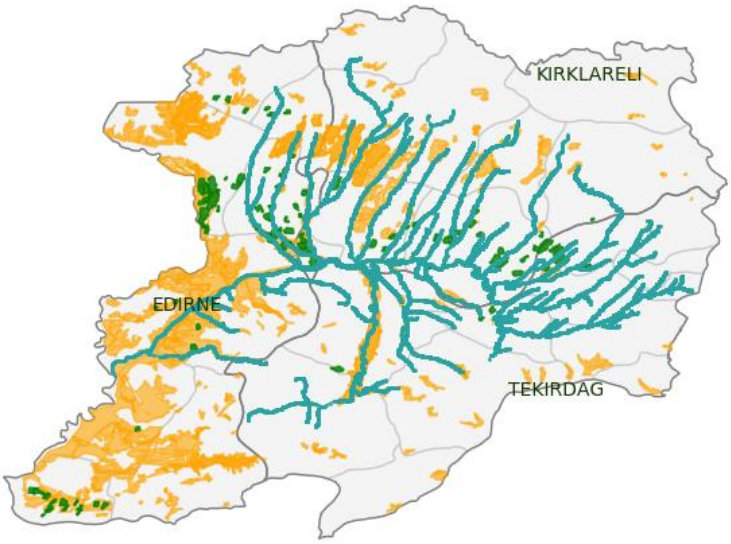

Figure 2.9. Distribution of agricultural land in Ergene Watershed.

Table 2.6. Consumption of different groups of pesticides in provinces.

Pesticide group	**Edirne**	**Tekirdağ**	**Kırklareli**
Insecticide	65.524	30.473	4.304
Fungicide	203.370	250.606	102.480
Herbicide	469.928	268.050	158.912
Acaricide	2.959	225	490
Rodenticide	6	888	10
Other pesticides	514	2.089	870
Total	**742.300**	**552.330,0**	**266.195**

As represented in Table 2.6, 552,330 kg pesticides are consumed in Tekirdağ region in 2016. This amount is applied on the area of 6,601,894 decares agricultural lands. Thus, the pesticides consumption in Tekirdağ region was approximately 83.7 g/decare. Kırklareli possessed the least pesticides consumption compared to other provinces. However, considering that 266,195 kg pesticides were applied on 2,84,052 decraes of agricultural lands, it had the highest pesticide application per decare of 93.5 g in 2016. 742,300 kg of different groups of pesticides were used in Edirne province and applied on larger area of agricultural lands (16,301,438 decares). The pesticide application was 45.5 g/decare in Edirne in 2016.

Considering urban, industrial and agricultural sectors in Ergene Watershed as well as poor treatment of the wastewaters generated in the abovementioned activities led to the extreme pollution of the water bodies in the region.

3. EVALUATION OF POLLUTION AND IDENTIFICATION OF POLLUTION SOURCES AND THEIR FINGERPRINT POLLUTANTS IN ERGENE RIVER

3.1. Introduction

Integrated watershed management (IWM) is an important process of organizing and managing of water, land, biota and other resources in a watershed to achieve ecological, social and economic goals (Wang et al., 2016a). In the past, while traditional watershed management was sector-oriented and mainly focused on water supply, irrigation, etc., the IWM prefers to cover all aspects of the management of the watershed including supply, usage, demand, etc. (Karpuzcu and Delipinar, 2011). IWM is "an approach that requires us to manage human activities and natural resources, together, on a watershed basis taking into consideration the connected interests and needs of the environment, economy and society" (Conservation Ontario). IWM is considered as the most important action to battle increasing problems such as environmental pollution and degradation resulted from socio-economic developments. As a holistic approach, IWM involves different aspects of a watershed such as water conservation, water quality management, land use, water reuse and recycling, biodiversity, human health and involvement, manufacturing and agriculture, water pollution control, sustainability, etc. (Karpuzcu and Delipinar, 2011).

Water as one of the most important components of watersheds requires wise managements and strategies. Nowadays, almost all surface water around the world are having problems with pollution originating from different sources. The sources are either natural or anthropogenic. The presence of the pollutants in surface water decrease its suitability for its further usage as drinking or irrigation water. Utilizing polluted water for irrigation can pollute the soil and agricultural products as well and further pose health risks for human and animals. Discharge of pollutants into surface water which is an important source of drinking water, may also transferred to human and animals via direct consumption. Therefore, quality of water needs substantial considerations in order to provide a safe life for human and environment (Che and Liu, 2014, Tröger et al., 2018).

Until very recently, conventional water quality parameters are used to obtain a general pollution statues of surface water. pH, temperature, chemical oxygen demand (COD), conductivity, turbidity, biochemical oxygen demand (BOD) and dissolved oxygen (DO) are among the conventional

parameters that are measured to evaluate the quality of surface water all around the world. In addition, nutrients such as ammonium, nitrate and phosphate are also other water quality parameters that are frequently monitored (Che and Liu, 2014, Irvine et al., 2005, Gholizadeh et al., 2016). Although conventional parameters give a general information about the contamination in water systems, they are limited in evaluation of risks on environment and human health associated with toxic, mutagenic, carcinogenic and estrogenic properties of the pollutants present in water which account for only a minor fraction of conventional water pollutants. Identification of those pollutants that accounts for only a minor portion are not only important to better understand the risk associated with the pollution but also to identify the source of pollution since every pollution source may release wastewater with a novel pollutant composition depending on the chemicals consumed and processes used (Ruff et al., 2015) .

Many organic chemicals such as hormones, PCPs and pharmaceuticals which have domestic origin; surfactants, corrosion inhibitors, dyes, flame retardants which are released from industrial facilities and pesticides from agricultural practices are detected at low microgram per liter concentrations in surface waters. Due to the range of concentration at which they are present in the environment, they are attributed as micropollutants (Luo et al., 2014). Altogether, about 1050 chemicals were listed in the EU Water Framework and NORMAN Network emerging contaminants list as contaminants to be monitored in surface water. In addition, some countries like Turkey has its own list of contaminants that need monitoring in Turkish surface waters. All those contaminants can be measured with advanced instrumental methods developed to specifically identify and quantify them. For instance, many PPCPs such as antibiotics (e.g. azithromycin, clarithromycin), analgesic drugs (e.g. acetaminophen, ibuprofen) and antibacterial agents (e.g. triclosan and triclocarban) can be identified and quantified by HPLC-MS/MS (Epa, 2007). Analysis performed to quantify known chemicals are called “targeted analysis”. On the other hand, as the high resolution mass spectroscopy advances, chemicals that are not in the list of chemicals to be monitored or produced *in situ* by the reaction of other known chemicals in a waterbody can also be identified by a methodology called “non-targeted analysis” Although targeted analysis of micropollutants can lead to detail information regarding the water contamination by identifying and quantifying the known organic chemicals, non-targeted analysis is the other essential method to identify the unknown chemicals and further understand the risk associated with those chemicals (Ruff et al., 2015).

Measuring conventional parameters along with targeted and non-targeted identification of the pollutants give valuable information about the source of pollutions. In fact, the main objective of the water quality control which is the key element of integrated watershed management is the prevention

of pollution at the source of generation. The pollution sources in a watershed include cities, industrial facilities, agricultural land, animal farms and landfills (Carpenter and Helbling, 2018, Fairbairn et al., 2016). Some of these sources which have discharges at a single or multiple points on a receiving body are classified as point sources. On the other hand, if the pollution is introduced to a waterbody over an area or a region, the source is called either diffuse source or non-point source. For instance, a discharge from an industrial wastewater treatment plant is a point source whereas agricultural runoff is a diffuse source of pollution. While point source are easy to identify and manage, non-point sources are difficult to control (Fairbairn et al., 2016, Kamarudzaman et al., 2011). Therefore, after measuring the pollutants in water, determining their sources is essential for further pollution preventions.

Given the fact that different activities are dominant in three major pollution sources, i.e. domestic, industrial and agricultural, the composition of the wastewater generated in these sources is different. For instance, PPCPs such as carbamazepine, erythromycin, sulfamethoxazole, 4-nonylphenol, etc. which are used as pharmaceuticals, surfactants or personal care products in houses are mainly derived from domestic wastewaters while pesticides such as atrazine, acetochlor, metalachlor, etc. are originated from agricultural lands where they are used to as herbicides (Karpuzcu et al., 2014). Industrial pollution sources however have higher variability in the types of pollutants they generate. Industrial wastewaters depending on the chemicals used in each process of the industry may lead to the discharge of different group(s) of pollutants such as COD, heavy metals, phenolic compounds, chlorinated organic compounds, sulfates, fluorine, etc. into surface water. For instance, Berehanu et al. (2015) compared the chemical composition of three industrial wastewaters (textile, ceramic and soft drink). In that study, COD of soft drink production and textile wastewaters (400 mg/L) were four times more than the COD of the ceramic factory's effluent. While sulfate concentration in the effluents of textile and soft drink production facilities did not exceed 100 mg/L, the sulfate concentration in the effluent of ceramic factory reached the value of 2,000 mg/L. Among the heavy metals analyzed, zinc had the highest concentration in all three effluents. However, the effluent of soft drink factory contained 102.1 mg/L of zinc while the value in the textile and ceramic effluents were 41 and 71.4 mg/L, respectively. Thus, considering the processes in industrial facilities and the chemicals specific for those processes, the types of pollutants produced are highly different (Berehanu et al., 2015).

Every pollution source may have pollutant profiles based on the major activities in that source and the chemicals used. "Pollutant fingerprints" term is used to describe the specific pollutant profile of a certain pollution source. By tracking the fingerprint contaminants that are specific to the sources, it would be possible to determine the impact of a pollution source on a receiving water body. The

concept of “pollutant fingerprinting” has only recently been introduced to the scientific literature, which is why the number of scientific studies in this field is very limited. One of these studies has been done in China (Zheng et al., 2013). In that study, scientists have conducted pollutant fingerprint analysis by measuring the pollutants in samples taken from a river (Huai river) that was exposed to rapid industrialization due to transfer of industries from industrial export zone (Yangtze Delta) to undeveloped lands (Henan region). Liquid chromatography-tandem mass spectroscopy (LC-MS^n) and gas chromatography-tandem mass spectroscopy (GC-MS^n) were used to determine the concentration of PCBs, PBDEs, plasticizers (phthalates), sulfonamides (e.g. sulfamethoxazole) and steroids in river water samples from two industrial areas in Eastern China and Central China. At the end of the pollutant fingerprint analysis, industrial pollution sources that contaminate the water as well as their pollution profiles with respect to time are determined. Their results showed that, pollutant fingerprints in highly polluted region of Henan had high relation to the ones in industrial export zone. For instance, PCBs and PBDEs were detected at respective concentration ranges of 0.07-12.6 µg/L and 0.01-0.07 µg/L in Yangtze Delta while the ranges were 0.4-16.1 µg/L and 0.02-0.08 µg/L in Henan region. In general, the pollutant fingerprints in samples from Henan were mostly similar to the ones in Yangtze Delta rather than to each other. In addition, no detection of PCBs and PBDEs in control region which did not have high number of industrial facilities, verified the high relativity of the water samples from Henan and Yangtze regions (Zheng et al., 2013).

In another study, Carpenter et al. (2018), detected 168 micropollutants in 17 sampling point along Hudson River Estuary during two years. Clustering the detected micropollutants considering their spatiotemporal occurrence in all samples resulted in three major clusters. The most important cluster included 60 core micropollutants since they were detected frequently in all samples as well as at all sampling times. Further, the core micropollutants were normalized using z-score normalization and clustered into four subclusters. One subcluster contained pesticides and their degradation products which also separated the sampling points into two areas. It was observed that these seven chemicals were originated from the sampling points where agricultural areas were dominant. Two other subclusters consisted of 39 compounds that were mainly derived from domestic usages such as PPCPs. The concentration of these two groups of chemicals were higher at STP outfalls than other sampling points. The last subcluster contained 13 chemicals. Those chemicals were either derived from agricultural activities or other wastewaters. For instance, carbaryl, simazine and prometon were categorized in this cluster as agricultural-derived chemicals. These chemicals have both commercial and residential usages. Some PhACs (e.g. albuterol) were also grouped in the last subcluster that are consumed both by human and animals. Therefore, based on the various usages of the micropollutants

in the last subcluster, they were classified as mixed sources-derived chemicals (Carpenter and Helbling, 2018).

A temporal-spatial study on the occurrence of 33 pharmaceutical compounds was conducted on the Lis River in Portugal where the scientists tried to quantify the concentrations of those chemicals in the influent and effluent of the WWTPs along the river and the river itself and further determine the contamination sources. 27 of them, were detected from which ibuprofen, ketoprofen, acetaminophen, fluoxetine and carbamazepine were the most important ones. The results represented that the main sources of these pharmaceuticals in Lis river were their usage by human and livestock and further excretion of them into the waters (Paiga et al., 2016).

Yang et al. (2015) detected triclosan in river water samples. They concluded that the source of the triclosan which is an antimicrobial agent used in various products is originated from the effluent of WWTP of a hospital discharged into the river (Yang et al., 2015). These recent studies show that the concept of "pollutant fingerprints" is a promising approach with many future applications since it is a very useful method in finding the source of pollution.

In the first part of the thesis research, pollution in the Ergene River was evaluated using conventional pollutants and micropollutants measured at 75 points along the Ergene River in four seasons using standard methods and LC-MS^n method developed in this study. Based on the measurements, pollution source zones on the river were identified. Fingerprint pollutants, which are chemicals mainly emitted from a particular source, were determined using flux and two-dimensional clustering analysis. In addition, a non-targeted analysis was performed to identify the most abundant organic pollutants rather than the selected micropollutants in the Ergene River.

3.2. Materials and Methods

3.2.1. Study Area and Sampling Points

Ergene Watershed located on the northwestern part of Turkey, where it is surrounded by Istanbul in the east, Greece and Bulgaria borders in the west and north with a total basin area of 12,438 km^2 is the study area of this research. It spans a length of 160 km from east to west and 140 km from north to south. The samples were taken from 75 points on the Ergene River and its tributaries. They were distributed along the main river as well as on tributaries to capture pollution source zones and to evaluate the transport of the contaminants (Figure 3.1). Therefore, every major tributary has at least

one sampling point on it. The number of sampling points are high at tributaries having more potential source zones such as organized industrial zones. About 18 sampling points were located on the mainstream before and after the main stream-tributary junctions to identify the specific contaminants coming from a particular tributary (Figure 3.2).

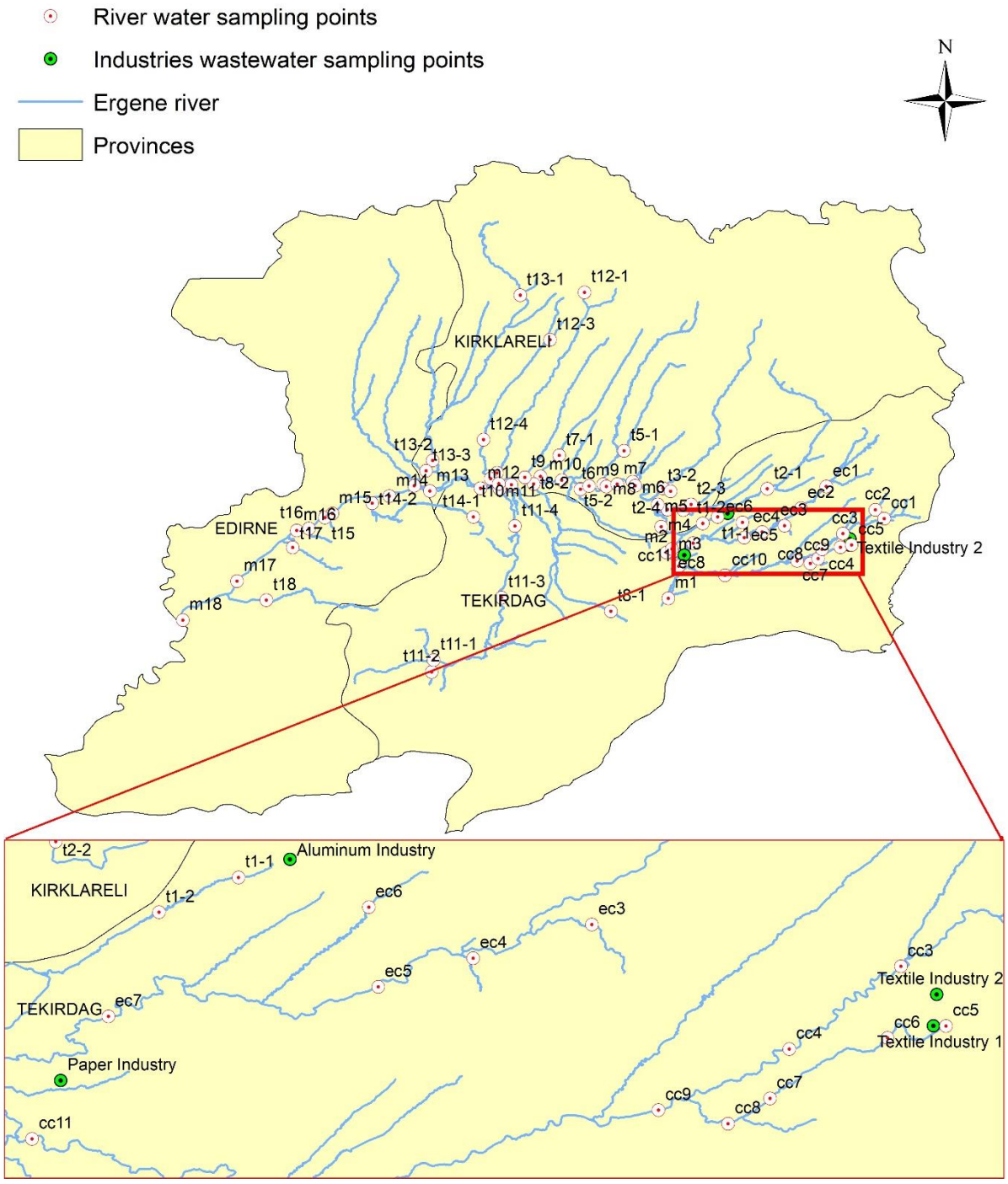

Figure 3.1. Map of Ergene river, its tributaries and the sampling points along the river and the industries.

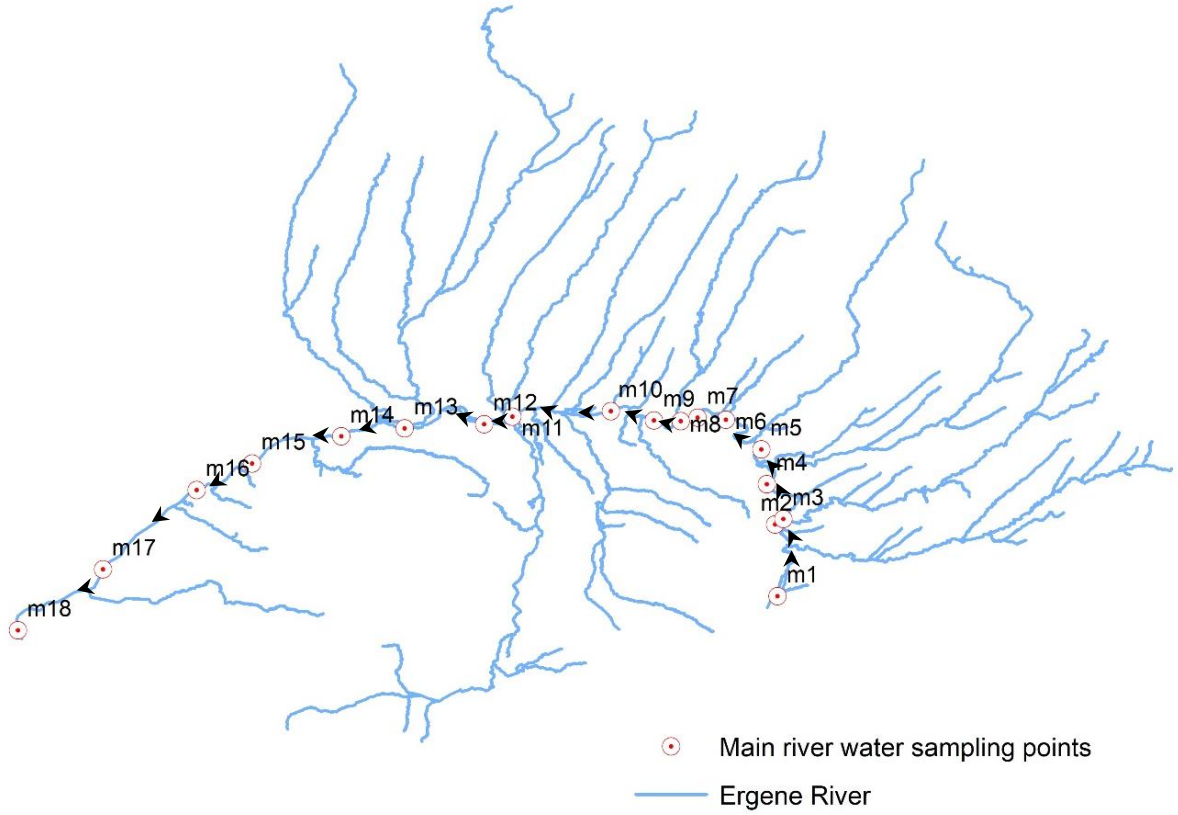

Figure 3.2. Sampling points located on main river.

The sampling points were numbered from 1 to 75 along with the prefixes (Table 3.1) representing their location or the type of sector and activity next to them. Table 3.2 and Table 3.3 summarized the location and coordinates of the river water and industrial wastewater sampling points, respectively.

Table 3.1. Abbreviations used in naming the sampling points.

Abbreviation	**Stream**
m	Main stream
cc	Çorlu Creek
ec	Ergene Creek
t	Tributary

Table 3.2. Location and coordinates of sampling points.

Sampling point	Latitude	Longitude	Province	City	Village/ District
m1	41° 5'21.19"N	27°28'6.23"E	Tekirdağ	Muratlı	Yesilsırt
cc1	41°16'20.11"N	27°57'50.45"E	Tekirdağ	Çerkezköy	Kızılpınar
cc2	41°17'32.67"N	27°56'37.70"E	Tekirdağ	Çerkezköy	Karaagaç
cc3	41°14'15.52"N	27°52'9.13"E	Tekirdağ	Çorlu	Velimeşe-Yalıboyu OIZ
cc4	41°12'6.54"N	27°49'15.05"E	Tekirdağ	Çorlu	Yulaflı
cc5	41°12'42.46"N	27°53'19.53"E	Tekirdağ	Çerkezköy	Veliköy OIZ
cc6	41°12'23.66"N	27°51'48.05"E	Tekirdağ	Çorlu	Velimeşe OIZ
cc7	41°10'49.52"N	27°48'44.80"E	Tekirdağ	Çorlu	Çorlu
cc8	41°10'9.98"N	27°47'39.51"E	Tekirdağ	Çorlu	Çorlu
cc9	41°10'31.03"N	27°45'50.82"E	Tekirdağ	Çorlu	Çorlu Leather OIZ
cc10	41°8'30.08"N	27°35'55.35"E	Tekirdağ	Muratlı	Kırkkepenekli
cc11	41° 9'46.33"N	27°29'33.33"E	Tekirdağ	Muratlı	Muratlı
m2	41°11'39.38"N	27°27'53.58"E	Tekirdağ	Muratlı	Inanlı
ec1	41°20'44.54"N	27°49'51.33"E	Tekirdağ	Çerkezköy	Uzunhacı
ec2	41°17'45.19"N	27°46'21.42"E	Tekirdağ	Ergene	Karamehmet
ec3	41°15'20.81"N	27°44'6.75"E	Tekirdağ	Ergene	Avrupa Serbest Bölgesi
ec4	41°14'28.36"N	27°41'1.73"E	Tekirdağ	Ergene	Ulaş
ec5	41°13'43.36"N	27°38'33.47"E	Tekirdağ	Çorlu	Esenler-Ergene 2 OIZ
ec6	41°15'47.95"N	27°38'18.71"E	Tekirdağ	Çorlu	Vakiflar-Ergene 1 OIZ
ec7	41°12'57.16"N	27°31'32.45"E	Tekirdağ	Muratlı	Ballihoca
ec8	41°11'40.11"N	27°28'34.66"E	Tekirdağ	Muratlı	Inanlı
m3	41°12'8.35"N	27°28'35.78"E	Tekirdağ	Muratlı	Inanlı
t1-1	41°16'34.25"N	27°34'55.32"E	Kırklareli	Lüleburgaz	Buyukkarıştıran OIZ
t1-2	41°15'39.99"N	27°32'51.32"E	Kırklareli	Lüleburgaz	Buyukkarıştıran
m4	41°15'12.95"N	27°27'9.01"E	Kırklareli	Lüleburgaz	Seyitler
t2-1	41°20'25.03"N	27°41'43.79"E	Tekirdağ	Saray	Beyazköy
t2-2	41°17'30.38"N	27°30'10.42"E	Kırklareli	Lüleburgaz	Buyukkarıştıran
t2-3	41°18'17.20"N	27°31'16.23"E	Kırklareli	Lüleburgaz	Buyukkarıştıran-Zentiva
t2-4	41°17'35.36"N	27°28'0.97"E	Kırklareli	Lüleburgaz	Çiftlikköy
m5	41°18'15.83"N	27°26'39.33"E	Kırklareli	Lüleburgaz	Karamusul
t3-1	41°20'29.82"N	27°27'22.53"E	Kırklareli	Lüleburgaz	Evrensekiz
t3-2	41°20'5.63"N	27°28'25.38"E	Kırklareli	Lüleburgaz	Evrensekiz-Akın Textile
m6	41°20'51.41"N	27°23'32.83"E	Kırklareli	Lüleburgaz	Eskibedir
t4	41°21'23.95"N	27°23'12.55"E	Kırklareli	Lüleburgaz	Eskibedir
m7	41°21'3.24"N	27°21'4.34"E	Kırklareli	Lüleburgaz	Durak
m8	41°20'45.44"N	27°19'34.22"E	Kırklareli	Lüleburgaz	Lüleburgaz
t5-1	41°25'39.96"N	27°22'0.72"E	Kırklareli	Lüleburgaz	Lüleburgaz
t5-2	41°21'2.86"N	27°19'9.80"E	Kırklareli	Lüleburgaz	Durak
m9	41°20'49.34"N	27°17'14.05"E	Kırklareli	Lüleburgaz	Düğüncübaşı
t6	41°20'21.89"N	27°16'1.67"E	Kırklareli	Lüleburgaz	Düğüncübaşı
m10	41°21'37.85"N	27°13'26.40"E	Kırklareli	Lüleburgaz	Oklalı
t7-1	41°25'1.19"N	27°13'7.21"E	Kırklareli	Babaeski	Kırıkköy-Bahçıvan Food industry
t7-2	41°22'8.17"N	27°10'31.38"E	Kırklareli	Babaeski	Düğüncülü

Table 3.2. Continued.

Sampling point	Latitude	Longitude	Province	City	Village/ District
t8-1	41°3'33.79"N	27°20'11.96"E	Tekirdağ	Suleymanpasa	Banarlı
t8-2	41°21'5.61"N	27°9'34.41"E	Kırklareli	Babaeski	Sinanlı
t9	41°22'0.50"N	27° 8'22.25"E	Kırklareli	Babaeski	Alpullu
t10	41°20'58.65"N	27° 6'31.83"E	Kırklareli	Babaeski	Mandıra
m11	41°21'8.52"N	27°4'46.91"E	Kırklareli	Babaeski	Mandıra
t11-1	40°56'51.53"N	26°55'49.87"E	Edirne	Malkara	Sarnıç
t11-2	40°55'13.51"N	26°55'32.04"E	Tekirdağ	Malkara	Gönence
t11-3	41° 5'27.81"N	27°5'9.38"E	Tekirdağ	Hayrabolu	Susuzmüsellim
t11-4	41°15'17.86"N	27°7'1.25"E	Tekirdağ	Hayrabolu	Çıkrıkçı
t11-5	41°20'24.36"N	27° 4'54.22"E	Tekirdağ	Hayrabolu	Karakavak
m12	41°20'29.33"N	27°2'17.36"E	Tekirdağ	Hayrabolu	Hedeyli
t12-1	41°47'27.79"N	27°16'36.31"E	Kırklareli	Merkez	Ahmetce
t12-2	41°22'37.71"N	27° 4'33.10"E	Kırklareli	Babaeski	Nadırlı
t12-3	41°40'56.06"N	27°11'51.44"E	Kırklareli	Merkez	Asilbeyli
t12-4	41°27'11.15"N	27° 2'41.21"E	Kırklareli	Babaeski	Babaeski
t12-5	41°21'49.48"N	27° 3'40.88"E	Kırklareli	Babaeski	Çiğdemli
m13	41°20'6.65"N	26°55'18.32"E	Kırklareli	Pehlivanköy	Akarca
t13-1	41°47'4.66"N	27° 7'43.69"E	Kırklareli	Merkez	Kayalıköy Dam
t13-2	41°24'19.62"N	26°55'42.34"E	Kırklareli	Pehlivanköy	Kumköy
t13-3	41°22'53.36"N	26°54'46.19"E	Kırklareli	Pehlivanköy	Hıdırca
t13-4	41°20'51.05"N	26°53'9.22"E	Edirne	Uzunköprü	Sazlımalkoç
m14	41°19'24.44"N	26°49'43.10"E	Edirne	Uzunköprü	Bayramlı
t14-1	41°16'32.83"N	27°1'7.40"E	Tekirdağ	Hayrabolu	Çerkezmüsellim
t14-2	41°18'27.74"N	26°47'20.97"E	Edirne	Uzunköprü	Bayramlı
m15	41°17'1.55"N	26°41'53.14"E	Edirne	Uzunköprü	Demirtaş
t15	41°16'27.79"N	26°40'51.64"E	Edirne	Uzunköprü	Uzunköprü
t16	41°14'57.90"N	26°38'39.96"E	Edirne	Uzunköprü	Uzunköprü
m16	41°14'41.33"N	26°36'59.52"E	Edirne	Uzunköprü	Çiftlikköy
t17	41°12'20.09"N	26°36'26.62"E	Edirne	Uzunköprü	Kavacık
m17	41° 7'43.79"N	26°28'46.28"E	Edirne	Uzunköprü	Kavakayazma
t18	41° 5'5.84"N	26°32'47.79"E	Edirne	Uzunköprü	Balabancık
m18	41° 2'22.10"N	26°21'17.70"E	Tekirdağ	Malkara	Balabancık

Table 3.3. Location and coordinates of industries where individual samples were taken.

Type of industry	Latitude	Longitude	Province	City	Village/District
Aluminum	41°17'02.5"N	27°36'15.5"E	Tekirdağ	Çorlu	Misinli-Ergene 1 OIZ
Paper	41°11'17.5"N	27°30'17.9"E	Tekirdağ	Muratlı	Muratlı OIZ
Textile 1	41°12'42.8"N	27°52'59.7"E	Tekirdağ	Çorlu	Velimeşe OIZ
Textile 2	41°13'31.6"N	27°53'04.8"E	Tekirdağ	Çorlu	Velimeşe OIZ

Based on the distribution of different possible potential pollution sources (industrial, domestic and agriculture) along the Ergene Watershed, the watershed was divided into three zones, 1) **industrial zone**, 2) ***transition zone*** and 3) ***agricultural zone*** (Figure 3.3). Each zone consists of 6 sampling points along the main stream and the rests are on the important tributaries. ***Industrial zone*** includes the sampling points *m1-m6* and the ***transition zone*** and ***agricultural zone*** cover the sampling points *m6-m12* and *m12-m18* on the main stream, respectively.

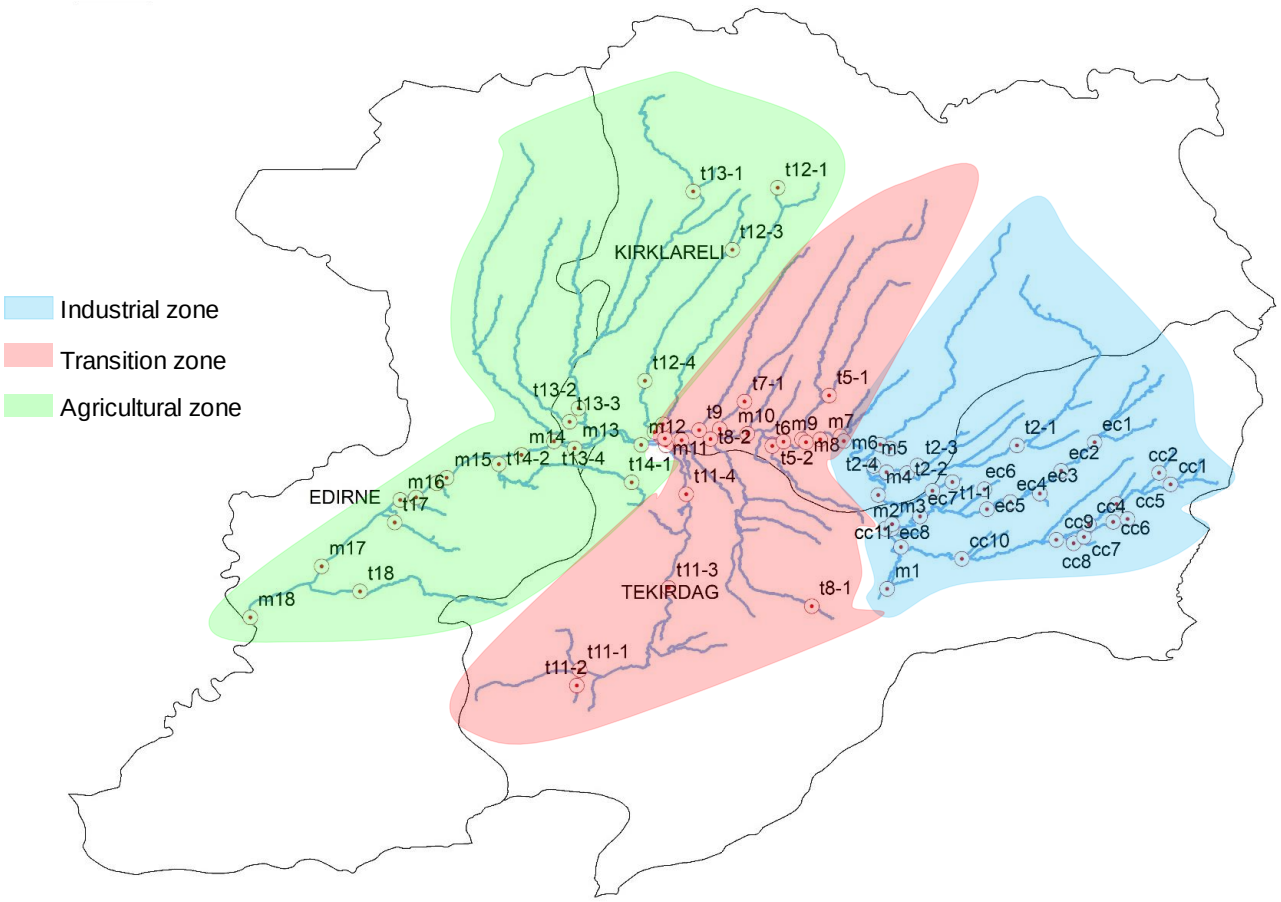

Figure 3.3. ***Industrial***, ***transition*** and ***agricultural zones*** in the Ergene Watershed.

3.2.2. Sampling and Sample Preparation

The sampling was performed by YABATAŞ Company following the procedures outlined under ISO 5667-Water Quality Sampling. In summary, 1-L samples were taken from 30-40 cm below the surface of the water into the pre-washed glass sample bottles with Teflon-lined screwcaps. The sample bottles were rinsed twice with the sample prior to the actual sampling. At the point of sampling, basic parameters such as the temperature and pH were measured. The samples were kept at a constant temperature of 4 ^{o}C during the transportation to the laboratory as well as in the laboratory at 2±2 ^{o}C until the measurements. The sampling was done for four seasons in the following order,

Summer 2017 (August 08- August 11), Fall 2017 (November 14- November 16), Winter 2018 (February 12- February 16) and Spring 2018 (May 14- May 15). The samples were aliquoted into four and processed for different analysis Table 3.4.

Table 3.4. Samples processing and analyses.

Sample Code	Analysis	Preparation Method
S01	Heavy metals measurements using ICP	50 mL falcon tubes containing 1 mL HNO_3 (65%) were filled with 30 mL water samples. they were then centrifuged at 4500 rpm for 10 minutes. The supernatant was filtered through 0.22 µm filters and stored at +4 ^oC for further ICP analysis.
S02	COD, TOC, ammonium nitrogen (NH_3-N) based on standard methods and Free phosphorus (PO_4^{3-} – P), sulfur (SO_4^{2-}), nitrate (NO_3^-) and nitrite (NO_2^-) using ion chromatography (IC)	50 mL of water samples were transferred from 1 L flask bottles to 50 mL falcon tubes, centrifuged at 4500 rpm for 10 minutes and further passed through 0.22 µm. The filtered samples were stored at -20 ^oC for further usage in COD, ammonium and other anions analysis.
S03	LC-MS/MS analysis for micropollutants measurements	10 mL of samples was taken from 1 L flask bottles and mixed with 10 mL methanol in 50 mL falcon tubes. After mixing using vortex, they were centrifuged at 4500 rpm for 10 minutes and further filtered through 0.22 µm filters. The prepared samples were stored in 20 mL amber glasses at -20 C^o for further analysis.
S04	Future storage	50 mL falcon tubes containing 1 mL H_2SO_4 were filled with samples taken from 1 L flask bottles and were stored at 4 ^oC.

3.2.3. Measurement of Conventional Parameters

3.2.3.1. pH. All pH measurements were performed potentiometrically with a calibrated microprocessor pH meter by YABATAŞ company right after taking the samples at the site.

3.2.3.2. Temperature. Temperature of water samples was measured using digital thermometer by YABATAŞ company right after taking the samples at the site.

3.2.3.3. Color. The color in river water samples was measured on 1 mL of filtered sample in 10 mm cuvettes. The color was measured using the American Dye Manufacturing Index (ADMI) method of HACH DR 3900 spectrophotometer instrument. Conventionally, Pt-Co method was used for color measurements. However, Pt-Co method is a visual color measurement method, while ADMI is

considered as a standard spectrophotometric method for analysis of water and wastewater color. Thus, ADMI method was used for color measurement of river water samples in this study.

3.2.3.4. Chemical oxygen demand. Chemical oxygen demand (COD) was measured using the closed reflux, colorimetric method as described in Standard Methods (Eaton et al., 2005). COD digestion solution was prepared for both high (300-1500 mg/L) and low (0-500 mg/L) ranges of COD values. For high-range COD, a digestion solution composed of 4.9 g $K_2Cr_2O_7$, 6 g $HgSO_4$, 6 g Ag_2SO_4 and 500 mL H_2SO_4 was prepared while in preparation of the low range COD digestion solution 1.63 gr $K_2Cr_2O_7$ was used. 3 mL of digestion solution was transferred to HACH COD digestion vials (HACH Company, Loveland, CO) and then 2 mL of sample was added to the vial. To measure the COD of river water samples, filtered samples (S02) as described in Table 3.4 were used and added to COD vials. After tumbling the vial for 4-8 times, the content in the vials was digested at 150^{o}C for 2 hours and then cooled down to the room temperature. The COD was calculated considering the absorbance measured at 620 and 490 nm for high and low ranges, respectively. The absorbance was measured with a HACH DR3900 spectrophotometer equipped with a diode array detector, deuterium and tungsten lamps and a 1 cm path length. All samples were prepared in triplicates. In addition, a calibration curve using different concentration prepared from a stock solution of 1000 mg COD/L potassium hydrogen phthalate (KHP) was constructed (Figure 3.4).

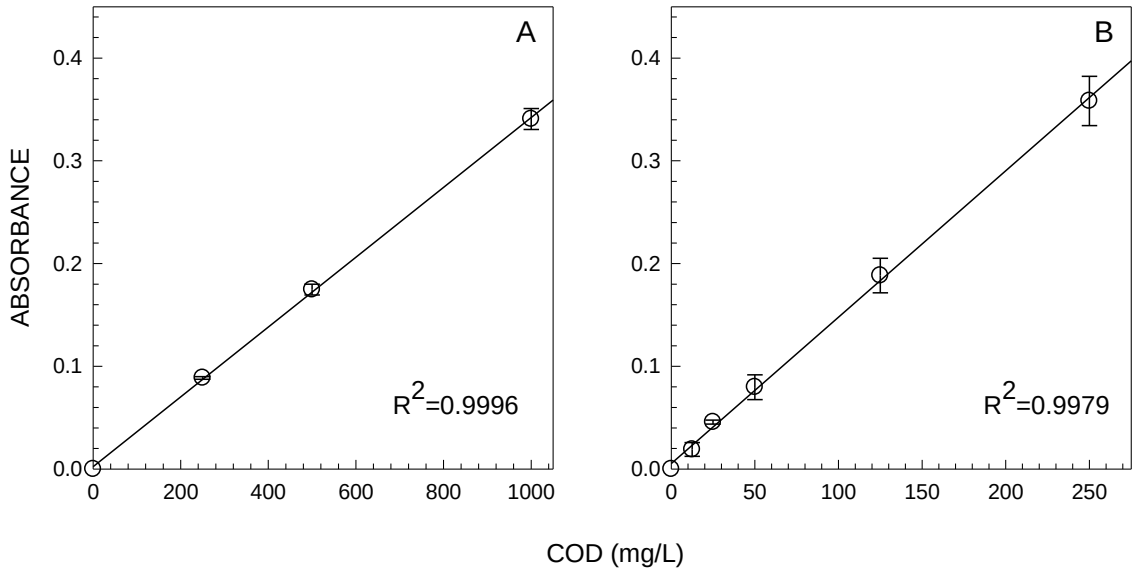

Figure 3.4. Calibration curves prepared for (A) high-range and (B) low-range COD measurements.

3.2.3.5. Total organic carbon. Total organic carbon (TOC) analysis were performed on S02 samples. A Shimadzu TOC-VWP analyzer was used for this purpose. Proper amount of S02 river water

samples were placed in vials and introduced to the instrument. The instrument was operated with the following parameters, phosphoric acid addition: 3mL, sparge time: 3 min and persulfate volume of 1.5 mL. The inject volume of the samples was 1250 µL.

3.2.3.6. Ammonia. 10 mL of S02 (Table 3.4) was used and ammonia concentration was determined using *Standard Methods* "4500-NH_3 Nitrogen" (Eaton et al., 2005). The distillation was performed using a VAPODEST (Gerhardt CO., Germany) instrument. The distillate was then titrated by 0.02 or 0.002 N H_2SO_4 according to the expected ammonia concentration in the sample. In addition, a stock solution of 1,000 mg/L of ammonium chloride was used to verify the accuracy and reproducibility of the method. The results were reported as ammonia-nitrogen (NH_3-N) in mg/L.

3.2.3.7. Anions. To determine the concentration of anions in water samples, S02 samples (Table 3.4) were analyzed with Ion Chromatography (IC). Fluoride (F^-), Chloride (Cl^-), bromide (Br^-), nitrite (NO_2^-), nitrate (NO_3^-), phosphate (PO_4^{3-}), and sulfate (SO_4^{2-}) anion concentrations were determined using a Dionex DX-100 ion chromatography unit (Dionex Coorporation, Sunnyvale, CA) equipped with a suppressed conductivity detector, a Dionex IonPac AG14A (4x50mm) precolumn, and a Dionex IonPac AS14A (4x250 mm) analytical column. The unit was operated in autosupression mode with 1mM $NaHCO_3$/8mM Na_2CO_3 eluent and a flow rate of 1 mL/min. All samples were filtered through 0.2 µm membrane filters prior to injection. The minimum detection limit for each anion listed above was 0.04, 0.2, 0.2, 0.2, 0.2, 0.4 and 0.2 mg/L, respectively.

3.2.3.8. Heavy metals. For the measurement of the heavy metals, S01 samples (Table 3.4) were used. Chromium (Cr), arsenic (As), cadmium (Cd), copper (Cu), aluminum (Al), lead (Pb), cobalt (Co), zinc (Zn), nickel (Ni), silver (Ag), antimony (Sb), tin (Sn), titanium (Ti), barium (Ba), beryllium (Be), Boron (B) and vanadium (V) were measured by Inductively Coupled Plasma Atomic Emission Spectroscopy (ICP-OES) instrument (Perkinelmer, MA, USA). Details of instrument specifications for the developed method to measure the abovementioned 17 heavy metals are summarized in Table 3.5. In addition, the LOD and maximum environmental limits for those metals are indicated in Table 3.6.

Table 3.5. Details of parameters for the measurements of heavy metals using ICP-OES instrument.

Parameter	Value/Type
Plasma gas	16 L/min*
Complementary gas	0.6 L/min
Nebulizer gas	0.6 L/min
Power	1450 W
Sample flow rate	1.5 mL/min
Plasma aerosol type	Wet

*Plasma gas emission of 17 L/min was used for silver (Ag).

Table 3.6. LOD of the heavy metals measured using the developed method along with their EQS assigned by the Turkish Ministry of Forestry and Water.

Heavy metal	LOD (µg/L)	EQS (µg/L)
As	4.0	53.0
Ba	0.3	680.0
Be	0.4	3.9
Zn	1.0	231.0
Cr	1.0	142.0
V	1.0	97.0
Co	1.0	2.6
Al	3.0	27.0
Cu	1.0	3.1
Pb	4.0	14.0
Ni	1.0	34.0
Cd	1.0	1.5
Ag	0.3	1.5
B	1.0	1472.0
Sn	2.0	13.0
Ti	2.0	42.0
Sb	6.0	103.0

3.2.3.9. Schematic analysis of the data. The acquired data from the seasonal analysis of the conventional parameters were interpreted via box plots. The box plots were constructed using Sigmaplot 10.0 software (Figure 3.5).

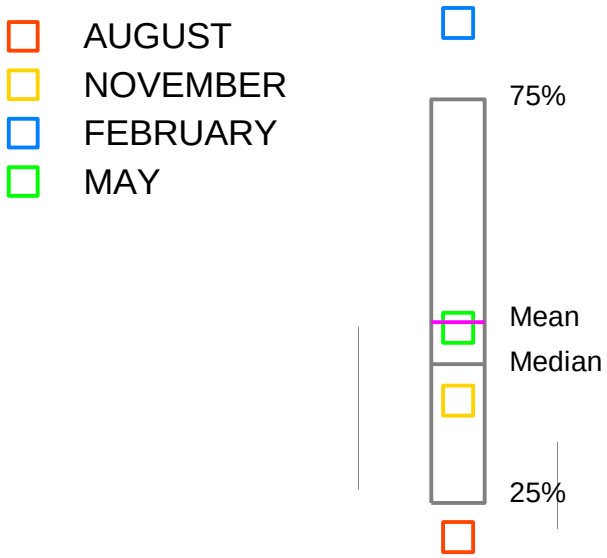

Figure 3.5. Box plots to show the seasonal measurements of the conventional parameters.

3.2.4. Measurement of The Selected Micropollutants

3.2.4.1. Identification and quantification of the selected micropollutants. A total of 222 chemical substances (Table A.1) selected among the list of "Priority Substances" of EU Water Framework Directive and contaminants of emerging concern of NORMAN Network were measured with A QTrap 4500 Linear Ion Trap mass spectrometer equipped with a TurboV IonSpray probe connected to an Eksigent Ekspert UltraLC 110 ultrahigh performance liquid chromatography system (AB SCIEX, Framingham, MA, USA) using scheduled multiple reaction monitoring (Table A.2).

First, 0.9 mL of filtered water sample was placed in an HPLC vial along with 0.1 mL of internal standard (IS) solution prepared at 0.5 µg/L (except for positive APCI ionization method where the IS concentration was prepared at 50 µg/L) concentration. Methyl-d3-triphenylphosphonium iodide (Sigma Aldrich) was used as IS for quantification of analytes that ionize positively and sodium lauroyl sarcosine (Amresco) was used as IS when MS was operated at negative ionization mode.

Separation of the analytes in the samples was achieved in UHPLC with a Kinetex C18 column (Phenomenex, 50 mm in length and 3 mm i.d.). A binary solvent system of MS grade methanol (Pump A) and MS grade water (Pump B) buffered with 0.1% formic acid and 0.1% formic acid with 10mM ammonium formate for the positive and negative ionization were used as mobile phases, respectively. The gradient elution was applied starting at 100% solvent B for 0-1.5 min, followed by 50% A (2-4 min.) and increased to 100% A (4-8 min.) and maintained at 100% A for the last 6 minutes. All the

analytes were detected in a total run time of 16 minutes with an initial equilibration of 2 minutes. The flow rate was constant at 0.5 mL/min, the column was kept at 40 ^{o}C and the injection volume was 10 µL.

Detection of analytes based on scheduled MRM (sMRM) was performed using ESI or APCI probes operating in positive or negative ionization modes. The source parameters for ESI positive/negative mode were as follows: curtain gas (CUR), 30; ion spray voltage (IS), 5500 V/ 4500 V; temperature (TEM), 550 ^{o}C; ion source gas 1 (GS1); 50 and ion source gas 2 (GS2), 60. In the APCI mode some parameters were operated differently as: GS1: 80; GS2: 0 and TEM: 500 ^{o}C (Figure 3.6). For the instrument control and data acquisition Analyst Software 1.6.2 (AB Sciex) and for the peak integration, MultiQuant 3.0.1 (AB Sciex) were used.

Preliminary recovery test was also performed to evaluate the effect of sample matrices on ionization enhancement and suppression. 5 ppb of recovery mixture of micropollutants was spiked to different polluted and non-polluted water samples. The recovery percentage for all the compounds was more than 84% indicating the high reliability of the developed method (Data not shown).

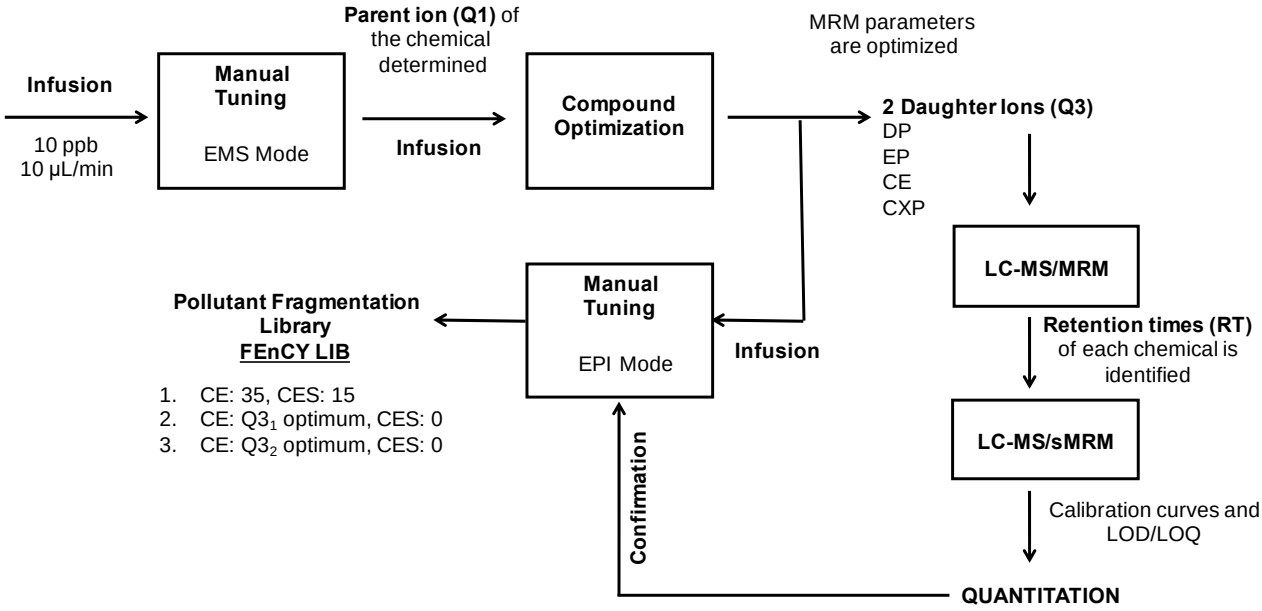

Figure 3.6. Optimum workflow for targeted and non-targeted analysis of chemicals in aqueous matrix.

3.2.4.2. Schematic and statistical analysis. The acquired data from the quantification of the selected micropollutants were depicted in box plots to show the range of the detected concentrations. The box plots were constructed using SigmaPlot 10.0 software (Figure 3.7).

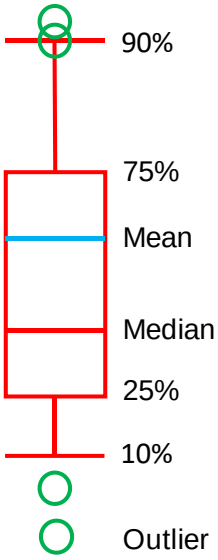

Figure 3.7. Box plots to show the concentration range of the selected micropollutants.

The selected micropollutants were further clustered using their spatiotemporal concentration. The clustering and heatmaps were constructed for the most frequently detected chemicals in each group by use of hierarchical clustering with *hclust* function (Ward.D2 agglomeration method and Euclidean distance method) in R statistical software v3.5.1.

3.2.5. Non-targeted Analysis of Water Samples

Ten µL formic acid was added to the processed river water sample. The acidified sample was infused into the MS via syringe at flow rate of 10 µL/min. The declustering potential (DP) was set to 70 eV and CAD was operated at low flow rate. For each water samples, the parent ions (Q1s) was scanned in the range of 100-600 Da. After acquiring the total ion chromatogram (TIC), five most abundant m/z were selected as important Q1s and each of them further were fragmented using Extracted Product Ion (EPI) method by scanning range of 50-Q1 Da. In this step, optimum collision energy (CE) at 35 eV was applied. The generated spectrum was then quarried from the Fragmentation Library.

3.3. Results and Discussions

3.3.1. Conventional Water Quality Parameters

The conventional water quality parameters including color, temperature, pH, inorganic anions, COD, ammonium, TOC and heavy metals were measured along the Ergene River. The maximum, minimum, mean, median and the number of sampling points (out of 75) at which the conventional parameters were detected are summarized in Table 3.7. Concentrations of each pollution parameter on the main stream and the tributaries of ***industrial*** (Figure 3.8), ***transition*** (Figure 3.9) and ***agricultural*** (Figure 3.10) zones were given and discussed, separately. Further, the potential pollution sources and their contribution to the pollution in the Ergene River were subsequently determined.

Table 3.7. Summary of conventional pollution parameters measured along the Ergene River in four seasons.

		August_2017				November_2017				February_2018				May_2018			
Parameter	**Unit**	**Max**	**Min**	**Mean**	**Median (Detected in (out of 75))**	**Max**	**Min**	**Mean**	**Median (Detected in (out of 75))**	**Max**	**Min**	**Mean**	**Median (Detected in (out of 75))**	**Max**	**Min**	**Mean**	**Median (Detected in (out of 75))**
pH		9.16	6.19	7.91	7.89 (75)	8.99	7.19	8.05	8.01 (75)	9.77	7.00	8.05	7.99 (75)	9.23	7.08	7.93	7.87 (75)
Temperature	^{o}C	35.40	19.50	27.53	27.4 (75)	29.00	11.80	16.28	14.9 (75)	23.50	5.00	8.44	7.70 (75)	33.30	12.90	21.98	22.10 (75)
Color	ADMI	1269.00	8.00	261.44	139 (75)	815.00	20.00	195.20	125 (75)	1037.00	7.00	88.57	55.00 (75)	833.00	23.00	194.64	139 (75)
TOC	mg C/L	532.23	0.00	85.13	58.33 (74)	528.88	5.59	50.28	28.25 (75)	101.49	0.36	19.34	16.03 (74)	165.14	4.23	36.45	27.03 (75)
COD	mg COD/L	1660.68	45.75	413.50	197.41 (75)	1075.67	21.96	323.71	201.98 (75)	726.83	17.38	138.98	53.07 (75)	952.27	23.10	300.17	165.15(75)
Ions																	
NH_3-N	mg N/L	270.8	0.0	13.5	7.8 (65)	95.2	0.3	10.2	6.2 (75)	29.4	0.0	2.5	1.1 (73)	32.8	0.0	5.8	3.4 (61)
NO_3	mg/L	97.62	0.00	3.42	0.00 (25)	103.45	0.00	4.96	0.33 (44)	42.32	0.07	11.31	9.81 (75)	112.03	0.00	7.97	0.86 (72)
NO_2	mg/L	4.27	0.00	0.17	0.00 (19)	5.59	0.00	0.28	0.00 (27)	7.96	0.00	0.43	0.21 (63)	2.27	0.00	0.35	0.00 (34)
Cl^-	mg/L	2427.70	15.41	674.16	577.41 (75)	2851.73	11.71	522.90	244.80 (75)	1080.58	0.00	102.14	57.38 (74)	2423.48	8.13	370.37	233.91 (75)
F^-	mg/L	30.56	0.08	1.16	0.38 (75)	7.65	0.09	0.51	0.34 (75)	0.92	0.00	0.23	0.22 (73)	7.63	0.25	0.61	0.47 (75)
Br^-	mg/L	4.42	0.00	0.62	0.48 (62)	1.76	0.00	0.56	0.58 (66)	0.51	0.00	0.18	0.16 (73)	2.54	0.00	0.60	0.62 (65)
SO_4^{2-}	mg/L	1946.15	2.83	177.18	115.97 (75)	1662.48	10.74	161.49	109.32 (75)	533.50	6.36	72.26	44.45 (75)	951.46	6.78	123.63	92.12 (75)
PO_4^{3-}	mg/L	8.27	0.00	2.46	1.92 (58)	68.00	0.00	4.23	2.41 (62)	4.07	0.00	0.68	0.42 (72)	13.06	0.00	1.99	1.655 (58)
Heavy metals																	
As	µg/L	62.33	0.00	5.06	0.69 (26)	35.45	0.00	3.49	1.98 (24)	65.17	0.00	3.70	1.99 (13)	94.82	0.00	5.41	0.00 (35)
Ba	µg/L	534.47	6.46	105.78	99.82 (75)	528.67	21.52	117.09	107.87 (75)	922.38	13.34	111.70	97.92 (75)	595.05	18.85	115.73	110.69 (75)
Be	µg/L	58.16	0.00	0.80	0.00 (1)	1.36	0.00	0.07	0.00 (2)	4.05	0.00	0.66	0.58 (62)	3.19	0.00	0.13	0.00 (10)
Zn	µg/L	1005.42	0.18	105.47	44.68(74)	10254.65	13.72	2176.10	1516.27 (75)	6212.12	149.83	1290.31	1144.82 (75)	33601.92	1123.60	16008.37	14958.24 (75)
Cr	µg/L	3628.89	0.24	184.47	8.75(67)	1222.82	0.20	57.01	5.59(66)	7138.61	0.00	212.92	0.82 (35)	1992.48	0.00	70.50	4.58 (60)
V	µg/L	50.43	1.75	12.46	11.74 (75)	35.01	0.00	8.74	6.35 (73)	62.84	0.00	7.34	5.63 (69)	164.65	0.00	4.11	0 (19)
Co	µg/L	11.91	0.15	1.61	1.42 (55)	16.28	0.05	1.77	1.16 (47)	33.64	0.00	1.79	0.92 (36)	17.96	0.00	2.10	1.72 (66)
Al	µg/L	12193.39	39.85	1462.00	540.38(75)	63755.14	50.61	2139.85	571.75 (75)	8961.58	56.41	1176.03	919.77 (75)	83899.38	35.07	3114.22	584.64 (75)
Cu	µg/L	993.00	2.65	52.47	27.55 (75)	4526.80	1.16	928.13	714.34 (75)	2851.59	78.58	918.90	696.65 (75)	14634.68	28.58	4124.76	3450.79 (75)
Pb	µg/L	2937.36	0.00	289.11	68.96 (74)	1848.09	8.02	491.73	429.56 (75)	840.82	53.56	259.04	220.23 (75)	5679.02	348.06	2141.63	1887.09 (75)
Ni	µg/L	2395.52	22.46	320.22	151.75 (75)	3807.74	133.04	1122.37	891.16 (75)	709.08	93.77	319.66	291.88 (75)	9711.04	551.20	3670.01	2977.54 (75)
Cd	µg/L	0.56	0.00	0.01	0.00 (0)	0.00	0.00	0.00	0.00 (0)	1.16	0.00	0.23	0.21 (1)	0.00	0.00	0.00	0.00 (0)
Ag	µg/L	0.65	0.00	0.03	0.00 (3)	0.86	0.00	0.08	0.00 (6)	0.07	0.00	0.00	0.00 (0)	2.76	0.00	0.19	0.00 (13)

Table 3.7. Continued.

Parameter	Unit	August_2017				November_2017				February_2018				May_2018			
		Max	Min	Mean	Median (Detected in (out of 75))	Max	Min	Mean	Median (Detected in (out of 75))	Max	Min	Mean	Median (Detected in (out of 75))	Max	Min	Mean	Median (Detected in (out of 75))
B	µg/L	2604.68	24.06	421.35	256.15 (75)	1150.79	28.66	298.23	231.62 (75)	260.73	12.86	86.00	67.77 (75)	1215.19	25.54	227.00	179.71 (75)
Sn	µg/L	571.73	1.33	38.71	9.43(71)	69.31	0.52	12.10	9.63 (74)	11.57	0.70	4.55	3.91 (67)	213.22	11.64	53.69	46.30 (75)
Ti	µg/L	44.99	0.00	5.81	4.02 (49)	70.85	0.25	7.14	3.58 (50)	31.53	0.38	5.96	4.93 (61)	80.39	0.00	6.95	3.48 (47)
Sb	µg/L	50.13	0.00	7.61	0.31 (22)	36.34	0.00	7.17	3.25 (30)	133.82	0.00	7.81	0.26 (15)	32.54	0.00	5.59	0.00 (31)

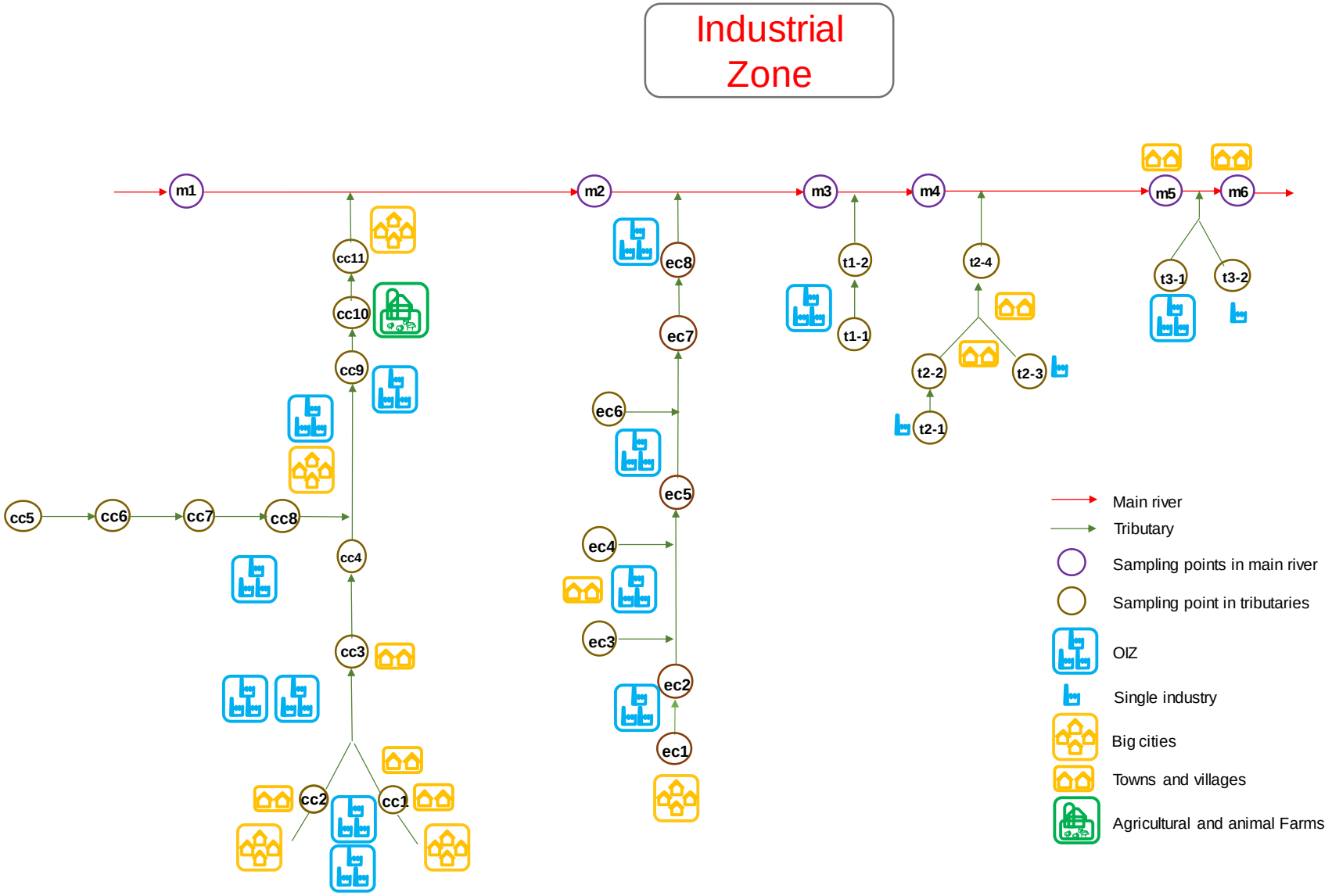

Figure 3.8. A simple illustration of "***industrial zone***".

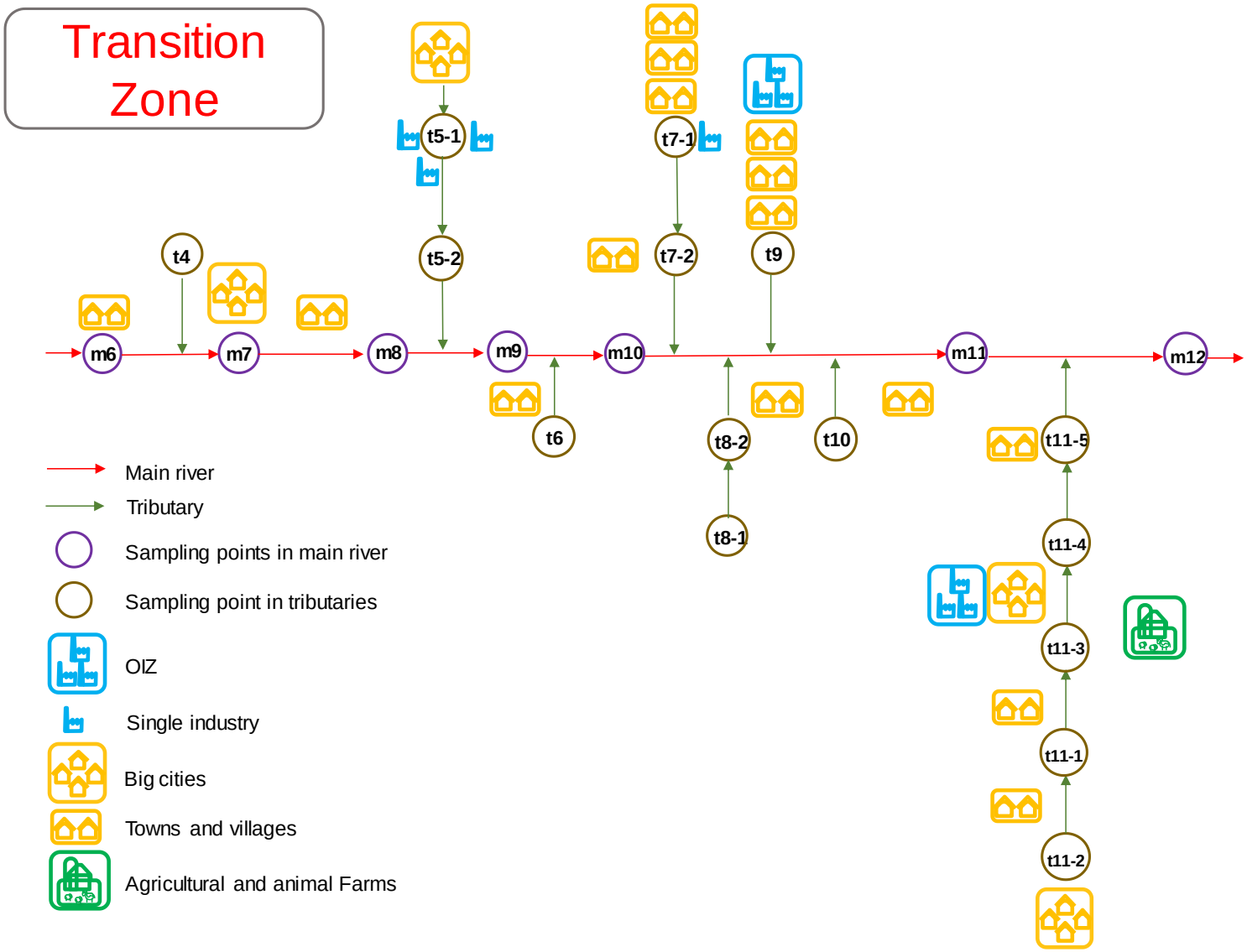

Figure 3.9. A simple illustration of "***transition zone***".

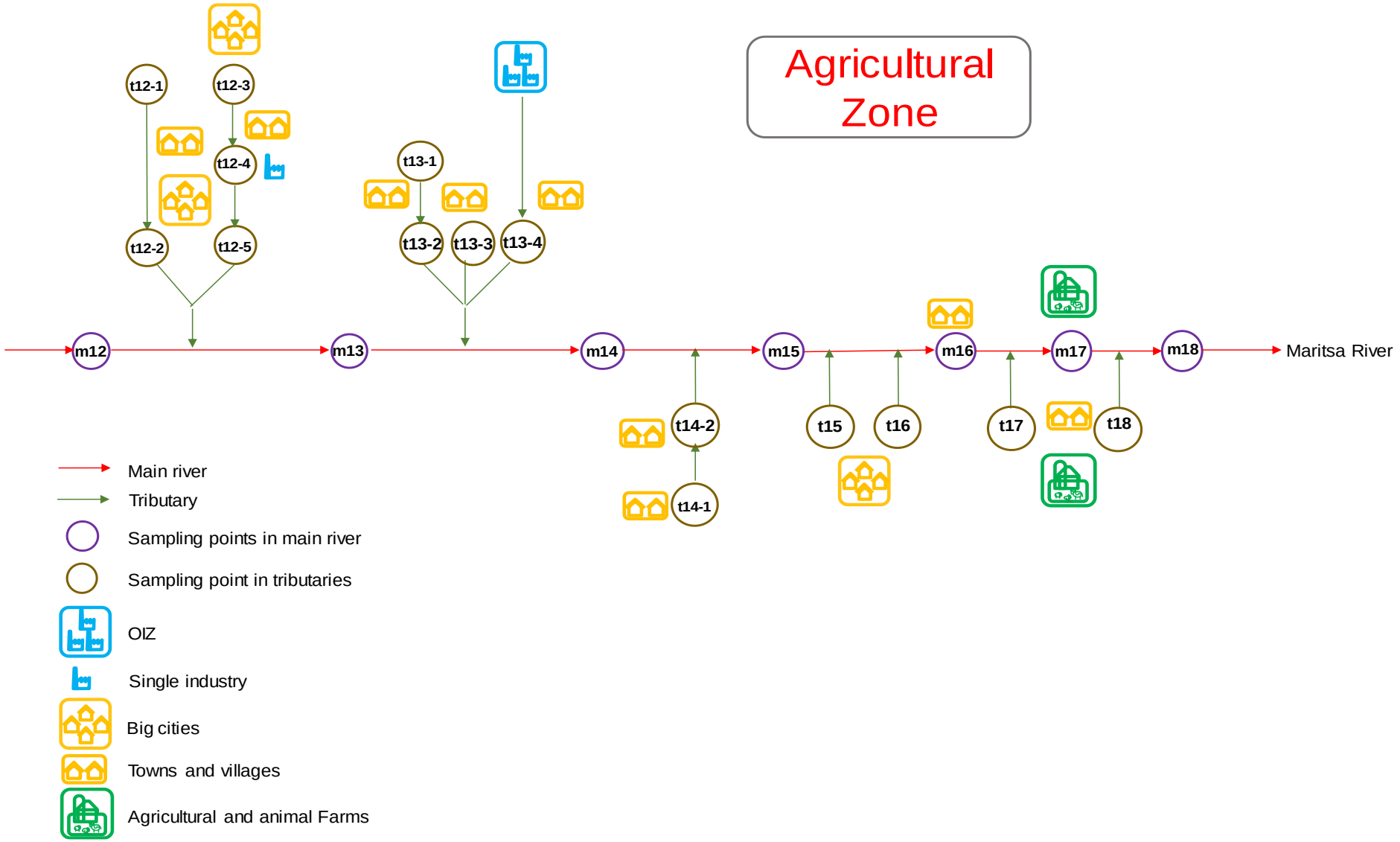

Figure 3.10. A simple illustration of "***agricultural zone***".

3.3.1.1. pH. The average pH of water samples taken from the Ergene River was in the range of 7 and 8 during different seasons which was in compliance with the EQS (pH: 6-9) set by the Turkish Ministry of Forestry and Water (Turkish Ministry of Forestry and Water, 2012). The seasonal profile of pH in three zones are shown in Figure 3.11, Figure 3.12 and Figure 3.13. The mean pH in ***industrial zone*** was 8.01, 8.12, 8.13 and 7.97 during summer, fall, winter and spring. respectively. In addition, in ***transition zone***, the mean pH was recorded as 7.81, 7.96, 8.03 and 7.91 and in ***agricultural zone*** was 7.85, 8.01, 7.93 and 7.89 in summer, fall, winter and spring, respectively. Therefore, the average pH in all three zones were in the same range set by the authorities.

Although being stable in the main stream of ***industrial zone***, the pH of water at some sampling points such as *cc7* and *cc8* on Çorlu Creek next to Velimeşe OIZ land *t1-1* and *t1-2* next to Büyükkarıştıran OIZ (Figure 3.11B) exceeded 9 which was over the EQS set by the Turkish Ministry of Forestry and Water. The mean pH at sampling point *cc7*, *t1-1* and *t1-2* were as high as 9.07, 9.02 and 9.18 during the year, respectively. The highest pH recorded during all sampling periods was 9.77 recorded at sampling point *cc7* on Çorlu Creek during winter. All those points are surrounded by industrial facilities such as metal, textiles, chemicals production, plastic and leather production. It was also reported that the average pH of the effluent from textile industries in Dhaka, Bangladesh was between 9.33 and 10.50 (Kamal et al., 2016). Sudden elevated pH at those points and their surroundings, can cause serious ecological problems to aquatic life. In addition to those points, the pH of river water taken from sampling point *t3-1* was as low as 6.19 during summer sampling although the annual average pH was 7.25. That sampling point is located next to Evrensekiz OIZ (Figure 3.14) and receives the effluents from brewery, tobacco, food and paper industries. A pH between 4.0-6.7 was reported for the effluent of a brewery industry in South Africa which indicates the effect of the industry on the pH of the close receiving water (Enitan et al., 2015).

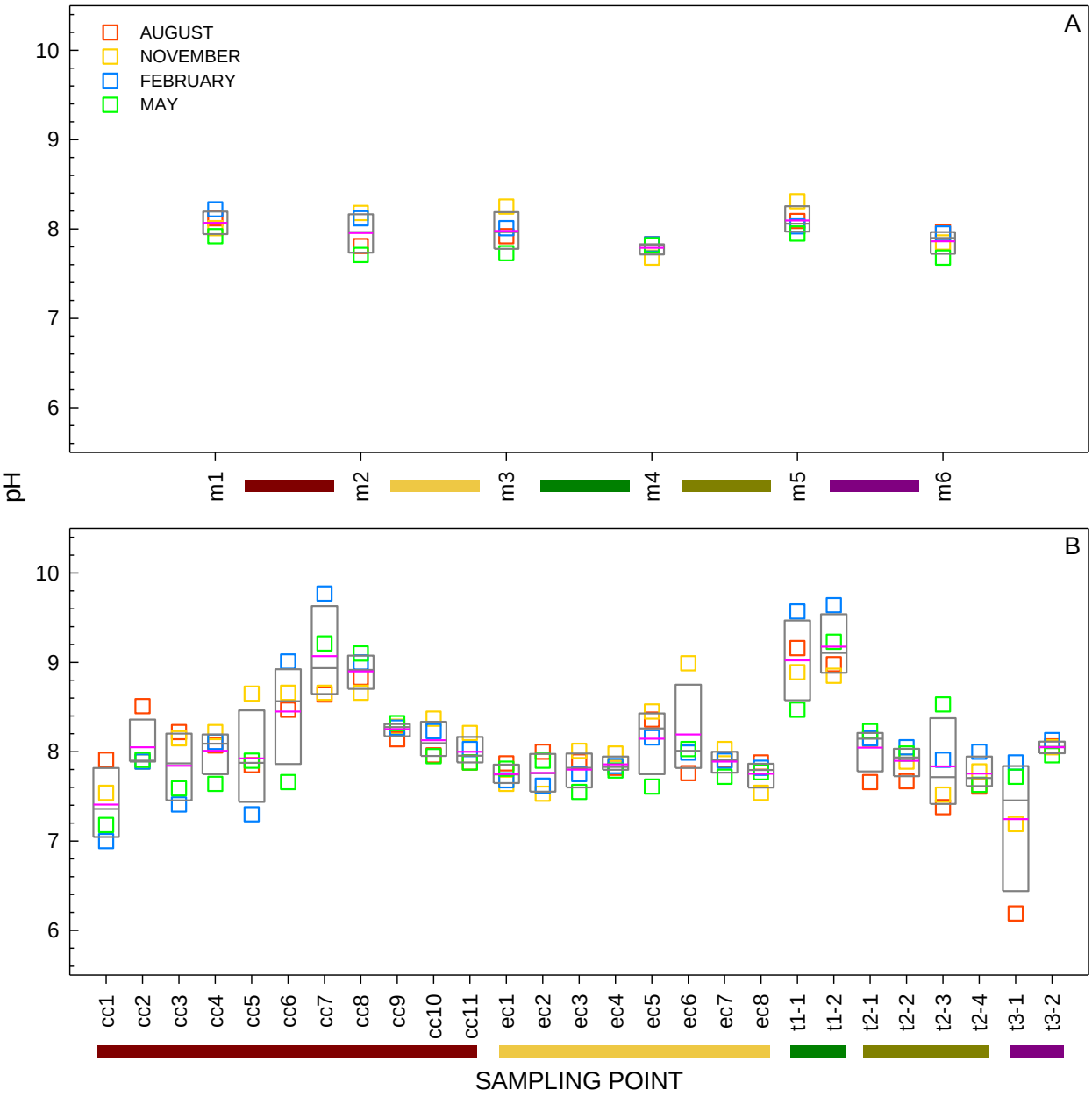

Figure 3.11. Seasonal profile of pH in (A) main stream and (B) tributary samples taken from the ***industrial zone***.

Considering the sampling points on the tributaries of ***transition zone*** (Figure 3.12B), pH of 6.19 was measured at sampling point *t7-1* during summer. That sampling point is also located next to a food industry (Figure 3.14) which is producing cheese products and discharge low pH effluent into the river. Discharging whey as a result of cheese production processes in dairy facilities can lower the pH to below 6.2. In addition to that, acidic pH range of 4.3-4.6 is the results of mineral acidic coagulation in cheese production facilities (Slavov, 2017).

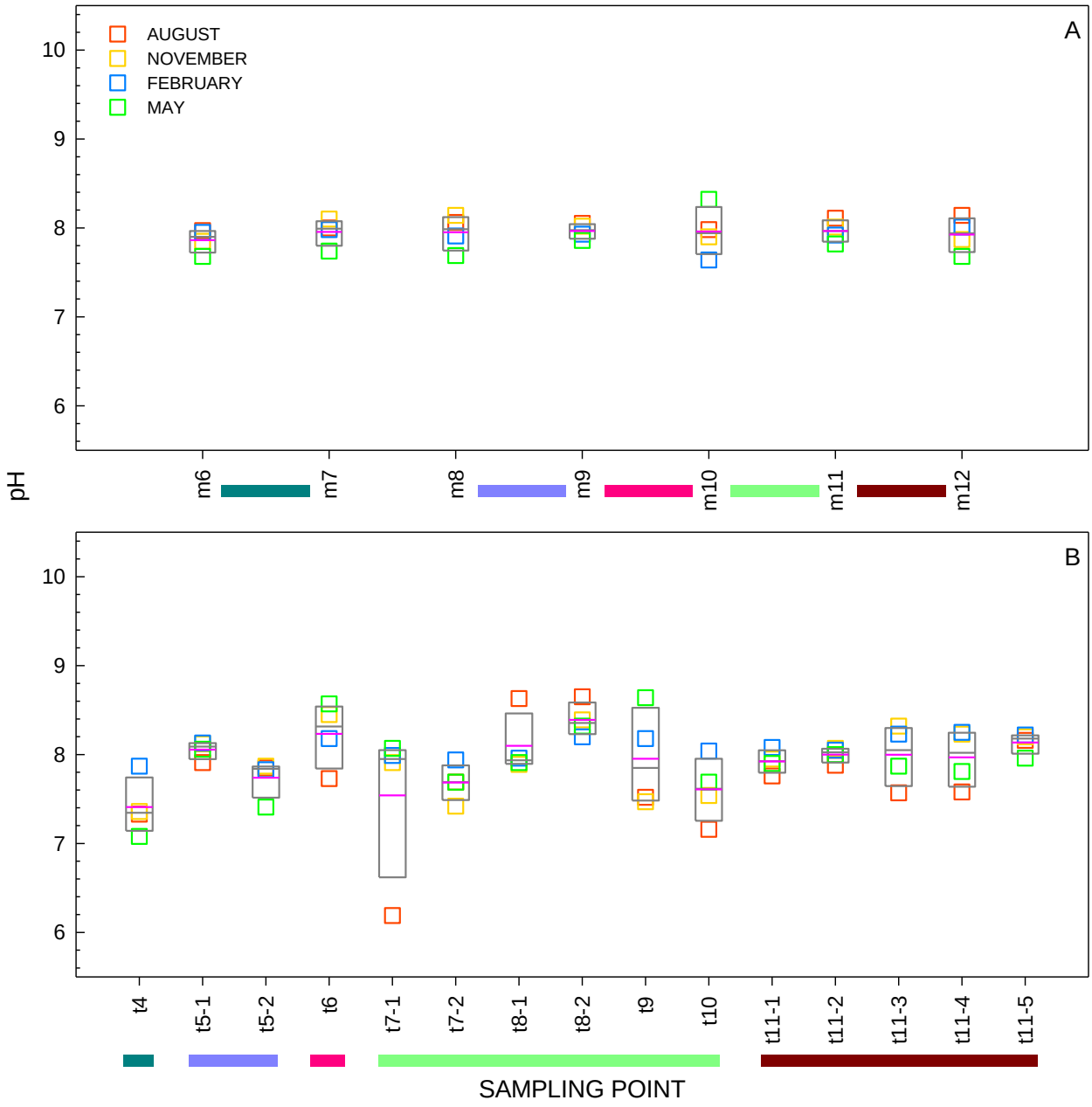

Figure 3.12. Seasonal profile of pH in (A) main stream and (B) tributary samples taken from the ***transition zone***.

Agricultural zone, on the other hand, had a more stable pH behavior when compared to other zones because of the lower number of industries located in that zone (Figure 3.13). The seasonal mean and median pH of sampling point *m18* as the last point in the Ergene River was 7.72 and 7.75.

In general, pH in the Ergene River was in the range recommended by the authorities except some sampling points with either very high or low pH that need serious actions.

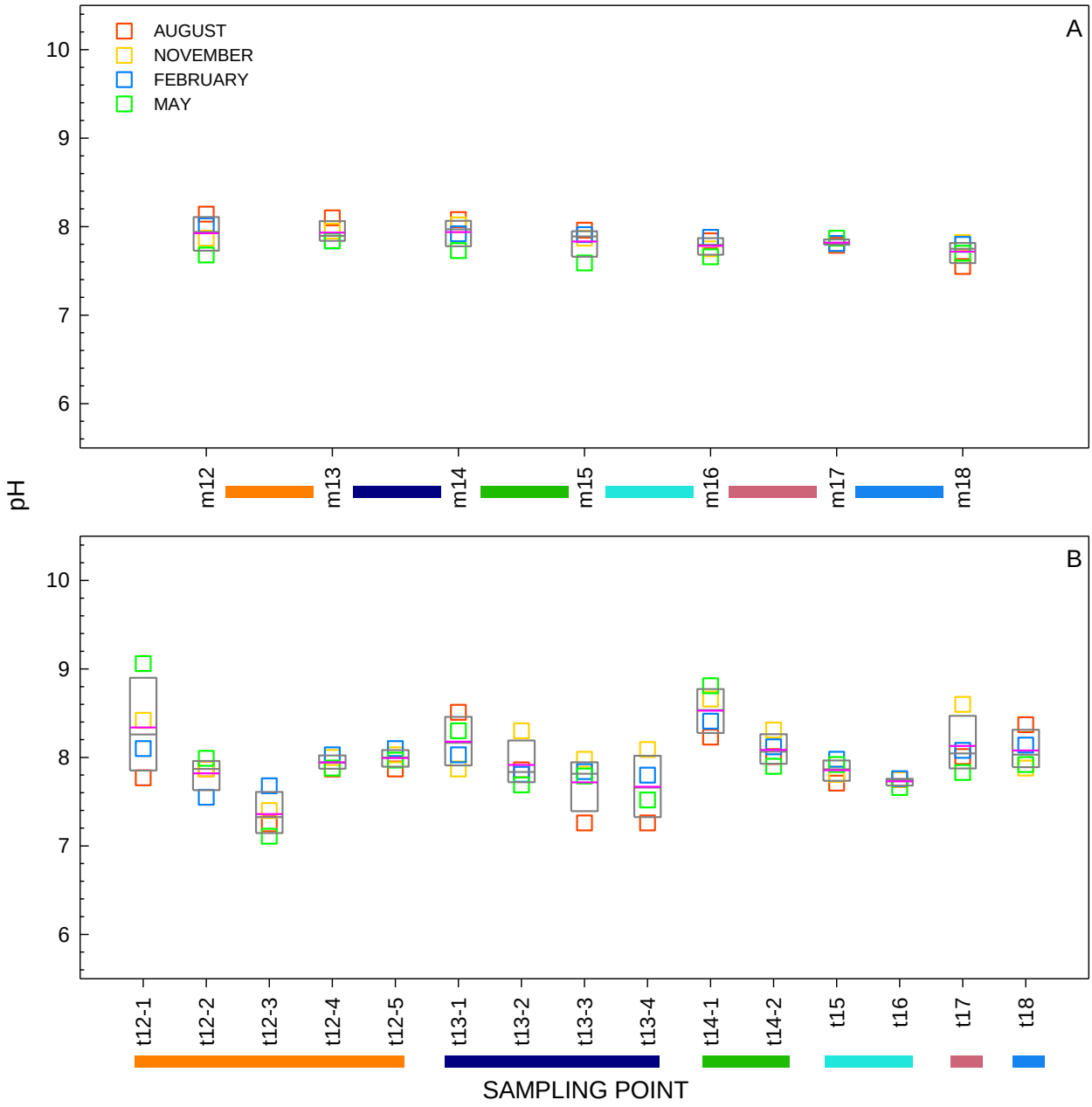

Figure 3.13. Seasonal profile of pH in (A) main steam and (B) tributary samples taken from the ***agricultural zone***.

Figure 3.14. Location of sampling points *t3-1* and *t7-1* with lowest pH values.

3.3.1.2. Temperature. The average temperature of the Ergene River water was 27.53, 16.28, 8.44 and 21.98 ^{o}C during summer, fall, winter and spring, respectively. Temperature of the river water samples in each season had direct correlation with the weather condition. The average temperature in ***Industrial zone*** was 28.85, 18.71, 8.44 and 22.05 ^{o}C during summer, fall, winter and spring respectively (Figure 3.15). In ***transition zone***, the average temperature was 26.18, 14.13, 8.81 and 22.91 ^{o}C during summer, fall, winter, and spring, respectively (Figure 3.16). Average temperatures of 26.81, 14.59, 8.08 and 20.95 ^{o}C in summer, fall, winter, and spring, were also recorded for the

agricultural zone, respectively (Figure 3.17). Therefore, temperature profile in each season followed a stable trend in most of the sampling points at all zones where lower temperatures were measured during the winter.

Investigating the ***industrial zone*** in detail indicated that *m1* as the first sampling point, representing the natural background in the watershed, had a seasonal mean temperature of 16.33 ^{o}C while the seasonal mean temperature at sampling points *m2-m6* was between 18.18 and 18.73 ^{o}C (Figure 3.15A). The increased temperature after *m1* was observed in all seasons. This suggested the high temperature water enters the main stream after that sampling point. The junction sampling points on Çorlu Creek (*cc11*), Ergene Creek (*ec8*), and tributaries next to Büyükkarıştıran OIZ (*t1-2*), Evrensekiz OIZ (*t3-1* and *t3-2*) with respective seasonal average temperature of 18.65, 19.13, 26.93 and 23.18 ^{o}C are the reason of temperature rise after *m1* in the main stream (Figure 3.15B). All of those sampling points and their associated tributaries are located next to OIZs. When investigated in detail (Figure 3.15B), the water taken from sampling points *t1-1* and *t1-2* next to Büyükkarıştıran OIZ with seasonal average temperature of 29.35 and 26.93 ^{o}C, *cc6* and *cc7* close to Velimeşe OIZ with 24.98 and 23.88 ^{o}C, *ec4* close to Ergene 2 OIZ with 21.4 ^{o}C and *ec6* next to Ergene 1 OIZ with 28.4 ^{o}C, respectively, were the main contributors of high temperature in their respective tributaries. Particularly, sampling points *ec6* on Ergene Creek with median temperature of 29.7 ^{o}C and *t1-1* and *t1-2* next to Büyükkarıştıran OIZ with respective median temperatures of 29.75 and 28.55 ^{o}C, were the points that the water temperature exceeded 19.1 ^{o}C, even in winter. Those three sampling points are located at the effluent discharge point of their respective OIZs. It was reported that temperature of effluents depends on the type of the industry and the processes performed in it. For instance, temperature of wastewater generated from a chemical production industry was 41 ^{o}C. Temperature of the effluents from textile, heavy electrical engineering, cooking oil production and food and beverages facilities were 28.5, 33.9, 21.4 and 27.4 ^{o}C, respectively in a study performed in Pakistan (Salman Afzal, 2018).

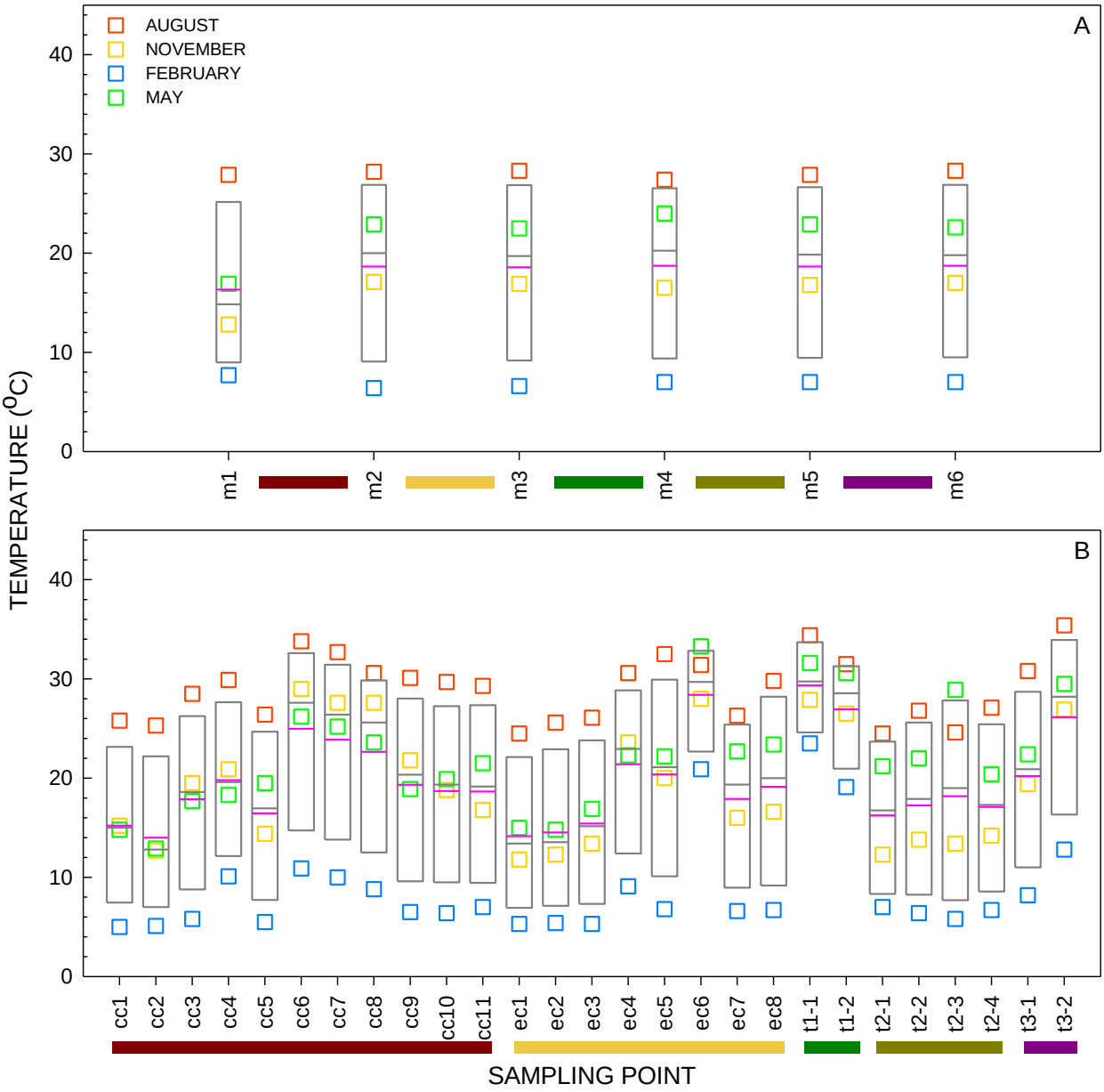

Figure 3.15. Seasonal profile of temperature in (A) main stream and (B) tributary samples taken from ***industrial zone***.

The temperature of water in ***transition zone*** remained stable along the main stream (Figure 3.16A). As shown, the seasonal mean and median temperatures at *m12* as the last sampling point of that zone was 19.0 and 19.5 ^{o}C, respectively that was not significantly different from *m6* as the first point in ***transition zone*** with respective seasonal mean and median temperatures of 18.73 and 19.8 ^{o}C (Figure 3.16A). In addition, the temperature of water taken from tributaries of that zone were correlated with the weather condition as well and no sudden increase or decrease in temperature was observed (Figure 3.16B).

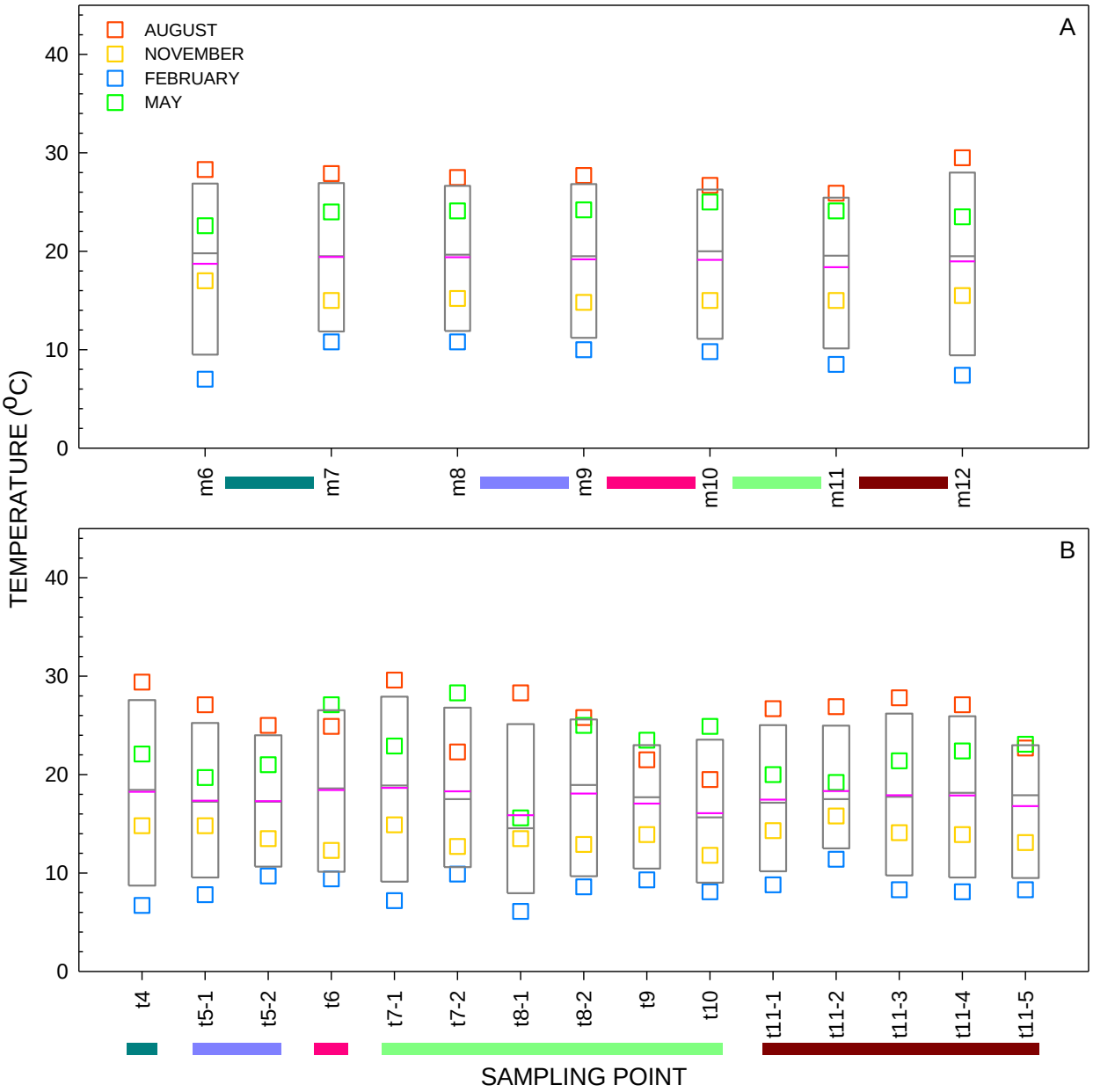

Figure 3.16. Seasonal profile of temperature in (A) main stream and (B) tributary samples taken from ***transition zone***.

The temperature profile in ***agricultural zone*** (Figure 3.17) was similar to ***transition zone***. Seasonal mean and median temperatures of 17.85 and 18.55 were measured at *m18* as the last sampling point. In this regard, the temperature in the main stream did not change significantly and stayed stable (Figure 3.17A). Moreover, the temperature of water samples in tributaries of ***agricultural zone*** indicated no exceptional pattern as well (Figure 3.17B).

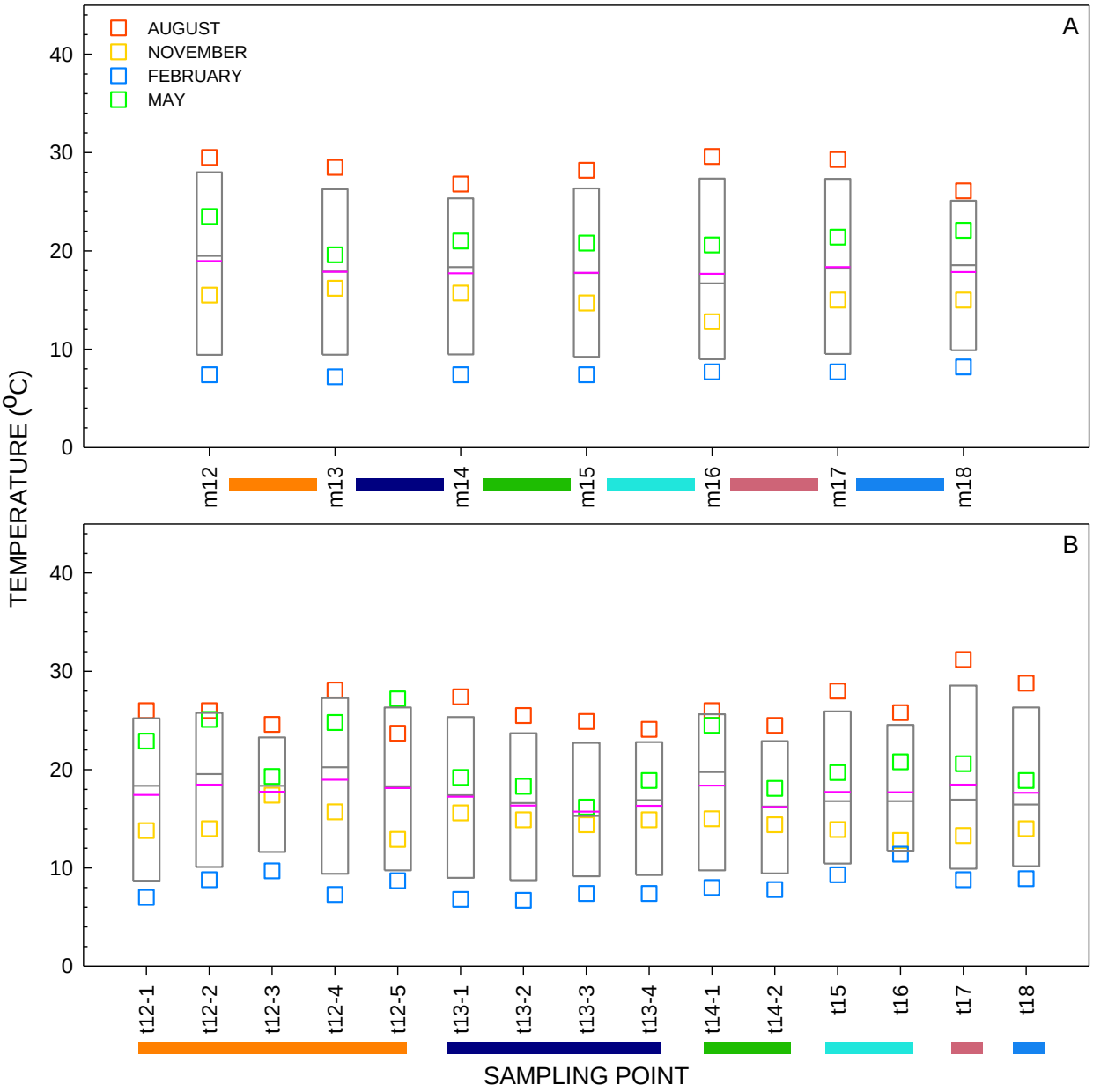

Figure 3.17. Seasonal profile of temperature in (A) main stream and (B) tributary samples taken from ***agricultural zone***.

As described above, the temperature seasonal temperature profiles indicated the direct correlation of water temperature with the weather conditions. However, industrial discharges in ***industrial zone*** affected the temperature of water in the tributaries and further the main stream. The high temperature in some of those points even in all seasons can influence the aquatic life.

3.3.1.3. Color. Color in the surface water is mainly due to presence of either natural materials or pollution. The natural materials are humic substance that are generated from the degradation of leaves and woods. The color of water may change due to the presence of suspended matters such as red clay

soils. In addition to those natural phenomena, the anthropogenic activities play an important role in coloring the surface waters. For instance, untreated or poorly treated effluents of textile industries which contain dyes or effluents of paper industries containing colored lignin derivatives are the sources of color in surface water (Sawyer, 2003).

The average color of Ergene River water was 261.44, 195.20, 88.57 and 194.64 ADMI during summer, fall, winter and spring, respectively. Considering zone by zone, the mean color of water in ***industrial zone*** was measured as 399, 293, 138 and 279 ADMI in summer, fall, winter and spring, respectively. As in ***transition zone***, the average color was 224, 155, 58 and 125 ADMI during summer, fall, winter and spring, respectively. Lower values of 83, 83, 41 and 131 ADMI in summer, fall, winter and spring, were observed in ***agricultural zone***, respectively. These results indicate that the average color of water was higher in ***industrial zone*** than the other two zones, suggesting the color stress applied by that zone on the whole river particularly the main stream.

In ***industrial zone***, the color of water samples taken from *m1* as the first point and natural background on the main stream of the Ergene River, was less than 200 ADMI (seasonal mean and median color of 65.5 and 56.5 ADMI, respectively) in all seasons. However, at the following sampling points along the main stream (*m2*-*m6*) of ***industrial zone*** (Figure 3.18A), color increased as much as three times. At *m6*, mean and median color of 268 and 317 ADMI was recorded in all seasons. Thus, as represented in Figure 3.18B, junction sampling points on Çorlu Creek (*cc11*), Ergene Creek (*ec8*), and tributaries next to Büyükkarıştıran OIZ (*t1-2*) and a single textile facility (*t3-2*) with respective seasonal average color of 283, 284, 758 and 298 ADMI, contributed the most to increased color values at sampling points after *m1*. Sampling points *cc6* and *cc7* with seasonal median color of 573 and 578 ADMI, respectively, had the highest color values in Çorlu Creek. In Ergene Creek, seasonal median color of 576 and 586 ADMI was measured at *ec4* and *ec6* (Figure 3.19), respectively, as well. Median color of 935 and 711 ADMI was also recorded at sampling points *t1-1* (Figure 3.19) and *t1-2* next to Büyükkarıştıran OIZ in ***industrial zone*** as well as all watershed. The common feature of all those points is the presence of many textile and dye industries around them releasing their untreated or poorly-treated wastewater into the Ergene River. These discharges resulted in color pollution in the main stream till the end of the ***industrial zone*** (*m6*). 22 out of 33 sampling points in industrial zone had color values more than the EQS (200 ADMI) defined by the authorities, during summer and fall.

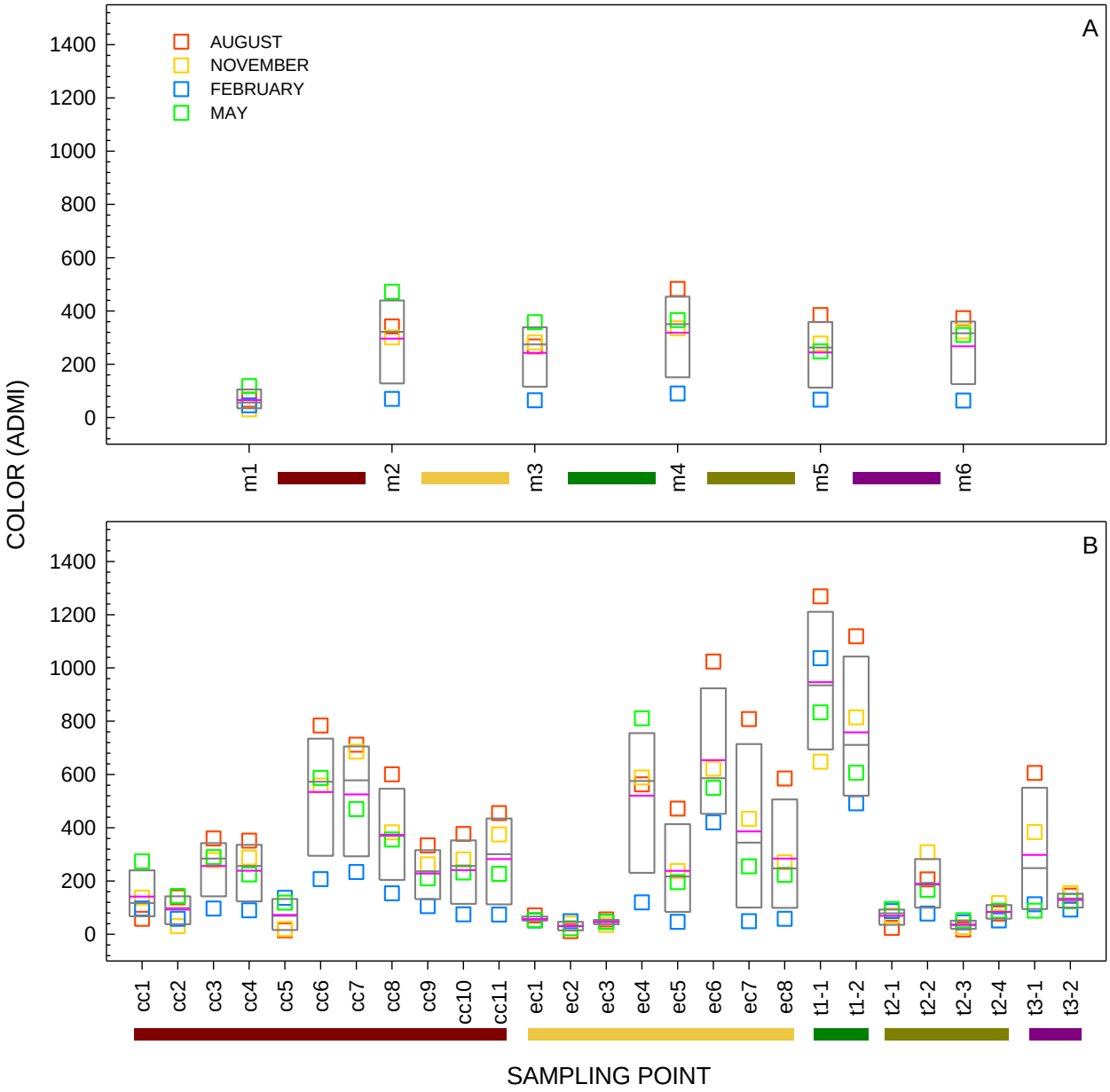

Figure 3.18. Seasonal profile of color in (A) main stream and (B) tributary samples taken from ***industrial zone***.

Figure 3.19. *ec6* and *t1-1* sampling points next to the Ergene 1 and Büyükkarıştıran OIZs with highest color values.

The color pollution resulted from the discharge of industrial effluents in ***industrial zone*** (*m2-m6*) was further transported to the ***transition zone*** via the main stream (Figure 3.20A) and sustained till the last point (*m12*) of that zone. Specially, during summer and fall when the dilution factor by precipitation is at its lowest level, higher color values were observed at main stream (Figure 3.20A). This fact is reflected at sampling point *m12* with the seasonal mean and median color at of 209 and 232 ADMI, respectively. Sampling points *t4* and *t7-2* on the tributaries also showed color values more than 400 ADMI during summer and fall, respectively (Figure 3.20B). Although those points did not affect the seasonal average color in the main stream significantly, they shall be considered as important pollution sources.

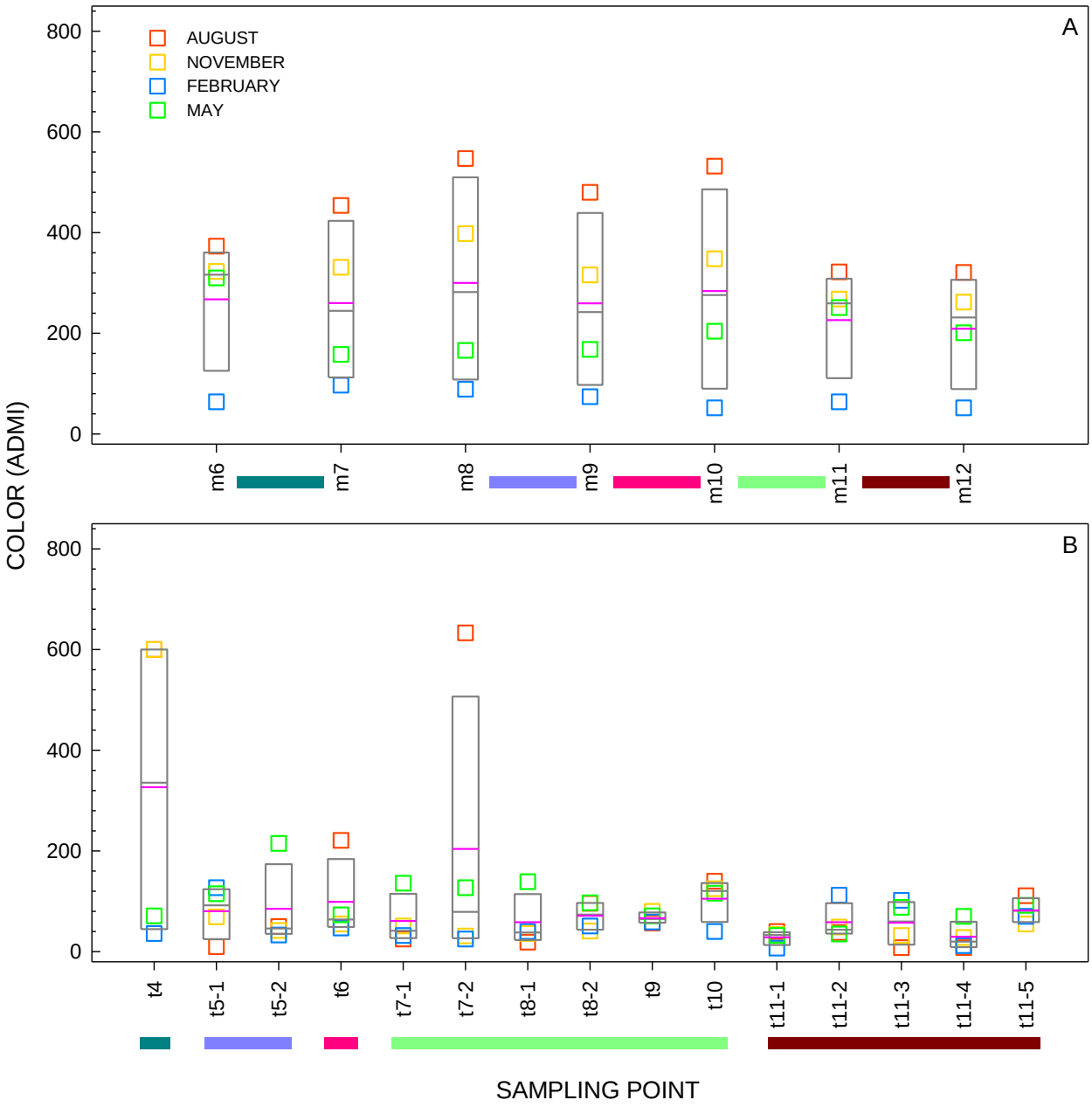

Figure 3.20. Seasonal profile of color in (A) main stream and (B) tributary samples taken from ***transition zone***.

Following the ***transition zone***, the sampling points on the main stream of ***agricultural zone*** (Figure 3.21A) had lower color values than the other two zones. This is due to lower number of industrial facilities in that zone together with the dilution factor along the main stream. Despite of lower color values on the main stream, the color values of the last point in ***agricultural zone*** (*m18*) was still more than 100 ADMI during fall and spring samplings which places the water in category A2 of surface water defined by directive 75/440/EC of European Commission. Besides, tributaries in ***agricultural zone*** had colors less than 200 ADMI (Figure 3.21B), suggesting not to have significant contribution to the color in the main stream.

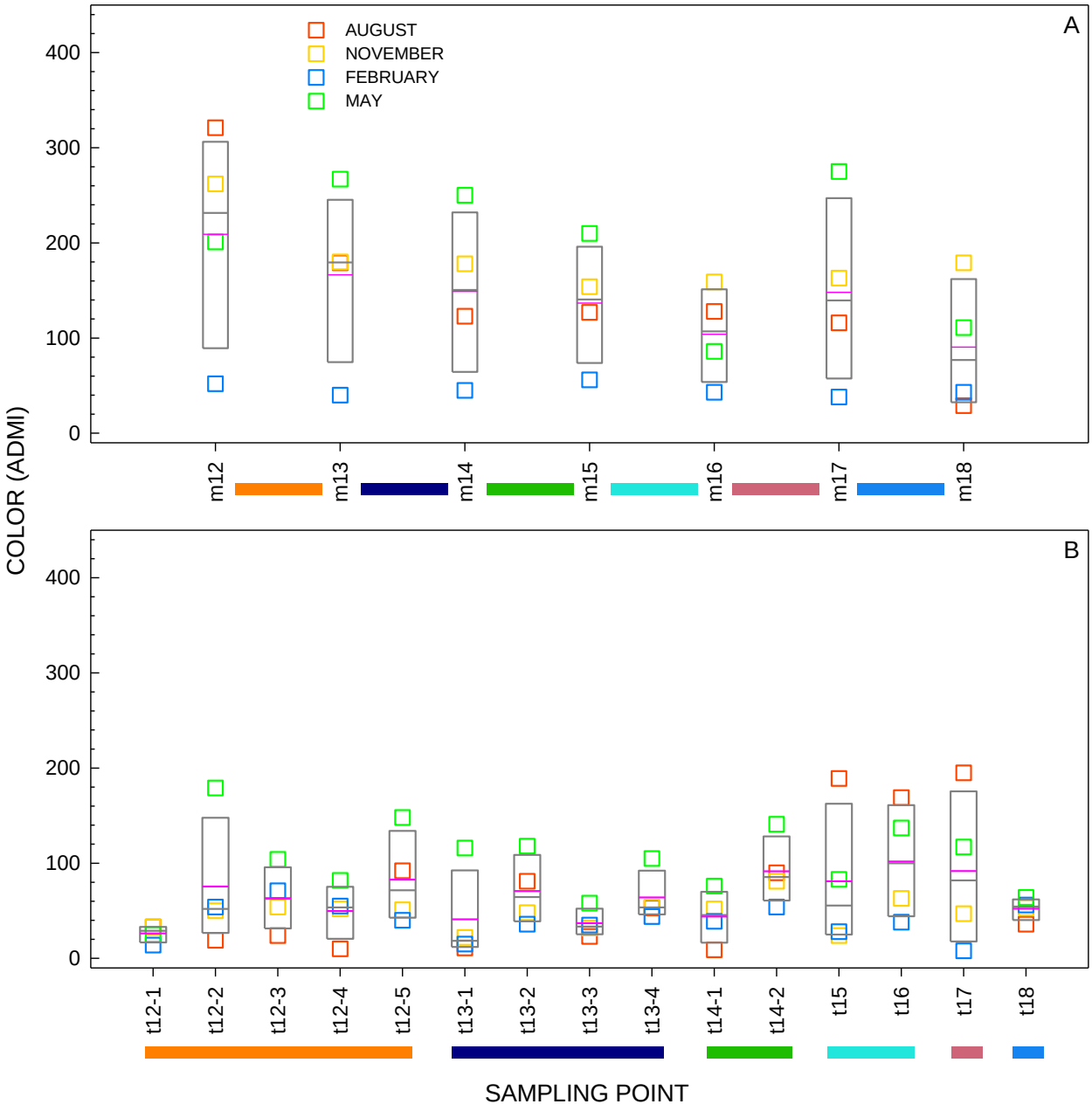

Figure 3.21. Seasonal profile of color in (A) main stream and (B) tributaries sampling points of agricultural zone.

Findings regarding the color of river water indicated that industrial discharges from dye and textile industries located on the Ergene Creek, Çorlu Creek and the tributary next to the Büyükkarıştıran OIZ located on ***industrial zone*** are the main sources of color pollution in the Ergene River (Figure 3.22).

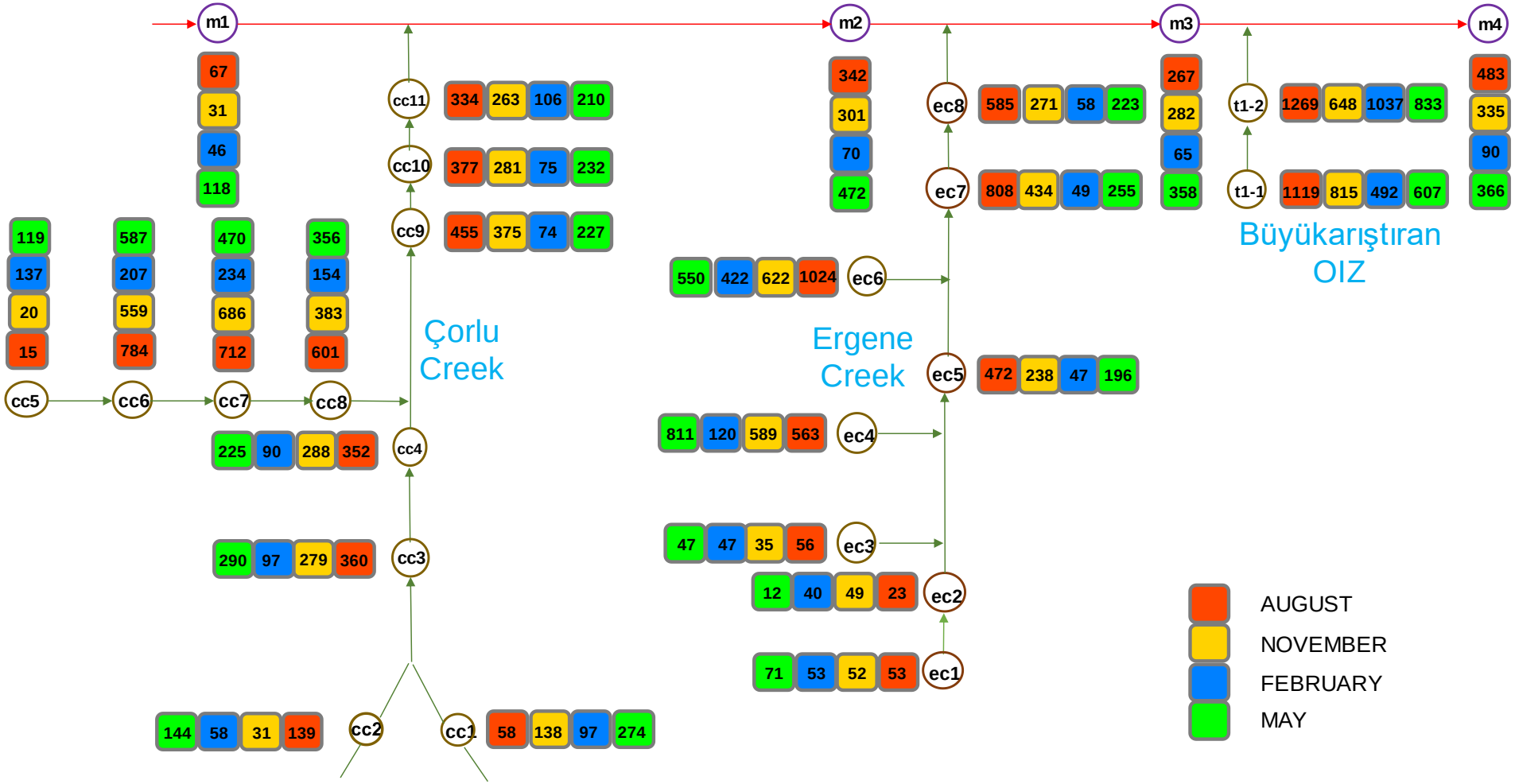

Figure 3.22. Seasonal color values of the main contributors of color pollution in Ergene River.

3.3.1.4. COD. Seasonal COD measurements along the Ergene River and its tributaries had close correlation to color profiles. The average COD in the Ergene River during summer, fall, winter and spring samplings was 413.50, 323.71, 138.98 and 300.17 mg/L, respectively. Considering the average COD during four seasons and the EQS for COD in surface water set by the Turkish Ministry of Forestry and Water (70 mg/L), the water of Ergene River is categorized in class 4 (highly polluted). Recorded COD in ***industrial zone*** was comparable to the following zones. The average COD in ***industrial zone*** was 603.1, 477.4, 216.8 and 468.7 mg/L in summer, fall, winter and spring, respectively, and in ***transition zone*** was 414.3, 270.5, 113.3 and 211.1 mg/L, respectively. Whereas ***agricultural zone*** was identified with lower average COD as 114.7, 135.4, 42.3 and 124.4 mg/L during summer, fall, winter and spring, respectively. Therefore, ***industrial zone*** had the highest COD in the watershed. In addition, considering the seasonal variations, the profiles of COD in three zones (Figure 3.23, Figure 3.24, Figure 3.25) showed low COD during winter considering the dilution factor as a results of increased precipitation during that season.

As represented in Figure 3.23A, the mean and median COD of water taken from *m1* which is the first sampling point along the main stream and can be considered as the natural background in the river, was 65.7 and 72.5 mg/L, respectively. While processing along the main river, the COD increased significantly to more than ten times in *m2* and sustained in the main stream till the last point of the ***industrial zone*** where seasonal mean and median COD as high as 563.1 and 618.5 mg/L, was measured at *m6*, respectively. Considering in detail, the water from sampling point *cc11* at the end of the Çorlu Creek (cc) mixes with the one from *m1* and reaches *m2* (Figure 3.23B). A seasonal mean COD as high as 540.8 mg/L for *c11* was measured suggesting the contribution of Çorlu Creek on high COD at *m2*. Similar to *cc11*, junction sampling points *ec8*, *t1-2*, *t3-1* and *t3-2* on the tributaries of ***industrial zone***, were quantified with seasonal average COD of 533.2, 728.3, 815.5 and 493.9 mg/L during the year, respectively. The elevated COD at those points are mainly originated from the OIZs located next to their respective tributary. On Çorlu Creek, sampling point *cc6* with seasonal mean and median COD of 800.4 and 891.5 mg/L, *cc7* with 774.2 and 894.5 mg/L and *cc8* with 608.8 and 672.4 mg/L, respectively, all located next to the Velimeşe OIZ, were the sampling points at which elevated COD values were measured. On the Ergene Creek, *ec4* next to Ergene 2 OIZ and *ec6* close to Ergene 1 OIZ also contained high COD. The seasonal mean and median COD of 635.2 and 705.0 for *ec4* and 773.9 and 789.5 mg/L for *ec6* was recorded, respectively. Sampling point *t1-1* next to Büyükkarıştıran OIZ with average mean and median COD of 831.8 and 838.6 mg/L, was the most important source of COD pollution in the river (Figure 3.23B). Besides, sampling points *t3-1* and *t3-2* next to Ervrensekiz OIZ and a single textile facility, respectively, were also determined with high COD. The seasonal mean and median COD at *t3-1* was 815.5 and 873.1 mg/L, respectively. The COD

pollution from all abovementioned tributaries resulted in high COD value in the main stream of ***industrial zone*** (Figure 3.23A).

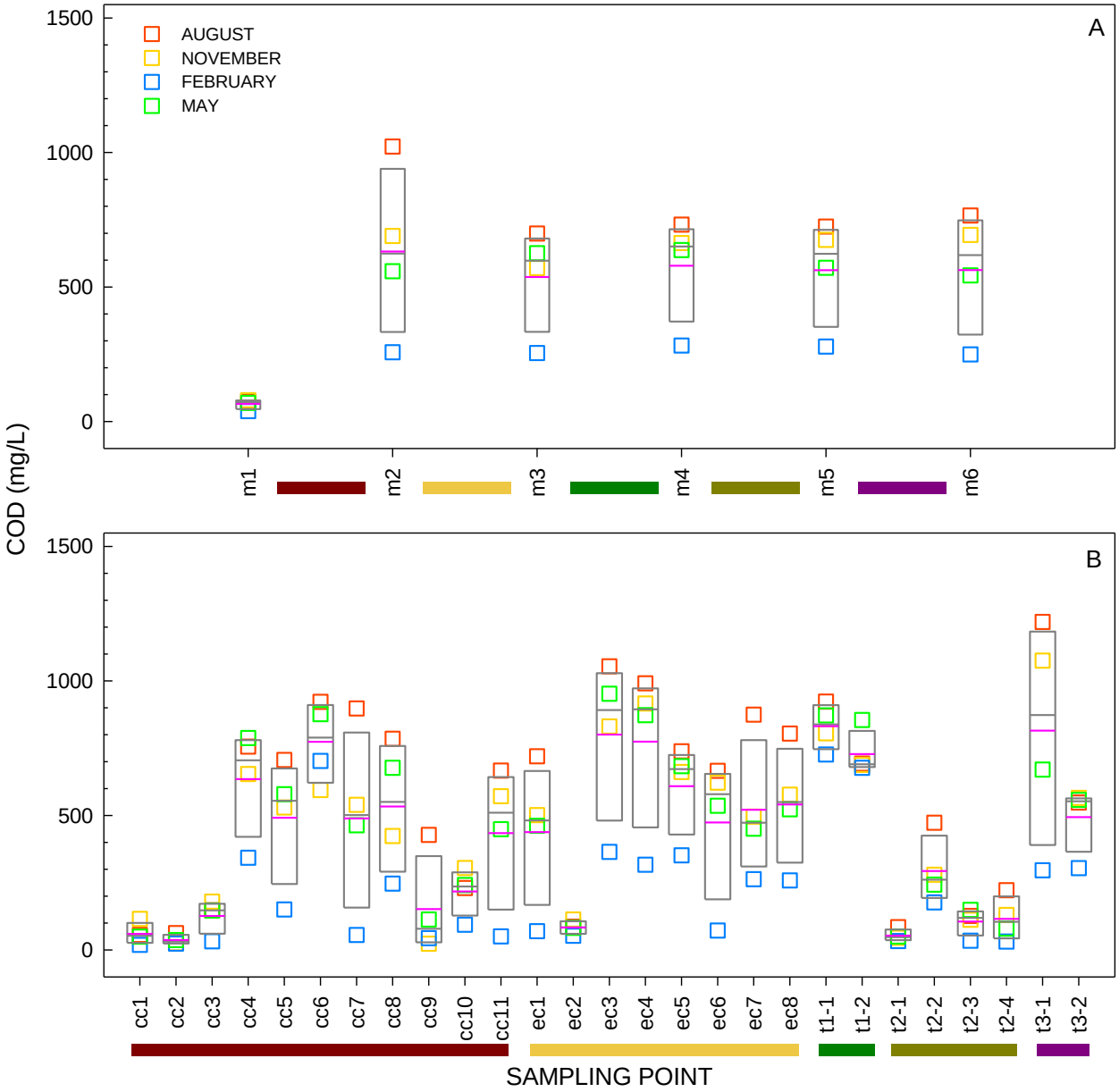

Figure 3.23. Seasonal profile of COD in (A) main stream and (B) tributary samples taken from ***industrial zone***.

Although the average COD values in ***transition zone*** during the four seasons were lower than ***industrial zone***, the sampling points on the main stream of ***transition zone*** (*m7-m12*) still contained high COD (Figure 3.24A). That is due to the COD pollution generated in ***industrial zone***, its transport to the ***transition zone*** via the main stream and slightly being diluted (Figure 3.24A). Seasonal mean and median COD of 514.8 and 523.7 mg/L at sampling point *m12* as the last sampling point of ***transition zone*** clarify that issue. Moreover, considering the tributaries (Figure 3.24B), water samples

taken from sampling points *t4* and *t7-1* had CODs of 981 and 1661 mg/L during summer. These sampling points are located next to flour production and dairy (cheese) production facilities, respectively. For instance, high COD ranges between 20,000 and 80,000 mg/L was reported for the wastewater of cheese production facilities in the literature as well. This amount can be treated to the lower COD of 1500 mg/L depending on the treatment conditions, although this amount is still more than the limit (250 mg/L) determined for the dairy effluent discharges (Lebrato et al., 1990, Shete and Shinkar, 2013). Therefore, measuring a high COD value at *t7-1* is not out of expectation.

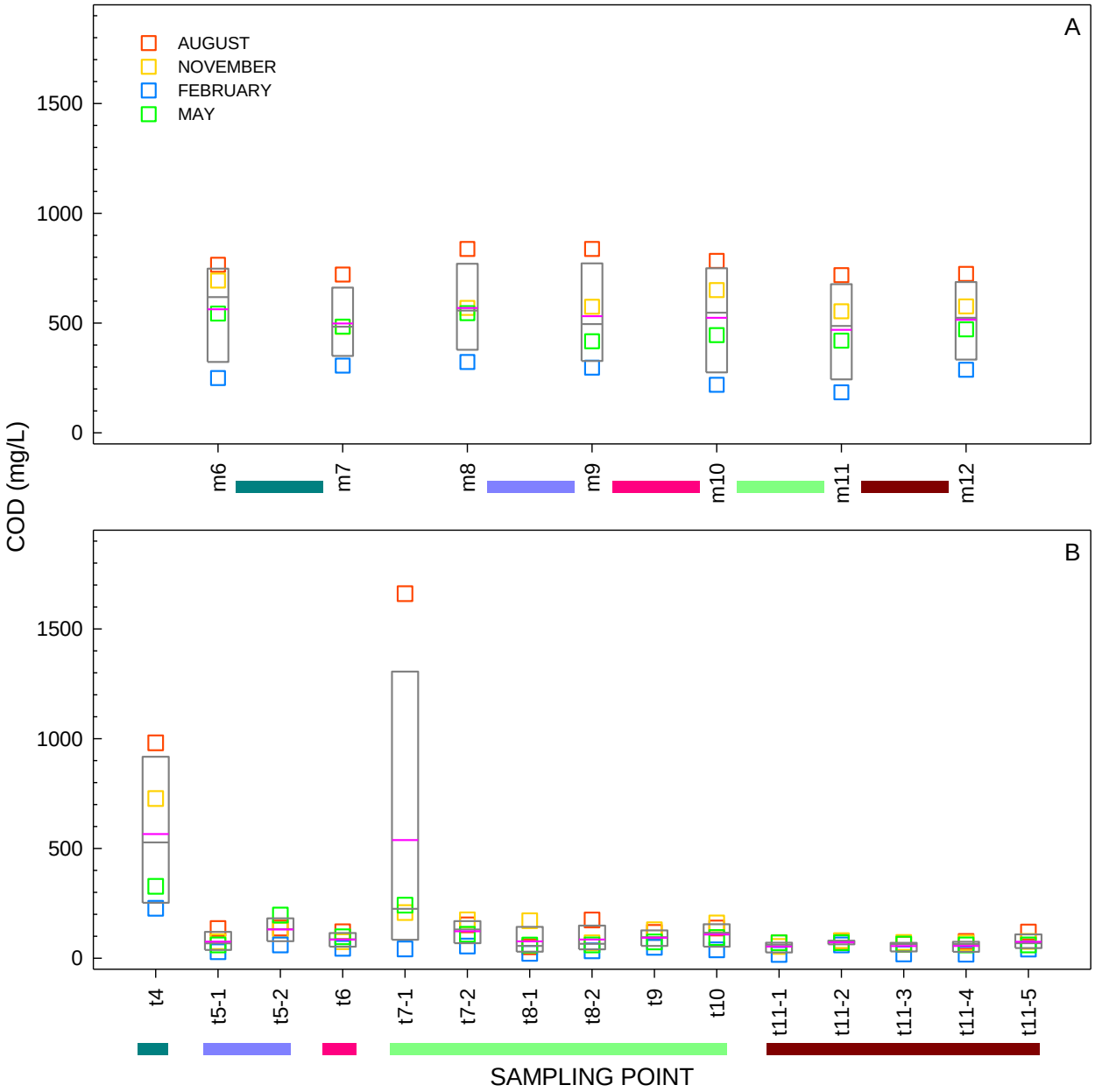

Figure 3.24. Seasonal profile of COD in (A) main stream and (B) tributary samples taken from ***transition zone***.

Following the ***transition zone***, COD of water samples from ***agricultural zone*** was lower than the previous two zones. As shown in Figure 3.25A, the COD values along the main river decreased due to the dilution factor. Although COD decreased in ***agricultural zone***, a seasonal mean and median COD of 121.7 and 99.2 mg/L was still determined at the last sampling point in the watershed (*m18*), respectively. Containing COD more than 70 mg/L (EQS) at *m18* reveals the level of pollution in the whole river.

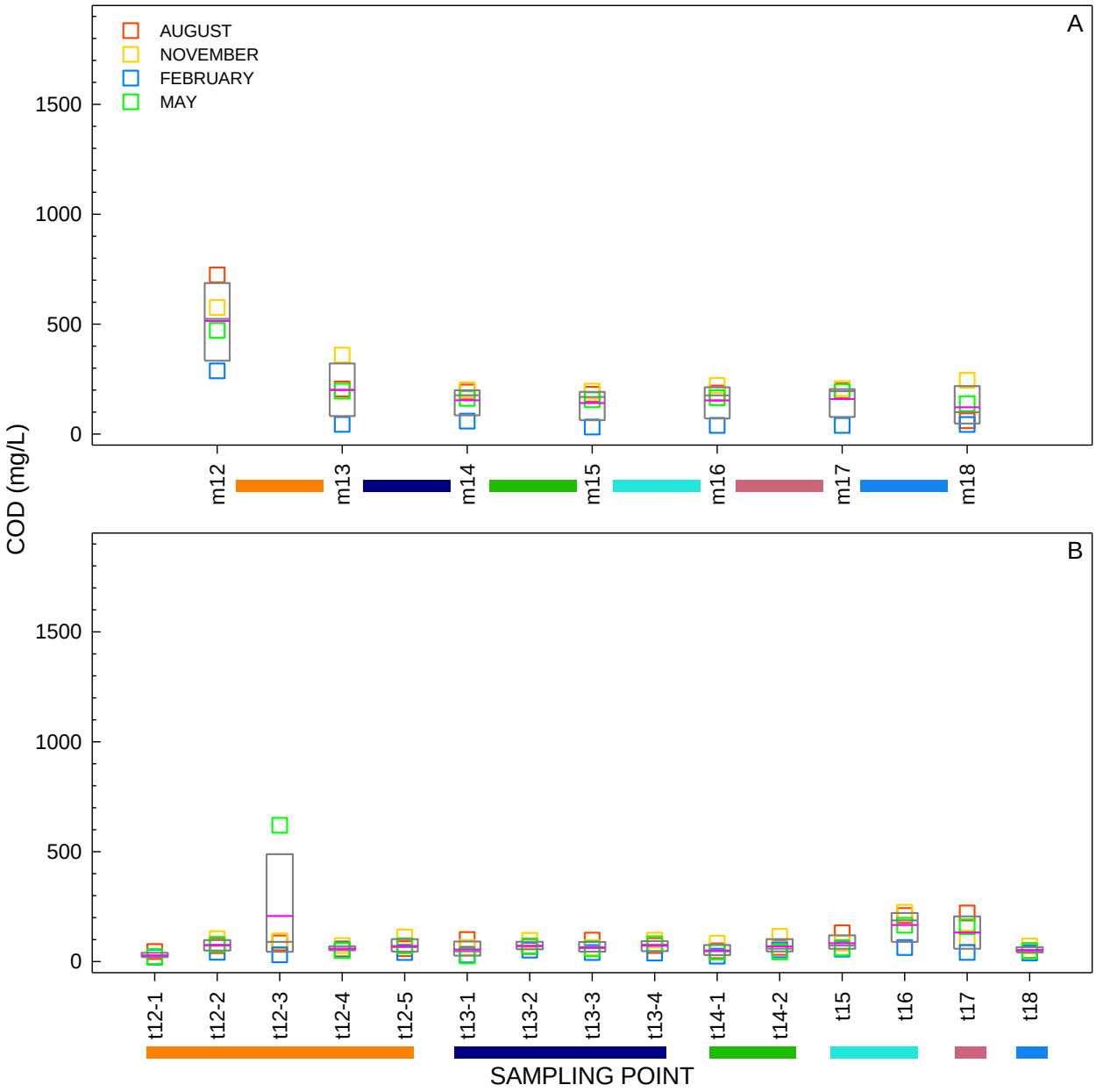

Figure 3.25. Seasonal profile of COD in (A) main stream and (B) tributary samples taken from ***agricultural zone***.

In addition to COD, total organic carbon (TOC) of river water samples was also measured. TOC of the samples had similar behavior as COD (APPNDIX B). The average TOC values were 85.13, 50.28, 19.34 and 36.45 mg/L during summer, fall, winter and spring respectively. Similar to COD, the highest TOC were observed at sampling points located in *industrial zone*. The high TOC was then sustained in the main stream till the last point, although it was decreasing gradually due to dilution factor. Industrial discharges are the main sources of COD and TOC pollutions in ***industrial zone*** as well as whole watershed.

3.3.1.5. Ions. Ammonium-nitrogen (NH_3-N), nitrate, nitrite, sulfate, phosphate, chloride, fluoride and bromide were quantified in river water samples.

Ammonium-nitrogen (NH_3-N): Ammonium-nitrogen (NH_3-N) was generally high in the Ergene River. The average NH_3-N was 13.5, 10.2, 2.6 and 5.8 during summer, fall, winter and spring, respectively, which were more than the limit (2 mg/L) set by the Turkish Ministry of Forestry and Water on quality of surface water for drinking water abstraction. Municipal wastewaters, industrial and agricultural wastewaters are the possible sources of NH_3-N occurrence in river water (Darwish, 2012). For instance, NH_3-N composes 60% of nitrogen in domestic wastewater (Purwono et al., 2017). In addition, ammonia is used in industrial processes as refrigerant in food industries, production of chemicals such as nitric acid, metal treating in metal industries as well as manufacturing of animals food. Therefore it can be discharged into the surface water in case of poor or no treatment of the abovementioned industrial wastewaters (Darwish, 2012). Agricultural runoffs may also contain NH_3-N due to usage of ammonium-containing fertilizers in agriculture (Darwish, 2012). In the Ergene River, average NH_3-N concentration of 12.9, 13.4, 4.2 and 9.0 mg/L in summer, fall, winter and spring, was measured in ***industrial zone***, respectively, while in ***transition zone*** 25.2, 11.5, 1.3 and 3.6 mg/L of NH_3-N was obtained. In ***agricultural zone***, presence of lower number of industrial facilities compared to the previous zones resulted in average NH_3-N of 2.8, 4.0, 1.1 and 2.9 mg/L in summer, fall, winter and spring, respectively. The results indicated that similar to COD and color, ***industrial zone*** was the main contributor of NH_3-N pollution in the river.

In ***industrial zone***, the seasonal mean and median concentrations of NH_3-N at sampling point *m1* was 0.5 and 0.4 mg/L, while at *m6* was 10.9 and 10.8 mg/L, respectively. The increased NH_3-N concentration in the main stream of ***industrial zone*** after *m1* (Figure 3.26A) was because of the pollution arrived from the tributaries. NH_3-N was present at mean and median concentrations of 14.3 and 13.2 mg/L at *cc11*, 7.4 and 6.4 mg/L at *ec8*, 25.1 and 24.2 at *t1-2* and 11.9 and 10.1 mg/L at *t3-1* as the junction sampling points of the tributaries, respectively (Figure 3.26B) suggesting the effects

of those tributaries on NH_3-N pollution in the main stream. Presence of different industries discharging their effluent into the Çorlu Creek, Ergene Creek, and the tributaries next to Büyükkarıştıran and Evrensekiz OIZs, resulted in high NH_3-N concentration not only at the sampling points on those tributaries but also on the main stream. In addition, *cc7* on the Çorlu Creek with seasonal mean and median NH_3-N concentrations of 21.1 and 22.4 mg/L, *ec6* on the Ergene Creek with 18.3 and 16.4 mg/L and *t1-1* on the tributary close to Büyükkarıştıran OIZ were identified as the main sources of NH_3-N in the Ergene River.

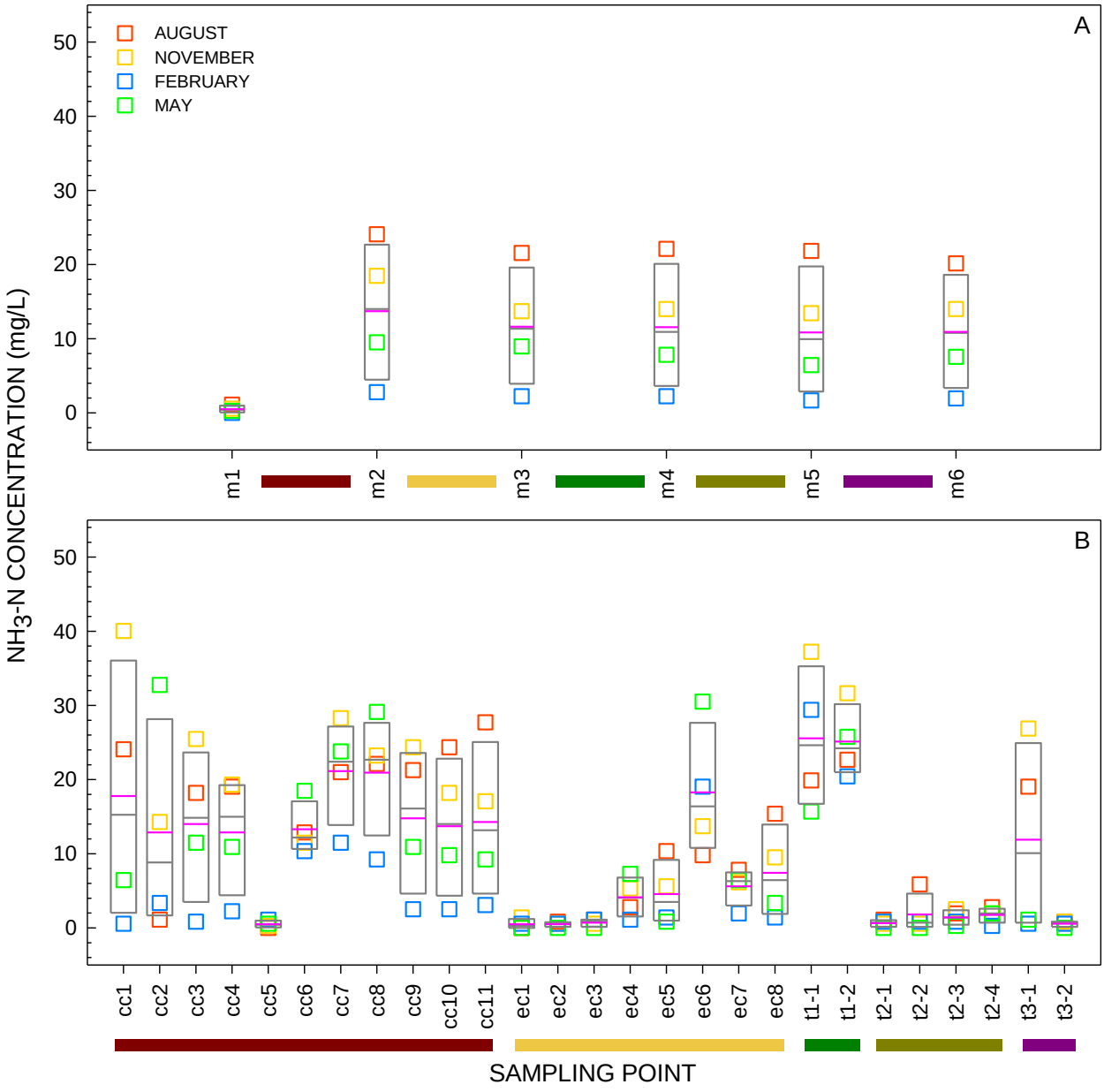

Figure 3.26. Seasonal profile of NH_3-N in (A) main stream and (B) tributary samples taken from ***industrial zone***.

The NH_3-N pollution in ***industrial zone*** sustained in the main stream and occurred in ***transition zone*** as well. As a result, mean and median NH_3-N concentrations of 9.3 and 8.8 mg/L were observed at *m12* as the last sampling of ***transition zone***, respectively (Figure 3.27A). Although NH_3-N concentration was stable in the main stream of that zone, the NH_3-N concentration exceeded 200 mg/L at some points. NH_3-N at concentration up to 270.8, 37.0 and 27.4 mg/L was present at sampling point *t4*, *t6* and *t7-2* in summer, respectively (Figure 3.27B). Those points are investigated to be located next to cities discharging their sewage into the river.

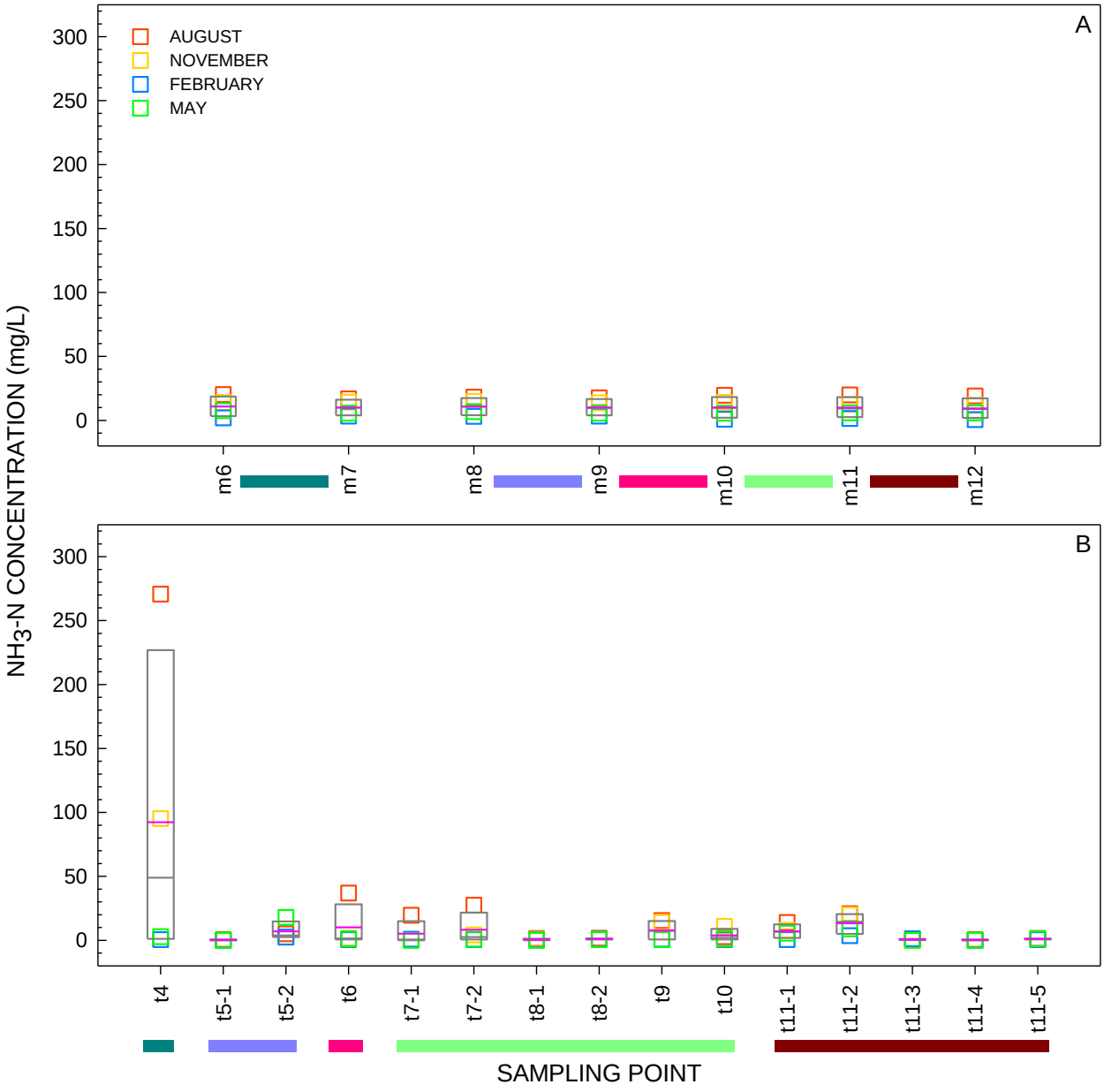

Figure 3.27. Seasonal profile of NH_3-N in (A) main stream and (B) tributary samples taken from ***transition zone***.

The average NH_3-N concentration in ***agricultural zone*** was lower compared to the two previous zones. Although it was decreased along the main stream due to dilution factor (Figure 3.28A), NH_3-N was still detected at *m18* as the last sampling point at seasonal mean and median concentrations of 3.9 and 2.9 mg/L, respectively (Figure 3.28A). On the tributaries of ***agricultural zone,*** *t12-3* next to Kırklareli City with mean and median NH_3-N concentrations of 5.7 and 6.2 mg/L, *t15* next to agricultural lands with 3.7 and 3.9 mg/L and *t16* close to Uzunköprü City and agricultural lands with 3.9 and 4.3 mg/L, respectively, were the sampling points at which the highest NH_3-N concentrations were measured (Figure 3.28B).

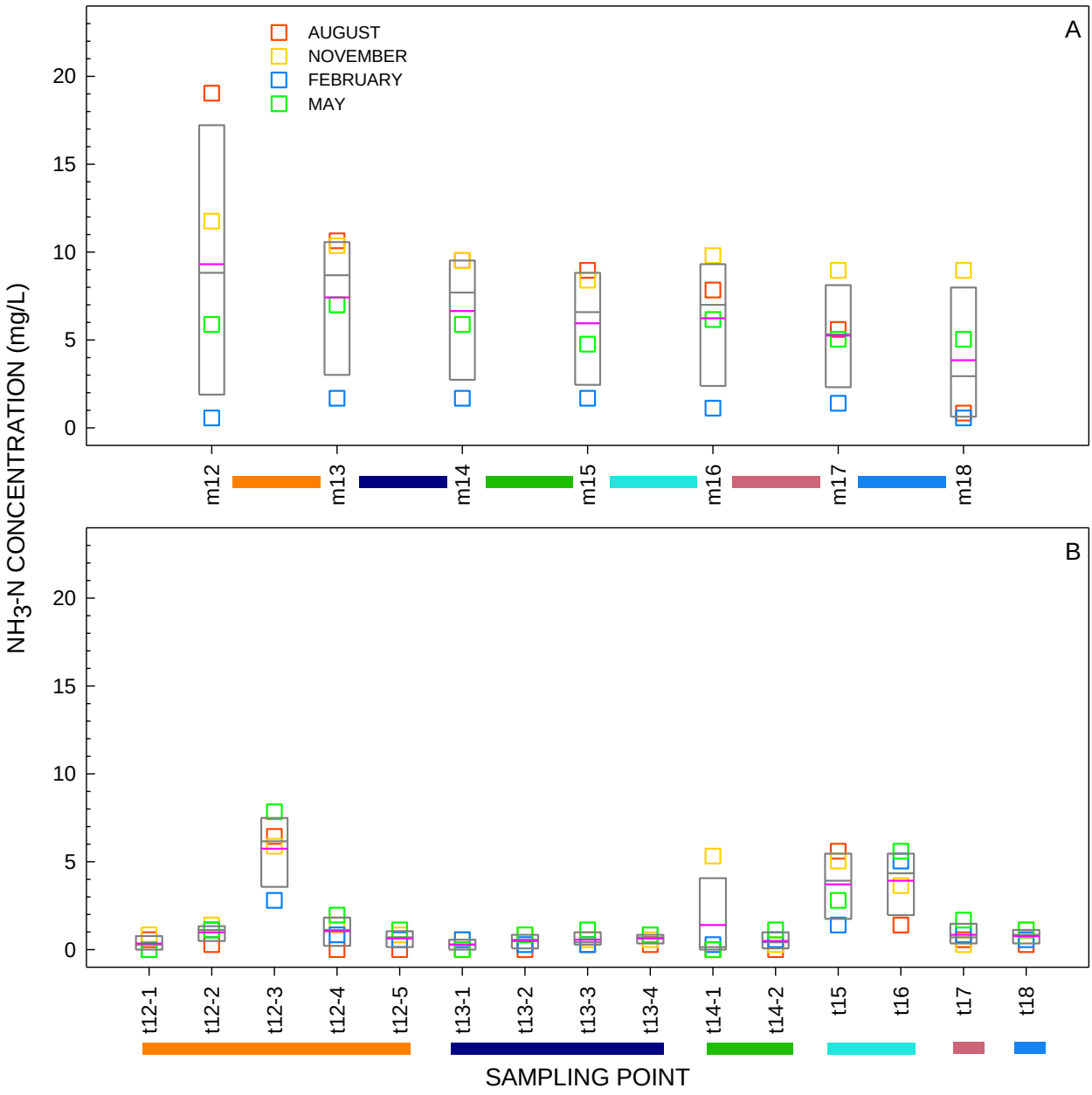

Figure 3.28. Seasonal profile of NH_3-N in (A) main stream and (B) tributary samples taken from ***agricultural zone***.

Considering seasonal NH_3-N concentration in the Ergene River exceeding the EQS, the water of the river is classified in category 4 (very polluted) defined by the Turkish Ministry of Forestry and Water. In addition, the pollution caused by elevated NH_3-N can endanger the aquatic life through eutrophication and decreasing the soluble oxygen in the water.

Nitrate: Nitrate (NO_3^-) concentration in the river was high in some points. The average nitrate concentration in the river was 3.42, 4.96, 11.31 and 7.97 mg/L during summer, fall, winter and spring, respectively. Although average nitrate concentration did not pass the EQS set by the Turkish Ministry of Forestry and Water (20 mg/L), some points including *t3-2* (next to a textile facility and surrounded by agricultural fields) in ***industrial zone*** and *t5-1* (next to dairy facility) in ***transition zone*** had nitrate concentrations of more than 20 mg/L in all seasons. Nitrate was present at seasonal mean and median concentrations of 88.9 and 100.5 mg/L at *t3-2* and 29.2 and 28.6 mg/L at *t5-1*, respectively. Untreated or poorly treated domestic wastewater as well as wastewater of industries such as textile, food industry, electroplating industries and power plants are known to be the main sources of nitrate in surface water (Su et al., 2017, Hussain et al., 2004, Park and Yoo, 2009). For instance, in a study on characterization of wastewaters of six textile industries in Bhilwara City in India, the nitrate concentration ranged between 120 and 627 mg/L (Hussain et al., 2004). The nitrate was present in the effluent from a dairy facility at concentration as high as 25.67 mg/L in a study performed in Cameron (Noukeu et al., 2016). In addition to domestic and industrial sources, nitrate in fertilizers can be carried to the surface water via run off from agricultural fields (Li et al., 2014). The detail seasonal profile of nitrate concentration in all three zones are shown in APPENDIX B.

Nitrite: In addition to nitrate, nitrite was measured in this study as well. The average nitrite concentration at 0.17, 0.28, 0.43 and 0.35 mg/L was measured in summer, fall, winter and spring, respectively. The concentration of nitrite did not exceed 8 mg/L throughout the watershed. Similar to nitrate, highest nitrite concentrations were observed in ***industrial zone***. Nitrite at highest concentration of 7.95 mg/L was measured during winter in sampling point *cc4* close to Veliköy OIZ (APPENDIX B).

Phosphate: The phosphate (PO_4^{3-}) concentration in most of the sampling points was more than EQS of 1.9 mg/L set by the Turkish Ministry of Forestry and Water and therefore, the Ergene River water is classified as class 4 (very polluted waters). The average concentration of phosphate was 2.46, 4.23, 0.68 and 1.99 mg/L during summer, fall, winter and spring, respectively throughout the watershed. ***Industrial zone*** where many facilities discharge their wastewater into the river, was identified with elevated phosphate concentration. The average phosphate concentration of 2.3, 3.3, 0.8 and 2.4 mg/L

was measured in that zone during summer, fall, winter and spring, respectively. In addition, phosphate was present at concentrations 3.7, 6.1, 0.6 and 1.9 mg/L in ***transition zone*** and 1.5, 3.9, 0.6 and 1.5 mg/L in ***agricultural zone*** during summer, fall, winter and spring, respectively. Average concentration in ***transition zone*** specially in fall was more than the other two zone because of high phosphate concentration measured in a tributary of that zone. Phosphate occurrence in surface waters is from various sources such as industrial wastewaters, detergents in domestic wastewaters as well as fertilizers and pesticides used in agriculture (Fadiran et al., 2008).

Industrial zone was the main contributor of phosphate pollution along the river since the phosphate concentration altered significantly from a mean concentration of 0.03 at sampling point *m1* to 2.46 mg/L at *m6* as the last sampling point in the main stream of that zone (Figure 3.29A). Sampling points *cc8* located on Çorlu Creek with mean and median concentrations of 3.08 and 3.62 mg/L, *ec4* on Ergene Creek with 5.25 and 5.32 mg/L and *t1-1* close to Büyükkarıştıran OIZ with 2.20 and 3.49 mg/L, respectively, were the main source of phosphate in those tributaries (Figure 3.29B).

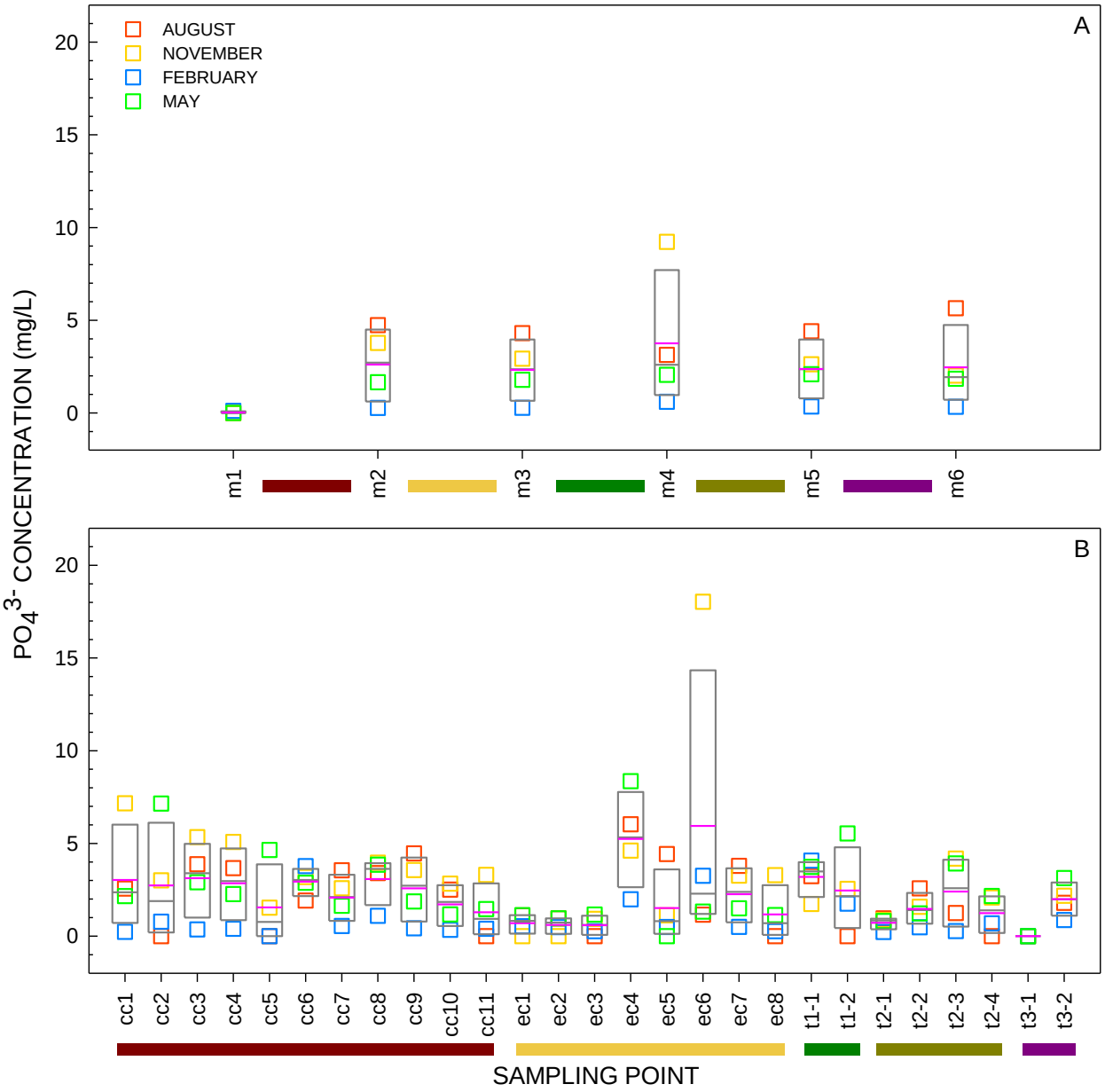

Figure 3.29. Seasonal profile of phosphate in (A) main stream and (B) tributary samples taken from ***industrial zone***.

In transition zone, the concentration of phosphate slightly increased after sampling point *m6* and sustained till *m12*. Phosphate was present at sampling point *m12* at seasonal mean and median concentrations of 3.14 and 2.15 mg/L, respectively (Figure 3.30A). The increased concertation after *m6* was due to the high phosphate-containing water from the tributary where sampling point *t4* is located (Figure 3.30B). In fall, concentration as high as 68.00 mg/L was measured in *t4* that is next to Lüleburgaz City.

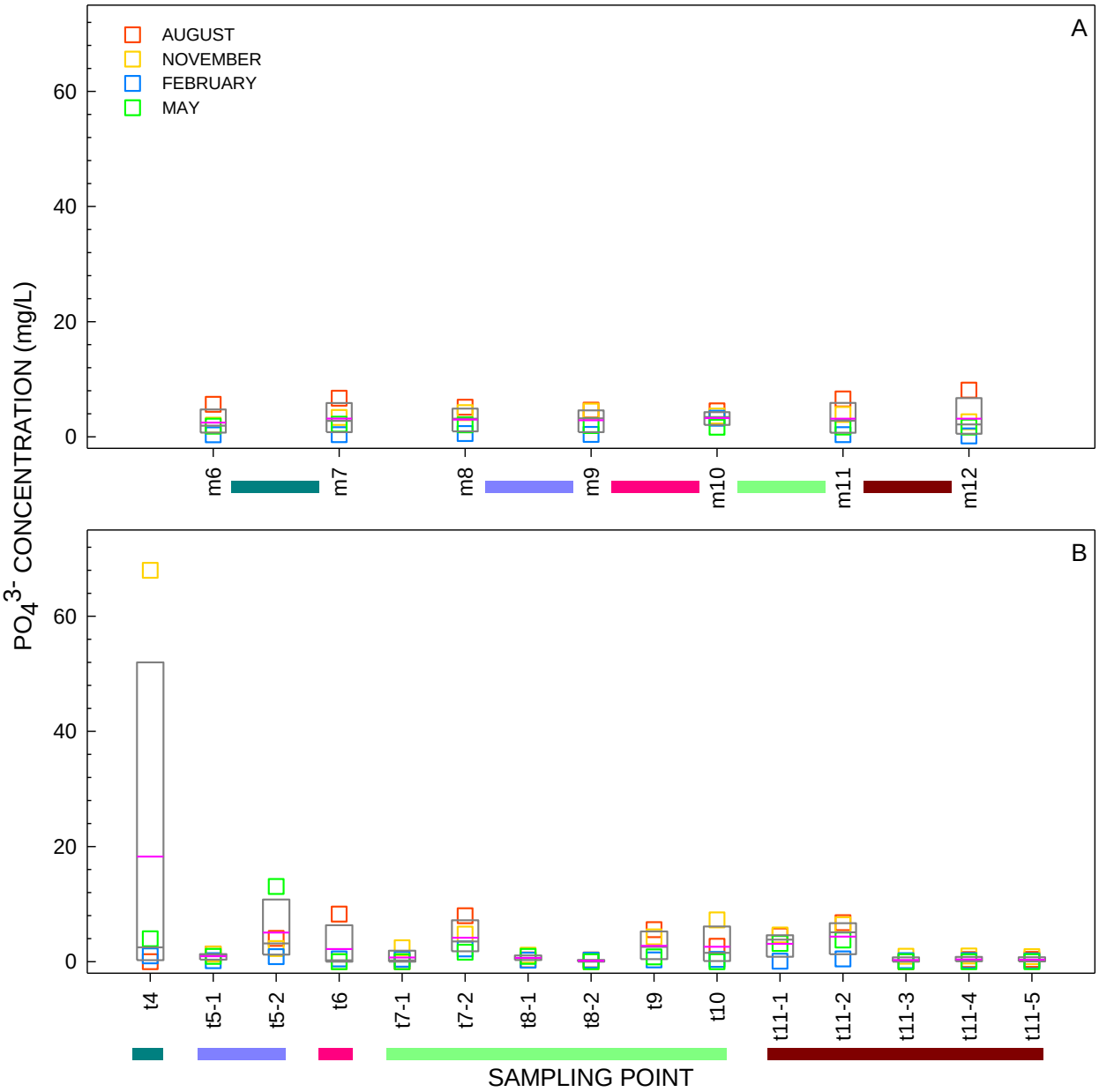

Figure 3.30. Seasonal profile of phosphate in (A) main stream and (B) tributary samples taken from ***transition zone***.

Phosphate concentration in the main stream of ***agricultural zone*** was decreased due to dilution factor. However, still seasonal mean and median concentrations of 1.13 and 1.23 mg/L of phosphate was detected at sampling *m18* where Ergene River meets Maritsa River (Figure 3.31A). Although tributaries in ***agricultural zone*** did not affect the phosphate concentration in the main stream, some sampling points such as *t16* (next to Uzunköprü City and agricultural fields) was recorded with 53.05 mg/L of phosphate during fall (Figure 3.31B).

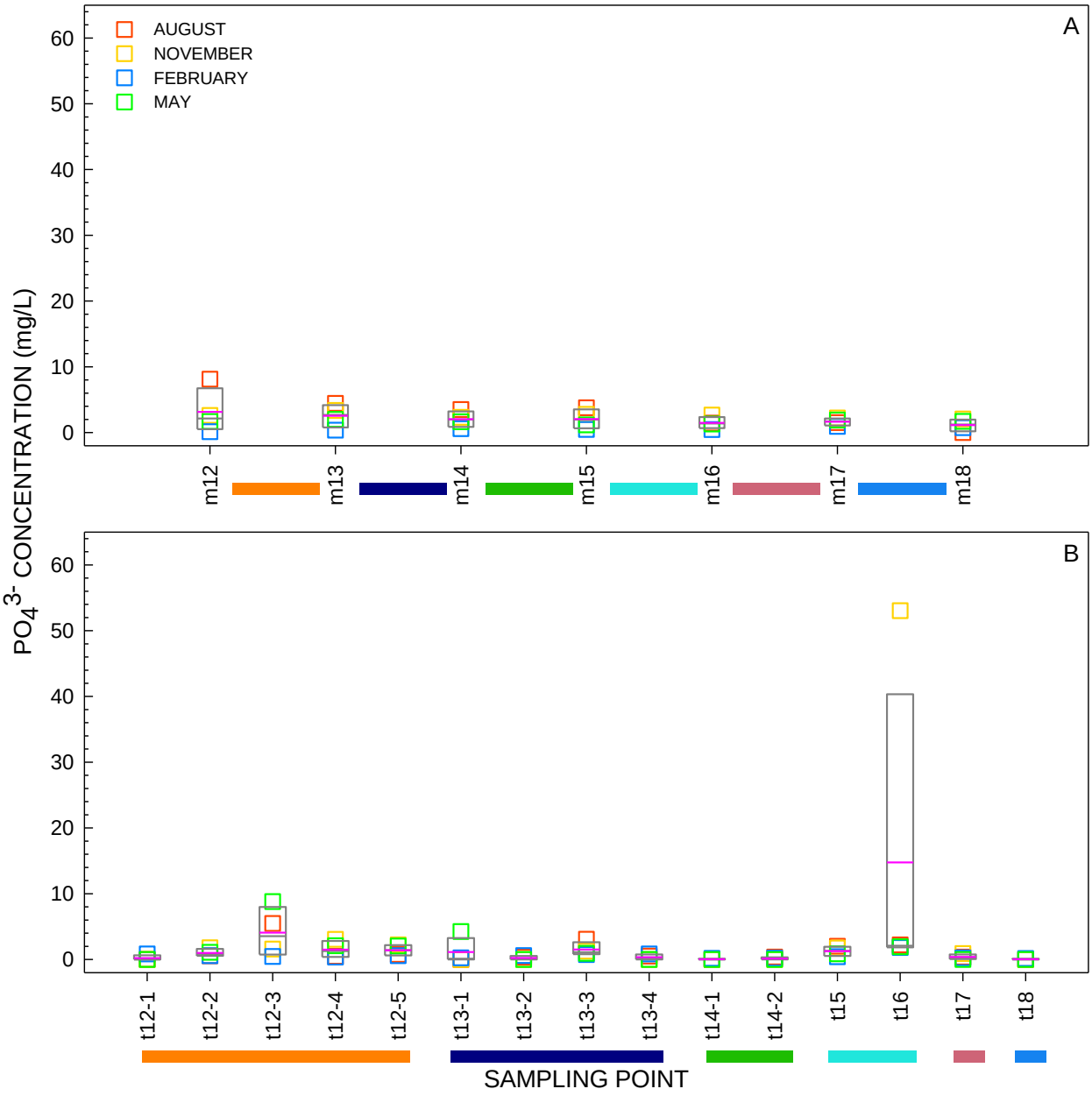

Figure 3.31. Seasonal profile of phosphate in (A) main river and (B) tributary samples taken from ***agricultural zone***.

Phosphate was present in Ergene River water at concentrations more than EQS (1.9 mg/L) that decreases its water quality. High concentration of phosphate can cause eutrophication and deplete dissolved oxygen in the surface water. In addition, high phosphate content water can induce digestive problems in human and aquatic animals (Fadiran et al., 2008).

Sulfate: Sulfate is an anion that its high concentration in water can cause different diseases. Sulfate mainly enters the surface water through discharge of industrial wastewaters. In Ergene River, the average sulfate concentration of 177.2, 161.5, 72.3 and 123.6 mg/L was measured in summer, fall,

winter and spring respectively. Similar to the distribution of other conventional parameters (e.g. color and COD), sulfate was measured at higher concentrations in ***industrial zone*** than the following zones. Sulfate was present in industrial zone at mean concentrations of 288.2, 233.1, 92.4 and 169.4 mg/L in summer, fall, winter and spring, respectively. However, lower sulfate concentrations as 115.2, 113.6, 72.1 and 93.8 mg/L in ***transition zone*** and 64.8, 96.9, 40.7 and 81.6 mg/L in ***agricultural zone*** was measured, respectively. According to the EQS set by the Turkish Ministry of Forestry and Water for sulfate in surface water (30 mg/L) as well as the seasonal profiles of sulfate in Ergene Watershed (Figure 3.32, Figure 3.33 and Figure 3.34), the water of Ergene River is classified in class 4 (very polluted).

As noticed in the main river of ***industrial zone*** (Figure 3.32A), sudden change is observed in sulfate concertation after the first sampling point (*m1*).The seasonal mean and median concentration of sulfate was 63.4 and 64.6 mg/L at *m1* while 162.4 and 130.7 mg/L was recorded at *m6* as the last sampling point of ***industrial zone***. Similar to previously explained parameters, sulfate pollution is emerged from the tributaries meet the main river in that zone. Mean sulfate concentrations of 164.39, 493.16 and 1273.40 mg/L during the year, were measured in junction sampling points on the tributaries, *cc11*, *t1-2* and *t3-2*, respectively. Sulfate at those points entered the main stream and as a result, the sampling points on the main river were identified with high sulfate concentrations than *m1*. In Çorlu Creek, Sampling points *cc6* with mean and median sulfate concentrations of 281.78 and 312.00 mg/L and *cc7* with 311.89 and 327.25 mg/L during the year were the main source of sulfate in Çorlu Creek. Sampling point *t1-1* close to Büyükkarıştıran OIZ with seasonal mean and median sulfate concentrations of 574.00 and 596.55 mg/L as well as sampling point *t3-2* close to a single textile facility with 1273.40 and 1306.97 mg/L, were the other important sources of sulfate (Figure 3.32B). All of those three sampling points were recognized to receive effluents from dye and textile industries. Therefore, high number of textile facilities in Ergene Watershed specially in ***industrial zone*** cause exceeded sulfate pollution along the main stream. Concentration ranges between 500 and 1000 mg/L of sulfate was reported for the effluent of textile and dye industries in the literature as well (Yaseen and Scholz, 2018).

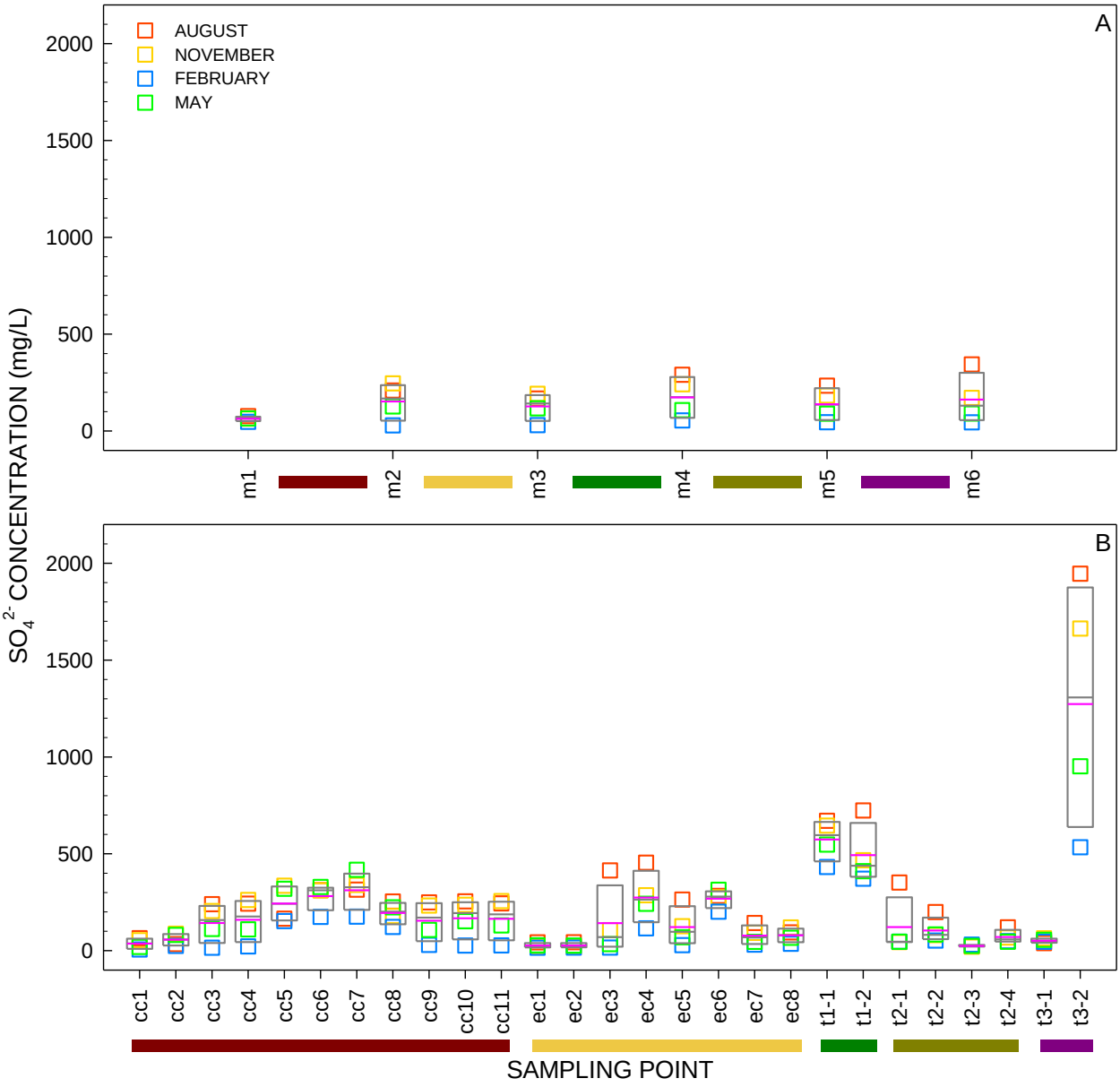

Figure 3.32. Seasonal profile of sulfate in (A) main stream and (B) tributary samples taken from ***industrial zone***.

The sulfate pollution originated from the ***industrial zone*** reached the ***transition zone***, although the average concentration was slightly lower than ***industrial zone*** because of dilution factor (Figure 3.33A). This was reflected by measuring seasonal mean and median sulfate concentrations of 114.7 and 86.5 mg/L at sampling point *m12* when compared to *m6* as the first sampling point of ***transition zone***. In addition, investigation of tributaries of ***transition zone*** revealed no significant high sulfate concentration of more than 200 mg/L in that zone (Figure 3.33B).

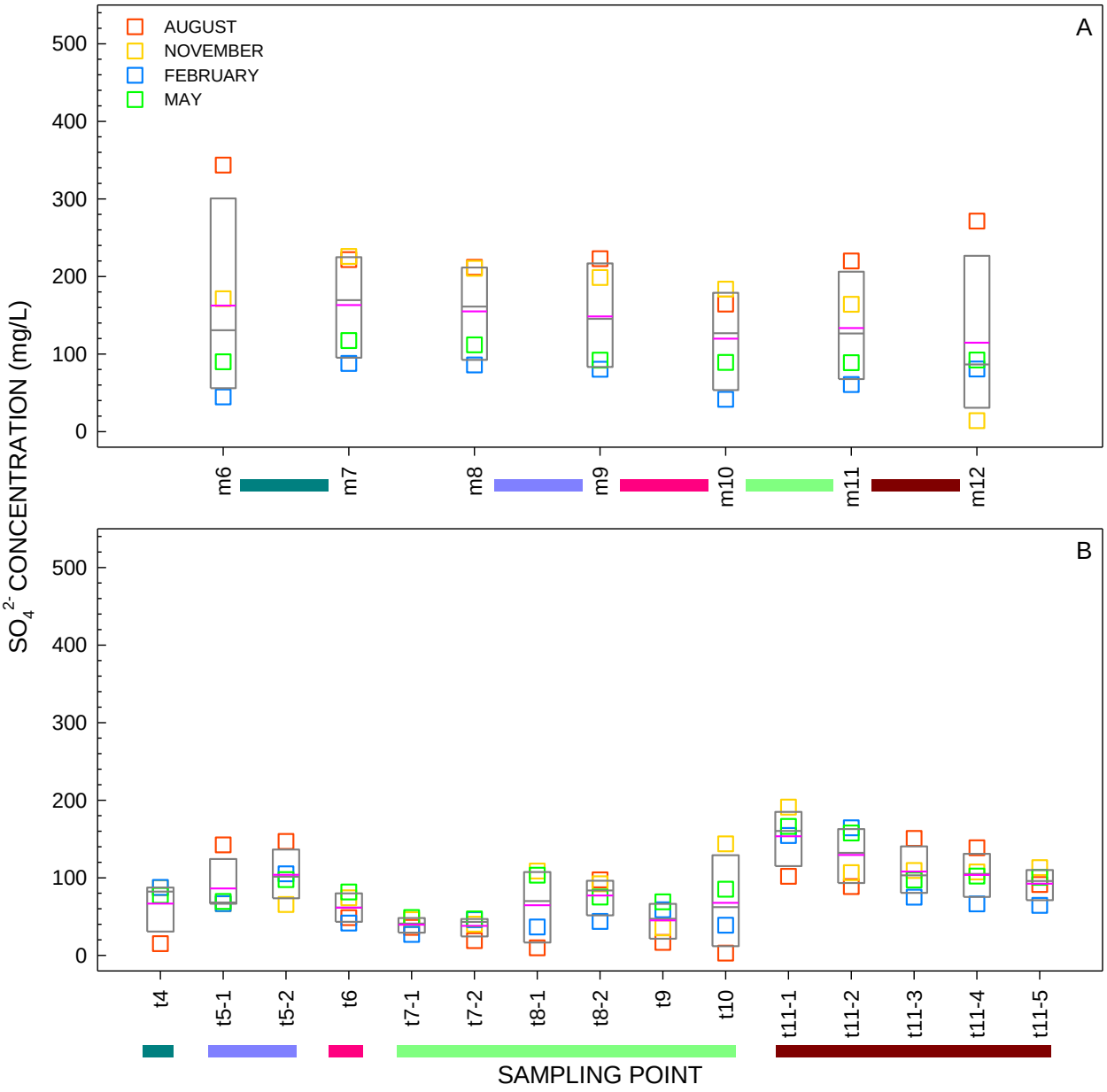

Figure 3.33. Seasonal profile of sulfate in (A) main stream and (B) tributary samples taken from ***transition zone***.

The sulfate concentration in the ***agricultural zone*** was lower than the previous two zone. On the main stream (Figure 3.34A), the sulfate concentration has not changed significantly and seasonal mean and median concentrations of 94.8 and 80.3 mg/L was recorded at *m18* (Figure 3.34A). In the tributaries of ***agricultural zone*** (Figure 3.34B), relatively higher sulfate concentrations were observed in sampling points *t16*, *t17* and *t18*. Sulfate was present at seasonal mean and median concentrations of 131.9 and 115.0 mg/L at t16, 103.0 and 100.0 mg/L at *t17* and 145.5 and 151.2 mg/L at *t18*, respectively. All of those points are next to agricultural lands which use sulfate in their fertilizers (Geurts et al., 2009, Khatri and Tyagi, 2014).

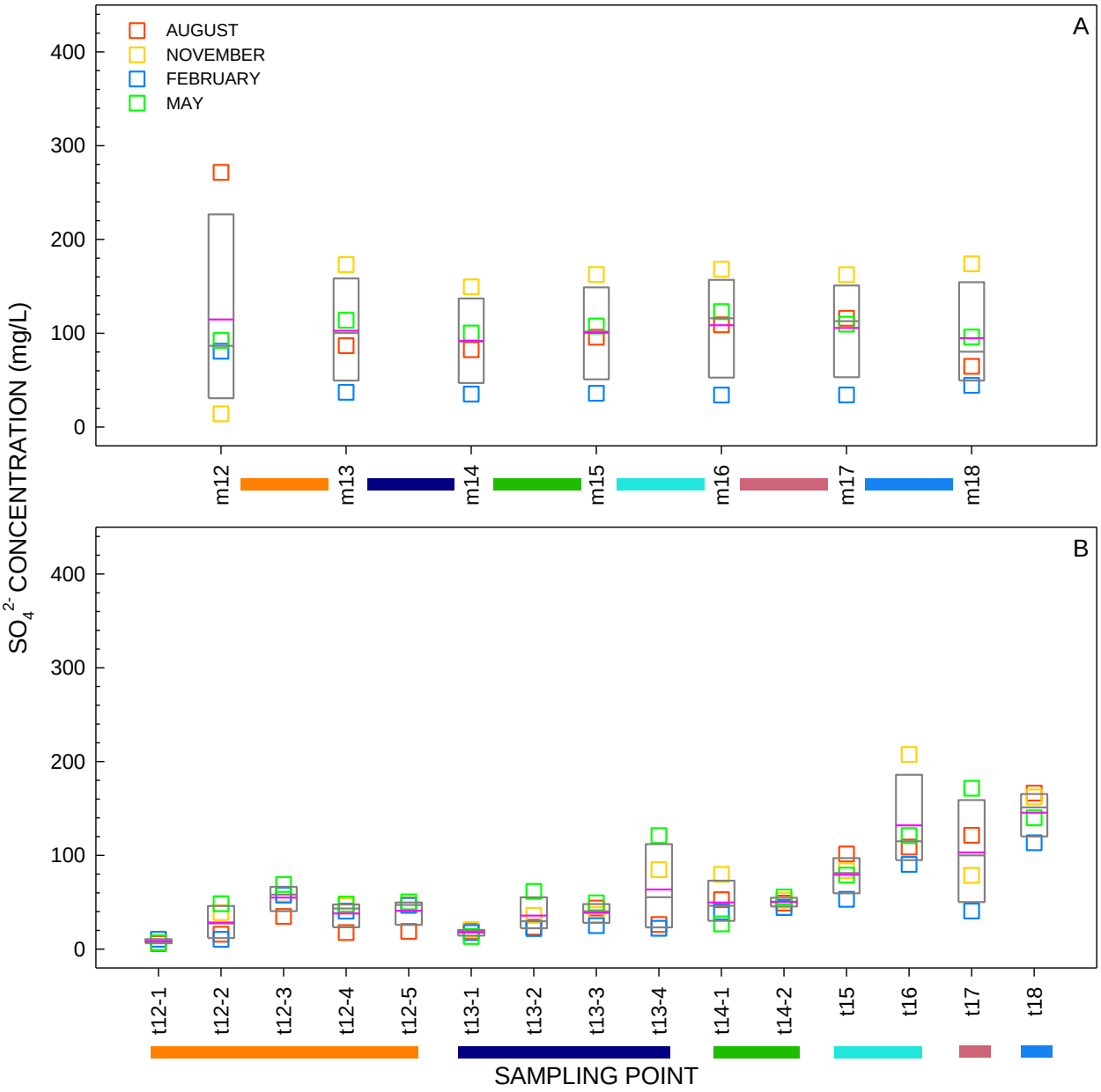

Figure 3.34. Seasonal profile of sulfate in (A) main stream and (B) tributary samples taken from ***agricultural zone***.

Moreover, considering the high COD value in Ergene River, especially in regions next to the OIZs, the river encounters low level oxygen and therefore anoxic condition evolves. Presence of sulfate in this condition, resulted in H_2S generation and an unpleasant smell.

Chloride: Ergene River was under intensive chloride stress. The average chloride concentration was 647.16, 522.90, 102.14 and 370.37 mg/L during summer, fall, winter and spring, respectively (Figure 3.35, Figure 3.36, Figure 3.37). The seasonal chloride concentration in Ergene River specially in ***industrial zone*** and the main stream exceeded the EQS (200 mg/L) recommended for surface water

by directive 75/440/EEC of European Commission. Chloride was present in ***industrial zone*** at mean concentrations of 1022.1, 840.4, 149.8 and 600.1 mg/L in summer, fall, winter and spring, respectively. However, 521.9, 312.0, 84.0 and 190.3 mg/L in ***transition zone*** and 64.8, 96.9, 40.7 and 81.6 mg/L in ***agricultural zone*** was recorded, respectively.

In ***industrial zone***, chloride concentration increased significantly in the main stream after sampling point *m1*. Chloride was present at seasonal mean and median concentrations of 80.7 and 85.1 mg/L at *m1* while 593.2 and 588.6 mg/L was recorded for sampling point *m6* at the end of that zone (Figure 3.35A). Seasonal average and mean chloride concentrations up to 1598.9 and 1819.4 mg/L in sampling point *cc6* on Çorlu Creek next to Velimeşe OIZ, 1570.8 and 1929.9 mg/L at *ec6* on Ergene Creek next to Ergene 1 OIZ and 1536.9 and 1627.8 mg/L at *t1-1* on the tributary next to Büyükkarıştıran OIZ, was measured, respectively (Figure 3.35B). Therefore, OIZs are the main sources of chloride pollution in Ergene River. Chloride is used as anti-icing agent for snow and ice removal as well as in food and chemicals production industries, battery production, paper industries and pesticides manufacturing (Apte Sagar et al., 2011, Strifling, 2018).

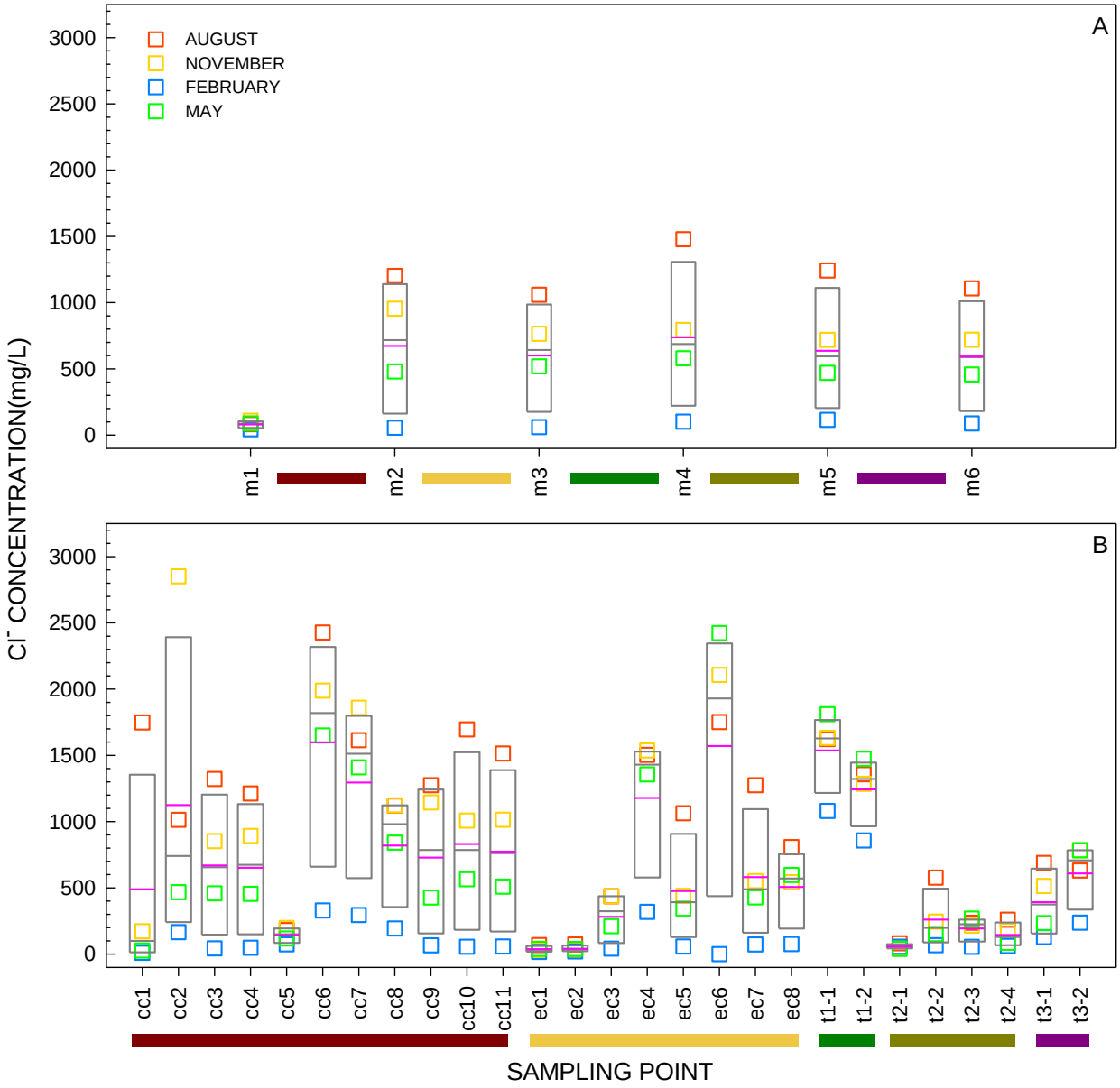

Figure 3.35. Seasonal profile of chloride in (A) main stream and (B) tributary samples taken from ***industrial zone***.

Chloride originated from ***industrial zone*** was sustained and transported to its following zone. After sampling point *m6* where ***transition zone*** starts, average chloride concentration has not changed till the last sampling point of that zone (*m12*). Chloride at seasonal mean and median concentrations of 728.5 and 465.4 mg/L was recorded at *m12*, respectively (Figure 3.36A). While high chloride concentration was detected in the main stream, the seasonal mean of chloride in samples taken from the tributaries of ***transition zone*** did not exceed 204.9 mg/L (Figure 3.36B)..

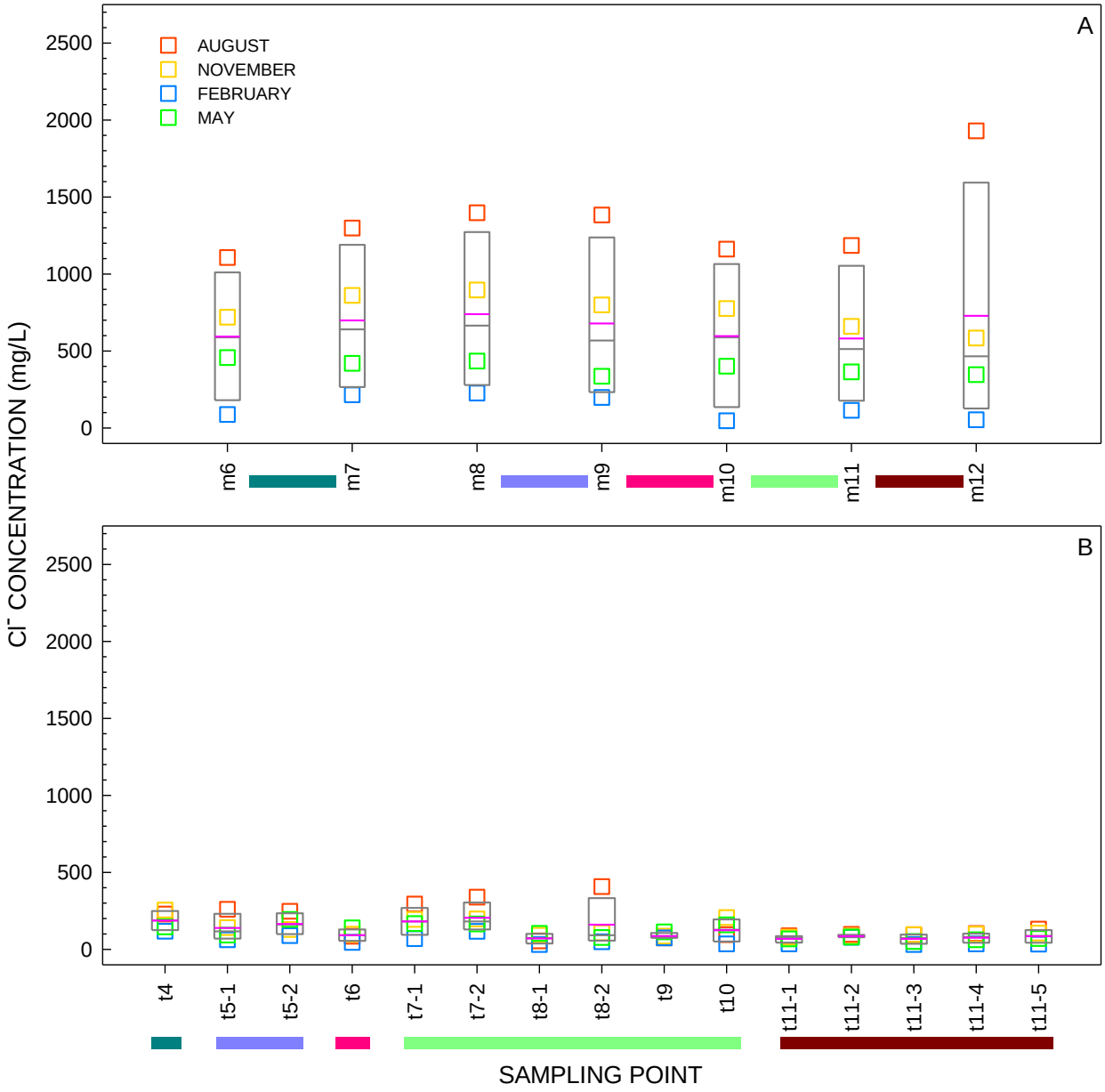

Figure 3.36. Seasonal profile of chloride in (A) main stream and (B) tributary samples taken from ***transition zone***.

Agricultural zone, on the other hand, had lower level of chloride compared to ***industrial*** and ***transition zones***. Even in the main stream, the chloride concentration decreased after *m12* (Figure 3.37A). The seasonal mean and median concentrations of chloride were 254.5 and 198.6 mg/L at *m18*, respectively (Figure 3.37A). In the tributaries of ***agricultural zone***, water samples taken from *t16*, *t17* and *t18* close to agricultural lands were recorded with seasonal average chloride concentrations of 317.9, 421.4 and 421.1 mg/L, respectively (Figure 3.37B). Chloride used as an ingredient of pesticide may be the source of high chloride in those points.

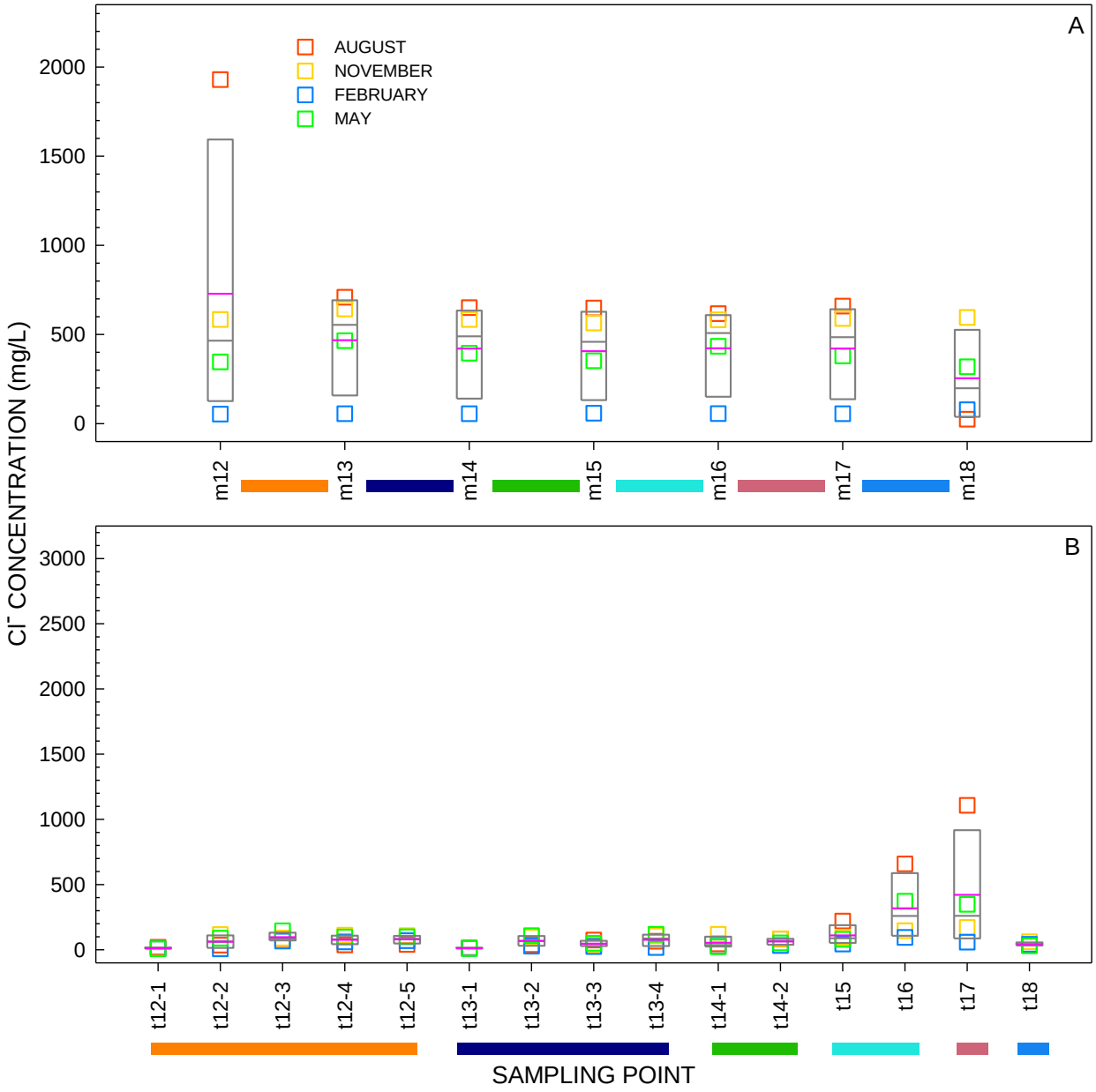

Figure 3.37. Seasonal profile of chloride in (A) main stream and (B) tributary samples taken from ***agricultural zone***.

Fluoride (F^-) and bromide (Br^-): F^- and Br^- concentration were also analyzed in the water samples taken from the Ergene River. The seasonal concentration profile of those two anions were also given in APPENDIX B. The average concentration of fluoride was 1.16, 0.51, 0.23 and 0.61 mg/L in summer, fall, winter and spring, respectively. The average concentration in the river have not exceeded the EQS (2 mg/L) set by the Turkish Ministry of Forestry and Water for surface water. However, some sampling points including *cc7* on Çorlu Creek, *ec3* on Ergene Creek, *t3-1* next to Evrensekiz OIZ in ***industrial zone*** and *t7-1* close to a dairy production facility in ***transition zone*** had the highest fluoride concentrations of 7.63, 12.22, 7.65 and 30.56 mg/L, respectively.

Bromide concentration on the other hand did not exceeded 3 mg/L throughout the watershed. Bromide was present at mean concentrations of 0.62, 0.56, 0.18 and 0.60 mg/L in the watershed during summer, fall, winter and spring, respectively. Similar to fluoride, industrial effluent discharges specially from Ergene 1 and Ergene 2 close to Ergene Creek in ***industrial zone*** were the main source of bromide. (APPENDIX B).

3.3.1.6. Heavy metals. Heavy metals are chemicals that have both natural and anthropogenic sources. Heavy metals can arise from natural environmental phenomena such as soil erosion, eruption of volcanoes and weathering while industrial processes such as metal processing facilities, combustion of wood, petroleum and coal, textiles and dyes facilities as well as plastic and paper industries are among the anthropogenic sources. In addition, mining applications and agricultural usages (pesticides) are among the other main sources of heavy metals. Although some of the heavy metals such as Cr, Ni, Cu and Zn are essential as nutrients in various biochemical reactions, their excess amount can cause serious health impacts on both organisms and human (Tchounwou et al., 2012).

In the Ergene River, aluminum (Al), zinc (Zn), copper (Cu), nickel (Ni), cobalt (Co), vanadium (V), antimony (Sb), silver (Ag), titanium (Ti), chromium (Cr), cadmium (Cd), lead (Pb), barium (Ba), beryllium (Be), arsenic (As), boron (B) and tin (Sn) were measured. Among the aforementioned heavy metals, Ba, Al, Zn, Cu, Ni, B and Pb were detected in all of the samples during all seasons.

The average aluminum concentration was between 1000-3000 µg/L during the year which was far more than the EQS value (27 µg/L) set by the Turkish Ministry of Forestry and Water. Although the highest measured concentrations of Al was different during the four seasons, they were all occurred in sampling points located next to the discharge point of the OIZs in ***industrial zone*** (Figure 3.38). Al was present at 2166.6, 3850.9, 1433.0 and 6134.6 mg/L in ***industrial zone*** during summer, fall, winter and spring, respectively. While 1410.7, 943.54, 1114.3 and 933.8 mg/L in ***transition zone*** and 406.2, 647.3, 833.9 and 548.3 mg/L in ***agricultural*** zone was recorded, respectively. Aluminum was reported as one of the most frequently detected heavy metals in different environment compartments in the literature as well. It is used in many industries such as production of housing and kitchen cabinets, manufacturing of cans and containers, cosmetics production and also as food additives (Barabasz et al., 2002). The occurrence of Al in Ergene River water suggested that Al pollution generated in ***industrial zone*** was transported to the following zones although the concentration decreased because of dilution factor.

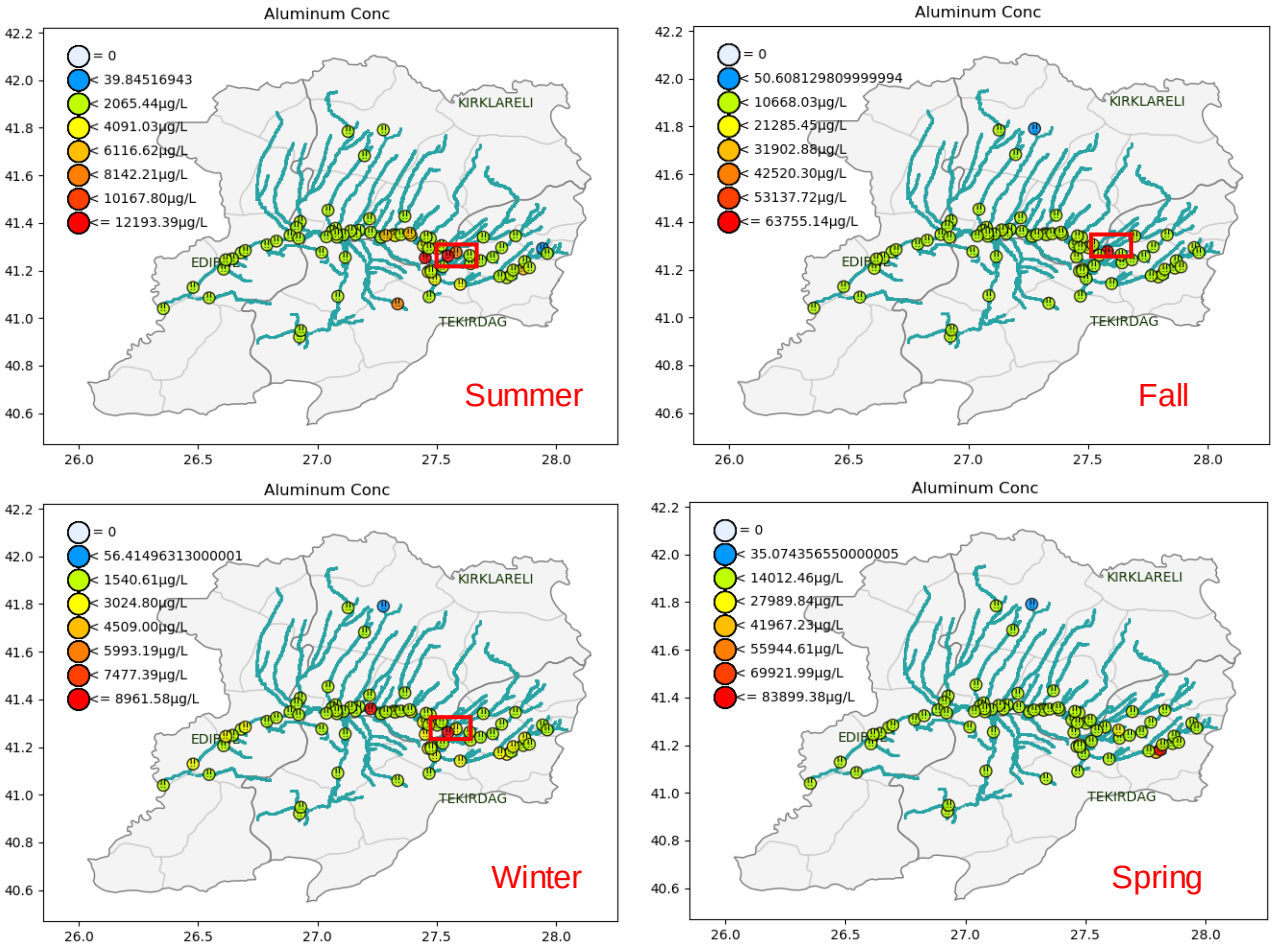

Figure 3.38. Seasonal aluminum concentration profile in Ergene River.

Al was present at concentrations between 35.1 and 83,889 µg/L in all seasons. Sampling point *t1-1* and *t1-2* in ***industrial zone*** were the main sources of Al during the year except spring when sampling point *cc7* (83,889 µg/L) close to Velimeşe OIZ had the highest Al concentration. The maximum recorded concentration of Al during summer sampling was 12,193 µg/L at sampling point *t1-2* located close to the Büyükkarıştıran OIZ while the value measured during the spring sampling was 63,755 µg/L at sampling point *t1-1* just before *t1-2*. This indicated that the effluent from the Büyükkarıştıran OIZ is one of the most major sources of Al in the watershed. In addition, the higher Al concentration in *t1-2* than *t1-1* (7,468 µg/L) during the summer was due to excess discharge of an aluminum industry located next to the *t1-2* (Figure 3.39).

Similar to Al, the other most frequently detected heavy metals were Cu, Pb, Zn, Ni and B. Cu was present at concentrations between 1.16 and 14634.7 µg/L in all seasons. The average concentration of Cu was 52.5, 928.1, 918.9 and 4,124 µg/L in summer, fall, winter and spring, respectively that was far more than its recommended EQS (3.1 µg/L) for surface water. The highest

concentration of Cu was 14,634.7 µg/L which was measured at sampling point *t7-2* in ***transition zone*** during spring.

The average concentration of Pb along the Ergene River and its tributaries was 289.1, 491.7, 259.0 and 2141.8 µg/L during summer, fall, winter and spring, respectively. The highest concentrations of Pb was measured in sampling points on Çorlu and Ergene Creeks in ***industrial zone*** as well as sampling point *t8-1* close to a solid waste disposal site in ***transition zone***. Zn with measured concentrations up to 33,601 µg/L and nickel up to 9,711 µg/L in ***industrial zone*** indicated the high discharge of industrial effluents from the OIZs to the Ergene river. The average concentration of Zn in Ergene River water during fall, winter and spring was more than 1000 µg/L. Nickel was also present at average concentration of 1122 and 3670 µg/L during fall and spring, respectively. Zn and Ni concentration in many sampling points exceeded the EQS.

Boron (B) was also frequently discharged into the Ergene River. Boron is used mainly as bleaching agent in textile industry as well as fertilizers in agriculture (Hasenmueller and Criss, 2013). The average concentration of B was 421.4, 298.2, 86.0 and 227.0 µg/L in summer, fall, winter and spring, respectively. boron was present at maximum concentrations of 2520 µg/L during summer at sampling point *ec8* during the year except winter. That sampling point is receiving the effluents from Muratlı OIZ. In addition, it is surrounded by many agricultural farms using pesticides that can be the reason of high B concentration in this sampling point.

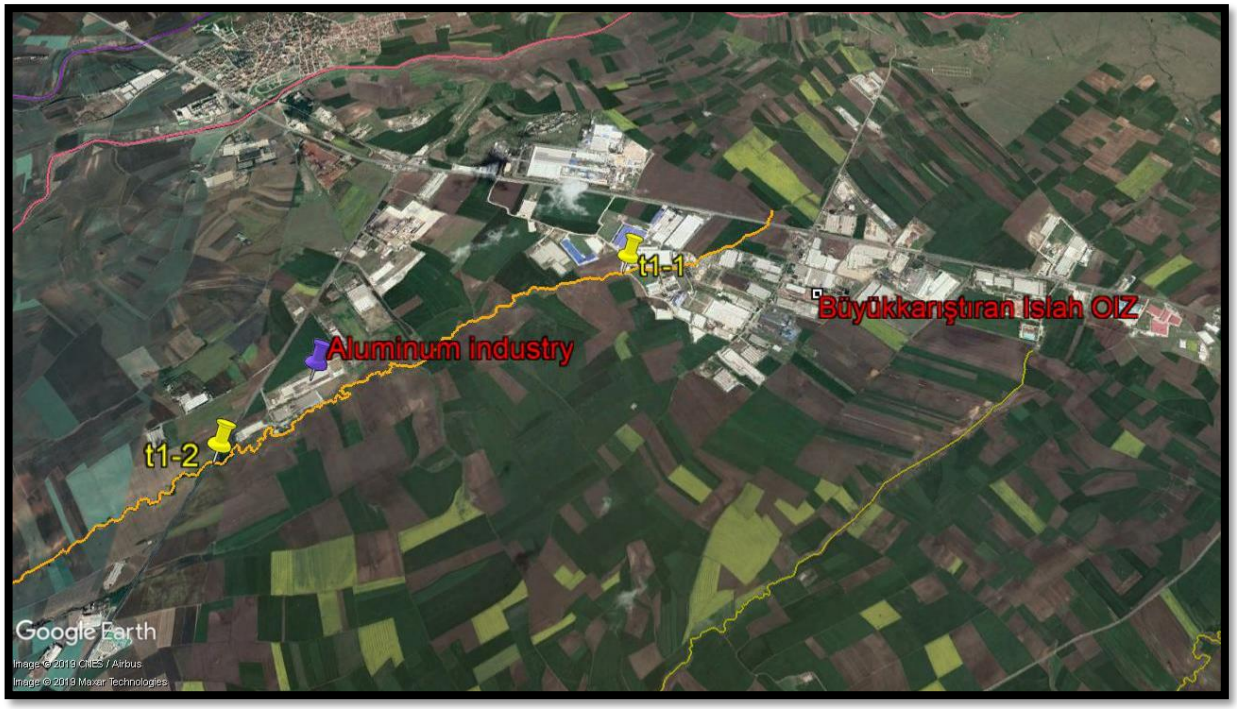

Figure 3.39. Location of sampling points *t1-1* and *t1-2* next to Büyükkarıştıran OIZ and presence of an aluminum industry between those two points.

Silver (Ag) was detected in 3, 6 and 13 samples out 75 sampling points analyzed in summer, fall and spring, respectively. It was mainly detected in sampling points on ***industrial zone*** including *cc2* and *cc3* receiving the effluents from yalıboyu and Çerkezköy OIZs and *cc6*, *cc7* and *cc8* next to Velimeşe OIZ, located on Çorlu Creek. Ag concentration at 1.76 µg/L was detected in sampling point *cc6* during spring which exceeded the EQS (1.5 µg/L). Industrial effluents discharges were the major reason of silver pollution in Ergene watershed. For instance, the discharge of industrial wastes to a river in India, was the main source of silver in groundwater (Vetrimurugan et al., 2016).

High concentration of chromium (Cr) exceeding its EQS of 142 µg/L for surface water, was determined in some sampling points during the year. Those sampling points were mainly located next to the effluent of Çorlu Leather OIZ (at 1,222 µg/L in *cc9* during fall), agricultural farms (at 2,252 µg/L in *cc10* during summer) (Figure 3.40) and solid waste disposal site (at 3,628 µg/L in *t8-1* during summer). Those sampling points are under high risk of Cr pollution. Chromium was reported to be utilized in different industrial processes such as tannery and steel production, metal industries, leather production and pesticides manufacturing (Ertani et al., 2017).

Figure 3.40. Location of sampling points cc9 and cc10 with high chromium concentration.

One of the most important heavy metals is arsenic. This metal was detected at its highest concentration at sampling points *t1-1* and *t1-2* located next to Büyükkarıştıran OIZ during the year (except spring). Arsenic was present at sampling point *t1-1* at 62.33 µg/L during summer which was more than its EQS value (53 µg/L). In addition, 94.82 µg/L of As was detected in water taken from *ec6* at the discharge point of Ergene1 OIZ in spring which was almost two times more than arsenic's EQS (53 µg/L) set by the Turkish Ministry of Forestry and Water for surface waters. All of the aforementioned three sampling points are located in ***industrial zone*** receiving the effluent from facilities specially textile and dyes manufacturing. Arsenic was reported to be used in different

industries such as production of pesticides, preservation of wood and veterinary drugs manufacturing which can be the other sources of arsenic (Tchounwou et al., 2012).

The concentration range of the heavy metals along with their detection frequency (out of 75) are shown in Figure B.22 in APPENDIX B. In general, the seasonal concentration of heavy metals in Ergene River water indicated that ***industrial zone*** is the main contributor of heavy metal pollution in the river. In addition, the pollution generated in that zone was transported to the ***transition*** and ***agricultural zones*** via the main stream.

3.3.2. Targeted Identification and Quantification of Micropollutants

3.3.2.1. Targeted analysis of the micropollutants in the Ergene River. Concentration of organic micropollutants in samples taken along the Ergene River was determined using LC-MS^n/sMRM method described above. This study, in which 222 chemicals were monitored in the water samples taken from the Ergene River in four seasons, was the first one to investigating the pollution in Ergene River. and Among 222 micropollutants screened in the river samples, 131, 135, 96 and 103 micropollutants were detected in at least one water sample during summer, fall, winter and spring, respectively. 64 micropollutants were detected in at least one point in all seasons (Figure 3.41). In addition, 12, 8, 6 and 5 micropollutants were specified for summer, fall, winter and spring, respectively (Figure 3.41). 1,2,5,6,9,10-hexabromocyclododecane, bisphenol-A, damscone, enthoprophos, fenamiphos, microcystin-LR, oxadixyl, penconazole, pentachlorobenzene, pyridaben, spiroxamine and trifloxystrobin were the micropollutants that were just detected in summer. Buprofezin, butylmethoxydibenzoylmethane, cypermethrin, dichlorvos, difenoconazole, hexythiazox, mandipropamid and prothioconazole were the eight micropollutants specific for fall season. In addition, our measurements indicated that 2-methylanthraquinone, 3-nitrobenaznthrone, diphenylamine, hexaconazole, n-methyl aniline and tetrabromobisphenol-A were just detected in winter while 2,4,4-tribromodiphenylether, ATII (traseolide), cybutryne, dodecyl sulfate and mesotrione were only identified in the spring. Among the micropollutants specifically detected in individual season, pesticides take an important place as they are seasonally applied and consumed.

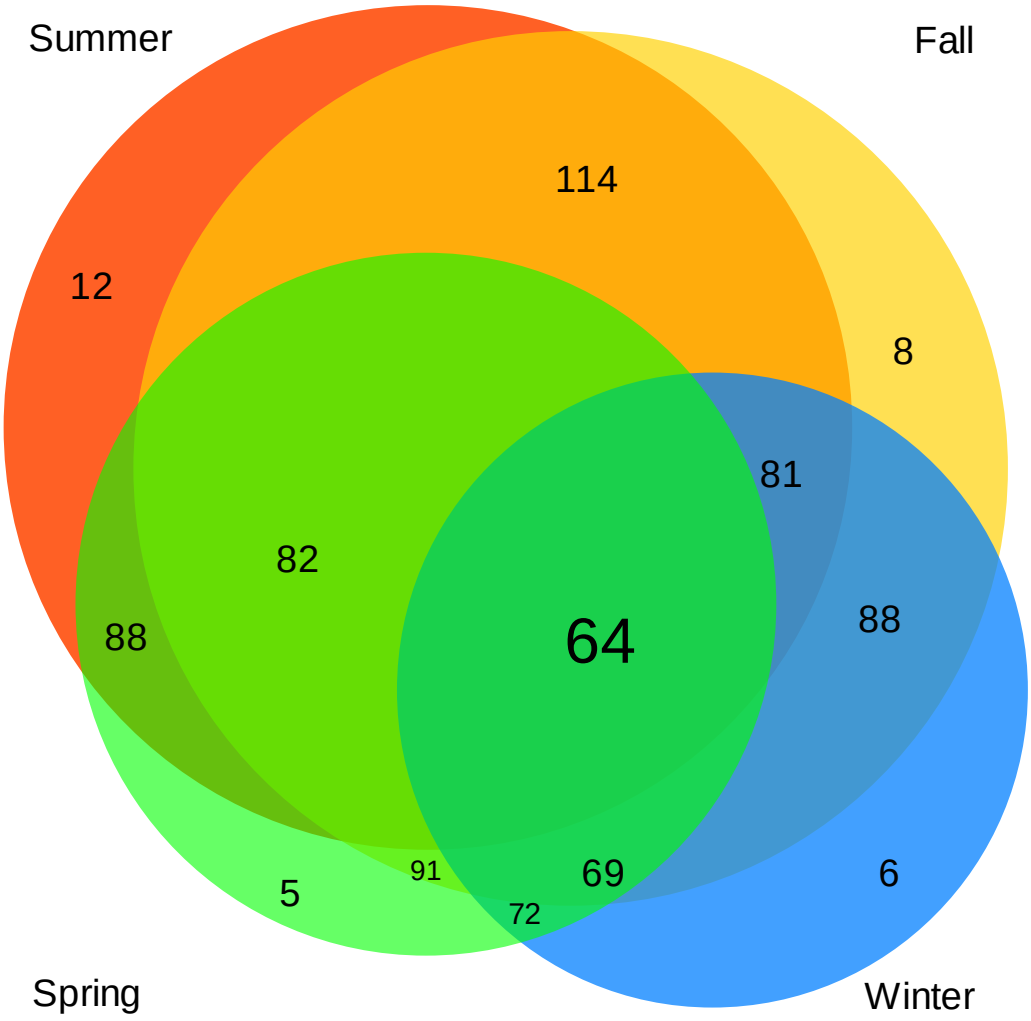

Figure 3.41. Number of specific and shared micropollutants detected in all seasons. The numbers represent the numbers of shared micropollutants in those seasons.

The highest number of micropollutants were detected in the samples taken in the August and November at which river flowrate was low (Figure 3.42). On the contrary, relatively few numbers of micropollutants were detected in the winter at which river flowrate was almost 20 times more than the latter seasons. Probably, some of the micropollutants just fell below the quantitation limit and could not get quantified in the winter due to dilution effect as a result of precipitation (Figure 3.42). Micropollutant discharges into the sampling points located on Çorlu Creek (*cc*) which connects the main stream between sampling points *m1* and *m2*, resulted in high number of micropollutants in sampling point *m2*. Number of micropollutants at *m1* was 19, 23, 19 and 13 in summer, fall, winter and spring, respectively, while at *m2* was 61, 61, 31 and 41, respectively. The sampling points on the Çorlu Creek are mainly collect the effluent of the industrial sectors in OIZs including Çerkezköy, Kapaklı, Yalıboyu, Veliköy, Velimeşe, Çorlu 1 and Çorlu Leather OIZs next to Çorlu creek (Figure 3.43).

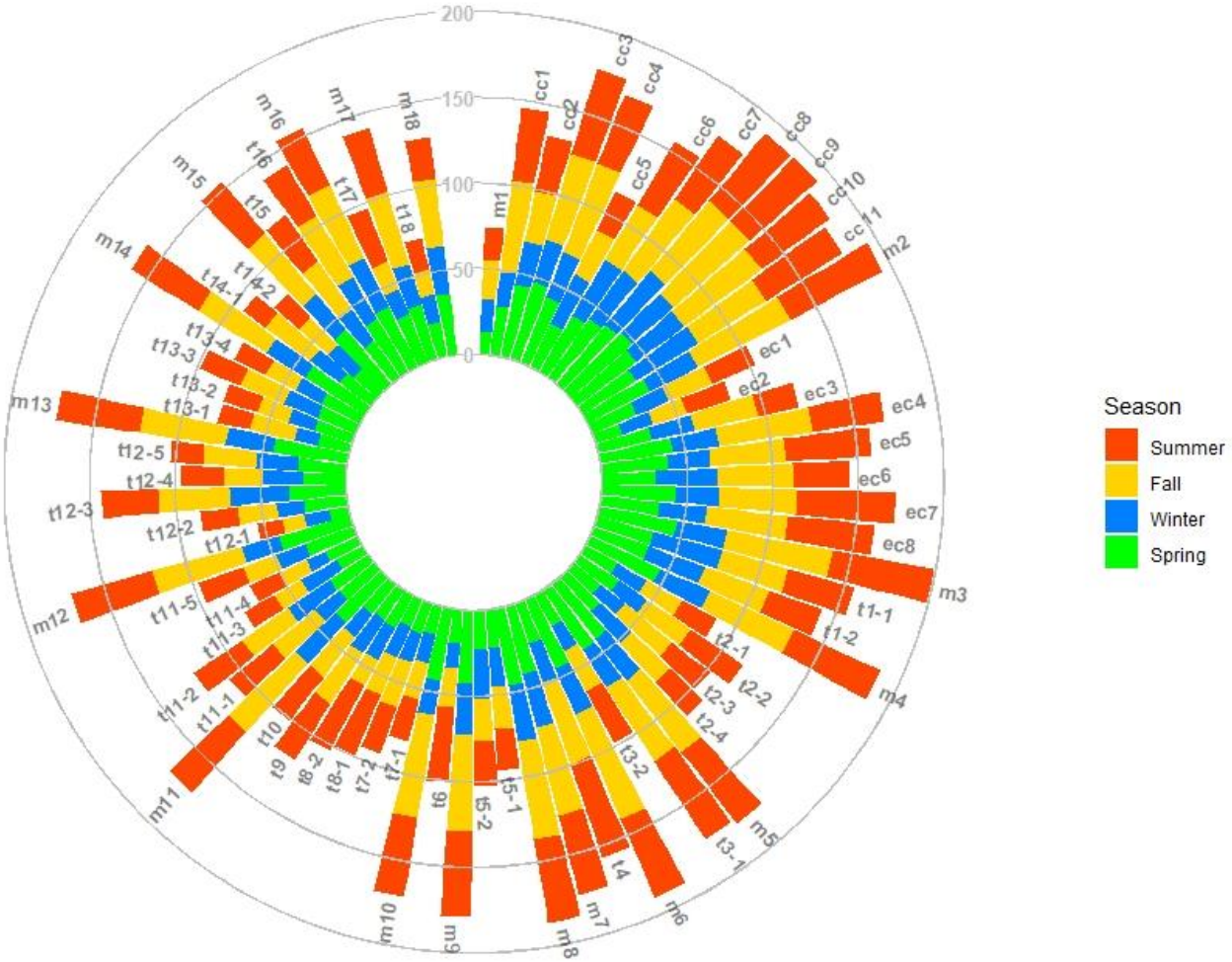

Figure 3.42. Seasonal frequency of detection of micropollutants in 75 sampling points on Ergene watershed.

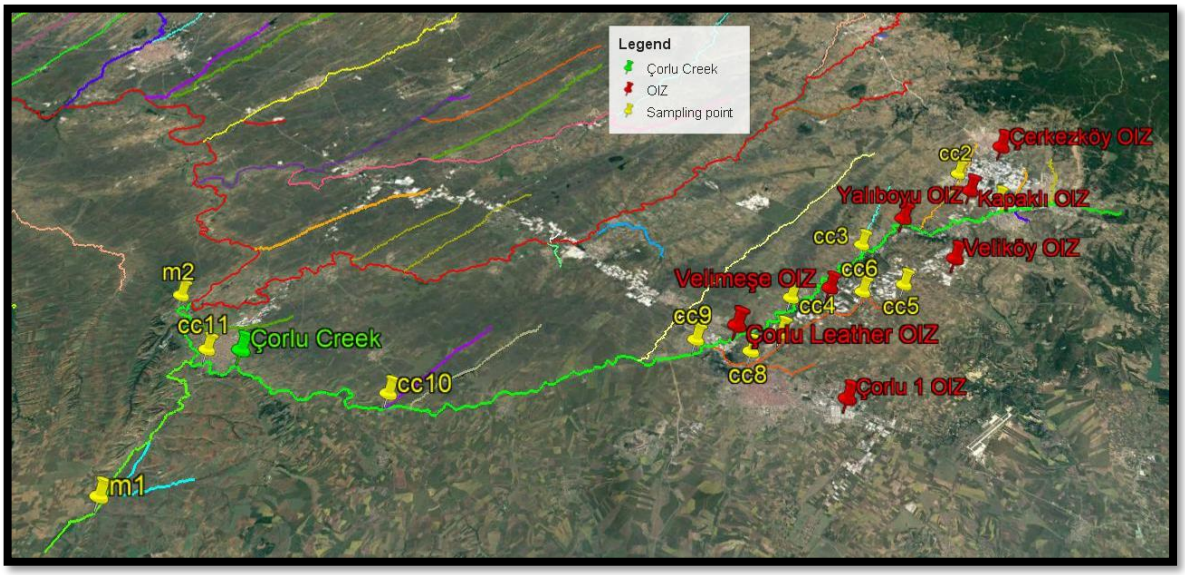

Figure 3.43. Location of OIZs and sampling points on Çorlu Creek.

In addition to the OIZs located on the Çorlu tributary of the Ergene River, the other main tributary that includes the sampling points *ec1* to *ec8* is Ergene Creek receives the effluents of Ergene 1, Ergene 2 and Muratlı OIZs. At *m3* on the main stream and after Ergene Creek meets the main stream, 60, 63, 30 and 46 micropollutants were detected in summer, fall, winter and spring, respectively. Sampling points *t1-1* and *t1-2* next to Büyükkarıştıran OIZ and *t3-1* and *t3-2* on the tributary next to Evrensekiz Islah OIZ are other important sampling points with high detection of micropollutants during the year (Figure 3.44). Further investigation of seasonal frequency of detection of micropollutants in the Ergene River and its tributaries indicates that the number of micropollutants in the sampling points on the main stream was more than the ones on the tributaries specially in ***transition*** (*m6-m12*) and ***agricultural*** (*m12-m18*) ***zones***. Besides, in ***transition zone***, sampling point *t4* was identified with high detection of micropollutants while in ***agricultural zone***, *t12-3* and *t16* receiving effluent from WWTPs of Kırklareli and Uzunköprü Cities, had the highest number of micropollutants. Furthermore, at *m18* where Ergene River meets Maritsa River, 24, 40, 28 and 36 micropollutants were detected during summer, fall, winter and spring, respectively. In addition, the maximum, minimum, mean, median concentration as well as the number of sampling points (out of 75) where the micropollutants are detected in the four seasons, are summarized in Table 3.8.

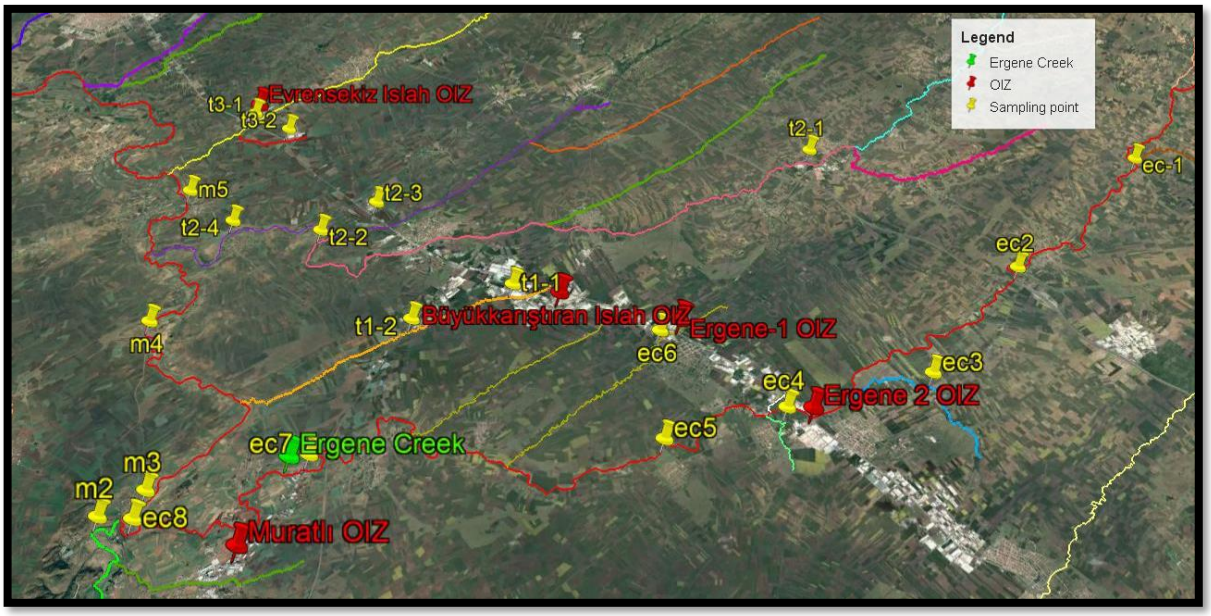

Figure 3.44. Location of other important OIZs and sampling points at which high number of micropollutants detected.

Table 3.8. Maximum, minimum, mean and median concentrations of detected organic micropollutants.

Chemical	August_2017				November_2017				February_2018				May_2018			
	Concentration (µg/L)			Median (µg/L) (Detected in (out of 75))	Concentration (µg/L)			Median (µg/L) (Detected in (out of 75))	Concentration (µg/L)			Median (µg/L) (Detected in (out of 75))	Concentration (µg/L)			Median (µg/L) (Detected in (out of 75))
	Max	Min	Mean		Max	Min	Mean		Max	Min	Mean		Max	Min	Mean	
1-Hydroxyibuprofen	95.60	7.51	24.77	16.18 (10)	19.37	8.64	13.64	11.49 (5)	n.d.*	n.d.	n.d.	n.d. (0)	n.d.	n.d.	n.d.	n.d. (0)
1,2,3-Benzotriazole	117.55	0.37	8.98	4.39 (68)	100.75	1.02	12.06	7.55 (51)	44.68	0.36	2.70	0.61 (46)	26.17	0.23	2.84	1.37 (54)
1,2,5,6,9,10-Hexabromocyclododecane	n.d.	n.d.	n.d.	n.d. (0)	0.16	0.16	0.16	0.16 (1)	n.d.	n.d.	n.d.	n.d. (0)	n.d.	n.d.	n.d.	n.d. (0)
1,3-Dinitropyrene	1.58	1.58	1.58	1.58 (1)	2.63	0.48	1.19	0.63 (6)	1.02	0.28	0.66	0.72 (5)	1.18	0.38	0.64	0.59 (5)
1,6-Dinitropyrene	1.23	0.43	0.83	0.83 (2)	2.71	0.26	0.86	0.44 (11)	1.02	0.19	0.65	0.67 (5)	0.73	0.11	0.39	0.30 (10)
1,8-Dinitropyrene	1.13	0.45	0.73	0.60 (3)	2.45	0.34	1.17	0.69 (5)	1.25	0.28	0.82	0.84 (5)	0.65	0.09	0.32	0.27 (9)
2-(2-Naphthalenyl) benzothiophene	22.87	2.30	11.01	10.28 (6)	18.62	1.25	6.52	3.83 (13)	23.19	23.19	23.19	23.19 (1)	25.20	0.73	6.41	3.40 (7)
2-Mercapto-benzothiazole	3.46	0.44	1.10	0.89 (20)	23.54	0.61	2.94	1.72 (23)	0.36	0.36	0.36	0.36 (1)	3.84	0.61	1.73	1.60 (51)
2-Methylanthraquinone	n.d.	n.d.	n.d.	n.d. (0)	n.d.	n.d.	n.d.	n.d. (0)	77.60	77.60	77.60	77.60 (1)	n.d.	n.d.	n.d.	n.d. (0)
2,2',4,4',5,5'-Hexabromo diphenyl ether	7.13	7.13	7.13	7.13 (1)	n.d.	n.d.	n.d.	n.d. (0)	n.d.	n.d.	n.d.	n.d. (0)	3.57	3.57	3.57	n.d. (1)
2,2',4,4',5,6'-Hexabromo diphenyl ether	n.d.	n.d.	n.d.	n.d. (0)	3.22	3.22	3.22	3.22 (1)	n.d.	n.d.	n.d.	n.d. (0)	7.43	4.26	5.85	5.85 (2)
2,3,3',4,4',5,5',6-Octabromodiphenyl ether	3.12	2.55	2.75	2.67 (4)	1.55	1.55	1.55	1.55 (1)	n.d.	n.d.	n.d.	n.d. (0)	n.d.	n.d.	n.d.	n.d. (0)
2,4-Dihydroxy benzophenone	2.53	0.16	0.59	0.45 (31)	0.99	0.16	0.51	0.51 (25)	0.11	0.11	0.11	0.11 (1)	3.94	0.04	0.32	0.12 (30)
2,4,4'-tribromodiphenylether	n.d.	n.d.	n.d.	n.d. (0)	n.d.	n.d.	n.d.	n.d. (0)	n.d.	n.d.	n.d.	n.d. (0)	1824.55	95.06	670.88	431.71 (5)
3-Chloroaniline	1.59	0.18	0.57	0.47 (29)	1.26	0.09	0.35	0.27 (29)	0.49	0.03	0.12	0.07 (16)	5.43	0.12	0.98	0.63 (36)
3-Nitrobenzanthrone	n.d.	n.d.	n.d.	n.d. (0)	n.d.	n.d.	n.d.	n.d. (0)	72.10	72.10	72.10	72.10 (1)	n.d.	n.d.	n.d.	n.d. (0)
4-Aminomethyl-benzenesulfonamide	0.90	0.11	0.42	0.25 (8)	1.02	0.07	0.23	0.17 (52)	0.35	0.02	0.07	0.06 (67)	0.83	0.04	0.17	0.16 (75)
4-Chloroaniline	2.05	0.07	0.54	0.44 (31)	1.52	0.08	0.34	0.27 (36)	0.43	0.06	0.15	0.08 (9)	5.84	0.08	1.02	0.60 (36)
4-Methyl-1H-benzotriazole	36.19	0.20	8.95	7.79 (58)	73.70	0.04	8.79	5.75 (58)	12.83	0.02	0.59	0.21 (57)	16.55	0.01	1.80	1.29 (64)
4-Methylbenzylidene camphor	34.90	0.68	3.74	1.54 (16)	15.60	0.55	1.99	0.87 (14)	n.d.	n.d.	n.d.	n.d. (0)	3.90	1.51	2.76	2.87 (3)
4-tert-Octylphenol diethoxylate	0.28	0.02	0.07	0.05 (43)	0.21	0.02	0.07	0.05 (36)	0.24	0.03	0.09	0.08 (74)	0.25	0.02	0.05	0.04 (65)
4,4'-Dichlorobenzophenone	3.68	0.16	1.51	1.40 (12)	1.71	0.26	0.84	0.83 (8)	1.91	0.12	0.54	0.23 (7)	5.15	0.90	2.21	1.40 (4)
5-Methyl-1H-benzotriazole	15.95	0.04	4.10	3.49 (63)	33.03	0.04	4.00	2.70 (65)	7.72	0.03	0.46	0.13 (38)	6.53	0.03	1.04	0.87 (62)
5,6-Dimethyl-1H-benzotriazole	20.86	0.25	4.77	2.86 (39)	118.29	0.30	5.69	2.25(41)	0.73	0.04	0.16	0.11 (32)	9.78	0.06	1.13	0.55 (36)
7H-Benzo(de) anthracen-7-one	30.31	0.20	3.12	1.15 (27)	4.95	0.13	1.38	0.74 (27)	4.18	0.41	1.67	0.73 (6)	2.15	0.06	0.42	0.22 (33)
8-Hydroxyquinoline	n.d.	n.d.	n.d.	n.d. (0)	0.63	0.07	0.18	0.12 (9)	0.07	0.02	0.04	0.04 (32)	123.51	0.09	15.13	8.29 (72)
Acetaminophen (Paracetamol)	107.26	0.06	7.78	2.83 (49)	96.23	0.07	9.06	2.86 (57)	8.99	0.05	0.90	0.28 (53)	111.05	0.09	4.16	0.68 (59)
Acetamiprid	1.93	0.03	0.22	0.13 (42)	2.86	0.08	0.23	0.13 (39)	0.99	0.03	0.12	0.04 (18)	1.92	0.04	0.19	0.08 (20)
Aclonifen	0.75	0.06	0.19	0.17 (32)	0.19	0.07	0.12	0.12 (18)	0.15	0.06	0.09	0.09 (13)	n.d.	n.d.	n.d.	n.d. (0)
ADBI (Celestolide)	0.70	0.06	0.24	0.16 (20)	1.25	0.03	0.36	0.24 (27)	0.18	0.05	0.11	0.09 (8)	0.55	0.12	0.30	0.24 (9)
AHDI (Phantolide)	3.44	0.08	0.72	0.49 (30)	4.01	0.22	0.86	0.53 (28)	0.53	0.12	0.35	0.38 (6)	1.34	0.32	0.64	0.46 (10)

Table 3.8. Continued.

Chemical	August_2017				November_2017				February_2018				May_2018			
	Concentration (µg/L)			Median (µg/L) (Detected in (out of 75))	Concentration (µg/L)			Median (µg/L) (Detected in (out of 75))	Concentration (µg/L)			Median (µg/L) (Detected in (out of 75))	Concentration (µg/L)			Median (µg/L) (Detected in (out of 75))
	Max	Min	Mean		Max	Min	Mean		Max	Min	Mean		Max	Min	Mean	
alpha-Terpineol	593.77	41.21	228.15	189.62 (10)	494.83	24.76	101.24	71.51 (16)	n.d.	n.d.	n.d.	n.d. (0)	365.02	20.62	96.10	56.85 (11)
Amoxicillin	n.d.	n.d.	n.d.	n.d. (0)	n.d.	n.d.	n.d.	n.d. (0)	0.64	0.36	0.50	0.50 (6)	2.41	0.61	1.37	1.33 (46)
Anthracene	851.00	27.54	183.05	95.82 (12)	309.02	17.99	91.39	46.37 (18)	824.63	11.04	154.11	114.29 (14)	97.02	9.14	41.35	39.61 (12)
ATII (Traseolide)	n.d.	n.d.	n.d.	n.d. (0)	n.d.	n.d.	n.d.	n.d. (0)	n.d.	n.d.	n.d.	n.d. (0)	2.65	1.24	1.94	1.94 (2)
Atrazine	0.05	0.01	0.02	0.02 (20)	1.02	0.02	0.13	0.03 (12)	n.d.	n.d.	n.d.	n.d. (0)	0.02	0.01	0.02	0.02 (2)
Atrazine-desethyl	9.56	0.02	0.39	0.05 (29)	0.43	0.02	0.07	0.05 (46)	0.08	0.03	0.05	0.04 (3)	n.d.	n.d.	n.d.	n.d. (0)
Azithromycin	7.86	0.07	0.86	0.29 (71)	1.33	0.08	0.41	0.24 (8)	2.23	0.18	0.87	0.21 (3)	0.49	0.21	0.35	0.35 (2)
Azoxystrobin	7.71	0.03	1.32	0.05 (6)	0.11	0.04	0.08	0.08 (2)	n.d.	n.d.	n.d.	n.d. (0)	0.10	0.03	0.06	0.06 (6)
Bayrepel	n.d.	n.d.	n.d.	n.d. (0)	n.d.	n.d.	n.d.	n.d. (0)	65.33	65.33	65.33	65.33 (1)	82.06	1.95	24.82	15.21 (5)
Benzenesulfonamide	71.87	71.87	71.87	71.87 (1)	9.53	8.01	8.77	8.77 (2)	4.70	3.26	3.98	3.98 (3)	n.d.	n.d.	n.d.	n.d. (0)
Benzo[a]anthracene	9.81	1.14	4.14	3.24 (6)	24.04	6.98	10.94	7.93 (6)	n.d.	n.d.	n.d.	n.d. (0)	n.d.	n.d.	n.d.	n.d. (0)
Benzo[a]pyrene	0.98	0.07	0.29	0.16 (22)	0.37	0.03	0.16	0.14 (8)	0.43	0.04	0.13	0.08 (11)	0.15	n.d.	0.03	0.01 (18)
Benzo[b]fluoranthene	4.38	0.70	2.05	1.07 (3)	4.00	1.43	2.72	2.72 (2)	0.52	0.27	0.39	0.39 (2)	n.d.	n.d.	n.d.	n.d. (0)
Benzo[ghi]perylene	10.62	0.89	4.79	3.82 (4)	61.43	5.53	27.07	20.67 (4)	5.48	2.03	3.67	3.50(3)	n.d.	n.d.	n.d.	n.d. (0)
Benzo[k]fluoranthene	3.01	0.02	0.87	0.65 (33)	1.43	0.07	0.53	0.44 (13)	n.d.	n.d.	n.d.	n.d. (0)	0.73	0.03	0.15	0.05 (13)
Benzothiazole	334.51	334.51	334.51	334.51 (1)	56.74	###	56.74	56.74 (1)	21.09	9.54	15.82	14.31 (11)	34.80	34.80	34.80	34.80 (1)
Benzylamine	0.74	0.07	0.20	0.10 (18)	0.33	0.10	0.19	0.18 (8)	0.08	0.02	0.03	0.03 (32)	n.d.	n.d.	n.d.	n.d. (0)
Benzyldimethyl dodecylammonium	23.89	0.05	4.20	0.64 (75)	110.42	0.03	6.70	1.95 (75)	78.51	0.03	2.32	0.31 (75)	116.65	0.01	5.69	0.31 (75)
Benzyldimethyltetradecyl ammonium	7.64	0.04	1.43	0.41 (75)	40.54	0.03	2.33	0.91 (75)	352.79	0.28	17.44	3.04 (75)	42.36	0.02	1.61	0.24 (73)
Benzyltrimethylammonium	0.33	0.01	0.11	0.09 (40)	0.92	0.03	0.40	0.39 (33)	0.13	0.03	0.08	0.09 (19)	0.07	0.01	0.03	0.02 (47)
Bisphenol-A	48.98	12.12	27.46	27.39 (8)	n.d.	n.d.	n.d.	n.d. (0)	n.d.	n.d.	n.d.	n.d. (0)	n.d.	n.d.	n.d.	n.d. (0)
Boisvelone / Iso-Esuper	13.51	1.66	3.77	2.99 (34)	9.35	1.69	3.93	3.16 (43)	3.85	2.00	2.85	2.66 (5)	3.56	2.42	2.88	2.64 (3)
Buprofezin	n.d.	n.d.	n.d.	n.d. (0)	0.06	0.06	0.06	0.06 (1)	n.d.	n.d.	n.d.	n.d. (0)	n.d.	n.d.	n.d.	n.d. (0)
Butylmethoxydibenzoylmethane	n.d.	n.d.	n.d.	n.d. (0)	0.40	0.40	0.40	0.40 (1)	n.d.	n.d.	n.d.	n.d. (0)	n.d.	n.d.	n.d.	n.d. (0)
Cadusafos	0.65	0.15	0.34	0.21 (3)	0.31	0.31	0.31	0.31 (1)	n.d.	n.d.	n.d.	n.d. (0)	0.57	0.08	0.18	0.16 (73)
Carbazole	1.66	1.63	1.65	1.65 (2)	0.54	0.31	0.43	0.43 (2)	0.11	0.11	0.11	0.11 (1)	n.d.	n.d.	n.d.	n.d. (0)
Carbendazim	6.33	0.04	1.19	0.55 (53)	3.21	0.03	0.80	0.55 (64)	1.16	0.03	0.21	0.08 (27)	2.43	0.03	0.54	0.24 (55)
Carbofuran	0.13	0.13	0.13	0.13 (1)	0.32	0.03	0.10	0.07 (7)	n.d.	n.d.	n.d.	n.d. (0)	0.04	0.02	0.03	0.03 (2)
Chloramphenicol	0.11	0.10	0.11	0.11 (2)	0.30	0.06	0.12	0.09 (5)	n.d.	n.d.	n.d.	n.d. (0)	n.d.	n.d.	n.d.	n.d. (0)
Chlorfenvinphos	0.44	0.44	0.44	0.44 (1)	n.d.	n.d.	n.d.	n.d. (0)	n.d.	n.d.	n.d.	n.d. (0)	0.44	0.44	0.44	0.44 (1)
Chloridazon	n.d.	n.d.	n.d.	n.d. (0)	0.68	0.31	0.53	0.62 (3)	0.14	0.14	0.14	0.14 (1)	0.55	0.55	0.55	0.55 (1)
Chlorpyrifos	0.67	0.13	0.35	0.31 (10)	0.50	0.14	0.26	0.23 (21)	0.39	0.13	0.22	0.19 (17)	1.72	0.19	0.70	0.20 (3)
Chlorsulfuron	n.d.	n.d.	n.d.	n.d. (0)	6.33	0.05	0.49	0.11 (22)	0.05	0.05	0.05	0.05 (2)	0.07	0.07	0.07	0.07 (1)
Ciprofloxacin	51.62	0.33	3.54	2.06 (63)	26.88	0.38	5.86	4.16 (75)	19.50	0.35	1.63	1.12 (56)	7.52	0.72	2.51	1.59 (25)
Clarithromycin	2.74	0.02	0.41	0.18 (58)	3.36	0.03	0.59	0.22 (39)	n.d.	n.d.	n.d.	n.d. (0)	n.d.	n.d.	n.d.	n.d. (0)
Cybutryne	n.d.	n.d.	n.d.	n.d. (0)	n.d.	n.d.	n.d.	n.d. (0)	n.d.	n.d.	n.d.	n.d. (0)	n.d.	n.d.	n.d.	n.d. (8)
Cyclopentadecanolide	n.d.	n.d.	n.d.	n.d. (0)	138.25	5.50	38.36	19.35 (14)	25.84	25.84	25.84	25.84 (1)	18.43	0.72	6.51	6.64 (35)
Cypermethrin	n.d.	n.d.	n.d.	n.d. (0)	6.24	6.24	6.24	6.24 (1)	n.d.	n.d.	n.d.	n.d. (0)	n.d.	n.d.	n.d.	n.d. (0)
Cyprodinil	0.29	0.04	0.10	0.05 (5)	0.16	0.04	0.08	0.07 (9)	n.d.	n.d.	n.d.	n.d. (0)	0.07	0.07	0.07	0.07 (1)

Table 3.8. Continued.

Chemical	August_2017				November_2017				February_2018				May_2018			
	Concentration (µg/L)			Median (µg/L) (Detected in (out of 75))	Concentration (µg/L)			Median (µg/L) (Detected in (out of 75))	Concentration (µg/L)			Median (µg/L) (Detected in (out of 75))	Concentration (µg/L)			Median (µg/L) (Detected in (out of 75))
	Max	Min	Mean		Max	Min	Mean		Max	Min	Mean		Max	Min	Mean	
Damascone	814.20	814.20	814.20	814.20 (1)	n.d.	n.d.	n.d.	n.d. (0)	n.d.	n.d.	n.d.	n.d. (0)	n.d.	n.d.	n.d.	n.d. (0)
Di(2- ethylhexyl)phthalate (DEHP)	69.92	3.06	19.92	17.12 (33)	100.65	2.87	24.56	19.73 (68)	70.35	3.58	25.96	21.62 (63)	160.62	3.23	21.46	13.48 (31)
Dichlorvos	n.d.	n.d.	n.d.	n.d. (0)	18.82	0.20	4.21	1.95 (9)	n.d.	n.d.	n.d.	n.d. (0)	n.d.	n.d.	n.d.	n.d. (0)
Dicyclohexylamine	5.13	0.02	0.40	0.14(62)	1.07	0.02	0.32	0.24 (56)	0.44	0.01	0.07	0.04 (41)	0.52	0.05	0.18	0.17 (46)
Difenoconazole	n.d.	n.d.	n.d.	n.d. (0)	0.04	0.04	0.04	0.04 (1)	n.d.	n.d.	n.d.	n.d. (0)	n.d.	n.d.	n.d.	n.d. (0)
Dimethoate	1.29	1.29	1.29	1.29 (1)	2.75	0.30	0.92	0.43 (5)	n.d.	n.d.	n.d.	n.d. (0)	0.27	0.27	0.27	0.27 (1)
Diphenylamine	n.d.	n.d.	n.d.	n.d. (0)	n.d.	n.d.	n.d.	n.d. (0)	0.29	0.22	0.26	0.27 (3)	n.d.	n.d.	n.d.	n.d. (0)
Diuron	2.64	0.04	0.81	0.85 (49)	2.05	0.09	0.75	0.72(43)	10.64	0.03	0.74	0.17 (28)	1.27	0.03	0.45	0.42 (40)
Dodecyl sulfate	n.d.	n.d.	n.d.	n.d. (0)	n.d.	n.d.	n.d.	n.d. (0)	n.d.	n.d.	n.d.	n.d. (0)	20.07	20.07	20.07	20.07 (1)
Doxycycline	3.22	0.36	1.05	0.58 (6)	2.36	0.15	0.97	0.79 (15)	0.26	0.04	0.14	0.13 (5)	n.d.	n.d.	n.d.	n.d. (0)
Drometrizole	1.03	0.03	0.50	0.40 (21)	2.03	0.06	0.84	0.77 (29)	1.67	0.02	0.52	0.43 (28)	0.71	0.07	0.36	0.33 (24)
Epoxiconazole	0.76	0.03	0.14	0.05 (18)	0.12	0.03	0.05	0.04 (9)	n.d.	n.d.	n.d.	n.d. (0)	0.16	0.03	0.06	0.05 (29)
Erythromycin	1.11	0.08	0.40	0.36 (11)	0.50	0.10	0.26	0.21 (9)	0.31	0.31	0.31	0.31 (1)	0.67	0.20	0.40	0.35 (3)
Ethoprophos	0.21	0.21	0.21	0.21 (1)	n.d.	n.d.	n.d.	n.d. (0)	n.d.	n.d.	n.d.	n.d. (0)	n.d.	n.d.	n.d.	n.d. (0)
Ethylhexylmethoxy cinnamate	13.86	0.17	1.49	0.59 (17)	n.d.	n.d.	n.d.	n.d. (0)	3.66	0.16	0.97	0.61 (27)	2.81	0.12	1.02	0.80 (46)
Fenamiphos	0.05	0.05	0.05	0.05 (1)	n.d.	n.d.	n.d.	n.d. (0)	n.d.	n.d.	n.d.	n.d. (0)	n.d.	n.d.	n.d.	n.d. (0)
Fenpropimorph	n.d.	n.d.	n.d.	n.d. (0)	0.06	0.06	0.06	0.06 (1)	n.d.	n.d.	n.d.	n.d. (0)	0.05	0.04	0.05	0.05 (2)
Fluoranthene	19.44	0.58	4.61	2.20 (13)	3.46	0.72	1.59	1.48 (9)	n.d.	n.d.	n.d.	n.d. (0)	1.26	0.16	0.79	0.81 (11)
Flutolanil	0.20	0.09	0.14	0.14 (2)	0.20	0.20	0.20	0.20 (1)	1.22	0.20	0.55	0.38 (4)	4.39	0.05	0.42	0.07 (14)
Flutriafol	0.33	0.11	0.18	0.15 (4)	0.22	0.22	0.22	0.22 (1)	0.08	0.08	0.08	0.08 (1)	n.d.	n.d.	n.d.	n.d. (0)
g-Methylionone	14.98	0.24	1.74	0.83 (30)	11.86	0.43	3.38	2.44 (20)	n.d.	n.d.	n.d.	n.d. (0)	n.d.	n.d.	n.d.	n.d. (0)
Galaxolide	n.d.	n.d.	n.d.	n.d. (0)	8.12	0.13	1.35	0.84 (66)	2.11	0.07	0.34	0.28 (52)	5.53	0.12	0.82	0.22 (13)
Hexa(methoxymethyl) melamine	329166.9	6.70	32814.6	10199.1 (66)	304783.9	13.81	22142.9	765.9 (74)	116123.9	6.85	4517.3	478.7 (65)	199177.5	11.23	16515.5	2653.2 (61)
Hexaconazole	n.d.	n.d.	n.d.	n.d. (0)	n.d.	n.d.	n.d.	n.d. (0)	0.03	0.02	0.03	0.03 (5)	n.d.	n.d.	n.d.	n.d. (0)
Hexylcinnamaldehyde	n.d.	n.d.	n.d.	n.d. (0)	1.10	1.10	1.10	1.10 (1)	n.d.	n.d.	n.d.	n.d. (0)	1.70	1.70	1.70	1.70 (1)
Hexythiazox	n.d.	n.d.	n.d.	n.d. (0)	0.16	0.16	0.16	0.16 (1)	n.d.	n.d.	n.d.	n.d. (0)	n.d.	n.d.	n.d.	n.d. (0)
Homosalate	124.42	5.96	29.58	19.58 (21)	n.d.	n.d.	n.d.	n.d. (0)	n.d.	n.d.	n.d.	n.d. (0)	16.11	5.94	8.73	7.37 (13)
Imazalil	2.92	0.34	1.19	0.75 (4)	1.94	0.21	0.86	0.42 (3)	n.d.	n.d.	n.d.	n.d. (0)	n.d.	n.d.	n.d.	n.d. (0)
Imazamox	0.76	0.04	0.18	0.13 (12)	0.50	0.04	0.11	0.06 (12)	0.07	0.07	0.07	0.07 (1)	n.d.	n.d.	n.d.	n.d. (0)
Imidacloprid	0.72	0.72	0.72	0.72 (1)	8.63	1.20	4.92	4.92 (2)	n.d.	n.d.	n.d.	n.d. (0)	n.d.	n.d.	n.d.	n.d. (0)
Indeno[1,2,3-cd]pyrene	110.02	2.33	23.28	10.52 (8)	109.22	3.29	24.28	16.33 (13)	12.18	4.37	7.54	6.81 (4)	n.d.	n.d.	n.d.	n.d. (0)
Lenacil	1.93	0.74	1.34	1.34 (2)	0.64	0.64	0.64	0.64 (1)	n.d.	n.d.	n.d.	n.d. (0)	n.d.	n.d.	n.d.	n.d. (0)
Mandipropamid	n.d.	n.d.	n.d.	n.d. (0)	0.04	0.04	0.04	0.04 (1)	n.d.	n.d.	n.d.	n.d. (0)	n.d.	n.d.	n.d.	n.d. (0)
Mepiquat chloride	0.64	0.11	0.27	0.24 (37)	1.16	0.19	0.37	0.35 (37)	0.12	0.07	0.10	0.10 (10)	0.58	0.08	0.31	0.30 (75)
Mesotrione	n.d.	n.d.	n.d.	n.d. (0)	n.d.	n.d.	n.d.	n.d. (0)	n.d.	n.d.	n.d.	n.d. (0)	0.63	0.08	0.39	0.42 (4)
Metalaxyl	0.10	0.05	0.08	0.08 (5)	0.04	0.04	0.04	0.04 (1)	n.d.	n.d.	n.d.	n.d. (1)	0.05	0.05	0.05	0.05 (1)
Methyl -iso-propylcyclohexenone	3.84	0.11	0.63	0.28 (15)	1.98	0.10	0.41	0.20 (20)	n.d.	n.d.	n.d.	n.d. (60)	0.45	0.12	0.21	0.17 (8)
Methyl paraben	4.31	0.18	1.27	0.76 (8)	0.33	0.09	0.14	0.13 (31)	1.89	1.89	1.89	1.89 (1)	1.71	0.18	0.71	0.32 (6)
Methyldihydrojasmonate	11.36	0.92	4.21	1.87 (9)	21.00	0.27	3.71	1.88 (73)	3.26	0.25	0.90	0.72 (60)	12.71	0.25	1.12	0.49 (59)

Table 3.8. Continued.

Chemical	August_2017				November_2017				February_2018				May_2018			
	Concentration (µg/L)			Median (µg/L) (Detected in (out of 75))	Concentration (µg/L)			Median (µg/L) (Detected in (out of 75))	Concentration (µg/L)			Median (µg/L) (Detected in (out of 75))	Concentration (µg/L)			Median (µg/L) (Detected in (out of 75))
	Max	Min	Mean		Max	Min	Mean		Max	Min	Mean		Max	Min	Mean	
Methylsalicylate	8.02	0.14	2.27	1.46 (8)	1.04	0.16	0.37	0.25 (12)	3.38	3.38	3.38	0.38 (1)	3.20	0.12	1.12	0.37 (7)
Metolachlor	0.13	0.02	0.05	0.05 (19)	0.21	0.03	0.07	0.05 (7)	0.03	0.03	0.03	0.03 (1)	0.15	0.02	0.05	0.04 (33)
Microcystin-LR	6.30	6.30	6.30	6.30 (1)	n.d.	n.d.	n.d.	n.d. (0)	n.d.	n.d.	n.d.	n.d. (0)	n.d.	n.d.	n.d.	n.d. (0)
Microcystin-RR	4.08	0.11	0.69	033 (19)	3.79	0.06	0.90	0.67 (20)	n.d.	n.d.	n.d.	n.d. (0)	n.d.	n.d.	n.d.	n.d. (0)
Molinate	3.49	0.04	0.76	0.36 (13)	0.82	0.04	0.24	0.20 (13)	0.11	0.04	0.06	0.05 (6)	211.38	0.12	15.56	1.89 (17)
Monocrotophos	0.05	0.02	0.03	0.03 (20)	0.07	0.02	0.03	0.02 (6)	n.d.	n.d.	n.d.	n.d. (0)	n.d.	n.d.	n.d.	n.d. (0)
Myclobutanil	1.38	0.20	0.45	0.38 (13)	0.35	0.04	0.11	0.09 (20)	0.08	0.01	0.04	0.04 (47)	n.d.	n.d.	n.d.	n.d. (0)
N-Benzyldimethylamine	3.79	0.01	0.31	0.06 (31)	8.48	0.01	0.49	0.14 (52)	0.90	0.01	0.08	0.03 (65)	0.05	0.04	0.05	0.05 (4)
N-Benzylmethylamine	0.37	0.04	0.16	0.15 (29)	0.37	0.04	0.16	0.16 (27)	0.31	0.04	0.10	0.07 (8)	n.d.	n.d.	n.d.	n.d. (0)
N-Ethyl-2-tolysulfonamide	0.55	0.04	0.14	0.09 (39)	0.36	0.03	0.11	0.09 (39)	0.31	0.03	0.06	0.05 (22)	0.24	0.03	0.06	0.04 (21)
N-methyl aniline	n.d.	n.d.	n.d.	n.d. (0)	n.d.	n.d.	n.d.	n.d. (0)	0.07	0.03	0.04	0.04 (26)	n.d.	n.d.	n.d.	n.d. (0)
N,N-Diethyl-m-toluamide	35.92	0.01	1.49	0.42 (75)	0.69	0.01	0.13	0.07 (75)	0.35	0.01	0.03	0.02 (70)	0.62	0.01	0.07	0.05 (71)
Nonylphenol diethoxylate	11.99	0.10	2.28	1.00 (47)	18.40	0.08	1.61	0.59 (51)	1.97	0.10	0.55	0.36 (64)	4.63	0.05	0.75	0.40 (44)
Norfloxacin	41.72	0.84	3.97	3.19 (69)	25.31	0.65	3.60	2.49 (39)	1.54	0.49	0.78	0.68 (40)	n.d.	n.d.	n.d.	n.d. (0)
Ofloxacin	530.39	0.04	8.05	0.55 (75)	88.40	0.03	2.33	0.75 (71)	80.13	0.08	2.30	0.23 (39)	824.37	0.15	24.82	0.47 (34)
Omethoate	1.46	0.09	0.26	0.13 (27)	0.91	0.15	0.29	0.20 (8)	0.14	0.09	0.11	0.11 (6)	0.10	0.09	0.09	0.09 (2)
Oxadiazon	1.42	0.40	0.72	0.64 (9)	0.60	0.58	0.59	0.59 (2)	0.48	0.42	0.45	0.45 (2)	4.32	0.39	1.50	1.22 (10)
Oxadixyl	2.72	2.72	2.72	2.72 (1)	n.d.	n.d.	n.d.	n.d. (0)	n.d.	n.d.	n.d.	n.d. (0)	n.d.	n.d.	n.d.	n.d. (0)
Oxybenzone	0.65	0.01	0.12	0.07 (39)	0.62	0.02	0.10	0.08 (40)	0.10	0.01	0.03	0.03 (33)	2.19	0.01	0.13	0.03 (57)
Penconazole	0.06	0.06	0.06	0.06 (1)	n.d.	n.d.	n.d.	n.d. (0)	n.d.	n.d.	n.d.	n.d. (0)	n.d.	n.d.	n.d.	n.d. (0)
Pendimethalin	0.10	0.03	0.06	0.06 (10)	0.05	0.03	0.04	0.04 (4)	0.06	0.02	0.04	0.03 (9)	2.60	0.02	0.18	0.04 (24)
Pentachlorobenzene	0.55	0.33	0.42	0.37 (3)	n.d.	n.d.	n.d.	n.d. (0)	n.d.	n.d.	n.d.	n.d. (0)	n.d.	n.d.	n.d.	n.d. (0)
Piperonylbutoxide	0.49	0.01	0.09	0.07 (65)	22.88	0.02	2.09	0.15 (43)	0.14	0.01	0.06	0.06 (16)	0.43	0.02	0.13	0.10 (35)
Pirimicarb	1.61	0.13	0.45	0.37 (24)	1.81	0.18	0.49	0.33 (8)	n.d.	n.d.	n.d.	n.d. (0)	0.17	0.17	0.17	0.17 (1)
Polychlorinated biphenyls	467.73	9.90	109.42	38.46 (75)	318.39	1.68	79.18	75.13 (69)	97.25	1.89	14.86	9.65 (30)	n.d.	n.d.	n.d.	n.d. (0)
Prochloraz	0.52	0.05	0.17	0.16 (41)	0.11	0.11	0.11	0.11 (1)	0.33	0.03	0.11	0.09 (23)	0.33	0.03	0.12	0.10 (45)
Prometryn	n.d.	n.d.	n.d.	n.d. (0)	0.10	0.01	0.06	0.06 (2)	n.d.	n.d.	n.d.	n.d. (0)	0.20	0.01	0.06	0.02 (5)
Propazine	0.01	0.01	0.01	0.01 (1)	0.02	0.02	0.02	0.02 (1)	n.d.	n.d.	n.d.	n.d. (0)	0.02	0.02	0.02	0.02 (1)
Propetamphos	0.47	0.25	0.33	0.26 (3)	0.40	0.40	0.40	0.40 (1)	n.d.	n.d.	n.d.	n.d. (0)	n.d.	n.d.	n.d.	n.d. (0)
Propiconazole	10.08	0.07	1.53	0.10 (7)	0.27	0.07	0.14	0.14 (21)	n.d.	n.d.	n.d.	n.d. (0)	0.16	0.10	0.12	0.11 (4)
Propyl paraben	0.51	0.51	0.51	0.51 (1)	0.04	0.04	0.04	0.04 (1)	n.d.	n.d.	n.d.	n.d. (0)	n.d.	n.d.	n.d.	n.d. (0)
Prothioconazole	n.d.	n.d.	n.d.	n.d. (0)	0.18	0.16	0.17	0.17 (2)	n.d.	n.d.	n.d.	n.d. (0)	n.d.	n.d.	n.d.	n.d. (0)
Pyraclostrobin	0.18	0.03	0.10	0.10 (4)	n.d.	n.d.	n.d.	n.d. (0)	n.d.	n.d.	n.d.	n.d. (0)	0.04	0.02	0.03	0.03 (2)
Pyridaben	0.03	0.01	0.02	0.02 (5)	n.d.	n.d.	n.d.	n.d. (0)	n.d.	n.d.	n.d.	n.d. (0)	n.d.	n.d.	n.d.	n.d. (0)
Pyriproxyfen	0.02	0.01	0.01	0.01 (10)	0.87	0.01	0.07	0.03 (28)	n.d.	n.d.	n.d.	n.d. (0)	n.d.	n.d.	n.d.	n.d. (0)
Quinalphos	1.03	0.04	0.35	0.29 (28)	1.04	0.09	0.37	0.33 (24)	0.12	0.12	0.12	n.d. (1)	1.05	0.09	0.38	0.30 (16)
Quinoxyfen	0.03	0.03	0.03	0.03 (1)	0.02	0.02	0.02	0.02 (1)	0.02	0.02	0.02	n.d. (1)	n.d.	n.d.	n.d.	n.d. (0)
Spiroxamine	0.24	0.06	0.15	0.15 (2)	n.d.	n.d.	n.d.	n.d. (0)	n.d.	n.d.	n.d.	n.d. (0)	n.d.	n.d.	n.d.	n.d. (0)
Sulfamethoxazole	3.27	0.08	0.53	0.40 (41)	1.60	0.07	0.37	0.34 (55)	0.10	0.04	0.06	0.06 (12)	0.76	0.04	0.19	0.16 (36)
Tebuconazole	0.21	0.06	0.14	0.14 (2)	1.40	0.04	0.26	0.14 (20)	n.d.	n.d.	n.d.	n.d. (0)	0.07	0.05	0.06	0.06 (5)
Terbuthylazine	0.04	0.02	0.03	0.02 (3)	0.12	0.12	0.12	0.12 (1)	n.d.	n.d.	n.d.	n.d. (0)	0.05	0.02	0.03	0.03 (4)
Terbutryn	0.03	n.d.	0.01	0.01 (36)	0.03	0.01	0.01	0.01 (11)	n.d.	n.d.	n.d.	n.d. (2)	0.01	n.d.	0.01	n.d. (6)
Tetraacetylethylenediamine	n.d.	n.d.	n.d.	n.d. (0)	18.77	18.77	18.77	18.77 (1)	2.73	1.10	1.81	1.71 (4)	n.d.	n.d.	n.d.	n.d. (0)

Table 3.8. Continued.

Chemical	August_2017				November_2017				February_2018				May_2018			
	Concentration (µg/L)			Median (µg/L) (Detected in (out of 75))	Concentration (µg/L)			Median (µg/L) (Detected in (out of 75))	Concentration (µg/L)			Median (µg/L) (Detected in (out of 75))	Concentration (µg/L)			Median (µg/L) (Detected in (out of 75))
	Max	Min	Mean		Max	Min	Mean		Max	Min	Mean		Max	Min	Mean	
Tetrabromobisphenol A	n.d.	n.d.	n.d.	n.d. (0)	n.d.	n.d.	n.d.	n.d. (0)	1.56	0.28	0.92	0.92 (2)	n.d.	n.d.	n.d.	n.d. (0)
Tetracycline	0.60	0.06	0.18	0.13 (13)	0.28	0.07	0.17	0.19 (7)	0.08	0.06	0.07	0.06 (3)	2.46	0.05	0.53	0.36 (16)
Thiacloprid	0.10	0.10	0.10	0.10 (1)	0.35	0.11	0.25	0.29 (3)	n.d.	n.d.	n.d.	n.d. (0)	0.42	0.19	0.28	0.21 (3)
Thiophanate-methyl	n.d.	n.d.	n.d.	n.d. (0)	0.06	0.03	0.04	0.04 (7)	0.50	0.03	0.21	0.16 (8)	n.d.	n.d.	n.d.	n.d. (0)
Tonalide	0.50	0.19	0.32	0.30 (7)	0.32	0.19	0.26	0.27 (4)	0.47	0.46	0.46	0.46 (2)	n.d.	n.d.	n.d.	n.d. (0)
Triazophos	0.37	0.13	0.22	0.19 (4)	1.29	0.32	0.96	1.27 (3)	0.18	0.11	0.15	0.17 (3)	0.32	0.05	0.15	0.11 (4)
Trifloxystrobin	0.20	0.20	0.20	0.20 (1)	n.d.	n.d.	n.d.	n.d. (0)	n.d.	n.d.	n.d.	n.d. (0)	n.d.	n.d.	n.d.	n.d. (0)
Trifluralin	2.16	2.16	2.16	2.16 (1)	n.d.	n.d.	n.d.	n.d. (0)	n.d.	n.d.	n.d.	n.d. (0)	0.31	0.04	0.21	0.28 (3)
Trimethoprim	0.20	0.03	0.13	0.14 (4)	0.45	0.03	0.11	0.09 (39)	0.08	0.01	0.03	0.03 (15)	0.14	0.02	0.07	0.05 (7)
Triphenylphosphineoxide	15.24	1.61	5.23	2.02 (4)	10.31	0.68	3.95	2.41 (4)	1.27	0.74	1.01	1.01 (2)	11.99	0.72	3.56	1.19 (5)
Tris(2-butoxyethyl) phosphate	270.17	0.04	21.00	5.32 (51)	527.43	0.03	54.19	1.46 (70)	90.26	0.03	6.64	2.77 (52)	565.22	0.03	33.36	9.11 (55)
Vancomycin	1.47	1.47	1.47	1.47 (1)	0.31	0.31	0.31	0.31 (1)	n.d.	n.d.	n.d.	n.d. (0)	n.d.	n.d.	n.d.	n.d. (0)

* not detected

3.3.2.2. Pharmaceuticals. We measured 20 chemicals classified as PhACs in the samples taken from Ergene River. Among them, dicloxacillin, thioridazine, 2-hydroxyibuprofen and three hormones (17-alpha-Estradiol, 17-alpha-Ethinylestradiol and 17-beta-Estradiol) were detected in none of the samples.

Antibiotics were detected frequently in the Ergene River in all seasons. The results show that the frequency of detection and concentration of quinolones (e.g. ofloxacin, ciprofloxacin, norfloxacin) and sulfonamide antibiotics (e.g. sulfamethoxazole) were higher than the tetracyclines (e.g. tetracycline, doxycycline) along the river (APPENDIX D). This difference can be explained by their consumption ratio as well as partitioning of the antibiotics between river water and sediment. For instance, tetracyclines have a higher tendency to absorb onto sediment and therefore a less concentration in water samples (Zhang et al., 2014). Ofloxacin found in 75, 71, 39 and 34 and ciprofloxacin present in 53, 75, 56 and 25 samples taken in summer, fall, winter and spring, respectively, were the most frequently detected antibiotics in the order of the frequency detection. Ofloxacin was detected in 79%, 73% and 70% of the samples from ***transition*** , ***industrial*** and ***agricultural zones***, respectively, at a concentration between 0.04-824.37 µg/L in all seasons (Figure 3.45). The highest concentration of ofloxacin was 530.9, 88.40, 80.13 and 824.37 µg/L during summer, fall, winter and spring occurred in the ***industrial zone***, respectively, measured at sampling point *t2-3* receives the effluents of a pharmaceutical industry (Figure 3.46). In ***transition zone***, the ofloxacin was detected up to 7.07 µg/L with the highest concentration at sampling points *t4* next to Lüleburgaz City while in ***agricultural zone***, was present up to 2.98 µg/L with the highest detected concentration at *t12-3* close to Kırklareli City (Figure 3.45 and Figure 3.47). Ofloxacin was also reported to be present at concentrations up to 990 ng/L in surface waters of Beijing, China (Sousa et al., 2018).

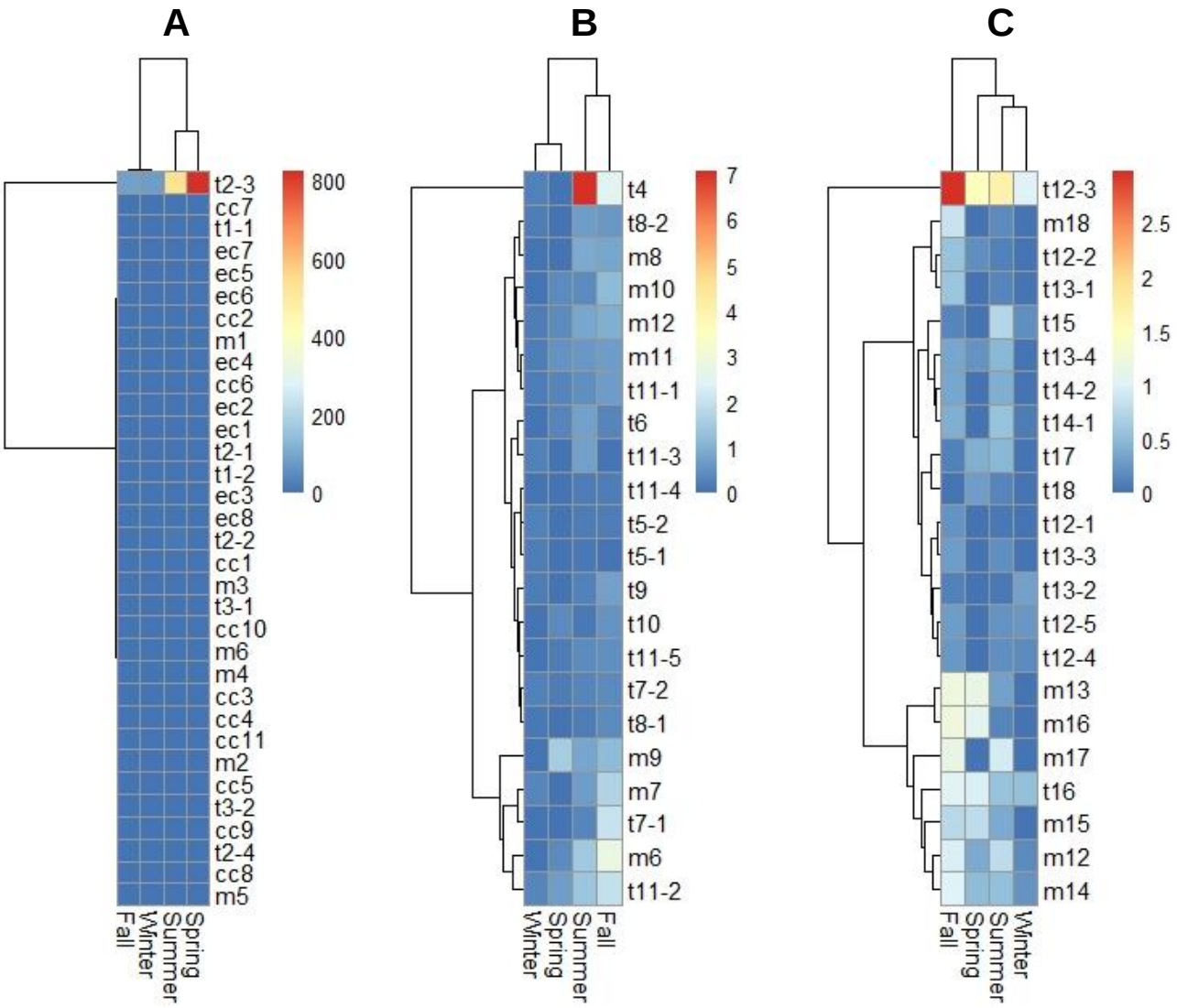

Figure 3.45. Heatmap of ofloxacin clustered by spatial-temporal concentration (µg/L) profiles in (A) ***industrial***, (B) ***transition*** and (C) ***agricultural zones***.

Ciprofloxacin is a fluoroquinolone antibiotic used in anticancer treatments was reported to be present as the most frequently detected antibiotic in wastewater and surface water (Mater et al., 2014). Ciprofloxacin was found in 80%, 78% and 60% of the samples from ***transition***, ***industrial*** and ***agricultural zones***, respectively, at concentrations between 0.35 and 51.62 µg/L during the year. The highest concentration of the ciprofloxacin was found at *t12-3* during all season except summer which was at *t4*. Sampling point *t12-3* is receiving the effluent of WWTP of Kırklareli City which is the main source of ciprofloxacin in that sampling point (Figure 3.47). Ciprofloxacin was among the antibiotics that was frequently reported in the literature. Ciprofloxacin at concentrations up to 13.58 µg/L was present in the Buyukcekmece Watershed in Turkey (Sousa et al., 2018).

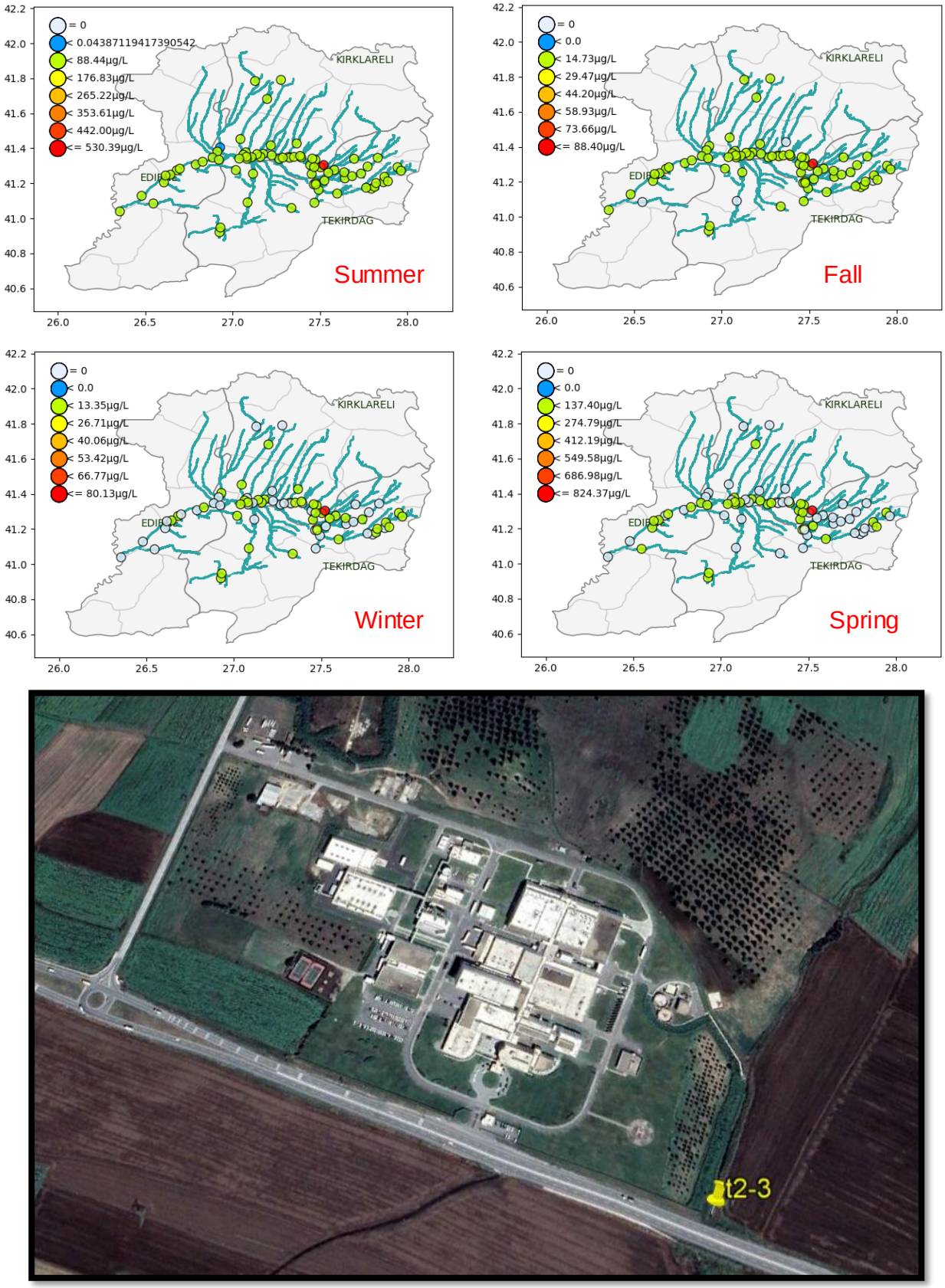

Figure 3.46. Seasonal profile of ofloxacin concentration in Ergene watershed, location of sampling point *t2-3* next to a pharmaceutical facility in ***industrial zone*** with the highest ofloxacin concentration.

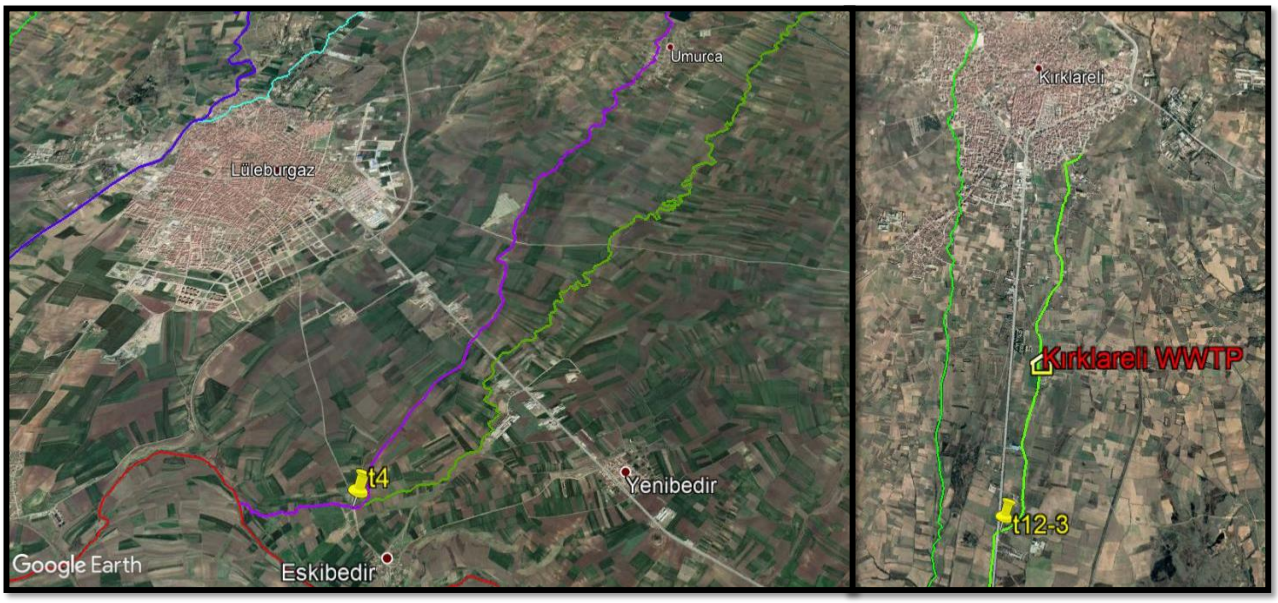

Figure 3.47. Location of sampling point *t4* in ***transition zone*** and *t12-3* in ***agricultural zone***.

In addition to these two antibiotics, others such as erythromycin, clarithromycin, sulfamethoxazole, norfloxacin and azithromycin were detected frequently along the main stream and its tributaries. The seasonal concentration range and detection frequency of PhACs are reported in APPENDIX D (Figure D.1).

Acetaminophen as an analgesic drug was detected in 49, 57, 53 and 50 sampling points during summer, fall, winter and spring, respectively. Acetaminophen's high detection frequency is due to extensive consumption of this analgesic drug and the fact that it does not require any prescription for consumption in Turkey. In literature, its frequent detection was reported in surface waters, ground waters as well as in sewage and industrial wastewater. Acetaminophen finds its way to these water environments via discharge through human excretion or the industrial sectors producing acetaminophen (Fram and Belitz, 2011, Al-Kaf et al., 2017). In the Ergene River, acetaminophen was detected in all zones in more than 79%, 79% and 70% of the samples taken from ***industrial***, ***transition*** and ***agricultural zones***, respectively. it was also measured at concentrations between 0.07 and 111.08 µg/L in all seasons. In ***industrial zone***, the highest concentration was determined at sampling point *t1-1* specially during summer and spring while, *t11-2* and *t12-3* in ***transition*** and ***agricultural zones***, respectively, had the highest acetaminophen concentration (Figure 3.48). Sampling point *t1-1* (Figure 3.49) is surrounded by many industries including a pharmaceutical industry and also located close to the WWTP of the Büyükkarıştıran OIZ. On the other hand *t11-2* (Figure 3.49) and *t12-3* (Figure 3.47) are receiving the effluent from WWTP of Malkara and Kırklareli Cities, respectively. In other studies, Acetaminophen was present in 46% of the water samples taken from Guadalquivir in Spain at

concentrations up to 9.61 µg/L while up to 30.42 µg/L was found in a study performed on Mojolinho River in Brazil (Sousa et al., 2018).

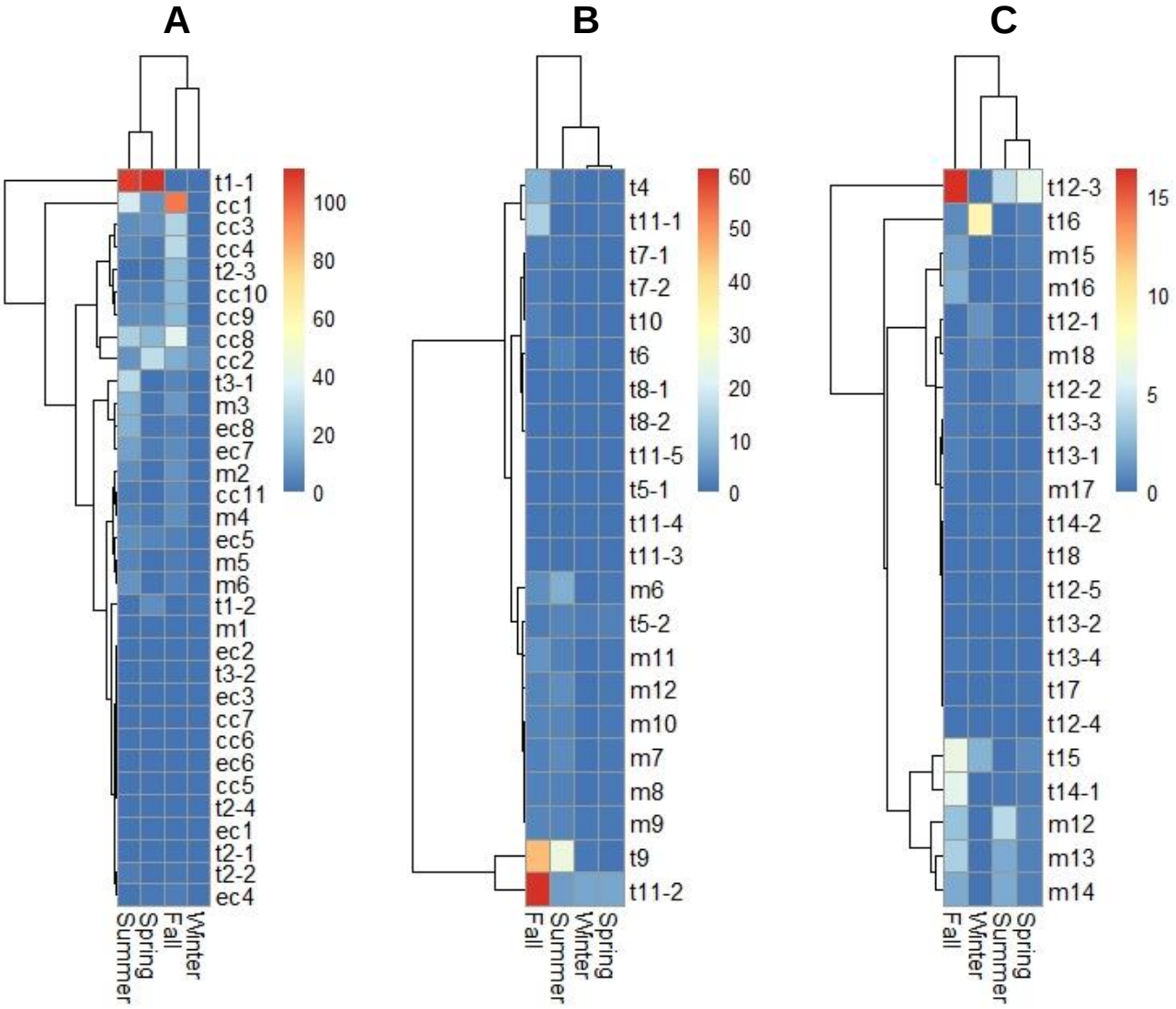

Figure 3.48. Heatmap of acetaminophen clustered by spatial-temporal concentration (µg/L) profiles in (A) ***industrial***, (B) ***transition*** and (C) ***agricultural zones***.

The complete seasonal concentration and frequency of the pharmaceuticals monitored in The Ergene River are given in APPENDIX D.

Figure 3.49. Location of sampling points *t1-1* and *t11-2* at which the highest acetaminophen concentration was detected.

3.3.2.3. Personal Care Products (PCPs). Fragrances are important ingredients of perfumes which are PCPs that are frequently used in daily life. Among the seventeen fragrances monitored in the Ergene River, nitro musk compounds including musk ambrette, musk ketone and musk xylene were

detected in none of the samples. Methyldihydrojasmoante detected at 9, 73, 60 and 59 samples in summer, fall, winter and spring, was the most frequently detected fragrance. Methyldihydrojasmonate is a fragrance that has insect repellence properties and has been used in the production of different perfumes. In addition it has flavoring properties and found in small amounts in fruits such as orange and tea (Zeng et al., 2018). In the Ergene River, methyldihydrojasmonate was detected at 70%, 68%, 61% of the samples taken from ***agricultural***, ***industrial*** and ***transition zones***, respectively. Its concentration in the river was between 0.25 and 21.00 µg/L in all seasons.

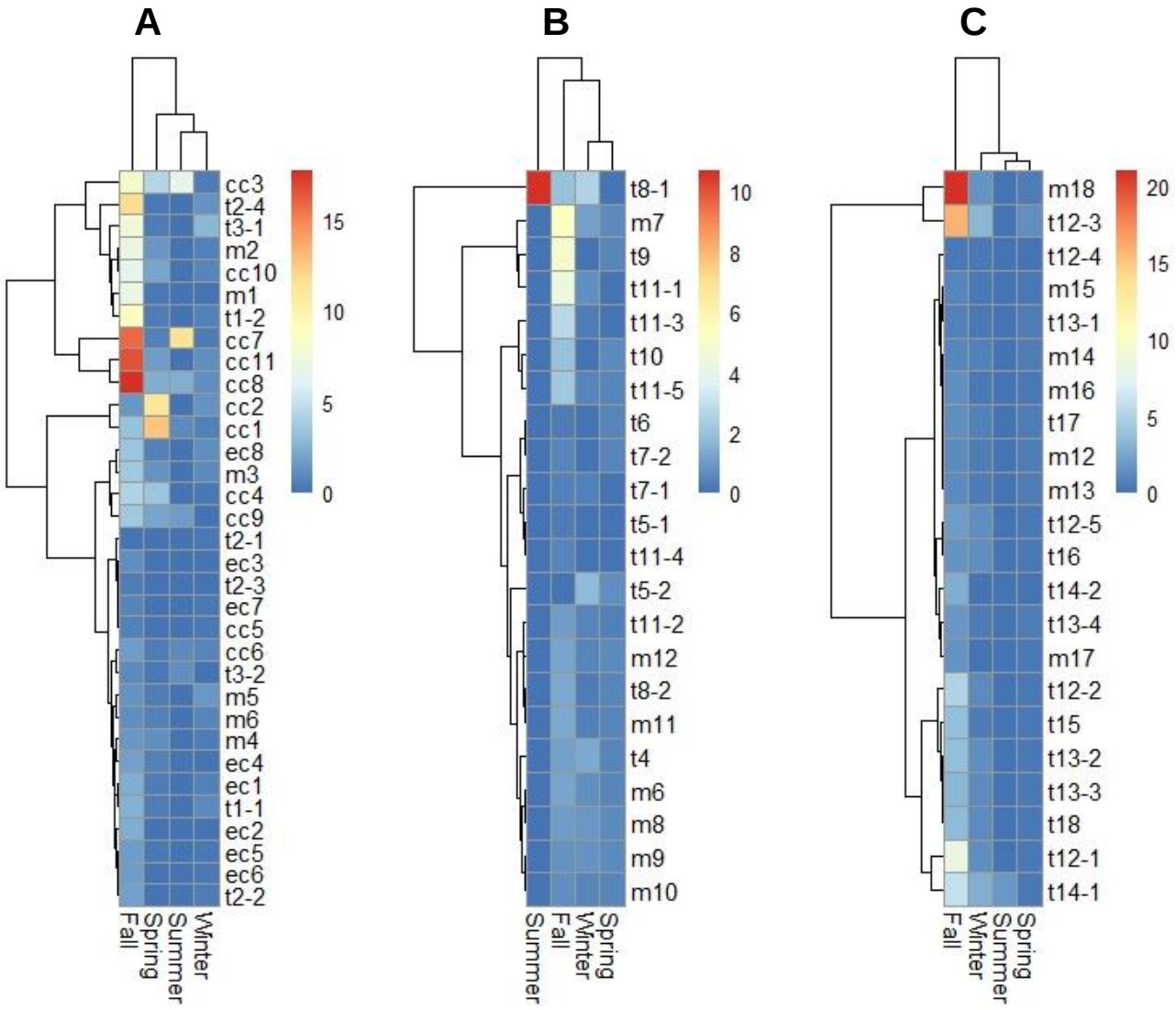

Figure 3.50. Heatmap of methyldihydrojasmonate clustered by spatial-temporal concentration (µg/L) profiles in (A) ***industrial***, (B) ***transition*** and (C) ***agricultural zones***.

In ***industrial zone***, presence a high number of food production and cosmetic facilities specially in OIZs close to Çorlu Creek may be the main sources of methyldihydrojasmonate (Figure 3.50 and Figure 3.51). While a solid waste disposal site close to *t8-1* in ***transition zone*** and WWTP effluent of

Kırklareli City next to *12-3* in ***agricultural zone*** resulted in high level of methyldihydrojasmonate at those points (Figure 3.50).

Polycyclic fragrances such as galaxolide are among the most consumed fragrances throughout the world (Villa et al., 2012). In Ergene River, galaxolide was the second most frequently detected fragrance. Although was not detected during summer, it was found in 66, 52 and 13 samples taken in fall, winter and spring, respectively, at concentrations between 0.07 and 8.12 µg/L. In particular, galaxolide was present at its highest concentrations in the ***industrial zone*** of Ergene Watershed where food and cosmetic facilities are located (Figure 3.51). Galaxolide was also reported to be present at 2.75 µg/L in a river in USA (Sousa et al., 2018) and at concentrations up to 1.14 µg/L in Molgora River in Italy (Villa et al., 2012).

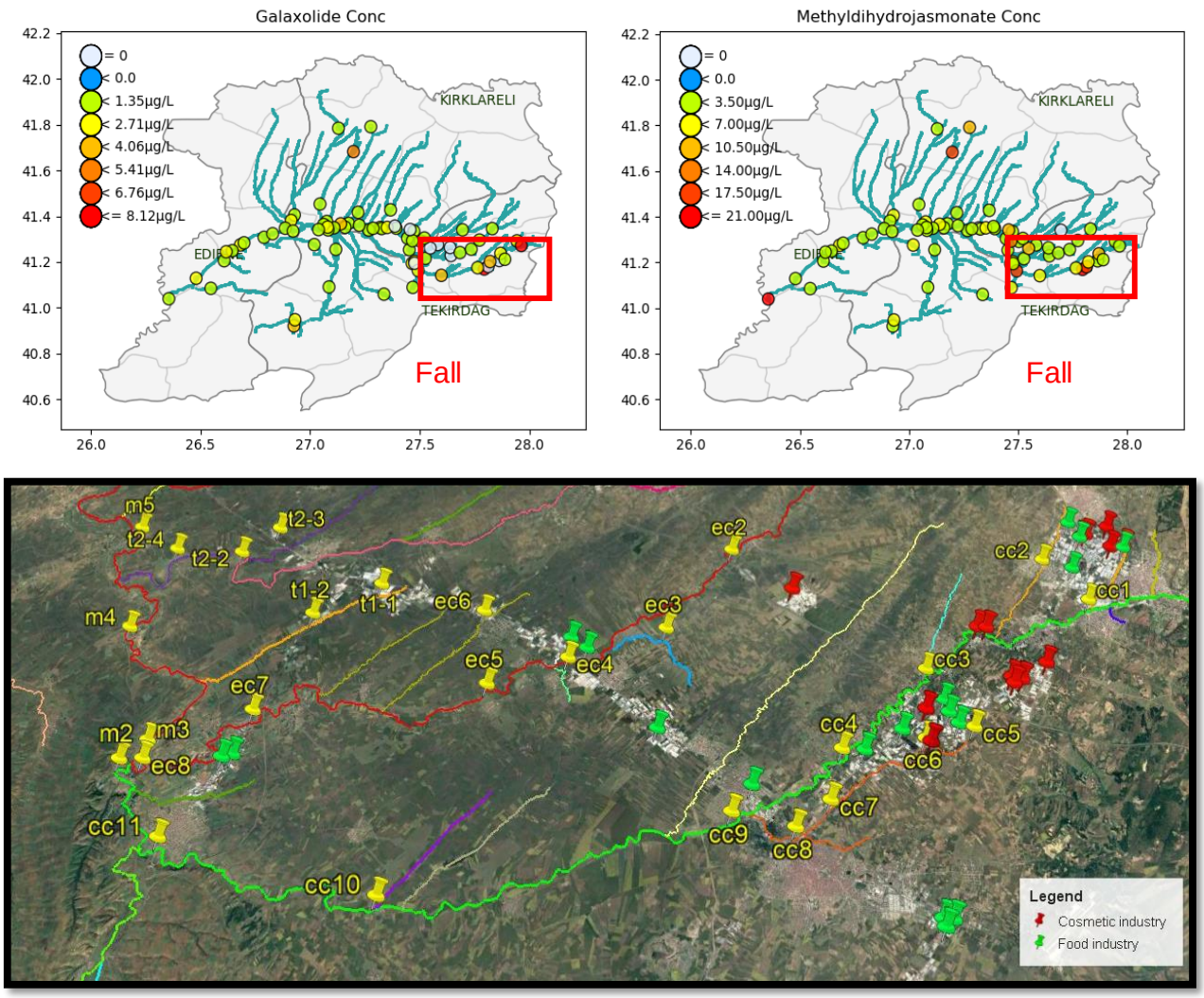

Figure 3.51. Concentration profile of galaxolide and methyldihydrojasmonate in Ergene River in fall, distribution of cosmetic and food facilities in ***industrial zone***.

In addition to the aforementioned chemicals, other fragrances and flavoring agents such as ADBI (celestolide), AHDI (phantolide), boisvelone, cyclopentadecanolide, damascene, hexylcinnamaldehyde, g-methylionone, methyl salicylate, tonalide and methyl-iso-propylcyclohexenone were also detected in the Ergene River (Figure D.2).

UV filters are chemicals that are used not only in sunscreens but also in cosmetic products, shampoos and other PCPs (Schneider and Lim, 2019). In Ergene River, seven UV filters including ethylhexylmethoxycinnamte, drometrizole, butylmehtoxydibenzoylmethane, 4-methulbenzylidene camphor, 2,4 dihydroxybenzophenone, oxybenzone and homosalate have been monitored. All of those UV filters were detected and among them oxybenzone found in 39, 40, 33 and 57 samples (out of 75) taken in summer, fall, winter and spring, respectively, was the most frequently detected one.

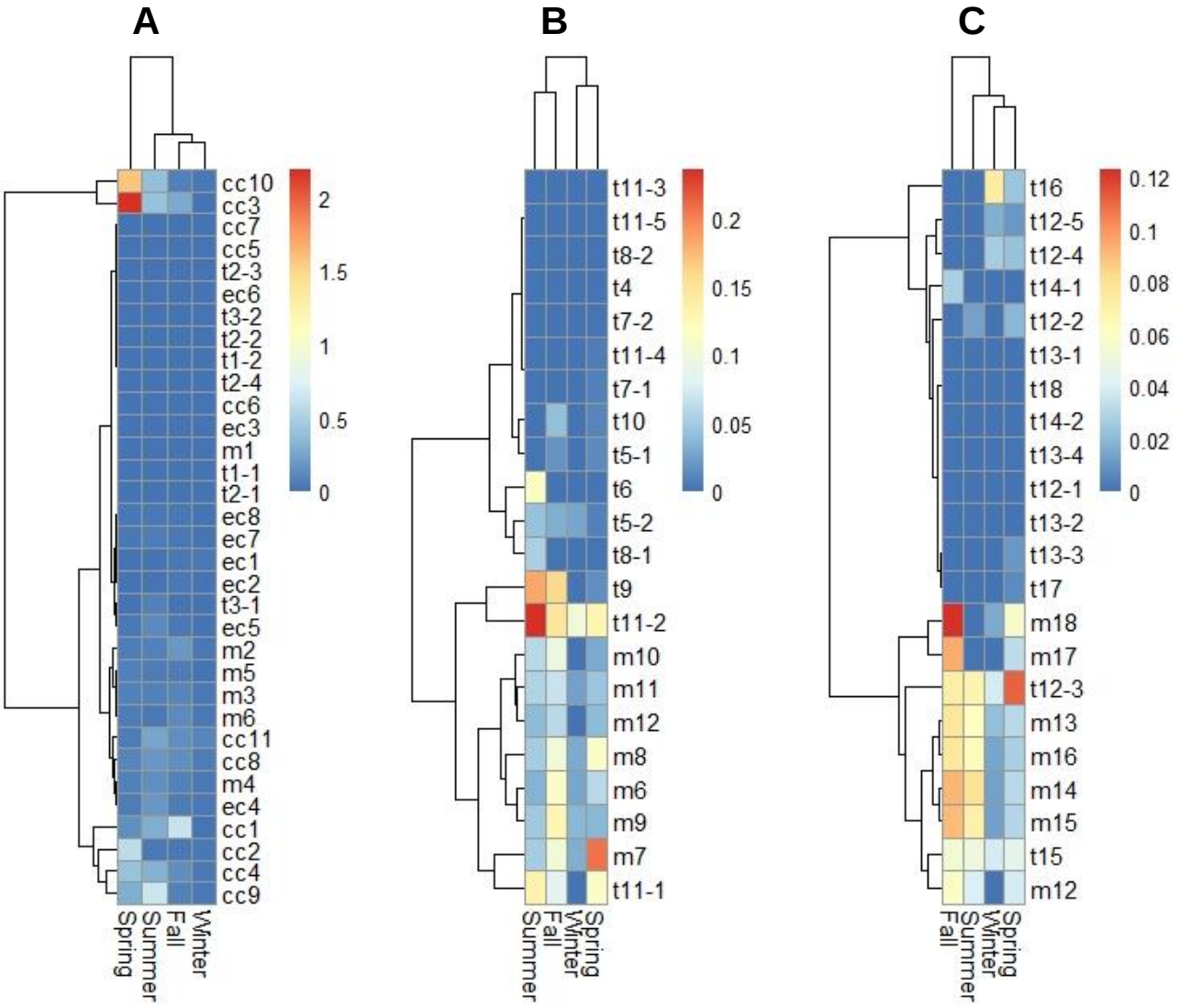

Figure 3.52. Heatmap of oxybenzone clustered by spatial-temporal concentration (µg/L) profiles in (A) ***industrial***, (B) ***transition*** and (C) ***agricultural zones***.

Oxybenzone also known as benzophenone-3 was mainly detected in the ***industrial zone***, (at 65% of the samples taken from that zone) at concentrations between 0.01 and 2.19 µg/L in all seasons. Whereas, it was only found in 53% and 48% of the samples taken from ***transition*** and ***agricultural zones***, respectively (Figure 3.52). In ***industrial zone***, the highest concentration of oxybenzone was measured at sampling points on the Çorlu Creek (*cc3*) close to Yalıboyu OIZ (Figure 3.52 and Figure 3.53). On the other hand, in ***transition zone***, sampling points *t9* (Figure 3.54) and *t11-2* (Figure 3.49) close to Alpullu and Malkara Cities and in ***agricultural zone***, sampling points *t12-3* (Figure 3.47) and *t16* (Figure 3.54) receiving the WWTP effluent of Kırklareli and Uzunköprü Cities, respectively, were the ones at which the highest oxybenzone concentration was recorded. Oxybenzone was also measured at concentrations up to 0.13 µg/L in swiss lakes (Liu et al., 2012) and at 0.05-0.14 µg/L in wastewater effluents in a study performed in Spain (Bueno et al., 2012).

The concentration ranges of other detected UV filter are given in APPENIX D (Figure D.3).

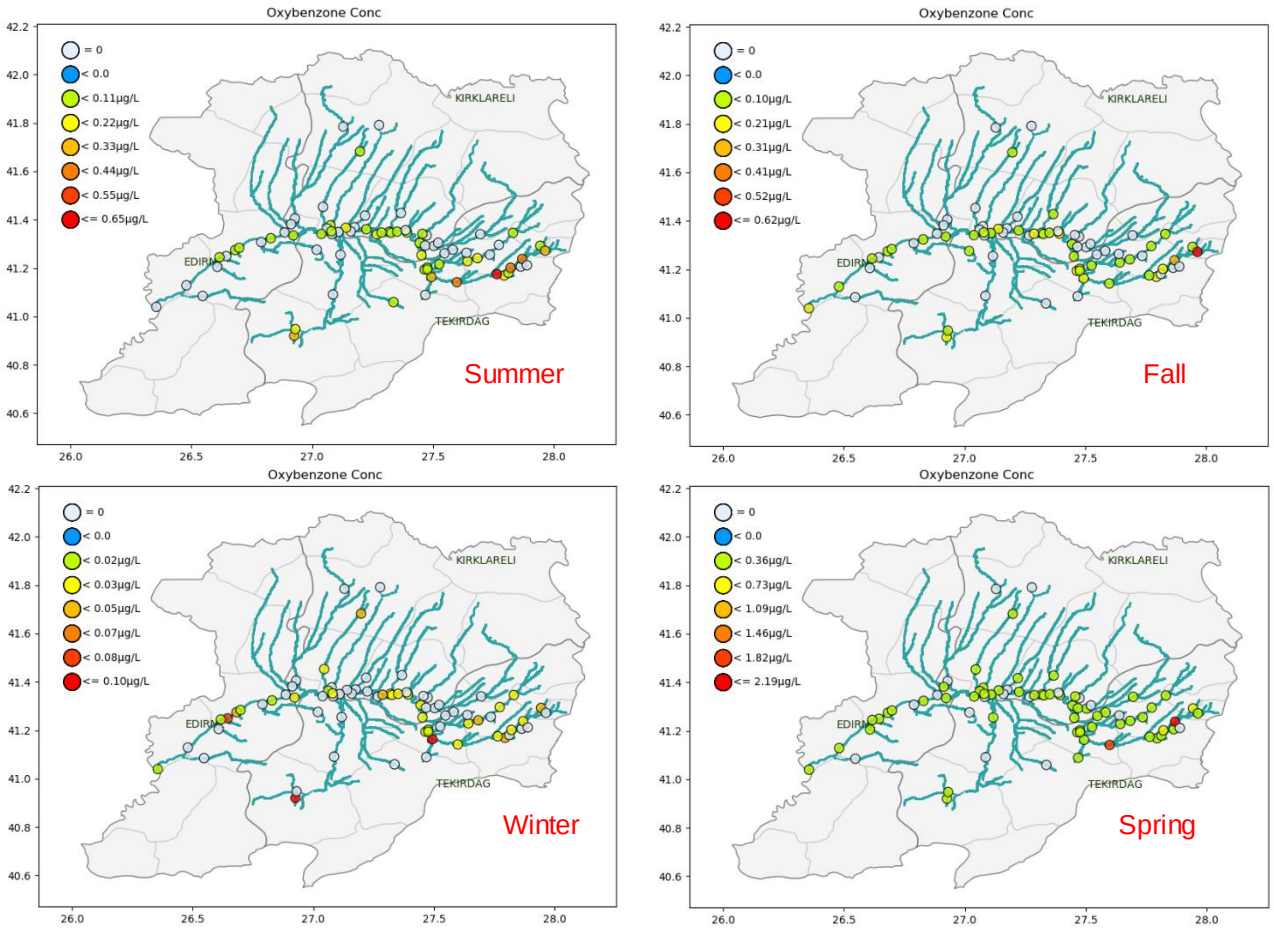

Figure 3.53. Seasonal profile of oxybenzone concentration in Ergene River.

Figure 3.54.. Location of sampling point *t16* and *t9*.

Methyl, ethyl, propyl and isobutyl paraben as widely used PCPs were monitored in the Ergene River. However, only methyl and propyl paraben were detected. Methyl paraben detected at 8, 31, 1 and 6 sampling points in summer, fall, winter and spring, respectively, was the most frequently

detected one. Propyl paraben, on the other hand, was just detected just in one sampling point during summer and fall. Methyl paraben was mainly detected in ***industrial zone*** (at 24% of samples taken in that zone) at 0.10-4.31 µg/L. In ***industrial zone***, the highest concentration of methyl paraben was recorded at sampling point *cc6* and *cc7* on Çorlu Creek and next to Velimeşe OIZ as well as *t1-2* on the tributary close to Büyükkarıştıran OIZ (Figure 3.55). Methyl paraben was reported to be frequently detected up to 144 ng/L in River Taff and up to 400 ng/L in River Ely, in UK (Kasprzyk-Hordern et al., 2008).

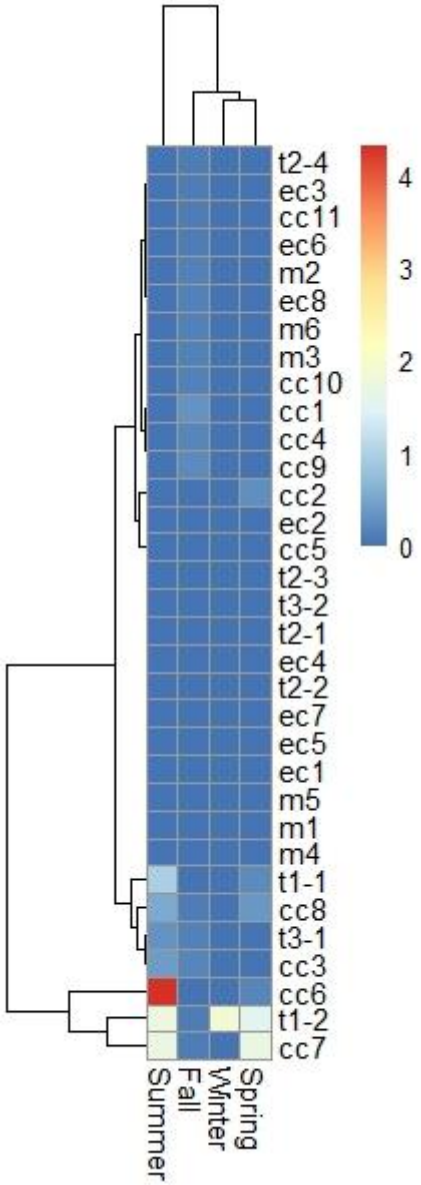

Figure 3.55. Heatmap of methyl paraben clustered by spatial-temporal concentration (µg/L) profile in ***industrial zone***.

Although methyl paraben was not detected frequently in ***transition zone***, the highest concentration of 0.33 µg/L was found at sampling point *t9* close to Alpullu City in fall (Figure 3.56).

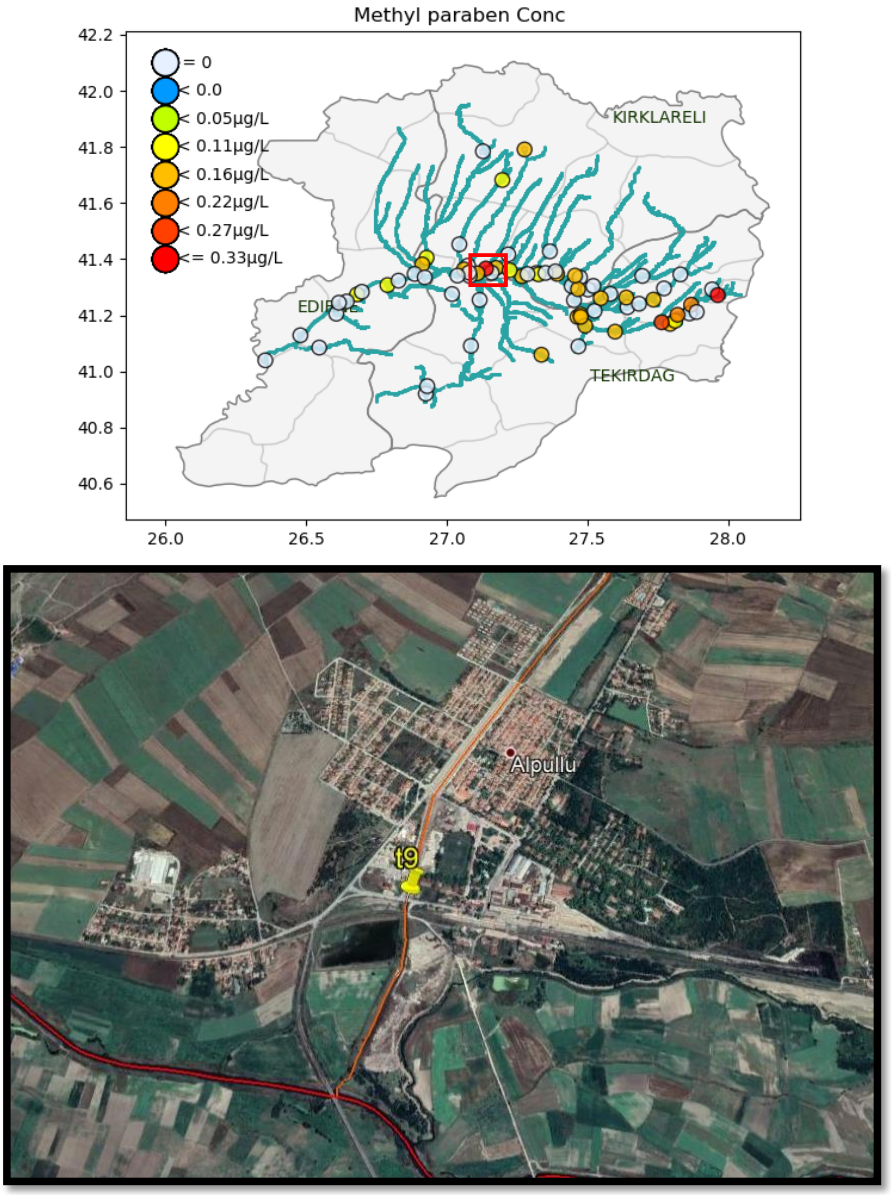

Figure 3.56. Concentration profile of methyl paraben in Ergene River in fall, Location of sampling point *t9* at which high methyl paraben concentration was detected.

The range of concentration as well as detection frequency of parabens are given in APPENDIX D (Figure D.4).

3.3.2.3. Surfactants. Surfactants are mainly used for cleaning and disinfection purposes in houses and various industries. Because of their disinfection properties, they are one of the most widespread chemicals in the environment (Ivankovic and Hrenovic, 2010). Out of nine surfactants measured in the Ergene River, 4-nonylphenoxy acetic acid, 4-tert-octylphenol monoethoxylate and benzyldimethylhexadecylammonium were detected in none of the samples. Quaternary ammonium compounds (QACs) specially benzyldimethyldodecylammonium (BDDDA) and benzyldimethyltetradecylammonium (BDTDA) were detected in almost all of the sampling points.

BDDDA was present in the Ergene River at concentrations between 0.02 and 116.65 µg/L in all seasons. Although found in all zones, the main sources of BDDDA are sampling points *t1-1* and *t1-2* close to Büyükkarıstıran OIZ in ***industrial zone*** (Figure 3.57, Figure 3.58 and Figure 3.59). In addition, the higher BDDDA concentration in *t1-2* than *t1-1* may be explained by excess discharge or untreated discharge of BDDDA from the textile industries around sampling point t1-2 (Figure 3.57, Figure 3.58 and Figure 3.59). Since, in addition to their disinfectant properties, BDDDA was reported to be widely used as coating agents in textile industries (Thorsteinsson et al., 2003).

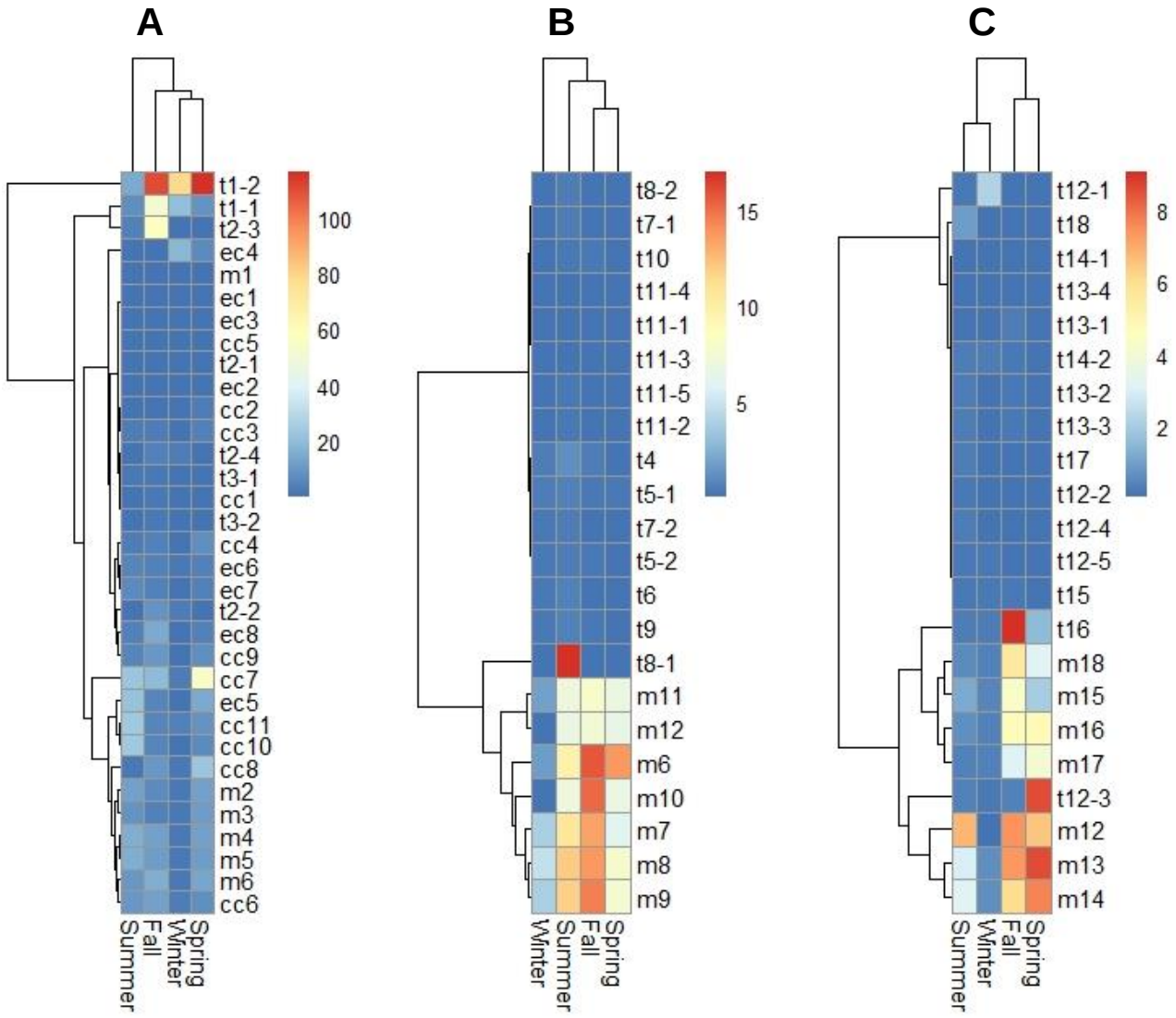

Figure 3.57. Heatmap of BDDDA clustered by spatial-temporal concentration (µg/L) profiles in (A) ***industrial***, (B) ***transition*** and (C) ***agricultural zones***.

In ***transition*** and ***agricultural zones***, the highest concentrations of BDDDA were mainly found at sampling points taken from the main stream of those zone (Figure 3.57) suggesting that BDDDA pollution is originated from the ***industrial zone*** (Figure 3.57). In addition, *t8-1* (Figure 3.59) in

transition zone and close to a solid waste disposal site and *t12-3* (Figure 3.47) and *t16* (Figure 3.54) in ***agricultural zone*** receiving the WWTP effluent of Kırklareli and Uzunköprü Cities, respectively, were other sampling points at which high concertation of BDDDA was measured (Figure 3.57).

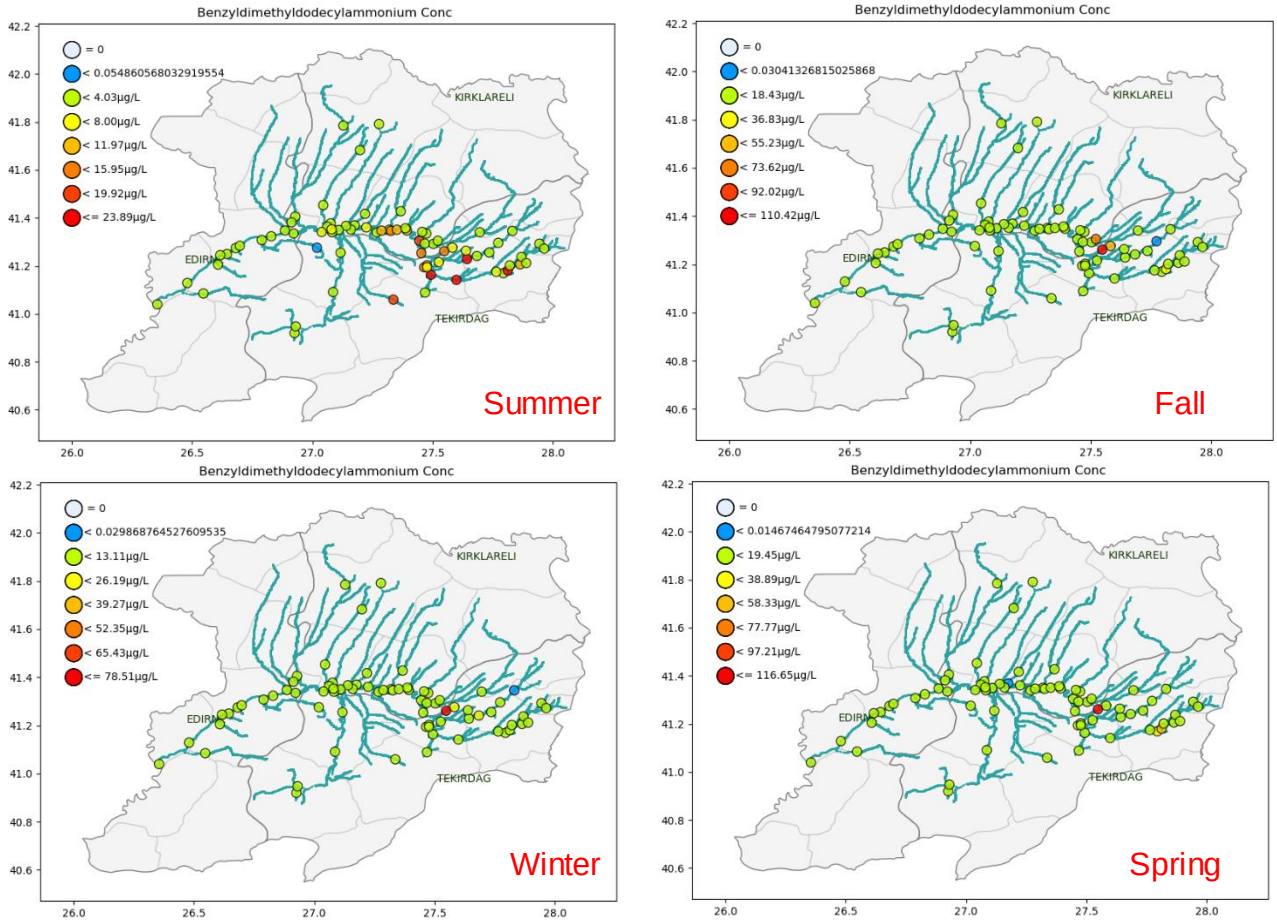

Figure 3.58. Seasonal BDDDA concentration profiles in Ergene River and its tributaries.

Figure 3.59. Location of sampling point *t1-2* in ***industrial zone*** and *t8-1* in ***transition zone***.

Following BDDDA and BDTDA, 4-tert octylphenol diethoxylate detected in 43, 36, 75 and 65 as well as nonylphenol diethoxylate found in 47, 51, 64 and 44 samples taken in summer, fall, winter and spring, respectively, were the other frequently detected surfactants. Both nonylphenols and octylphenols are listed as PS in WFD by European Commission and their presence leads to endocrine disrupting in living organisms (Petrovic et al., 2002). Although 4-tert octylphenol was present at a mean concentration of 0.05 µg/L in all seasons, its concentration at *cc4* (0.17 µg/L) on the Çorlu Creek and *t2-3* (0.12 µg/L) close to a pharmaceutical industry, exceeded its AA-EQS (0.1 µg/L) set by the European Commission.

In Ergene River, nonylphenol diethoxylate was present at a mean concentration of 0.86 µg/L in all seasons. Nonylphenol diethoxylate was mainly detected in ***industrial zone*** (at 79% of the samples taken from that zone) at 0.05-18.40 µg/L in all seasons. The highest concentration of nonylphenol diethoxylate in ***industrial zone*** was recorded at sampling points *cc6* (up to 18.40 µg/L), *ec6* (up to 11.99 µg/L) and *t1-2* (up to 10.88 µg/L) on Çorlu Creek, Ergene Creek and the tributary next to Büyükkarıştıran OIZ, respectively (Figure 3.60). On the other hand, in ***transition*** and ***agricultural zones***, samples taken from the main stream had the highest concentration of nonylphenol diethoxylate suggesting that it is originated from the ***industrial zone*** (Figure 3.60). Nonylphenol are also reported in many studies throughout the world. Nonyl phenol was present at 0.02-1.4 µg/L in Huangpu River and 0.34-0.3.56 µg/L in Pearl River in China. It was also determined at concentrations up to 0.79 µg/L in Tagus River, in Portugal (Sousa et al., 2018).

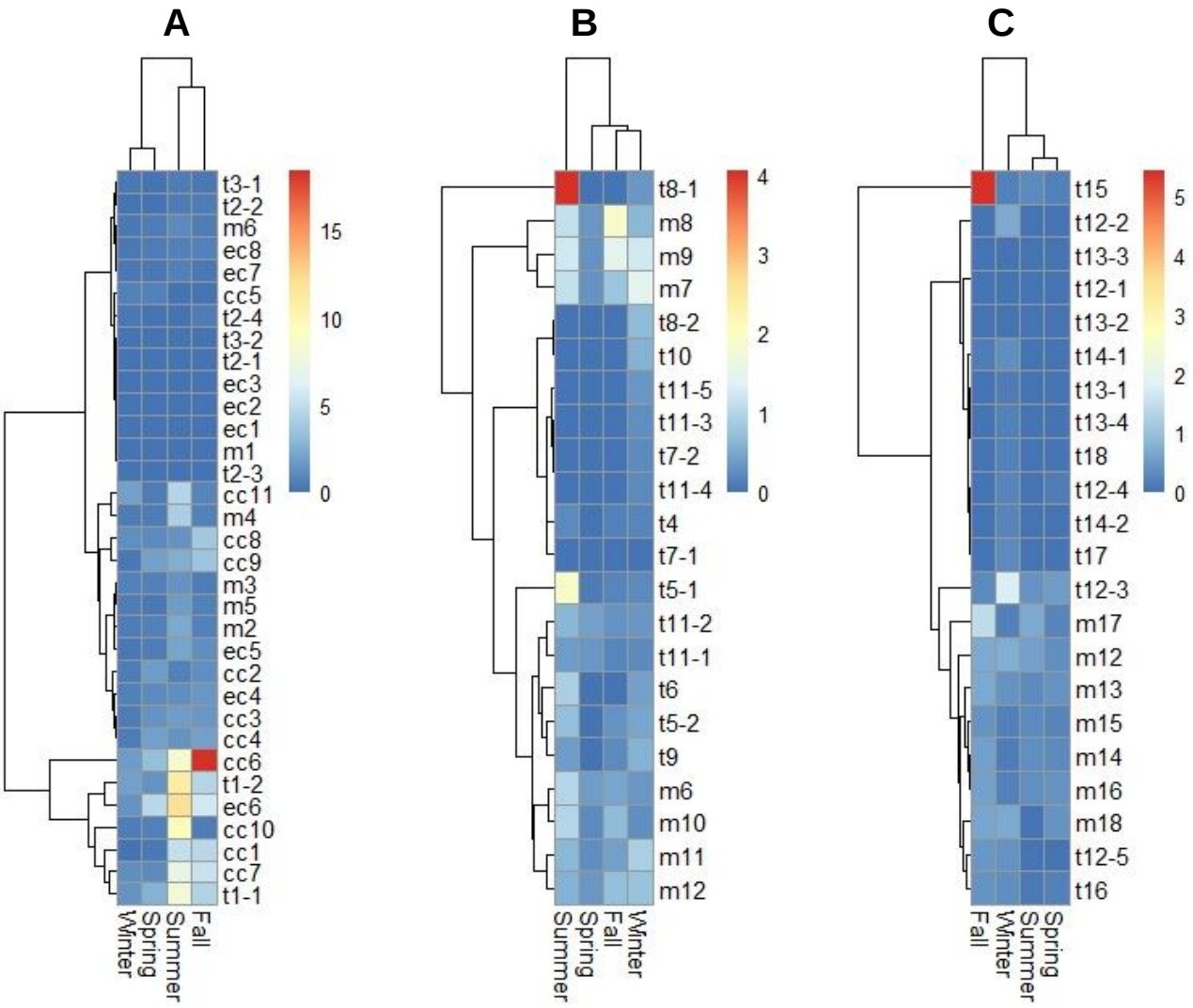

Figure 3.60. Heatmap of nonylphenol diethoxylate clustered by spatial-temporal concentration (µg/L) profiles in (A) ***industrial***, (B) ***transition*** and (C) ***agricultural zones***.

The detection frequency of surfactants as well as their concentration ranges are given in APPENDIX D (Figure D.5).

3.3.2.4. Industrial chemicals. *Flame retardants:* We measured 16 flame retardants in the samples taken from the Ergene River. Among them, 2,2,3,4,4,5,5,6-nonabromodiphenyl ether, 2,2,3,3,4,4,5,5,6,6-decabromodiphenyl ether, 2,2,3,4,4,5,6-heptabromodiphenyl ether, 2,2,4,4-tetrabromodiphenyl ether, 2,4-dibromophenol, 2,4,6-tribromophenol and tris(1-chloro-2-propanyl) phosphate were not detected. Tris(2-butoxyethyl) phosphate (TBEP) detected in 51, 70, 52 and 55 out of 75 samples in summer, fall, winter and spring, respectively, was the most frequently found flame retardant. TBEP is one of the most widely used OP flame retardants after banning the PBDEs. Its annual production ranged 5000 to 6000 tons throughout the world and is used in textiles, plastics, polishes and electronic equipment productions (Han et al., 2014, Jin et al., 2016). In Ergene River, TBEP was mainly detected in ***industrial zone*** (88% of the samples taken from that zone) at concentrations between 0.03 and 565.22 µg/L in all seasons (Figure 3.61). While it was found in only 68% and 67% of the samples in ***transition*** and ***agricultural zones***, respectively. The highest concentration of TBEP in ***industrial zone*** was often measured at *cc6*, *cc7* and *cc8* on Çorlu Creek (Figure 3.61 and Figure 3.62) and close to Velimeşe OIZ. In ***transition*** and ***agricultural zones***, the highest concentrations of TBEP were recorded on the main stream (Figure 3.61) suggesting that TBEP pollution is as a result of industrial activities in the ***industrial zone***. In fact, TBEP was sustained along the main stream and even was present up to 137.14 µg/L at sampling point *m18* as the last sampling point. TBEP was also reported in a study on the surface waters of Germany at concentrations up to 0.65 µg/L (Regnery and Puttmann, 2010). In another study, TBEP up to 80 ng/L was recorded in Elbe River in Germany (Bollmann et al., 2012). Compared to other studies, Ergene River is under serious stress of TBEP pollution.

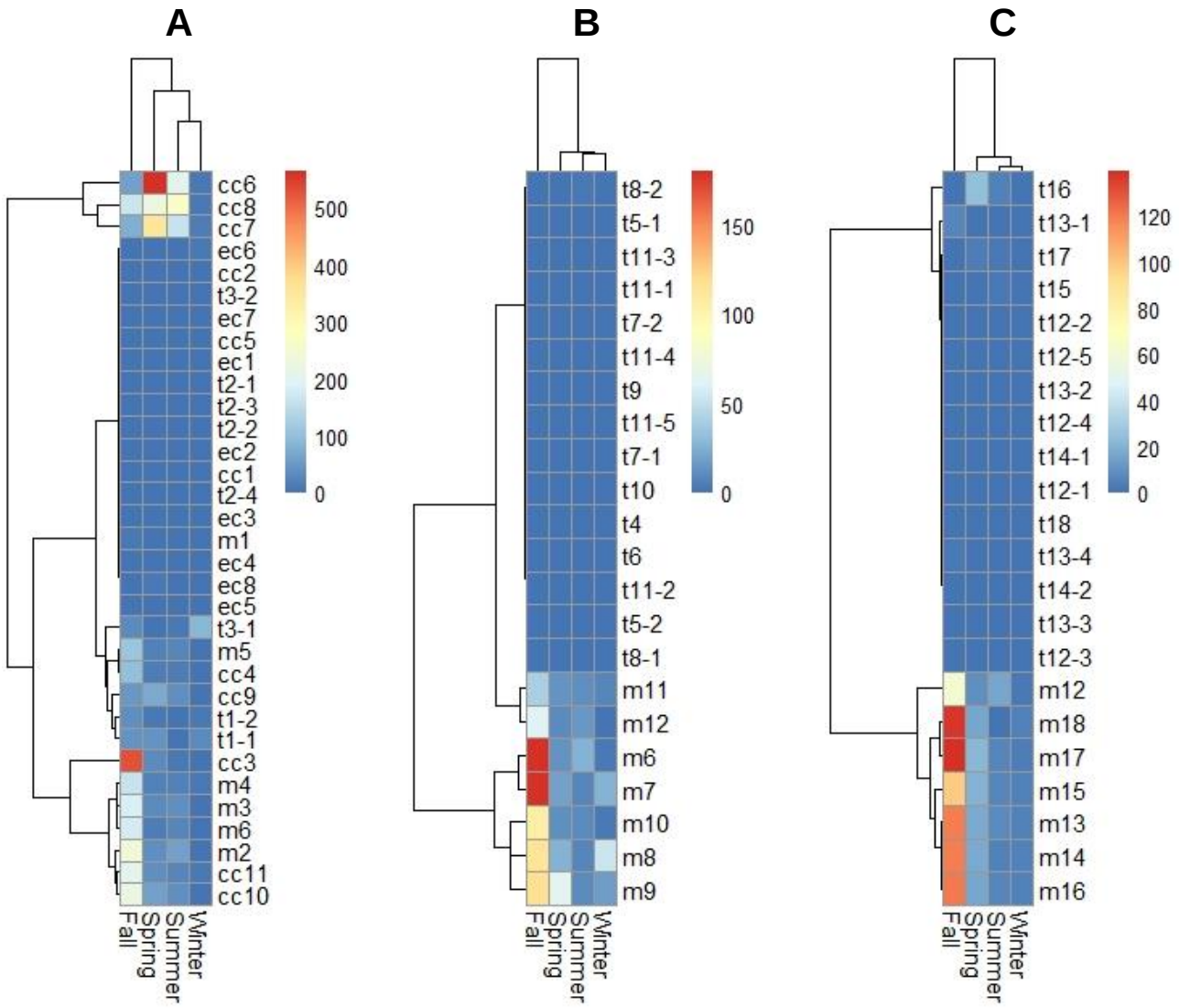

Figure 3.61. Heatmap of TBEP clustered by spatial-temporal concentration (µg/L) profiles in (A) ***industrial***, (B) ***transition*** and (C) ***agricultural zones***.

PBDEs are another group of flame retardants included in the list of PS by European Commission. Although their usage has been phased out or decreased (Jin et al., 2016), they were detected at some sampling points. 2,2',4,4',5,5'-Hexabromodiphenyl ether or BDE-153 was present at 7.13 and 3.57 µg/L at sampling point *cc9* receiving the effluent of WWTP of Çorlu Leader OIZ, during summer and spring, respectively (Figure 3.63). In addition to its high bioaccumulation and persistency in the environment, BDE-153 is an endocrine disruptor compound (Lu et al., 2018). Other than BDE-153, BDE-154 (2,2',4,4',5,6'-Hexabromodiphenyl ether) was found at sampling point *cc8* (3.22 µg/L) in fall and at *cc6* next to Velimeşe OIZ and *t1-2* next to Büyükkarıştıran OIZ in spring at respective concentrations of 7.43 and 4.26 µg/L, respectively. 0.59 µg/L of BDE-203 (2,2',3,4,4',5,5',6-Octabromodiphenyl ether) was found at sampling point *t2-3* close to a pharmaceutical industry. BDE-205 (2,3,3',4,4',5,5',6-Octabromodiphenyl ether) was found mainly in summer at three sampling

points in ***industrial zone***. It was present at 2.63, 2.55 and 2.71 at sampling points *cc6*, *ec4* and *t1-1*, respectively. Our results indicated that the main source of PBDEs are the facilities located on ***industrial zone***. In addition, the detected concentration of all aforementioned PBDEs exceeded their maximum EQS (0.14 µg/L) set by directive 2013/39/EU. Therefore, presence of PBDEs at those points can lead to health problems for both humans and living organisms. In the literature, PBDEs were studied in several monitoring programs, however, the measured concentrations did not exceed 0.16 ng/L (Sousa et al., 2018).The seasonal concentration profile and the number of sampling points at which flame retardants were detected are given in APPENDIX D (Figure D.6).

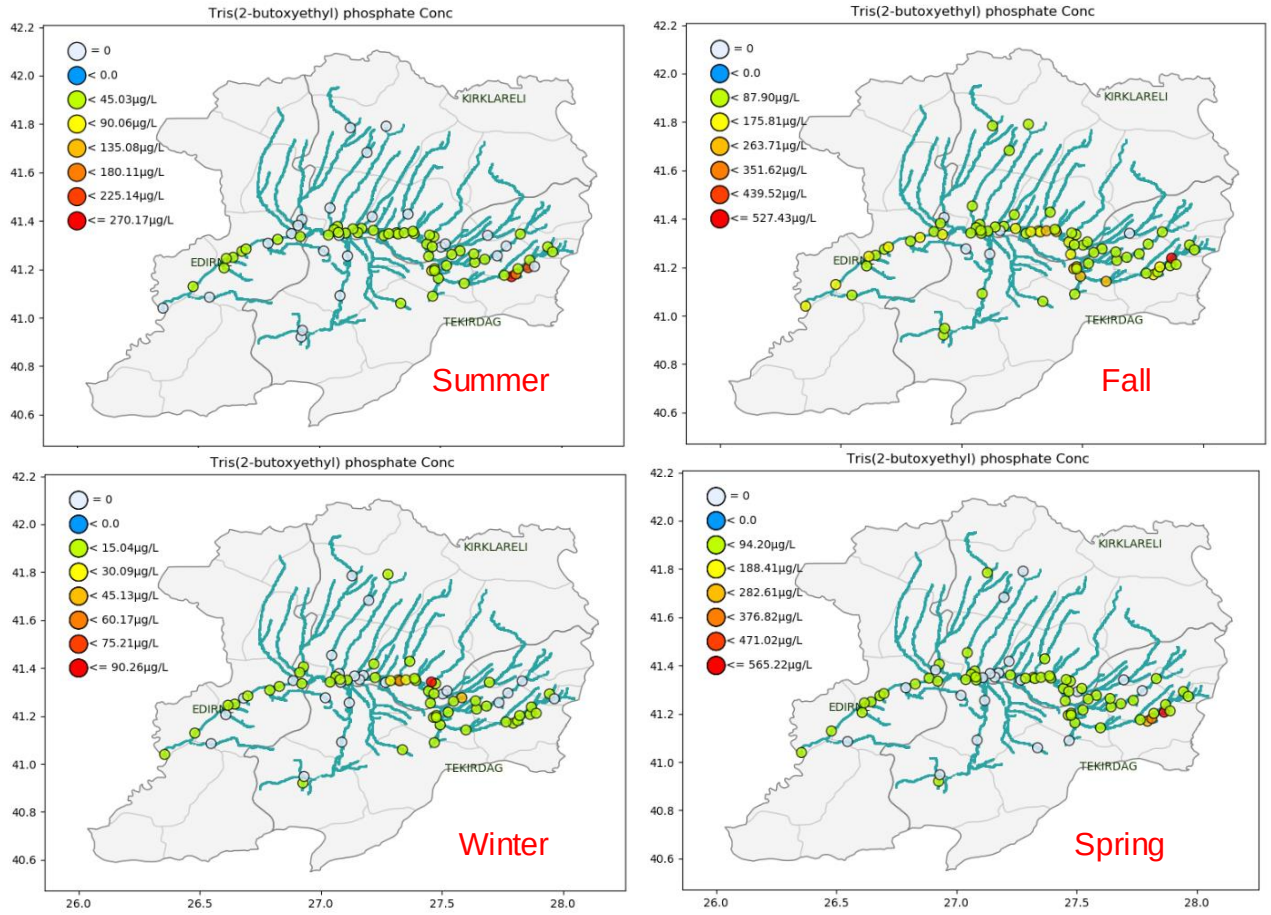

Figure 3.62. Seasonal concentration profiles of TBEP in the Ergene River.

Figure 3.63. Sampling point cc9 representing high BDE-153 concentration during summer and spring samplings.

Plasticizers. Phthalate esters as plasticizers are among the most important and widely used compounds. Among phthalates, DEHP is listed as PS by European Commission. In the literature, DEHP was reported to have the highest concentration in different aquatic environments compared to other phthalates (Edjere et al., 2016, Olujimi et al., 2014). That is why it was monitored in the Ergene River in the course of this study. DEHP was detected in all zone but mainly in ***transition zone*** at 73% of the samples taken from that zone at concentrations between 3.06 and 70.35 µg/L. In ***industrial*** and ***agricultural zones***, this phthalate ester was detected at 64% and 58% of the sampling points in those zones, respectively (Figure 3.64). The highest concentration of DEHP in ***transition zone*** was observed at sampling point *t8-1* which is close to a solid waste disposal site. Whereas *cc8* close to Velimeşe OIZ in ***industrial zone*** and *t13-2* in ***agricultural zone*** close to residential places had the highest DEHP concentrations (Figure 3.64). Giving the fact that DEHP is not bound to the polymers, it is released into the water bodies through WWTPs of industrial facilities using or manufacturing DEHP or leaching from the products. Therefore, it is mainly found in surface waters close to domestic and industrial sectors (Fatoki et al., 2010). For instance, DEHP concentrations as high as 69.92 and 48.69 µg/L was present at *t12-3* and *t16* during summer sampling which are receiving the effluent of WWTP of Kırklareli and Üzünköprü Cities, respectively. In addition, sampling points *t8-2*, *t9*, *t10* and *t11-5* which are also located next to small towns, had relatively high DEHP concentrations (Figure 3.65). The seasonal concentration profile along with the number of sampling points where the DEHP was detected are shown in Figure D.7.

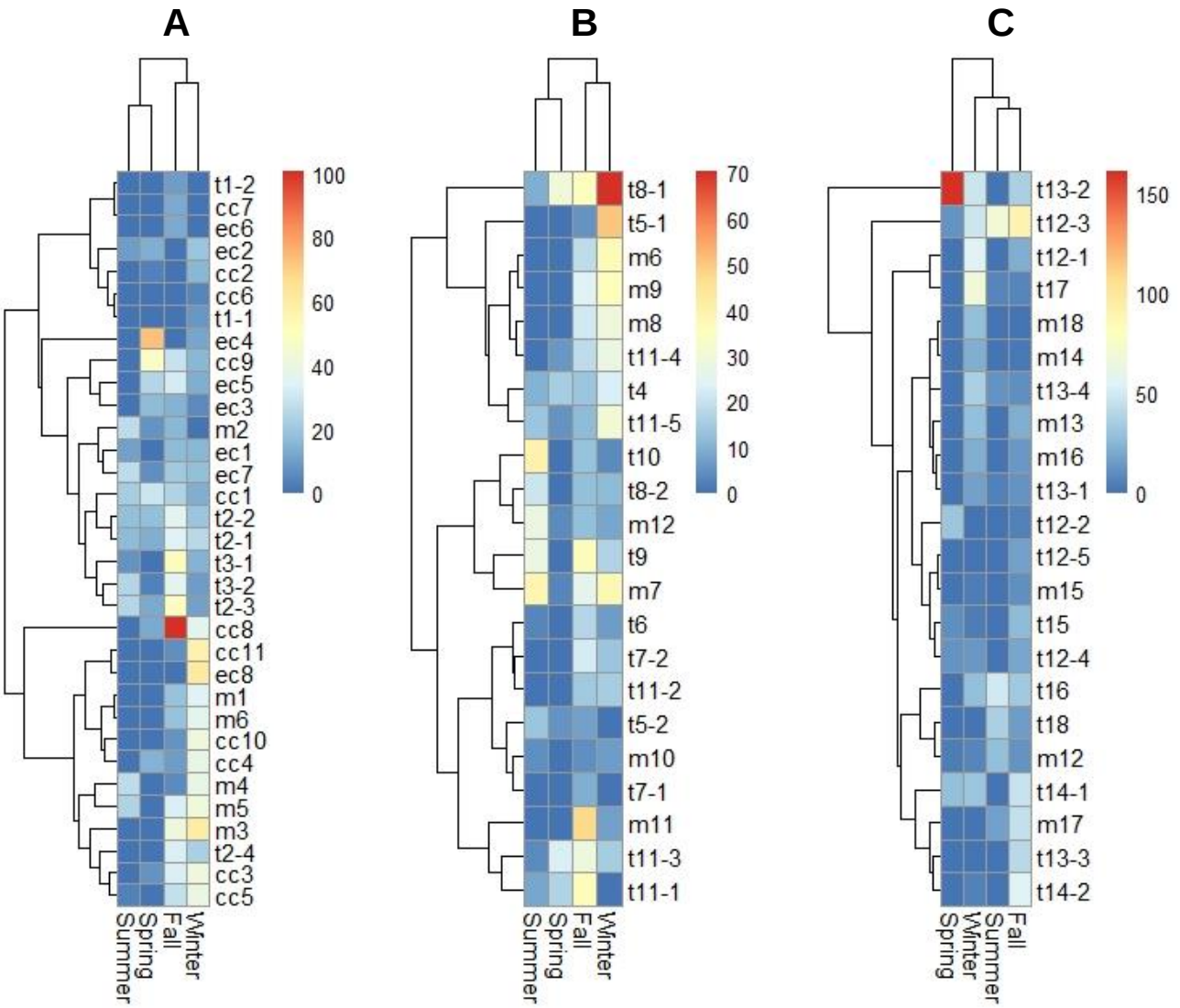

Figure 3.64. Heatmap of DEHP clustered by spatial-temporal concentration (µg/L) profiles in (A) ***industrial***, (B) ***transition*** and (C) ***agricultural zones***.

DEHP concentration at most of the sampling points exceeded its MAC-EQS value of 1.3 µg/L. For instance, DEHP was detected at 68 sampling points during fall and all of them had DEHP concertation more than 1.3 µg/L. Considering inevitable pollution of Ergene River by DEHP, the ecosystem is suffering from the carcinogenic and endocrine disrupting risks of this chemical. A review on the occurrence of DEHP in surface waters throughout the world also revealed the high concentration of this phthalate ester in different WWTPs of different countries (Net et al., 2015). For instance, DEHP was reported to be frequently present (93% of the samples) at concentrations up to 6.35 µg/L, in China (Liu et al., 2014). Other studies performed on Hun River (Li et al., 2015) and Pearl River (Li et al., 2016) in China also reported DEHP at concentration 0.31-34.20 µg/L and up to 8.84 µg/L, respectively.

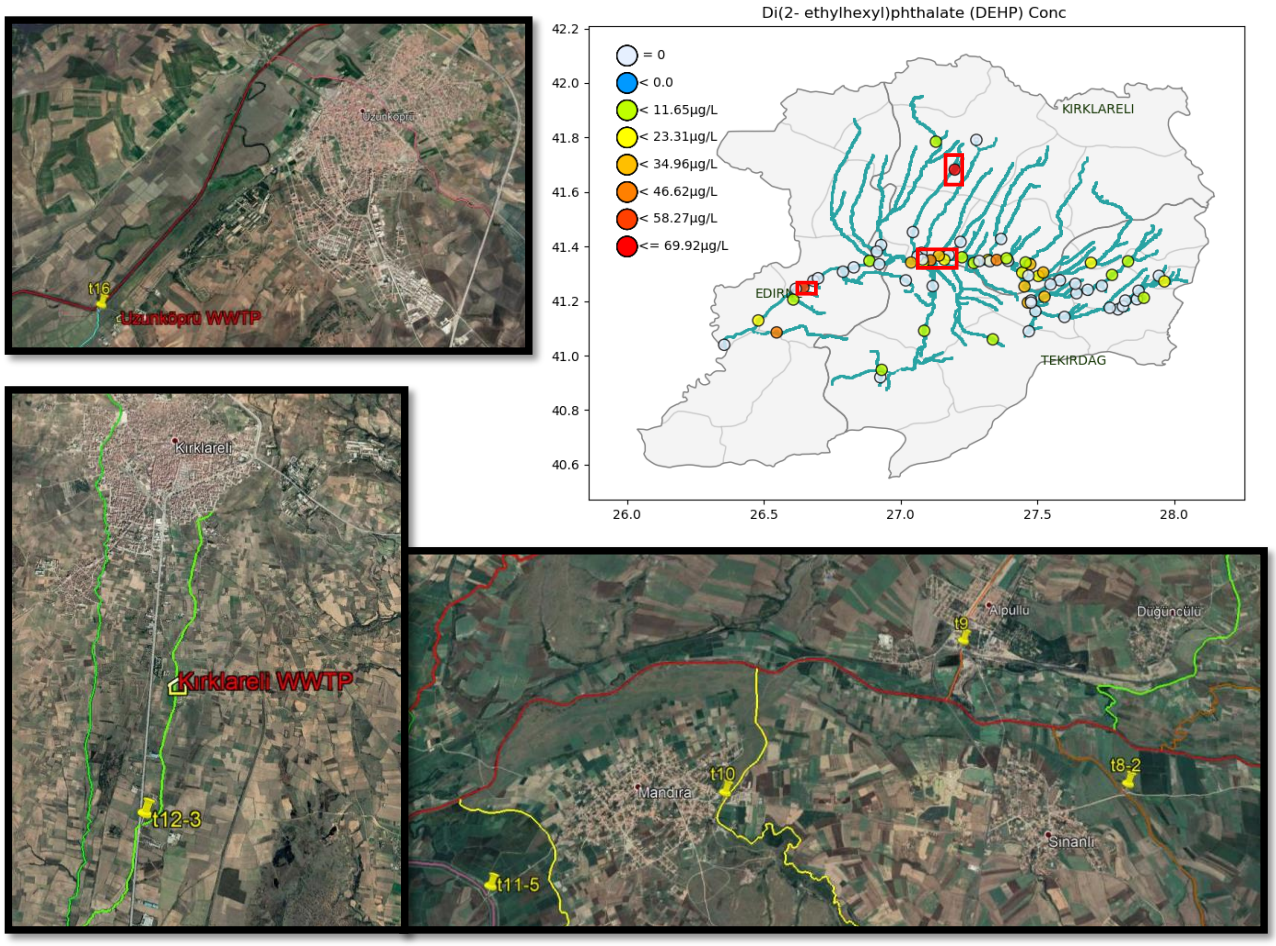

Figure 3.65. Profile of DEHP concentration in summer, Location of sampling points next to cities having high DEHP concentration.

Polychlorinated biphenyls (PCBs). PCBs are anthropogenic pollutants that were used intensively during 1930 and 1980 in electrical equipment (Jing et al., 2018). They are among the initial Persistent Organic Pollutants (POPs) released by Stockholm Convention and are also included in the list of PSs by European Commission. Although their production and usage has been banned, they are still illegally found and used in mainly old electrical utilities (Stockholm Convention, 2008, Eurpean Commission, 2013). In addition to that, they are used in other industrial applications such as production of pesticides, plasticizers, flame retardants and other organic products (Safe, 1994). PCBs were detected in 75, 69 and 30 samples taken from the Ergene River in summer, fall and winter, respectively. PCBs were detected in 61%, 60% and 52% of the analyzed samples taken from ***industrial***, ***transition*** and ***agricultural zones***, respectively. Although detected in all zones, PCBs were present at higher concentrations (up to 467.73 µg/L) in ***industrial zone*** where OIZs are located (Figure 3.66 and Figure 3.67). In ***industrial zone***, the highest concentration of PCBs was mainly measured at sampling points on the Çorlu Creek. In addition, sampling points *ec4* and *ec6* on Ergene Creek, close to Ergene 2 and Ergene 1 OIZs, respectively, *t1-1* and *t1-2* next to Büyükkarıştıran OIZ

as well as *t3-2* next to a textile industry had high PCBs concentrations, particularly in summer and fall (Figure 3.66 and Figure 3.67). On the contrary, in ***transition*** and ***agricultural zones***, PCBs were often present at their highest concentrations at sampling points on the main stream suggesting that PCBs are originated from ***industrial zone***. High concentrations of PCBs up to 379.57 µg/L at *t4* in ***transition zone*** and up to 199.02 µg/L at *t16* in ***agricultural zone*** were also determined. The seasonal concentration profile along with the number of sampling points at which PCBs were detected are given in Figure D.8.

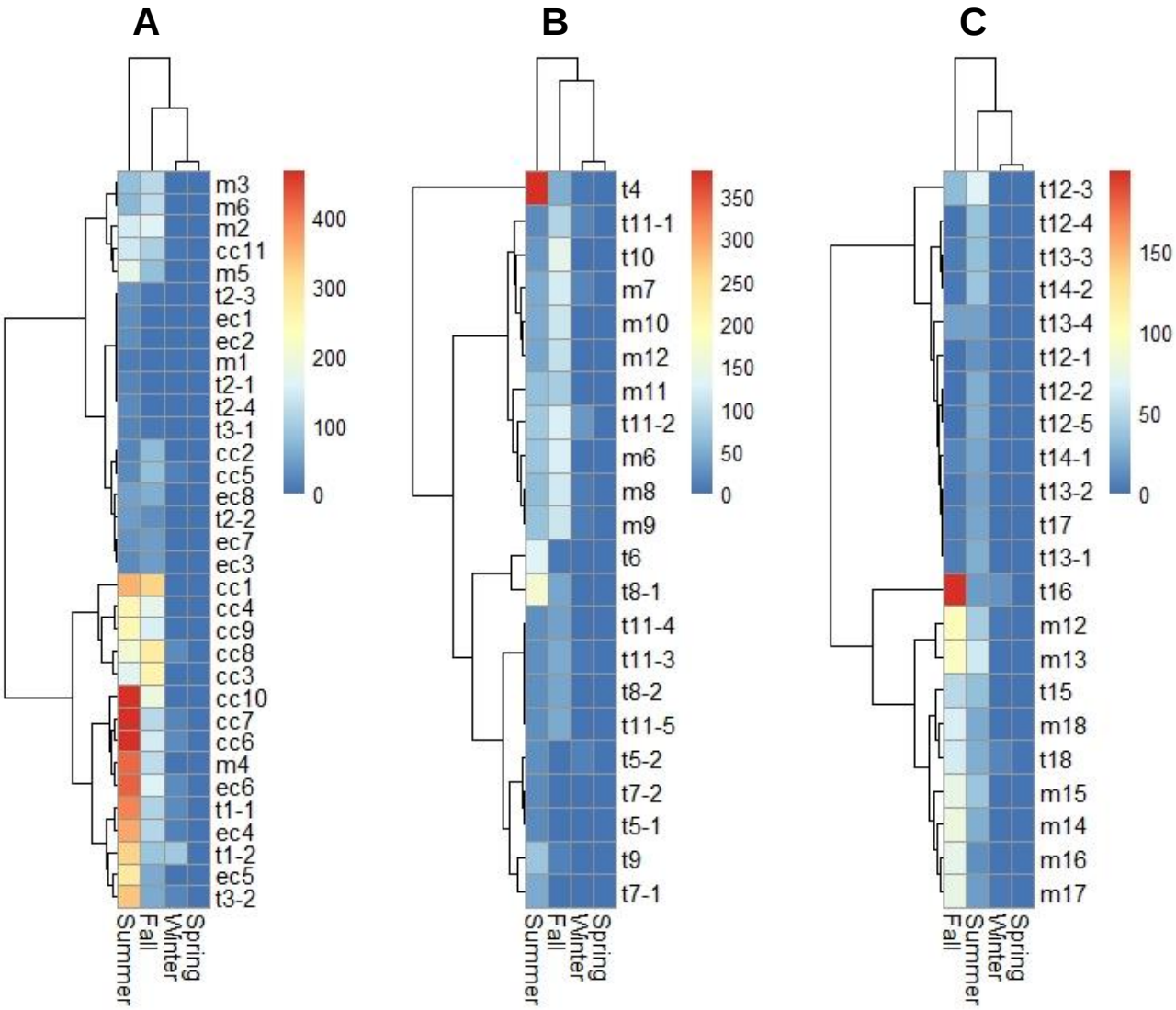

Figure 3.66. Heatmap of PCBs clustered by spatial-temporal concentration (µg/L) profiles in (A) ***industrial***, (B) ***transition*** and (C) ***agricultural zones***.

PCBs as important PSs were also reported in some studies. For instance, PCBs at 1.58 -62.7 ng/L in surface waters in Beijing, China (Shao et al., 2016) and 0.8-6.4 ng/L in Chenab River in Pakistan (Eqani et al., 2015) was reported. In Europe, PCBs were determined at concentration between 0.12

and 0.24 ng/L in surface water in Bosna river in Bosnia and Herzegovina (Harman et al., 2013) and between 0.41 and 2.17 ng/L in surface waters of Brno, Czech Republic (Jalova et al., 2013).

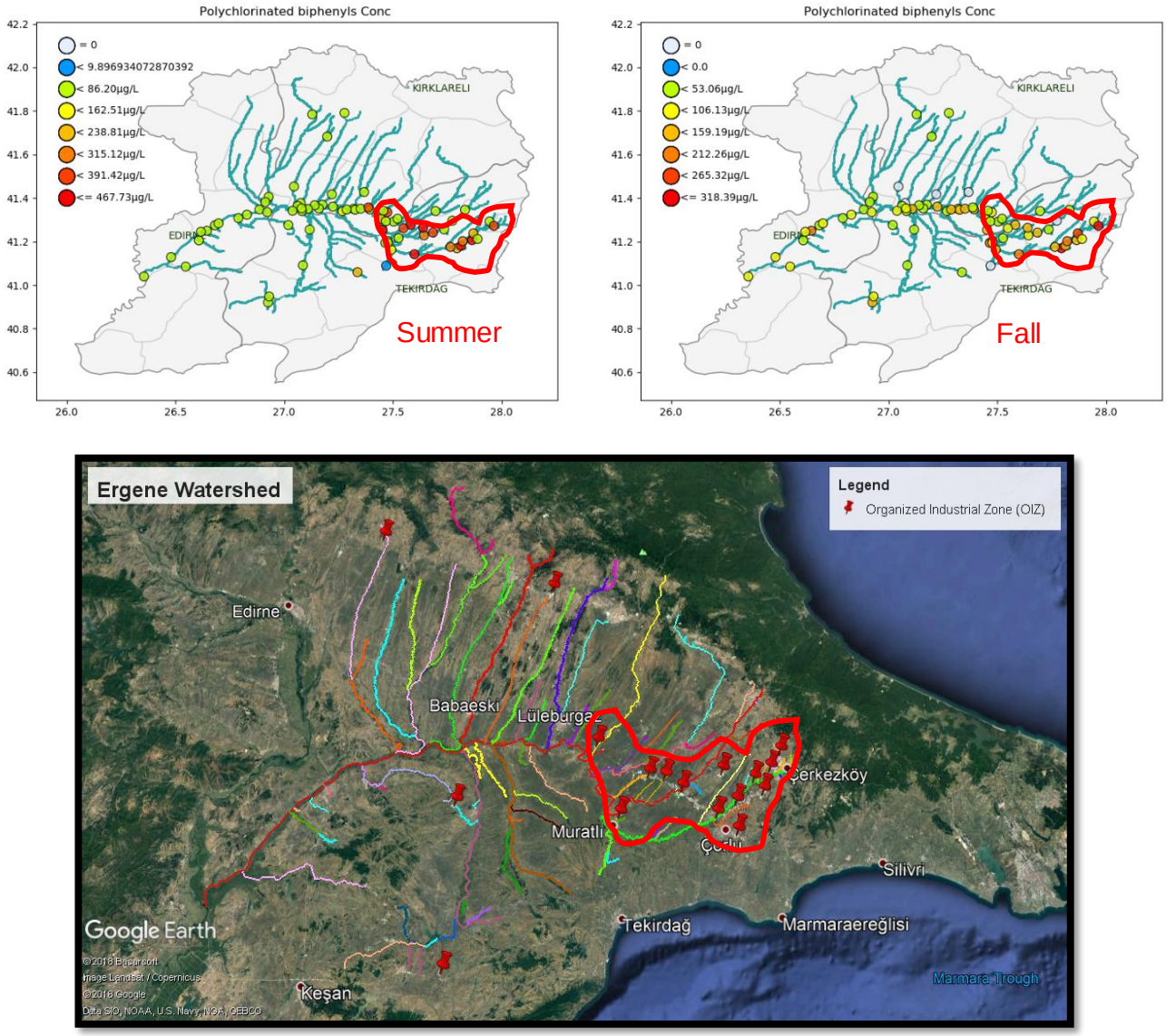

Figure 3.67. Concentration profile of PCBs in summer and fall, location of OIZs in the Ergene Watershed.

Polycyclic Aromatic Hydrocarbons (PAHs) as Combustion Byproducts. Listed as PS by European Commission (EC), PAHs are chemicals mainly generated during natural or anthropogenic combustion processes. Considering their anthropogenic generation, PAHs are released by various industries such as refineries, power plants, aluminum industries, food processing, paper industries and other sectors that involve the combustion of coal, wood and fuels (Gupta, 2018, Manzetti, 2013, Abdel-Shafy and Mansour, 2016). In Ergene River, 13 PAHs were monitored. All of them were detected in the samples taken from the Ergene River. Among them, benzo[a]pyrene detected at 22, 8, 11 and 18 and anthracene at 12, 18, 14 and 12 sampling points in summer, fall, winter and spring,

respectively, were the most frequently detected PAHs. Both of them were mainly detected in ***industrial zone***. In ***industrial zone***, benzo[a]pyrene was detected in 27% of the samples taken from that zone at concentrations between 0.01 and 0.98 µg/L while anthracene was in 28% at 9.41-851 µg/L in all seasons (Figure 3.68). The highest concentrations of benzo[a]pyrene were measured at sampling points *t1-2* and *t1-1* close to Büyükkarıştıran OIZ, *t3-1* close to Evrensekiz OIZ, *cc7* next to Velimeşe OIZ and *ec8* close to Muralı OIZ which was more than its MAC-EQS (0.27 µg/L) (Figure 3.68). In other regions of the world, benzo[a]pyrene was present at concentrations between 0.9 and 11.3 ng/L in Slotan Abad River Iran (Kafilzadeh, 2015) and up to 1.35 µg/L in the Great Lakes tributaries in USA (Baldwin et al., 2016).

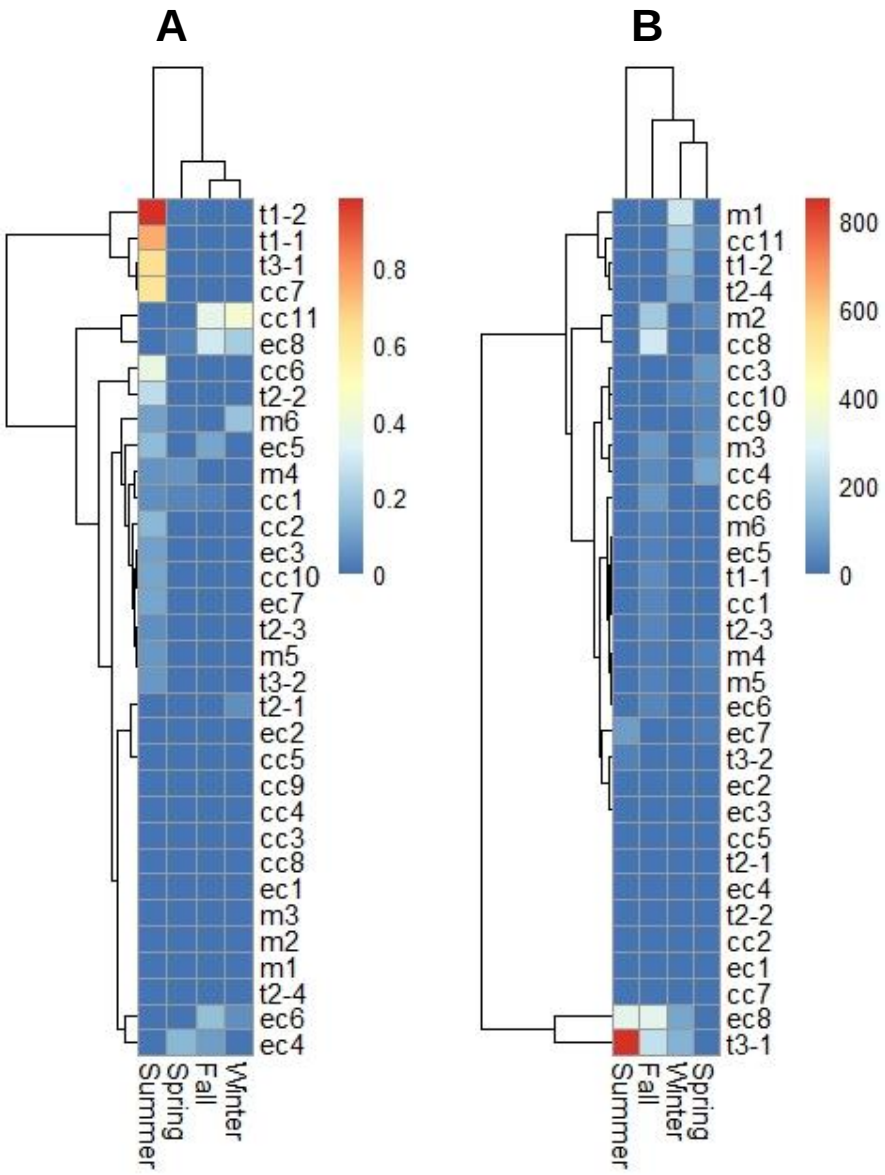

Figure 3.68. Heatmap of (A) benzo[a]pyrene (B) anthracene clustered by spatial-temporal concentration (µg/L) profiles in ***industrial zone***.

Anthracene was present in the Ergene River at mean concentrations of 29.29, 21.93, 28.77 and 6.62 µg/L in summer, fall, winter and spring samplings, respectively, exceeded its AA-EQS (0.1 µg/L) set by European Commission.

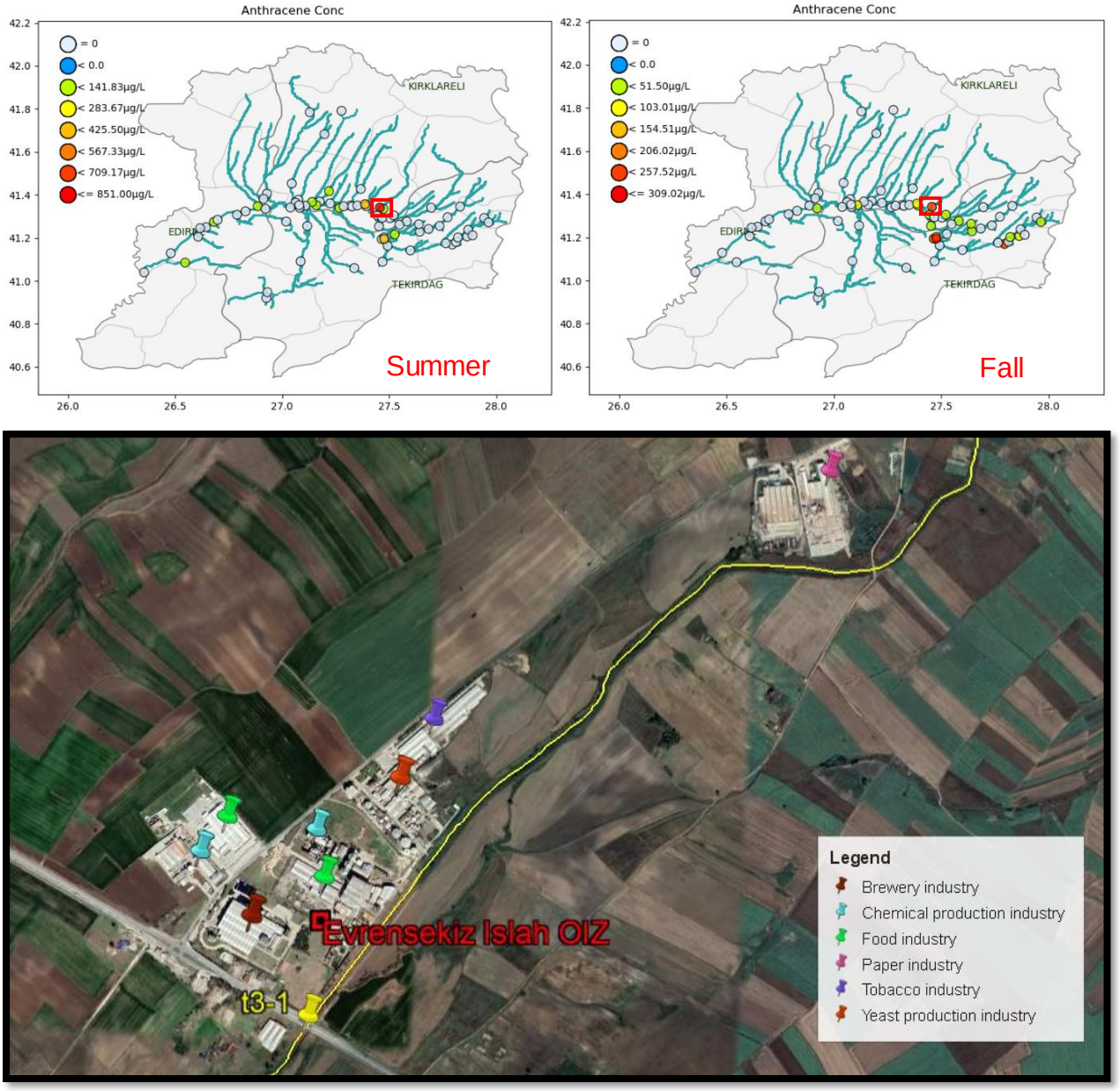

Figure 3.69. Concentration profile of anthracene in summer and fall, location of sampling point *t3-1* next to the Evrensekiz OIZ in ***industrial zone***.

In addition, anthracene was present at its highest concentrations in samples taken from *t3-1* and *ec8* in ***industrial zone***. Sampling point *t3-1* which is located next to the Evrensekiz OIZ consisting of food processing, chemicals production, tobacco and paper industries (Figure 3.69), is the main source of the PAHs. Anthracene up to 0.43 µg/L in Cauca River in Columbia (Sarria-Villa et al., 2016) and up to 2.5 µg/L in Ovia River in Nigeria was reported in the literature (Tongo et al., 2017).

In addition to anthracene and bezno[a]pyrene, fluoranthene at concentration as high as 19.44 µg/L was measured at that point. Fluoranthene was also detected at sampling points located next to Velimeşe OIZ, Çorlu Leather OIZ and Ergene 1 OIZ and its concentration at those points was more than its recommended MAC-EQS of 0.12 µg/L.

1,3-dinitropyrene, 1,6-dinitropyrene, 1,8-dinitropyrene as nitro-PAHs (NPAHs) were only detected in ***industrial zone***, but in all seasons. They were present at concentrations up to 2.63, 2.71 and 2.45 µg/L, respectively (Figure 3.70). Sampling points *t1-1* close to Büyükkarıştıran OIZ, *ec4* close to Ergene 2 OIZ, *ec6* next to Ergene 1 OIZ and *cc6* close to Velimeşe OIZ were points at which high concentrations of NPAHs were measured (Figure 3.70). All of the aforementioned OIZs consist of high number of textile and dye facilities using NPAHs in their processes (Arlt, 2005).

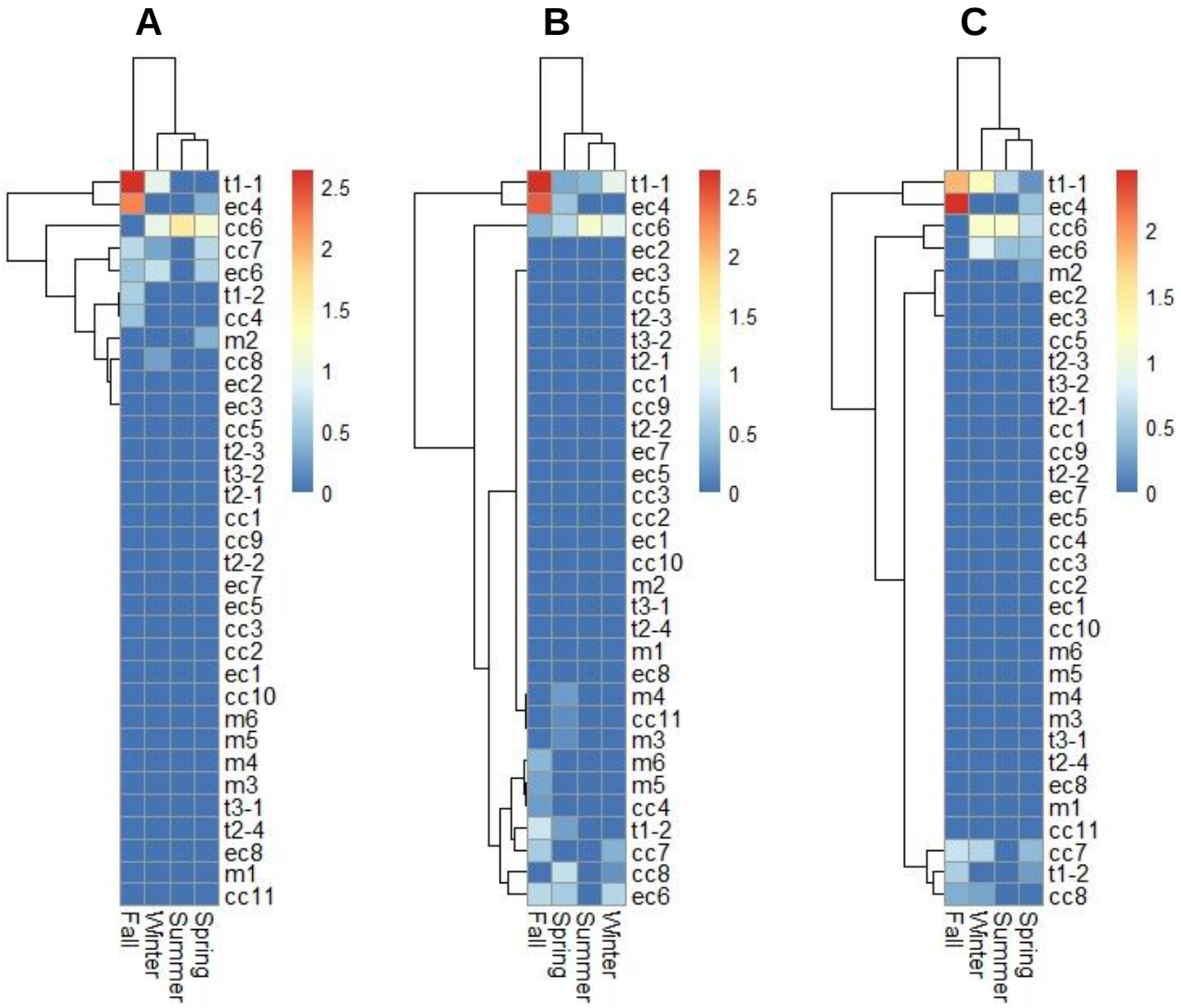

Figure 3.70. Heatmap of (A) 1,3-dinitropyrene, (B) 1,6-dinitropyrene and (C) 1,8-dinitropyrene clustered by spatial-temporal concentration (µg/L) profiles in ***industrial zone***.

Based on the occurrence and distribution of PAHs in the Ergene River, it is concluded that the region is under high exposure to PAHs. In addition, giving the fact that PAHs are carcinogen, mutagen and persistent chemicals, therefore human and aquatic lives face inevitable risks. The seasonal concentration profile along with the number of sampling points where the aforementioned PAHs and others including 3-nitro-benzanthrone, 2-(2-Naphthalenyl)-benzothiophene, benzo[b]-fluoranthene, benzo[a]-anthracene, indeno[1,2,3-cd]-pyrene, benzo[k]-fluoranthene and benzo[ghi]-perylene were detected, are given in Figure D.9.

Corrosion inhibitors. Four benzotriazoles and dicyclohexylamine in the group of corrosion inhibitors were monitored in the Ergene River. Among them, benzotriazoles were the most abundantly detected ones. Benzotriazoles are chemical substances that are mainly used as corrosion inhibitor in metal coatings, textiles, dishwasher detergents and other industries and they also have endocrine disrupting properties (Wang et al., 2016b, Avagyan et al., 2015, Liu et al., 2017a). Benzotriazoles have been detected in municipal wastewaters emerged from the laundering of the clothes in houses, as well (Avagyan et al., 2015). Thus, their wide usage in different industrial processes and domestic activities have resulted in their high occurrence in the Ergene River, as well. Among them, 1,2,3-B found in 68, 51, 46 and 54, 4-M-1H-B in 58, 58, 57 and 64 and 5-M-1H-B in 63, 65, 38 and 63 samples taken from the Ergene River in summer, fall, winter and spring, respectively, were the most frequently corrosion inhibitors. It was reported that 4-M-1H-B and 5-M-1H-B as the derivatives of 1,2,3-B are introduced in a mixture which clarifies their similar detection frquency (Herzog et al., 2014). The average concentration of 1,2,3-B in the Ergene River was 8.14, 8.20, 1.66 and 2.04 µg/L in summer, fall, winter and spring, respectively. In each season, the average concentration of 1,2,3-B was more than 4-1H-M-B, and 5-1H-M-B which shows the wide usage of 1,2,3-B compared to its derivatives. Moreover, the degradation of 4-1H-M-B and 5-1H-M-B may result in the production of 1,2,3-B (Liu et al., 2013c) which can be another major source of 1,2,3-B's higher concentration. 1,2,3-B was mainly found in ***industrial zone*** (90% of the samples taken from that zone) at 0.23-117.55 µg/L, in all seasons while it was only detected at 62% and 58% of the sampling points in ***transition*** and ***agricultural zone***, respectively (Figure 3.71 and Figure 3.72). In ***industrial zone***, the highest concentrations of 1,2,3-B were measured at sampling point *cc5*, *cc8* and *ec4* close to Veliköy, Velimeşe and Ergene Creek OIZs, respectively (Figure 3.71 and Figure 3.72). While in ***transition*** and ***agricultural zones***, the highest 1,2,3-B concentrations were observed in the samples taken from the main stream suggesting that this chemical is originated from the ***industrial zone*** (Figure 3.71 and Figure 3.72). Different industries including metals, textiles and dyes are responsible for benzotriazoles discharge into the Ergene River in those points. Benzotriazoles presence in the surface waters have been reported in different regions in the literature as well. Reemtsma et al. (2010) found

concentrations between less than 0.05 and 0.5 µg/L and between 0.2 and 0.5 µg/L of 1,2,3-B and 4-M-1H-B in the Rhine and Elbe Rivers in Germany, respectively (Reemtsma et al., 2010). 1,2,3-B and 5-M-1H-B in seven rivers in Switzerland were studied where the highest mean concentration of 2.68 and 0.47 µg/L in Glatt River was quantified and recorded (Giger et al., 2006). 1,2,3-B, 4-M-1H-B and 5-M-1H-B were present at respective concentration ranges of 38-1,474 ng/L, 25-952 ng/L and 25-281 ng/L in Hengstbach and Hegbach Rivers in Germany as well (Kiss and Fries, 2009).

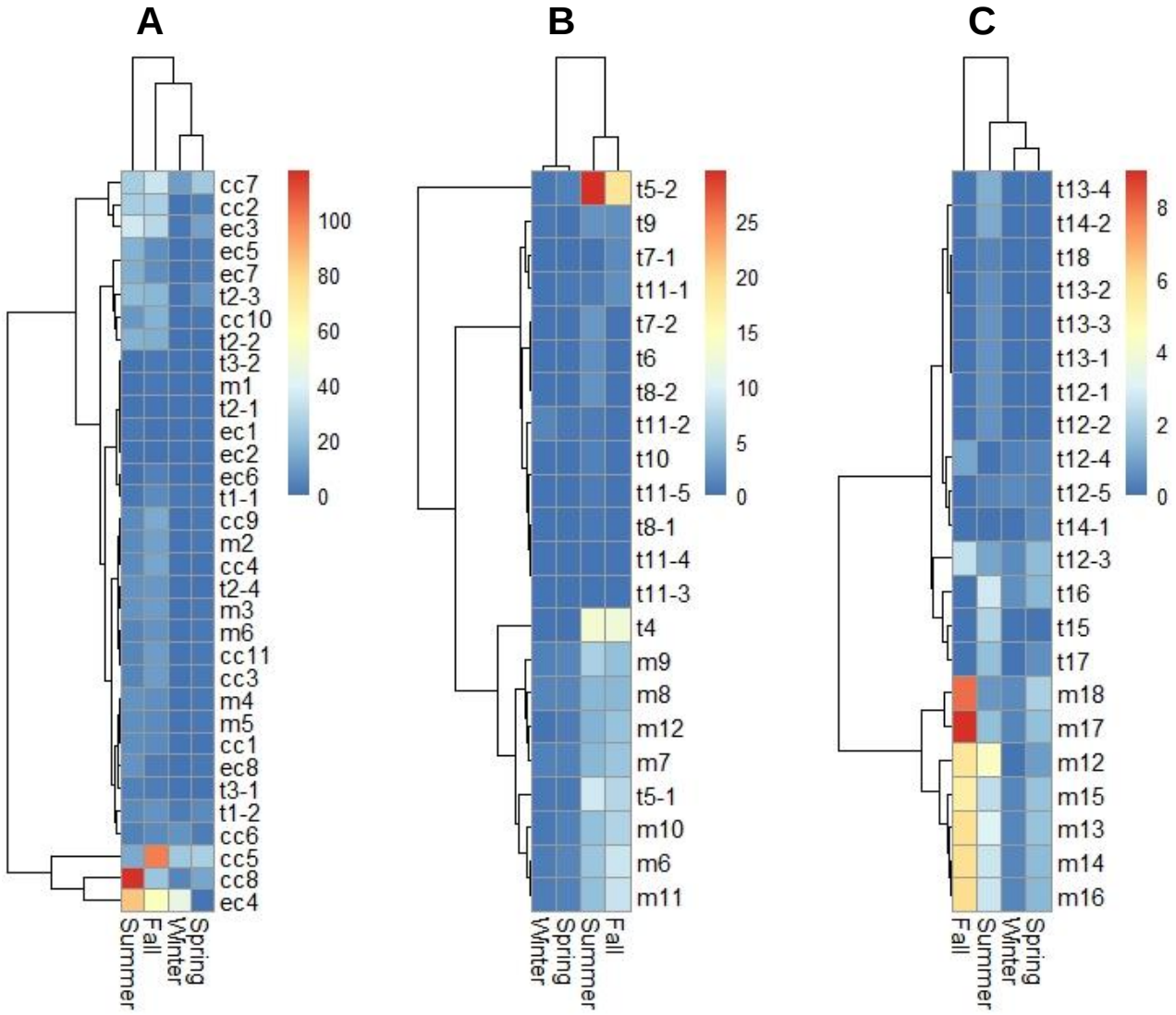

Figure 3.71. Heatmap of 1,2,3-B clustered by spatial-temporal concentration (µg/L) profiles in (A) ***industrial***, (B) ***transition*** and (C) ***agricultural zones***.

The seasonal concentration profile of the aforementioned three benzotriazoles as well as 5,6-D-1H-B and dicyclohexylamine, along with the number of sampling points where they were detected, are given in APPENDIX D (Figure D.10).

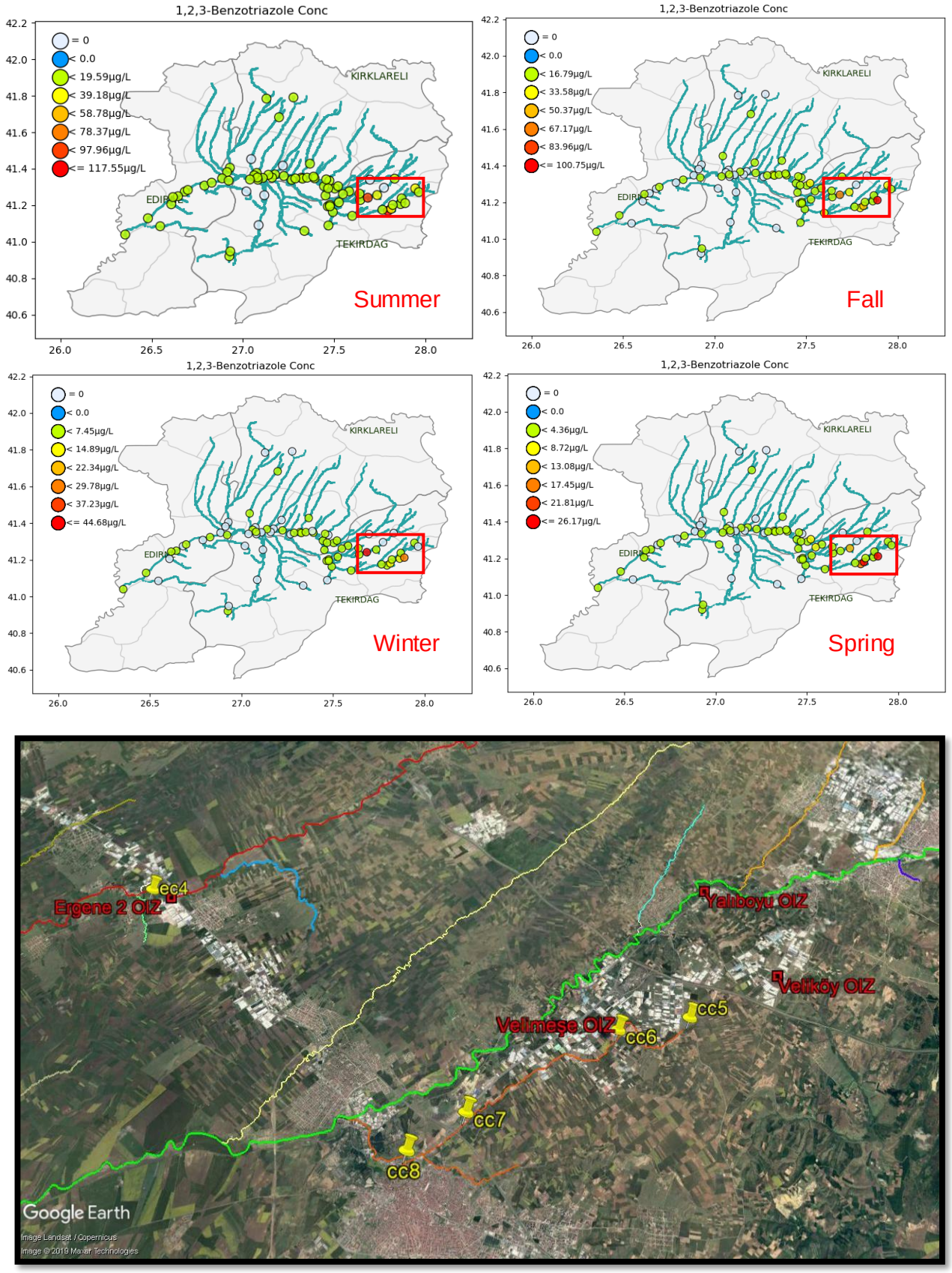

Figure 3.72. Seasonal distribution of 1,2,3-B in Ergene watershed, OIZs in Ergene creek and Çorlu creek and Büyükkarıştıran OIZ and Evrensekiz OIZ responsible for benzotriazoles discharges.

Chemicals in production of different products. These industrial chemicals are mainly used as the main ingredient in the manufacturing of other products such as dyes, chemicals, rubbers, pesticides, etc. Sixteen chemicals classified in this group including HMMM, chloroanilines, benzothiazoles, benzylamines and etc. were monitored in the Ergene River. Among them, N-phenyl-2-naphthylamine, hexachlorobenzene and 2,4-dinitrophenol were detected in none of the samples while hexamethoxymethylmelamine (HMMM) and chloroanilines were found in most of the samples. HMMM was detected in 66, 74, 65 and 61 samples taken from the Ergene River. In addition, HMMM was the chemical that was present at highest concentration compared to other chemicals analyzed in the course of this research. Although found in most of the samples, HMMM was mainly detected in ***industrial zone*** (97% of the samples taken from that zone) in all seasons at concentrations between 6.70 and 329,166 µg/L (Figure 3.73 and Figure 3.74). In ***industrial zone***, the highest concentrations of HMMM was recorded at mainly *t1-1* and *t1-2* on the tributary next to Büyükkarıştıran OIZ as well as at *cc6*, *cc7* and cc8 on the Çorlu Creek, close to Velimeşe OIZ, respectively (Figure 3.73, Figure 3.74 and Figure 3.75). HMMM is mainly used as coating agent in textile, metal, paper and plastic industries in those OIZs. On the other hand, in ***transition*** and ***agricultural zones***, the highest HMMM concentrations were recorded at the sampling points on the main stream (Figure 3.73). This represents that HMMM released as a result of industrial activities in ***industrial zone*** was carried to the following zones by the main stream and reached the Maritsa river (*m18*) at which HMMM as high as 15,580.49 µg/L was measured. HMMM was also reported in a study performed on the German rivers where it was present in 51% of the samples at concentrations up to 0.88 µg/L (Dsikowitzky and Schwarzbauer, 2015).

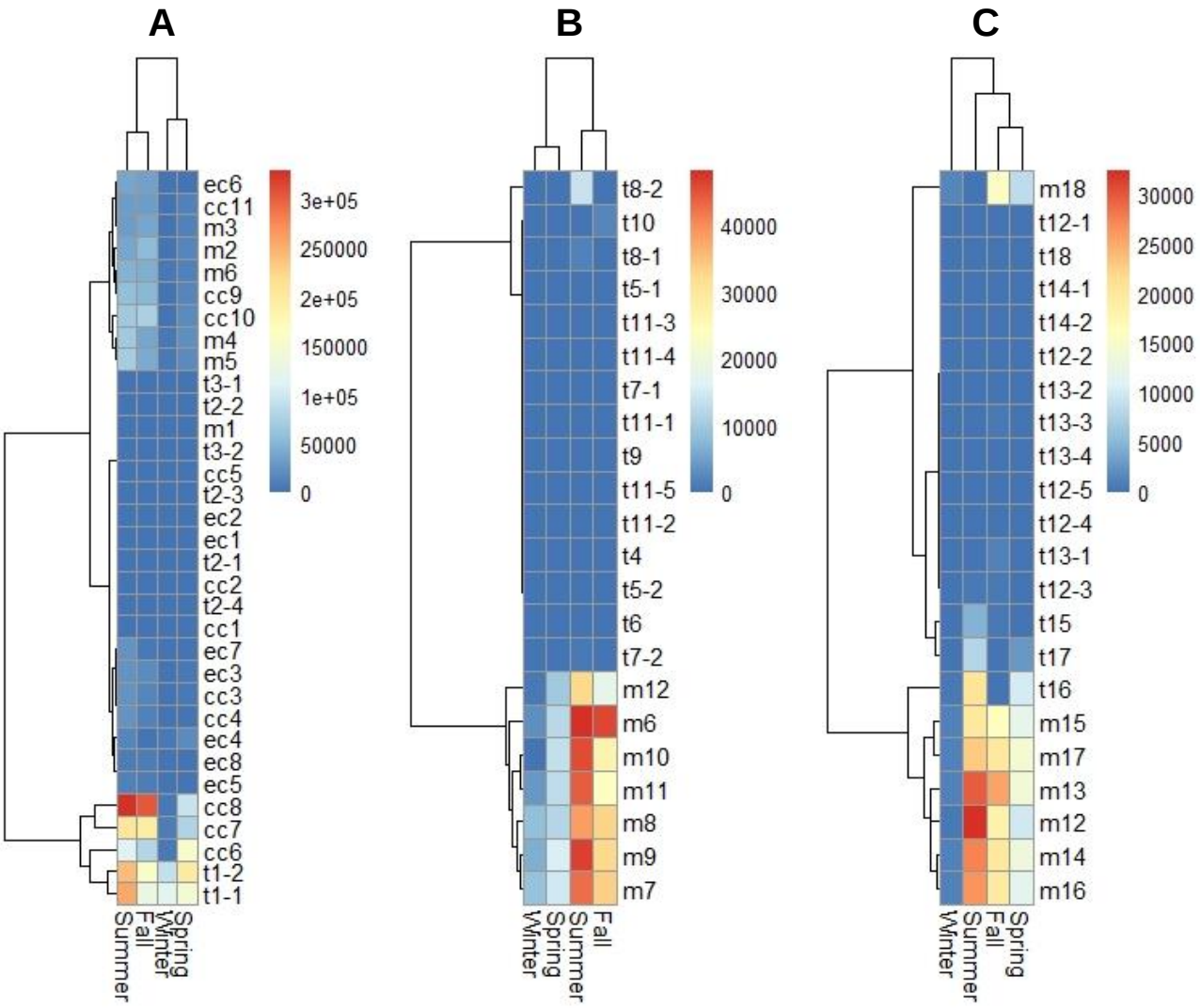

Figure 3.73. Heatmap of HMMM clustered by spatial-temporal concentration (µg/L) profiles in (A) ***industrial***, (B) ***transition*** and (C) ***agricultural zones***.

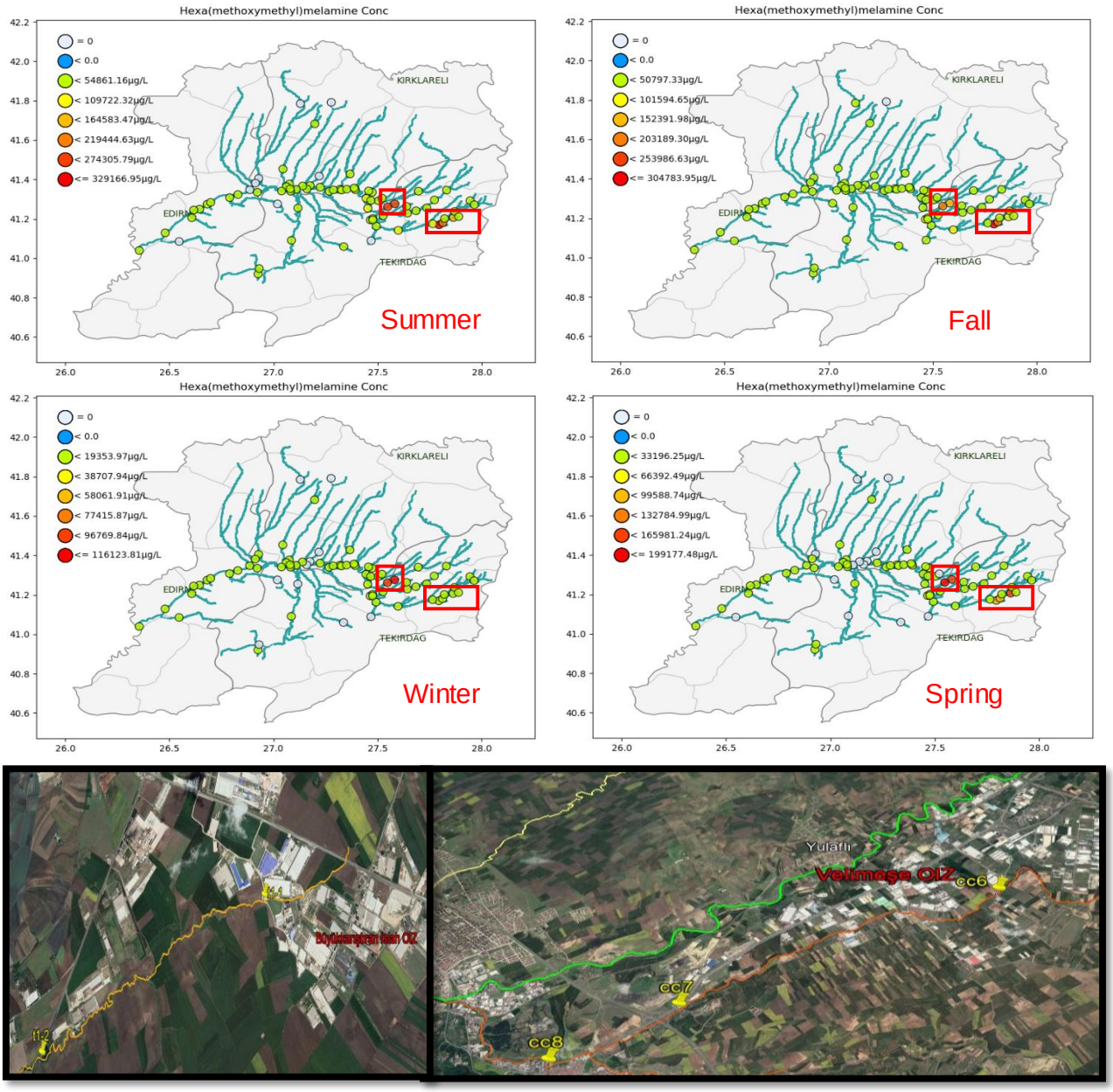

Figure 3.74. Seasonal concentration profile of HMMM in Ergene River, location of the main sources of HMMM next to Velimeşe OIZ (sampling points *cc7* and *cc8*) and Büyükkarıştıran OIZ (sampling points *t1-1* and *t1-2*).

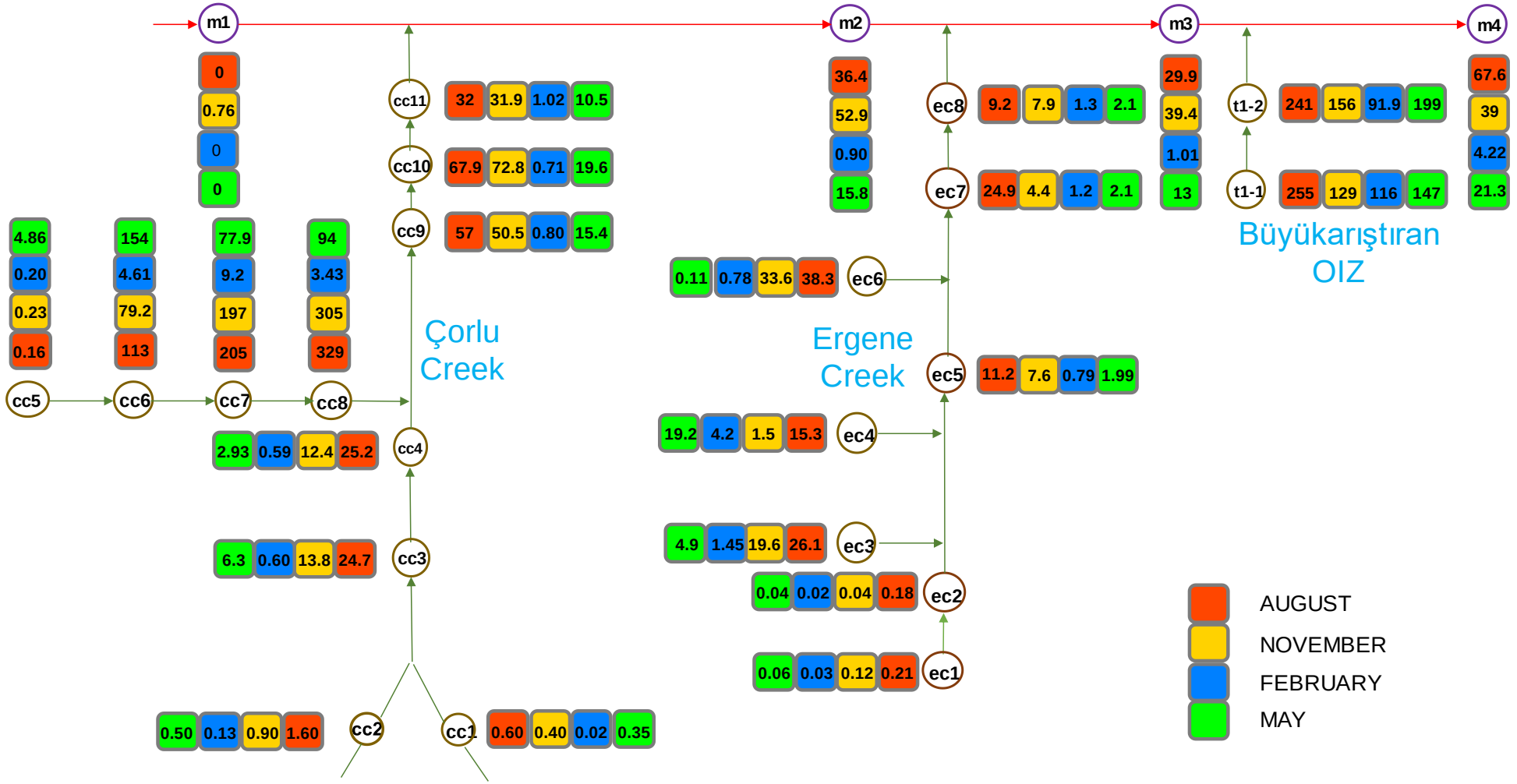

Figure 3.75. Seasonal HMMM concentration (mg/L) in sampling points located next to the three main contributors of HMMM contamination.

3-chloroaniline and 4-chloroaniline are chloroanilines that are used in the production of dyes, pesticides and pharmaceutical drugs. Therefore, their sources can be either the industrial effluents or the metabolism of the pesticides in the environment (Hwang et al., 1987, Okumura et al., 1996). Although both of them has genotoxicity and carcinogenic effects, the latter has higher toxicity (Bohencke et al., 2003).

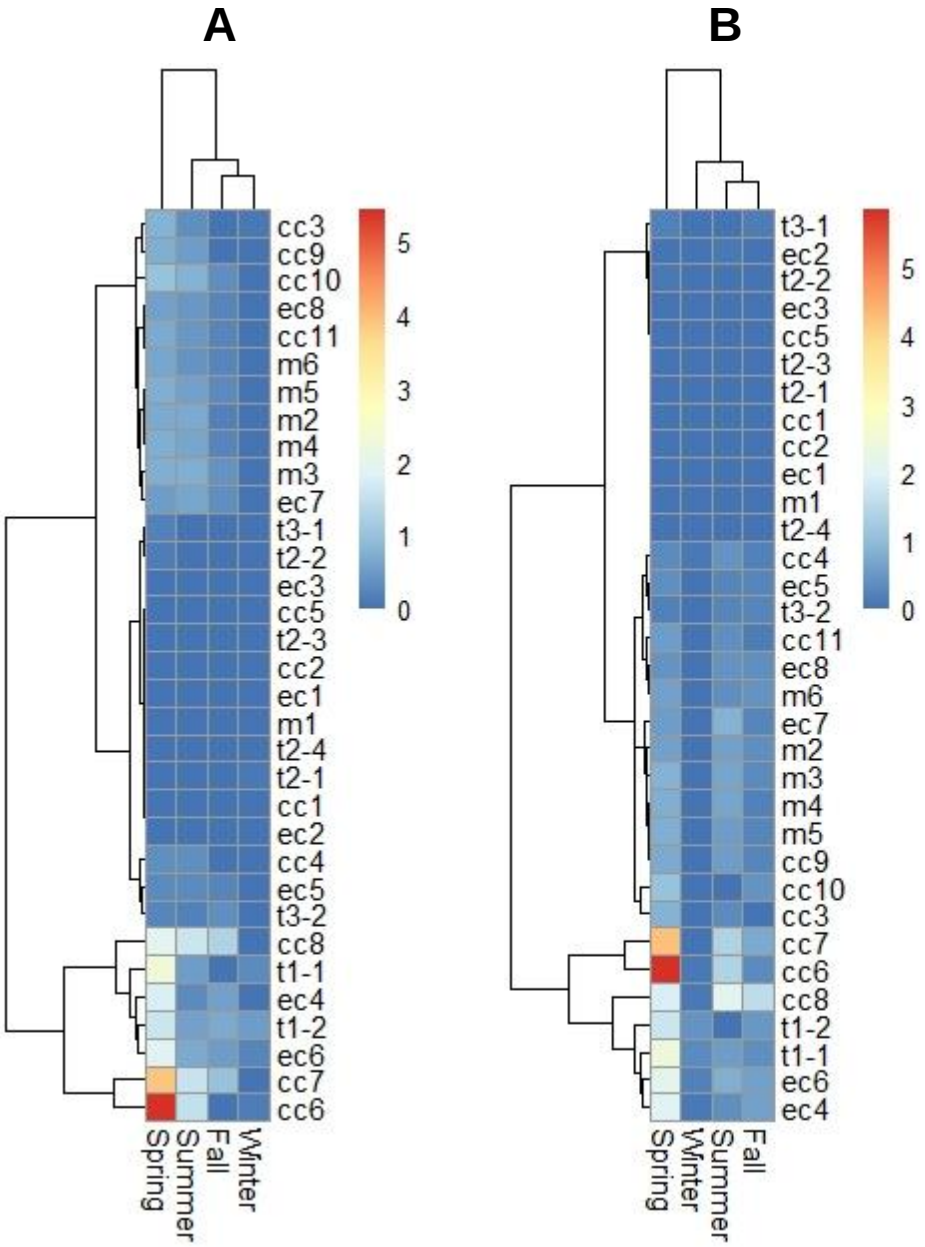

Figure 3.76. Heatmap of (A) 3-chloroaniline (B) 4-chloroaniline clustered by spatial-temporal concentration (µg/L) profiles in ***industrial zone***.

3-chloroaninline was detected in 29, 29, 16 and 36 while 4-chloroaniline in 31, 36, 9 and 36 samples taken from the Ergene River. Both of the chloroanilines were mainly occurred in ***industrial***

zone. During the sampling year, 3-chloroaninline was detected in 53% of the samples taken from ***industrial zone*** at 0.05-5.43 µg/L while 4-chloroaniline was present in 55% of those samples at concentrations between 0.06 and 5.84 µg/L exceeded its EQS (0.005 µg/L). The highest concentration of the two chloroanilines in ***industrial zone*** were mostly measured at sampling point *cc6* and *cc7* on Çorlu Creek close to Velimeşe OIZ (Figure 3.76 and Figure 3.77). In addition, *ec4* (Ergene 2 OIZ) and *ec6* (Ergene 1 OIZ) on Ergene Creek as well as *t1-1* and *t1-2* on the tributary next to Büyükkarıştıran OIZ, were identified as sampling points at which high concentrations of chloroanilines were recorded (Figure 3.76 and Figure 3.77). 3-chloroaniline and 4-chloroaniline were also measured at 0.59 and 2.0 µg/L in a river water in Italy, respectively (Gosetti et al., 2010).

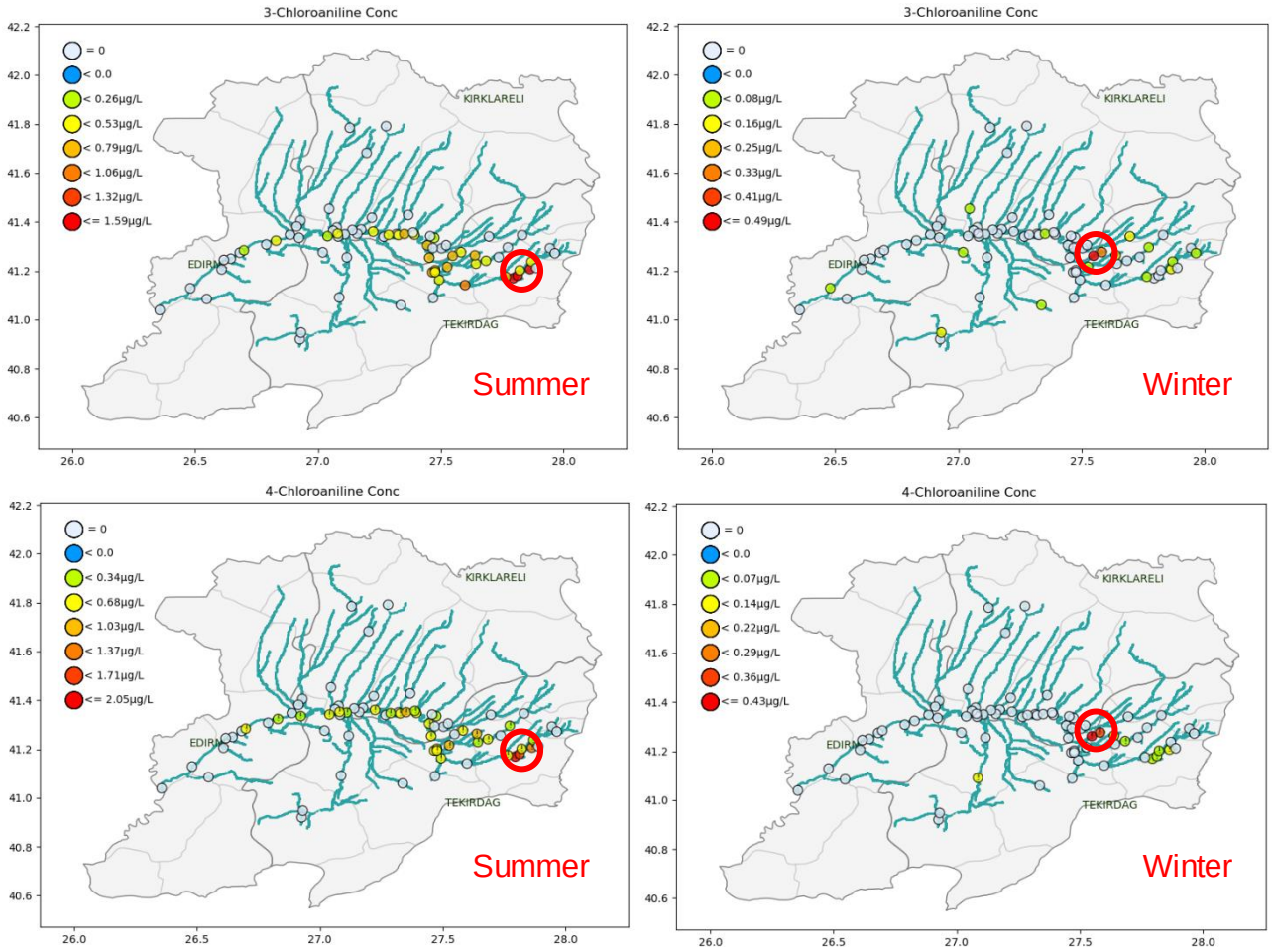

Figure 3.77. Concentration profiles 3-chloroaniline and 4-chloroanailine in the Ergene River in summer and winter.

Benzothiazoles are important ingredients used in the rubber production. Benzothiazoles are also reported to be used as antifogging agent and corrosion inhibitors too (Wang et al., 2016b). Benzothiazole and 2-mercapto benzothiazole are benzothiazole compounds that were analyzed in this study. Among those two, 2-mercapto benzothiazole detected in 20, 23, 1 and 51 out of 75 samples,

whereas benzothiazole was present at maximum 11 sampling points in all seasons. 2-mercapto-benzothiazole was mainly found in ***industrial zone*** (33% of the samples taken from that zone) at concentrations between 0.36 and 23.54 µg/L (Figure 3.78). The highest concentration of 2-mercapto-benzothiazole in ***industrial zone*** was recorded at *cc2* close to Çerkezköy OIZ. In addition, benzothiazole at concentrations as high as 334.51 and 56.74 µg/L was measured at *cc2* as well, indicating this sampling point as the main source of benzothiazoles (Figure 3.78 and Figure 3.79). Benzothiazole was also measured in the surface waters of Netherlands at a mean concentration of 0.01 µg/L (Van Leerdam et al., 2009).

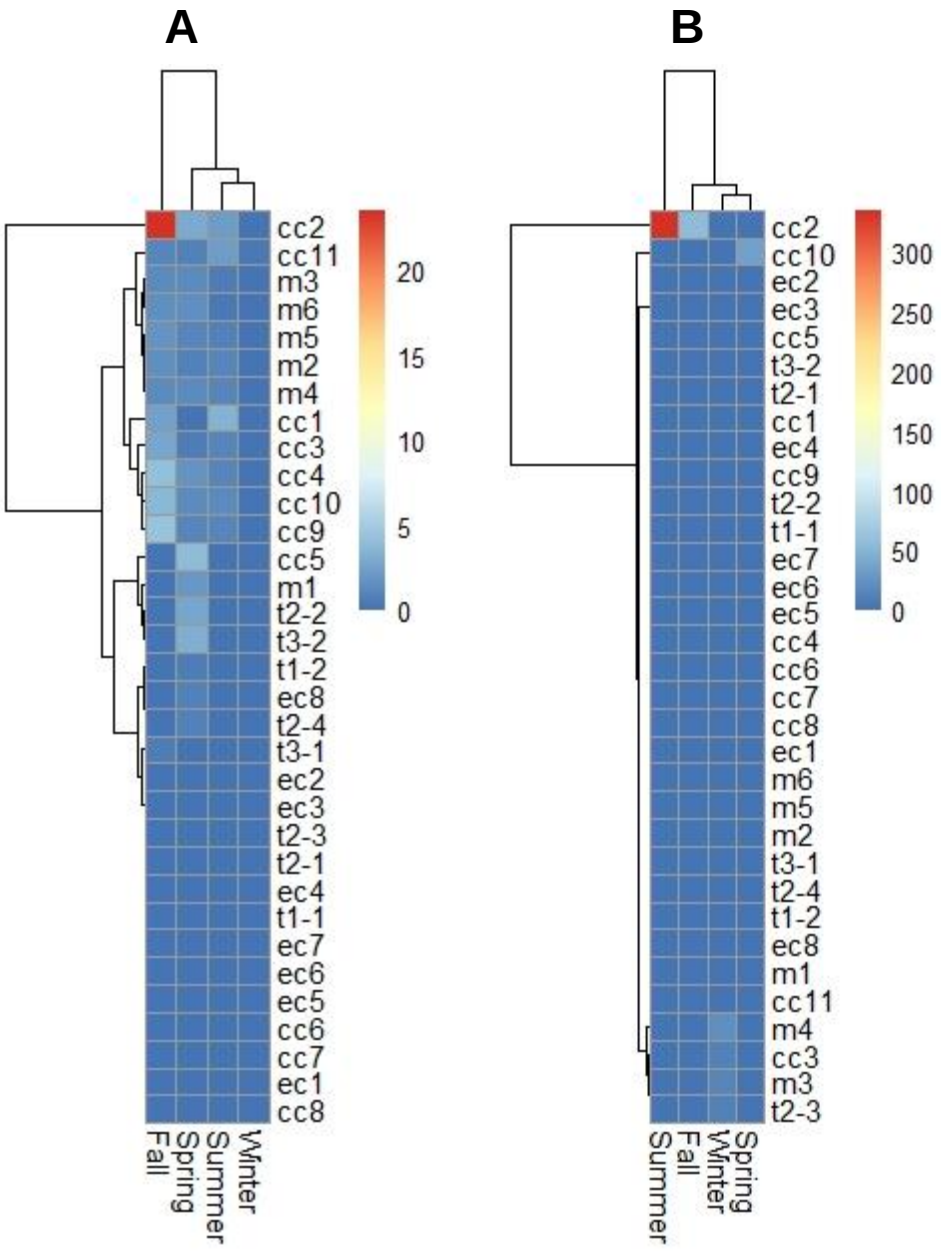

Figure 3.78. Heatmap of (A) 2-mercapto-benzothiazole and (B) benzothiazole clustered by spatial-temporal concentration (µg/L) profiles in ***industrial zone***.

Figure 3.79. Location of sampling point *cc2* at which high concentration of benzothiazoles was detected.

The seasonal concentration profile along with the number of sampling points where the HMMM, chloroanilines, benzothiazoles and others were detected, are given in Figure D.11.

3.3.2.5. Pesticides. Pesticides are mainly used in agricultural applications to repel different groups of pests. In this study, we analyzed the presence of 103 pesticides. Among them, acetochlor, alachlor, azinphos-methyl, bifenox, boscalid, clofentazine, chlothianidin, cyromazine, diazinon, dimethomorph, ethofumesate, fenarimol, fenthion, fluopyram, fluquinconazole, fosthiazate, isoproturon, linuron, malathion, methamidophos, methidathion, methomyl, methoxyfenozide, metrafenone, pinoaden, pyrimethanil, simazine, tolfenpyrad, triasulfuron, triclosan and triphenyltin were not detected. Out of 72 pesticides found in the Ergene River, acetamiprid, carbendazim, diuron and N,N-diethyl-m-toluamide were the most frequently detected ones.

Acetamiprid is among the eight pesticides in the Watch List introduced by the European Commission. Acetamiprid detected in 42, 39, 18 and 20 samples taken from the Ergene River in summer, fall, winter and spring, respectively. It was mainly detected in ***industrial zone*** (56% of the samples taken from that zone) at concentrations between 0.03 and 2.86 µg/L in all seasons (Figure 3.80). In ***industrial zone***, the highest concentration of acetamiprid was recorded at sampling point *cc5* in all seasons (Figure 3.80). The sources of this pesticide can be the agricultural fields as well as

industrial effluents from chemical (pesticide) production facilities located in OIZs next to *cc5* (Figure 3.81). Acetamiprid up to 0.03 µg/L in Pinios River in Greece (Tsaboula et al., 2016) and up to 0.38 µg/L in the rivers of Sydney, Australia (Sanchez-Bayo and Hyne, 2014).

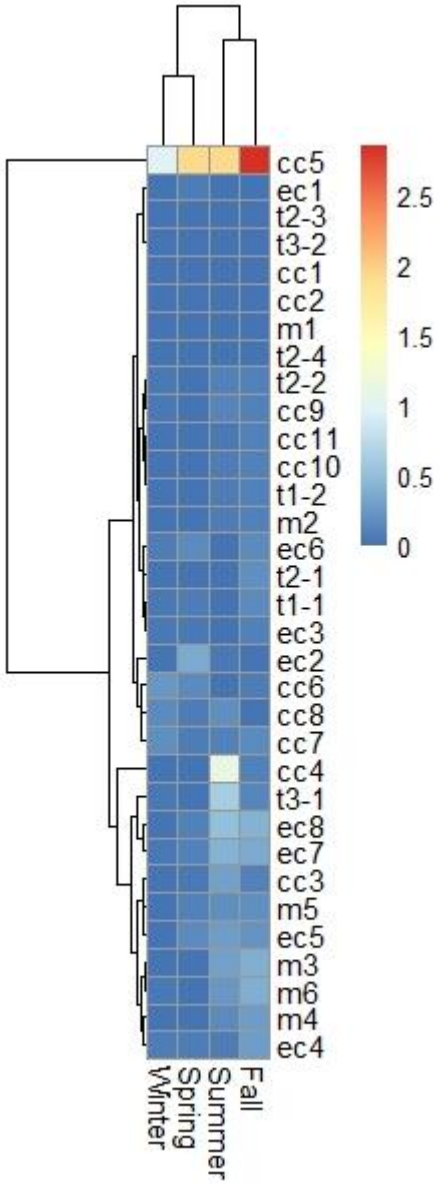

Figure 3.80. Heatmap of acetamiprid clustered by spatial-temporal concentration (µg/L) profile in ***industrial zone***.

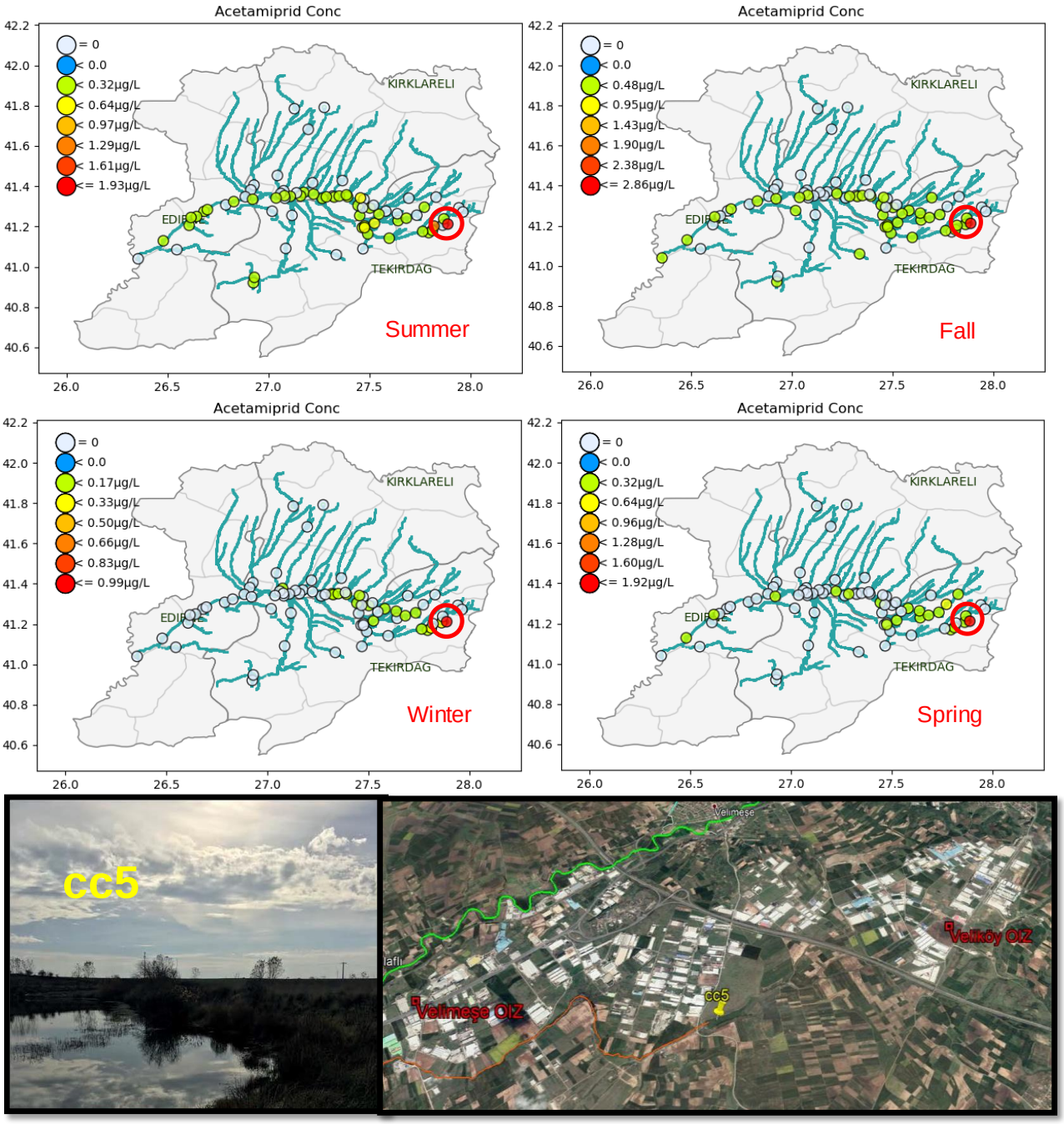

Figure 3.81. Seasonal concentration profiles of acetamiprid, Location of sampling point *cc5* next to agricultural fields and Veliköy OIZ.

Diuron as a PS was detected in 49, 43, 28 and 40 samples taken from the Ergene River. It was mainly detected in ***industrial zone*** (71% of the samples taken from that zone) at concentrations between 0.03 and 10.64 µg/L in all seasons (Figure 3.82). The recorded concentrations of diuron in the Ergene River specially in ***industrial zone*** exceeded its AA-EQS (0.2 µg/L) set by the WFD. In ***industrial zone***, diuron was present at its highest concentration in the sample taken from *cc5* close to Veliköy OIZ (Figure 3.81). In addition to *cc5*, diuron was measured at relatively high levels at other sampling points located next to OIZs (Ergene 1, Ergene 2, Büyükkarıştıran and Evrensekiz) of

industrial zone. Although detected in ***transition*** and ***agricultural zones*** as well, it was only found at 38% and 42% of the sampling points in those zones in all seasons, respectively. In addition, occurrence of diuron in ***transition*** and ***agricultural zones*** was mainly at sampling points on the main stream suggesting that this chemical is originated from the ***industrial zone*** and was carried to the following zones via the main stream (Figure 3.82). In ***agricultural zone***, *t15* and *t16* next to the agricultural lands were also measured with relatively high diuron concentrations (Figure 3.83). In other regions of the world, diuron was reported to be present at concentrations up to 19.60 ng/L in Alqueva Reservoir in Portugal (Palma et al., 2014), up to 39 ng/L in Pinios River in Greece (Tsaboula et al., 2016) and at 3.45-159.53 ng/L in Llobregat River in Spain (Masia et al., 2015).

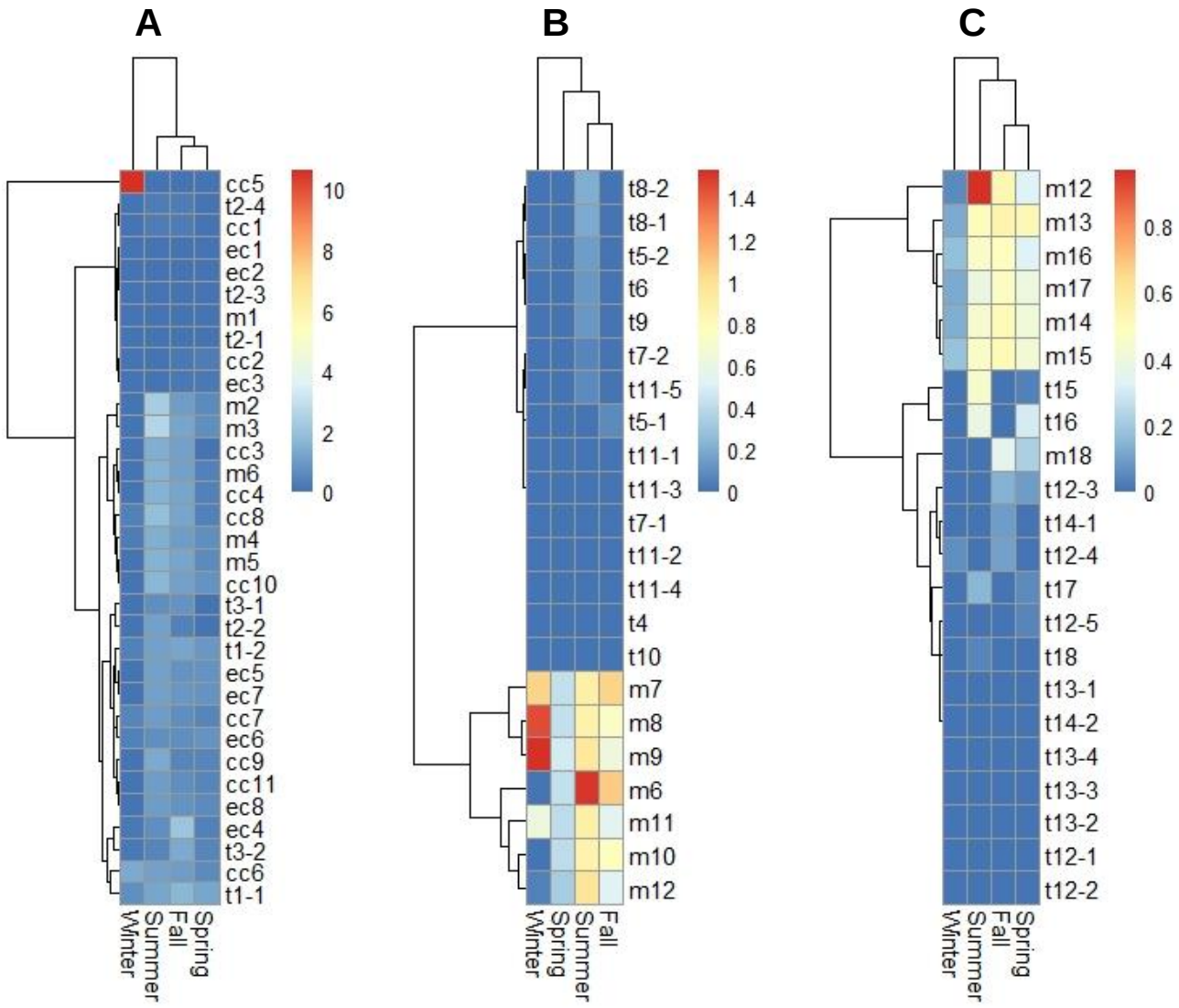

Figure 3.82. Heatmap of diuron clustered by spatial-temporal concentration (µg/L) profiles in (A) ***industrial***, (B) ***transition*** and (C) ***agricultural zones***.

Figure 3.83. Location of sampling points *t15* and *t16* in ***agricultural zone***.

Other pesticides listed as PS by European Commission (Directive 2013/39/EU) such as chlorpyrifos, atrazine, chlofenvinphos, terbutryn, cypermethrine, aclonifen, quinoxyfen, dichlorvos and trifluralin were also detected in some sampling points. Among the aforementioned pesticides, chlorpyrifos was detected at 10, 21, 17 and 3 sampling points in the Ergene River in August, November, February and May, respectively and its concentration exceeded its MAC-EQS of 0.1 µg/L. Cypermethrine was detected at concentration as high as 6.28 µg/L in the sample taken from sampling point *t16* (Figure 3.83) in fall, that was far more than its MAC-EQS of 0.0006 µg/L. Other priority pesticides whose concentrations exceeded their MAC-EQS are aclonifen, chlorfenvinphos, dichlorvos and trifluralin.

Carbendazim as a CEC was frequently found in the Ergene River. It is used to protect the agricultural farms from fungi as well as in industrial applications as biocide for preservation of leather, rubber and construction materials. Therefore, carbendazim can be found in surface water emerged from industrial effluents, agricultural runoff as well as municipal wastewaters (Merel et al., 2018). In Ergene River, carbendazim was detected in 53, 64, 27 and 55 samples taken from the river in summer, fall, winter and spring, respectively. Carbendazim was mainly detected in ***industrial zone*** (73% of the samples taken from that zone) and also in ***transition*** and ***agricultural zones*** at 63% and 60% sampling point located on those zones, respectively. It was present at 0.03-6.33 µg/L in ***industrial zone*** in which the highest concentration was measured at *cc10* that is surrounded by

agricultural lands (Figure 3.84, Figure 3.85 and Figure 3.86). In ***transition*** and ***agricultural zone***s, carbendazim was mainly present at high levels in the samples taken from the main stream representing the importance of ***industrial zone*** on the carbendazim pollution (Figure 3.84, Figure 3.85). Beside the sampling points on the main stream, sampling points *t12-3* close to Kırklareli City as well as *t16* (Figure 3.83) and *t17* (Figure 3.86) surrounded by agricultural lands were identified with high carbendazim concentrations. In other studies, carbendazim at concentrations up to 232 ng/L in Pinios River in Greece (Tsaboula et al., 2016), up to 269 ng/L in Danube River in Serbia (Antić et al., 2015) and at 9-45 ng/L in Arade River in Portugal (Gonzalez-Rey et al., 2015), was reported.

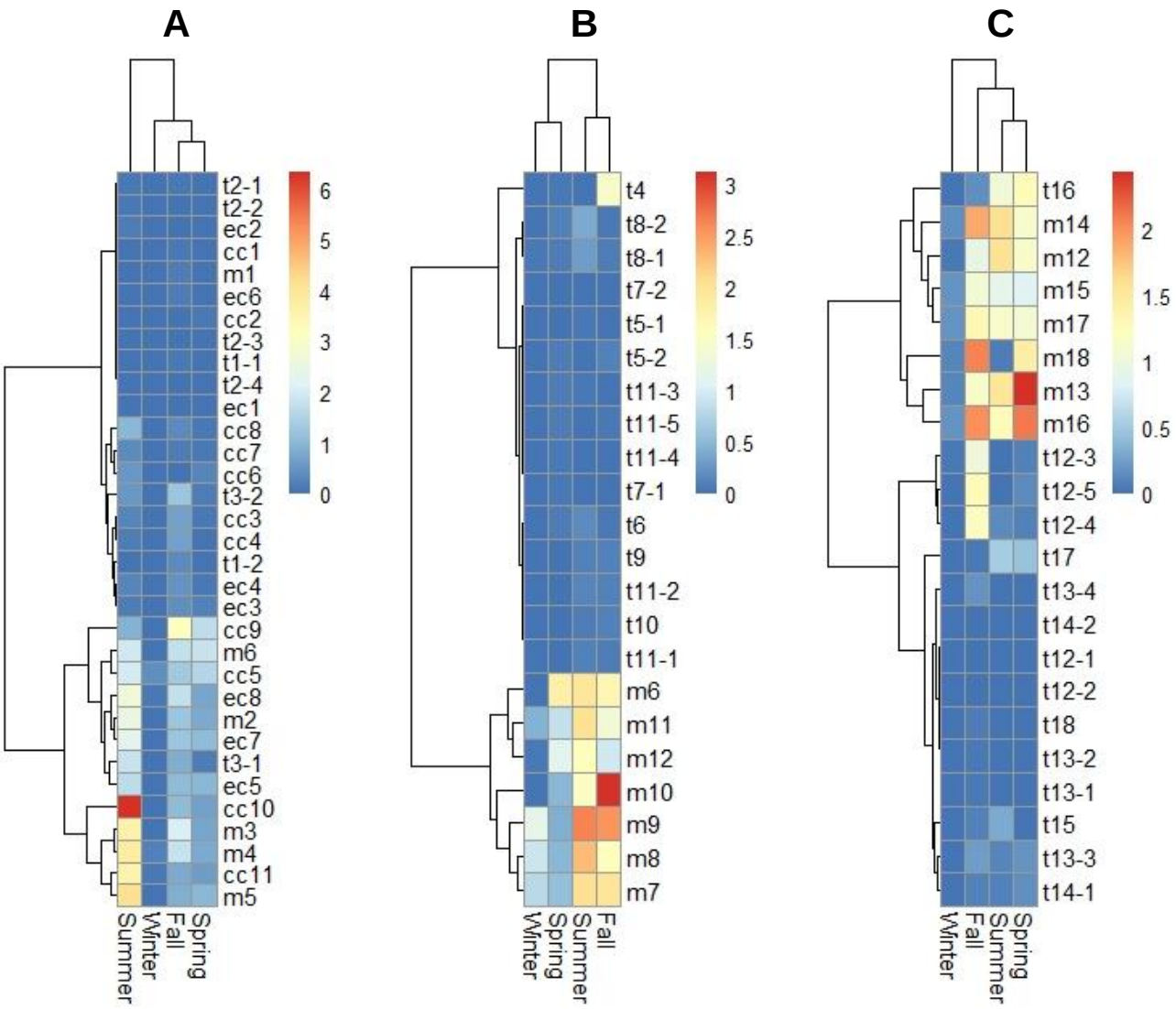

Figure 3.84. Heatmap of carbendazim clustered by spatial-temporal concentration (µg/L) profiles in (A) ***industrial***, (B) ***transition*** and (C) ***agricultural zones***.

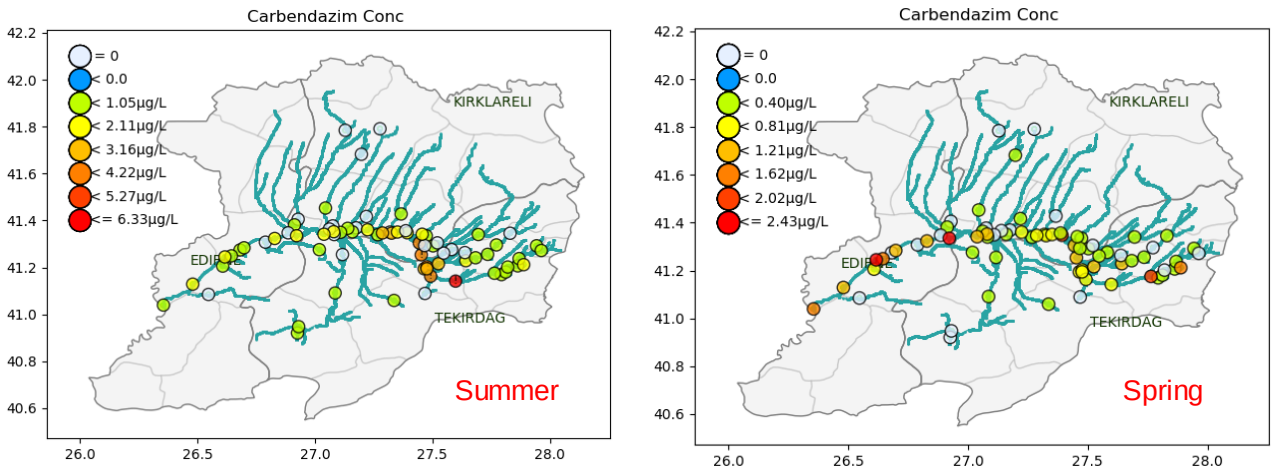

Figure 3.85. Concentration profile of carbendazim in the Ergene River in summer and spring.

Figure 3.86. Location of sampling point *cc10* in industrial zone and *t17* in ***agricultural zone***.

N,N-diethyl-m-toluamide (DEET) is a pesticide that is used mainly as insect repellent in houses as well as resin solvent and plasticizer in industries. It is also reported to be used as antifeedant on crops (Aronson et al., 2012). DEET was detected in 75, 75, 70 and 71 out of 75 samples taken from the Ergene River in summer, fall, winter and spring, respectively. Although detected in all zones, the highest concentrations of DEET was observed at *t6* (27.45 µg/L) and *t9* (35.92 µg/L) close to Düğüncücübaşı and Alpullu Cities in the ***transition zone*** in summer, respectively (Figure 3.87 and Figure 3.88). In ***industrial zone***, samples on the Çorlu Creek, Ergene Creek and the tributary next to Evrensekiz OIZ, had relatively high DEET concentrations. On the contrary, in ***agricultural zone***, *t12-3*, *t15* and *t16* close to cities and agricultural lands were determined with higher DEET concentrations (Figure 3.87).

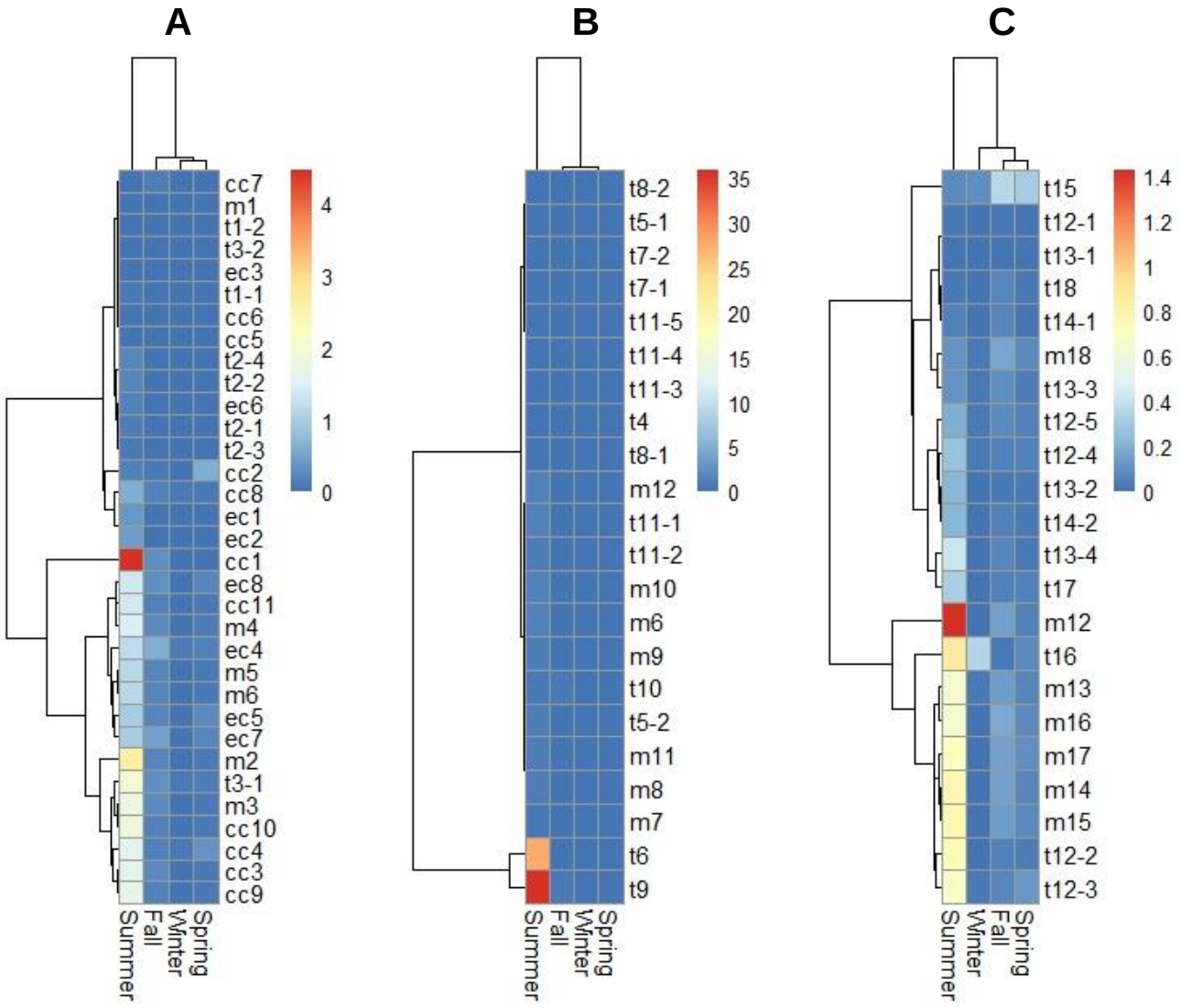

Figure 3.87. Heatmap of N,N-diethyl-m-toluamide clustered by spatial-temporal concentration (µg/L) profiles in (A) ***industrial***, *(B)* ***transition*** *and (C)* ***agricultural zones***.

In other studies, DEET up to 0.14 µg/L in the river waters of Japan (Komori et al., 2013), up to 1.36 µg/L in the samples taken from Beiyun River in china (Ma et al., 2017) and up to 2.67 µg/L in Great Lakes tributaries in USA (Baldwin et al., 2016) was measured and reported.

The seasonal concentration profile along with the number of sampling points where the pesticides were detected, are shown in Figure D.12.

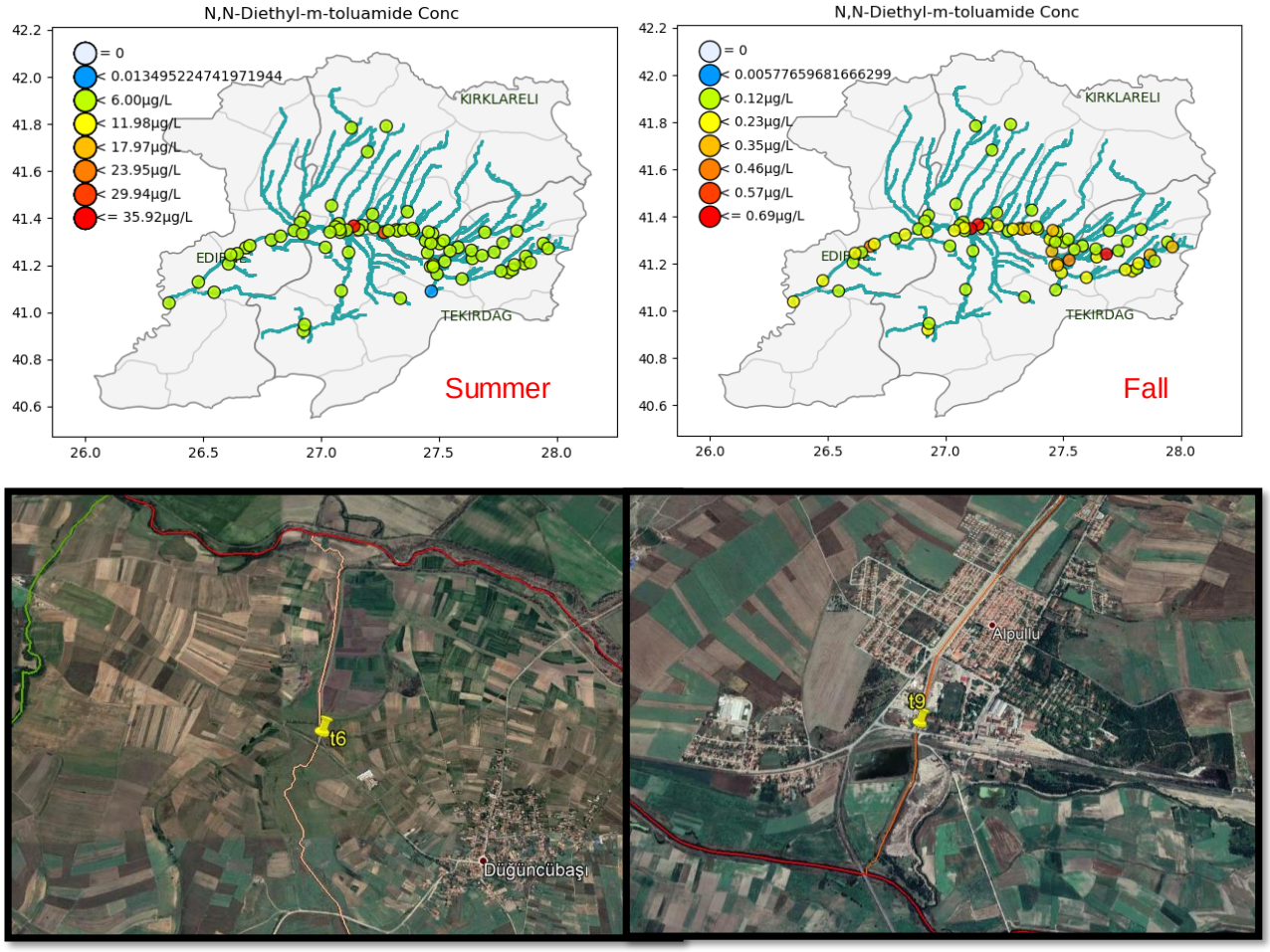

Figure 3.88. Concentration profiles of DEET in the Ergene River in summer and fall, Location of sampling point *t6* and *t9* in ***transition zone***.

3.3.2.6. Natural Chemicals. The presence of three microcystins as naturally occurring pollutants, was studied in the Ergene River. Among them, microcystin-YR was detected in none of the samples. microcystin-LR and microcystin-RR were found from which the former was just detected at sampling point *cc8* at a concentration of 6.30 µg/L during summer that was 6 times higher than the recommended value by WHO (1 µg/L). Microcystin-RR, on the other hand, was detected in 19/75 and 20/75 samples taken from the Ergene River in summer and fall, respectively. Microcystin-RR was mainly found in ***industrial zone*** (16% of the samples taken from that zone) at concentrations

between 0.14 and 4.08 µg/L. The highest concentration of Microcystin-RR in ***industrial zone*** was recorded at *t2-3* in both seasons (Figure 3.89, Figure 3.90 and Figure 3.91). Both sampling points *cc8* and *t2-3* are receiving the water from shallow algal blooms (Figure 3.92).

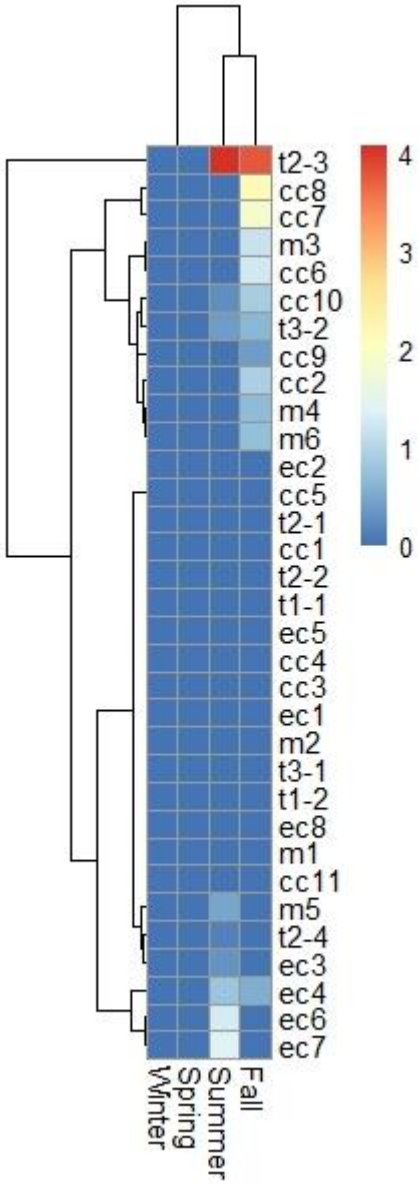

Figure 3.89. Heatmap of microcystin-RR clustered by spatial-temporal concentration (µg/L) profile in ***industrial zone***.

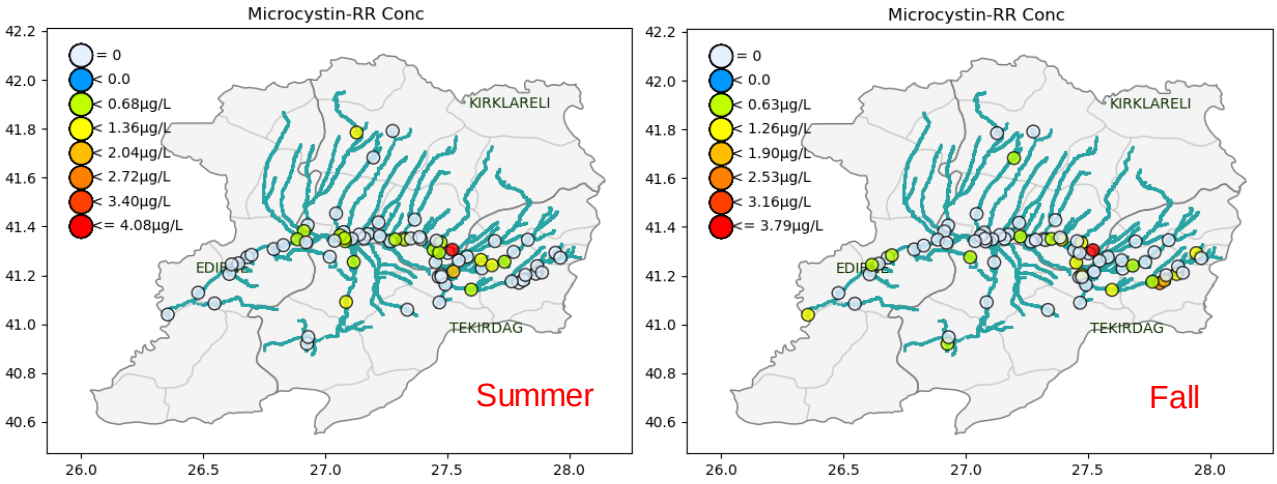

Figure 3.90. Concentration profiles of microcystin-RR in Ergene River in summer and fall.

Figure 3.91. Location of sampling points *cc8* and *t2-3* in ***industrial zone***.

Figure 3.92. Sampling point *cc8* next to an algal bloom and with the highest microcystin-LR concentration.

The seasonal concentration profile along with the number of sampling points at which the microcystins were detected, are given in Figure D.13.

3.3.3. Important Micropollutants Sources and Their Fingerprint Pollutants

Z-score for a micropollutant at each sampling point based on its concentration and load at that point.
Concentration of micropollutants and heavy metals measured at every sampling point were used for clustering sampling points as well as pollutants. Cluster analysis were useful to understand which sampling point are related to each other in terms of micropollutants, if they share common pollution sources as well as the pollutant fingerprint of those pollution sources. In addition, it also gave an insight on which micropollutants co-occur and the sources they are emitted. Z-scores derived for each

micropollutant at each sampling point was used to construct the dendrograms and heatmaps using *h-clust* package on R statistical software v3.5.1 with Ward.D2 agglomeration method and Euclidean distance method (Carpenter and Helbling, 2018).

$$Z_{i,x} = \frac{P_{i,x} - \mu_i}{\sigma_i} \qquad \text{(Eqn. 1)}$$

where Z is the z-score of a pollutant i at sampling point x, P is the concentration of a pollutant at a sampling point, μ is the mean concentration of a pollutant in the Ergene River and σ is the standard deviation of a pollutant measured in the Ergene River.

Sampling points formed distinct clusters based on the z-scores of the micropollutants at different seasons. In summer (Figure 3.93) and fall (Figure 3.94), sampling points were grouped into three and four main clusters, respectively. In general, these clusters were composed of 1) sampling point *t4* close to Lüleburgaz City (Figure 3.93, cluster A), 2) sampling points on the main stream (*m*), Büyükkarıştıran tributary (*t1-1* and *t1-2*), tributary next to Evrensekiz OIZ (*t3-1*), Çorlu Creek (*cc*) and Ergene Creek (*ec*) (Figure 3.93, cluster C) and 3) the rest of the sampling points mainly the ones on the tributaries in the ***transition*** and ***agricultural zones*** (Figure 3.93, cluster B). In fall, the composition of the clusters was almost the same as summer with a difference that sampling points *cc6* and *cc7* were separated because of high concentration of some micropollutants (Figure 3.94, cluster B). In May (Figure 3.96), the tributaries in ***transition*** and ***agricultural zones*** were clustered together (Figure 3.96, cluster C), while the sampling points on the main stream (*m*), Büyükkarıştıran tributary (*t1-1* and *t1-2*), Çorlu Creek (*cc*) and Ergene Creek (*ec*) were in other subclusters (Figure 3.96, clusters A, B, D, E and F). The sampling points hierarchical clustering during spring had almost the same trend as in summer and fall.

On the contrary, the sampling points on the Çorlu Creek (*cc5*, *cc6*, *cc7*, *cc8* and *cc11*), Ergene Creek (*ec6*) and the tributary next to Büyükkarıştıran OIZ (*t1-1* and *t1-2*) representing the sampling points with the highest concentrations of more than 50% of the chemicals, were separated from the rest of the sampling points in the winter (Figure 3.95, cluster B). In addition, unlike the rest of the year, sampling points along the main stream (*m1-m18*) were not clustered with the aforementioned sampling points due to high flowrate of water and further dilution of micropollutants after released from their sources in winter (Figure 3.95). Considering all seasons, the heatmaps as well as hierarchical clustering indicated that Çorlu Creek (*cc*), Ergene Creek (*ec*) and the tributary close to

Büyükkarıştıran OIZ (*t1-1* and *t1-2*) located in ***industrial zone***, were the main possible sources of pollution in the Ergene River.

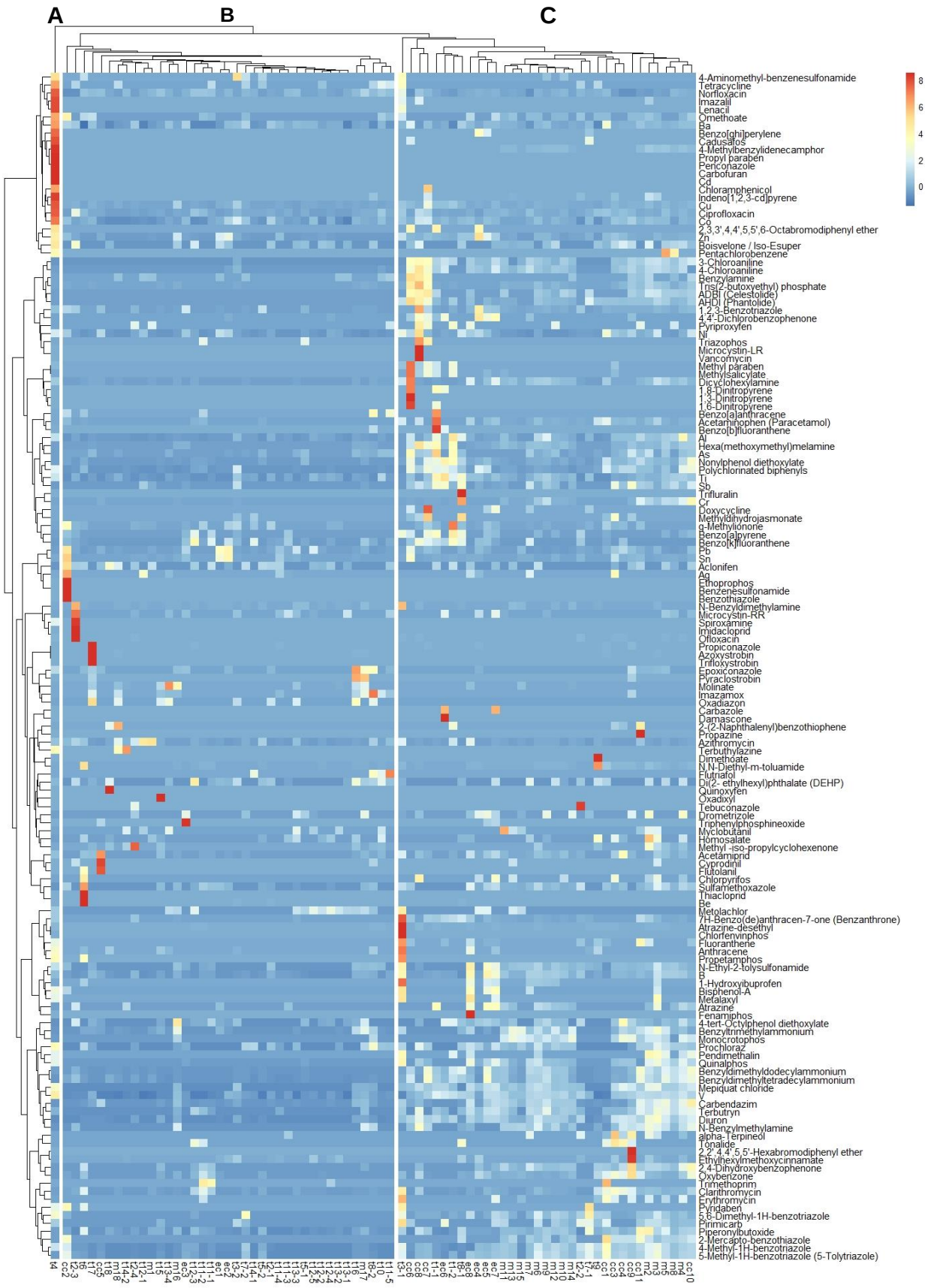

Figure 3.93. Heatmap of micropollutants clustered by spatial z-score normalized concentration profiles in all samples taken in summer. The color of each cell represents the z-score value calculated for a pollutant at a sampling point.

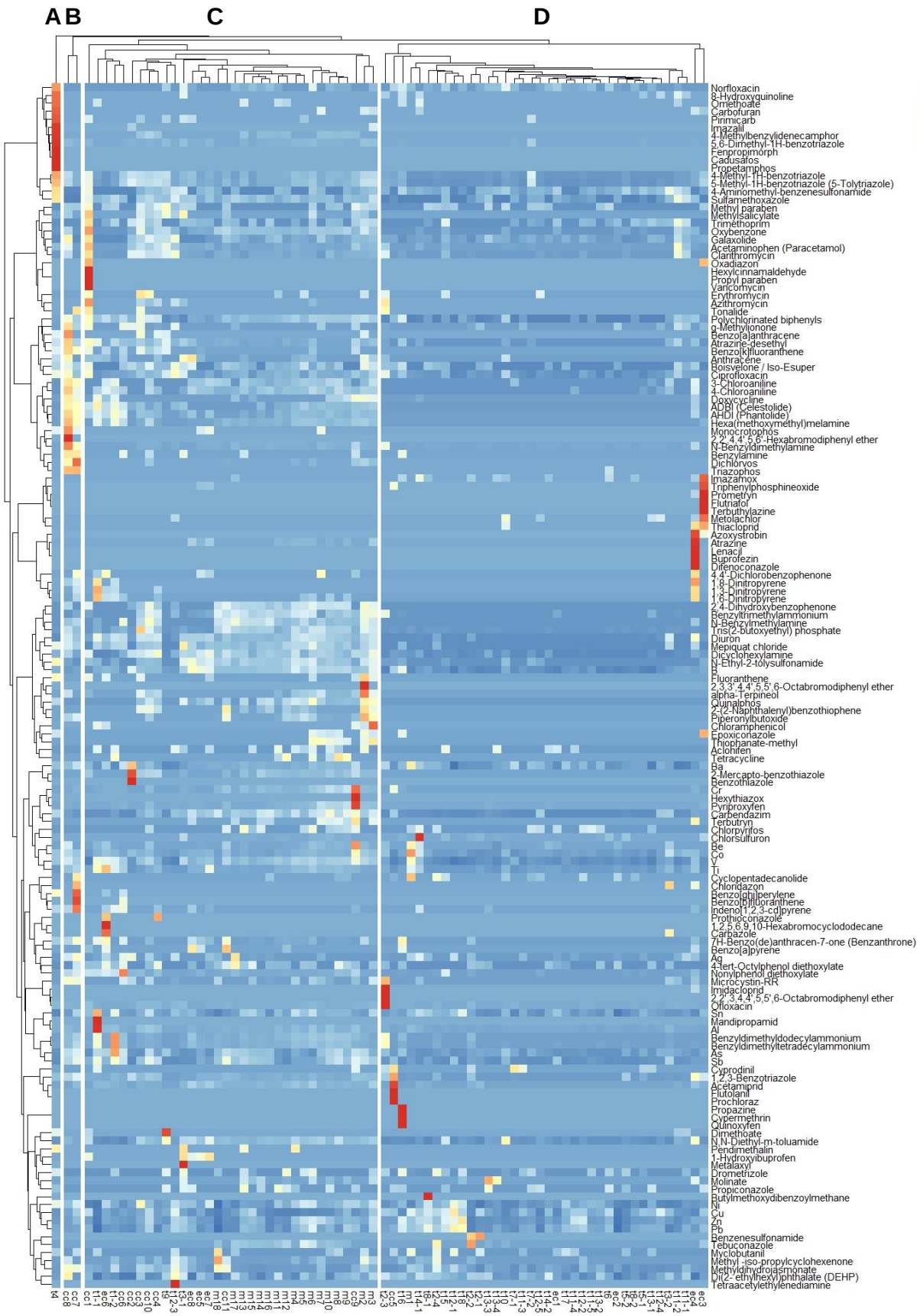

Figure 3.94. Heatmap of micropollutants clustered by spatial z-score normalized concentration profiles in all samples taken in fall. The color of each cell represents the z-score value calculated for a pollutant at a sampling point.

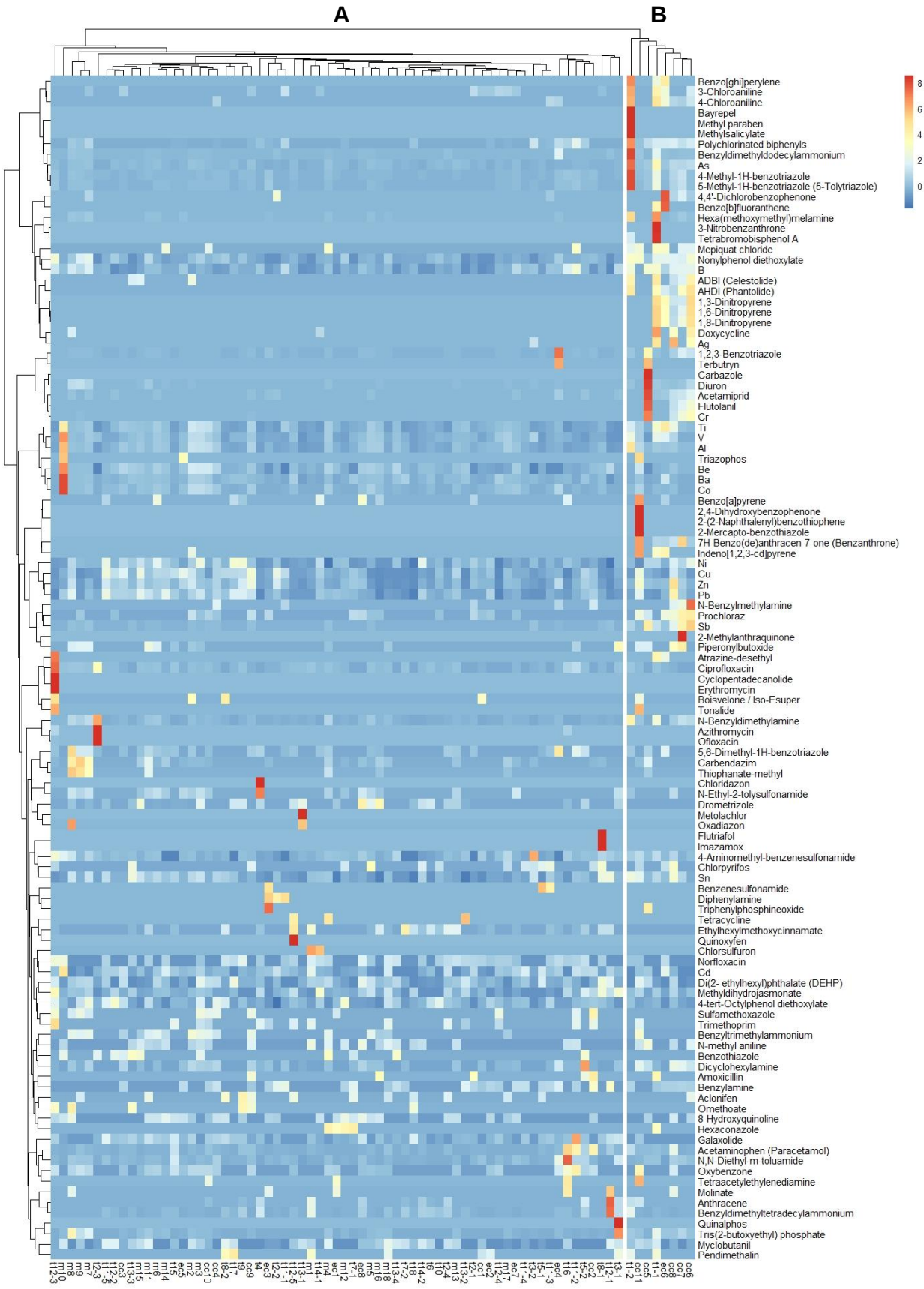

Figure 3.95. Heatmap of micropollutants clustered by spatial z-score normalized concentration profiles in all samples taken in winter. The color of each cell represents the z-score value calculated for a pollutant at a sampling point.

Figure 3.96. Heatmap of micropollutants clustered by spatial z-score normalized concentration profiles in all samples taken in spring. The color of each cell represents the z-score value calculated for a pollutant at a sampling point.

The pollution distribution in the main stream of the Ergene River is of high importance since it collects the pollution from its tributaries as well. Thus, the sampling points on the main stream (*m1-m18*) were investigated in details to elucidate the correlation between those sampling points on the basis of the micropollutants concentration. In this regard, detected micropollutants were clustered using spatial z-score normalized concentration profiles in the samples taken from the main stream (*m1-m18*) in all seasons (Figure 3.97-Figure 3.100). In general, the sampling points after *m1* in the ***industrial zone*** specially *m2*, *m3* and *m4* after Çorlu Creek, Ergene Creek and the tributary close to Büyükkarıştıran OIZ connects the main stream, respectively, were clustered together. In summer, cluster C composed of *m2* and *m3* was separated from the rest (Figure 3.97). In fall, in which the highest number of micropollutants were detected, *m2*, *m3* and *m6* (the last sampling point in industrial zone) were embedded in the same cluster (Figure 3.98, cluster A). In spring, *m2*, *m3* and *m4* were separated from the rest of the sampling points located on the main stream (Figure 3.100, cluster A). On the contrary, no specific pattern was identified in winter due to precipitation effects and dilution of micropollutants in the water (Figure 3.99). Therefore, at the most time of the year, the occurrence and distribution of the micropollutants in the main stream resulted in separation of sampling points in the ***industrial zone*** (*m2-m6*) from the ones in the following zones (*m7-m18*).

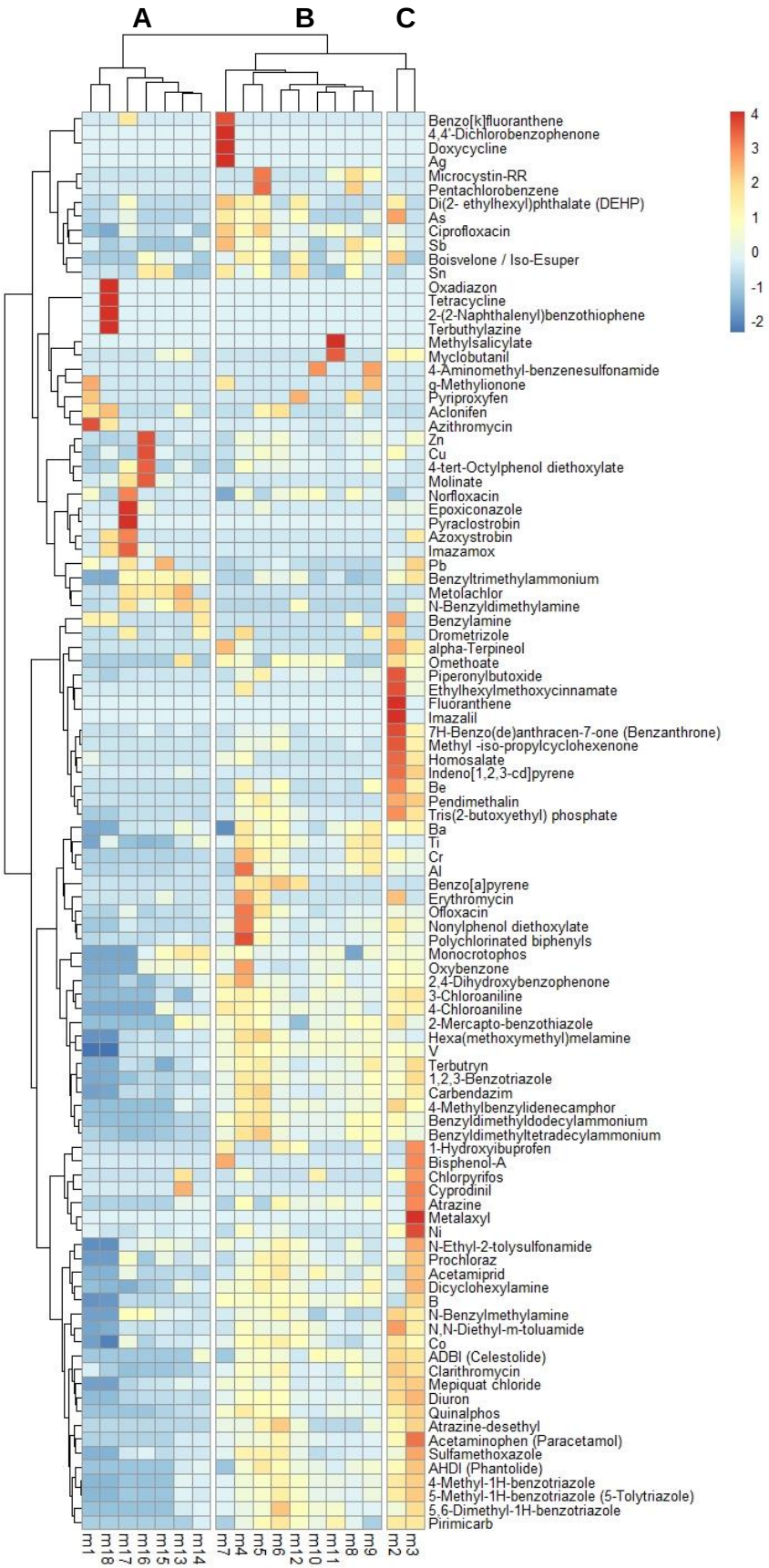

Figure 3.97. Heatmap of micropollutants clustered by spatial z-score normalized concentration profiles in the samples taken from the main stream in summer. The color of each cell represents the z-score value calculated for a pollutant at a sampling point.

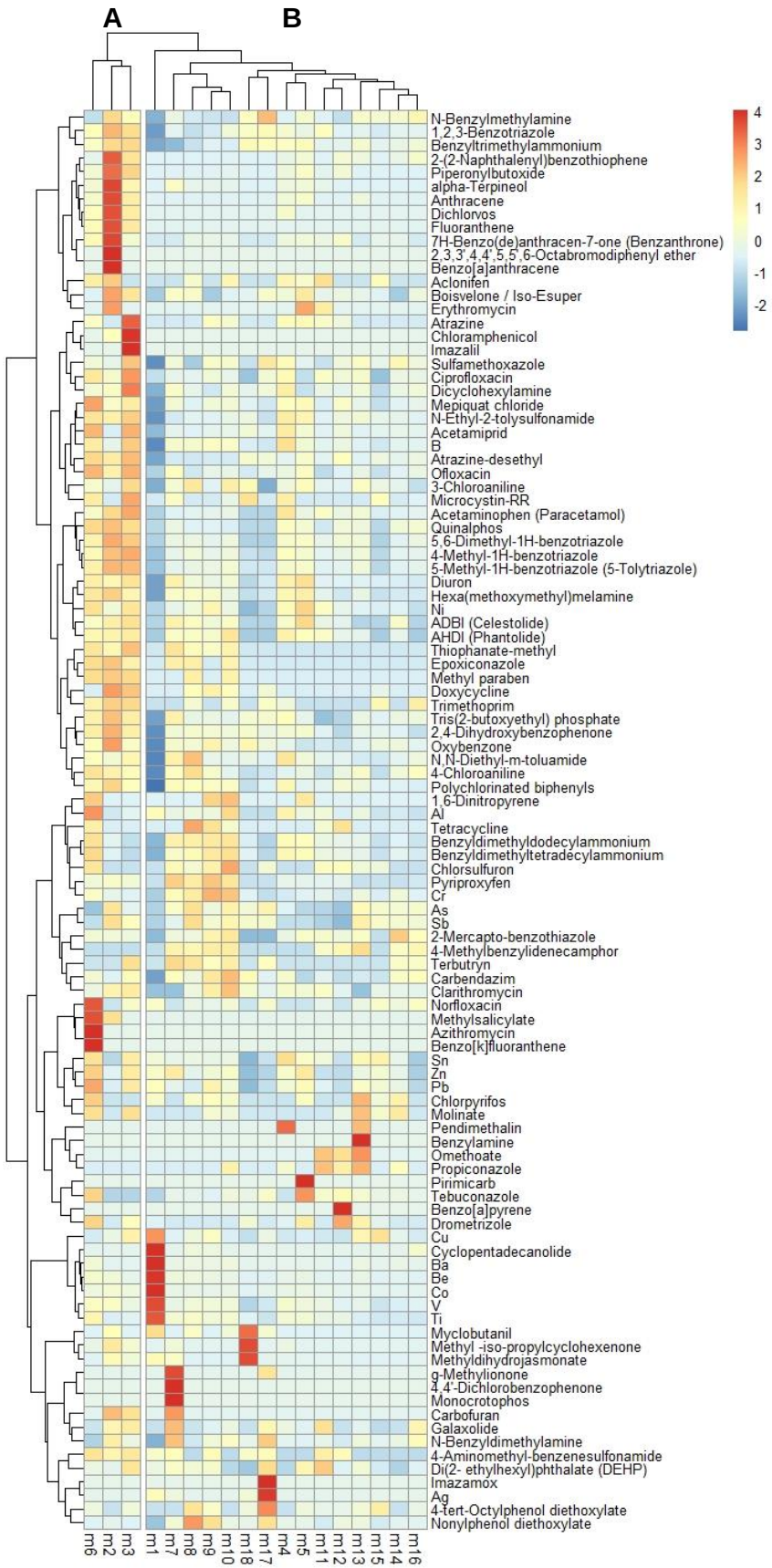

Figure 3.98. Heatmap of micropollutants clustered by spatial z-score normalized concentration profiles in the samples taken from the main stream in fall. The color of each cell represents the z-score value calculated for a pollutant at a sampling point.

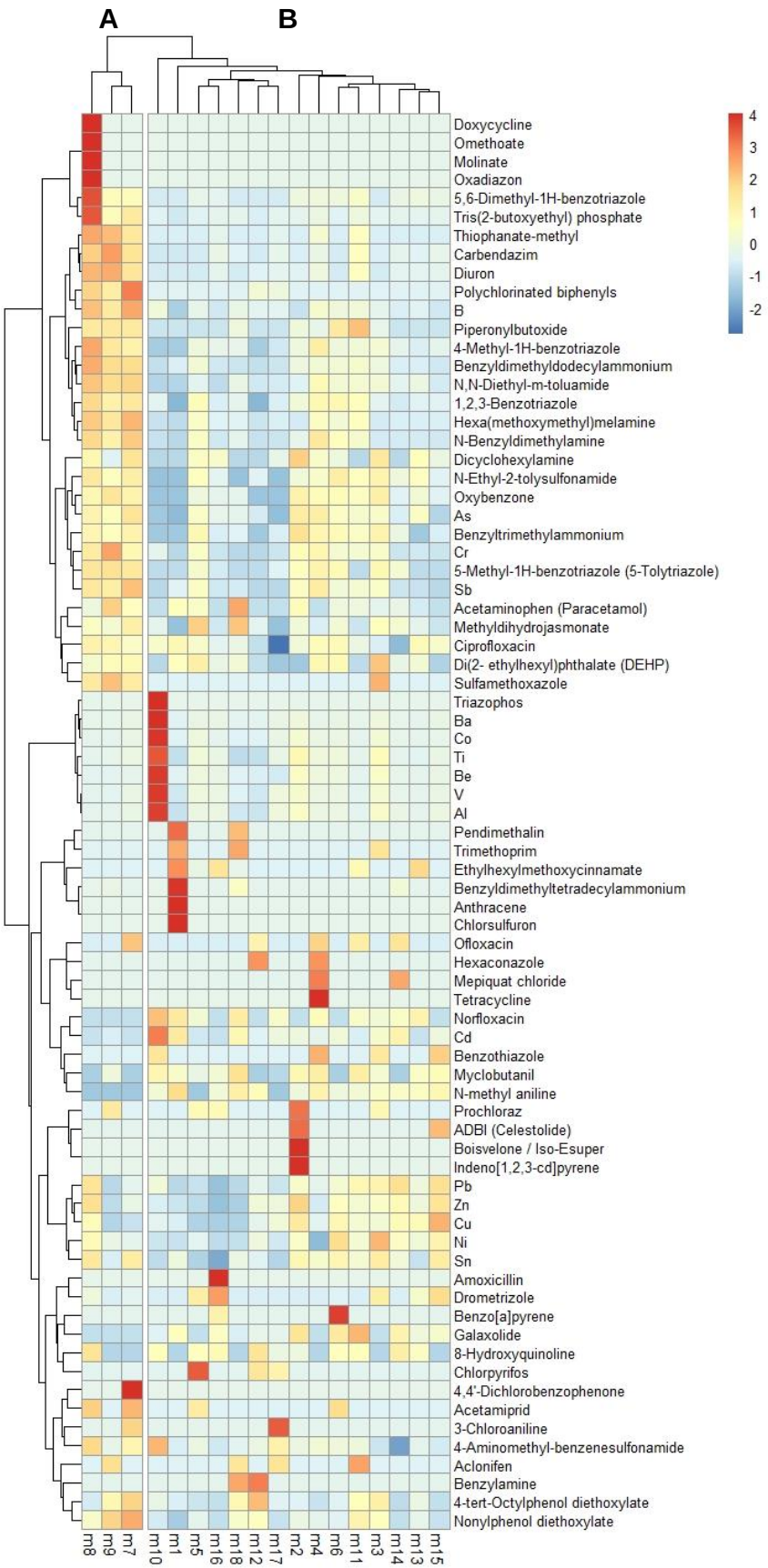

Figure 3.99. Heatmap of micropollutants clustered by spatial z-score normalized concentration profiles in the samples taken from the main stream in winter. The color of each cell represents the z-score value calculated for a pollutant at a sampling point.

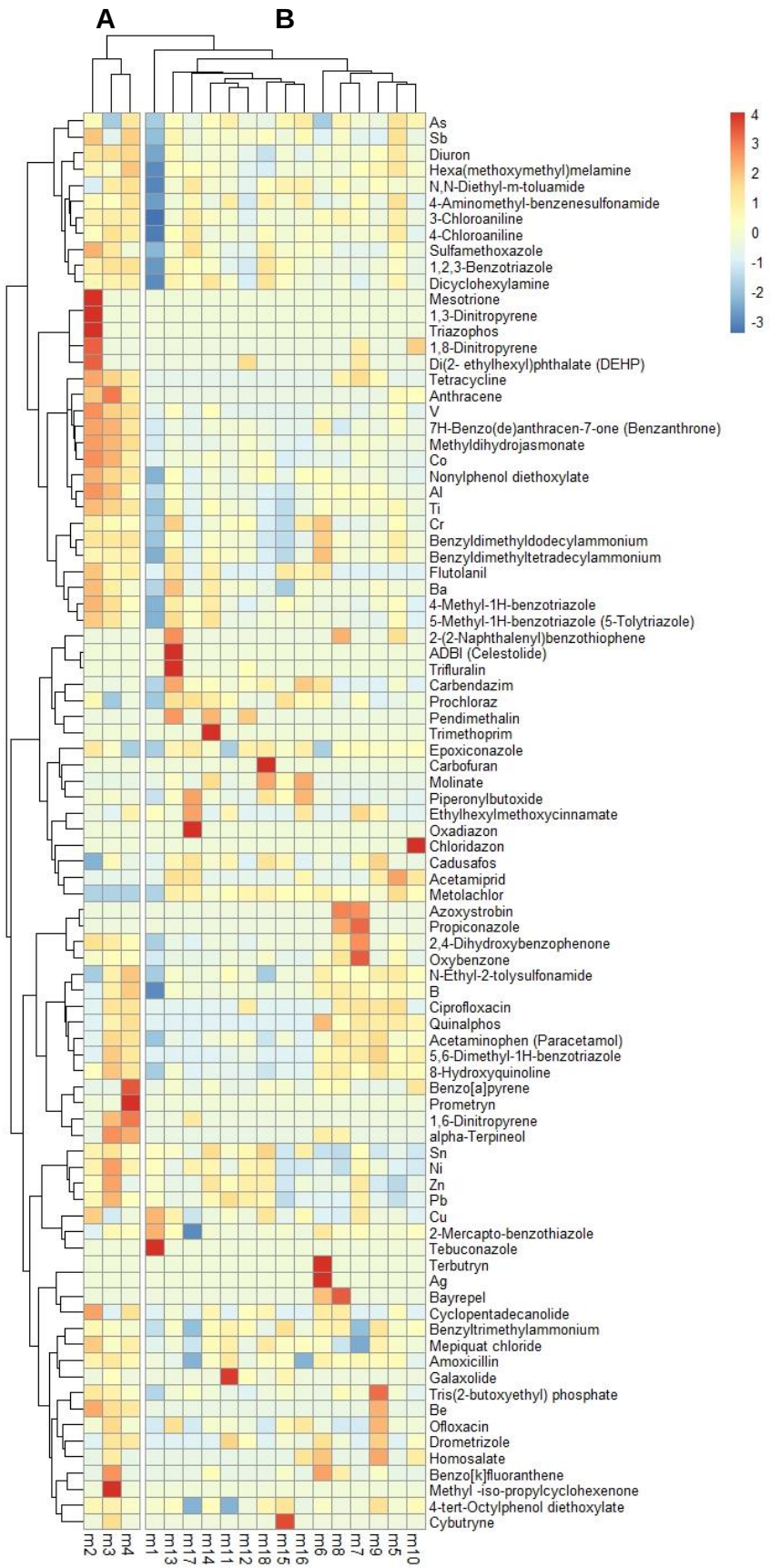

Figure 3.100. Heatmap of micropollutants clustered by spatial z-score normalized concentration profiles in the samples taken from the main stream in spring. The color of each cell represents the z-score value calculated for a pollutant at a sampling point.

The next step was to recognize the effects of the tributaries on the pollution in the main stream specially the ones in the ***industrial zone***. Therefore, a clustering analysis was constructed using the load profiles of the micropollutants in the samples taken from the junction sampling points of the tributaries and the main stream (Figure 3.101-Figure 3.104). In summer (Figure 3.101) and fall (Figure 3.102), the junction sampling points were mainly grouped into two namely 1) junction sampling points of the Çorlu Creek (*cc11*), Ergene Creek (*ec8*), the tributaries next to Büyükkarıştıran OIZ (*t1-2*), next to Evrensekiz OIZ (*t3-1*) and the one close to Lüleburgaz City (*t4*) (Figure 3.101, cluster B and Figure 3.102, cluster B) and 2) the junction sampling points of the rest of the tributaries and the main stream (Figure 3.101, cluster A and Figure 3.102, cluster A). The same pattern was also observed in winter and spring with a difference that the tributaries on which *t3-1* and *t4* are located were not determined as the main pollution contributors (Figure 3.103, cluster B, C and D and Figure 3.104, cluster A and C). Combining the results from clustering of the sampling points on the main stream using the junction sampling points indicated that the pollution in the main stream is originated from mainly Çorlu Creek, Ergene Creek and the tributaray next to Büyükkarıştıran OIZ in all season. In addition, the two tributaries next to Evrensekiz OIZ and the one close to Lüleburgaz City are other important contributors, particularly in dry seasons (summer and fall).

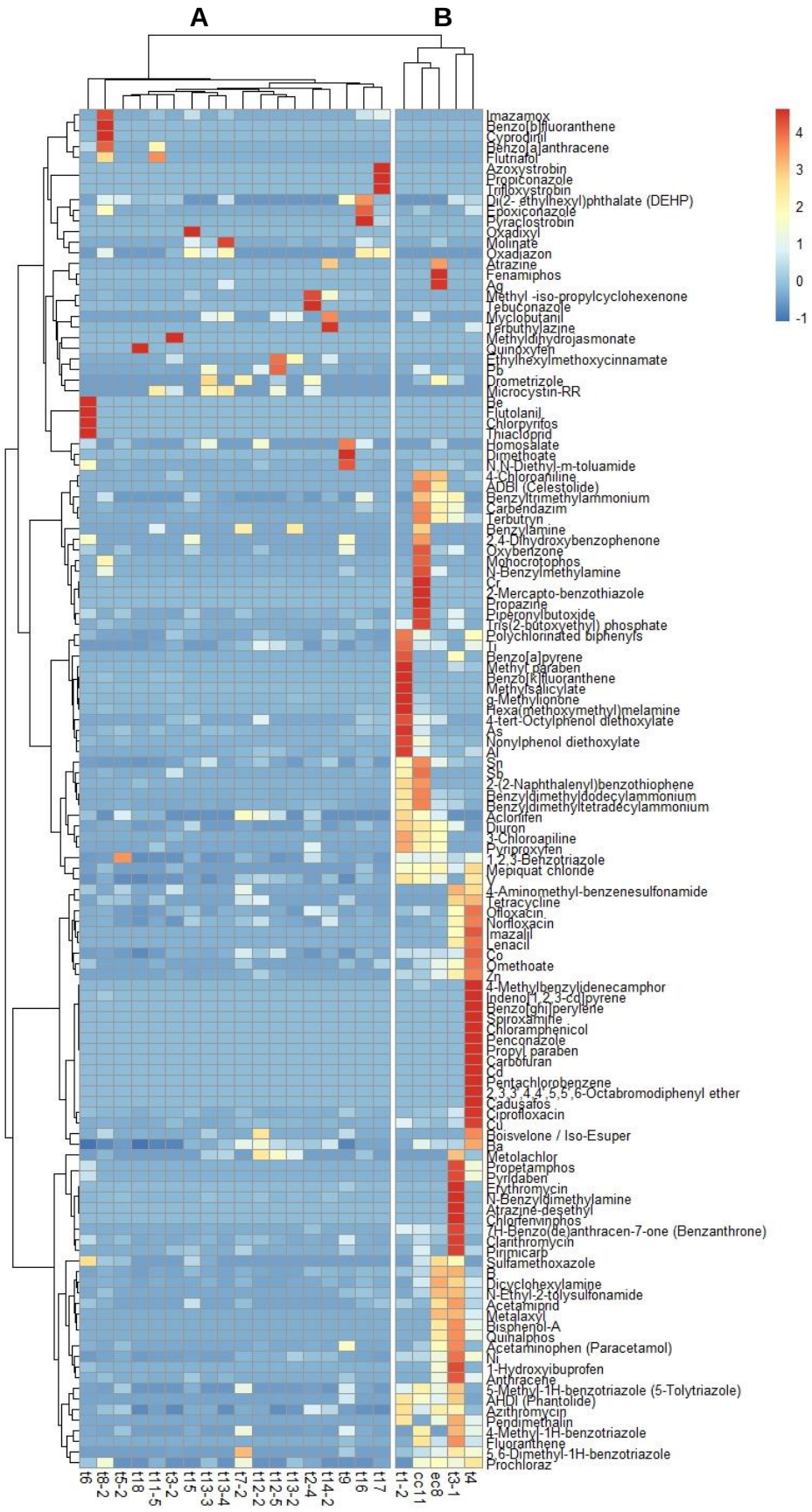

Figure 3.101. Heatmap of micropollutants clustered by spatial z-score normalized load profiles in the samples taken from the junction sampling points of all tributaries and the main stream in summer. The color of each cell represents the z-score value calculated for a pollutant at a sampling point.

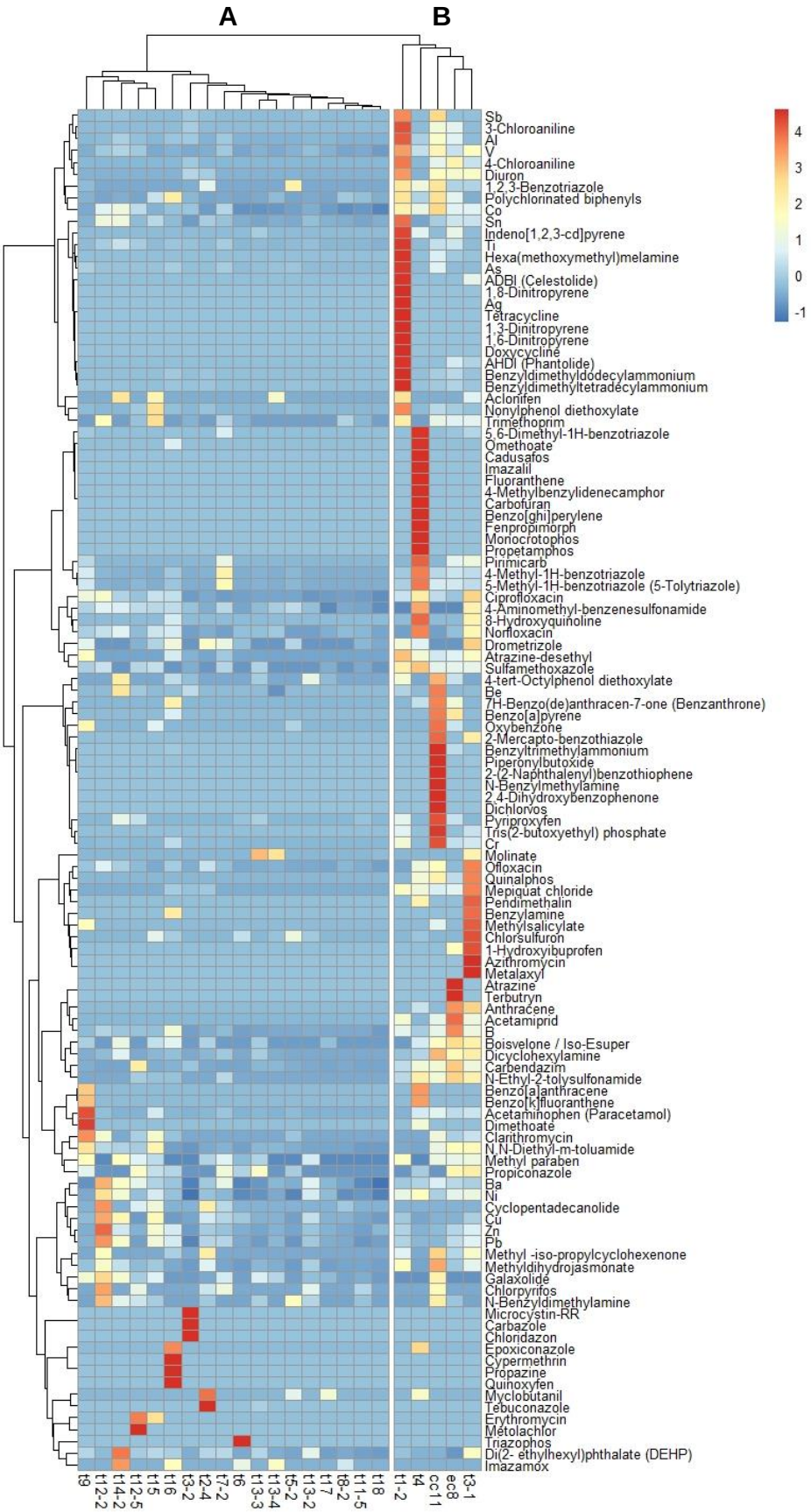

Figure 3.102. Heatmap of micropollutants clustered by spatial z-score normalized load profiles in the samples taken from the junction sampling points of all tributaries and the main stream in fall. The color of each cell represents the z-score value calculated for a pollutant at a sampling point.

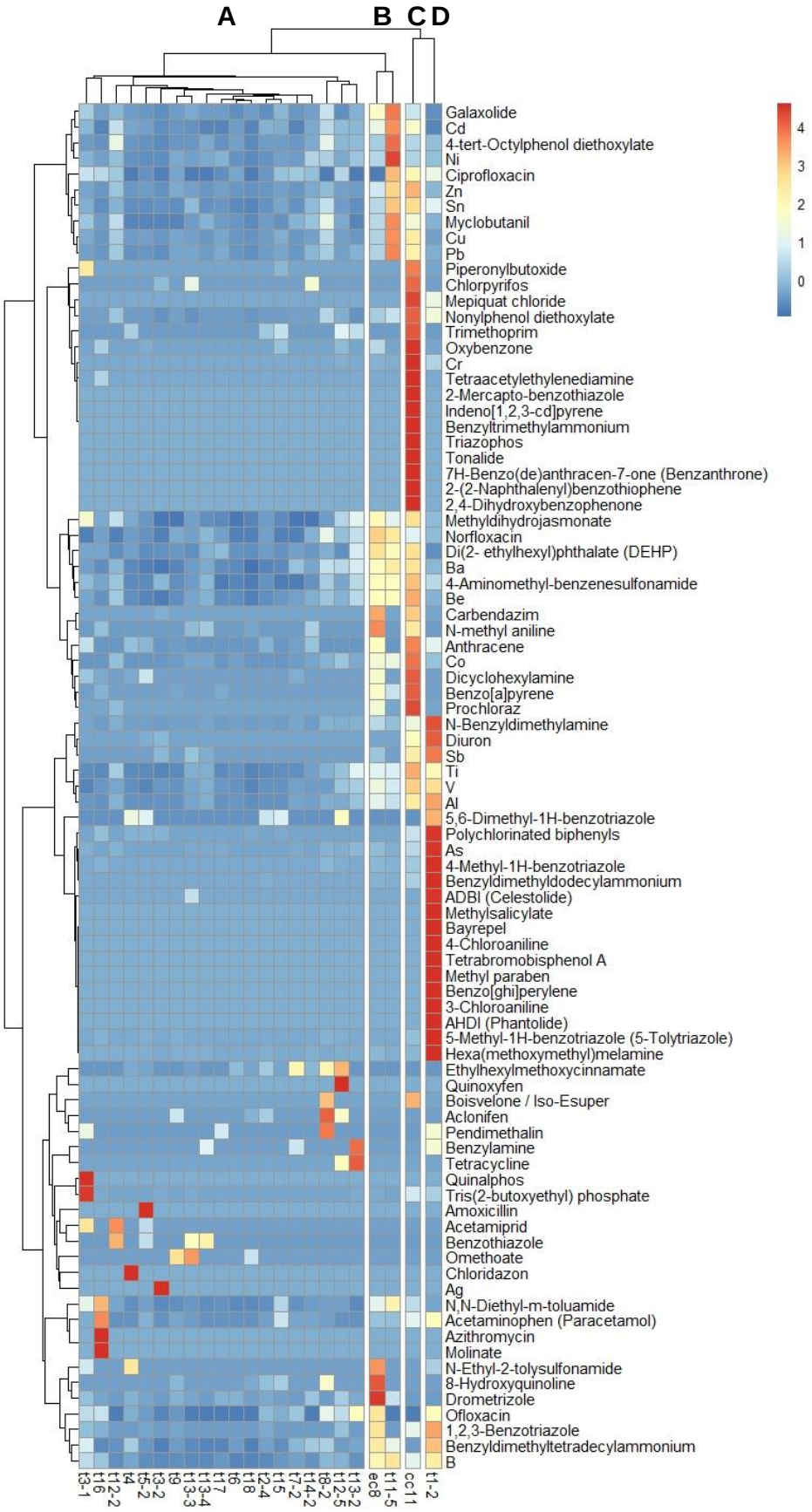

Figure 3.103. Heatmap of micropollutants clustered by spatial z-score normalized load profiles in the samples taken from the junction sampling points of all tributaries and the main stream in winter. The color of each cell represents the z-score value calculated for a pollutant at a sampling point.

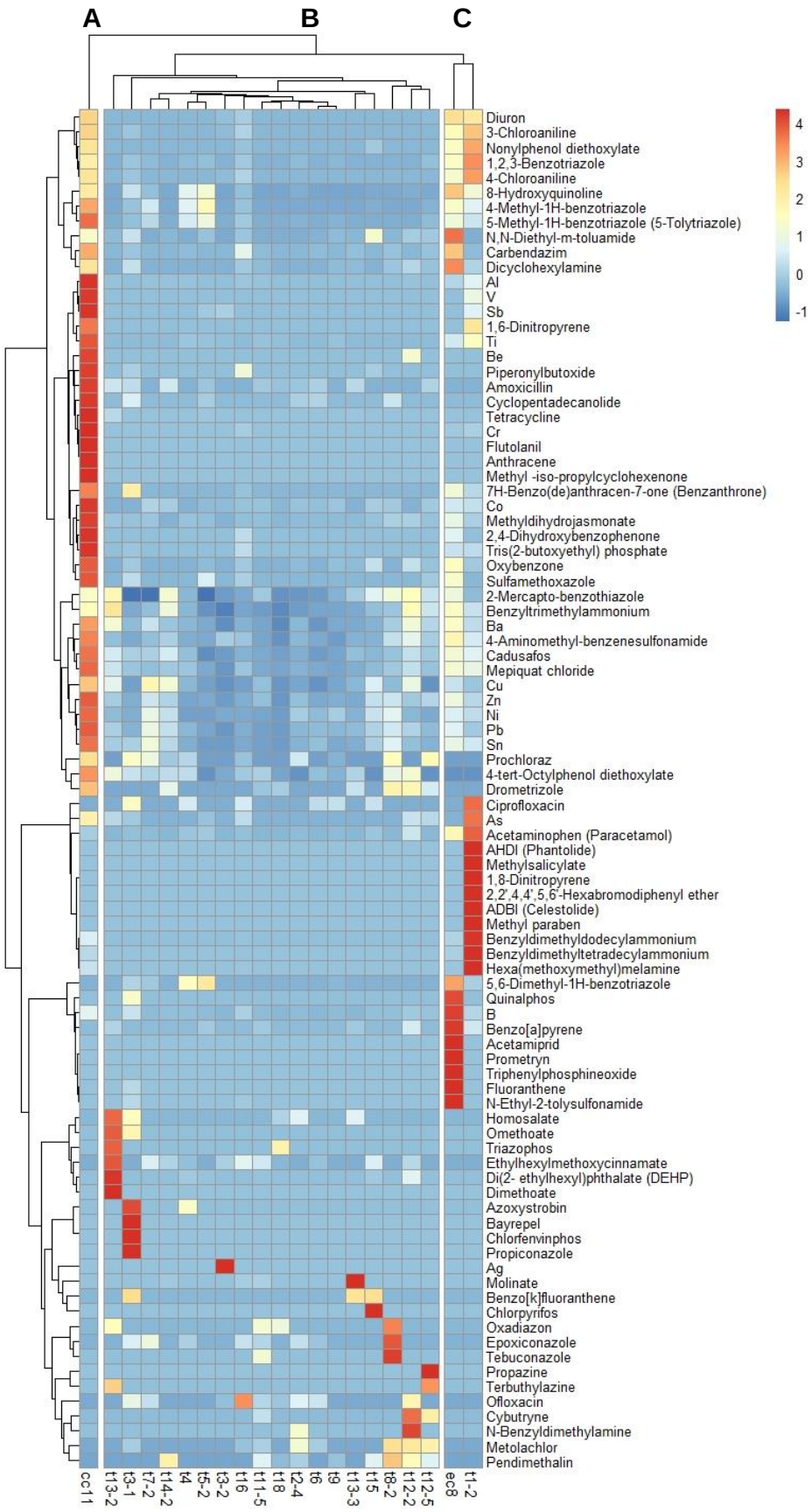

Figure 3.104. Heatmap of micropollutants clustered by spatial z-score normalized load profiles in the samples taken from the junction sampling points of all tributaries and the main stream in spring. The color of each cell represents the z-score value calculated for a pollutant at a sampling point.

To understand whether the pollution from the ***industrial zone*** affects the following zones or not, heatmaps of micropollutants clustered by the z-score normalized concentration profiles in all of the samples taken from ***transition*** and ***agricultural zones*** in a dry season (fall) (Figure 3.105 and Figure 3.106) and a wet season (spring) (Figure 3.107 and Figure 3.108) were constructed. The clustering analysis indicated that sampling points on the main stream are separated from the ones on the tributaries in both zones. For instance, in fall, sampling points on the main stream of the ***transition zone*** (*m6-m12*) (Figure 3.105, cluster A) were separated from the ones on the tributaries. The same pattern was also achieved for the samples taken from the ***transition zone*** in spring as well (Figure 3.107, cluster A). Similar to the ***transition zone***, the sampling points on the main stream of the ***agricultural zone*** (*m12-m18*) (Figure 3.106, cluster A and Figure 3.108, cluster C) were grouped in one cluster in both seasons while the ones on the tributaries were in the other cluster. These results suggested that sampling points on the main river have the same composition. In other words, the pollution released in ***industrial zone*** from the industrial facilities mainly close to Çorlu Creek, Ergene Creek and the tributaray next to Büyükkarıştıran OIZ was further transported to the ***transition*** and ***agricultural zones*** via the main stream.

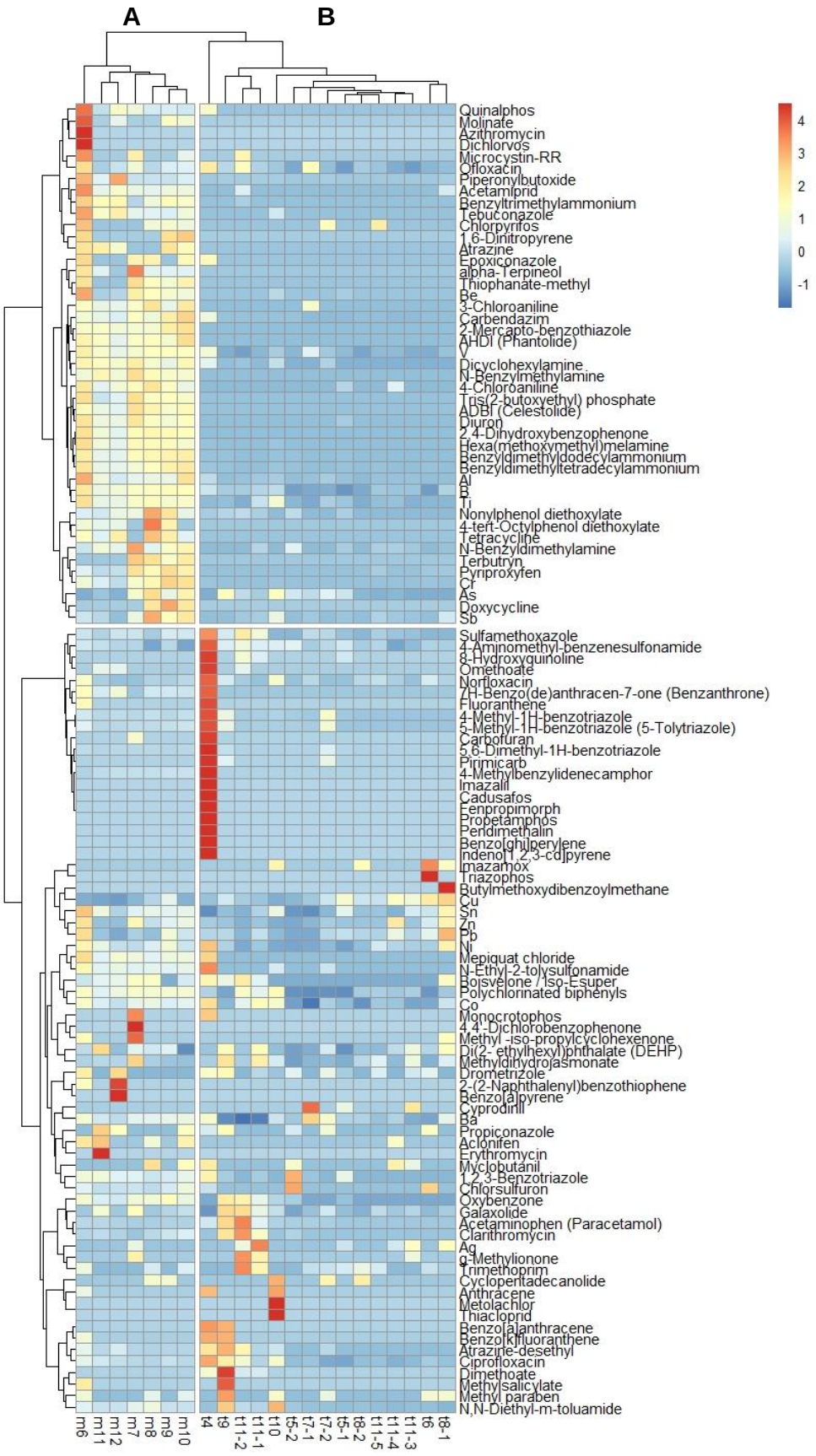

Figure 3.105. Heatmap of micropollutants clustered by spatial z-score normalized concentration profiles in all samples taken from the ***transition zone*** in fall. The color of each cell represents the z-score value calculated for a pollutant at a sampling point.

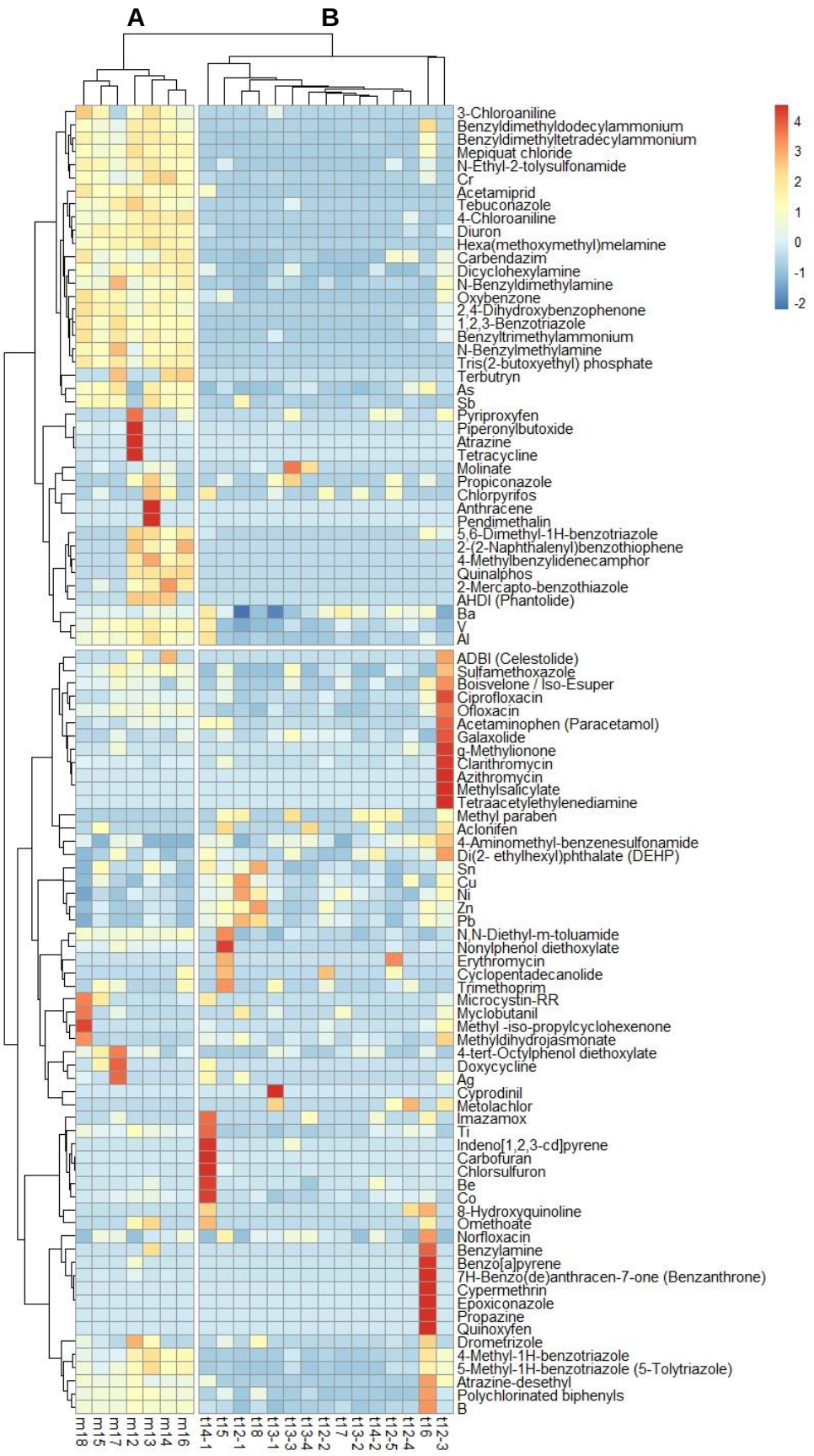

Figure 3.106. Heatmap of micropollutants clustered by spatial z-score normalized concentration profiles in all samples taken from the ***agricultural zone*** in fall. The color of each cell represents the z-score value calculated for a pollutant at a sampling point.

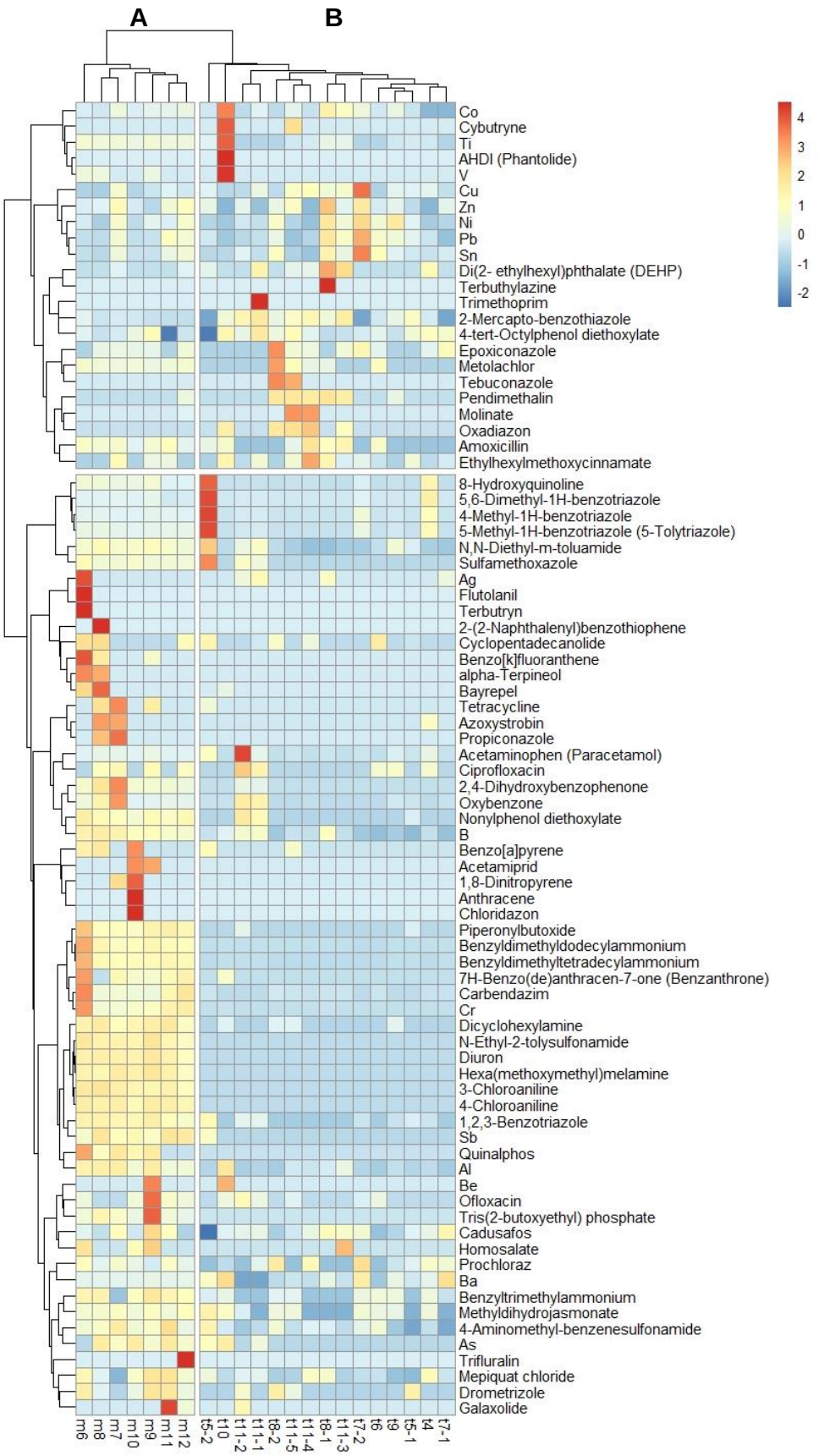

Figure 3.107. Heatmap of micropollutants clustered by spatial z-score normalized concentration profiles in all samples taken from the ***transition zone*** in spring. The color of each cell represents the z-score value calculated for a pollutant at a sampling point.

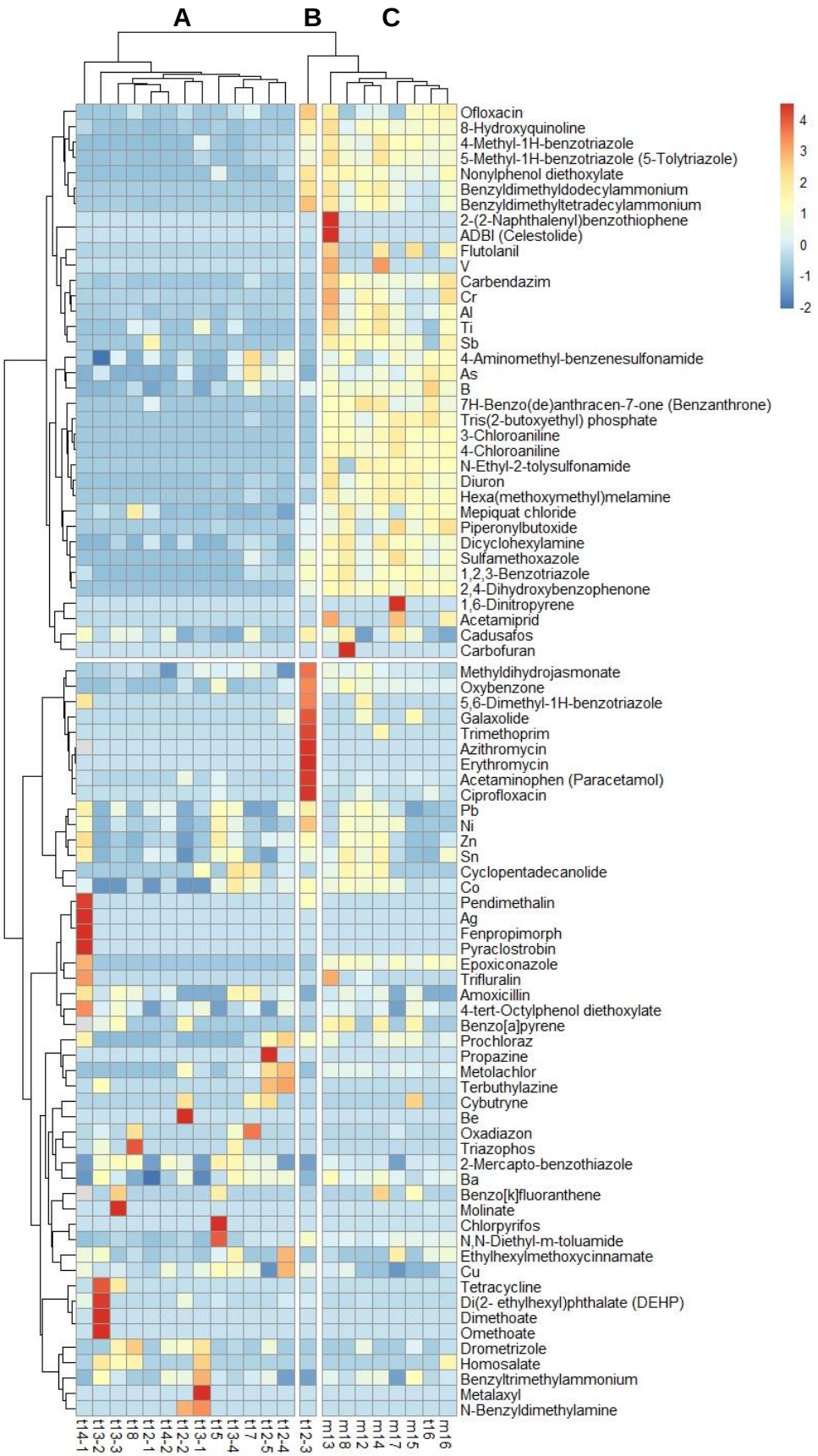

Figure 3.108. Heatmap of micropollutants clustered by spatial z-score normalized concentration profiles in all samples taken from the ***agricultural zone*** in spring. The color of each cell represents the z-score value calculated for a pollutant at a sampling point.

Yet, it was concluded that the sampling points on the Çorlu Creek, Ergene Creek as well as the tributary next to Büyükkarıştıran OIZ in the ***industrial zone*** are the main contributors of the pollution in the Ergene River. However, which sampling points on those creeks are the main sources of pollution is not clear. Therefore, further analysis was performed on each creek for all seasons, individually. For that, z-score normalized concentration profiles of the micropollutants at the sampling points on the Çorlu Creek (*cc1-cc11*) and Ergene creek (*ec1-ec8*) was used.

Sampling points on the Çorlu Creek were mainly grouped into two clusters in all seasons. Sampling points *cc6*, *cc7* and *cc8* in summer (Figure 3.109, cluster A), *cc7* and *cc8* in fall (Figure 3.110. cluster A), *cc5*, *cc6*, *cc7* and *cc8* in winter (Figure 3.111, cluster A) and *cc6*, *cc7* and *cc8* in spring (Figure 3.112, cluster A) were separated from the other sampling points (cluster B in all seasons) on the creek. Those sampling points (cluster A in all seasons) were the ones at which most of the micropollutants were detected mainly at high concentration. Among them, sampling point *cc7* and *cc8* were common in all seasons placing them as the main sources of micropollutants in the Çorlu Creek. In addition, both of those points are located close to Velimeşe OIZ which consists of different industrial facilities including metals, textile, plastic and etc. Following these two sampling points, sampling point *cc1* close to Çekezköy OIZ and *cc2* next to Kapaklı OIZ are the most important pollution sources.

Sampling points on the Ergene Creek were subjected to hierarchical clustering, as well. Although sampling points were not grouped in the same way in all seasons, *ec4*, *ec6* and *ec8* were separated from the rest of the sampling points on the creek at the most time of the year. Specially in fall where the highest number of sampling points were detected, sampling points *ec4* and *ec6* (Figure 3.114, cluster A) were placed in a separate cluster than others. In summer and fall, *ec8* was the third most important sampling point that was separated from the others. The abovementioned sampling points are located next to Ergene 2 OIZ (*ec4*), Ergene 1 OIZ (*ec6*) and Muratlı OIZ (*ec8*).

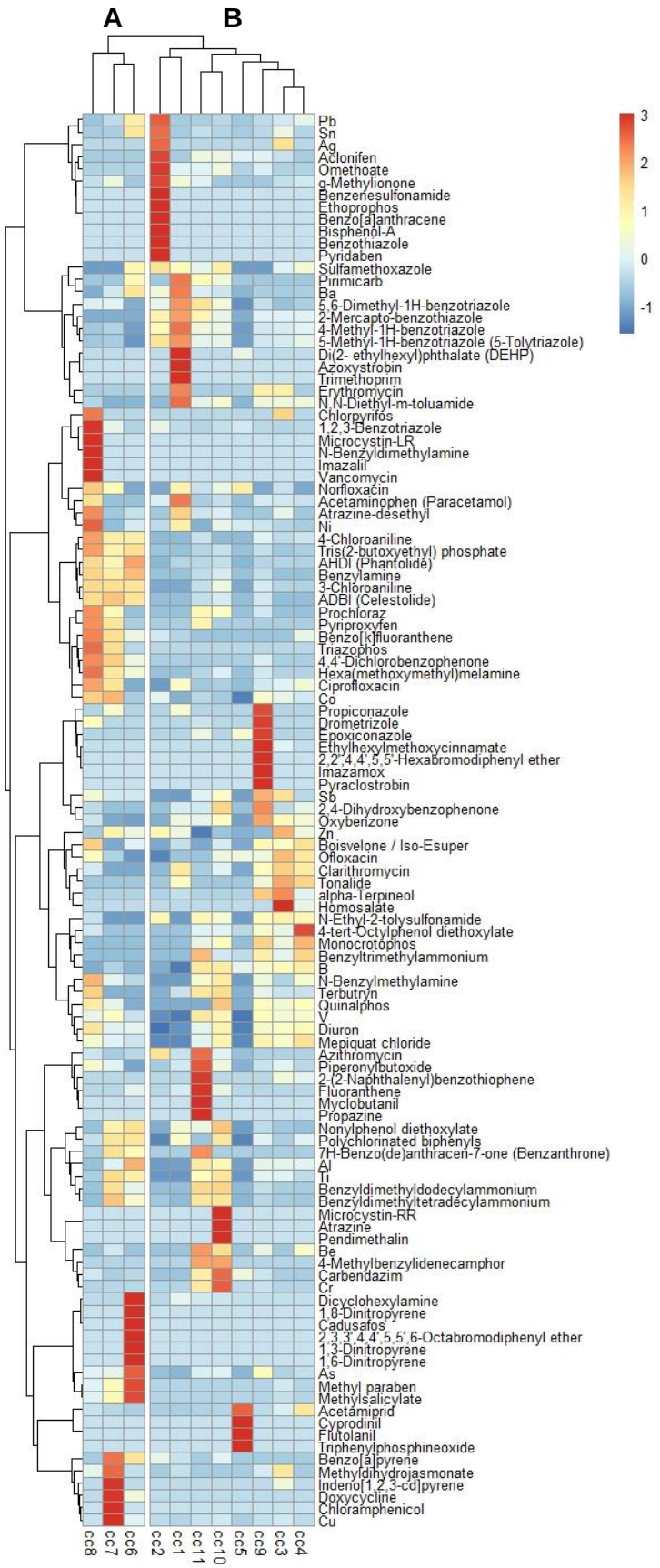

Figure 3.109. Heatmap of micropollutants clustered by spatial z-score normalized concentration profiles in the samples taken from the Çorlu Creek in summer. The color of each cell represents the z-score value calculated for a pollutant at a sampling point.

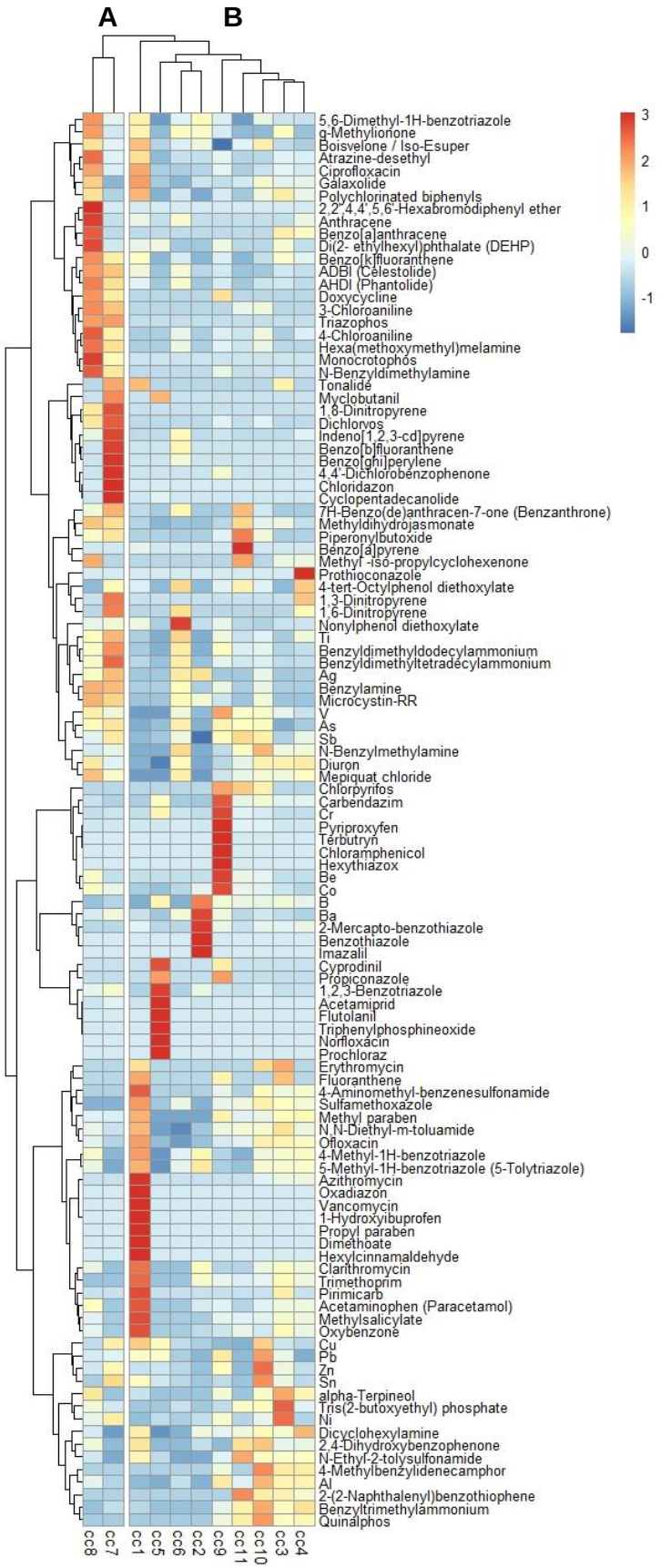

Figure 3.110. Heatmap of micropollutants clustered by spatial z-score normalized concentration profiles in the samples taken from the Çorlu Creek in fall. The color of each cell represents the z-score value calculated for a pollutant at a sampling point.

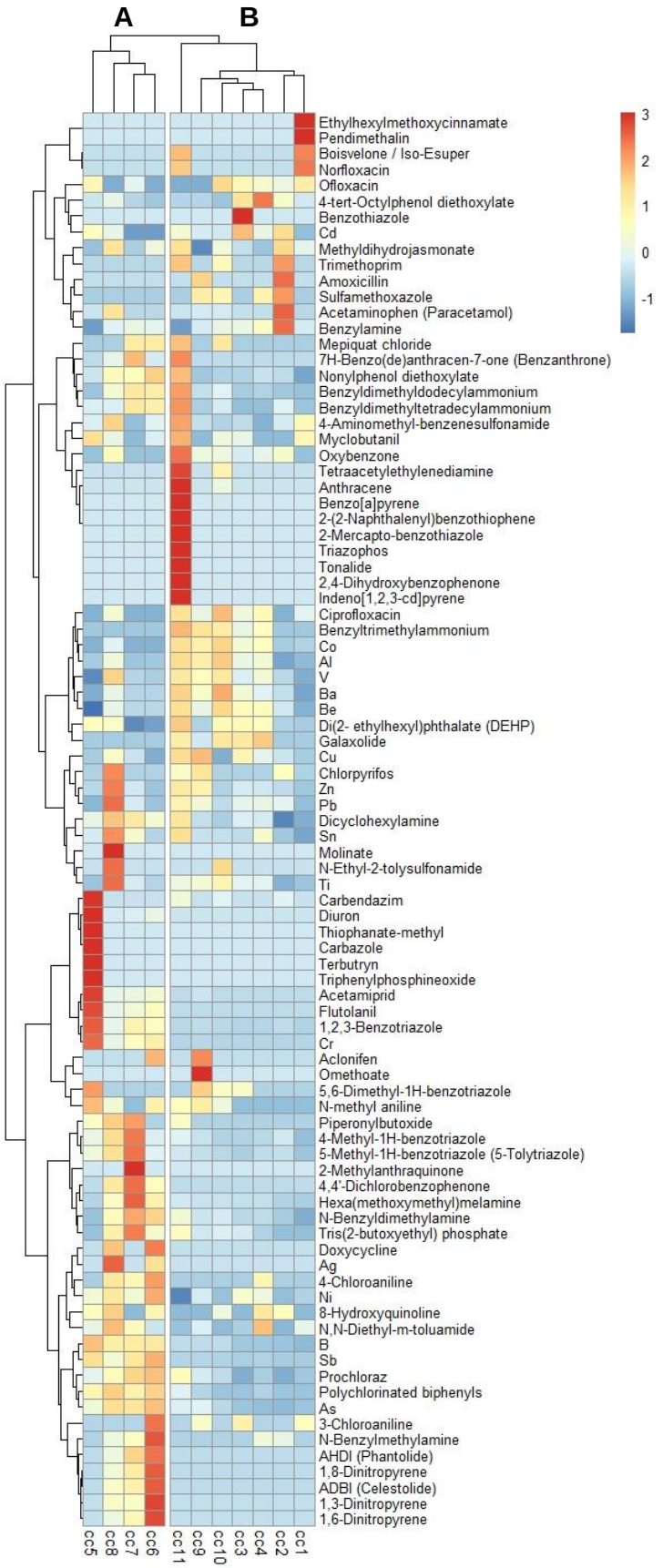

Figure 3.111. Heatmap of micropollutants clustered by spatial z-score normalized concentration profiles in the samples taken from the Çorlu Creek in winter. The color of each cell represents the z-score value calculated for a pollutant at a sampling point.

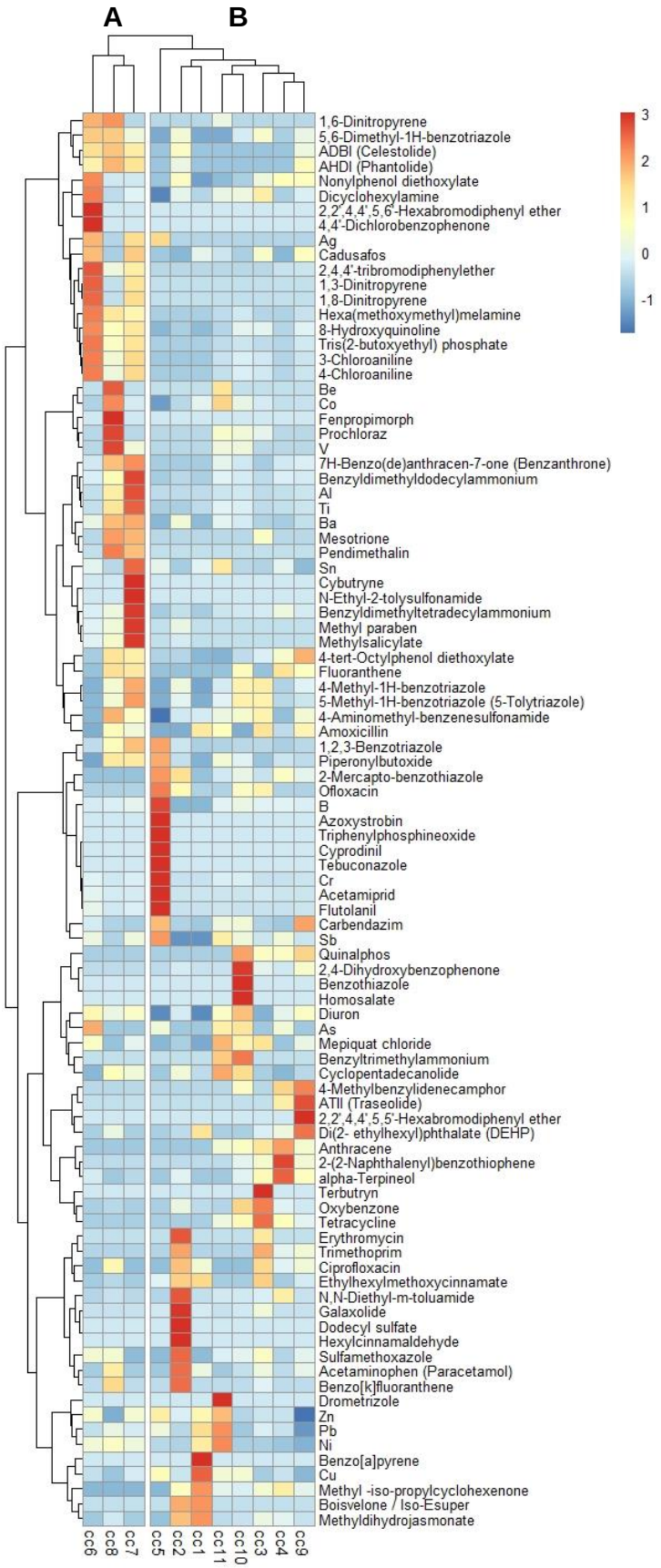

Figure 3.112. Heatmap of micropollutants clustered by spatial z-score normalized concentration profiles in the samples taken from the Çorlu Creek in spring. The color of each cell represents the z-score value calculated for a pollutant at a sampling point.

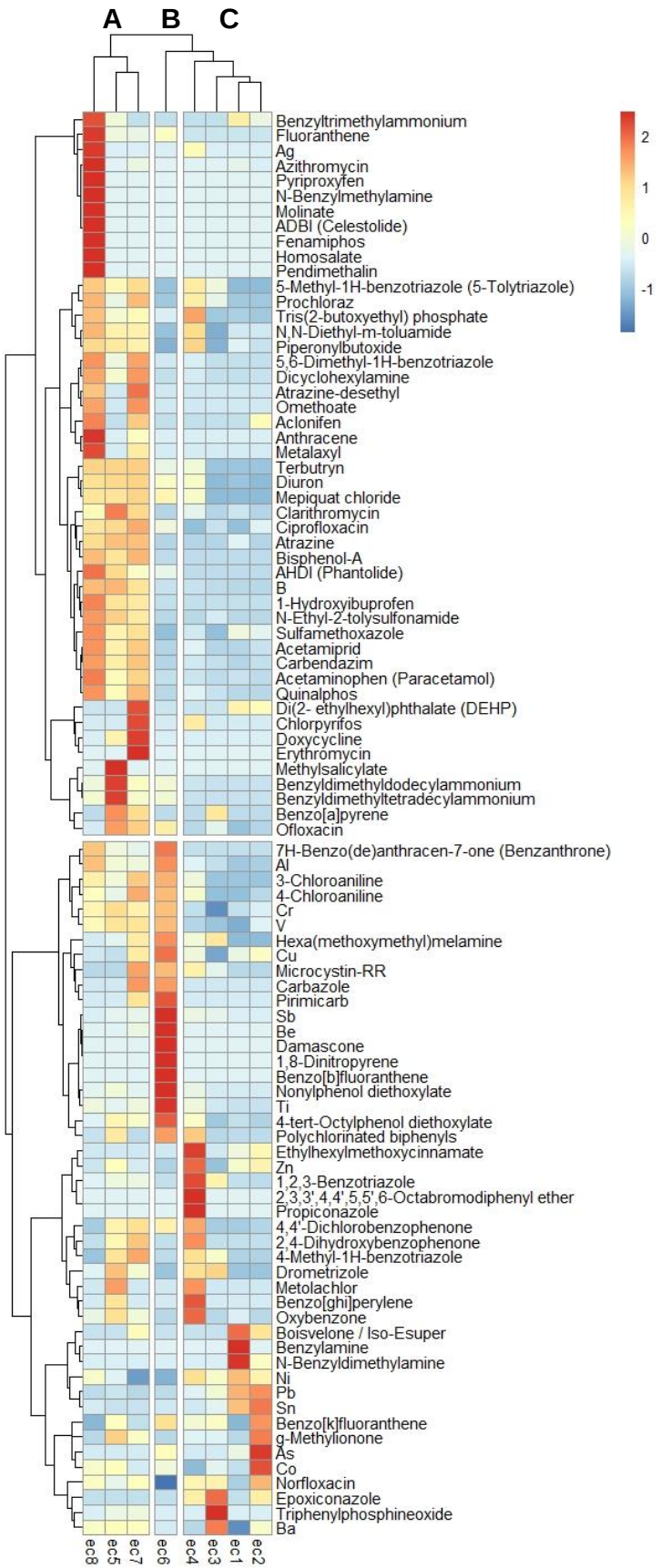

Figure 3.113. Heatmap of micropollutants clustered by spatial z-score normalized concentration profiles in the samples taken from the Ergene Creek in summer. The color of each cell represents the z-score value calculated for a pollutant at a sampling point.

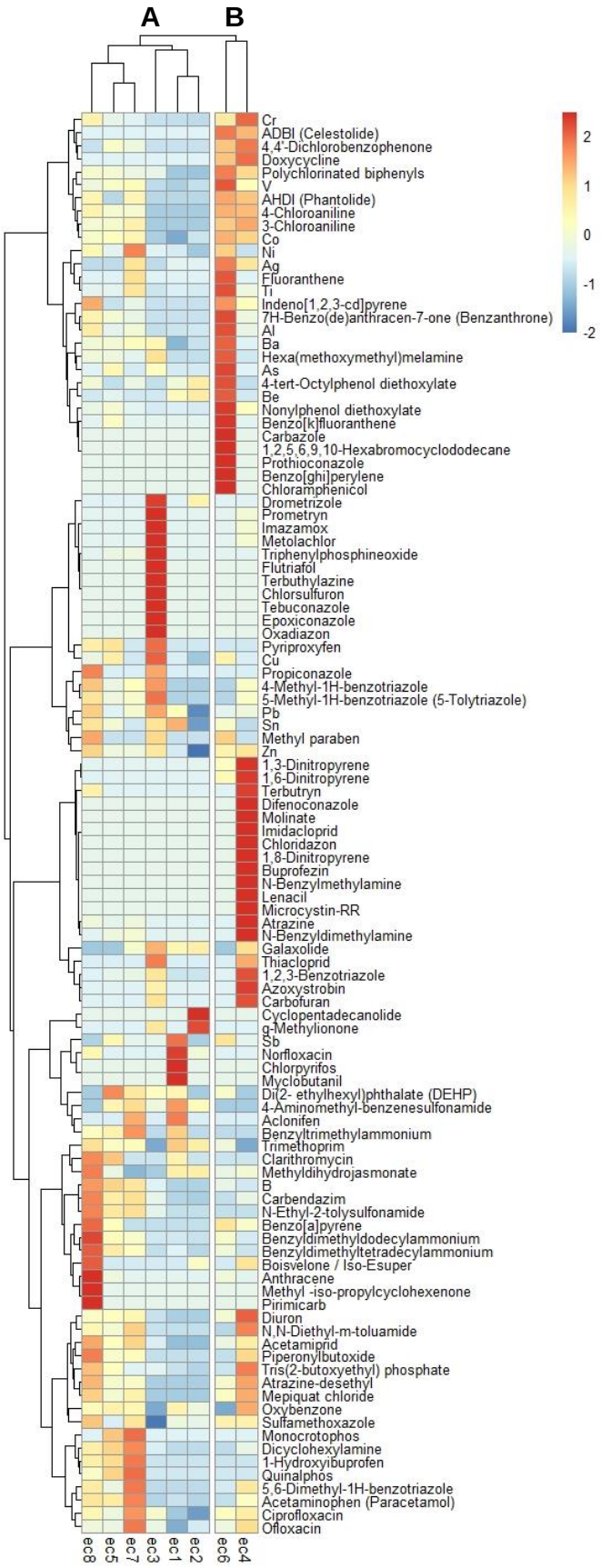

Figure 3.114. Heatmap of micropollutants clustered by spatial z-score normalized concentration profiles in the samples taken from the Ergene Creek in fall. The color of each cell represents the z-score value calculated for a pollutant at a sampling point.

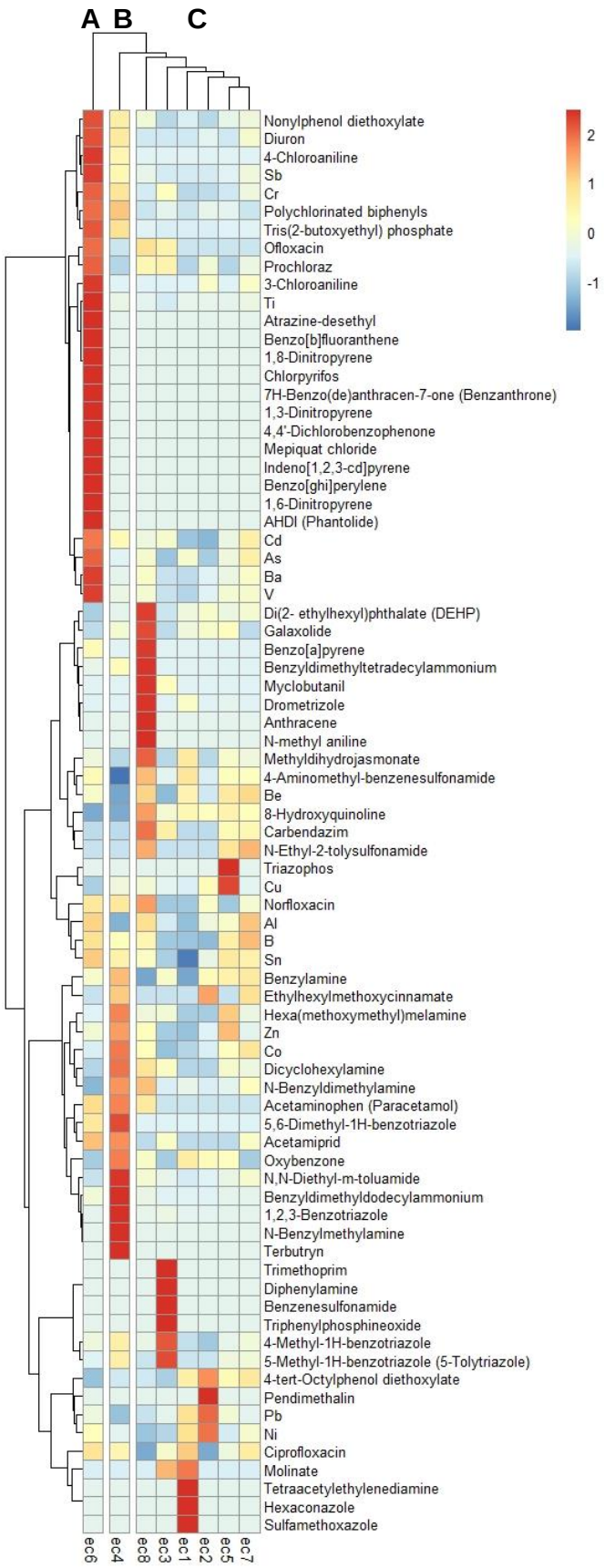

Figure 3.115. Heatmap of micropollutants clustered by spatial z-score normalized concentration profiles in the samples taken from the Ergene Creek in winter. The color of each cell represents the z-score value calculated for a pollutant at a sampling point.

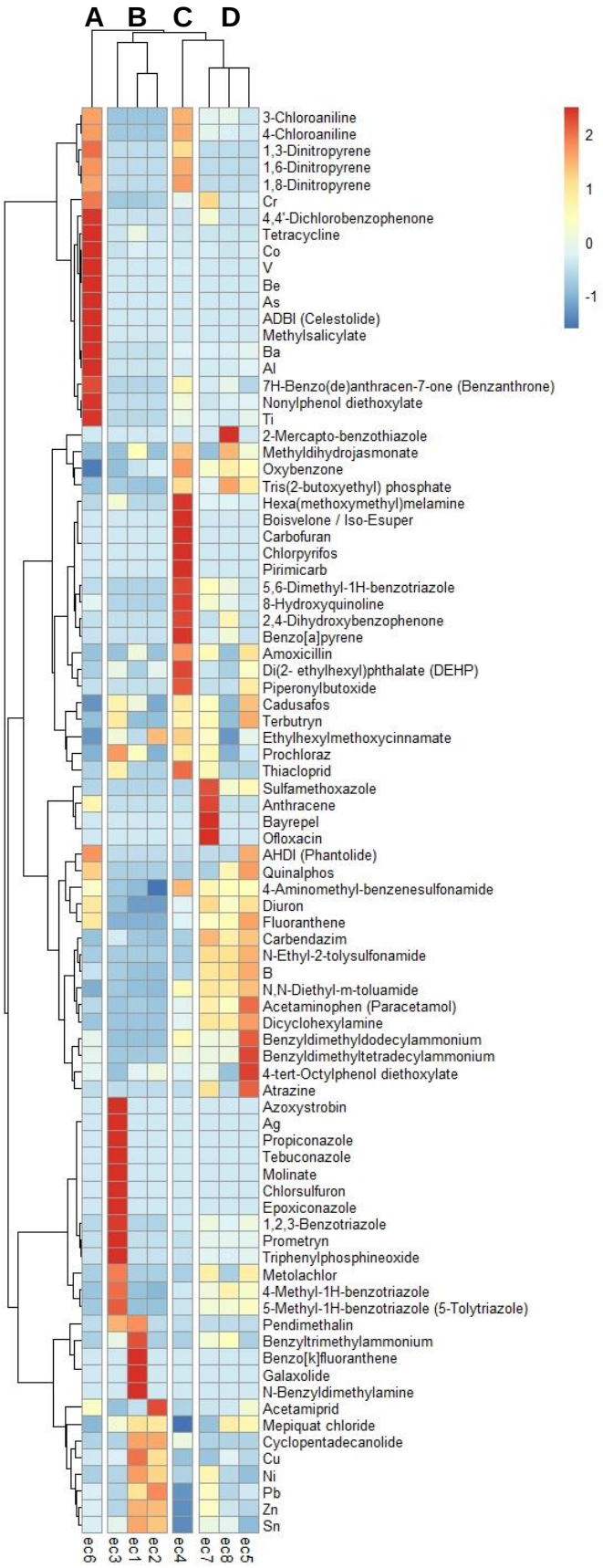

Figure 3.116. Heatmap of micropollutants clustered by spatial z-score normalized concentration profiles in the samples taken from the Ergene Creek in spring. The color of each cell represents the z-score value calculated for a pollutant at a sampling point.

The clustering results described above revealed that the sampling points located next to the OIZs in ***industrial zone*** are the main sources of pollution in the Ergene River (Figure 3.117). However, considering the detection frequency and concentration of micropollutants (particularly in fall that the highest number of micropollutants were detected), *cc7* on the Çorlu Creek, *ec6* on the Ergene Creek and *t1-1* on the tributary next to Büyükkarıştıran OIZ, were identified as the most important pollution sources.

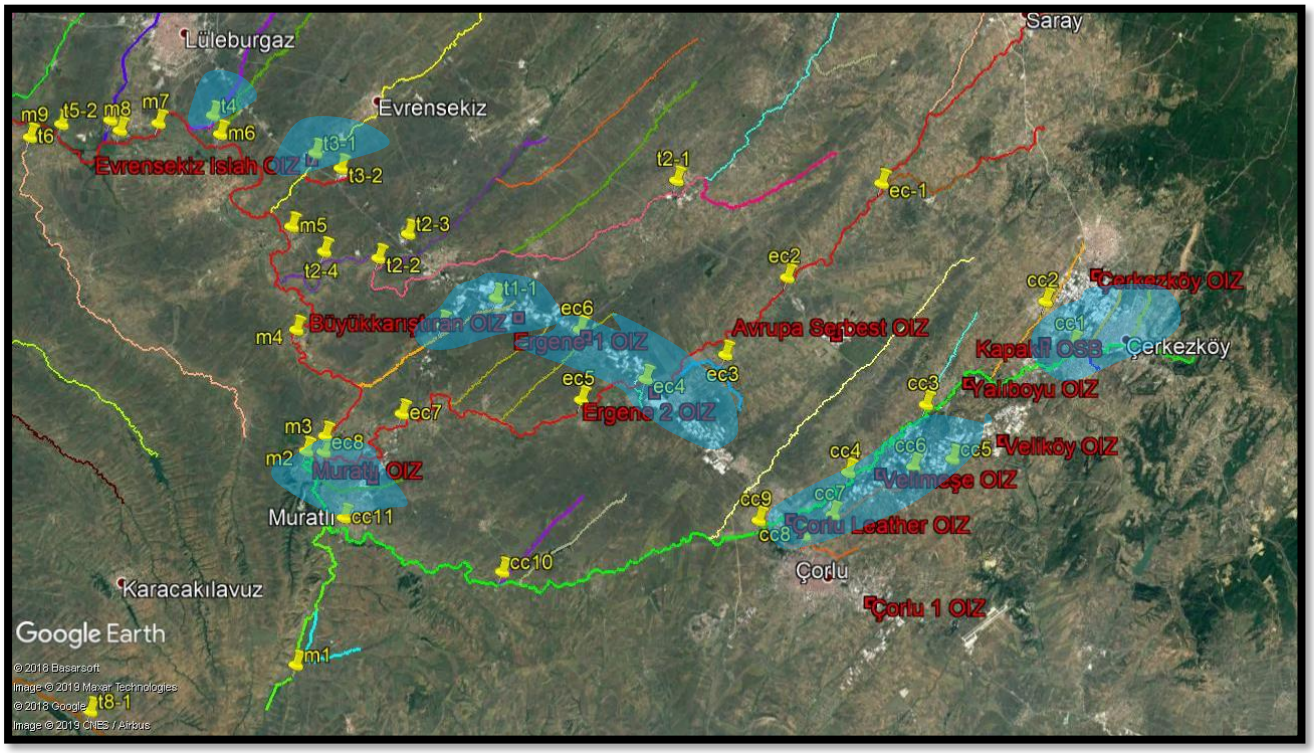

Figure 3.117. Zones of Pollution sources in the Ergene River.

Sampling point *cc7* is located next to Velimeşe OIZ that consists of textiles, metals, plastic production, chemical manufacturing as well as electrical equipment production industries. Considering the clustering analysis of all sampling points (Figure 3.93-Figure 3.96) as well as the sampling points on the Çorlu Creek in all seasons (Figure 3.109-Figure 3.112), the most important micropollutants detected in that sampling point are listed in Table 3.9. In addition, considering the occurrence of those micropollutants in more than three seasons of the year, micropollutants including 1,2,3-benzotriazole, 3-chloroaniline, 4,4-dichlorobenzophenone, 4-chloroaninline, 7H-benzo(de)anthracen-7-one (Benzanthrone), ADBI (Celestolide), AHDI (Phantolide), benzyldimethyldodecylammonium, benzyldimethyltetradecylammonium, hexa(methoxymethyl)melamine, methyldihydrojasmonate and tris-(2-butoxyethyl) phosphate were the fingerprint pollutants of this pollution source.

Table 3.9. List of micropollutants with high concentration in sampling point *cc7* in all season.

Sampling point *cc7*			
Summer	**Fall**	**Winter**	**Spring**
3-chloroaniline	1,2,3-benzotriazole	1,2,3-Benzotriazole	1,2,3-Benzotriazole
4,4-Dichlorobenzophenone	1,3-Dinitropyrene	2-methylanthaquinone	1,3-Dinitropyrene
4-chloroaniline	1,6-Dinitropyrene	4,4-Dichlorobenzophenone	1,8-Dinitropyrene
7H-benzo(de)anthracen-7-one (Benzanthrone)	1,8-Dintropyrene	4-chloroaniline	2,4,4-tribromodiphenylether
ADBI (Celestolide)	3-chloroaniline	4-methyl-1H-benzotriazole	3-chloroaniline
AHDI (Phantolide)	4,4-Dichlorobenzophenone	5-methyl-1H-benzotriazole	4-aminomethyl-benzenesulfonamide
Benzo[k]fluoranthene	4-chloroaniline	7H-benzo(de)anthracen-7-one (Benzanthrone)	4-chloroaniline
Benzyldimethyl dodecylammonium	7H-benzo(de)anthracen-7-one (Benzanthrone)	Benzyldimethyl dodecylammonium	4-methyl-1H-benzotriazole
Benzyldimethyl tetradecyl ammonium	ADBI (Celestolide)	Benzyldimethyl tetradecyl ammonium	4-tert-octylphenol diethoxylate
chloramphenicol	Ag	Cr	5-methyl-1H-benzotriazole
Ciprofloxacin	AHDI (Phantolide)	Hexa(methoxymethyl)melamine	7H-benzo(de)anthracen-7-one (Benzanthrone)
Co	As	Mepiquat chloride	8-hydroxyquinoline
Cu	Ba	N.N-diethyl-m-toluamide	ADBI (Celestolide)
Doxycycline	Benzo[b]fluoranthene	N-benzyldimethylamine	Ag
Hexa(methoxymethyl) melamine	Benzo[ghi]perylene	Nonylphenol diexthoxylate	AHDI (Phantolide)
Methyldihydrojasmonate	Benzo[k]fluoranthene	Piperonylbutoxide	Al
Nonylphenol diexthoxylate	Benzylamine	Polychlorinated biphenyls	Amoxicillin
Norfloxacin	Benzyldimethyl dodecylammonium	Tris-(2-butoxyethyl) phosphate	Ba
Polychlorinated byphenils	Benzyldimethyl tetradecyl ammonium	-	Benzyldimethyl dodecylammonium
Prochloraz	Chloridazon	-	Benzyldimethyl tetradecyl ammonium
Propiconazole	Cu	-	Cadusafos
Pyriproxyfen	Cyclopentadecanolide	-	Cybutryne
Qunialphos	Dichlorvos	-	Fluoranthene
Ti	Doxycycline	-	Hexa(methoxymethyl) melamine
Triazophos	Hexa(methoxymethyl) melamine	-	Mesotrione
Tris-(2-butoxyethyl)phosphate	Indeno[1,2,3]perylene	-	Methyl paraben
V	Mepiquat chloride	-	Methyldihydrojasmonate
Zn	Methyldihydrojasmonate	-	Methylsalicylate

Table 3.9. Continued.

Sampling point *cc7*			
Summer	**Fall**	**Winter**	**Spring**
-	Microcystin-RR	-	N-ethyl-2-tolysulfonamide
-	Monocrotophos	-	Pendimethalin
-	Myclobutanil	-	Piperonylbutoxide
-	N-benzyldimethylamine	-	Sn
-	Ni	-	Ti
-	Sb	-	Tris-(2-butoxyethyl) phosphate
-	Sn	-	-
-	Tonalide	-	-
-	Triazophos	-	-
-	Zn	-	-

Sampling point *ec6* is the other most substantial pollution source in the Ergene River that is located next to Ergene 1 OIZ composed of mainly textile industries. The high color value of water sample taken from *ec6* showed the discharges of textile effluents from the Ergene 1 OIZ into that point. Based on the clustering analysis of all sampling points (Figure 3.93-Figure 3.96) as well as the ones on the Ergene Creek (Figure 3.113-Figure 3.116), the micropollutants at elevated concentration detected in *ec6* are summarized in Table 3.10. Considering the occurrence of the pollutants during the year, 1,8-dinitropyrene, 3-chloroaniline, 4-chloroaniline, 7H-benzo(de)anthracen-7-one (Benzanthrone), AHDI (Phantolide), Al, Ba, Cr, hexa(methoxymethyl)melamine, nonylphenol diethoxylate, polychlorinated biphenyls, Ti and V were identified as the fingerprint micropollutants released from the sampling point *ec6*.

Table 3.10. List of micropollutants with high concentration in sampling point *ec6* in all season.

Sampling point *ec6*			
Summer	**Fall**	**Winter**	**Spring**
1,8-Dinitropyrene	1,2,5,6,9,10-Hexabromocyclododecane	1,3-dinitropyrene	1,3-dinitropyrene
3-chloroaniline	3-chloroaniline	1,6-dinitropyrene	1,6-dinitropyrene
4-chloroaniline	4,4-Dichlorobenzophenone	1,8-dinitropyrene	1,8-dinitropyrene
4-tert-octylphenol diethoxylate	4-chloroaniline	3-chloroaniline	3-chloroaniline
7H-benzo(de)anthracen-7-one (Benzanthrone)	7H-benzo(de)anthracen-7-one (Benzanthrone)	4-chloroaniline	4,4-Dichlorobenzophenone
Al	ADBI (celestolide)	5,6-dimethyl-1H-benzotriazole	4-chloroaniline
Benzo[b]fluoranthene	Ag	7H-benzo(de)anthracen-7-one (Benzanthrone)	7H-benzo(de)anthracen-7-one (Benzanthrone)
Benzo[b]fluoranthene	AHDI (phantolide)	Acetaminophen	Acetamiprid
Carbazole	Al	Acetamiprid	ADBI (celestolide)
Cr	Ba	AHDI (phantolide)	AHDI (phantolide)
Cu	Benzo[a]pyrene	Al	Al
Damascone	Benzo[ghi]perylene	As	As
Hexa(methoxymethyl) melamine	Benzo[k]fluoranthene	Atrazine-desethyl	Ba
Microcystin-RR	Carbazole	B	Be
Nonylphenol diethoxylate	Chloramphenicol	Ba	Co
Pirmicarb	Co	Benzo[b]fluoranthene	Cr
Polychlorinated biphenyls	Cr	Cd	Diuron
Sb	Doxycycline	Chlorpyrifos	Fluoranthene
Ti	Fluoranthene	Cr	Methylsalicylate
V	Hexa(methoxymethyl) melamine	Diuron	Nonylphenol diethoxylate
-	Indeno[1,2,3-cd]pyrene	Hexa(methoxymethyl) melamine	Quinalphos
-	Methyl paraben	Nonylphenol diethoxylate	Tetracycline
-	Ni	Norfloxacin	Ti
-	Nonylphenol diethoxylate	Ofloxacin	V
-	Polychlorinated biphenyls	Polychlorinated biphenyls	-
-	Prothioconazole	Prochloraz	-
-	Sulfamethoxazole	Sb	-
-	Ti	Sn	-
-	V	Ti	-
-	Zn	Tris-(2-butoxyethyl) phosphate	-
-	-	V	-

One of the most important sampling points at which micropollutants were detected at high detection and concentration during the year was sampling *t1-1*. This sampling point is located next to

Büyükkarıştıran OIZ and is surrounded by mainly textiles as well as electrical equipment manufacturing, power plant, plastic production, metal and pharmaceutical industries. Clustering analysis of all sampling points (Figure 3.93-Figure 3.96) indicated that, important micropollutants observed in *t1-1* are the ones listed in Table 3.11. In addition, micropollutants including 1,3-dinitropyrene, 1,6-dinitropyrene and 1,8-dinitropyrene, 3-chloroaniline, 4-chloroaniline, 7H-benzo(de)anthracen-7-one (Benzanthrone), ADBI (celestolide), AHDI (phantolide), Al, As, benzyldimethyldodecylammonium, benzyldimethyltetradecylammonium, diuron, hexa(methoxymethyl)melamine, mepiquat chloride, Sb, Sn, Ti and V were recognized as the fingerprint pollutants belong to sampling point *t1-1* during the year.

Table 3.11. List of micropollutants with high concentration in sampling point *t1-1* in all season.

Sampling point *t1-1*			
Summer	**Fall**	**Winter**	**Spring**
1,6-Dinitropyrene	1,3-Dinitropyrene	1,3-Dinitropyrene	1,3-Dinitropyrene
1,8-dinitropyrene	1,6-Dinitropyrene	1,6-Dinitropyrene	1,6-Dinitropyrene
2,3,3,4,4,5,5,6-octabromodiphenyl ether	1,8-dinitropyrene	1,8-dinitropyrene	1,8-dinitropyrene
3-chloroaniline	4-chloroaniline	3-chloroaniline	3-chloroaniline
4-chloroaniline	7H-Benzo(de)anthracen-7-one (Benzanthrone)	3-nitrobenzanthrone	4,4-Dichlorobenzophenone
Acteaminophen (paracetamol)	Aclonifen	4-aminomethyl-benzenesulfonamide	4-aminomethyl-benzenesulfonamide
ADBI (Celestolide)	ADBI (Celestolide)	4-chloroaniline	4-chloroaniline
AHDI (Phantolide)	AHDI (Phantolide)	4-methyl-1H-benzotriazole	4-methyl-1H-benzotriazole
Al	Al	5-methyl-1H-benzotriazole	4-tert-octylphenol diethoxylate
As	Anthracene	7H-Benzo(de)anthracen-7-one (Benzanthrone)	5-methyl-1H-benzotriazole
Atrazine	Atrazine-desethyl	ADBI (Celestolide)	7H-Benzo(de)anthracen-7-one (Benzanthrone)
Benzo[a]pyrene	Benzyldimethyldodecyl ammonium	Ag	Acetaminophen (paracetamol)
Benzo[b]fluoranthene	Benzyldimethyltetradecyl ammonium	AHDI (Phantolide)	Acetamiprid
Benzo[k]fluoranthene	Chloramphenicol	Amoxicillin	ADBI (Celestolide)
Benzyldimethyldodecyl ammonium	Cyprodinil	As	Ag
Benzyldimethyltetradecyl ammonium	Diuron	Atrazine-desethyl	AHDI (Phantolide)
Diuron	Doxycycline	B	Al

Table 3.11. Continued.

Sampling point *t1-1*			
Summer	**Fall**	**Winter**	**Spring**
Hexa(methoxymethyl)melamine	Hexa(methoxymethyl)melamine	Benzo[b]fluoranthene	As
Mepiquat chloride	Mandipropamid	Benzo[ghi]perylene	B
Methayl paraben	Mepiquat chloride	Benzyldimethyldodecyl ammonium	Benzyldimethyldodecyl ammonium
Methylsalicylate	Nonylphenol diethoxylate	Co	Benzyldimethyltetradecyl ammonium
Nonylphenol diethoxylate	Omethoate	Doxycycline	Cadusfos
Polychlorinated biphenyls	Sb	Hexa(methoxymethyl)melamine	Ciprofloxacin
Sb	Sn	Hexaconazole	Co
Terbutryn	Ti	Indeno-[1,2,3-cd]pyrene	Cu
Ti	V	Mepiquat chloride	Cyclopentadecanolide
V	-	Methyldihydrojasmonate	Diuron
-	-	Myclobutanil	Hexa(methoxymethyl)melamine
-	-	N-benzyldimethylamine	Methyl paraben
-	-	Ni	Methyl salicylate
-	-	Nonylphenol diethoxylate	Ni
-	-	Pendimethalin	Pb
-	-	Polychlorinated biphenyls	Sb
-	-	Sb	Sn
-	-	Sn	Ti
-	-	Tetrabisphenol A	Tris-(2-butoxyethyl) phosphate
-	-	Ti	V
-	-	Tris-(2-butoxyethyl) phosphate	Zn
-	-	V	-
-	-	-	-

Sampling point *t3-1* was determined with high detection frequency of micropollutants in summer and fall. That sampling point receives the effluent from Evrensekiz OIZ as well as domestic and agricultural wastewaters around it. Therefore, the micropollutants specific to this pollution source embraced broad spectrum of industrial, agricultural as well as domestic chemicals. Clustering analysis of the all samples (Figure 3.93-Figure 3.96) indicated that micropollutants listed in Table 3.12 are specific to sampling point *t3-1*. Detail investigation of micropollutants for summer and fall seasons demonstrated that 1-hydroxyibuprofen, 4-aminomethyl-benzenesulfonamide, 4-methyl-1H-benzotriazole, 5-mehyl-1H-benzotriazole, 7H-benzo(de)anthracen-7-one (Benzanthrone), AHDI (phantolide), anthracene, atrazine-desethyl, azithromycin, B, carbendazim, ciprofloxacin, di-(2-

ethylhexl)phthalate, dicyclohexylamine, diuron, metalaxyl, methyl paraben, N,N-diethyl-m-toluamide, N-ethyl-2-tolysolfunamide, Ni, norfloxacin, omethoate, pendimethalin, piperonylbutoxide, pirimicarb, quinalphos, sulfamethoxazole and Zn, were the fingerprint pollutants for sampling point *t3-1* during fall and summer.

Table 3.12. List of micropollutants with high concentration in sampling point *t3-1* in all season.

Sampling point *t3-1*			
Summer	**Fall**	**Winter**	**Spring**
1-hydroxyibuprofen	1-Hydroxyibuprofen	4-methyl-1H-benzotriazole	5,6-dimethyl-1H-benzotriazole
4-aminomethyl-benzenesulfonamide	4-aminomethyl-benzenesulfonamide	5-methyl-1H-benzotriazole	7H-Benzo(de)anthracen-7-one (Benzanthrone)
4-methyl-1H-benzotriazole	4-methyl-1H-benzotriazole	Acetamiprid	8-hydroxyquinoline
5,6-dimehtyl-1H-benzotriazole	5-methyl-1H-benzotriazole	Anthracene	Amoxicillin
5-methyl-1H-benzotriazole	7H-Benzo(de)anthracen-7-one (Benzanthrone)	B	Azoxytrobin
7H-Benzo(de)anthracen-7-one (Benzanthrone)	8-hydroxyquinoline	Benzyldimehtyltetradecyl ammonium	B
Acetaminophen (paracetamol)	Aclonifen	Ciprofloxacin	Bayrepel
Acetamiprid	ADBI (Celestolide)	Dicyclohexylamine	Benzo[k]fluoranthene
AHDI (Phantolide)	AHDI (Phantolide)	Drometrizole	Cadusafos
Anthracene	Anthracene	Galaxolide	Chlorfenvinphos
Atrazine-desethyl	Atrazine-desethyl	Methyldihydrojasmonate	Ciprofloxacin
Azithromycin	Azithromycin	Myclobutanil	Cyclopentadecanolide
B	B	N,N-diethyl-m-toluamide	Dicyclohexylamine
Benzo[a]pyrene	Benzylamine	N-ethyl-2-tolysulfonamide	Eposxiconazole
Benzyltrimethylamine	Boisvelone/Iso-Esuper	Pendimethalin	Homosalate
Bisphenol-A	Carbendazim	Piperonylbutoxide	N,N-diethyl-m-toluamide
Carbendazim	Ciprofloxacin	Quinalphos	N-ethyl-2-tolysulfonamide
Chlorfenvinphos	Di-(2-ethylhexyl)phthalate (DEHP)	Tris(2-butoxyethyl) phosphate	Omethoate
Ciprofloxacin	Dicyclohexylamine	-	Piperonylbutoxide
Clarithromycin	Diuron	-	Prochloraz
Co	Drometrizole	-	Propiconazole
Di-(2-ethylhexyl)phthalate (DEHP)	Mepiquat chloride	-	Qunialphos
Dicyclohexylamine	Metalaxyl	-	Sulfamethoxazole
Diuron	methyl paraben	-	-
Erythromycin	Methyldihydrojasmonate	-	-
Fluoranthene	Methyl-iso-propylcyclohexenone	-	-

Table 3.12. Continued.

Sampling point *t3-1*			
Summer	**Fall**	**Winter**	**Spring**
Imazalil	methylsalicylate	-	-
Lenacil	Molinate	-	-
Metalaxyl	N,N-diethyl-m-toluamide	-	-
Methyl paraben	N-ethyl-2-tolysulfonamide	-	-
Metolachlor	Ni	-	-
N-benzyldimethylammonium	Norfloxacin	-	-
N-ethyl-2-tolysulfonamide	Omethoate	-	-
Ni	Pb	-	-
Norfloxacin	Pendimethalin	-	-
Omethoate	Pirmicarb	-	-
Pendimethalin	Propiconazole	-	-
Piperonylbutoxide	Quinalphos	-	-
Pirmicarb	Sulfamethoxazole	-	-
Prochloraz	Trimethoprm	-	-
Propetamphos	V	-	-
Pyridaben	Zn	-	-
Qunialphos	-	-	-
Sulfamethoxazole	-	-	-
Terbutryn	-	-	-
Tetracycline	-	-	-
Zn	-	-	-

Similar to sampling point *t3-1*, *t4* was also separated from the other sampling point in hierarchical clustering analysis during summer and fall. Sampling point *t4* is located next to Lülebürgaz city and surrounded by agricultural lands in the region. In addition, some single industrial facilities are in close distance to *t4*. Therefore, domestic, industrial as well as agricultural-specific chemicals were found in the samples taken from that sampling point specially in summer and fall. Clustering analysis of all samples (Figure 3.93-Figure 3.96) indicated that chemicals listed in Table 3.13 are originated from *t4*. Micropollutants including 4-aminomethyl-benzenesulfonamide, 4-methyl-1H-benzotriazole, 4-methylbenzyldenecamphor, 5,6-dimethyl-1H-benzotriazole, anthracene, benzo[ghi]perylene, boisvelone/iso Esuper, cadusafos, ciprofloxacin, Co, epoxiconazole, fluoranthene, imazalil, N-ethyl-2-tolysulfonamide, Ni, omethoate, pendimethalin, propetamphos and quinalphos were the fingerprint pollutants of sampling point *t4*.

Table 3.13. List of micropollutants with high concentration in sampling point *t4* during all season.

Sampling point *t4*			
Summer	**Fall**	**Winter**	**Spring**
1,2,3-benzotriazole	4-aminomethyl-benzenesulfonamide	5,6-dimethyl-1H-benzotriazole	4-methyl-1H-benzotriazole
2,3,3,4,4,5,5,6-Octabromodiphenyl ether	4-methyl-1H-benzotriazole	Anthracene	5,6-dimethyl-1H-benzotriazole
4-aminomethyl-benzenesulfonamide	4-methylbenzyldenecamphor	B	5-methyl-1H-benzotriazole
4-methyl-1H-benzotriazole	5,6-dimethyl-1H-benzotriazole	Benzyldimethyltetradecyl ammonium	8-hydroxyquinoline
4-methylbenzyldenecamphor	5-methyl-1H-benzotriazole	Chloridazon	Azoxystrobin
5,6-dimethyl-1H-benzotriazole	8-hydroxyquinoline	Drometrizole	Epoxiconazole
7H-Benzo(de)anthracen-7-one (Benzanthrone)	Anthracene	Methyldihydrojasmonate	Mepiquat chloride
Al	Atrazine-desethyl	N-Ethyl-2-tolysulfonamide	Prochloraz
Anthracene	Benzo[a]anthracene	Trimethoprim	-
Ba	Benzo[ghi]perylene	-	-
Benzo[ghi]perylene	Benzo[k]fluoranthene	-	-
Bisphenol-A	Boisvelone/Iso Esuper	-	-
Boisvelone/Iso Esuper	Cadusafos	-	-
Cadusafos	Carbendazim	-	-
Carbofuran	Carbuforan	-	-
Cd	Ciprofloxacin	-	-
Chloramphenicol	Co	-	-
Ciprofloxacin	Dimethoate	-	-
Co	Drometrizole	-	-
Cu	Epoxiconazole	-	-
Dicyclohexylamine	Fenpropimorph	-	-
Epoxiconazole	Fluoranthene	-	-
Fluoranthene	Imazalil	-	-
Imazalil	Mepiquat chloride	-	-
Indeno[1,2,3-cd]pyrene	Monocrotophos	-	-
Lenacil	Myclobutanil	-	-
Mepiquat chloride	N-Ethyl-2-tolysulfonamide	-	-
Metalaxyl	Ni	-	-
N-Ethyl-2-tolysulfonamide	Norfloxacin	-	-
Ni	Omethoate	-	-
Omethoate	Pendimethalin	-	-
Penconazole	Pirimicarb	-	-
Pendimethalin	Propetamphos	-	-
Pentachlorobenzene	Propiconazole	-	-
Polychlorinated biphenyls	Quinalphos	-	-
Prochloraz	Sulfamethoxazole	-	-
Propetamphos	-	-	-

Table 3.13. Continued.

Sampling point *t4*			
Summer	**Fall**	**Winter**	**Spring**
Propyl paraben	-	-	-
Pyridaben	-	-	-
Quinalphos	-	-	-
Spiroxamine	-	-	-
Terbuthylazine	-	-	-
Terbutryn	-	-	-
Tetracycline	-	-	-
Ti	-	-	-
V	-	-	-
Zn	-	-	-

Analysis of wastewater samples taken from four industries located in industrial zone: To verify our founding, we analyzed wastewater samples taken from an aluminum industry, a paper industry and two textile industries located in the ***industrial zone***. Those industries were selected since there are the most abundant industries in the Ergene Watershed. The analysis of the wastewaters indicated that textile industries possessing high COD are the main contributors of COD pollution in the Ergene River (Table 3.14). This fact was in compliance with high CODs measured at the main pollution sources stated above. COD at average concentrations of 774.20, 773.96 and 831.7 mg/L was measured at sampling points *cc7*, *ec6* and *t1-1* which are surrounded by textile and dye industries, respectively. In addition to COD, heavy metals including As, Ba, Cr, Ti and Sb as well as organic micropollutants mainly HMMM, BDDDA, BDTDA, nitropyrenes and chloroanilines were present at their highest concentrations in the wastewater taken from the textile industries (Table 3.14). Those pollutants were also present at high levels at sampling points *cc7*, *ec6* and *t1-1* identified as the most important pollution sources. For instance, mean concentrations of 122,301.38, 18,180.41 and 161,575.92 µg/L of HMMM was measured at sampling points *cc7*, *ec6* and *t1-1*, respectively.

Heavy metals such as Zn, Al, Cu, Pb and Ni were measured at high concentrations in the wastewater sample taken from a metal industry (Table 3.14). These metals were also present at their highest concentrations at sampling points on the Çorlu Creek (cc) as well as the tributary close to Büyükkarıştıran OIZ (*t1-1* and *t1-2*) that are surrounded by OIZs at which metal industries are present. For instance, Al was measured at mean concentrations of 20,396.91 and 21,995.76 µg/L in the samples taken from *t1-1* and *cc7* in all seasons, respectively, indicating the effect of metal industries on the elevated Al concentration at those points. In addition to heavy metals, benzotriazoles

(1,2,3-B, 4-M-1H-B and 5-M-1H-B) were present in the wastewater of the metal industry at high levels (Table 3.14). This pattern was also valid for the sampling points on Çorlu Creek and close to the OIZs. For instance, 1,2,3-B was found at high average concentrations of 23.65 and 47.51 µg/L at *cc7* and *ec4* close to Velimeşe and Ergene 2 OIZs, respectively.

The wastewater taken from the paper industry had boron (B) concentration as high as 5114.50 µg/L (Table 3.14). B at high mean concentrations of 1,291.63 and 909.49 µg/L was also measured at *ec8* and *t3-1* located close to Muratlı OIZ and Evrenskiz OIZ, respectively. Those OIZs also have paper industries.

In general, OIZs present in the industrial zone of Ergene Watershed have the highest contribution to the pollution in the Ergene River. Characterizations of the wastewater samples of the main industries revealed that textile and dye industries as the dominant industries, are the main sources of industrial chemicals not only at the sampling points next to them but in some cases in the whole river. In addition, textiles together with other facilities predominantly metal, plastic as well as chemical production discharging their untreated or poorly-treated wastewaters into the Ergene River resulted in inevitable pollution stress in the region.

Table 3.14. Characterization of wastewater samples taken from four industries.

Parameter	Aluminum industry	Paper industry	Textile industry 1	Textile industry 2
Conventional				
COD (mg/L)	390.62	262.36	**1074.70**	509.17
Heavy metals (µg/L)				
As	0.00	0.00	**13.34**	1.40
Ba	65.53	44.18	**169.08**	111.19
Zn	**3948.12**	1849.22	1702.65	2374.51
Cr	1.79	2.95	11.33	**50.92**
Co	1.39	**2.31**	0.52	0.48
Al	**2275.10**	172.10	810.76	117.82
Cu	**1438.56**	1007.99	510.07	980.72
Pb	**1190.12**	708.26	644.60	1181.04
Ni	**3455.06**	1113.86	1227.34	2301.61
Ag	0.27	0.60	0.39	0.10
B	172.73	**5114.50**	230.28	102.70
Sn	**30.53**	21.37	19.26	17.95
Ti	1.27	0.16	**3.19**	1.48
Sb	2.71	1.19	38.16	**597.13**
Organic micropollutants (µg/L)				
1,2,3-Benzotriazole (1,2,3-B)	**1.45**	0.62	0.34	0.00
1,3-Dinitropyrene	0.00	0.00	0.00	**0.37**
1,6-Dinitropyrene	0.00	0.00	0.00	**0.38**
1,8-Dinitropyrene	0.00	0.00	0.00	**0.58**
3-Chloroaniline	0.00	0.00	**1.34**	0.24
4-Chloroaniline	0.00	0.00	**1.51**	0.24
4-Methyl-1H-benzotriazole (4-M-1H-B)	**13.85**	1.41	0.06	0.67
4-tert-Octylphenol diethoxylate	**0.04**	0.03	0.03	**0.04**
5-Methyl-1H-benzotriazole (5-M-1H-B)	**9.15**	0.85	0.05	0.43
7H-Benzo(de)anthracen-7-one (Benzanthrone)	0.00	0.00	0.00	**1.73**
Benzyldimethyldodecylammonium (BDDDA)	0.16	0.29	**0.61**	0.58
Benzyldimethyltetradecylammonium (BDTDA)	0.36	0.47	**0.93**	0.91
Hexa(methoxymethyl)melamine (HMMM)	81.84	39574.62	**245484.28**	21408.04
Nonylphenol diethoxylate	**0.32**	0.00	0.00	0.00

3.3.4. Non-targeted Analysis of Micropollutants in The Ergene River

The non-targeted analysis was conducted for 30 out of 75 sampling points from fall sampling. The selected sampling points represented the point and non-point sources as well as they were located on the main stream and important tributaries (Figure 3.118). After manual infusion of the acidified river water samples to the MS of the instrument, further ionization using positive ESI method, the five most abundant ions in the samples which were not detected in the blank (methanol) were selected for further fragmentation (EPI method). Using EPI method, the selected ions were fragmented individually and the generated spectrum was further compared with the library.

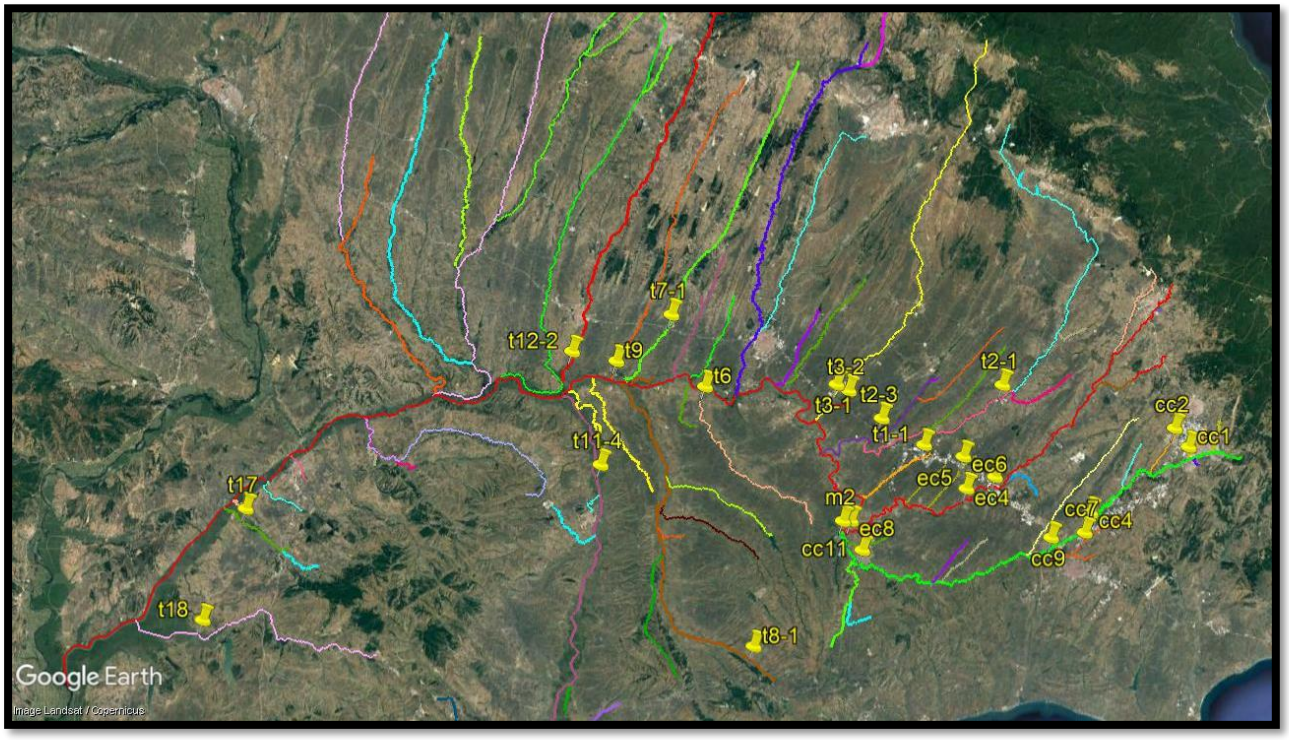

Figure 3.118. Location of 24 sampling points selected for non-targeted analysis.

Out of 24 sampling points selected, 13 sampling points had significant difference compared to blank. These sampling points include sampling points *m2*, *cc4*, *cc7*, *cc9*, *cc11*, *ec4*, *ec5*, *ec6*, *ec8*, *t1-1*, *t2-3*, *t3-1* and *t3-2* which were also among the most polluted sampling points during the targeted analysis of the micropollutants. The aforementioned sampling points were mainly located next to the industrial facilities in the Ergene watershed. The detail of the mass spectrum of the samples is shown in Figure E.1. in APPENDIX E.

After acquiring the mass spectrum of the samples, the five most abundant ions were fragmented. It should be mentioned that, not all of the selected abundant ions have been identified, since the library

does not cover all of the chemicals. Therefore, the chemicals with high similarity with the mass spectrum of the selected ions in the samples were explained in this study.

The fragmented mass of each precursor ion ($[M+H]^+$) for every individual sample is presented in APPENDIX E. For instance, Figure 3.119 shows the comparison of mass spectrum of water sample from sampling point cc11 and the blank (methanol).

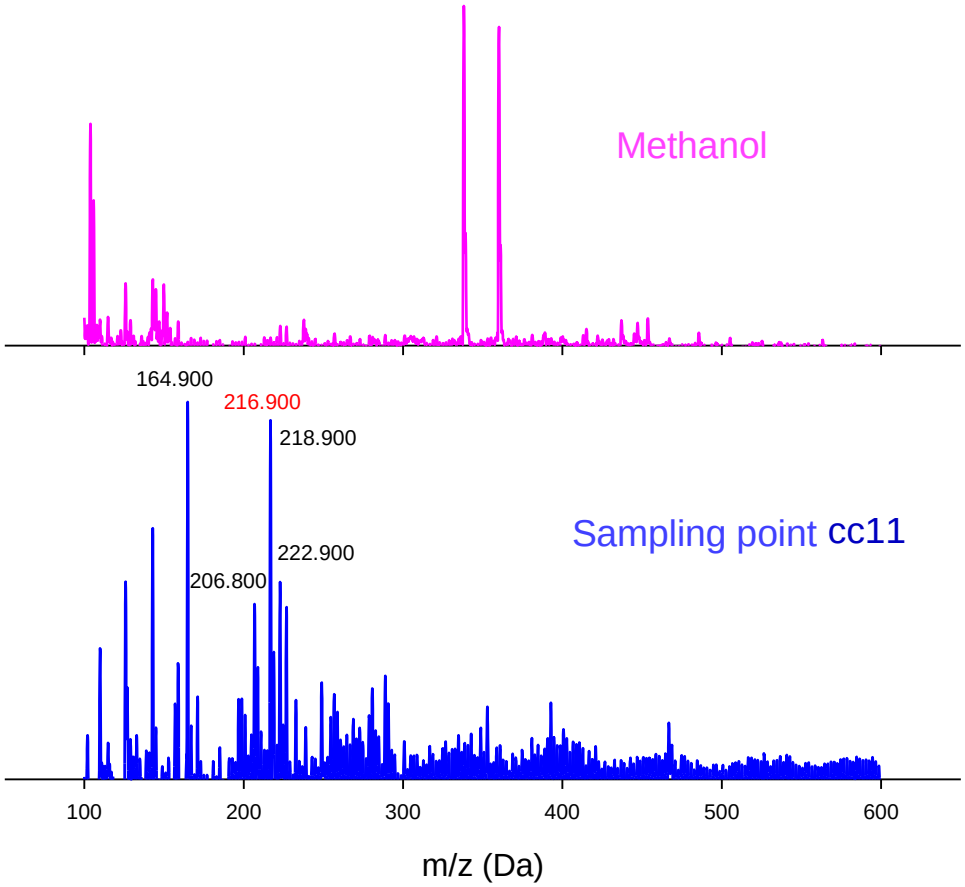

Figure 3.119. Comparison of the mass spectrum of water sample taken from *cc11* with blank.

Comparing the intensities of the mass spectra with the blank, the five most abundant ones selected for sampling point *cc11* were the ones with m/z values of 164.900, 206.800, 216.900, 218.900 and 222.900. Among the precursor ions fragmented in all of the samples, the one with m/z value of 216.900 was observed in the water samples taken from the 13 sampling points except *t3-1*. The library search of the MS^2 spectrum of this precursor ion resulted from the analysis of the water sample taken from *cc11* was compatible with the one of the chemical detomidine carboxylic acid (Figure 3.120). This chemical is the metabolite of detomidine which is used as a sedative and analgesic drug in mainly horses and also to immobilize calves in other animals such as cattle (Salonen

et al., 1992, Re et al., 2011). Detomidine carboxylic acid was determined as the metabolite of detomidine in the urine of the horses after 5 to 12 hours oral introduction to the horses. In addition, the chemicals was also detected in the urine of rats (Salonen et al., 1988, Salonen et al., 1992).

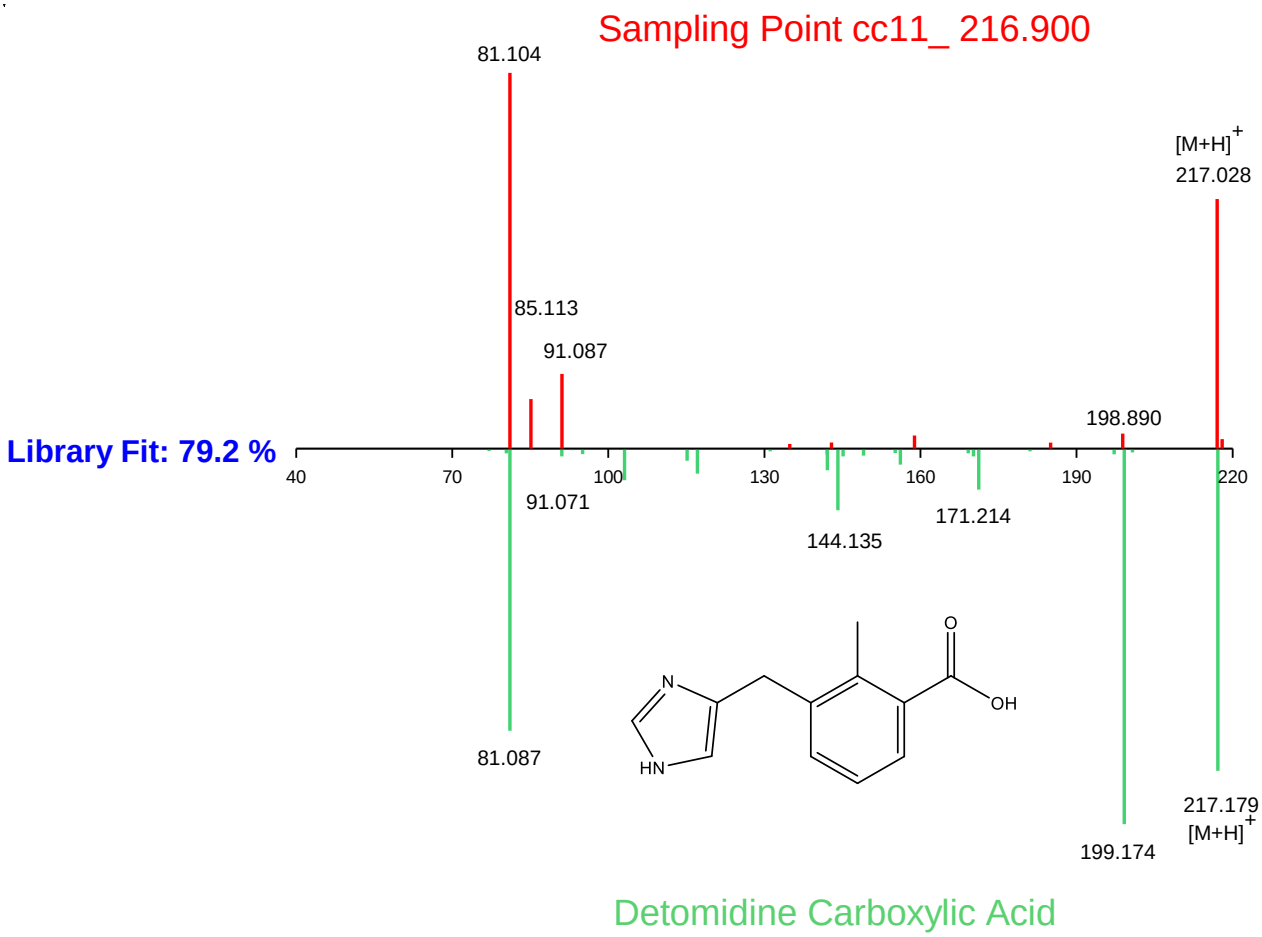

Figure 3.120. MS^2 comparison of precursor ion 216.900 in the water sample taken from *cc11* and detomidine carboxylic acid.

The library fit of the MS^2 spectrum of the same precursor (216.900 Da) resulted from the ionization of the other sampling points including *cc4*, *cc7*, *cc9*, *m2*, *ec4*, *ec5*, *ec6*, *t1-1*, *t2-3* and *t3-2* with detomidine carboxylic acid was 91.6%, 82.1%, 79.3%, 70.3%, 91.8%, 73.5%, 69.4%, 88.3%, 89.0% and 81.9%, respectively.

In the water sample taken from *cc4*, out of the most abundant ions, the one with m/z value of 248.900 Da, had 98.2% similarity with MS^2 spectrum of difenzoquat based on the library search (Figure 3.121). Difenzoquat is used as herbicide to remove wild weeds in agricultural lands. Due to its persistency, European Union (EU) has placed it in the list of priority compounds of potential concern. Furthermore, the extensive usage of difenzoquat resulted in its presence in surface water although it has a high hydrophobicity (Rytwo et al., 2004, Ibanez et al., 1996). High abundancy of

this chemicals in the water sample taken from *cc4* may be as result of its widely usage in agricultural farms around this sampling point.

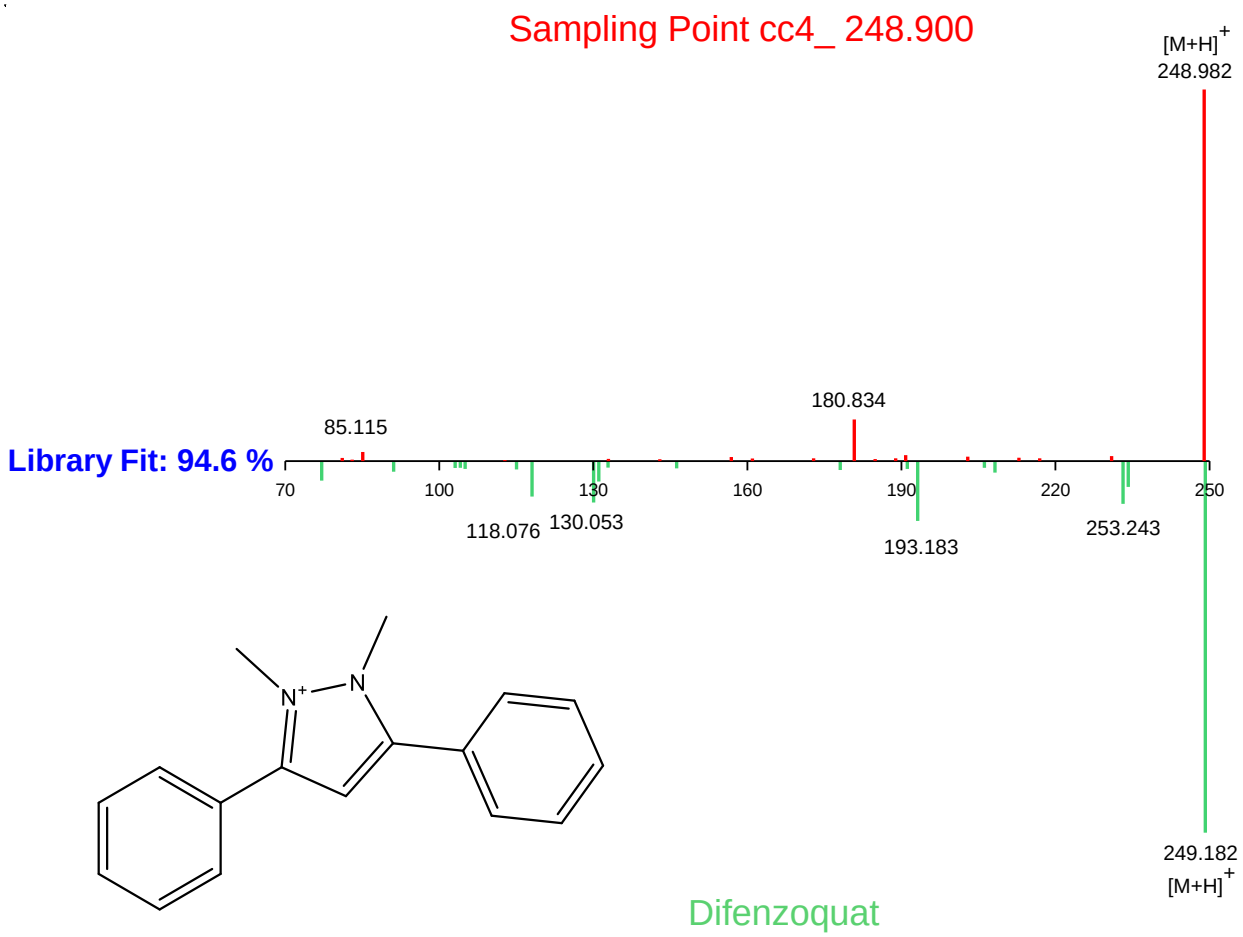

Figure 3.121. MS^2 spectra comparison of precursor ion 248.900 Da in the water sample taken from *cc4* and difenzoquat.

Precursor ion with m/z value of 288.900 Da acquired from the ionization of the water sample taken from *cc4* had MS^2 spectrum with 93.8% similarity with tetrazepam (Figure 3.122**).** Tetrazepam is a drug mainly used as muscle relaxant. Tetrazepam presence in the environment may have toxic effects on the organisms. Its effective dose (ED_{50}) was reported to be 70 times more than diazepam (Perez-Guerrero et al., 1997, Keane et al., 1988). Sampling point cc4 is close to OIZs that also include pharmaceutical industries which are producing drugs, can be a possible source of this chemical.

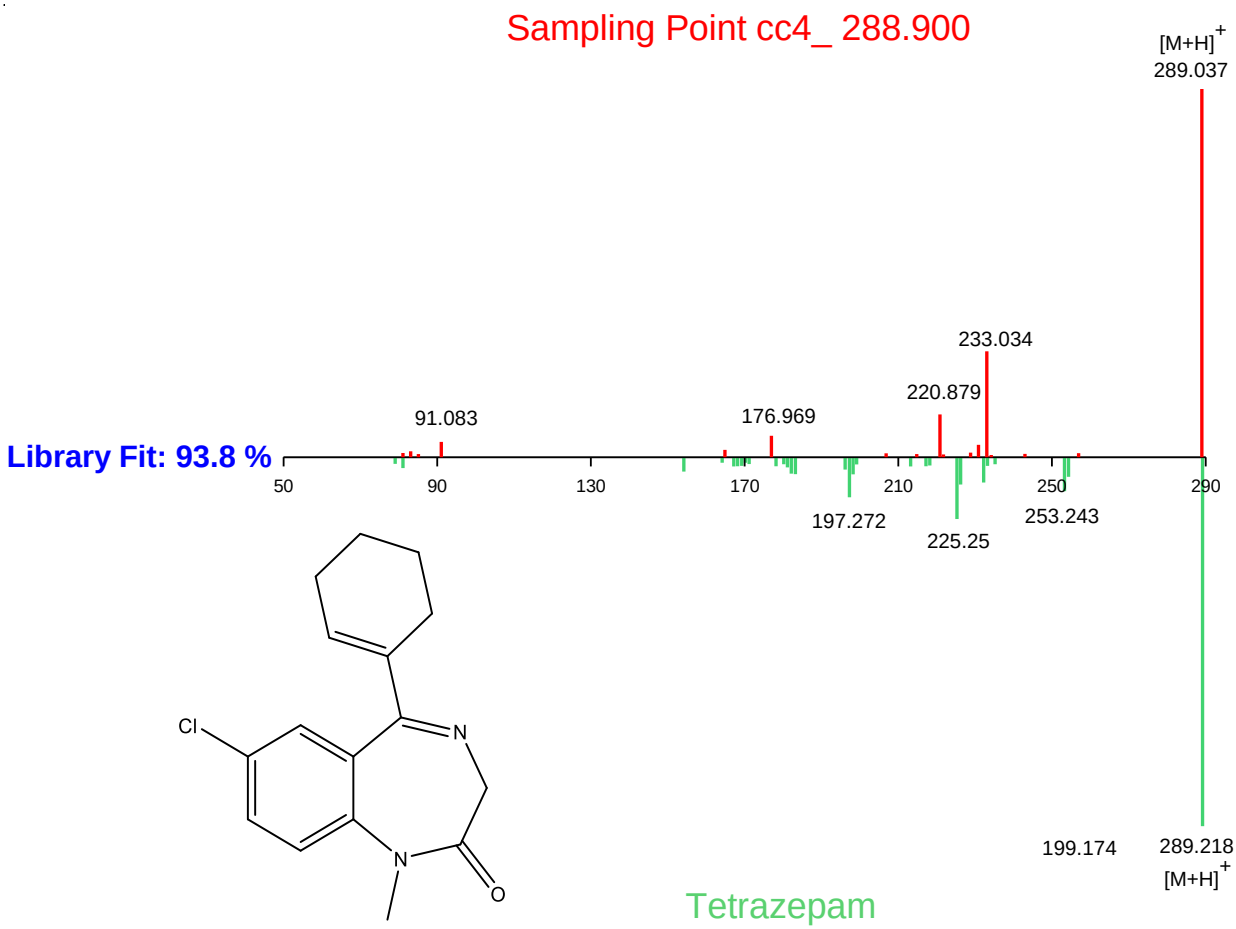

Figure 3.122. MS^2 spectra comparison of precursor ion 288.900 Da in the water sample taken from *cc4* and tetrazepam.

The MS^2 spectrum of the chemical 6β-hydroxyfluoxymestrone represented 86.0% similarity with the MS^2 spectrum of the precursor ion 353.100 Da from the ionization of the water sample taken from *cc7* (Figure 3.123). 6β-hydroxyfluoxymestrone is reported to be the 6β-hydroxylation metabolite of the anabolic steroid fluoxymestrone which was determined in the urine samples. Fluoxymestrone is used as anabolic androgenic steroid for muscle bulking in human or in animals such as cattle (Furstenberger et al., 2012, Schanzer et al., 1995, Vanoosthuyze et al., 1994). In the Ergene Watershed, illegal and misusage of this steroid in cattle and other animals in animal farms can be the possible source of 6β-hydroxyfluoxymestrone.

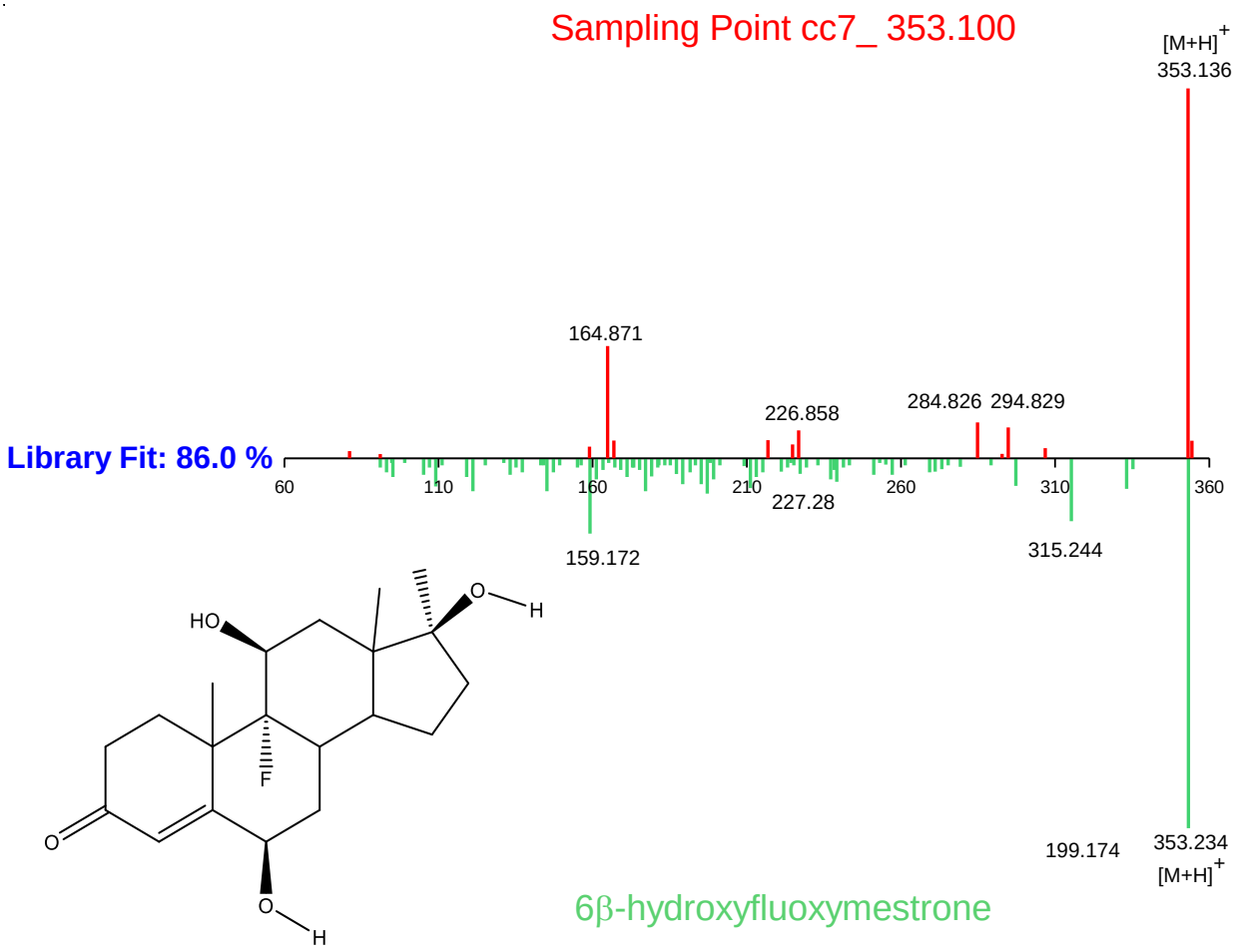

Figure 3.123. MS^2 spectra comparison of precursor ion 353.100 Da in the water sample taken from *cc7* and 6β-hydroxyfluoxymestrone.

Ionization of the water sample taken from *ec5* which is located on the Ergene Creek resulted in five most abundant precursor ions with m/z values of 185.100, 216.900, 392.900, 164.900 and 229.100 Da. The MS^2 spectrum of the ion with m/z value of 185.100 Da showed a similarity of 79.9% with the one of fuberidazole (Figure 3.124). Fuberidazole is a pesticide that is mainly used to kill fungi species. It is also reported to have carcinogenic and moderate acute toxicity effects (Saleh et al., 2013, Melo and Pina, 1992). Sampling point *ec5* is surrounded by agricultural farms where the run off of fuberidazole from them can be the source of this chemical in sampling point ec5.

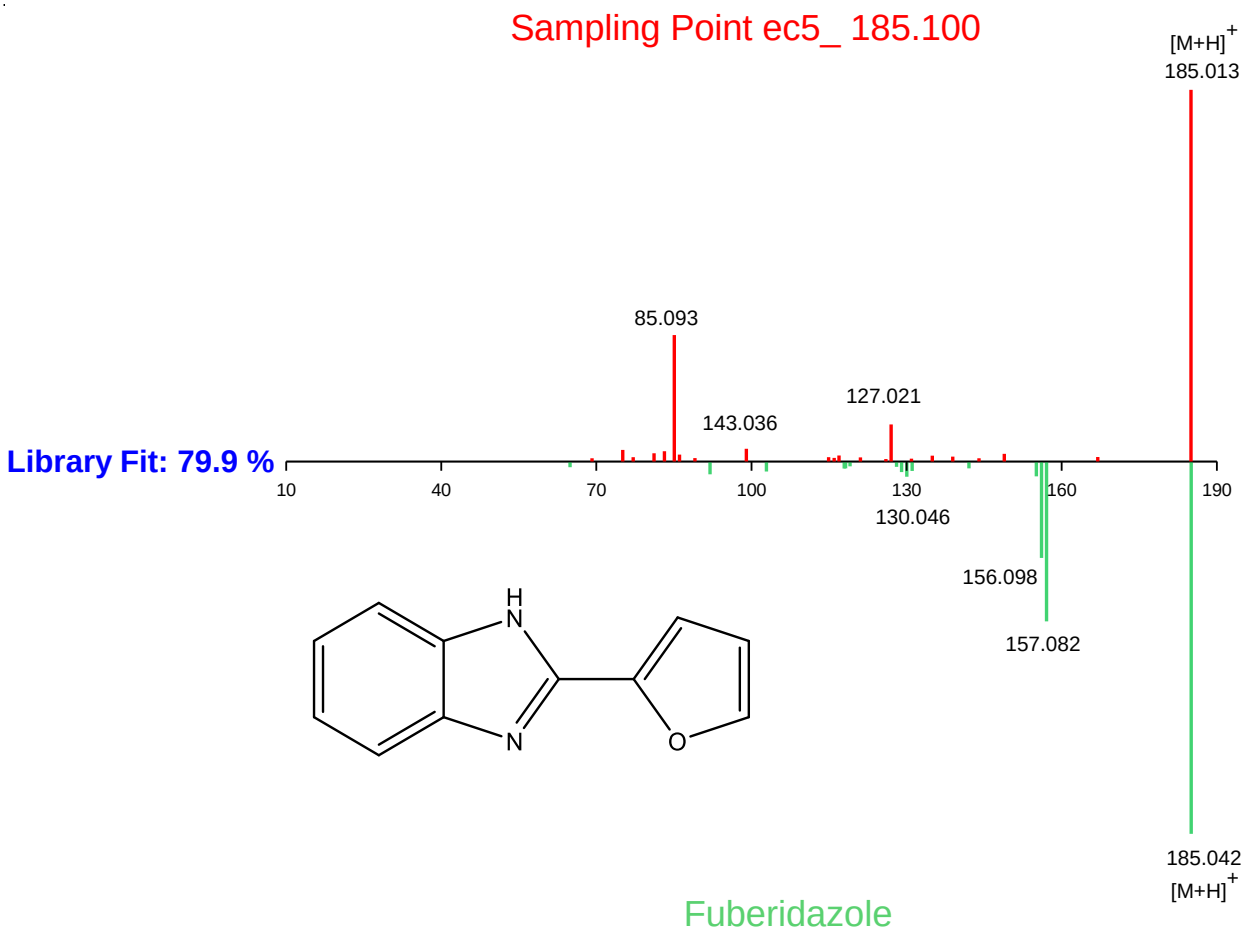

Figure 3.124. MS^2 spectra comparison of precursor ion 185.100 Da in the water sample taken from *ec5* and Fuberidazole.

Considering the mass spectrum of the water sample taken from *ec8*, precursor ion with m/z value of 134.000 Da had MS^2 library fit of 99.1% with 4-M-1H-B (Figure 3.125), which was also identified and quantified in targeted analysis. That chemical mainly used as corrosion inhibitor in different industries (Herzog et al., 2014), was among the micropollutants that was measured at high concentrations up to 10.83 µg/L at *ec8*. This sampling point receives the effluent from different industrial facilities including textiles and metals and automotive located at Muratlı OIZ next to this sampling point.

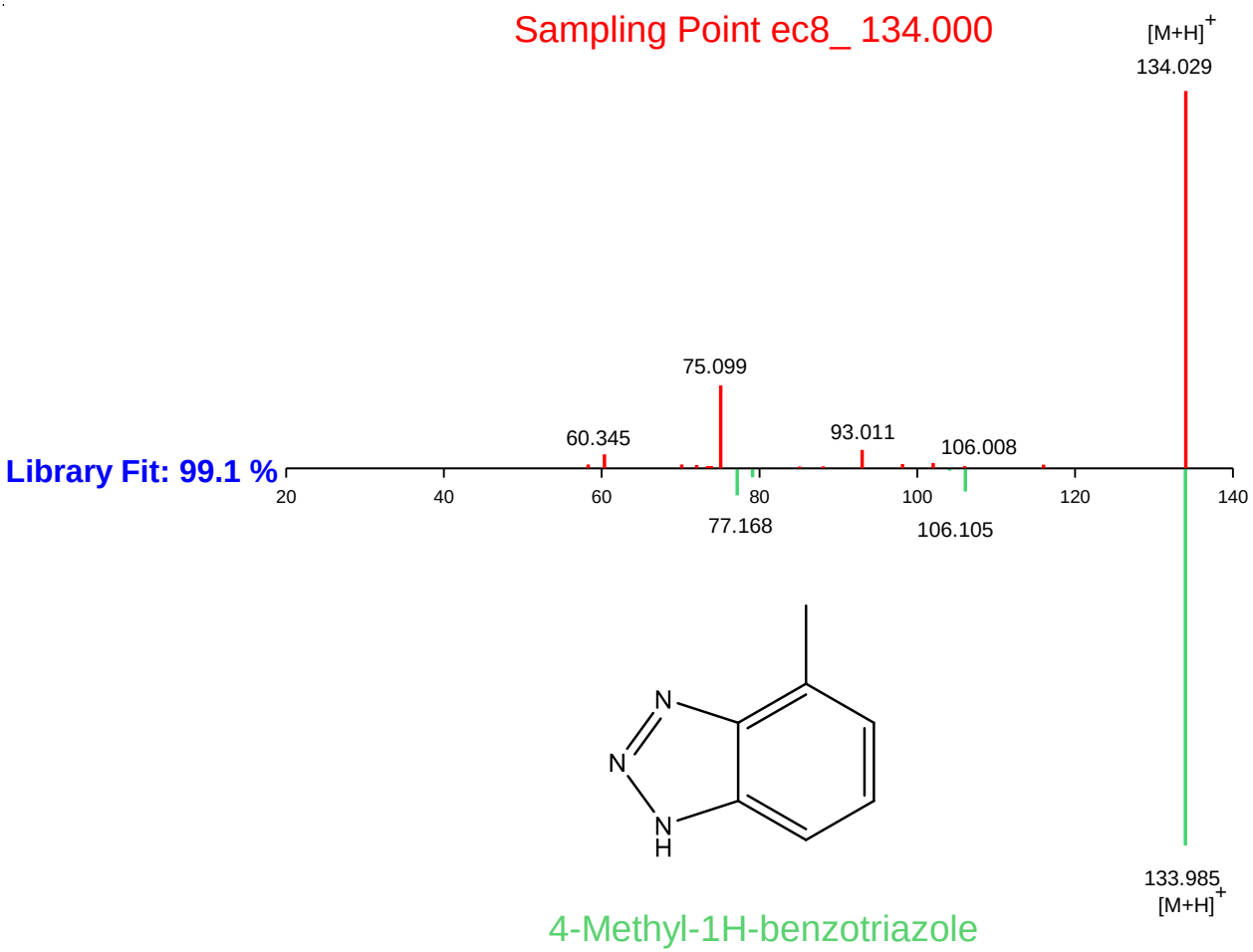

Figure 3.125. MS^2 spectra comparison of precursor ion 134.000 in the water sample taken from *ec8* and 4-M-1H-B.

Considering the ESI ionization of the water sample taken from sampling point *t2-3*, the MS^2 spectrum of the precursor ion with m/z value of 304.200 Da had 99.8% similarity with MS^2 spectrum of BDDDA (Figure 3.126). BDDDA is a widely used benzalkonium compound which has antimicrobial properties (Tezel and Pavlostathis, 2015). In addition, it is used in industrial processes including pharmaceuticals (Noecker and Miller, 2011). BDDDA was studied in targeted analysis of the micropollutants in this research. In fall, its concentration was as high as 57.77 µg/L at sampling point *t2-3* which was 6.5 times more than its average concentration throughout the watershed. Sampling point *t2-3* is located next to a pharmaceutical facility which discharge its effluent to the Ergene River.

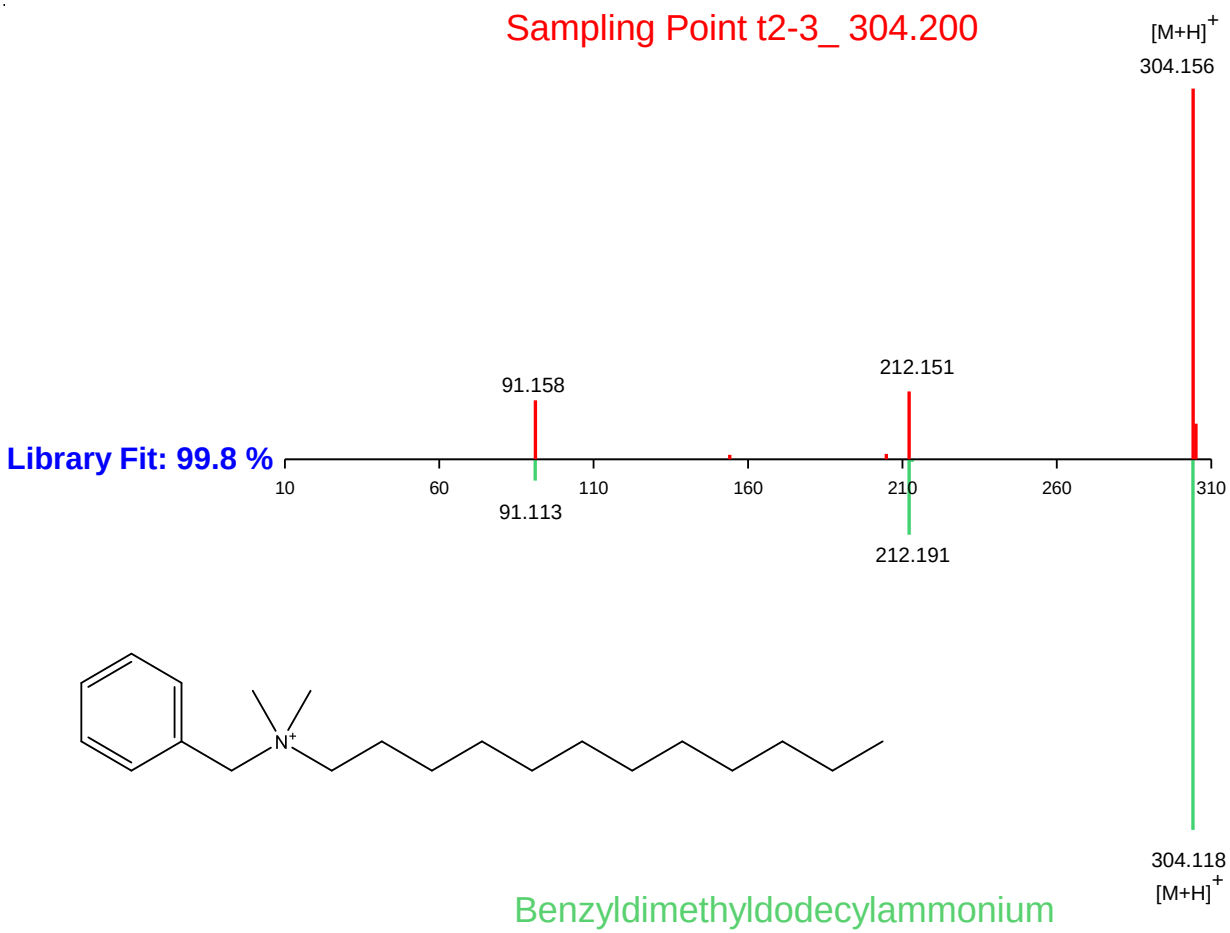

Figure 3.126. MS^2 spectra comparison of precursor ion 304.200 Da in the water sample taken from *t2-3* and BDDDA.

Precursor ion with m/z value of 370.100 Da acquired from the ionization of the water sample taken from *t2-3* had MS^2 spectrum similarity of 99.5% with the one of prajmalium (Figure 3.127). Prajmalium is a derivative of ajmaline and is used to cure arrhythmic disease. Despite of its pharmaceutical usages, it is considered as a toxic compound. Its toxicity effects on different animals has been investigated where the LD_{50} of 3.4 mg/kg in rats was reported (Alvarez and Vassort, 1993, Padrini, 1987). The high abundancy of this chemical at sampling point *t2-3* is originated from the industrial effluent of the pharmaceutical facility next to this point.

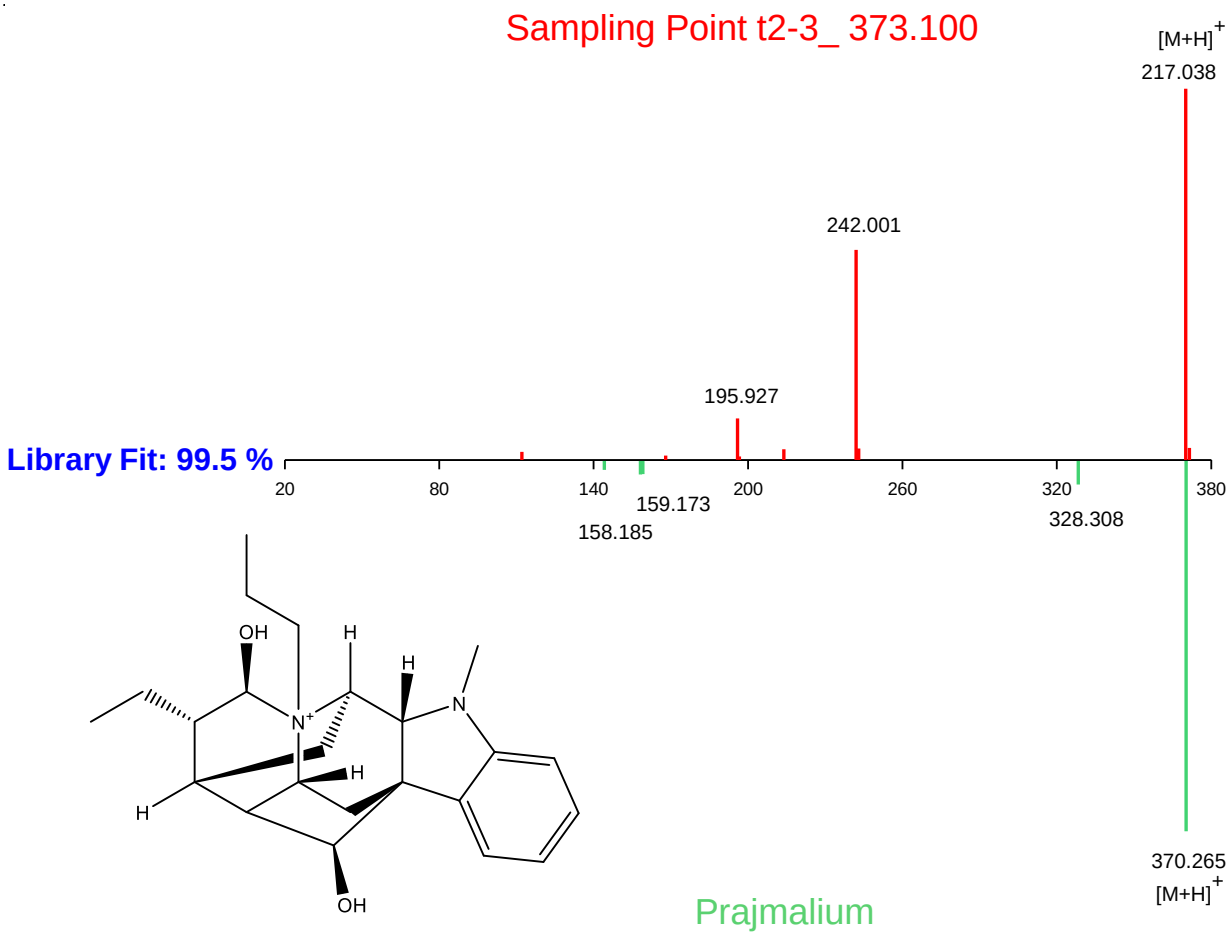

Figure 3.127. MS^2 spectra comparison of precursor ion 370.100 Da in the water sample taken from *t2-3* and prajmalium.

Considering the ESI ionization of the water sample taken from sampling point *t3-1*, the MS^2 spectrum of the precursor ion with m/z value of 117.900 Da had 88.4% similarity with MS^2 spectrum of betaine (Figure 3.128). Betaine is a compound that is found in different organisms specially marine invertebrates. In addition to its nutritional properties, it is used as an additive to detergents to reduce their irritating effects on skin (Nicandar et al., 2003, Craig, 2004). Although it has low toxicity effects, however, its high dosage can cause problems. For instance, the lethal dose (LD_{50}) of betaine on rats was reported to be 11g/kg of the body weight (Efsa, 2005). Betaine is manufactured in a chemical facility in Evrensekiz OIZ (next to *t3-1*) to use as ingredient in detergents.

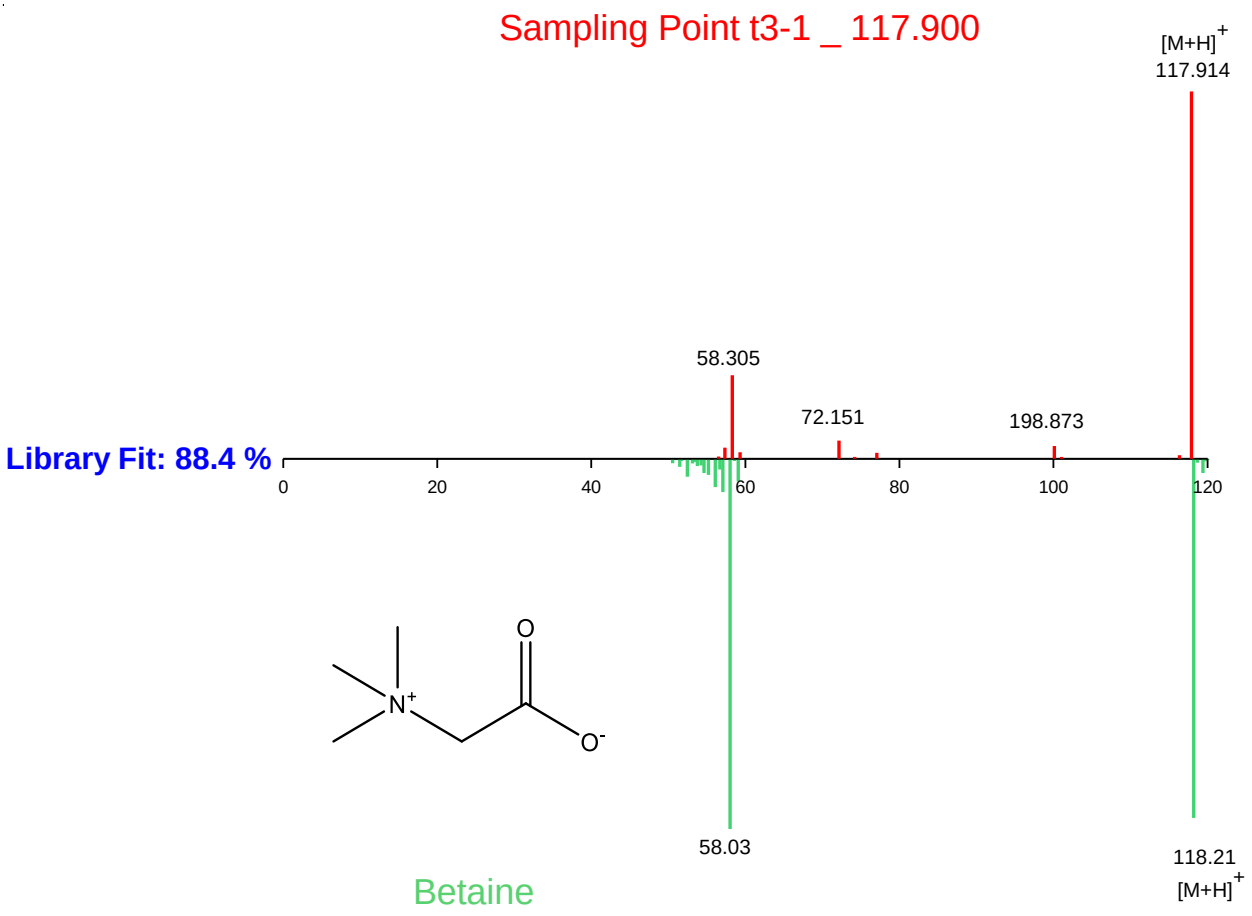

Figure 3.128. MS^2 spectra comparison of precursor ion 117.900 in the water sample taken from *t3-1* and betaine.

As comprehensively explained in this chapter, Ergene River is highly polluted with different groups of pollutants. The high pollution is mainly originated from the OIZs located close to Ergene and Çorlu Creeks as well as the single facilities. In addition, agricultural and animal farms located in the Ergene Watershed, extensively contribute to the pharmaceuticals and pesticides presence in the river water. Considering the results of this study, serious strategies should be considered to alleviate the quality of the water.

4. BIOTRANSFORMATION OF MICROPOLLUTANTS UNDER ANAEROBIC AND SULFATE REDUCING CONDITIONS

4.1. Introduction

Surface waters around the world are encountering high level of pollution day by day which reduces biodiversity and ecological richness of those habitats. The pollution is mainly originated from the anthropogenic activities in domestic, industrial and agricultural settings. Therefore, those activities introduce various groups of organic pollutants to the environment (Volker et al., 2017, Gioia et al., 2011).

When they enter into a surface water, organic pollutants undergo various environmental processes such as evaporation, sorption, hydrolysis and biodegradation. Identification and evaluation of those processes help us to predict the fate of micropollutants in the environment and associated risk to environment and human health (Jaffe, 1991, Dvořák et al., 2017, Löffler et al., 2005).

Biodegradation of a pollutant in the river environment is an important transformation process at which the pollutant may be completely biodegraded (e.g. to carbon dioxide), converted to non-toxic products or in some cases it may generate products with a higher toxicity level than themselves. Biodegradation of the pollutants in the river can occur either in water phase and/or on the sediment particles. Therefore, biodegradation of an organic pollutant highly depends on the physical-chemical properties of the pollutant such as solubility and water-sediment partitioning. For instance, hydrophilic chemicals with high solubility tend to stay in the water phase of the river while hydrophobic ones with high water-sediment partitioning coefficient prefer to attach onto the particles and sediments (Cui et al., 2011, Dvořák et al., 2017, Delle Site, 2001). Many organic pollutants detected in the Ergene River are hydrophobic chemicals. Therefore, they may sorb on the sediment of the river. Other than physical-chemical properties of the pollutants, properties of the sediment particles such as particle size distribution, organic content and the surface area as well as flowrate of the river water affect the biodegradation process. For instance, when an organic pollutant is sorbed on the sediment, it may desorb to the water phase due to sudden turbulence in the water flow and be degraded by the microorganisms presents in the water phase. In another case, since the sediment itself consists of a diverse microbial community, the organic pollutant can be uptaken by the

microorganisms of the sediment depending on the bioavailability of the organic pollutant to the microorganisms (Meggo and Schnoor, 2011).

Several factors affect the biotransformation of organic pollutants in the river among which redox condition and nutrition and the organic pollutant availability are the most important ones. Redox condition in the rivers highly correlated to the depth of the water. For shallow rivers, oxygen is available in the most parts of the river and therefore aerobic condition is dominant. While in deep rivers, as go deeper, anaerobic condition is the main redox condition due to absence of the oxygen. In deep rivers, depending on the abundancy of the electron acceptor, the biodegradation may occur under nitrate, sulfate or methanogenic conditions. For instance, water streams receiving the effluent of industrial facilities such as textiles, paper industries, solid waste processing sites, petroleum and oil refineries and food processing are reported to have high sulfate concentration (Huang et al., 2011, Holliger and Zehnder, 1996, Ghattas et al., 2017, Hussain et al., 2016). Therefore, sulfate reducing condition is dominant in those surface waters and may lead to the biotransformation of the micropollutants. Sulfate reducing bacteria (SRBs) are the microorganisms which fulfill the biodegradation of the organic pollutants under sulfate reducing conditions. SRBs attain their energy for growth by reducing the sulfate to H_2S gas while oxidizing the organic pollutants (Marietou, 2016). In addition, the produced H_2S gas will react with the metals in the water and can lead to their precipitation as their sulfide form (Hussain et al., 2016).

In the Ergene River, different groups of micropollutants have been detected due to the high density of industrial, agricultural and domestic activities in that region which completely described in Chapter 3. Giving the fact that sulfate was one of the most important ions due to its high concentration in the river, the condition may be favorable for the anaerobic biotransformation of the micropollutants under sulfate reducing condition. Moreover, among the micropollutants measured in the Ergene River, the ones with higher concentrations and detection frequency in both water and sediment phase were selected for the biotransformation assay. Thus, the objective of this chapter was to investigate the biotransformation of the selected micropollutants under anaerobic and sulfate reducing conditions during a 100 days incubation period.

4.2. Materials and Methods

4.2.1. Chemicals and Solutions

The chemicals including methanol, ethyl acetate, silver nitrate, acetonitrile as well as the selected analytes were purchased from Sigam Aldrich and Merck companies. In addition, several standard solutions were prepared during the course of this chapter.

Sulfate standard solution. 30,000 mg/L of sulfate standard solution was prepared by adding 4.44 gr of sodium sulfate (Na_2SO_4-MW=142.04g/mole) to 100 mL DI water.

Molybdate standard solution. 12.1 gr of sodium molybdate dihydrate ($Na_2MoO_4.2H_2O$-MW=241.95 g/mole) will be added to 100 mL DI water to prepare 0.5 M molybdate solution.

4.2.2. Sediment and Water Samples Collection

In order to test the biotransformation potential of the detected micropollutants under sulfate reducing condition in the river, several sampling points were chosen that represented the following criteria, (a) sampling points should contain high number of micropollutants, (b) each sampling point should have different micropollutant profile from each other representing different pollution sources and (c) sulfate concentration should be high at the selected sampling point.

According to the concentration profile of the micropollutants in the Ergene River and considering the criteria stated above, sampling points *m2*, *ec8*, *t1-1*, intersect of *t3-1* and *t3-2*, and *m10* were selected as the potential candidates for sediment sampling (Figure 4.1). The selected points had high number of micropollutants, from different groups of chemicals (Table 4.1**)** as well as relatively high sulfate concentrations (Figure 4.2). The highest sulfate concentration was detected at sampling points *t3-2* and *t1-1* with measured concentrations of 1946.15 and 670.77 mg/L during Summer 2017, respectively (Figure 4.2). After selecting the ideal sampling point, the sediments were taken using a Ponar dredge from 5-10 cm upper layer of the sediment in those sampling points. The samples were then kept in an ice bath and further transported to the laboratory and stored at 2±2^{o}C. The sampling was performed in 15th September 2018. It has to be mentioned that due to the difficulties in grabbing the sediment from the intersect of *t3-1* and *t3-2*, the sediment was taken from sampling point *t3-2*. In addition to sediment samples, the associated waters of the sediments from those sampling points were also collected. 2×1-L samples were taken from 30-40 cm below the surface of the water into the pre-

washed glass sample bottles with Teflon-lined screwcaps. The sample bottles were rinsed three times with the water sample prior to the actual sampling. The associated water samples were placed in an ice bath, transported to the laboratory and then stored at 2±2^{o}C.

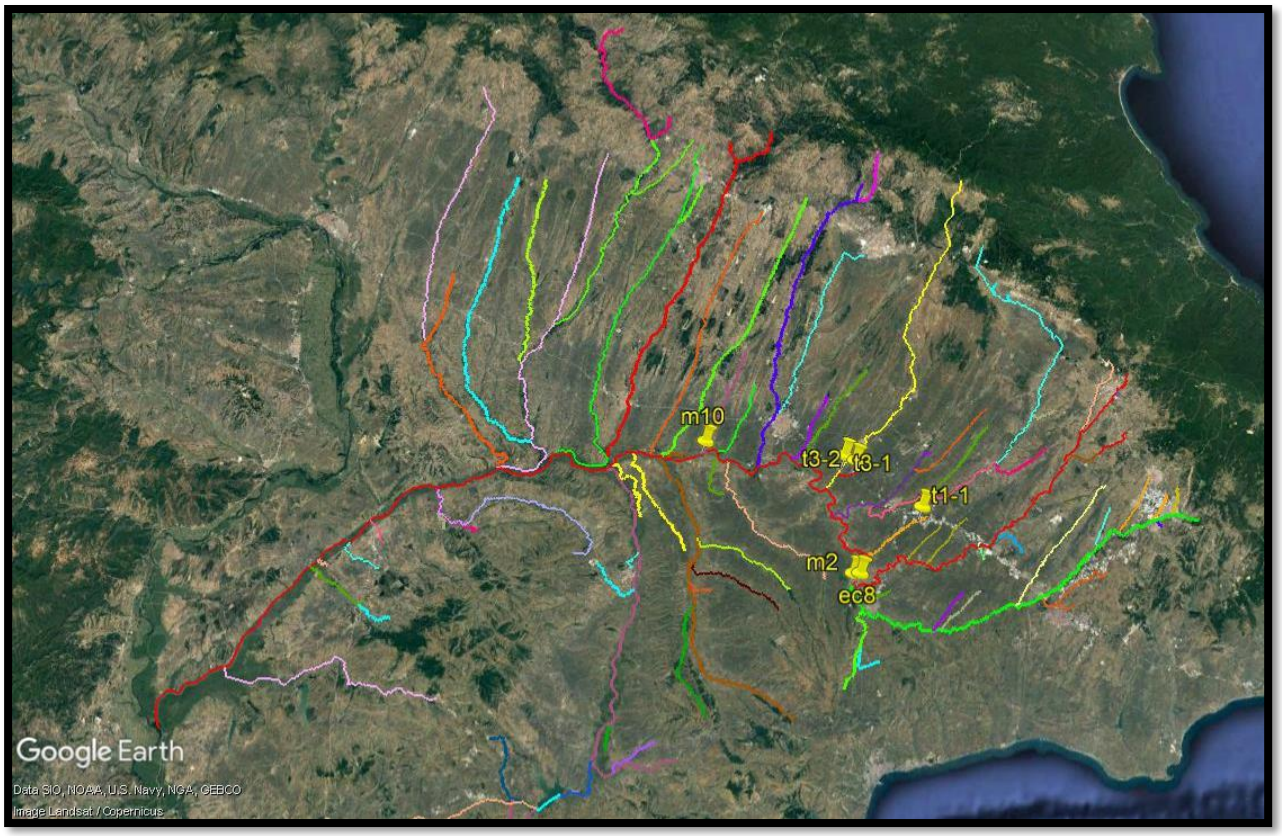

Figure 4.1. Selected sampling points for testing the anaerobic biodegradation of pollutants under anaerobic and sulfate reducing conditions.

Although a lot of micropollutants have been detected and quantified in water samples at the selected sampling points, the ones that have been frequently detected and have high application in different industrial processes were monitored in the course of biotransformation assays. Based on the results of the previous chapter regarding the concentration of the micropollutants, the chemicals including 1,2,3-benzotriazole (1,2,3-B), 4-methyl-1H-benzotriazole (4-M-1-H), 5,6-dimethyl-1H-benzotriazole monohydrate (5,6-D-1H-B), and 5-methyl-1H-benzotriazole (5-M-1H-B) as corrosion inhibitors (Asimakopoulos et al., 2013), tris(2-butoxyethyl) phosphate (TBEP) as flame retardant and plasticizers (Bacaloni et al., 2007), benzyldimethyldodecylammonium (BDDDA) and benzyldimethyltetradecylammonium (BDTDA) as surfactants (Tezel and Pavlostathis, 2015) and hexa(methoxymethyl)melamine (HMMM) used for coating of cans and automobiles and production of melamine nanoparticles (Dsikowitzky and Schwarzbauer, 2015), were selected. The structure of those chemicals along with their properties and usages are summarized in Table 4.2.

Table 4.1. List of chemicals detected during summer 2017 in selected sampling points for testing the anaerobic biodegradation of pollutants under sulfate-reducing and anerobic conditions.

Sampling point / **Pollutants**	***ec8***	***t3-1***	***m2***	***m10***	***t1-1***	***t3-2***	**Reference(s) on biodegradation, biotransformation or removal under sulfate-reducing conditions**
As			+		+	+	(Sun et al., 2016, Serrano and Leiva, 2017)
Ba	+	+	+	+	+	+	-
Be			+		+	+	-
Zn	+	+	+	+	+	+	(Liu et al., 2017b), (Jong and Parry, 2003, Kiran et al., 2017, Steed et al., 2000)
Cr	+	+	+	+	+	+	(Wijaya, 1993, Qian et al., 2016)
V	+	+	+	+	+	+	-
Co	+	+	+	+	+	+	(Sitte et al., 2010, Krumholz et al., 2003)
Al	+	+	+	+	+	+	(Mccauley et al., 2009)
Cu	+	+	+	+	+	+	(Liu et al., 2017b, Jong and Parry, 2003, Kiran et al., 2017, Wijaya, 1993, Steed et al., 2000)
Pb	+	+	+	+	+	+	(Kiran et al., 2017, Wijaya, 1993, Zhang et al., 2016, Hoa et al., 2007)
Ni	+	+	+	+	+	+	(Jong and Parry, 2003, Kiran et al., 2017)
Ag	+						-
B	+	+	+	+	+	+	-
Sn	+	+	+	+	+	+	-
Ti	+	+	+	+	+	+	-
Sb			+	+	+	+	(Wang et al., 2013)
Chlorfenvinphos		+					-
Fenamiphos	+						-
Lenacil		+					-
1,6-Dinitropyrene					+		-
Propetamphos		+					-
benzo(b)fluoranthene					+		-
1,8-Dinitropyrene					+		-
Imazalil		+	+				-
2,3,3’,4,4’,5,5’,6-Octabromodiphenyl ether					+		-
4-tert-Octylphenol diethoxylate			+	+		+	-
Metalaxyl	+	+					-

Table 4.1. Continued.

Pollutants \ Sampling point	*ec8*	*t3-1*	*m2*	*m10*	*t1-1*	*t3-2*	**Reference(s) on biodegradation, biotransformation or removal under sulfate-reducing conditions**
Pyridaben		+					-
Benzo(a)anthracene					+		(Lu et al., 2012)
4-Aminomethyl-benzenesulfonamide		+		+		+	-
Methyl Paraben		+			+		(Wu et al., 2017)
Methylsalicylate					+		-
indeno pyrene			+				(Nuñal et al., 2017)
Bisphenol-A	+	+					(Yang et al., 2015, Sarmah and Northcott, 2008)
Methyldihydrojasmonate						+	-
Pyriproxifen	+						-
Chlorpyrifos			+	+			-
Pendimethalin	+	+	+				-
1-HydroxyIbuprofen	+	+					-
alpha-Terpineol			+				-
Erythromycin		+	+				(Dutta et al., 2014)
4,4'-Dichlorobenzophenone					+		-
Anthracene	+	+				+	(Yuan and Chang, 2007, Genthner et al., 1997)
Tetracycline		+					-
Molinate	+						-
Myclobutanil			+				-
Fluoranthene	+	+	+				(Kumar et al., 2009)
Methyl -iso-propylcyclohexenone			+				-
4-Methylbenzylidenecamphor	+	+	+	+			(Liu et al., 2013d)
Ethylhexylmethoxycinnamate			+			+	(Liu et al., 2013d)
Tonalide			+				-
4-Nonylphenol monoethoxylate	+			+	+		(Lu et al., 2008, Chang et al., 2004)
Benzylamine			+				-
Epoxiconazole			+				-
Microcystin-RR						+	-
Metolachlor		+					(Stamper and Tuovinen, 1998)
ADBI (Celestolide)	+		+	+	+		-
Atrazine	+		+	+	+		(Wilber and Parkin, 1995, Boopathy, 2017)
Monocrotophos			+	+			-
Drometrizole	+	+	+				-
Homosalate	+		+				-
benzo(a) pyrene		+			+	+	(Rothermich et al., 2002)

Table 4.1. Continued.

Pollutants \ Sampling point	*ec8*	*t3-1*	*m2*	*m10*	*t1-1*	*t3-2*	Reference(s) on biodegradation, biotransformation or removal under sulfate-reducing conditions
2-Mercapto-benzothiazole			+	+			-
Pirimicarb		+	+	+		+	-
Oxybenzone			+	+			-
Omethoate	+	+	+	+			-
7H-Benzo(de)anthracen-7-one (Benzanthrone)	+	+	+	+	+		-
Quinalphos	+	+	+	+			-
3-Chloroaniline	+		+	+	+	+	-
N-Benzylmethylamine	+		+	+			-
Atrazine-desethyl	+	+	+		+		-
AHDI (Phantolide)	+	+	+	+	+		-
g-Methylionone					+	+	-
4-Chloroaniline	+		+	+	+	+	-
2,4-Dihydroxybenzophenone			+	+			-
N-Benzyldimethylamine	+	+					-
Aclonifen	+				+		-
Di(2- ethylhexyl)phthalate (DEHP)		+	+	+		+	(Chang et al., 2005)
benzo(k)fluoranthene					+	+	-
Boisvelone / Iso-Esuper			+				-
Terbutryn	+	+	+	+	+		-
Mepiquat chloride	+	+	+	+	+	+	-
5,6-Dimethyl-1H-benzotriazole monohydrate	+	+	+	+	+	+	-
N-Ethyl-2-tolysulfonamide	+			+			-
Benzyltrimethylammonium	+	+	+	+			-
Sulfamethoxazole	+	+	+	+			(Jia et al., 2017, Falås et al., 2016, Mohatt et al., 2011)
Prochloraz	+	+	+	+			-
Acetamiprid	+	+	+	+			-
Piperonylbutoxide	+	+	+	+			-
N,N-Diethyl-m-toluamide	+	+	+	+			-
Acetaminophen (Paracetamol)	+	+	+	+			(Falås et al., 2016)
Nonylphenol diethoxylate	+	+	+	+	+	+	(Lu et al., 2008)
Diuron	+	+	+	+	+	+	-
Tris(2-butoxyethyl) phosphate	+	+	+	+	+	+	-
Carbendazim	+	+	+	+		+	-
Benzyldimethyldodecylammonium	+	+	+	+	+	+	-
Benzyldimethylhexadecylammonium	+	+	+		+		-
4-Methyl-1H-benzotriazole		+	+	+	+		-
Clarithromycin	+	+	+	+			(Jelic et al., 2015)
Dicyclohexylamine	+	+	+	+	+	+	-
5-Methyl-1H-benzotriazole (5-Tolytriazole)	+	+	+	+	+	+	(Liu et al., 2011a)

Table 4.1. Continued.

Pollutants \ Sampling point	*ec8*	*t3-1*	*m2*	*m10*	*t1-1*	*t3-2*	Reference(s) on biodegradation, biotransformation or removal under sulfate-reducing conditions
Ciprofloxacin	+	+	+	+	+	+	(Dutta et al., 2014)
Hexa(methoxymethyl)melamine	+	+	+	+	+	+	-
1,2,3-Benzotriazole	+	+	+	+	+	+	(Liu et al., 2011a)
Norfloxacin	+	+	+	+	+	+	-
Benzyldimethyltetradecylammonium	+	+	+	+	+	+	-
Azithromycin	+	+	+	+	+	+	-
Ofloxacin	+	+	+	+	+	+	(Dutta et al., 2014)
Polychlorinated biphenyls	+	+	+	+	+	+	(Chang et al., 2001)

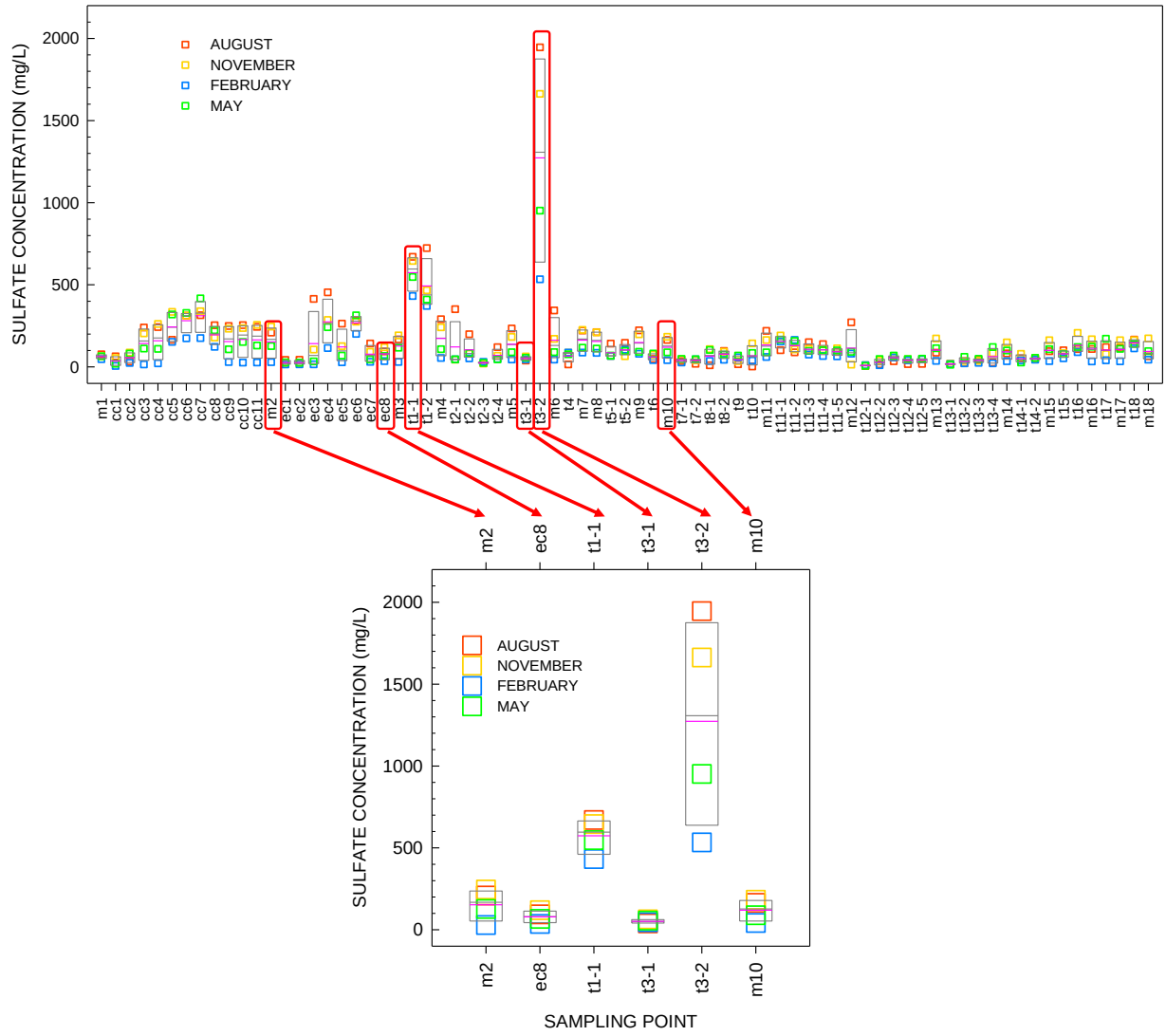

Figure 4.2. Sulfate concentration profile in 75 sampling points and the selected sampling points.

Table 4.2. Selected chemicals for biotransformation assays.

CAS#	Chemical Name	Molecular Structure	Formula	MW	LogP	Solubility in water (ppm)	Type
95-14-7	1,2,3-benzotriazole (1,2,3-B)		$C_6H_5N_3$	119.12	1.34	20000	
29385-43-1	4-methyl-1H-benzotriazole (4-M-1H-B)		$C_7H_7N_3$	133.15	1.80	3069	Corrosion inhibitor, Drug precursor, Antifreeze
4184-79-6	5,6-dimethyl-1H-benzotriazole (5,6-D-1H-B)	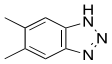	$C_8H_9N_3$	147.18	2.26	914.20	
136-85-6	5-methyl-1H-benzotriazole (5-M-1H-B)	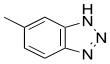	$C_7H_7N_3$	133.15	1.80	3069	
78-51-3	Tris-(2-butoxyethyl) phosphate (TBEP)	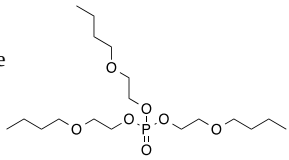	$C_{18}H_{39}O_7P$	398.47	4.30	1100	Flame Retardant, Solvent, Manufacture of paints, Manufacture of coatings
68002-20-0	Hexa(methoxymethyl)melamine (HMMM)	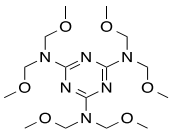	$C_{15}H_{30}N_6O_6$	390.44	3.07	149.30	Manufacture of paints, Coating agent, Textile, Leather
139-07-1	Benzyldimethyldodecylammonium (BDDDA)	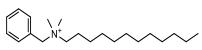	$C_{21}H_{38}N$	304.30	2.93	1000000	Surfactant, Disinfectant, Biocide
139-08-2	Benzyldimethyltetradecylammonium (BDTDA)	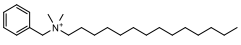	$C_{23}H_{46}NO_2$	332.33	3.91	1000	

Several studies have reported the occurrence and distribution of the benzotriazoles (Reemtsma et al., 2010, Van Leerdam et al., 2009, Giger et al., 2006, Kiss and Fries, 2009), benzalkonium chlorides (Ding and Liao, 2001, Ferrer and Furlong, 2001), TBEP (Kim and Kannan, 2018, Cristale et al., 2013a, Shi et al., 2016, Bollmann et al., 2012) and HMMM (Dsikowitzky and Schwarzbauer, 2015, Bobeldijk et al., 2002, De Hoogh et al., 2006, Schwarzbauer and Ricking, 2010) in surface waters. In those studies, the concentration of all the selected chemicals were in ng/L ranges, while the concentration ranges determined in the Ergene River during Summer 2017 was several µg/L or

higher. In addition, the selected chemicals had the highest detection frequencies in Ergene watershed compared to other analytes monitored.

Table 4.3. Maximum, minimum and mean concentration (µg/L) and frequency detection of the most detected micropollutants in the samples taken from the Ergene River in Summer 2017.

Chemical name	Maximum concentration.	Minimum Concentration.	Mean Concentration	Detection Frequency (out of 75)
1,2,3-B	117.55	0.00	8.14	68
4-M-1H-B	36.19	0.00	6.92	58
5,6-D-1H-B	20.86	0.00	2.48	39
5-M-1H-B	15.95	0.00	3.45	63
HMMM	329166.95	0.00	28876.90	66
TBEP	270.17	0.00	14.28	51
BDDDA	23.89	0.00	4.20	75
BDTDA	7.64	0.00	1.43	75

4.2.3. Characterization of The Sediment Samples

4.2.3.1. Total and volatile solids (TS and VS). Total and volatile solids were measured according to method 2540 of the *standard methods* (Eaton et al., 2005). Sediment samples were firstly weighed in pre-ignited crucibles and further dried at 105^{o}C for one day. The dried samples were then placed in desiccator till cooled. Further, their dry weight was measured and considered for TS calculation. In order to measure the volatile solids, the crucibles were then placed in a furnace set to 550 ^{o}C, for 20 minutes. After ignition, the samples were cooled and transferred to a desiccator. The weight was then measured to calculated the VS.

4.2.3.2. Sediment particle size classification. The particle size distribution of sediments were determined using *ASTM D422* "Standard test method for particle size analysis of soils". For that, the samples were firstly dried at 105^{o}C and further kept in desiccator. An appropriate amount of the dried sediments was weighted. For the analysis, sieves with attributed numbers of 4 (4.750 mm), 10 (2.000 mm), 20 (0.850 mm), 70 (0.425 mm), 140 (0.106 mm) and 200 (0.075 mm) were utilized. The weight of all of the sieves were measured individually and recorded. Further, the sieves were placed up on each other, considering their number, on a shaker. The sample was then poured on the first sieve from the top. After shaking for 5 minutes, the weight of each sieve was recorded and the difference was used to calculate the size distribution.

4.2.3.3. Micropollutants content. The presence of organic micropollutants in the sediments was initially extracted using methanol as solvent. For that, the sediment samples were placed into 50 mL falcon tubes and further centrifuged at 10,000 rpm for 10 minutes and the excess water was removed. Further 10 mL methanol was added to 10 gr of excess water-removed sediment and agitated on an orbital shaker at 130 rpm for one day. The following day, the content was firstly vortexed, mixed and then centrifuged at 10,000 rpm for 10 minutes. The resulted supernatant was further processed and diluted relatively and analyzed with LC-MS/MS as described in Chapter 3 to quantify the micropollutants in the sediment samples.

4.2.4. Extraction of Micropollutants from Sediment Samples

Based on the results on particle size distribution as well as micropollutants content of the sediments, two sediments that had the highest potential of micropollutants biotransformation were selected. Further, to optimize and select the most favorable solvent or solvent mixture to extract the selected micropollutants from the sediment samples, a preliminary desorption assay was conducted. The assay was accomplished by testing water, methanol, methanol + acetonitrile (50:50), acetonitrile + 50 mM phosphate buffer (60:40), and silver nitrate solution + acetonitrile + ethyl acetate (20:30:50) as solvents to extract the chemicals from sediments. The total volume for all of the used solvent or mixture of solvents were two times more than the amount of the sediment except the last one with the final volume of 10 mL for 2 gr sediment. After each day mixing, the content was vortexed and centrifuged and further the chemicals in the supernatant were analyzed. Further, the same amount of solvent was added to the remained pellet and the procedure was repeated for at least five days. Using the amount of desorbed chemicals in each day, a consecutive desorption profile was constructed. Using them and after selection the proper solvent(s), recovery of the selected micropollutants was performed by spiking standard solutions (considering their initial concentration in the sediment) into 1 gr sediment.

4.2.5. Biotransformation of Selected Micropollutants under Anaerobic and Sulfate Reducing Conditions at Water-Sediment System

The batch biotransformation assays were conducted in two sets each lasting 100 days, according to OECD guideline for the testing of chemicals (*OECD-308*, aerobic and anaerobic transformation in aquatic sediment systems). The sets were prepared and organized in a way that can elucidate the activity and performance of the sediments in both synthetic and real conditions. Therefore, the sets were performed using the two selected sediments as inoculum and 1) spiked synthetic chemicals mix

and 2) associated water of the sediment, as chemical sources. 40 mL amber glass vials were used in this study to eliminate the potential photodegradation (Figure 4.3). Each set contained 6 reactors (40 mL amber vials) in duplicates for each sampling time. One reactor in each set was opened at each sampling time and treated for micropollutant analysis and other parameters. In addition, reactors were sacrificed for analysis at 0, 5, 10, 25, 60 and 100 days after starting the experiment.

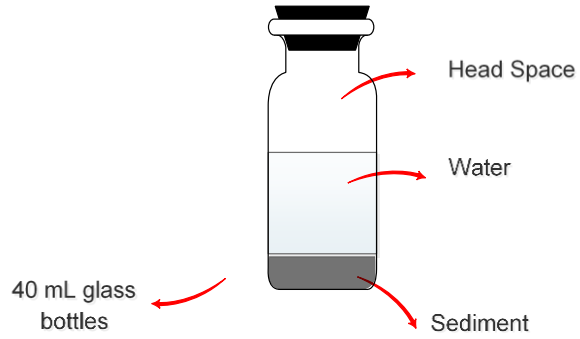

Figure 4.3. 40 mL amber glass vials used in setting up the reactors.

4.2.5.1. Biotransformation potential of the selected micropollutants under anerobic and sulfate-reducing conditions using synthetic chemicals mix (SET 1). A batch set was conducted to investigate the biodegradation of the most detected micropollutants under sulfate reducing and anaerobic conditions using the two selected sediment as the inoculum. In this set, the reactors were prepared by placing 10 gr water-discarded sediments into the 40 mL amber glass vials. Further the prepared synthetic mix (based on the data of August 2017 sampling) of the selected chemicals (Table 4.4) and sulfate were amended to the vials (REACTOR-S) ($V_{Aqueous}/W_{Sediment}$ =3). Another set of amber glass vials with the same composition as reactors but also containing sodium molybdate, were also prepared as the control set (CONTROL-S). The role of sodium molybdate is to deactivate the SRBs. A set of vials without any sediment were also prepared as reference (REF-S).

Table 4.4. Concentration of the analytes amended to the reactors in SET 1.

Chemical	**Concentration (µg/L)**
1,2,3-B	93.86±2.25
4-M-1H-B	114.71±3.42
5,6-D-1H-B	148.89±6.53
5-M-1H-B	110.80±2.26
HMMM	11495.53±505.82
TBEP	114.06±10.48
BDDDA	148.98±3.59
BDTDA	97.97±4.54

4.2.5.2. Biotransformation potential of the selected micropollutants under anaerobic and sulfate-reducing conditions using associated water (SET 2). The second batch assay was conducted to elucidate the biotransformation potential of the most detected micropollutants in the two selected sampling points using the associated water of the sediments. The reactors vials were prepared similar to the SET 1 except that the associated water (Table 4.5) was added instead of the synthetic mix of the chemicals. A set of vials containing only associated water, without any sediment were also prepared as reference (REF-A).

Table 4.5**.** Initial concentration of the analytes in associated water of the sediments *t1-1* and *t3-2*.

	Associated Water	
Chemical	***t1-1***	***t3-2***
1,2,3-B	-	-
4-M-1H-B	1.69±0.09	7.50±1.86
5,6-D-1H-B	0.94±0.015	1.76±0.50
5-M-1H-B	0.91±0.001	4.83±1.24
HMMM	196606.21±7571.84	3089.66±11.53
TBEP	58.89±5.80	21.26±7.61
BDDDA	53.29±4.13	2.48±0.19
BDTDA	22.15±1.58	1.37±0.11

For both sets, two reference vials (REF-0 and REF-1) were also prepared which contains either no sediment or no addition of chemicals. The reactors set up in both sets are summarized in Table 4.6. The batch assay was conducted in 40 mL amber glass vials. Further, all of the vials were flushed with helium for 3 minutes to provide anaerobic condition. The vials were then placed on an orbital shaker and agitated at 30 rpm at room temperature.

Table 4.6. Components of reactors in detailed biotransformation assay.

Reactor	Sediment (g)	Sulfate (mL) from 30,000 mg/L stock	Molybdate (mL) from 0.5M Stock	Chemicals mix (mL)	Associated Water	DI Water	Total water phase (mL)
SET 1: Synthetic mix							
CONTROL-S	+	+	+	+	-	+	30
REACTOR-S	+	+	-	+	-	+	30
REF-S	-	+	-	+	-	+	30
SET 2: Associated water							
CONTROL-A	+	+	+	-	+	-	30
REACTOR-A	+	+	-	-	+	-	30
REF-A	-	+	-	-	+	-	30
Common References							
REF-0	+	-	-	-	-	+	30
REF-1	+ (Autoclaved)	-	-	+	-	+	30

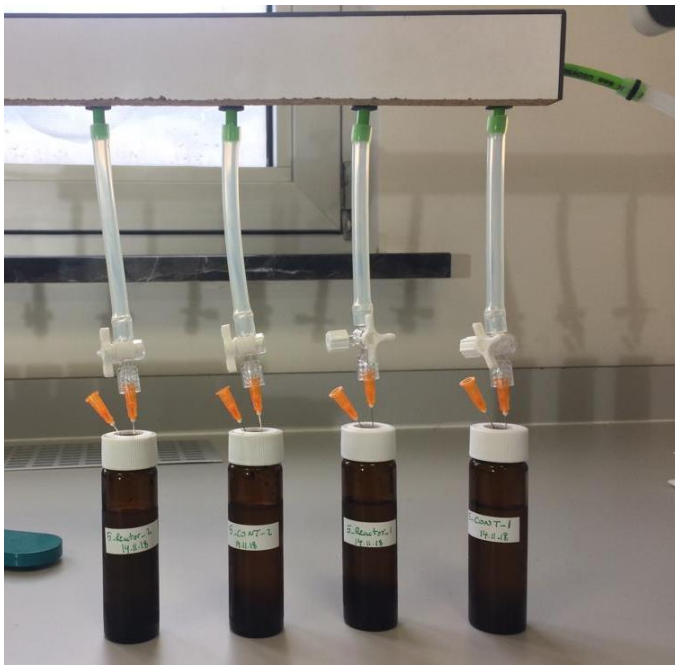

Figure 4.4. Flushing of 40 mL vials with helium to provide anaerobic conditions.

4.2.5.3. Total gas, pH, sulfate and selected micropollutants analysis. At each sampling time, total produced gas, pH, sulfate concentration and selected analytes were analyzed.

Total gas Production. In each sampling time, the total gas production of the 40 mL amber vials was measured before opening their caps using a VWR pressure/vacuum transducer with an accuracy of 0.002 atm.

pH. The pH was measured using a pH meter as stated in Chapter 3.

Sulfate. After pH measurements, the contents of the vials were transferred to 50 mL falcon tubes. The falcon tubes were centrifuged at 10,000 rpm for 10 minutes. An aliquot of the supernatant was then filtered through 0.2 µm filters for sulfate measurements as described in Chapter 3.

Micropollutants quantification in vials. The micropollutants concentration was measured in both supernatant and pellet of the 50 mL falcon tubes as following:

1. 5 mL of supernatant was mixed with 5 mL methanol, vortexed and further filter through 0.2 µm filters. The processed sample was then analyzed using LC-MS/MS as described in Chapter 3.
2. After discarding the supernatant, for the quantification of selected micropollutants in sediment part of the vials, the proper solvent or solvents mixture was used for extraction purpose. For that, 1 gr of centrifuged sediment was transferred to a 15 mL falcon tube, further mixed with a proper amount of the solvent or solvent mixtures and agitated on an orbital shaker at 130 rpm for one day. The next day, the content of the falcon tubes were centrifuged at 10,000 rpm for 10 minutes. 1 mL aliquot of the supernatant was diluted and further analyzed with LC-MS/MS to measure the concentration of the micropollutants extracted from the sediment part of the reactors. The extraction assays were conducted in triplicates.

4.3. Results and Discussions

4.3.1. Characterization of The Sediments

The characterization of the five selected sediment samples including TS, VS, particle size distribution and their micropollutant content, are summarized in Table 4.7.

Table 4.7. Characterization of sediment samples.

Parameter	Sediment *ec8*	Sediment *m2*	Sediment *m10*	Sediment *t1-1*	Sediment *t3-2*
Solids					
TS (%)	83.99 ± 0.67	79.63 ± 0.72	81.76 ± 0.22	49.61 ± 5.14	20.59 ± 0.47
VS (%)	0.26 ± 0.11	0.51 ± 0.15	0.32 ± 0.01	3.46 ± 0.32	3.09 ± 0.10
Particle Size Distribution (%)					
Gravel	4.00	0.00	0.20	0.00	0.00
Coarse sand	18.50	1.50	3.90	0.00	0.60
Medium sand	69.00	84.90	81.10	8.30	42.20
Fine sand	8.50	13.40	14.80	62.90	51.30
Fines (silt + clay)	0.00	0.10	0.00	28.80	5.90
Chemical (µg/g)					
1,2,3-Benzotriazole	0.005	0.005	0.004	0.005	0.006
2-Mercapto-benzothiazole	0.094	0.090	0.107	0.041	0.016
3-Chloroaniline	0.003	0.002	0.001	0.027	0.115
4,4'-Dichlorobenzophenone	-	-	-	0.004	-
4-Chloroaniline	0.003	0.002	0.001	0.027	0.121
4-Methyl-1H-benzotriazole	0.004	0.008	0.004	0.013	0.005
4-tert-Octylphenol diethoxylate	-	-	0.001	-	-
5,6-Dimethyl-1H-benzotriazole monohydrate	-	-	-	0.002	0.074
5-Methyl-1H-benzotriazole (5-Tolytriazole)	0.002	0.005	0.003	0.008	0.003
Acetaminophen (Paracetamol)	-	-	-	-	0.002
ADBI (Celestolide)	0.015	-	0.010	-	-
AHDI (Phantolide)	0.069	-	0.049	-	-
Azoxystrobin	-	-	-	-	0.001
Bayrepel	0.542	0.379	0.358	-	-
Benzydimehtyldodecylammonium	0.592	0.709	0.670	1.200	0.346
Benzyldimethyltetradecylammonium	0.404	0.513	0.470	1.391	0.196
Boisvelone / Iso-Esuper	-	0.071	-	-	-
Cadusafos	0.004	0.004	0.003	0.002	0.002
Carbazole	0.003	0.003	-	-	-
Carbendazim	0.002	0.002	0.002	-	0.002
Di(2- ethylhexyl)phthalate (DEHP)	3.164	0.287	1.915	0.000	0.162
Dicyclohexylamine	0.002	0.023	0.003	0.003	0.002
Difenoconazole	-	-	-	-	0.001
Diuron	0.001	0.001	0.001	0.016	0.001
Drometrizole	0.002	-	-	-	-
Epoxiconazole	-	-	-	-	0.001
Fenpropimorph	0.001	0.001	0.001	-	0.002
Hexa(methoxymethyl)melamine	2.612	17.968	16.339	304.241	0.525
N,N-Diethyl-m-toluamide	0.001	0.001	0.001	-	0.001
N-Benzyldimethylamine	0.001	0.003	0.003	0.026	0.001
N-Benzylmethylamine	-	-	-	0.002	-
N-Ethyl-2-tolysulfonamide	0.001	-	-	-	0.001
N-methyl-Aniline	-	-	-	-	-

Table 4.7. Continued.

Parameter	Sediment *ec8*	Sediment *m2*	Sediment *m10*	Sediment *t1-1*	Sediment *t3-2*
Nonylphenol diethoxylate	0.002	0.003	0.004	0.034	0.023
N-phenyl-2-napthylamine	-	-	-	-	-
Pendimethalin	0.003	-	0.002	-	-
Piperonylbutoxide	0.000	0.001	0.002	-	0.002
Prochloraz	0.002	0.002	0.003	0.001	0.015
Propiconazole	-	-	-	-	0.004
Tebuconazole	-	-	-	-	0.001
Terbutryn	-	-	-	-	-
Trimethoprim	-	-	-	0.001	-
Tris(2-butoxyethyl) phosphate	0.019	0.019	0.017	1.170	0.083

As presented in Table 4.7, sediment samples taken from sampling points *ec8*, *m2* and *m10* have high TS, however, the VS portion of these sediments is so low compared to sediment *t1-1* and *t3-2*. In addition, the particle size distribution of the sediments taken from sampling points *ec8*, *m2* and *m10* were mainly composed of medium sand while sediment *t1-1* and *t3-2* composed of mainly fine sand, silt and clay (Figure 4.5).

Extraction using methanol as solvent resulted in detection of 43 organic pollutant in the sediment samples. Among them, benzotriazoles, HMMM, BACs and TBEP were the ones present at the highest concentrations as also determined for water samples in chapter 3. In addition, they were detected in particular at the highest recorded concentrations in sediments *t1-1* and *t3-2*. Therefore, considering the frequency and concentration of these chemicals, their biotransformation may occur under anaerobic and sulfate reducing conditions using the sediments as inoculum.

In general, among the sediment samples, sediments *t1-1* and *t3-2* had the highes VS content, high concentration of selected analytes as well as the highest sulfate concentration in their associated water. In addition, they have finer particles (more clay and silt)) which may lead to higher surface area and further sorption of the selected analytes onto these two sediments (Delle Site, 2001). It was reported that fine silt and clay can provide a larger area for microorganisms to be attached (Xia and Wang, 2008). Moreover, sorption of the chemicals onto the sediment particles leads to a higher concentration of them on the sediment particles which can induce the activity of the microorganisms. Several studies reported the direct usage of the sorbed chemicals by the bacteria (Cui et al., 2011). Thus, based on the results attained from the characterization of the sediment samples, sediments taken

from sampling points *t1-1* and *t3-2* were chosen as the best candidates for biotransformation assay of selected analytes.

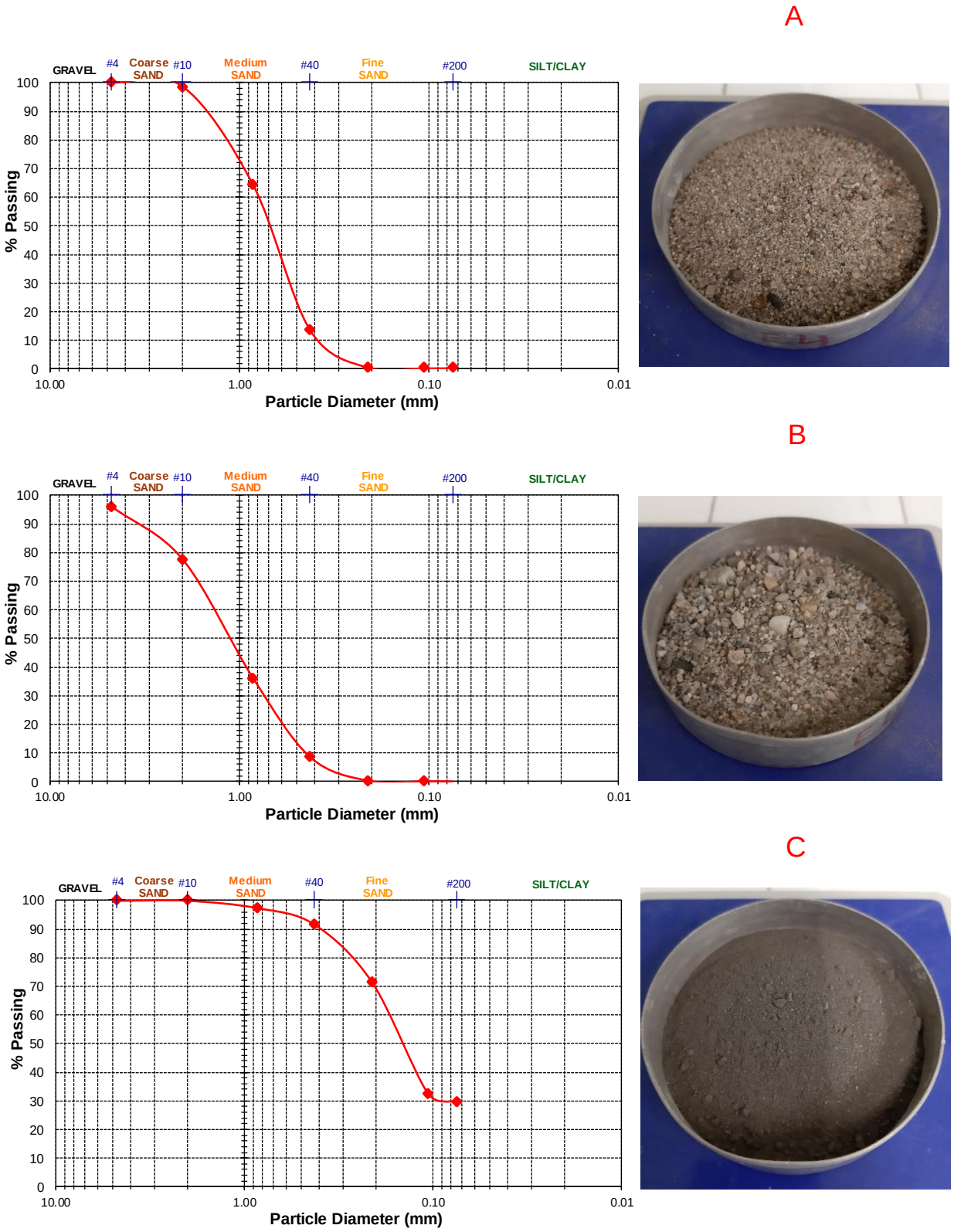

Figure 4.5. Detail profile of particle size distribution of sediments A) *m2*, B) *ec8* and C) *t1-1*, D) *t3-2* and E) *m10*.

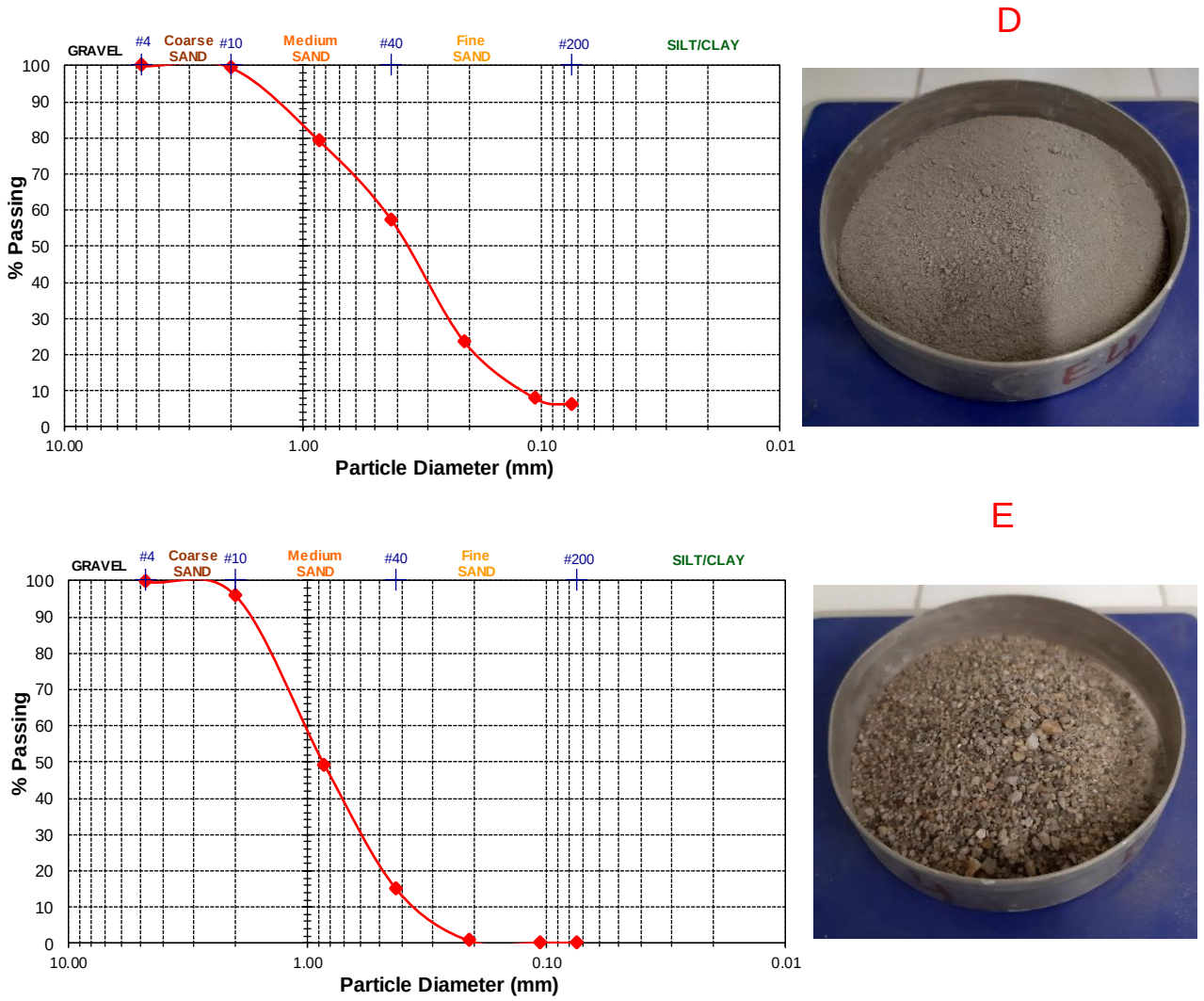

Figure 4.5. Continued.

4.3.2. Optimizing the Extraction of Micropollutants from The Sediment Samples

Mechanical shaking using different solvent/solvent mixtures were tested to select the proper solvent for achieving high recovery of the selected chemicals in sediments *t1-1* and *t3-2*. Desorption of the selected chemicals from the sediment matrix of *t1-1* by water (Figure 4.6A) indicated that the chemicals are continuously released into the water phase. Besides, desorption of chemicals by water can increase the concentration of those chemicals in the water phase. Based on the desorption profiles (Figure 4.6), sediment *t1-1* was extensively polluted by BDDDA, BDTDA, HMMM and TBEP. The high amount of those chemicals may be due to their extensive discharge into that point and higher LogP values compared to others as well as the small particle size of the sediment. Benzalkonium chlorides (BACs) were reported to be mainly found in the sediments of the rivers than the water itself due to the high interaction of their ammonium head with the natural particles of the sediments. BDDDA was detected at 32,800 ng/g while BDTDA's amount was 8760 ng/g at sediment *t1-1*. The

measured values were far higher than the other studies in the literature. For instance, the range of total BACs in the sediments taken from Pearl River Estuary in China was between 49.3 and 1050 ng/g (Li et al., 2014). A mean concentration of 140 and 440 ng/g of BDDDA and BDTDA were reported in the sediment samples from lower Hudson river (Li and Brownawell, 2010). In another study in Austria, BDDDA was responsible for most of the pollution in sediments compared to other BACs, similar to what we determined in this study for the Ergene River (Martinez-Carballo et al., 2007). In sediment sample taken from sampling point *t1-1*, the results showed that benzotriazoles were efficiently extracted by the solvents containing methanol and acetonitrile. BDDDA and BDTDA extraction were the highest when the solvents contain acetonitrile (Figure 4.6C, D and E**)**. Although TBEP and HMMM were extracted by the most of the solvents, the highest efficiency was determined using the mixture of silver nitrate, acetonitrile and ethyl acetate (Figure 4.6E). Thus, the suitability of a solvent for extraction was selected based on the amount of the chemical to be extracted at the first day of extraction. According to the Figure 4.6, the appropriate solvent to extract benzotriazoles was the mixture of methanol and acetonitrile (1:1). In addition, mixture of 100 mM silver nitrate, acetonitrile and ethyl acetate was used for the extraction of TBEP, HMMM, BDDDA and BDTDA from the sediment matrix. The recovery of the aforementioned chemicals using the suitable solvents mixture was conducted for both sediments taken from sampling points *t1-1* and *t3-2*. The recovery accomplished by spiking standard solutions of chemicals to 1gr of sediment to give a final concentration of 10 µg/g (except for BDDDA and HMMM which was 100 and 1000 µg/g) (Table 4.8).

Table 4.8. Recovery (%) of the selected micropollutants from sediments taken from sampling points *t1-1* and *t3-2*.

	Methanol + Acetonitrile	
Chemical	Sampling Point *t1-1*	Sampling Point *t3-2*
1,2,3-B	60.47±0.79	75.21±5.25
4-M-1H-B	71.92±6.04	78.67±7.58
5,6-D-1H-B	56.07±3.06	57.87±2.45
5-M-1H-B	72.47±6.92	78.03±7.64
	100 mM $AgNO_3$ + Acetonitrile + Ethyl acetate	
	Sampling Point *t1-1*	Sampling Point *t3-2*
HMMM	76.21±10.70	85.22±5.78
TBEP	77.84±6.70	100.95±5.77
BDDDA	84.11±6.49	85.51±7.21
BDTDA	73.95±5.22	69.14±2.30

The Recovery tests were conducted in triplicates.

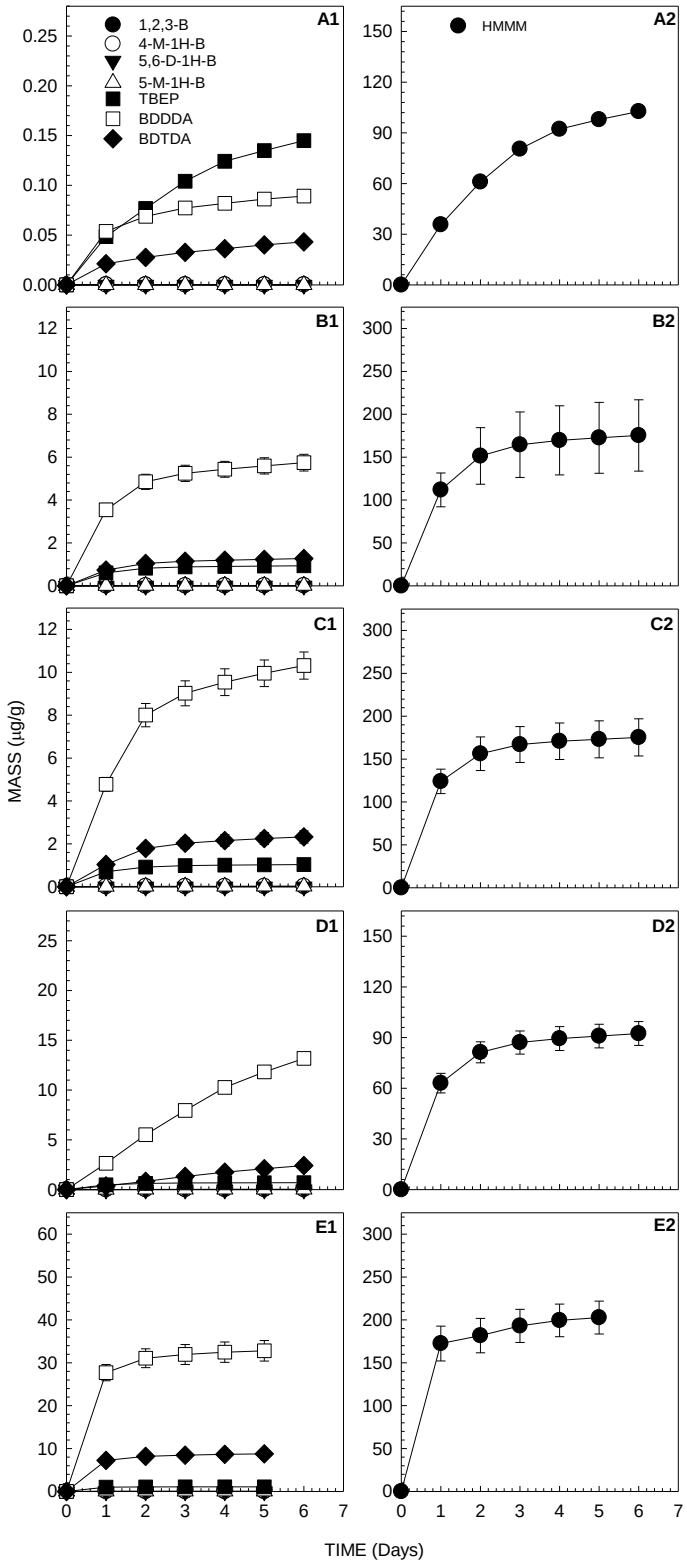

Figure 4.6. Desorption profile of micropollutants from sediment from sampling point *t1-1* by (A) water, (B) methanol, (C) methanol + acetonitrile (50:50), (D) acetonitrile + 50 mM phosphate buffer (60:40) and (E) silver nitrate solution + acetonitrile + ethyl acetate (20:30:50).

4.3.3. Biotransformation of Selected Micropollutants under Anaerobic and Sulfate Reducing Conditions at Water-Sediment System

4.3.2.1. pH. The pH value of the vials for both of the sets was variable between 6.9 and 8.7. The lower pH of the ones containing the synthetic water (Figure 4.7.A1 and B1) at the beginning of the test was due to the low pH of the synthetic water which was 5.98 ± 0.06. By passing time, the pH of the contents in the vials reached the aforementioned range in the vials.

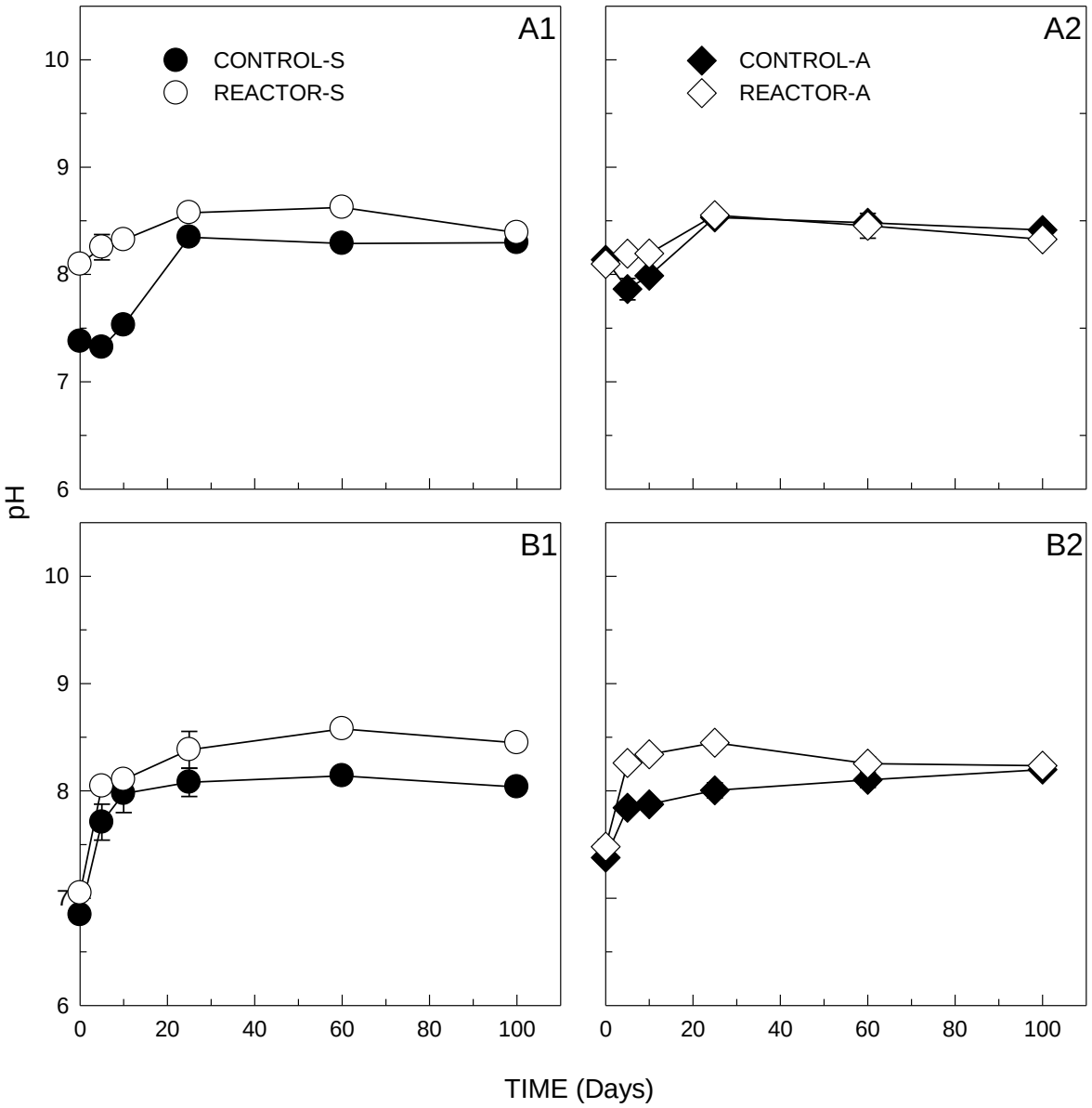

Figure 4.7. pH profiles in vials containing sediment from sampling point (A) *t1-1* and (B) *t3-2*, along with (1) synthetic water and (2) associated water.

4.3.2.2. Total gas production. Figure 4.8 shows that the total gas production in SET 1 and SET 2 for the vials containing sediment *t3-2* had a similar trend (Figure 4.8B). While the ones containing sediment *t1-1* had higher gas production in the vials with the synthetic water (Figure 4.8A1). This may be occurred due to the higher pollution and presence of the toxic chemicals in the associated water of the sediment *t1-1* than the synthetic water, resulted in deactivating the responsible microorganisms (Table 4.5). In addition, vials containing the sediment from sampling point *t3-2* produced more gas due to higher microbial activity in sediment and associated water of that sampling point (Figure 4.8B2).

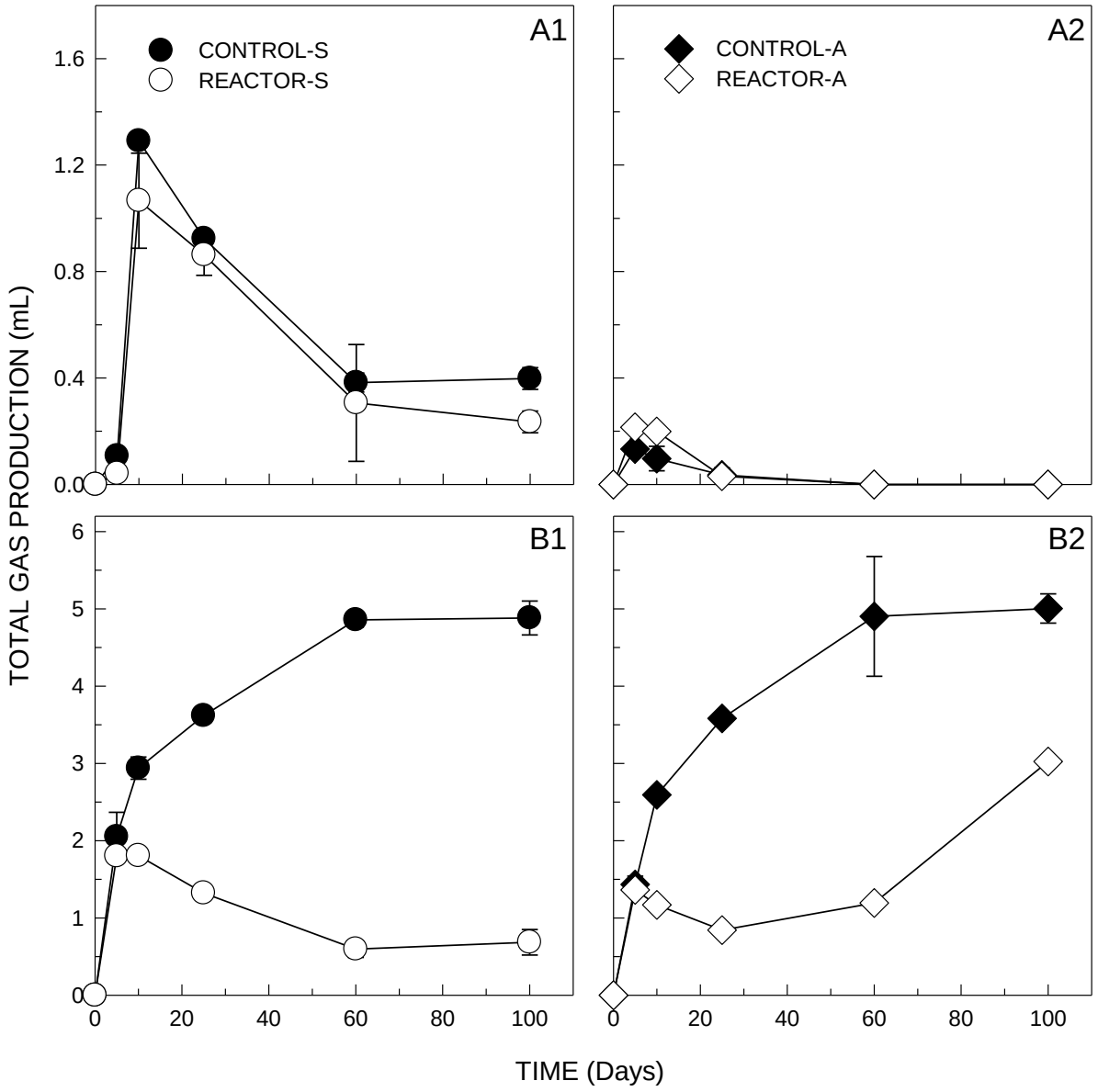

Figure 4.8. Total gas production (mL) profiles in vials containing sediment from sampling point (A) *t1-1* and (B) *t3-2*, along with (1) synthetic water and (2) associated water.

4.3.2.3. Sulfate. The sulfate removal in the vials was calculated using Eqn.2:

$$[Total\ Removal\ (Sulfate)\ (\%)]_t = \frac{[CONC_{Supernatant}]_0 - [CONC_{Supernatant}]_t - [(CONC_REF_S)_0 - (CONC_REF_S)_t]}{[CONC_{Supernatant}]_0} \times 100 \quad \text{Eqn. 2}$$

where: $[TOTAL\ SULFATE\ Removal\ (\%)]_t$ is the total sulfate removal in the vial, $CONC_{Supernatant}$ is the concentration of sulfate in supernatant part of the vials, and $CONC_REF_S$ is the concentration of sulfate in REF-S containing only the synthetic mix of the chemicals and sulfate.

The sulfate removal was calculated for both CONTROL and REACTOR vials and their difference was considered as the total sulfate removal. As shown in Figure 4.9, sulfate concentration did not change in any of the vials containing sediment from sampling point *t1-1* (Figure 4.9A). While the ones containing sediment from *t3-2* showed sulfate reductions of 96.22 ± 0.45 % and 91.18 ± 5.43% when synthetic mix and associated water were used, respectively. In addition, the higher rate of sulfate reduction in the vials containing the associated water (Figure 4.9.B2) reveals the presence of SRBs in the associated water of *t3-2*.

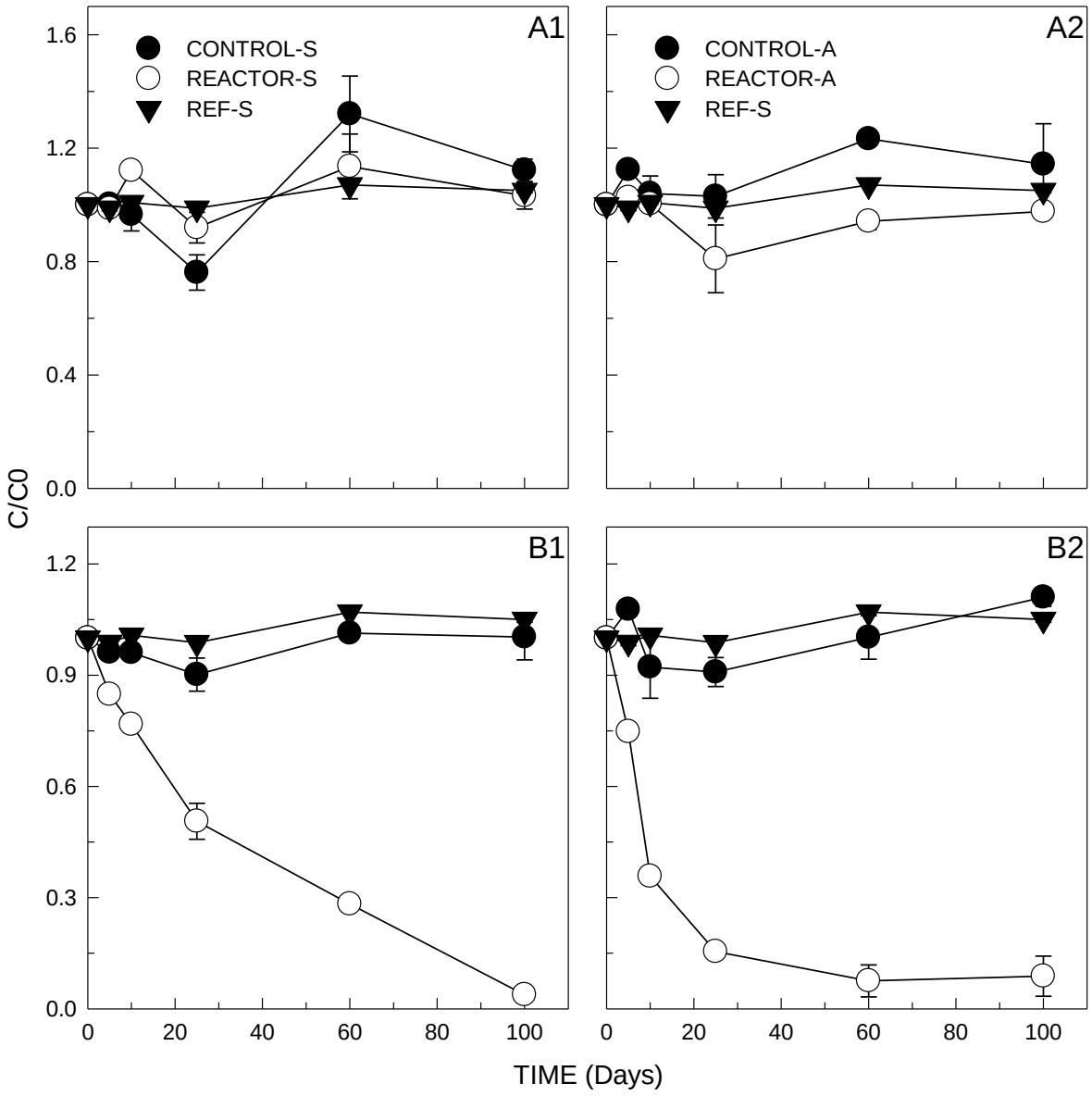

Figure 4.9. Sulfate reduction profiles in vials containing sediment from sampling point (A) *t1-1* and (B) *t3-2*, along with (1) synthetic water and (2) associated water.

4.3.2.4. Micropollutants. Micropollutants biotransformation under anaerobic and sulfate reducing condition was studies during 100 days batch experiment. In order to determine the biotransformation of each chemical, their concentration reduction in the aqueous phase (supernatant) as well as their total mass reduction in the whole vial (aqueous and sediment) were recognized based on the following equations (Eqn 3 and Eqn 4):

$$[Removal\ in\ Aqueous\ Phase\ (\%)]_t = \frac{[CONC_{Supernatant}]_0 - [CONC_{Supernatant}]_t - \{[CONC_{Supernatant}]_0 \left[1 - \frac{(CONC_{REF_S})_t}{(CONC_{REF_S})_0}\right]\}}{[CONC_{Supernatant}]_0} \times 100 \quad \text{Eqn. 3}$$

Where, $CONC_{Supernatant}$ is the concentration of the chemical in the aqueous phase, $CONC_{REF_S}$ is the concentration of the chemical in REF-S which contains only the synthetic mix solution of the chemicals.

$$[Total\ Biodegradation\ (\%)]_t = \frac{[MASS_{Supernatant} + MASS_{Pellet}]_0 - [MASS_{Supernatant} + MASS_{Pellet}]_t - \{[MASS_{Supernatant} + MASS_{Pellet}]_0 \left[1 - \frac{(MASS_{REF_S})_t}{(MASS_{REF_S})_0}\right]\}}{[MASS_{Supernatant} + MASS_{Pellet}]_0} \times 100 \quad \text{Eqn. 4}$$

where, $MASS_{Supernatant}$ is the mass of the chemical in the aqueous part of the vials, $MASS_{Pellet}$ is the mass of the chemical in the solid part (sediment) of the vials, $MASS_{REF_S}$ is the mass of the chemical in REF-S which only contains synthetic mix solution of the chemicals.

The removal in aqueous phase and total biodegradation was calculated for both CONTROL and REACTOR vials. Further, the differences in total masses in CONTROL and REACTOR were considered as the biodegradation percentage accomplished by SRBs.

Benzotriazoles. In the vials containing sediment from sampling point *t1-1*, the concentration of benzotriazoles, considering their solubility and logP, decreased to up to 70% of their initial concentration in the aqueous phase of the vials (Figure 4.10). The vials containing sediment from *t1-1* along with the synthetic mix showed between 59.08 % and 69.78 % concentration reduction in the aqueous phase, for all of the benzotriazoles after 100 days incubation time (Figure 4.10.1). However, the total mass losses (Figure 4.11) show that, except 5,6-D-1H-B which had a higher logP than the other benzotriazoles, between 40% and 45% of the benzotriazoles are sorbed on the sediment. This value was about 61% for 5,6-D-1H-B.

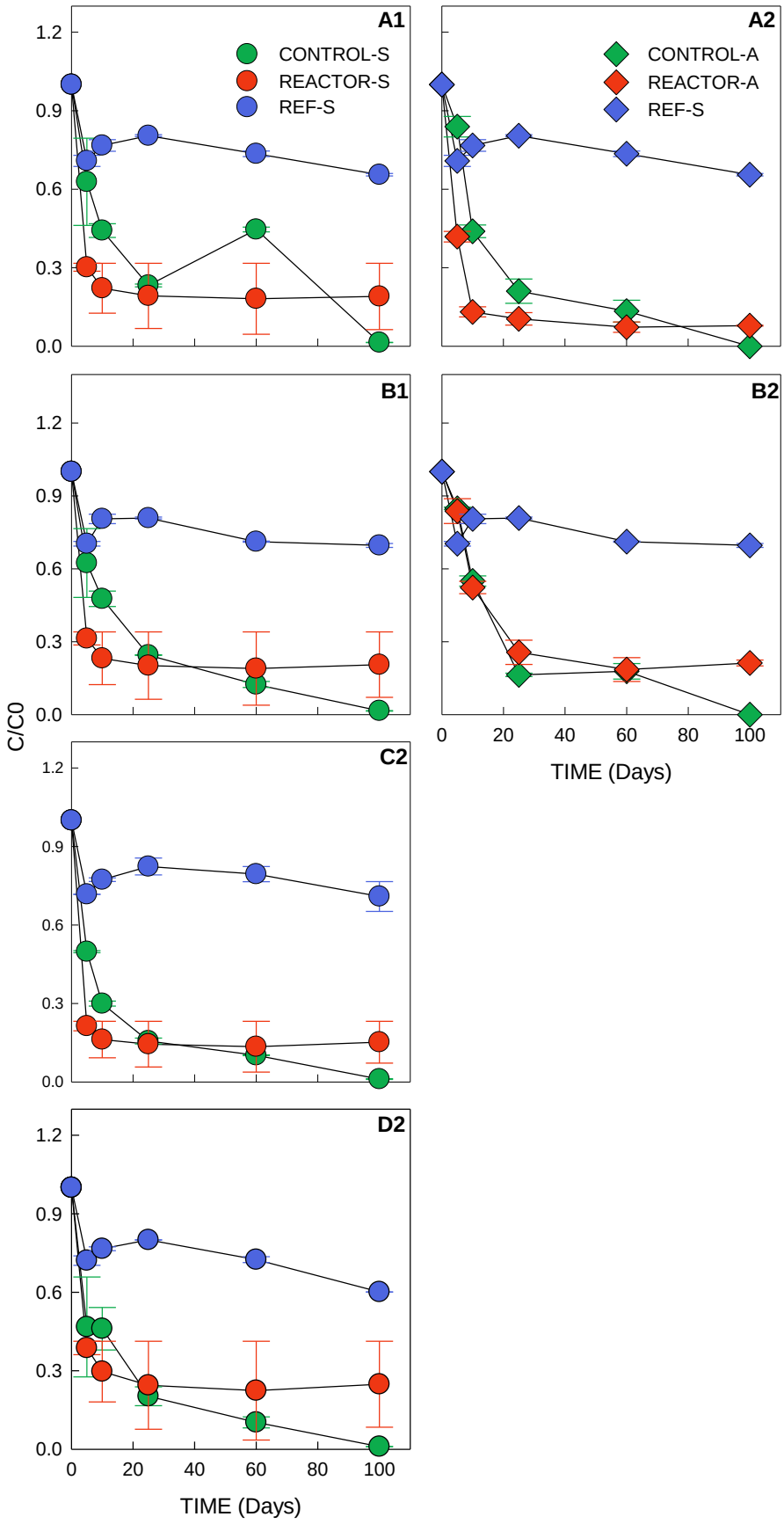

Figure 4.10. Concentration reduction profile of (A) 4-M-1H-B, (B) 5-M-1H-B, (C) 5,6-D-1H-B and (D) 1,2,3-B in aqueous phase of the vials containing sediment *t1-1* along with (1) synthetic water and (2) associated water.

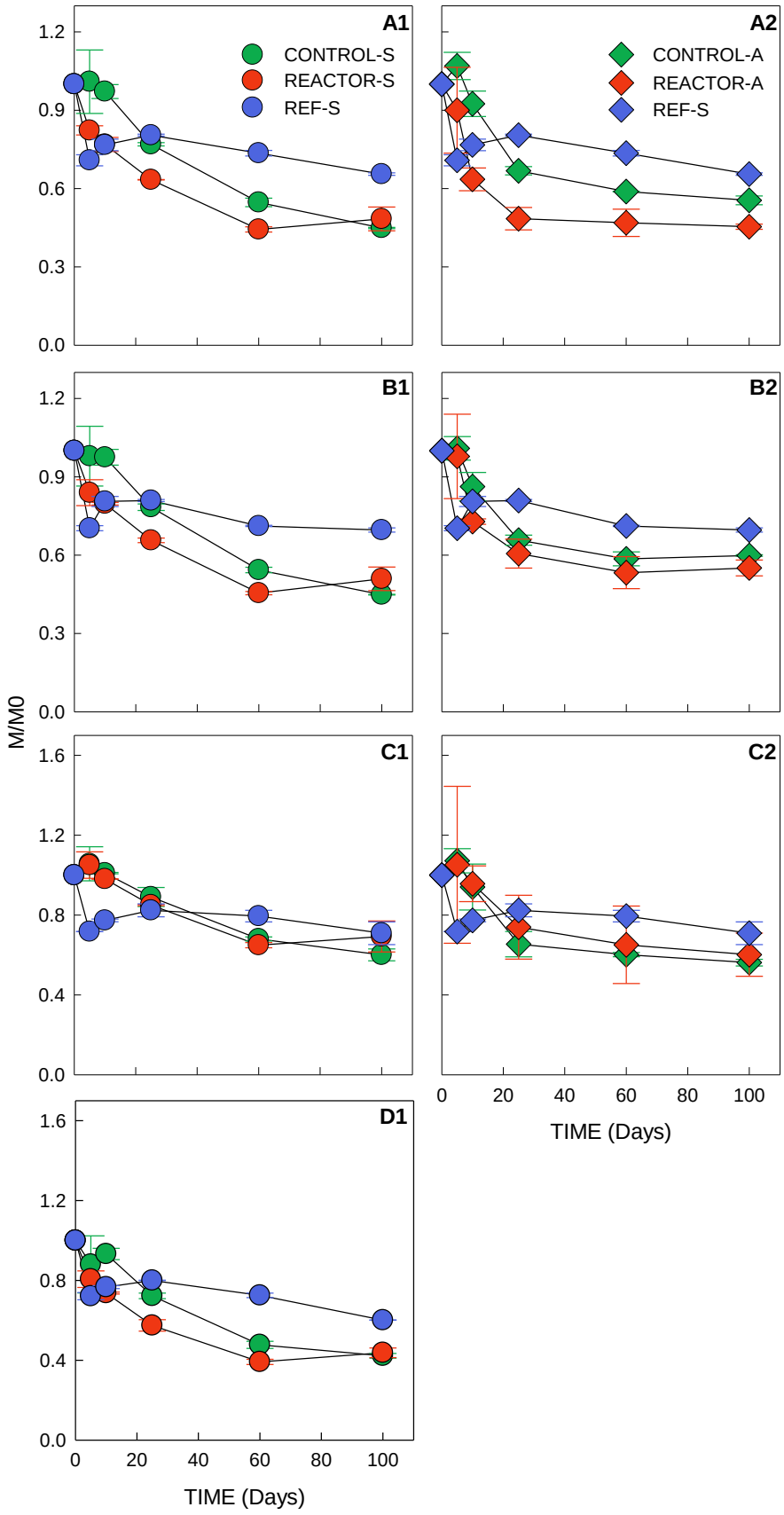

Figure 4.11. Total mass reduction profile of (A) 4-M-1H-B, (B) 5-M-1H-B, (C) 5,6-D-1H-B and (D) 1,2,3-B in the vials containing sediment *t1-1* along with (1) synthetic water and (2) associated water.

In addition, the difference in total biodegradation in CONTROL and REACTOR vials was not significant which represents that other anaerobes (non-SRB) were responsible for the biodegradation of the benzotriazoles in the vials containing sediment *t1-1*. Comparing total mass losses in CONTROL and REACTOR vials with associated water (Figure 4.11) indicated that 4-M-1H-B (10.08%) and 5-M-1H-B (4.75%) were slightly biodegraded by SRB after 100 days incubation time (Figure 4.11.A2 and B2**)**. This can be due to the presence of SRB microorganisms in the associated water of sampling point *t1-1*.

In the vials containing sediment taken from *t3-2*, the benzotriazoles concentration reduction in aqueous phase for both synthetic and associated water, was the same as the ones with sediment *t1-1* (Figure 4.12). Moreover, total mass losses showed that, sediment *t3-2* along with its the associated water, was able to biodegrade up to 55.38%, 41.04% and 56.92% of 4-M-1H-B, 5,6-D-1H-B and 5-M-1H-B, respectively (Figure 4.13.2). Although SRBs were not responsible for this biotransformation, other anaerobes are still present in sediment *t3-2* which are capable of biotransforming those benzotriazoles. The concentration reduction as well as the total mass losses of the studied benzotriazoles are given in Table 4.9.

Biotransformation of benzotriazoles by sediment under anaerobic and sulfate reducing conditions indicated that, these compounds have affinity to attach on the sediment particles. In addition, different biodegradation patterns of benzotriazoles in water-sediment system of *t1-1* and *t3-2* delineate that the sediment as well as their associated water plays an important role due to their microbial diversity. In the literature, it was reported that 1,2,3-B and 5-M-1H-B showed a higher biodegradation by aquifer sediment under anaerobic condition compared to nitrate and sulfate reducing conditions, which confirms the importance of redox condition on the biodegradability of the benzotriazoles (Liu et al., 2013c, Liu et al., 2011b). In another study, 1,2,3-B, 4-M-1-H and 5-M-1-H biodegradation under nitrate and sulfate reducing conditions using activated sludge was investigated. No biodegradation of the three benzotriazoles was observed in that study (Herzog et al., 2014). Thus, considering the other studies and this research, the microbial community is one of the major factors affecting the biotransformation of the benzotriazoles.

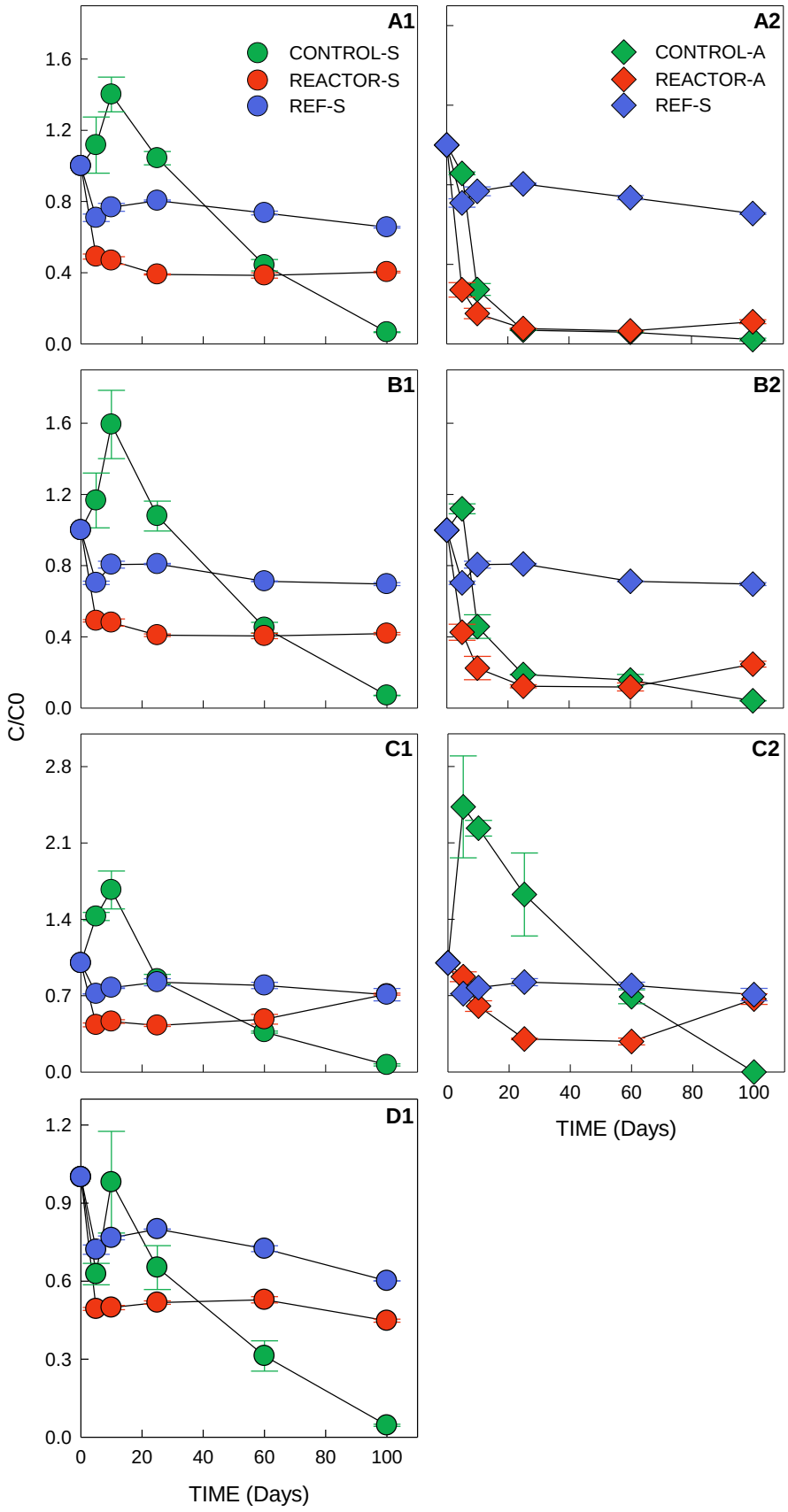

Figure 4.12. Concentration reduction profile of (A) 4-M-1H-B, (B) 5-M-1H-B, (C) 5,6-D-1H-B and (D) 1,2,3-B in aqueous phase of the vials containing sediment *t3-2* along with (1) synthetic water and (2) associated water.

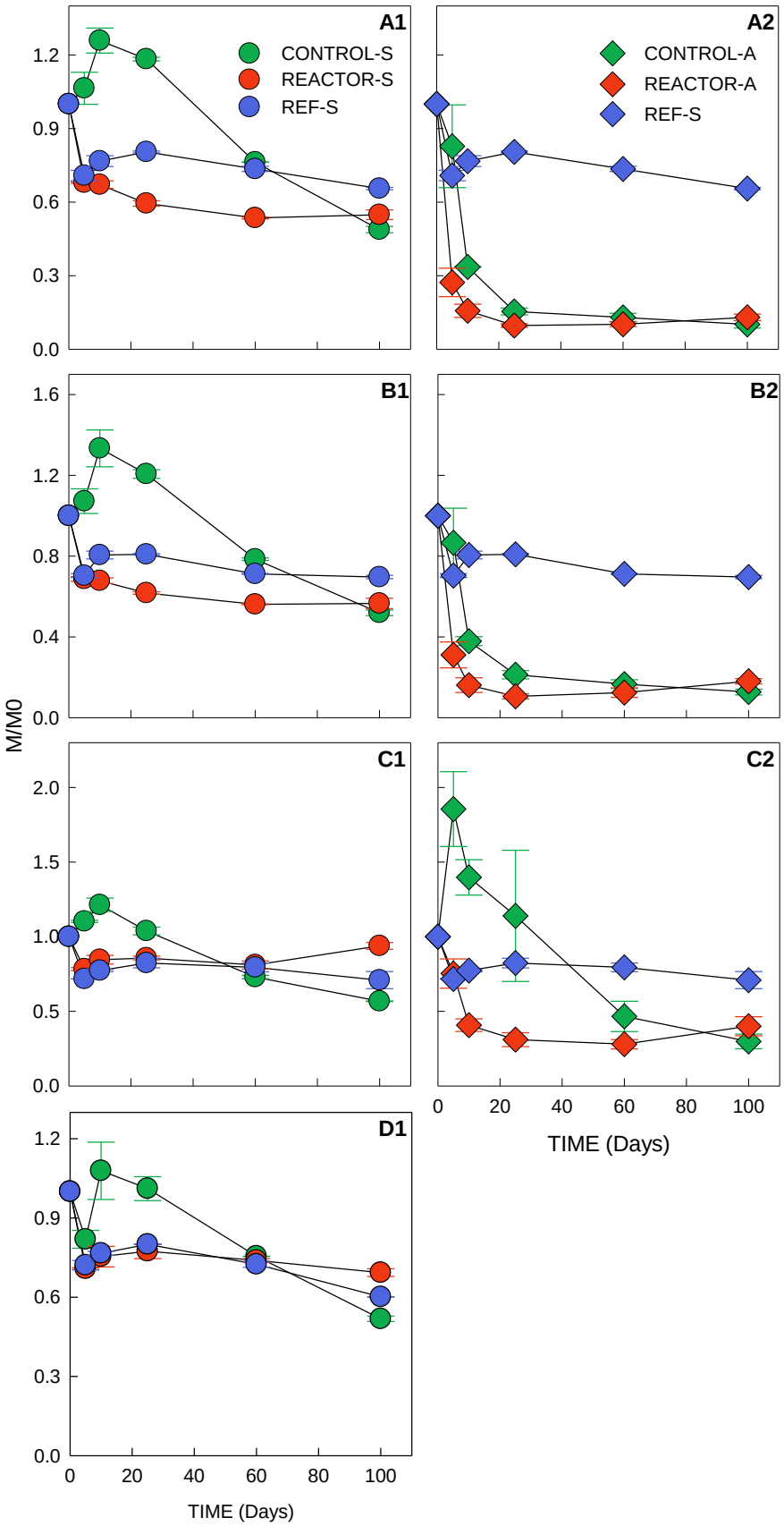

Figure 4.13. Total mass reduction profile of (A) 4-M-1H-B, (B) 5-M-1H-B, (C) 5,6-D-1H-B and (D) 1,2,3-B in the vials containing sediment *t3-2* along with (1) synthetic water and (2) associated water.

HMMM, TBEP, BDDDA and BDTDA. The concentration of HMMM in REF-S containing the only the synthetic mix revealed that HMMM disappeared after 100 days (Figure 4.14.A). Despite of its higher concentration (10,000 µg/L) than the other chemicals, HMMM was completely removed from the systems. This may happen due to other transformation mechanisms such as hydrolysis although there is not enough information regarding the degradation of HMMM by different mechanism in the literature.

In the vials containing the sediment taken from sampling point *t1-1*, the total mass reduction of HMMM was lower in CONTROL and REACTOR vials when compared to REF-S. This may occur because of high concentration of HMMM both in sediment and associated water of *t1-1* (Figure 4.15.A). The same trend was also noticed for the vials containing sediment from sampling point *t3-2* (Figure 4.17.A). Based on the results, HMMM was not biodegraded under anerobic and sulfate reducing conditions.

Although TBEP concentration in aqueous phase of the vials containing sediment *t1-1* decreased (Figure 4.14.B), the total mass losses showed that it was mainly sorbed on the sediment particles (Figure 4.15.B). 28.38% and 18.8% of TBEP was biodegraded by sediment *t1-1* (non-SRB) along with synthetic water and associated water, respectively (Figure 4.15.B). However, in the case of sediment *t3-2*, TBEP was mainly degraded in the CONTROL vials containing the associated water (Figure 4.17.B2). TBEP showed a total biodegradation of 35.58% after 100 days incubation time in those vials. The higher biodegradation may be due to the presence of TBEP-degrading anaerobes in the associated water of *t3-2*. Because of its high hydrophobicity, TBEP also showed a low biodegradability in a study on the aquifer system (Fries and Püttmann, 2003).

BDDDA and BDTDA which are benzalkonium compounds, have high hydrophobicity. In the vials containing the sediment *t1-1*, more than 51% and 23% of BDDDA and BDTDA was removed from the aqueous phase, respectively (Figure 4.14.C and D). Those values were less (more than 34% and 4.7%, respectively) in the vials containing sediment *t3-2* (Figure 4.16.C and D) which may be resulted from the larger particles of sediment *t3-2* than *t1-1*. Despite of removal in the aqueous phase, the results of mass losses for both sets either using sediment *t1-1* or sediment *t3-2* (Figure 4.15.C and D, Figure 4.17.C and D) indicated no biodegradation of BDDDA and BDTDA after 100 days incubation. Till today, no study reported the biodegradation of BDDDA and BDTDA under anaerobic condition, although they can be utilized by microorganisms under aerobic conditions (Tezel and Pavlostathis, 2015).

The removal percentages of the selected chemicals in the aqueous phase of the vials as well as their total biodegradation percentages are given in Table 4.9.

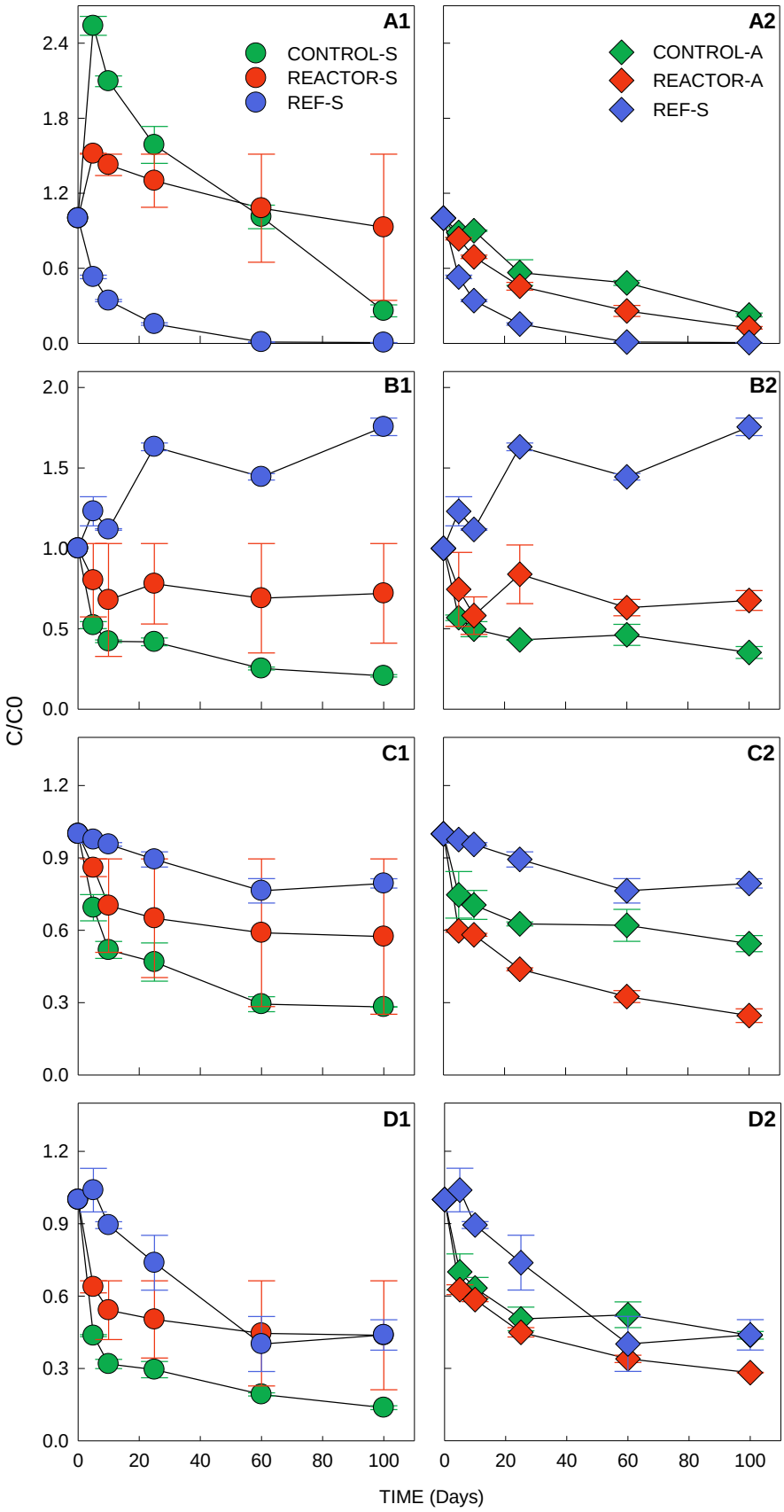

Figure 4.14. Concentration reduction profile of (A) HMMM, (B) TBEP, (C) BDDDA and (D) BDTDA in aqueous phase of the vials containing sediment *t1-1* along with (1) synthetic water and (2) associated water.

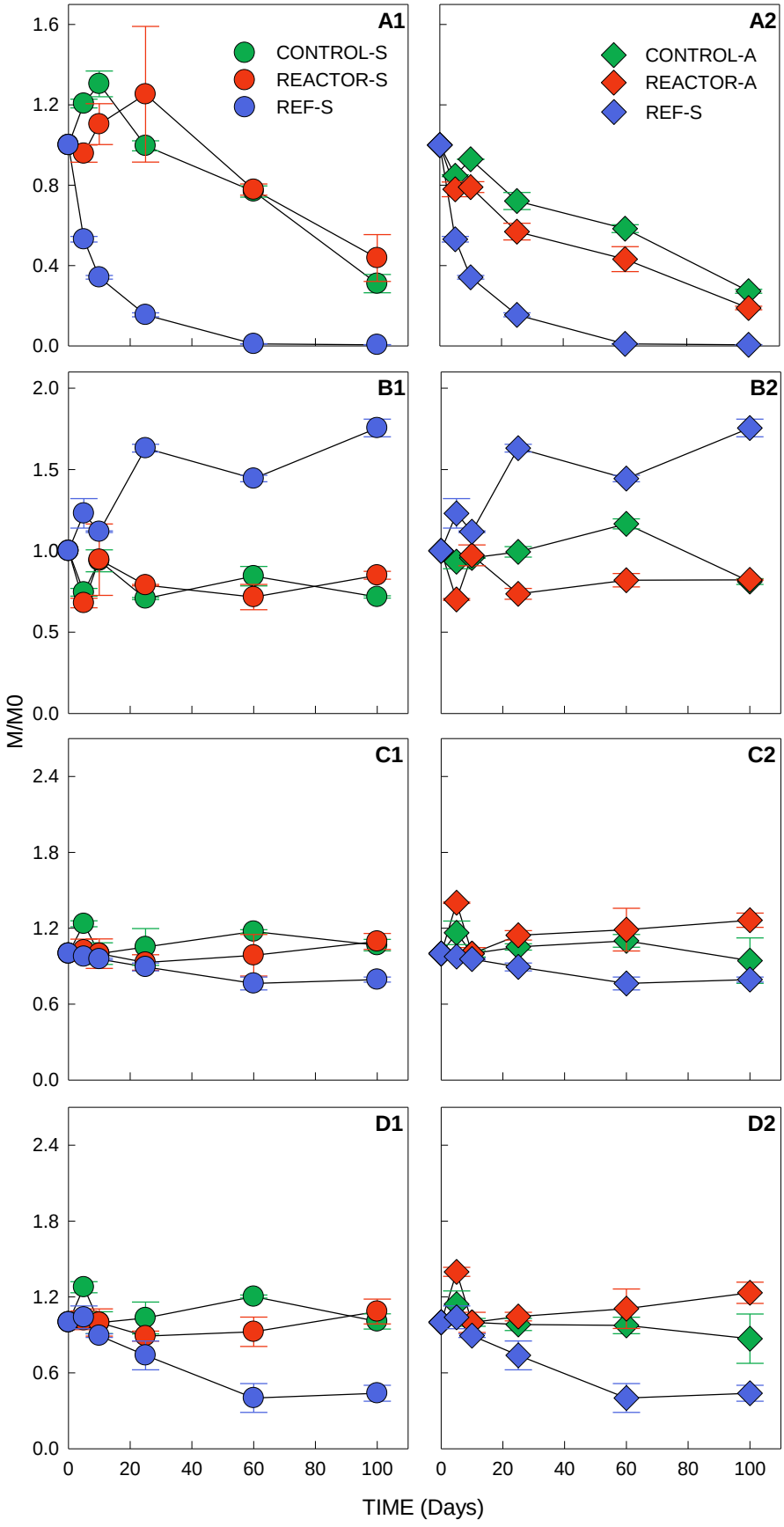

Figure 4.15. Total mass reduction profile of (A) HMMM, (B) TBEP, (C) BDDDA and (D) BDTDA in the vials containing sediment *t1-1* along with (1) synthetic water and (2) associated water.

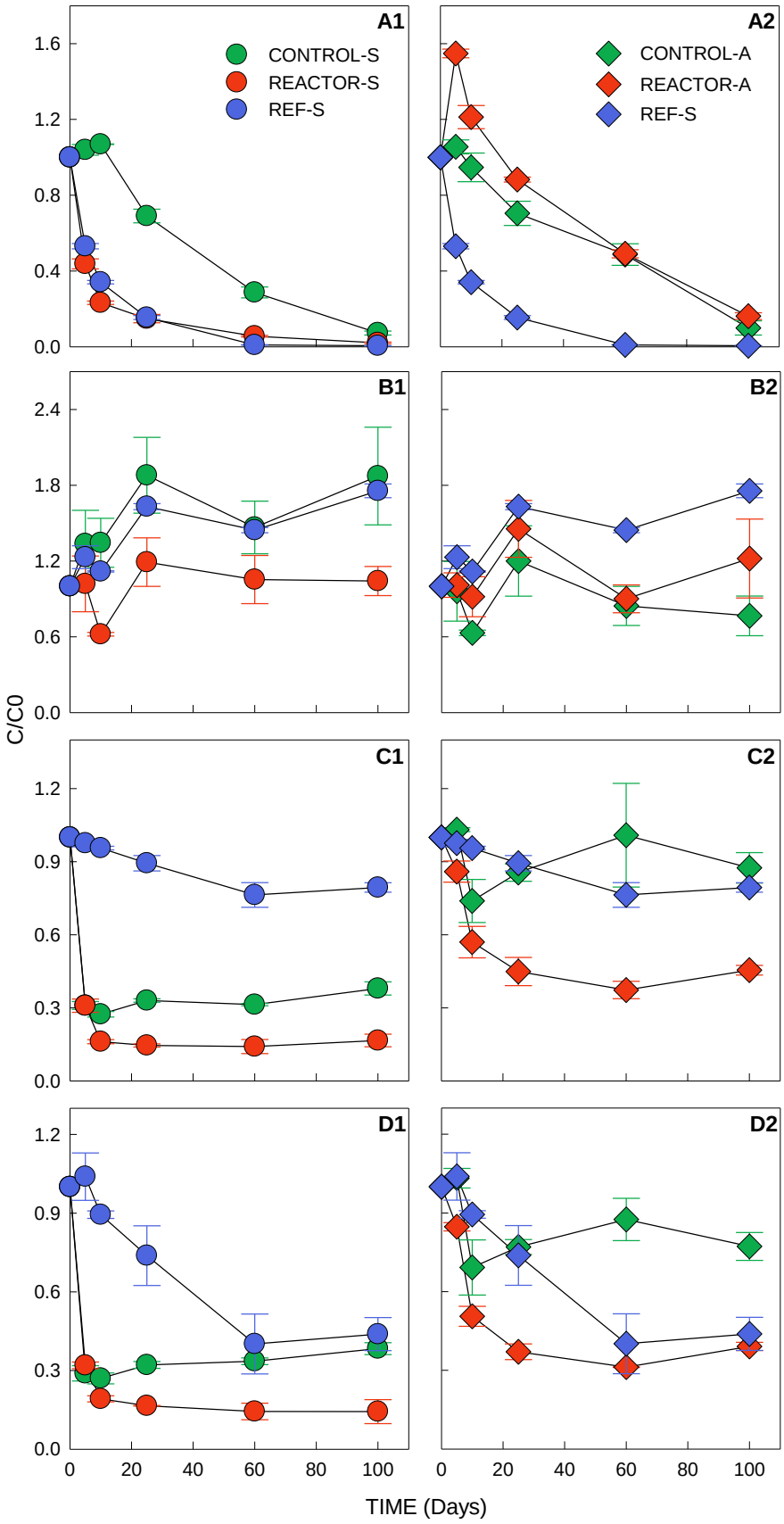

Figure 4.16. Concentration reduction profile of (A) HMMM, (B) TBEP, (C) BDDDA and (D) BDTDA in aqueous phase of the vials containing sediment *t3-2* along with (1) synthetic water and (2) associated water.

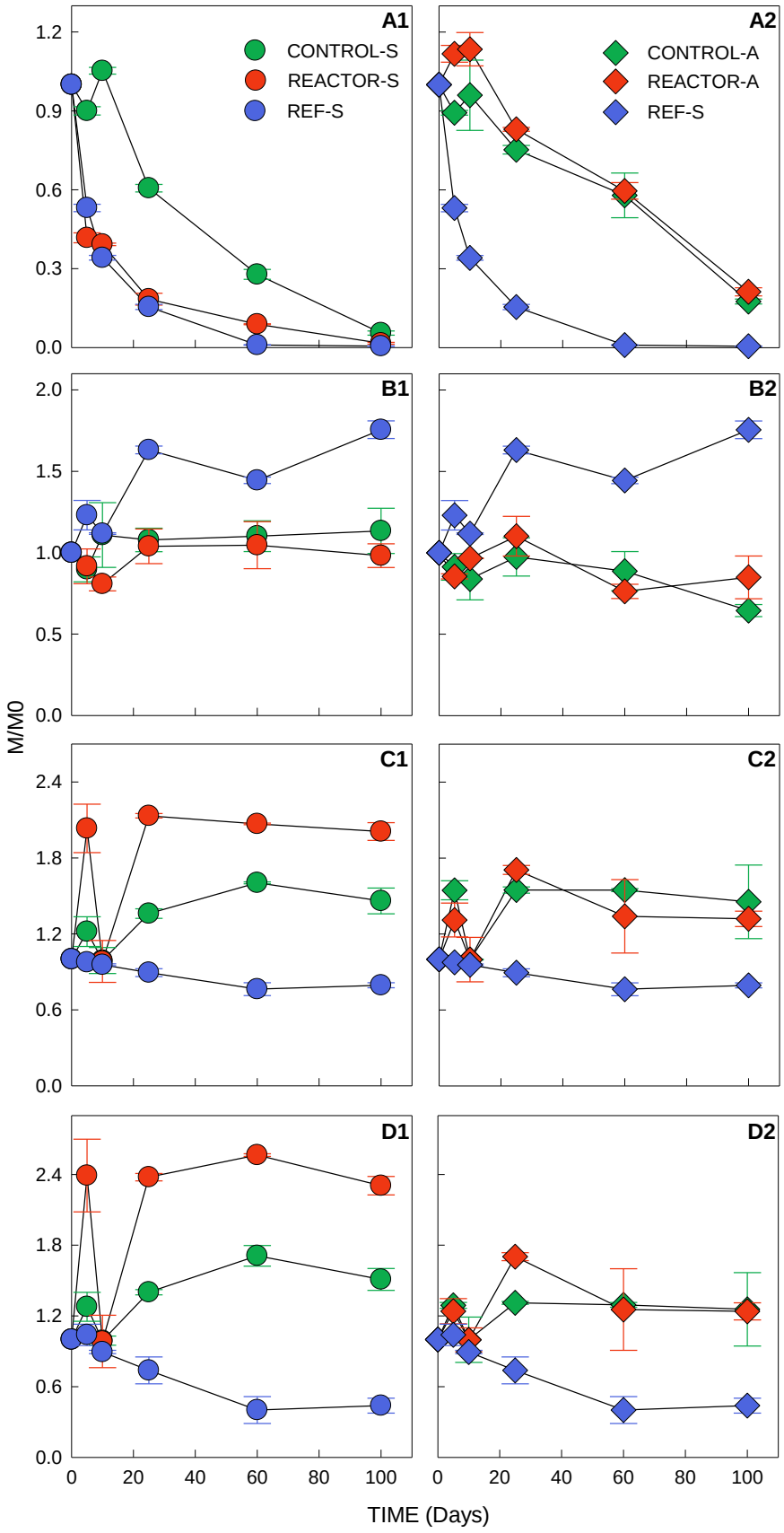

Figure 4.17. Total mass reduction profile of (A) HMMM, (B) TBEP, (C) BDDDA and (D) BDTDA in the vials containing sediment *t3-2* along with (1) synthetic water and (2) associated water

Table 4.9. Removal (%) of micropollutants in aqueous phase and their total biodegradation (%).

Sediment from sampling point *t1-1*

	Synthetic Water					Associated Water				
	Removal in Aqueous Phase		Total Biodegradation (%)		Biodegradation by SRB (%)	Removal in Aqueous Phase		Total Biodegradation (%)		Biodegradation by SRB (%)
Chemical	CONTROL-S	REACTOR-S	CONTROL-S	REACTOR-S		CONTROL-A	REACTOR-A	CONTROL-A	REACTOR-A	
1,2,3-B	59.08±0.01	52.28±0.59	17.85±1.18	16.35±2.42	0.00	-	-	-	-	-
4-M-1H-B	64.12±0.07	58.44±0.74	20.63±0.23	17.17±4.56	0.00	65.55±0.00	57.68±0.17	10.07±1.70	20.14±0.99	10.08
5,6-D-1H-B	69.78±0.15	63.86±0.82	10.85±2.98	1.63±7.74	0.00	70.90±0.00	70.90±0.00	14.73±1.68	10.75±10.84	0.00
5-M-1H-B	68.09±0.13	61.62±0.89	24.76±0.15	18.69±4.49	0.00	69.63±0.00	48.39±1.21	9.78±0.30	14.53±3.04	4.75
HMMM	0.00	0.00	0.00	0.00	0.00	0.00	0.00	0.00	0.00	0.00
TBEP	79.30±0.75	51.80±7.14	28.38±0.70	15.02±2.38	0.00	64.78±3.71	32.41±6.16	18.89±1.79	17.84±0.37	0.00
BDDDA	51.20±0.06	54.79±0.55	0.00	0.00	0.00	24.96±3.33	54.82±2.81	0.00	0.00	0.00
BDTDA	30.16±0.78	23.65±0.92	0.00	0.00	0.00	0.19±1.56	15.67±0.11	0.00	0.00	0.00

Sediment from sampling point *t3-2*

	Synthetic Water					Associated Water				
	Removal in Aqueous Phase		Total Biodegradation (%)		Biodegradation by SRB (%)	Removal in Aqueous Phase		Total Biodegradation (%)		Biodegradation by SRB (%)
	CONTROL-S	REACTOR-S	CONTROL-S	REACTOR-S		CONTROL-A	REACTOR-A	CONTROL-A	REACTOR-A	
1,2,3-B	55.52±0.41	15.31±0.60	8.29±1.01	0.00	0.00	-	-	-	-	-
4-M-1H-B	58.97±0.22	25.15±0.43	16.74±1.30	10.69±1.95	0.00	63.34±0.64	54.38±0.98	55.38±1.51	52.52±1.31	0.00
5,6-D-1H-B	64.31±0.97	0.00	14.12±0.23	0.00	0.00	70.90±0.00	4.13±4.87	41.04±4.90	30.86±6.41	0.00
5-M-1H-B	62.58±0.15	27.79±0.64	17.68±1.37	13.05±2.56	0.00	65.52±0.09	44.95±1.66	56.92±1.44	51.57±1.30	0.00
HMMM	0.00	0.00	0.00	0.00	0.00	0.00	0.00	0.00	0.00	0.00
TBEP	0.00	0.00	0.00	0.00	0.00	23.41±15.68	0.00	35.58±34.12	15.09±13.11	0.00
BDDDA	41.45±2.70	62.80±2.61	0.00	0.00	0.00	0.00	33.96±1.98	0.00	0.00	0.00
BDTDA	5.53±2.27	29.55±4.56	0.00	0.00	0.00	0.00	4.78±1.57	0.00	0.00	0.00

5. CONCLUSION

The study presented here identified and quantified the conventional water quality parameters and organic micropollutants in the Ergene River, determined the most important pollution sources and their fingerprint pollutants, and finally assessed the biotransformation and biodegradation of micropollutants under anaerobic and sulfate reducing conditions.

Ergene watershed located in the Thrace region in Turkey has encounter pollution due to rapid population and industrial growth. To understand the level of pollution and its sources, seasonal samplings of 75 sampling points located on the main stream as well as its tributaries were accomplished. Conventional water quality parameters including color, pH, temperature, COD, TOC, ammonium nitrogen, sulfate, phosphate and other important anions as well as heavy metals were measured in those samples. The values of conventional parameters reached high values at sampling points located next to the discharge of the OIZs in the ***industrial zone***. Discharge of industrial effluents from OIZs into the river lessened the quality of water. Reddish color, elevated temperature, high COD (1,660 mg/L), high anions concentration (1990 mg/L of sulfate) and elevated heavy metals (more than 10 mg/L for Al, Zn and Cu) were the characteristics of critical sampling points next to the industrial facilities.

Although conventional parameters indicated the high pollution in the Ergene River, organic micropollutants identification and quantification gives more comprehensive and detailed information about the toxicity and other adverse effects of the pollution in the river. Out of 222 organic micropollutants selected from the list of priority substances (WFD) as well as NORMAN list of CECs during targeted analysis of micropollutants, 131, 135, 96 and 103 chemicals were detected in at least one sampling point during summer, fall, winter and spring samplings, respectively. Those pollutants embraced a wide spectrum of chemicals originated from various industrial, agricultural and domestic activities which also possess carcinogenic, mutagenic and other toxic effects. Among them, flame retardants (TBEP: 565.22 µg/L), fragrances (methydihydrojasmonate: 21 µg/L), plasticizers (DEHP: 69.92 µg/L), surfactants (BACs: 116.7 µg/L), combustion byproducts (anthracene: 851 µg/L), corrosion inhibitors (1,2,3-B: 117 µg/L), and chemicals used in the manufacturing of different products (HMMM: 329,166 µg/L) were the most frequently detected as well as the ones with higher concentration than the rest of the chemicals analyzed. Similar to conventional parameters, micropollutants were mainly detected at the sampling points close to the discharge point of OIZs (***industrial zone***), specially the ones located on the Çorlu Creek (*cc*), Ergene Creek (*ec*) and the

tributaries close to the Büyükkarıştıran (*t1-1*) and Evrensekiz OIZs (*t3-1*). Pharmaceutical (ofloxacin: 824.37 µg/L) and personal care products were intensively found either next to the discharge of their manufacturing point or close to the residential regions. In addition to industrial and domestic-derived micropollutants, pesticides (diuron: 10.64 µg/L) were intensively observed in sampling points surrounded by agricultural lands. In addition, the concentration of detected chemicals such as PSs (PAHs, PBDE, Pesticides, etc) at some sampling points exceeded the recommended EQS by the authorities indicating the high pollution stress and potential health risk in the watershed.

Heatmaps of micropollutants clustered using the normalized concentration profiles of sampling points on the main river, tributaries, Çorlu creek and Ergene creek were constructed to elucidate the main sources. The results indicated that sampling points located in ***industrial zone*** specially the ones located ones on the Çorlu creek (*cc*), Ergene Creek (*ec*), the tributaries close to Büyükkarıştıran (*t1-1*) and Evrensekiz OIZs (*t3-1*) and sampling pint *t4* were the important pollution sources. In addition, clustering analysis of ***transition*** and ***agricultural zone***s during fall (dry season) and spring (wet season) demonstrated that the pollution generated in the ***industrial zone*** was transported to the ***transition*** and ***agricultural zones*** via the main stream till the last sampling point where the Ergene River connects the Maritsa river. Out of the abovementioned sampling points, *cc7* next to Velimeşe OIZ, *ec6* next to Ergene 1 OIZ, *t1-1* close to Büyükkarıştıran OIZ were selected as the most important pollution sources in all seasons. The fingerprint pollutants of those sampling points were identified as well. HMMM, BACs, benzotriazoles and PAHs were the common fingerprint pollutants in the aforementioned sampling points. Discharge of different industrial effluents around those sampling points specially textile and dye facilities as well as chemical production, plastic, metal, etc. into those sampling points were the reason of pollution. Sampling points *t3-1* and *t4* were also considered as most important sampling point during summer and fall. Those two sampling points were receiving domestic, industrial and agricultural wastewaters and that is why the fingerprint pollutants consisted of chemicals specific for those activities.

Beside targeted analysis, unknown screening of river water samples was also accomplished for non-targeted analysis. 24 sampling points located on the main stream and important tributaries were subjected to unknown screening using the developed method and further five most abundant ions were investigated in detail for identification. The mass spectrum of 13 out of 24 sampling points were significantly different from the blank (methanol). In addition, further fragmentation and identification of the most abundant precursor ions indicated that detomidine carboxylic acid was identified in most of those samples. Other than that, chemicals such as fuberidazole, tetrazepam, difenzoquat and prajmaline mainly as sedative drugs and pesticides were also identified.

Considering the concentration of the most frequently detected micropollutants in the Ergene River, their biotransformation potential under anaerobic and sulfate reducing conditions in water-sediment system was studied. Eight chemicals from different groups including benzotriazoles (1,2,3-B, 4-M-1H-B, 5,6-D-1H-B, 5-M-1H-B), HMMM, TBEP, BDDDA and BDTDA that had high detection frequencies and concentrations, were chosen as candidates for biotransformation assays. In addition, five sediment samples taken from sampling points *m2*, *ec8*, *t1-1*, *t3-2* and *m10* were selected as SRBs sources. However, sediments characterization elucidated that sediments *t1-1* and *t3-2* composed of finer particles as well as high VS and micropollutants. That is why, those sediments were selected for the biotransformation tests.

Biotransformation assay was conducted in two sets using sediment *t1-1* and *t3-2* along with their associated water and prepared synthetic water. The 100 days biotransformation assay delineate that benzotriazoles are mainly biodegraded by non-sulfate reducing organisms (non-SRB) although 4-M-1H-B (10.08%) and 5-M-1H-B (4.75%) were slightly biodegraded by SRBs. HMMM on the other hand, was completely disappeared from the system due to its probable hydrolysis. TBEP showed 28.38% and 35.58% biodegradation by non-SRB anaerobes present in sediment *t1-1* and *t3-2*, respectively. BDDDA and BDTDA were not biodegraded under anaerobic and sulfate reducing conditions.

The results of this study revealed that the Ergene River is polluted by different micropollutants that are emerged from industrial, domestic and agricultural activities in the watershed. Particularly, abundant number of industrial facilities in the region (OIZs and single facilities) resulted in high concentration of industrial-derived chemicals such as HMMM, BDDDA, BDTDA, TEHP, benzotriazoles, PAHs, etc. in the river. Identified pollution sources and their fingerprint pollutants can be utilized to prevent the discharge of those chemicals into the river. In addition, giving the fact that current remediation progress on the Ergene River which aims to divert polluted streams to Marmara Sea and let the river replenish itself naturally is not going to alleviate the level of pollution since the chemicals which are sorbed on the sediment and not biodegradable will still remain in the river. Therefore, other strategies along with stringent regulation should be assigned to battle the pollution in the Ergene Watershed.

REFERENCES

Abdel-Shafy, H.I., Mansour, M.S.M., 2016. A review on polycyclic aromatic hydrocarbons: Source, environmental impact, effect on human health and remediation. Egyptian Journal of Petroleum, 25, 107-123.

Al-Kaf, A.G., Naji, K.M., Abdullah, Q.Y.M., Edrees, W.H.A., 2017. Occurrence of paracetamol in aquatic environments and transformation by microorganisms: A review. Chronicles of Pharmaceutical Science, 1, 341-355.

Albergamo, V., Helmus, R., De Voogt, P., 2018. Direct injection analysis of polar micropollutants in natural drinking water sources with biphenyl liquid chromatography coupled to high-resolution time-of-flight mass spectrometry. Journal of Chromatography A, 1569, 53-61.

Aldenberg, T.,Jaworska, J.S., 2000. Uncertainty of the hazardous concentration and fraction affected for normal species sensitivity distributions. Ecotoxicology and Environmental Safety, 46, 1-18.

Alder, A.C., Schaffner, C., Majewsky, M., Klasmeier, J., Fenner, K., 2010. Fate of beta-blocker human pharmaceuticals in surface water: Comparison of measured and simulated concentrations in the Glatt valley watershed, Switzerland. Water Research, 44, 936-48.

Alotaibi, M.D., McKinley, A.J., Patterson, B.M., Reeder, A.Y., 2015. Benzotriazoles in the aquatic environment: A review of their occurrence, toxicity, degradation and analysis. Water, Air, and Soil Pollution, 226.

Alvarez, J.L.,Vassort, G., 1993. Prajmalium. Cardiovascular Drugs Review, 11, 385-410.

Amé, M.V., Galanti, L.N., Menone, M.L., Gerpe, M.S., Moreno, V.J., Wunderlin, D.A., 2010. Microcystin–LR, –RR, –YR and –LA in water samples and fishes from a shallow lake in Argentina. Harmful Algae, 9, 66-73.

Antić, N., Radišić, M., Radović, T., Vasiljević, T., Grujić, S., Petković, A., Dimkić, M., Laušević, M., 2015. Pesticide residues in the danube river basin in serbia - a survey during 2009-2011. CLEAN - Soil, Air, Water, 43, 197-204.

Apte Sagar, S., Apte Shruti, S., Kore, V.S., Kore, S.V., 2011. Chloride removal from wastewater by biosorption with the plant biomass. Universal Journal of Environmental Research and Technology, 1, 416-422.

Arlt, V.M., 2005. 3-nitrobenzanthrone, a potential human cancer hazard in diesel exhaust and urban air pollution: A review of the evidence. Mutagenesis, 20, 399-410.

Aronson, D., Weeks, J., Meylan, B., Guiney, P.D., Howard, P.H., 2012. Environmental release, environmental concentrations, and ecological risk of n,n-diethyl-m-toluamide (DEET). Integrated Environmental Assessment and Management, 8, 135-66.

Asimakopoulos, A.G., Wang, L., Thomaidis, N.S., Kannan, K., 2013. Benzotriazoles and benzothiazoles in human urine from several countries: A perspective on occurrence, biotransformation, and human exposure. Environment International, 59, 274-81.

Avagyan, R., Luongo, G., Thorsen, G., Ostman, C., 2015. Benzothiazole, benzotriazole, and their derivates in clothing textiles--a potential source of environmental pollutants and human exposure. Environmental Science and Pollution Research, 22, 5842-9.

Aydin, E., Talinli, I., 2013. Analysis, occurrence and fate of commonly used pharmaceuticals and hormones in the buyukcekmece watershed, turkey. Chemosphere, 90, 2004-12.

Aziz, F., Syed, J.H., Malik, R.N., Katsoyiannis, A., Mahmood, A., Li, J., Zhang, G., Jones, K.C., 2014. Occurrence of polycyclic aromatic hydrocarbons in the soan river, pakistan: Insights into distribution, composition, sources and ecological risk assessment. Ecotoxicology and Environmental Safety, 109, 77-84.

Aznar-Alemany, O., Trabalon, L., Jacobs, S., Barbosa, V.L., Tejedor, M.F., Granby, K., Kwadijk, C., Cunha, S.C., Ferrari, F., Vandermeersch, G., Sioen, I., Verbeke, W., Vilavert, L., Domingo, J.L., Eljarrat, E., Barcelo, D., 2017. Occurrence of halogenated flame retardants in commercial seafood species available in European markets. Food and Chemical Toxicology, 104, 35-47.

Bacaloni, A., Cavaliere, C., Foglia, P., Nazzari, M., Samperi, R., Lagana, A., 2007. Liquid chromatography/tandem mass spectrometry determination of organophosphorus flame retardants and

plasticizers in drinking and surface waters. Rapid Communications in Mass Spectrometry, 21, 1123-30.

Baldwin, A.K., Corsi, S.R., De Cicco, L.A., Lenaker, P.L., Lutz, M.A., Sullivan, D.J., Richards, K.D., 2016. Organic contaminants in Great Lakes tributaries: Prevalence and potential aquatic toxicity. Science of the Total Environment, 554-555, 42-52.

Barabasz, W., Albinska, D., Jaskowska, J., Lipiec, J., 2002. Ecotoxicology of aluminium. Polish Journal of Environmental Studies, 11, 199-203.

Belfroid, A.C., Van Der Host, A., Vethaak, A.D., Schafer, A.J., Rijs, G.B.J., Wegener, J., Cofino, W.P., 1999. Analysis and occurrence of estrogenic hormones and their glucuronides in surface water and waste water in the Netherlands. The Science of Total Environment, 225, 101-108.

Berehanu, B., Lemma, B., Tekle-Giorgis, Y., 2015. Chemical composition of industrial effluents and their effect on the survival of fish and eutrophication of lake Hawassa, Southern Ethiopia. Journal of Environmental Protection, 06, 792-803.

Bobeldijk, I., Stoks, P.G.M., Vissers, J.P.C., Emke, E., Van Leerdam, J.A., Muilwijk, B., Berbee, R., Noij, T.H.M., 2002. Surface and wastewater quality monitoring: Combination of liquid chromatography with (geno)toxicity detection, diode array detection and tandem mass spectrometry for identification of pollutants. Journal of Chromatography A,, 970, 167-181.

Bohencke, A., Kielhorn, J., Konnecker, G., Pohlenz-Michel, C., Mangelsdorf, I. 2003. Concise international chemical assessment document 48: 4-chloroaniline.

Bollmann, U.E., Moller, A., Xie, Z., Ebinghaus, R., Einax, J.W., 2012. Occurrence and fate of organophosphorus flame retardants and plasticizers in coastal and marine surface waters. Water Research, 46, 531-8.

Boopathy, R., 2017. Anaerobic degradation of atrazine. International Biodeterioration & Biodegradation, 119, 626-630.

Bueno, M.J., Gomez, M.J., Herrera, S., Hernando, M.D., Aguera, A., Fernandez-Alba, A.R., 2012. Occurrence and persistence of organic emerging contaminants and priority pollutants in five sewage treatment plants of spain: Two years pilot survey monitoring. Environmental Pollution, 164, 267-73.

Buratti, F.M., Testai, E., 2015. Species- and congener-differences in microcystin-LR and -RR gsh conjugation in human, rat, and mouse hepatic cytosol. Toxicology Letters, 232**,** 133-40.

Careghini, A., Mastorgio, A.F., Saponaro, S., Sezenna, E., 2015. Bisphenol a, nonylphenols, benzophenones, and benzotriazoles in soils, groundwater, surface water, sediments, and food: A review. Environmental Science and Pollut Research, 22**,** 5711-41.

Carey, J.H. Transformation processes of contaminants in rivers. May 1993 1993 Rostov-on-Don, Russia. IAHS 41-50.

Carpenter, C.M.G., Helbling, D.E., 2018. Widespread micropollutant monitoring in the hudson river estuary reveals spatiotemporal micropollutant clusters and their sources. Environmental Science and Technology, 52**,** 6187-6196.

Cecen, F., 2018. Removal and behavior of hazardous pollutants in biological treatment systems. In*:* Cecen, F., Tezel, U. (Eds.) Hazardous pollutants in biological treatment systems. London, UK: IWA Publishing.

Cespedes, R., Lacorte, S., Ginebreda, A., Barcelo, D., 2006. Chemical monitoring and occurrence of alkylphenols, alkylphenol ethoxylates, alcohol ethoxylates, phthalates and benzothiazoles in sewage treatment plants and receiving waters along the ter river basin (catalonia, n. E. Spain). Anal Bioanal Chem, 385**,** 992-1000.

Chang, B.V., Chang, I.T., Yuan, S.Y., 2008. Anaerobic degradation of phenanthrene and pyrene in mangrove sediment. Bulletin of Environmental Contamination and Toxicology, 80**,** 145-149.

Chang, B.V., Liao, C.S., Yuan, S.Y., 2005. Anaerobic degradation of diethyl phthalate, di-n-butyl phthalate, and di-(2-ethylhexyl) phthalate from river sediment in Taiwan. Chemosphere, 58**,** 1601-1607.

Chang, B.V., Liu, W.G., Yuan, S.Y., 2001. Microbial dechlorination of three PCB congeners in river sediment. Chemosphere, 45**,** 849-856.

Chang, B.V., Yu, C.H., Yuan, S.Y., 2004. Degradation of nonylphenol by anaerobic microorganisms from river sediment. Chemosphere, 55**,** 493-500.

Charalampous, A.C., Miliadis, G.E., Koupparis, M.A., 2015. A new multiresidue method for the determination of multiclass pesticides, degradation products and PCBs in water using LC–MS/MS and GC–$MS^{(n)}$ systems. International Journal of Environmental Analytical Chemistry, 95**,** 1283-1298.

Che, H., Liu, S., 2014. Contaminant detection using multiple conventional water quality sensors in an early warning system. Procedia Engineering, 89**,** 479-487.

Chen, B., Xuan, X., Zhu, L., Wang, J., Gao, Y., Yang, K., Shen, X., Lou, B., 2004. Distributions of polycyclic aromatic hydrocarbons in surface waters, sediments and soils of hangzhou city, china. Water Research, 38**,** 3558-68.

Chen, C.I., Taylor, R.T., 1997. Thermophilic biodegradation of btex by two consortia of anaerobic bacteria. Applied Microbiology and Biotechnology, 48**,** 121-128.

Chen, K., Zhou, J.L., 2014. Occurrence and behavior of antibiotics in water and sediments from the huangpu river, shanghai, china. Chemosphere, 95**,** 604-12.

Conservation Ontario. Integrated watershed management, protecting water resources and addressing environmental challenges [Online]. Available: https://conservationontario.ca/policy-priorities/integrated-watershed-management/ [Accessed 5th September 2019].

Craig, S.A., 2004. Betaine in human nutrition. American Journal of Clinical Nutrition, 80**,** 539-549.

Cristale, J., Garcia Vazquez, A., Barata, C., Lacorte, S., 2013a. Priority and emerging flame retardants in rivers: Occurrence in water and sediment, daphnia magna toxicity and risk assessment. Environment International, 59, 232-43.

Cristale, J., Katsoyiannis, A., Sweetman, A.J., Jones, K.C., Lacorte, S., 2013b. Occurrence and risk assessment of organophosphorus and brominated flame retardants in the river Aire (UK). Environmental Pollution, 179, 194-200.

Cui, X., Hunter, W., Yang, Y., Chen, Y., Gan, J., 2011. Biodegradation of pyrene in sand, silt and clay fractions of sediment. Biodegradation, 22, 297-307.

Czajka, C.P., Londry, K.L., 2006. Anaerobic biotransformation of estrogens. Science of the Total Environment, 367, 932-941.

Czarczynska-Goslinska, B., Zgola-Grzeskowiak, A., Jeszka-Skowron, M., Frankowski, R., Grzeskowiak, T., 2017. Detection of bisphenol a, cumylphenol and parabens in surface waters of Greater Poland Voivodeship. Journal of Environmental Management, 204, 50-60.

Darwish, M.S., 2012. Characterization of ammonia removal from municipal wastewater using microwave energy. Master of Science, The Islamic University-Gaza.

De Hoogh, C.J., Wagenvoort, A.J., Jonker, F., Van Leerdam, J.A., Hogenboom, A.C., 2006. HPLC-DAD and Q-TOF ms techniques identify cause of daphnia biomonitor alarms in the river meuse. Environmental Science and Technology, 40, 2678-2685.

De Wilt, A., He, Y., Sutton, N., Langenhoff, A., Rijnaarts, H., 2018. Sorption and biodegradation of six pharmaceutically active compounds under four different redox conditions. Chemosphere, 193, 811-819.

Delle Site, A., 2001. Factors affecting sorption of organic compounds in natural sorbentõ water systems and sorption coefficients for selected pollutants. A review. Journal of Physical and Chemical Reference Data, 30, 187-431.

Deng, W., Li, N., Zheng, H., Lin, H., 2016. Occurrence and risk assessment of antibiotics in river water in hong kong. Ecotoxicology and Environmental Safety, 125, 121-7.

DeWeerd, K.A., Mandelco, L., Tanner, R.S., Woese, C.R., Suflita, J.M., 1990. *Desulfomonile tiedjei* gen. Nov. And sp. Nov., a novel anaerobic, dehalogenating, sulfate-reducing bacterium. Archives of Microbiology, 154, 23-30.

Diamond, J.M., Latimer, H.A., Munkittrick, K.R., Thornton, K.W., Bartell, S.M., Kidd, K.A., 2011. Prioritizing contaminants of emerging concern for ecological screening assessments. Environmental Toxicology and Chemistry, 30, 2385-94.

Dich, j., Zahm, S.H., Hanberg, A.,Adami, H.O., 1997. Pesticides and cancer. Cancer Causes and Control, 8, 420-443.

Diez-Quijada, L., Puerto, M., Gutierrez-Praena, D., Llana-Ruiz-Cabello, M., Jos, A., Camean, A.M., 2019. Microcystin-RR: Occurrence, content in water and food and toxicological studies. A review. Environmental Research, 168, 467-489.

Ding, W., Liao, Y.H., 2001. Determination of alkylbenzyldimethylammonium chlorides in river water and sewage effluent by solid-phase extraction and gas chromatography/mass spectrometry. Analytical Chemistry, 73, 36-40.

Dom, I., Bire, R., Hort, V., Lavison-Bompard, G., Nicolas, M., Guerin, T., 2018. Extended targeted and non-targeted strategies for the analysis of marine toxins in mussels and oysters by (LC-HRMS). Toxins (Basel), 10.

Dsikowitzky, L., Schwarzbauer, J., 2015. Hexa(methoxymethyl)melamine: An emerging contaminant in german rivers. Water Environment Research, 87, 461-469.

Dulio, V., Slobodnik, J., 2009. Norman-network of reference laboratories, research centres and related organisations for monitoring of emerging substances. Environmental Science and Pollution Research International, 16 Suppl 1, S132-5.

Dulio, V., van Bavel, B., Brorstrom-Lunden, E., Harmsen, J., Hollender, J., Schlabach, M., Slobodnik, J., Thomas, K., Koschorreck, J., 2018. Emerging pollutants in the EU: 10 years of norman in support of environmental policies and regulations. Environmental Science Europe, 30, 5.

Dutta, K., Lee, M.-Y., Lai, W.W.-P., Lee, C.H., Lin, A.Y.-C., Lin, C.-F., Lin, J.-G., 2014. Removal of pharmaceuticals and organic matter from municipal wastewater using two-stage anaerobic fluidized membrane bioreactor. Bioresource Technology, 165, 42-49.

Dvořák, T., Száková, J., Vondráčková, S., Košnář, Z., Holečková, Z., Najmanová, J., Tlustoš, P., 2017. Content of inorganic and organic pollutants and their mobility in bottom sediment from the orlík water reservoir (vltava river, czech republic). Soil and Sediment Contamination: An International Journal, 26, 584-604.

Eaton, A.D., Clesceri, L.S., Rice, E.W., Greenberg, A.E., Franson, M.A.H., 2005. Standard methods for the examination of water and wastewater, Washangton, DC, American Public Health Association, American Water Works Association, and Water Environment Federation.

Edjere, O., Asibor, I.G., Otolo, S.E., 2016. Evaluation of the levels of phthalate ester plasticizers in surface water of ethiope river system, delta state, nigeria. Journal of Applied Sciences and Environmental Management, 20, 608.

EFSA, 2005. Opinion of the scientific panel on dietetic products, nutrition and allergies on a request from the commission related to an application concerning the use of betaine as a novel food in the EU. The EFSA Journal, 191, 1-17.

Eisler, R. 1987. Polycyclic aromatic hydrocarbon hazards to fish, wildlife, and invertebrates: A synoptic review.

Elersek, T., Zenko, M.,Filipic, M., 2018. Ecotoxicity of disinfectant benzalkonium chloride and its mixture with antineoplastic drug 5-fluorouracil towards alga pseudokirchneriella subcapitata. PeerJ, 6, e4986.

Enitan, A.M., Adeyemo, J., Kumari, S., Swalaha, F.M.,Bux, F., 2015. Characterization of brewery wastewater composition. International Journal of Environmental and Ecological Engineering, 9, 1073-1076.

EPA 2007. Method 1694: Pharmaceuticals and personal care products in water, soil, sediment, and biosolids by HPLC/MS/MS. Washington, USA: U.S. Environmental Protection Agency.

Eqani, S.A., Cincinelli, A., Mehmood, A., Malik, R.N., Zhang, G., 2015. Occurrence, bioaccumulation and risk assessment of dioxin-like pcbs along the chenab river, pakistan. Environmental Pollution, 206, 688-95.

Ertani, A., Mietto, A., Borin, M., Nardi, S., 2017. Chromium in agricultural soils and crops: A review. Water, Air, & Soil Pollution, 228.

Esminger, M.P., Budd, R., Kelley, K.C., Goh, K.S., 2013. Pesticide occurrence and aquatic benchmark exceedances in urban surface waters and sediments in three urban areas of california, USA, 2008–2011. Environmental Monitoring and Assessment, 185, 3697–3710.

EU 2003. Integrated pollution prevention and control: Reference document on best available techniques for the textiles industry. EU, BREF.

European Commission, 2000. Directive 2000/60/EC of the european parliament and of the council of 23 october 2000 establishing a framework for community action in the field of water policy. official Journal of the European Union.

European Commission, 2008. European union, environmental quality standards in the field of water policy, 2008/105/EC. official Journal of the European Union.

European Commission 2009. Common implementation strategy for the water framework directive (2000/60/EC). Luxembourg: Office for Official Publications of the European Communities.

European Commission, 2015. Decision 495/2015/EU of 20 march 2015 establishing a watch list of substances for union-wide monitoring in the field of water policy pursuant to directive 2008/105/EC of the european parliament and of the council, off. official Journal of the European Union.

Eurpean Commission, 2013. Directive 2013/39/EU of the european parliament and of the council of 12august 2013 amending directives 2000/60/EC and 2008/105/EC as regardspriority substances in the field of water policy. official Journal of the European Union, 226, 1-17.

Fadiran, A.O., Dlamini, S.C., Mavuso, A., 2008. A comparative study of the phosphate levels in some surface and ground water bodies of swaziland. Bulletin of the Chemical Society of Ethiopia, 22, 197-206.

Fairbairn, D.J., Arnold, W.A., Barber, B.L., Kaufenberg, E.F., Koskinen, W.C., Novak, P.J., Rice, P.J., Swackhamer, D.L., 2016. Contaminants of emerging concern: Mass balance and comparison of

wastewater effluent and upstream sources in a mixed-use watershed. Environmental Science and Technology, 50, 36-45.

Falås, P., Wick, A., Castronovo, S., Habermacher, J., Ternes, T.A., Joss, A., 2016. Tracing the limits of organic micropollutant removal in biological wastewater treatment. Water Research, 95, 240-249.

Fatoki, O.S., Bornman, M., Ravandhalala, L., Chimuka, L., Genthe, B., Adeniyi, A., 2010. Phthalate ester plasticizers in freshwater systems of venda, south africa and potential health effects. Water SA, 36, 117-126.

Fent, K., Zenker, A., Rapp, M., 2010. Widespread occurrence of estrogenic UV-filters in aquatic ecosystems in switzerland. Environmental Pollution, 158, 1817-24.

Fernandez, M.B., Sicre, M.A., Boireau, A., Tronczynski, J., 1997. Polyaromatic hydrocarbon (pah) distributions in the seine river and its estuary. Marine Pollution Bulletin, 34, 857-867.

Ferrer, I., Furlong, E.T., 2001. Identification of alkyl dimethylbenzylammonium surfactants in water samples by solid-phase extraction followed by ion trap LC/MS and LC/MS/MS. Environmental Science and Technology, 35, 2583-2588.

Ferrer, I.,Thurman, E.M., 2012. Analysis of 100 pharmaceuticals and their degradates in water samples by liquid chromatography/quadrupole time-of-flight mass spectrometry. J Chromatogr A, 1259, 148-57.

Finizio, A., Azimonti, G., Villa, S., 2011. Occurrence of pesticides in surface water bodies: A critical analysis of the italian national pesticide survey programs. Journal of Environmental Monitoring, 13, 49-57.

Fram, M.S., Belitz, K., 2011. Occurrence and concentrations of pharmaceutical compounds in groundwater used for public drinking-water supply in california. Science of the Total Environment, 409, 3409-17.

Freixa, A., Rubol, S., Carles-Brangari, A., Fernandez-Garcia, D., Butturini, A., Sanchez-Vila, X., Romani, A.M., 2016. The effects of sediment depth and oxygen concentration on the use of organic

matter: An experimental study using an infiltration sediment tank. Science of the Total Environment, 540, 20-31.

Fries, E., Püttmann, W., 2003. Monitoring of the three organophosphate esters TBP, TCEP and TBEP in river water and ground water (Oder, Germany). Journal of Environmental Monitoring, 5, 346-352.

Furstenberger, C., Vuorinen, A., Da Cunha, T., Kratschmar, D.V., Saugy, M., Schuster, D., Odermatt, A., 2012. The anabolic androgenic steroid fluoxymesterone inhibits 11beta-hydroxysteroid dehydrogenase 2-dependent glucocorticoid inactivation. Toxicological Sciences, 126, 353-61.

Gabet-Giraud, V., Miege, C., Jacquet, R., Coquery, M., 2014. Impact of wastewater treatment plants on receiving surface waters and a tentative risk evaluation: The case of estrogens and beta blockers. Environmental Science and Pollution Research International, 21, 1708-1722.

Gakuba, E., Moodley, B., Ndungu, P., Birungi, G., 2015. Occurrence and significance of polychlorinated biphenyls in water, sediment pore water and surface sediments of umgeni river, kwazulu-natal, south africa. Environmental Monitoring and Assessment, 187, 568.

Galinaro, C.A., Pereira, F.M.,Vieira, E.M., 2015. Determination of parabens in surface water from mogi guaçu river (são paulo, brazil) using dispersive liquid-liquid microextraction based on low density solvent and LC-DAD. Journal of the Brazilian Chemical Society.

Gangadharan Puthiya Veetil, P., Vijaya Nadaraja, A., Bhasi, A., Khan, S., Bhaskaran, K., 2012. Degradation of triclosan under aerobic, anoxic, and anaerobic conditions. Applied Biochemistry and Biotechnology, 167, 1603-12.

Genthner, B.R.S., Townsend, G.T., Lantz, S.E., Mueller, J.G., 1997. Persistence of polycyclic aromatic hydrocarbon components of creosote under anaerobic enrichment conditions. Archives of Environmental Contamination and Toxicology, 32, 99-105.

Geurts, J.J., Sarneel, J.M., Willers, B.J., Roelofs, J.G., Verhoeven, J.T., Lamers, L.P., 2009. Interacting effects of sulphate pollution, sulphide toxicity and eutrophication on vegetation development in fens: A mesocosm experiment. Environmental Pollution, 157, 2072-81.

Ghattas, A.-K., Fischer, F., Wick, A., Ternes, T.A., 2017. Anaerobic biodegradation of (emerging) organic contaminants in the aquatic environment. Water Research, 116, 268-295.

Gholizadeh, M.H., Melesse, A.M., Reddi, L., 2016. A comprehensive review on water quality parameters estimation using remote sensing techniques. Sensors (Basel), 16.

Giebultowicz, J., Tyski, S., Wolinowska, R., Grzybowska, W., Zareba, T., Drobniewska, A., Wroczynski, P., Nalecz-Jawecki, G., 2018. Occurrence of antimicrobial agents, drug-resistant bacteria, and genes in the sewage-impacted Vistula River (Poland). Environmental Science and Pollution Research International, 25, 5788-5807.

Gieg, L.M., Davidova, I.A., Duncan, K.E., Suflita, J.M., 2010. Methanogenesis, sulfate reduction and crude oil biodegradation in hot Alaskan oilfields. Environmental Microbiology, 12, 3074-3086.

Giger, W., 2009. Hydrophilic and amphiphilic water pollutants: Using advanced analytical methods for classic and emerging contaminants. Analytical and Bioanalytical Chemistry, 393, 37-44.

Giger, W., Schaffner, C., Kohler, H.P.E., 2006. Benzotriazole and tolyltriazole as aquatic contaminants. 1. Input and occurrence in rivers and lakes. Environmental Science and Technology, 40, 7186-7192.

Gioia, R., Dachs, J., Nizzetto, L., Berrojalbiz, N., Galban, C., Del Vento, S., Mejanelle, L., Jones, K.C., 2011. Sources, transport and fate of organic pollutants in the oceanic environment. In*:* Quante, M. (ed.) Persistent pollution – past, present and future. Springer.

Glinski, D.A., Purucker, S.T., Van Meter, R.J., Black, M.C., Henderson, W.M., 2018. Analysis of pesticides in surfacewater, stemflow, and throughfall in an agricultural area in south georgia, USA. Chemosphere, 209, 496-507.

Gogoi, A., Mazumder, P., Tyagi, V.K., Tushara Chaminda, G.G., An, A.K., Kumar, M., 2018. Occurrence and fate of emerging contaminants in water environment: A review. Groundwater for Sustainable Development, 6, 169-180.

Goktas, R.K.,MacLeod, M., 2018. Hazardous pollutants in the environment. In*:* Cecen, F. & Tezel, U. (eds.) Hazardous pollutants in biological treatment systems. London, UK: IWA publishing.

Gonzalez-Alonso, S., Merino, L.M., Esteban, S., Lopez de Alda, M., Barcelo, D., Duran, J.J., Lopez-Martinez, J., Acena, J., Perez, S., Mastroianni, N., Silva, A., Catala, M., Valcarcel, Y., 2017. Occurrence of pharmaceutical, recreational and psychotropic drug residues in surface water on the Northern Antarctic Peninsula region. Environmental Pollution, 229, 241-254.

Gonzalez-Rey, M., Tapie, N., Le Menach, K., Devier, M.H., Budzinski, H., Bebianno, M.J., 2015. Occurrence of pharmaceutical compounds and pesticides in aquatic systems. Marine Pollution Bulletin, 96, 384-400.

Gosetti, F., Chiuminatto, U., Zampieri, D., Mazzucco, E., Marengo, E., Gennaro, M.C., 2010. A new on-line solid phase extraction high performance liquid chromatography tandem mass spectrometry method to study the sun light photodegradation of mono-chloroanilines in river water. Journal of Chromatography A, 1217, 3427-34.

Gumbi, B.P., Moodley, B., Birungi, G.,Ndungu, P.G., 2017. Detection and quantification of acidic drug residues in south african surface water using gas chromatography-mass spectrometry. Chemosphere, 168, 1042-1050.

Gupta, H., 2018. Pah determination in effluent and sludge samples of paper industry. Environmental Technology and Innovation, 9, 115-121.

Gurbuz, F., Uzunmehmetoglu, O.Y., Diler, O., Metcalf, J.S., Codd, G.A., 2016. Occurrence of microcystins in water, bloom, sediment and fish from a public water supply. Science of the Total Environment, 562, 860-868.

Haag, A.M., 2016. Mass analyzers and mass spectrometers. Adv Exp Med Biol, 919, 157-169.

Häggblom, M.M.,Young, L.Y., 1990. Chlorophenol degradation coupled to sulfate reduction. Applied and Environmental Microbiology, 56, 3255-3260.

Halder, J., Islam, N., 2015. Water pollution and its impact on the human health. Journal of Environment and Human, 2, 36-46.

Han, X., Zhou, T.X., Xu, S.W., Li, Y., Wang, Y.F., Liu, Y., 2017. Removal of Cr (VI) and phenol coupled with the reduction of sulfate by sulfate-reducing bacteria sludge. International Journal of Environmental Science and Technology, 1-8.

Han, Z., Wang, Q., Fu, J., Chen, H., Zhao, Y., Zhou, B., Gong, Z., Wei, S., Li, J., Liu, H., Zhang, X., Liu, C., Yu, H., 2014. Multiple bio-analytical methods to reveal possible molecular mechanisms of developmental toxicity in zebrafish embryos/larvae exposed to tris(2-butoxyethyl) phosphate. Aquatic Toxicology, 150, 175-81.

Hanif, N.M., Adnan, S.N.N., Latif, M.T., Zakaria, Z., Abudallah, M.P., Othman, M.R., 2012. The composition of surfactants in river water and its influence to the amount of surfactants in drinking water. World Applied Sciences Journal, 17, 970-975.

Harman, C., Grung, M., Djedjibegovic, J., Marjanovic, A., Sober, M., Sinanovic, K., Fjeld, E., Rognerud, S., Ranneklev, S.B.,Larssen, T., 2013. Screening for stockholm convention persistent organic pollutants in the Bosna river (Bosnia and Herzogovina). Environmental Monitoring and Assessment, 185, 1671-83.

Harms, G., Zengler, K., Rabus, R., Aeckersberg, F., Minz, D., Rosselló-Mora, R., Widdel, F., 1999. Anaerobic oxidation of o-xylene, m-xylene, and homologous alkylbenzenes by new types of sulfate-reducing bacteria. Applied and Environmental Microbiology, 65, 999-1004.

Hasenmueller, E.A., Criss, R.E., 2013. Multiple sources of boron in urban surface waters and groundwaters. Science of the Total Environment, 447, 235-47.

Hassani, G., Babaei, A.A., Takdastan, A., Shairmardi, M., Yousefian, F., Mohammadi, M.J., 2016. Occurrence and fate of 17β-estradiol in water resources and wastewater in Ahvaz, Iran. Global NEST Journal, 18, 855-866.

Heimann, A., Jakobsen, R., Blodau, C., 2010. Energetic constraints on H_2-dependent terminal electron accepting processes in anoxic environments: A review of observations and model approaches. Environmental Science and Technology, 44, 24-33.

Hepsağ Güneş, E., 2009. Havzalar için zehirlilik parametresi İle deşarj etki İndeksi geliştirilmesi.

Herrero-Hernández, E., Andrades, M.S., Álvarez-Martín, A., Pose-Juan, E., Rodríguez-Cruz, M.S., Sánchez-Martín, M.J., 2013. Occurrence of pesticides and some of their degradation products in waters in a spanish wine region. Journal of Hydrology, 486, 234-245.

Herzog, B., Lemmer, H., Huber, B., Horn, H., Muller, E., 2014. Xenobiotic benzotriazoles biodegradation under meso- and oligotrophic conditions as well as denitrifying, sulfate-reducing, and anaerobic conditions. Environmental Science and Pollution Research International, 21, 2795-804.

Hoa, T.T.H., Liamleam, W., Annachhatre, A.P., 2007. Lead removal through biological sulfate reduction process. Bioresource Technology, 98, 2538-2548.

Hoh, E., Zhu, L., Hites, R.A., 2006. Dechlorane plus, a chlorinated flame retardant, in the great lakes. Environmental Science and Technology, 40, 1184-1189.

Holcapek, M., Jirasko, R.,Lisa, M., 2012. Recent developments in liquid chromatography-mass spectrometry and related techniques. J Chromatogr A, 1259, 3-15.

Holliger, C., Zehnder, A.J.B., 1996. Anaerobic biodegradation of hydrocarbons. Current Opinion in Biotechnology, 7, 326-330.

Holvoet, K.M.A., Seuntjens, P., Vanrolleghem, P.A., 2007. Monitoring and modeling pesticide fate in surface waters at the catchment scale. Ecological Modeling, 209, 53-64.

Huang, D.-Y., Zhou, S.-G., Chen, Q., Zhao, B., Yuan, Y., Zhuang, L., 2011. Enhanced anaerobic degradation of organic pollutants in a soil microbial fuel cell. Chemical Engineering Journal, 172, 647-653.

Hussain, A., Hasan, A., Javid, A., Qazi, J.I., 2016. Exploited application of sulfate-reducing bacteria for concomitant treatment of metallic and non-metallic wastes: A mini review. 3 Biotech, 6, 1-10.

Hussain, J., Hussain, I., Arif, M., 2004. Characterization of textile wastewater. Journal of Industrial Pollution Control, 20, 137-144.

Hwang, H.M., Hodson, R.E., Lee, R.F., 1987. Degradation of aniline and chloroaniline by sunlight and microbes in estuarine water. Water Research, 21, 309-316.

Ibanez, M., Pico, Y.,Mans, J., 1996. On-line liquid chromatographic trace enrichment and high-performance liquid chromatographic determination of diquat, paraquat and difenzoquat in water. Journal of Chromatography A, 728, 325-331.

Iklim Su 2016. İklim değişikliğinin su kaynaklarına etkisi projesi. T. C. Orman ve Su İşleri Bakanlığı Su Yönetimi Genel Müdürlüğü.

Inyinbor Adejumoke, A., Adebesin Babatunde, O., Oluyori Abimbola, P., Adelani-Akande Tabitha, A., Dada Adewumi, O., Oreofe Toyin, A., 2018. Water pollution: Effects, prevention, and climatic impact.

Irvine, K.N., McCorkhill, G., Caruso, J., 2005. Continuous monitoring of conventional parameters to assess receiving water quality in support of combined sewer overflow abatement plans. Water Environment Research, 77, 543-552.

Ivankovic, T., Hrenovic, J., 2010. Surfactants in the environment. Archives of Industrial Hygiene and Toxicology, 61, 95-110.

Jaffe, R., 1991. Fate of hydrophobic organic pollutants in the aquatic environment: A review. Environmental Pollution, 69, 237-257.

Jahin, H.S., Barsoum, B.N., Tawfic, T.A., Headley, J.V., 2009. Occurrence and distribution of polycyclic aromatic hydrocarbons in the egyptian aquatic environment. Journal of Environmental Science and Health, Part A: Toxic/ Hazardous Substances Environmental Engineering, 44, 1237-43.

Jalova, V., Jarosova, B., Blaha, L., Giesy, J.P., Ocelka, T., Grabic, R., Jurcikova, J., Vrana, B., Hilscherova, K., 2013. Estrogen-, androgen- and aryl hydrocarbon receptor mediated activities in passive and composite samples from municipal waste and surface waters. Environment International, 59, 372-83.

James, C.A., Brandenberger, J.A., Dutch, M., Hardy, J., Lester, D., Norton, D., O'Neill, S.M., Redman, S., Schultz, I.R., Sulliven, C., West, J.W. 2015. Contaminants of emerging concern: A prioritization framework for monitoring in Puget Sound. Puget Sound Ecosystem Monitoring Program.

Jelic, A., Rodriguez-Mozaz, S., Barceló, D., Gutierrez, O., 2015. Impact of in-sewer transformation on 43 pharmaceuticals in a pressurized sewer under anaerobic conditions. Water Research, 68, 98-108.

Jia, H., Sun, Y., Liu, X., Yang, M., Wang, D., Qi, H., Shen, L., Sverko, E., Reiner, E.J., Li, Y.F., 2011. Concentration and bioaccumulation of dechlorane compounds in coastal environment of northern china. Environmental Science and Technology, 45, 2613-8.

Jia, Y., Khanal, S.K., Zhang, H., Chen, G.-H., Lu, H., 2017. Sulfamethoxazole degradation in anaerobic sulfate-reducing bacteria sludge system. Water Research, 119, 12-20.

Jiang, W., Fan, W., 2008. Bioremediation of heavy metal–contaminated soils by sulfate-reducing bacteria. Annals of the New York Academy of Sciences, 1140, 446-454.

Jin, Y., Chen, G., Fu, Z., 2016. Effects of tbep on the induction of oxidative stress and endocrine disruption in tm3 leydig cells. Environmental Toxicology, 31, 1276-86.

Jing, R., Fusi, S., Kjellerup, B.V., 2018. Remediation of polychlorinated biphenyls (PCBs) in contaminated soils and sediment: State of knowledge and perspectives. Frontiers in Environmental Science, 6.

Jong, T., Parry, D.L., 2003. Removal of sulfate and heavy metals by sulfate reducing bacteria in short-term bench scale upflow anaerobic packed bed reactor runs. Water Research, 37, 3379-3389.

Jurado-Sanchez, B., Ballesteros, E., Gallego, M., 2012. Occurrence of aromatic amines and n-nitrosamines in the different steps of a drinking water treatment plant. Water Research, 46, 4543-55.

Jurado, A., Gago-Ferrero, P., Vàzquez-Suñé, E., Carrera, J., Pujades, E., Díaz-Cruz, M.S., Barceló, D., 2014. Urban groundwater contamination by residues of UV filters. Journal of Hazardous Materials, 271, 141-149.

Kafilzadeh, F., 2015. Distribution and sources of polycyclic aromatic hydrocarbons in water and sediments of the Soltan Abad river, Iran. The Egyptian Journal of Aquatic Research, 41, 227-231.

Kamal, A.K.I., Ahmed, F., Hassan, M., Uddin, M.K., Hossain, S.M., 2016. Characterization of textile effluents from dhaka export processing zone (depz) area in Dhaka, Bangladesh. Pollution, 2, 153-161.

Kamarudzaman, A.N., Feng, V.K., Aziz, R.A., Ab Jalil, M.F. 2011. Study of point and non point sources pollution – a case study of timah tasoh lake in perlis, malaysia. International Conference on Environmental and Computer Science. Singapore: IACSIT Press.

Karpuzcu, M., Delipinar, S., 2011. Integrated watershed management: Socio-economic prespective. The Online Journal of Science and Technology, 1, 1-7.

Karpuzcu, M.E., Fairbairn, D., Arnold, W.A., Barber, B.L., Kaufenberg, E., Koskinen, W.C., Novak, P.J., Rice, P.J., Swackhamer, D.L., 2014. Identifying sources of emerging organic contaminants in a mixed use watershed using principal components analysis. Environmental Sciences: Processes and Impacts, 16, 2390-2399.

Kasprzyk-Hordern, B., Dinsdale, R.M., Guwy, A.J., 2008. The occurrence of pharmaceuticals, personal care products, endocrine disruptors and illicit drugs in surface water in south wales, UK. Water Research, 42, 3498-518.

Katsoyiannis, A., 2006. Occurrence of polychlorinated biphenyls (PCBs) in the soulou stream in the power generation area of eordea, Northwestern Greece. Chemosphere, 65, 1551-61.

Keane, P.E., Simiand, J., Morre, M., Biziere, K., 1988. Tetrazepam: A benzodiazepine which dissociates sedation from other benzodiazepine activities. I. Psychopharmacological profile in rodents. Journal of Pharmacology and Experimental Therapeutics, 245, 692-698.

Khatri, N., Tyagi, S., 2014. Influences of natural and anthropogenic factors on surface and groundwater quality in rural and urban areas. Frontiers in Life Science, 8, 23-39.

Kibbey, T.C.G., Paruchury, R., Sabatini, D.A., Chen, L., 2007. Adsorption of beta blockers to environmental surfaces. Environmental Science and Technology, 41, 5349-5356.

Kim, M.-K., Zoh, K.-D., 2016. Occurrence and removals of micropollutants in water environment. Environmental Engineering Research, 21, 319-332.

Kim, U.J., Kannan, K., 2018. Occurrence and distribution of organophosphate flame retardants/plasticizers in surface waters, tap water, and rainwater: Implications for human exposure. Environmental Science and Technology, 52, 5625-5633.

Kiran, M.G., Pakshirajan, K., Das, G., 2017. Heavy metal removal from multicomponent system by sulfate reducing bacteria: Mechanism and cell surface characterization. Journal of Hazardous Materials, 324, 62-70.

Kiss, A., Fries, E., 2009. Occurrence of benzotriazoles in the rivers main, Hengstbach, and Hegbach (Germany). Environmental Sciencea and Pollution Research International, 16, 702-10.

Klein, W. 1999. Revised proposal for a list of priority substances in the context of the water frame directive (commps procedure). Fraunhofer-Institut Umweltchemie und Ökotoxikologie, Schmallenberg, Germany.

Kloepfer, A., Jekel, M., Reemtsma, T., 2005. Occurrence, sources, and fate of benzothiazoles in municipal wastewater treatment plants. Environmental Science and Technology, 39, 3792-3798.

Kocaman, I., Konukcu, F., Isanbulluoglu, A., Albut, S., 2015. Effect of irrigation with Maritza and Ergene rivers water on soil contamination and heavy metal accumulation in rice crop. Bulgarian Journal of Agricultural Science, 21, 71-77.

Komori, K., Suzuki, Y., Minamiyama, M., Harada, A., 2013. Occurrence of selected pharmaceuticals in river water in Japan and assessment of their environmental risk. Environmental Monitoring and Assessment, 185, 4529-36.

Kovacevic, S., Miloradov, M.V., Spanik, I., Dimkic, M., Dogo, M., Popovic, M., 2013. Screening analysis of selected plasticizers as emerging substances in the surface waters. International Journal of Engineering, 247-250.

Krauss, M., Hug, C., Bloch, R., Schulze, T., Brack, W., 2019. Prioritising site-specific micropollutants in surface water from lc-hrms non-target screening data using a rarity score. Environmental Sciences Europe, 31.

Krumholz, L.R., Elias, D.A., Suflita, J.M., 2003. Immobilization of cobalt by sulfate-reducing bacteria in subsurface sediments. Geomicrobiology Journal, 20, 61-72.

Kumar, A., Xagoraraki, I., 2010. Pharmaceuticals, personal care products and endocrine-disrupting chemicals in U.S. Surface and finished drinking waters: A proposed ranking system. Science of the Total Environment, 408, 5972-89.

Kumar, M., Wu, P.C., Tsai, J.C., Lin, J.G., 2009. Biodegradation of soil-applied polycyclic aromatic hydrocarbons by sulfate-reducing bacterial consortium. Journal of Environmental Science and Health, Part A, 44, 12-20.

Lebrato, J., Perez-Rodriguez, J.L., Maqueda, C., Morillo, E., 1990. Cheese factory wastewater treatment by anaerobic semicontinuous digestion. Resources, Conservations and Recycling, 3, 193-199.

Lee, I.S., Kim, U.J., Oh, J.E., Choi, M., Hwang, D.W., 2014. Comprehensive monitoring of synthetic musk compounds from freshwater to coastal environments in korea: With consideration of ecological concerns and bioaccumulation. Science of the Total Environment, 470-471, 1502-8.

Lee, Y.M., Lee, J.E., Choe, W., Kim, T., Lee, J.Y., Kho, Y., Choi, K., Zoh, K.D., 2019. Distribution of phthalate esters in air, water, sediments, and fish in the Asan lake of Korea. Environment International, 126, 635-643.

Lehutso, R.F., Daso, A.P., Okonkwo, J.O., 2017. Occurrence and environmental levels of triclosan and triclocarban in selected wastewater treatment plants in Gauteng Province, South Africa. Emerging Contaminants, 3, 107-114.

Li, B., Hu, X., Liu, R., Zeng, P., Song, Y., 2015. Occurrence and distribution of phthalic acid esters and phenols in hun river watersheds. Environmental Earth Sciences, 73, 5095-5106.

Li, J., Li, F., Liu, Q., Suzuki, Y., 2014. Nitrate pollution and its transfer in surface water and groundwater in irrigated areas: A case study of the piedmont of South Taihang mountains, China. Environmental Science: Processes and Impacts, 16, 2764-73.

Li, X., Brownawell, B.J., 2010. Quaternary ammonium compounds in urban estuarine sediment environments - a class of contaminants in need of increased attention? Environmental Science and Technology, 44, 7561-7568.

Li, X., Luo, X., Mai, B., Liu, J., Chen, L., Lin, S., 2014. Occurrence of quaternary ammonium compounds (QACs) and their application as a tracer for sewage derived pollution in urban estuarine sediments. Environmental Pollution, 185, 127-33.

Li, X., Yin, P., Zhao, L., 2016. Phthalate esters in water and surface sediments of the Pearl river estuary: Distribution, ecological, and human health risks. Environmental Science and Pollution Research International, 23, 19341-9.

Lien, G.W., Chen, C.Y., Wu, C.F., 2007. Analysis of polycyclic aromatic hydrocarbons by liquid chromatography/tandem mass spectrometry using atmospheric pressure chemical ionization or electrospray ionization with tropylium post-column derivatization. Rapid Communication in Mass Spectrometry, 21, 3694-700.

Liu, W., Xue, J., Kannan, K., 2017a. Occurrence of and exposure to benzothiazoles and benzotriazoles from textiles and infant clothing. Science of the Total Environment, 592, 91-96.

Liu, X., Shi, J., Bo, T., Zhang, H., Wu, W., Chen, Q.,Zhan, X., 2014. Occurrence of phthalic acid esters in source waters: A nationwide survey in China during the period of 2009-2012. Environmental Pollution, 184, 262-70.

Liu, Y.S., Ying, G.G., Shareef, A., Kookana, R.S., 2011a. Biodegradation of three selected benzotriazoles under aerobic and anaerobic conditions. Water Research, 45, 5005-5014.

Liu, Y.-S., Ying, G.G., Shareef, A., Kookana, R.S., 2012. Biodegradation of the ultraviolet filter benzophenone-3 under different redox conditions. Environmental Toxicology and Chemistry, 31, 289-295.

Liu, Y.-S., Ying, G.-G., Shareef, A., Kookana, R.S., 2013a. Degradation of six selected ultraviolet filters in aquifer materials under various redox conditions. Groundwater Monitoring & Remediation, 33, 79-88.

Liu, Y., Chen, Z., Shen, J., 2013b. Occurrence and removal characteristics of phthalate esters from typical water sources in Northeast China. Journal of Analytical Methods in Chemistry, 2013, 419349.

Liu, Y.S., Ying, G.G., Shareef, A., Kookana, R.S., 2011b. Biodegradation of three selected benzotriazoles under aerobic and anaerobic conditions. Water Research, 45, 5005-14.

Liu, Y.S., Ying, G.G., Shareef, A., Kookana, R.S., 2013c. Biodegradation of three selected benzotriazoles in aquifer materials under aerobic and anaerobic conditions. Journal of Contaminant Hydrology, 151, 131-9.

Liu, Y.S., Ying, G.G., Shareef, A., Kookana, R.S., 2013d. Degradation of six selected ultraviolet filters in aquifer materials under various redox conditions. Groundwater Monitoring and Remediation, 33, 79-88.

Liu, Z., Li, L., Li, Z., Tian, X., 2017b. Removal of sulfate and heavy metals by sulfate reducing bacteria in an expanded granular sludge bed reactor. Environmental Technology, 1-31.

Livingstone, D.R., 1998. The fate of organic xenobiotics in aquatic ecosystems: Quantitative and qualitative differences in biotransformation by invertebrates and fish. Comparative Biochemistry and Physiology Part A, 120, 43-49.

Löffler, D., Römbke, J., Meller, M., Ternes, T.A., 2005. Environmental fate of pharmaceuticals in water/sediment systems. Environmental Science and Technology, 39, 5209-5218.

Lu, G., Liu, J., Zhang, F., Nkoom, M., Wu, D., 2018. Interactive effects of BDE-153 and its metabolite 2,4-DBP on biochemical status in crucian carp (*Carassius auratus*). Polish Journal of Environmental Studies, 27, 1155-1163.

Lu, J., Jin, Q., He, Y., Wu, J., Zhao, J., 2008. Biodegradation of nonylphenol polyethoxylates under sulfate-reducing conditions. Science of the Total Environment, 399, 121-127.

Lu, X.-Y., Li, B., Zhang, T., Fang, H.H.P., 2012. Enhanced anoxic bioremediation of PAHs-contaminated sediment. Bioresource technology, 104, 51-58.

Lung, S.C., Liu, C.H., 2015. Fast analysis of 29 polycyclic aromatic hydrocarbons (pahs) and nitro-pahs with ultra-high performance liquid chromatography-atmospheric pressure photoionization-tandem mass spectrometry. Scientific Reports, 5, 12992.

Luo, Y., Guo, W., Ngo, H.H., Nghiem, L.D., Hai, F.I., Zhang, J., Liang, S., Wang, X.C., 2014. A review on the occurrence of micropollutants in the aquatic environment and their fate and removal during wastewater treatment. Science of the Total Environment, 473, 619-641.

Lv, Y., Yuan, T., Hu, J., Wang, W., 2010. Seasonal occurrence and behavior of synthetic musks (SMs) during wastewater treatment process in Shanghai, China. Science of the Total Environment, 408, 4170-6.

Ma, L., Yates, S.R., Ashworth, D., 2016. Parent and conjugated estrogens and progestagens in surface water of the Santa ana river: Determination, occurrence, and risk assessment. Environmental Toxicology and Chemistry, 35, 2657-2664.

Ma, R., Wang, B., Yin, L., Zhang, Y., Deng, S., Huang, J., Wang, Y., Yu, G., 2017. Characterization of pharmaceutically active compounds in Beijing, China: Occurrence pattern, spatiotemporal distribution and its environmental implication. Journal of Hazardous Materials, 323, 147-155.

Mabey, W., Mill, T., 1978. Critical review of hydrolysis of organic compounds in water under environmental conditions. Journal of Physical and Chemical Reference Data, 7, 383-415.

Madigan, M.T., Martinko, J.M., Dunlap, P.V.,Clark, D.P., 2008. Brock biology of microorganisms 12th edn. International. Microbiology, 11, 65-73.

Malik, A., Verma, P., Singh, A.K., Singh, K.P., 2011. Distribution of polycyclic aromatic hydrocarbons in water and bed sediments of the Gomti River, India. Environmental Monitoring and Assessment, 172, 529-45.

Manoli, E., Samara, C., Konstantinou, I., Albanis, T., 2000. Polycyclic aromatic hydrocarbons in bulk precepitaion and surface waters of Northern Greece. Chemosphere, 41, 1845-1855.

Manzetti, S., 2013. Polycyclic aromatic hydrocarbons in the environment: Environmental fate and transformation. Polycyclic Aromatic Compounds, 33, 311-330.

Marietou, A., 2016. Nitrate reduction in sulfate-reducing bacteria. FEMS Microbiology Letters, 363.

Martinez-Carballo, E., Gonzalez-Barreiro, C., Sitka, A., Kreuzinger, N., Scharf, S.,vGans, O., 2007. Determination of selected quaternary ammonium compounds by liquid chromatography with mass spectrometry. Part II. Application to sediment and sludge samples in Austria. Environmental Pollution, 146, 543-7.

Masia, A., Campo, J., Navarro-Ortega, A., Barcelo, D., Pico, Y., 2015. Pesticide monitoring in the basin of Llobregat River (Catalonia, Spain) and comparison with historical data. Science of the Total Environment, 503-504, 58-68.

Mater, N., Geret, F., Castillo, L., Faucet-Marquis, V., Albasi, C., Pfohl-Leszkowicz, A., 2014. In vitro tests aiding ecological risk assessment of ciprofloxacin, tamoxifen and cyclophosphamide in range of concentrations released in hospital wastewater and surface water. Environment International, 63, 191-200.

McCauley, C.A., O'Sullivan, A.D., Milke, M.W., Weber, P.A., Trumm, D.A., 2009. Sulfate and metal removal in bioreactors treating acid mine drainage dominated with iron and aluminum. Water Research, 43, 961-970.

McMahon, P.B., Bruce, B.W., 1997. Distribution of terminal electron-accepting processes in an aquifer having multiple contaminant sources. Applied Geochemistry, 12, 507-516.

Megahed, A.M., Dahshan, H., Abd-El-Kader, M.A., Abd-Elall, A.M., Elbana, M.H., Nabawy, E., Mahmoud, H.A., 2015. Polychlorinated biphenyls water pollution along the river Nile, Egypt. ScientificWorld Journal, 2015, 389213.

Meggo, R.E., Schnoor, J.L., 2011. Abiotic and biotic factors affecting the fate of organic pollutants in soils and sediments. In*:* Xing, B., Sensei, N., Huang, P.M. (Eds.) Biophysico-chemical processes of anthropogenic organic compounds in environmental systems. John Wiley and Sons,.

Melo, M.J., Pina, F., 1992. Photochemistry of 2-(2-furyl)-benzimidazole (fuberidazole). The Zeitschrift für Naturforschung, 47.

Merel, S., Benzing, S., Gleiser, C., Di Napoli-Davis, G., Zwiener, C., 2018. Occurrence and overlooked sources of the biocide carbendazim in wastewater and surface water. Environmental Pollution, 239, 512-521.

Middleburg, J.J., Levin, L.A., 2009. Coastal hypoxia and sediment biogeochemistry. Biogeosciences, 6, 1273-1293.

Mohatt, J.L., Hu, L., Finneran, K.T., Strathmann, T.J., 2011. Microbially mediated abiotic transformation of the antimicrobial agent sulfamethoxazole under iron-reducing soil conditions. Environmental Science and Technology, 45, 4793-4801.

Morasch, B., Schink, B., Tebbe, C.C., Meckenstock, R.U., 2004. Degradation of o-xylene and m-xylene by a novel sulfate-reducer belonging to the genus *desulfotomaculum*. Archives of Microbiology, 181, 407-417.

Moreno-Gonzalez, R., Rodriguez-Mozaz, S., Gros, M., Perez-Canovas, E., Barcelo, D., Leon, V.M., 2014. Input of pharmaceuticals through coastal surface watercourses into a mediterranean lagoon (Mar Menor, Spain): Sources and seasonal variations. Science of the Total Environment, 490, 59-72.

Moukas, A.I., Thomaidis, N.S., Calokerinos, A.C., 2014. Determination of polychlorinated biphenyls by liquid chromatography-atmospheric pressure photoionization-mass spectrometry. Journal of Mass Spectrometry, 49, 1096-107.

Munoz, G., Labadie, P., Botta, F., Lestremau, F., Lopez, B., Geneste, E., Pardon, P., Dévier, M.-H., Budzinski, H., 2017. Occurrence survey and spatial distribution of perfluoroalkyl and polyfluoroalkyl surfactants in groundwater, surface water, and sediments from tropical environments. Science of the Total Environment, 607-608, 243-252.

Musolff, A., Leschik, S., Moder, M., Strauch, G., Reinstorf, F., Schirmer, M., 2009. Temporal and spatial patterns of micropollutants in urban receiving waters. Environmental Pollution, 157, 3069-77.

Nagy, A.S., Szabo, J.,Vass, I., 2013. Occurrence and distribution of polycyclic aromatic hydrocarbons in surface water of the Raba River, Hungary. Journal of Environmental Science and Health, Part A, Toxic/Hazardous Substances and Environmental Engineering, 48, 1190-200.

Net, S., Sempere, R., Delmont, A., Paluselli, A., Ouddane, B., 2015. Occurrence, fate, behavior and ecotoxicological state of phthalates in different environmental matrices. Environmental Science and Technology, 49, 4019-35.

Nicandar, I., Aberg, P., Ollmar, S., 2003. The use of different concentrations of betaine as a reducing irritation agent in soaps monitored visually and non-invasively. Skin Research and Technology, 9, 43-49.

Noecker, R., Miller, K.V., 2011. Benzalkonium chloride in glaucoma medications. The Ocular Surface, 9, 159-162.

NORMAN. 2016. Emerging substances [Online]. Available: https://www.norman-network.net/ [Accessed 3 March 2019].

Noukeu, N.A., Gouado, I., Priso, R.J., Ndongo, D., Taffouo, V.D., Dibong, S.D., Ekodeck, G.E., 2016. Characterization of effluent from food processing industries and stillage treatment trial with *Eichhornia crassipes* (Mart.) and *Panicum maximum* (Jacq.). Water Resources and Industry, 16, 1-18.

NuÑAl, S.N., Santander-De Leon, S.M.S., Hongyi, W.E.I., Regal, A.A., Yoshikawa, T., Okunishi, S., Maeda, H., 2017. Hydrocarbon degradation and bacterial community responses during remediation of sediment artificially contaminated with heavy oil. Biocontrol Science, 22, 187-203.

Okumura, T., Imamura, K., Nishikawa, Y., 1996. Determination of anilines in river water, sediment, and fish samples by gas chromatography–mass spectrometry. Journal of Chromatographic Science, 34, 190-198.

Olkowska, E., Ruman, M., Polkowska, Z., 2014. Occurrence of surface active agents in the environment. Journal of Analytical Methods in Chemistry, 2014, 769708.

Olujimi, O.O., Aroyeun, A.O., Akinhanmi, T.F., Arowolo, T.A., 2014. Occurrence and concentration of phthalate esters in river sediment around Covenant oxidation ponds, Covenant university, Ota, Ogun state. International Journal of Environment and Sustainability, 3, 1-7.

Olutona, G.O., Oyekunle, J.A.O., Ogunfowokan, A.O., Fatoki, O.S., 2017. Concentrations of polybrominated diphenyl ethers (PBDEs) in water from Asunle stream, Ile-ife, Nigeria. Toxics, 5.

Padhye, L.P., Sun, P., Huang, C.H., 2018. Quantification of hazardous pollutants in biological systems. In*:* Cecen, F. and Tezel, U. (eds.) Hazardous pollutants in biological treatment systems. London, UK: IWA Publishing.

Padrini, R., 1987. Column liquid chromatographic determination of prajmalium in plasma and urine by direct sample injection. Journal of Chromatography, 415, 183-187.

Paiga, P., Santos, L., Ramos, S., Jorge, S., Silva, J.G., Delerue-Matos, C., 2016. Presence of pharmaceuticals in the Lis river (Portugal): Sources, fate and seasonal variation. Science of the Total Environment, 573, 164-177.

Palma, P., Kock-Schulmeyer, M., Alvarenga, P., Ledo, L., Barbosa, I.R., Lopez de Alda, M., Barcelo, D., 2014. Risk assessment of pesticides detected in surface water of the Alqueva reservoir (Guadiana basin, Southern of Portugal). Science of the Total Environment, 488-489, 208-19.

Papadakis, E.N., Tsaboula, A., Kotopoulou, A., Kintzikoglou, K., Vryzas, Z., Papadopoulou-Mourkidou, E., 2015. Pesticides in the surface waters of lake Vistonis basin, Greece: Occurrence and environmental risk assessment. Science of the Total Environment, 536, 793-802.

Park, J.Y., Yoo, Y.J., 2009. Biological nitrate removal in industrial wastewater treatment: Which electron donor we can choose. Applied Microbiology and Biotechnology, 82, 415-29.

Perez-Guerrero, C., Suarez, J., Herrera, M.D., Marhuenda, E., 1997. Spasmolytic effects of tetrazepam on rat duodenum and guinea- pig ileum. Pharmacological Research, 35.

Petrovic, M., Fernandez-Alba, A.R., Borrull, F., Marce, R.M., Mazo, E.G., Barcelo, D., 2002. Occurrence and distribution of nonionic surfactants, their degradation products, and linear alkylbenzene sulfonates in coastal waters and sediments in Spain. Environmental Toxicology and Chemistry, 21, 37-46.

Planas, C., Caixach, J., Santos, F.J., Rivera, J., 1997. Occurrence of pesticides in spanish surface waters. Analysis by high resolution gas chromatography coupled to mass spectrometry. Chemosphere, 34, 2393-2406.

Purwono, Rezagama, A., Hibbaan, M., Budihardjo, M.A., 2017. Ammonia-nitrogen (nh3-n) and ammonium-nitrogen (nh4 +-n) equilibrium on the process of removing nitrogen by using tubular plastic media. Journal of Materials and Environmental Sciences, 8, 4915-4922.

Qian, J., Wei, L., Liu, R., Jiang, F., Hao, X., Chen, G.H., 2016. An exploratory study on the pathways of Cr (VI) reduction in sulfate-reducing up-flow anaerobic sludge bed (UASB) reactor. Scientific Reports, 6, 23694.

Raman, D.R., Williams, E.L., Layton, A.C., Burns, R.T., Easter, J.P., Daugherty, A.S., Mullen, M.D., Sayler, G.S., 2004. Estrogen content of dairy and swine wastes. Environmental Science and Technology, 38, 3567-3573.

Re, M., Blanco-Murcia, F.J., Gomez de Segura, I.A., 2011. Chemical restraint and anaesthetic effects of a tiletamine-zolazepam/ketamine/detomidine combination in cattle. The Veterinary Journal, 190, 66-70.

Reemtsma, T., Miehe, U., Duennbier, U., Jekel, M., 2010. Polar pollutants in municipal wastewater and the water cycle: Occurrence and removal of benzotriazoles. Water Research, 44, 596-604.

Regnery, J., Puttmann, W., 2010. Occurrence and fate of organophosphorus flame retardants and plasticizers in urban and remote surface waters in Germany. Water Research, 44, 4097-104.

Renz, L., Volz, C., Michanowicz, D., Ferrar, K., Christian, C., Lenzner, D., El-Hefnawy, T., 2013. A study of parabens and bisphenol a in surface water and fish brain tissue from the greater Pittsburgh area. Ecotoxicology, 22, 632-41.

Robles-Molina, J., Gilbert-Lopez, B., Garcia-Reyes, J.F., Molina-Diaz, A., 2014. Monitoring of selected priority and emerging contaminants in the Guadalquivir river and other related surface waters in the province of Jaen, South East Spain. Science of the Total Environment, 479-480, 247-57.

Rockne, K.J., Strand, S.E., 1998. Biodegradation of bicyclic and polycyclic aromatic hydrocarbons in anaerobic enrichments. Environmental Science and Technology, 32, 3962-3967.

Rothermich, M.M., Hayes, L.A., Lovley, D.R., 2002. Anaerobic, sulfate-dependent degradation of polycyclic aromatic hydrocarbons in petroleum-contaminated harbor sediment. Environmental Science and Technology, 36, 4811-4817.

Ruff, M., Mueller, M.S., Loos, M., Singer, H.P., 2015. Quantitative target and systematic non-target analysis of polar organic micro-pollutants along the river Rhine using high-resolution mass-spectrometry--identification of unknown sources and compounds. Water Research, 87, 145-54.

Ruggeri, G., Ghigo, G., Maurino, V., Minero, C., Vione, D., 2013. Photochemical transformation of ibuprofen into harmful 4-isobutylacetophenone: Pathways, kinetics, and significance for surface waters. Water Research, 47, 6109-21.

Rytwo, G., Tavasi, M., Afuta, S., Nir, S., 2004. Adsorption of difenzoquat on montmorillonite: Model calculations and increase in hydrophobicity. Applied Clay Science, 24, 149-157.

Safe, S.H., 1994. Polychlorinated biphenyls (PCBs) : Environmental impact, biochemical and toxic responses, and implications for risk assessment. Critical Reviews in Toxicology, 42, 87-149.

Sakai, H., Hao, A., Iseri, Y., Wang, S., Kuba, T., Zhang, Z., Katayama, H., 2013. Occurrence and distribution of microcystins in lake Taihu, China. ScientificWorld Journal, 2013, 838176.

Saleh, N.i., Ajeb, S.M., Sham, A., AbuQamar, S.F., 2013. Enhancement of in vitro fungicidal activity of fuberidazole to botrytis cinerea by cucurbiturils. Journal of Inclusion Phenomena and Macrocyclic Chemistry, 79, 301-309.

Salgueiro-González, N., López de Alda, M.J., Muniategui-Lorenzo, S., Prada-Rodríguez, D., Barceló, D., 2015. Analysis and occurrence of endocrine-disrupting chemicals in airborne particles. TrAC Trends in Analytical Chemistry, 66, 45-52.

Salman Afzal, M., 2018. Characterization of industrial effluents and groundwater of Hattar industrial estate, Haripur. Advances in Agriculture and Environmental Science: Open Access (AAEOA), 1.

Salonen, J.S., Vuorilehto, L., Eloranta, M., Karjalainen, A., 1988. Metabolism of detomidine in the rat ii. Characterisation of metabolites in urine. European Journal Of Drug Metabolism And Pharmacokinetics, 13, 59-65.

Salonen, J.S., Vuorilehto, L., Gilbert, M., Maylin, G.A., 1992. Identification of detomidine carboxylic acid as the major urinary metabolite of detomidine in the horse. European Lournal Of Drug Metabolism And Pharmacokinetics, 17, 13-20.

Sánchez-Avila, J., Bonet, J., Velasco, G., Lacorte, S., 2009. Determination and occurrence of phthalates, alkylphenols, bisphenol A, PBDEs, PCBs and PAHs in an industrial sewage grid discharging to a municipal wastewater treatment plant. Science of the Total Environment, 407, 4157-4167.

Sanchez-Bayo, F., Hyne, R.V., 2014. Detection and analysis of neonicotinoids in river waters--development of a passive sampler for three commonly used insecticides. Chemosphere, 99, 143-51.

Sarmah, A.K., Northcott, G.L., 2008. Laboratory degradation studies of four endocrine disruptors in two environmental media. Environmental Toxicology and Chemistry, 27, 819-827.

Sarria-Villa, R., Ocampo-Duque, W., Paez, M., Schuhmacher, M., 2016. Presence of PAHs in water and sediments of the colombian cauca river during heavy rain episodes, and implications for risk assessment. Science of the Total Environment, 540, 455-65.

Sawyer, C.N., 2003. Chemistry for environmental engineering and science, McGraw Hill.

Schanzer, W., Horning, S., Donike, M., 1995. Metabolism of anabolic steroids in humans: Synthesis of 6β-hydroxy metabolites of 4-chloro-l,2-dehydro- 17 alpha -methyltestosterone, fluoxymesterone, and metandienone. Steroids, 60, 353-366.

Schlabach, M., Haglund, P., Rostkowski, P., Dye, C. 2013. Non-target screening – a powerful tool for selecting environmental pollutants. NILU.

Schmidt, N., Page, D., Tiehm, A., 2017. Biodegradation of pharmaceuticals and endocrine disruptors with oxygen, nitrate, manganese (IV), iron (III) and sulfate as electron acceptors. Journal of Contaminant Hydrology, 203, 62-69.

Schneider, S.L., Lim, H.W., 2019. Review of environmental effects of oxybenzone and other sunscreen active ingredients. Journal of American Academy of Dermatology, 80, 266-271.

Schwarzbauer, J., Ricking, M., 2010. Non-target screening analysis of river water as compound-related base for monitoring measures. Environmental Science and Pollution Research International, 17, 934-47.

Schwarzenbach, R.P., Escher, B.I., Fenner, K., Hofstetter, T.B., Johnson, C.A., Von Gunten, U., Wehreli, B., 2006. The challenge of micropollutants in aquatic systems. Science, 313, 1072-1077.

Schwarzenbach, R.P., Gschwend, P.M., Imboden, D.M., 2003. Air-organic solvent and air-water partitioning. Environmental organic chemistry. 2nd ed.: John Wiley and Sons, Inc.

Scoglio, S., 2018. Microcystins in water and in microalgae: Do microcystins as microalgae contaminants warrant the current public alarm? Toxicology Reports, 5, 785-792.

Segev, O., Kushmaro, A., Brenner, A., 2009. Environmental impact of flame retardants (persistence and biodegradability). International Journal of Environmental Research and Public Health, 6, 478-91.

Serrano, J., Leiva, E., 2017. Removal of arsenic using acid/metal-tolerant sulfate reducing bacteria: A new approach for bioremediation of high-arsenic acid mine waters. Water, 9, 994.

Shang, L., Feng, M., Xu, X., Liu, F., Ke, F., Li, W., 2018. Co-occurrence of microcystins and taste-and-odor compounds in drinking water source and their removal in a full-scale drinking water treatment plant. Toxins (Basel), 10.

Shao, Y., Han, S., Ouyang, J., Yang, G., Liu, W., Ma, L., Luo, M., Xu, D., 2016. Organochlorine pesticides and polychlorinated biphenyls in surface water around Beijing. Environmental Science and Pollution Research, 23, 24824-24833.

Shete, B.S., Shinkar, N.P., 2013. Dairy industry wastewater sources, characteristics & its effects on environment. International Journal of Current Engineering and Technology, 3, 1611-1615.

Shi, Y., Gao, L., Li, W., Wang, Y., Liu, J., Cai, Y., 2016. Occurrence, distribution and seasonal variation of organophosphate flame retardants and plasticizers in urban surface water in Beijing, China. Environmental Pollution, 209, 1-10.

Shi, Z.Q., Liu, Y.S., Xiong, Q., Cai, W.W., Ying, G.G., 2019. Occurrence, toxicity and transformation of six typical benzotriazoles in the environment: A review. Science of the Total Environment, 661, 407-421.

Sitte, J., Akob, D.M., Kaufmann, C., Finster, K., Banerjee, D., Burkhardt, E.-M., Kostka, J.E., Scheinost, A.C., Büchel, G., Küsel, K., 2010. Microbial links between sulfate reduction and metal retention in uranium-and heavy metal-contaminated soil. Applied and Environmental Microbiology, 76, 3143-3152.

Skutlarek, D., Exner, M., Färber, H., 2006. Perfluorinated surfactants in surface and drinking waters (9 pp). Environmental Science and Pollution Research - International, 13, 299-307.

Slavov, A.K., 2017. General characteristics and treatment possibilities of dairy wastewater – a review. Food Technology and Biotechnology, 55, 14-28.

Smith, R., Harris, J.S., 2007. Determining the terminal electron-accepting reaction in the saturated subsurface. Manual of environmental microbiology. 3 ed.: ASM Press.

Somsamak, P., Cowan, R.M., Häggblom, M.M., 2001. Anaerobic biotransformation of fuel oxygenates under sulfate-reducing conditions. FEMS Microbiology Ecology, 37, 259-264.

Sosa-Ferrera, Z., Mahugo-Santana, C., Santana-Rodríguez, J.J., 2012. New developments in liquid chromatography mass spectrometry for the determination of micropollutants. Chromatography Research International, 2012, 1-18.

Sousa, J.C.G., Ribeiro, A.R., Barbosa, M.O., Pereira, M.F.R., Silva, A.M.T., 2018. A review on environmental monitoring of water organic pollutants identified by EU guidelines. Journal of Hazardous Materials, 344, 146-162.

Stamper, D.M., Tuovinen, O.H., 1998. Biodegradation of the acetanilide herbicides alachlor, metolachlor, and propachlor. Critical Reviews in Microbiology, 24, 1-22.

Starner, K., Kuivila, K.M., Jennings, B., Moon, G.E. Degradation rates of six pesticides in water from the Sacramento River, California. U.S. Gelogical Survey Toxic Substances Hydrology Program, March 8-12 1999 Xharleston, South Carolina.

Steed, V.S., Suidan, M.T., Gupta, M., Miyahara, T., Acheson, C.M., Sayles, G.D., 2000. Development of a sulfate-reducing biological process to remove heavy metals from acid mine drainage. Water Environment Research, 72, 530-535.

Stockholm Convention. 2008. Progress towards the 2028 target of the Stockholm Convention [Online].Switzerland.Available:http://chm.pops.int/Implementation/IndustrialPOPs/PCBs/Overview/tabid/273/Default.aspx.

Strempel, S., Scheringer, M., Ng, C.A., Hungerbuhler, K., 2012. Screening for pbt chemicals among the "existing" and "new" chemicals of the EU. Environmental Science and Technology, 46, 5680-7.

Strifling, D., 2018. Reducing chloride discharges to surface water and groundwater: A menu of options for policymakers. Environmental Law, 167-210.

Su, L., Li, K., Zhang, H., Fan, M., Ying, D., Sun, T., Wang, Y., Jia, J., 2017. Electrochemical nitrate reduction by using a novel Co_3O_4/Ti cathode. Water Research, 120, 1-11.

Sumner, N.R., Guitart, C., Fuentes, G., Readman, J.W., 2010. Inputs and distributions of synthetic musk fragrances in an estuarine and coastal environment; a case study. Environmental Pollution, 158, 215-22.

Sun, J., Quicksall, A.N., Chillrud, S.N., Mailloux, B.J., Bostick, B.C., 2016. Arsenic mobilization from sediments in microcosms under sulfate reduction. Chemosphere, 153, 254-261.

Tahri, N., Bahafid, W., Sayel, H., El Ghachtouli, N., 2013. Biodegradation: Involved microorganisms and genetically engineered microorganisms. 289-320.

Tchounwou, P.B., Yedjou, C.G., Patlolla, A.K.,Sutton, D.J., 2012. Heavy metal toxicity and the environment. NIH Public Access, 101, 133-64.

Tezel, U., Pavlostathis, S.G., 2015. Quaternary ammonium disinfectants: Microbial adaptation, degradation and ecology. Current Opinion in Biotechnology, 33, 296-304.

Thorsteinsson, T., Loftsson, T., Masson, M., 2003. Soft antibacterial agents. Current Medicinal Chemistry, 10, 1129-1136.

Tiwari, B., Sellamuthu, B., Ouarda, Y., Drogui, P., Tyagi, R.D., Buelna, G., 2017. Review on fate and mechanism of removal of pharmaceutical pollutants from wastewater using biological approach. Bioresouruce Technology, 224**,** 1-12.

Tongo, I., Ezemonye, L., Akpeh, K., 2017. Distribution, characterization, and human health risk assessment of polycyclic aromatic hydrocarbons (PAHs) in Ovia River, Southern Nigeria. Environmental Monitoring and Assessment, 189**,** 247.

Tousova, Z., Oswald, P., Slobodnik, J., Blaha, L., Muz, M., Hu, M., Brack, W., Krauss, M., Di Paolo, C., Tarcai, Z., Seiler, T.-B., Hollert, H., Koprivica, S., Ahel, M., Schollée, J.E., Hollender, J., Suter, M.J.F., Hidasi, A.O., Schirmer, K., Sonavane, M., Ait-Aissa, S., Creusot, N., Brion, F., Froment, J., Almeida, A.C., Thomas, K., Tollefsen, K.E., Tufi, S., Ouyang, X., Leonards, P., Lamoree, M., Torrens, V.O., Kolkman, A., Schriks, M., Spirhanzlova, P., Tindall, A., Schulze, T., 2017. European demonstration program on the effect-based and chemical identification and monitoring of organic pollutants in European surface waters. Science of the Total Environment, 601-602**,** 1849-1868.

Tran, N.H., Urase, T., Ta, T.T., 2014. A preliminary study on the occurrence of pharmaceutically active compounds in hospital wastewater and surface water in Hanoi, Vietnam. CLEAN - Soil, Air, Water, 42**,** 267-275.

Tröger, R., Klöckner, P., Ahrens, L., Wiberg, K., 2018. Micropollutants in drinking water from source to tap - method development and application of a multiresidue screening method. Science of the Total Environment, 627**,** 1404-1432.

Tsaboula, A., Papadakis, E.N., Vryzas, Z., Kotopoulou, A., Kintzikoglou, K., Papadopoulou-Mourkidou, E., 2016. Environmental and human risk hierarchy of pesticides: A prioritization method, based on monitoring, hazard assessment and environmental fate. Environment Interantional, 91**,** 78-93.

Tsai, J.C., Kumar, M., Lin, J.G., 2009. Anaerobic biotransformation of fluorene and phenanthrene by sulfate-reducing bacteria and identification of biotransformation pathway. Journal of Hazardous Materials, 164**,** 847-855.

Turkish Ministry of Enviornment and Forestry 2008a. Ergene havzası çevre yönetimi master planı. T. C. Çevre ve Orman Bakanlığı.

Turkish Ministry of Enviornment and Forestry 2008b. Meriç-ergene havzası koruma eylem planı. T. C. Çevre Ve Orman Bakanlığı Çevre Yön. Genel Müdürlüğü.

Turkish Ministry of Forestry and Water, 2012. Yerüstü su kalİtesİ yönetmelİğİnde değİşİklİk yapilmasina daİr yönetmelİk taslağı.

Van Leerdam, J.A., Hogenboom, A.C., Van der Kooi, M.M.E., De Voogt, P., 2009. Determination of polar 1H-benzotriazoles and benzothiazoles in water by solid-phase extraction and liquid chromatography ltq ft orbitrap mass spectrometry. International Journal of Mass Spectrometry, 282, 99-107.

Vanoosthuyze, K., Daeseleire, E., Van Overbeke, A., Van Peteghem, C., 1994. Survey of the hormones used in cattle fattening based on the analysis of belgian injection sites. Analyst, 119, 2655-2658.

Velicu, M., Suri, R., Fu, H., Andaluri, G., Chimchirian, R. 2007. Occurrence of estrogen hormones in environmental systems. World Environmental and Water Resources Congress. Tampa, Florida.

Venkatesan, A.K., Pycke, B.F., Barber, L.B., Lee, K.E., Halden, R.U., 2012. Occurrence of triclosan, triclocarban, and its lesser chlorinated congeners in Minnesota freshwater sediments collected near wastewater treatment plants. Journal of Hazardous Materials, 229-230, 29-35.

Vetrimurugan, E., Brindha, K., Elango, L., Ndwandwe, O.M., 2016. Human exposure risk to heavy metals through groundwater used for drinking in an intensively irrigated river delta. Applied Water Science, 7, 3267-3280.

Villa, S., Assi, L., Ippolito, A., Bonfanti, P., Finizio, A., 2012. First evidences of the occurrence of polycyclic synthetic musk fragrances in surface water systems in italy: Spatial and temporal trends in the molgora river (Lombardia region, Northern Italy). Science of the Total Environment, 416, 137-41.

Vincent, S.G.T., Reshmi, R.R., Hassan, S.J., Nair, K.D., Varma, A., 2017. Predominant terminal electron accepting processes during organic matter degradation: Spatio-temporal changes in Ashtamudi estuary, Kerala, India. Estuarine, Coastal and Shelf Science, 198, 508-517.

Volker, J., Vogt, T., Castronovo, S., Wick, A., Ternes, T.A., Joss, A., Oehlmann, J., Wagner, M., 2017. Extended anaerobic conditions in the biological wastewater treatment: Higher reduction of toxicity compared to target organic micropollutants. Water Research, 116, 220-230.

von der Ohe, P.C., Dulio, V., Slobodnik, J., De Deckere, E., Kuhne, R., Ebert, R.U., Ginebreda, A., De Cooman, W., Schuurmann, G., Brack, W., 2011. A new risk assessment approach for the prioritization of 500 classical and emerging organic microcontaminants as potential river basin specific pollutants under the European water framework directive. Science of the Total Environment, 409, 2064-77.

Vrzel, J., Vukovic-Gacic, B., Kolarevic, S., Gacic, Z., Kracun-Kolarevic, M., Kostic, J., Aborgiba, M., Farnleitner, A., Reischer, G., Linke, R., Paunovic, M., Ogrinc, N., 2016. Determination of the sources of nitrate and the microbiological sources of pollution in the Sava river basin. Science of the Total Environment, 573, 1460-1471.

Wang, G., Mang, S., Cai, H., Liu, S., Zhang, Z., Wang, L., Innes, J.L., 2016a. Integrated watershed management: Evolution, development and emerging trends. Journal of Forestry Research, 27, 967-994.

Wang, H., Chen, F., Mu, S., Zhang, D., Pan, X., Lee, D.J., Chang, J.-S., 2013. Removal of antimony (Sb (V)) from sb mine drainage: Biological sulfate reduction and sulfide oxidation–precipitation. Bioresource Technology, 146, 799-802.

Wang, L., Zhang, J., Sun, H., Zhou, Q., 2016b. Widespread occurrence of benzotriazoles and benzothiazoles in tap water: Influencing factors and contribution to human exposure. Environmental Science and Technology, 50, 2709-17.

Watkinson, A.J., Murby, E.J., Kolpin, D.W., Costanzo, S.D., 2009. The occurrence of antibiotics in an urban watershed: From wastewater to drinking water. Science of the Total Environment, 407, 2711-23.

Wijaya, S.C., 1993. Optimization of dissolved heavy metals removal using sulfate-reducing bacteria in the upflow anaerobic fixed film reactor.

Wilber, G.G., Parkin, G.F., 1995. Kinetics of alachlor and atrazine biotransformation under various electron acceptor conditions. Environmental Toxicology and Chemistry, 14, 237-244.

Wilkinson, J., Hooda, P.S., Barker, J., Barton, S., Swinden, J., 2017. Occurrence, fate and transformation of emerging contaminants in water: An overarching review of the field. Environmental Pollution, 231, 954-970.

Wu, Y., Sun, Q., Wang, Y.W., Deng, C.X.,Yu, C.P., 2017. Comparative studies of aerobic and anaerobic biodegradation of methylparaben and propylparaben in activated sludge. Ecotoxicology and Environmental Safety, 138, 25-31.

Wurl, O., Lam, P.K., Obbard, J.P., 2006. Occurrence and distribution of polybrominated diphenyl ethers (pbdes) in the dissolved and suspended phases of the sea-surface microlayer and seawater in Hong Kong, China. Chemosphere, 65, 1660-6.

Xia, X., Wang, R., 2008. Effect of sediment particle size on polycyclic aromatic hydrocarbon biodegradation: Importance of the sediment–water interface. Environmental Toxicology and Chemistry, 27, 119-125.

Yan, C., Yang, Y., Zhou, J., Liu, M., Nie, M., Shi, H., Gu, L., 2013. Antibiotics in the surface water of the Yangtze Estuary: Occurrence, distribution and risk assessment. Environmental Pollution, 175, 22-9.

Yang, G.C., Tsai, H.J., Chang, F.K., 2015. Occurrence of triclosan in the tropical rivers receiving the effluents from the hospital wastewater treatment plant. Environmental Monitoring and Assessment, 187, 151.

Yang, J.F., Ying, G.G., Yang, L.H., Zhao, J.L., Liu, F., Tao, R., Yu, Z.Q., Peng, P., 2009. Degradation behavior of sulfadiazine in soils under different conditions. Journal of Environmental Science and Health, Part B, 44, 241-8.

Yang, Y., Ok, Y.S., Kim, K.H., Kwon, E.E.,Tsang, Y.F., 2017. Occurrences and removal of pharmaceuticals and personal care products (PPCPs) in drinking water and water/sewage treatment plants: A review. Science of the Total Environment, 596-597, 303-320.

Yang, Y., Wang, Z., He, T., Dai, Y., Xie, S., 2015. Sediment bacterial communities associated with anaerobic biodegradation of bisphenol A. Microbial Ecology, 70, 97-104.

Yang, Z., Shen, Z., Gao, F., Tang, Z., Niu, J., 2009. Occurrence and possible sources of polychlorinated biphenyls in surface sediments from the Wuhan reach of the Yangtze River, China. Chemosphere, 74, 1522-30.

Yaseen, D.A., Scholz, M., 2018. Textile dye wastewater characteristics and constituents of synthetic effluents: A critical review. International Journal of Environmental Science and Technology, 16, 1193-1226.

Yuan, S.Y., Chang, B.V., 2007. Anaerobic degradation of five polycyclic aromatic hydrocarbons from river sediment in Taiwan. Journal of Environmental Science and Health Part B, 42, 63-69.

Zeng, F., Xu, P., Tan, K., Zarbin, P.H.G., Leal, W.S., 2018. Methyl dihydrojasmonate and lilial are the constituents with an "off-label" insect repellence in perfumes. Plos One, 13, e0199386.

Zhang, L., Lin, X., Wang, J., Jiang, F., Wei, L., Chen, G., Hao, X., 2016. Effects of lead and mercury on sulfate-reducing bacterial activity in a biological process for flue gas desulfurization wastewater treatment. Scientific Reports, 6.

Zhang, X., Li, Y., Liu, B., Wang, J., Feng, C., Gao, M., Wang, L., 2014. Prevalence of veterinary antibiotics and antibiotic-resistant *Escherichia coli* in the surface water of a livestock production region in Northern China. Plos One, 9, e111026.

Zhang, Z., Huang, J., Yu, G., Hong, H., 2004. Occurrence of pahs, pcbs and organochlorine pesticides in the tonghui river of Beijing, China. Environmental Pollution, 130, 249-61.

Zheng, W., Wang, X., Tian, D., Jiang, S., Andersen, M.E., He, G., Crabbe, M.J.C., Zheng, Y., Zhong, Y., Qu, W., 2013. Water pollutant fingerprinting tracks recent industrial transfer from coastal to inland China: A case study. Scientific Reports, 3, 1031.

Ziylan, A., Ince, N.H., 2011. The occurrence and fate of anti-inflammatory and analgesic pharmaceuticals in sewage and fresh water: Treatability by conventional and non-conventional processes. Journal of Hazardous Materials, 187, 24-36.

APPENDIX A

Table A.1. Properties of analytes in this study.

Chemical Name	CAS #	Molecular Formula	Molecular Structure	Solubility (mg/L)	LogP
1-HydroxyIbuprofen	53949-53-4	$C_{13}H_{18}O_3$	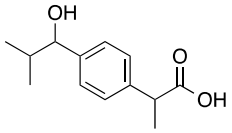	-	1.89
1,2,3-Benzotriazole	95-14-7	$C_6H_5N_3$	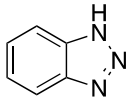	20000	1.34
1,2,5,6,9,10-Hexabromocyclododecane	3194-55-6	$C_{12}H_{18}Br_6$	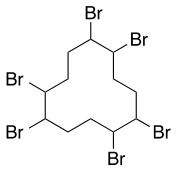	-	6.63
1,3-Dinitropyrene	75321-20-9	$C_{16}H_8N_2O_4$	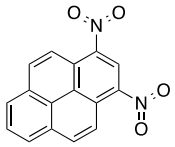	4.00	4.57
1,6-Dinitropyrene	42397-64-8	$C_{16}H_8N_2O_4$	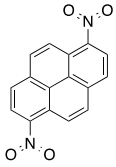	0.01	4.63
1,8-Dinitropyrene	42397-65-9	$C_{16}H_8N_2O_4$	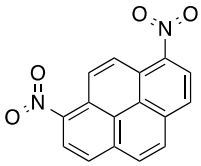	0.05	4.63
17-alpha-Estradiol	57-91-0	$C_{18}H_{24}O_2$	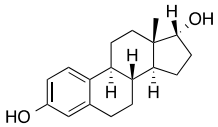	3.90	3.94
17-alpha-Ethinylestradiol	57-63-6	$C_{20}H_{24}O_2$	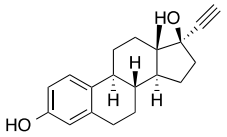	11.30	3.67
17-beta-Estradiol	50-28-2	$C_{18}H_{24}O_2$	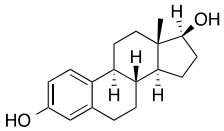	3.90	4.01
2-(2-Naphthalenyl) benzothiophene	17164-77-1	$C_{18}H_{12}S$	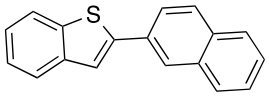	0.01	7.52
2-HydroxyIbuprofen	51146-55-5	$C_{13}H_{18}O_3$	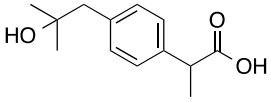	2974	2.29

Table A.1. Continued.

Chemical Name	CAS #	Molecular Formula	Molecular Structure	Solubility (mg/L)	LogP
2-Mercapto-benzothiazole	149-30-4	$C_7H_5NS_2$	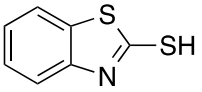	118	2.41
2-Methylanthraquinone	84-54-8	$C_{15}H_{10}O_2$	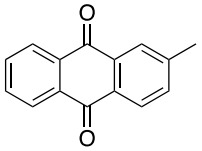	1.23	3.84
2,2',3,3',4,4',5,5',6-Nonabromodiphenyl ether	63936-56-1	$C_{12}HBr_9O$	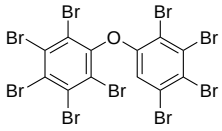	-	10.70
2,2',3,3',4,4',5,5',6,6'-Decabromodiphenyl ether	1163-19-5	$C_{12}Br_{10}O$	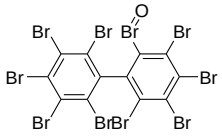	-	9.97
2,2',3,4,4',5,5',6- Octabromodiphenyl ether	337513-72-1	$C_{12}H_2Br_8O$	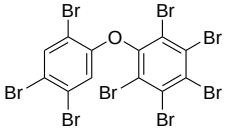	0.01	8.71
2,2',3,4,4',5',6- Heptabromodiphenyl ether	207122-16-5	$C_{12}H_3Br_7O$	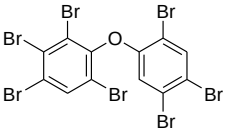	-	9.49
2,2',4,4'-Tetrabromodiphenyl ether	5436-43-1	$C_{12}H_6Br_4O$	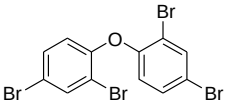	-	7.39
2,2',4,4',5,5'-Hexabromodiphenyl ether	68631-49-2	$C_{12}H_4Br_6O$	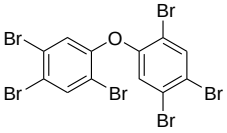	-	8.98
2,2',4,4',5,6'-Hexabromodiphenyl ether	207122-15-4	$C_{12}H_4Br_6O$	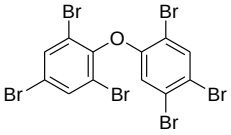	-	8.83
2,3,3',4,4',5,5',6-Octabromodiphenyl ether	446255-56-7	$C_{12}H_2Br_8O$	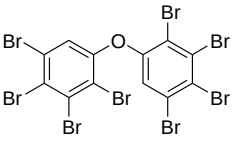	-	6.29
2,4-Dibromophenol	615-58-7	$C_6H_4Br_2O$	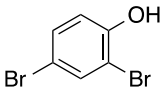	1900	3.43
2,4-Dihydroxybenzophenone	131-56-6	$C_{13}H_{10}O_3$	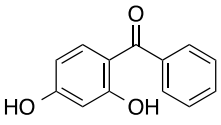	413.40	3.17
2,4-Dinitrophenol	51-28-5	$C_6H_4N_2O_5$	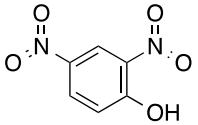	2790	1.74

Table A.1. Continued.

Chemical Name	CAS #	Molecular Formula	Molecular Structure	Solubility (mg/L)	LogP
2,4,4'-Tribromodiphenylether	41318-75-6	$C_{12}H_7Br_3O$	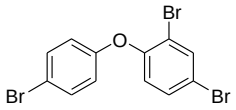	0.03	6.70
2,4,6-Tribromophenol	118-79-6	$C_6H_3Br_3O$	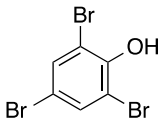	70	4.13
3-Chloroaniline	108-42-9	C_6H_6ClN	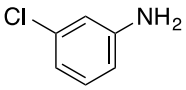	5400	1.81
3-Nitrobenzanthrone	17117-34-9	$C_{17}H_9NO_3$	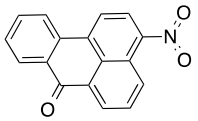	0.07	4.54
4-Aminomethyl-benzenesulfonamide	138-37-4	$C_7H_{10}N_2O_2S$	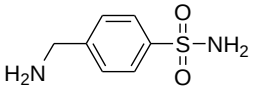	390000	-0.55
4-Chloroaniline	106-47-8	C_6H_6ClN	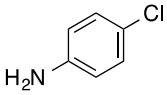	3900	1.76
4-Methyl-1H-benzotriazole	29878-31-7	$C_7H_4D_3N_3$	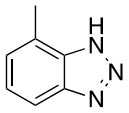	3069	1.80
4-Methylbenzylidenecamphor	36861-47-9	$C_{18}H_{22}O$	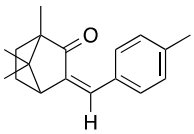	0.20	4.95
4-Nonylphenol monoethoxylate	104-35-8	$C_{17}H_{28}O_2$	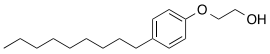	1.10	5.58
4-Nonylphenoxy acetic acid	3115-49-9	$C_{17}H_{26}O_3$	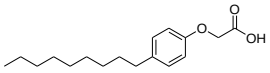	0.45	5.80
4-tert-Octylphenol diethoxylate	2315-61-9	$C_{18}H_{30}O_3$	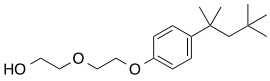	5.16	4.59
4-tert-Octylphenol monoethoxylate	2315-67-5	$C_{16}H_{26}O_2$	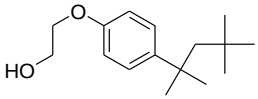	5.36	4.86
4,4'-Dichlorobenzophenone	90-98-2	$C_{13}H_8Cl_2O$	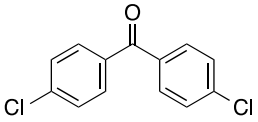	3.80	4.62
5-Methyl-1H-benzotriazole (5-Tolytriazole)	136-85-6	$C_7H_7N_3$	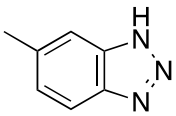	3069	1.80
5,6-Dimethyl-1H-benzotriazole	1354973-50-4	$C_8H_9N_3$	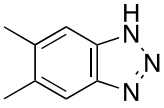	914.20	2.26

Table A.1. Continued.

Chemical Name	CAS #	Molecular Formula	Molecular Structure	Solubility (mg/L)	LogP
7H-Benzo(de)anthracen-7-one (Benzanthrone)	82-05-3	$C_{17}H_{10}O$	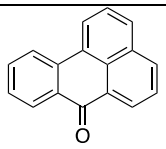	0.18	4.81
8-hydroxyquinoline	148-24-3	C_9H_7NO	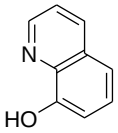	556	1.85
Acetaminophen (Paracetamol)	103-90-2	$C_8H_9NO_2$	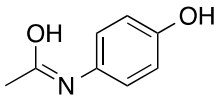	14000	0.46
Acetamiprid	135410-20-7	$C_{10}H_{11}ClN_4$	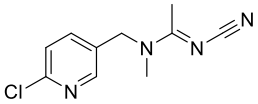	4250	0.80
Acetochlor	34256-82-1	$C_{14}H_{20}ClNO_2$	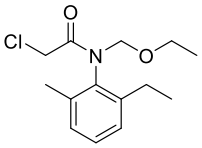	233	4.14
Aclonifen	74070-46-5	$C_{12}H_9ClN_2O_3$	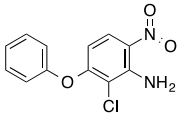	6.95	4.04
ADBI (Celestolide)	13171-00-1	$C_{17}H_{24}O$	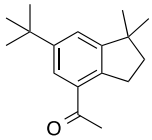	0.22	5.51
AHDI (Phantolide)	15323-35-0	$C_{17}H_{24}O$	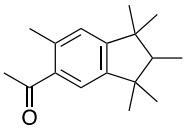	0.75	5.80
Alachlor	15972-60-8	$C_{14}H_{20}ClNO_2$	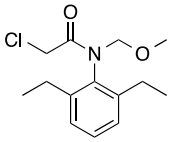	240	3.52
alpha-Terpineol	98-55-5	$C_{10}H_{18}O$	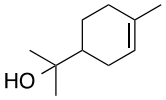	710	2.79
Amoxicillin	26787-78-0	$C_{16}H_{19}N_3O_5S$	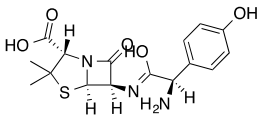	3433	0.97
Anthracene	120-12-7	$C_{14}H_{10}$	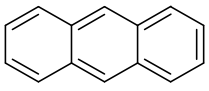	0.04	4.45
ATII (Traseolide)	68140-48-7	$C_{18}H_{26}O$	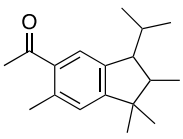	0.26	6.14
Atrazine	1912-24-9	$C_8H_{14}ClN_5$	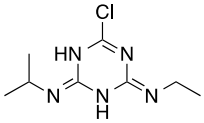	34.70	2.61

Table A.1. Continued.

Chemical Name	CAS #	Molecular Formula	Molecular Structure	Solubility (mg/L)	LogP
Atrazine-desethyl	6190-65-4	$C_6H_{10}ClN_5$	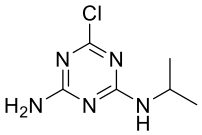	3200	1.51
Azinphos-methyl	86-50-0	$C_{10}H_{12}N_3O_3PS_2$	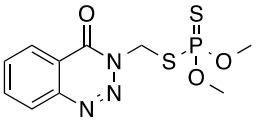	20.90	2.75
Azithromycin	83905-01-5	$C_{38}H_{72}N_2O_{12}$	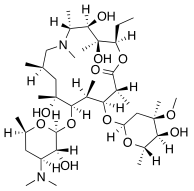	2.37	3.33
Azoxystrobin	131860-33-8	$C_{22}H_{17}N_3O_5$	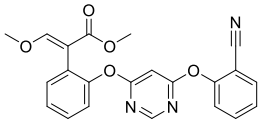	6.00	2.50
Bayrepel	658051-75-3	$C_{12}H_{23}NO_3$	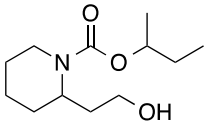	8200	1.56
Banzaldehyde, (phenylmethylene)hydrazone	588-68-1	$C_{14}H_{12}N_2$	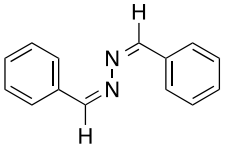	5.95	4.01
Benzenesulfonamide	98-10-2	$C_6H_7NO_2S$	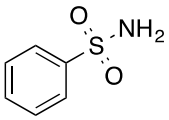	4300	0.33
Benzo(a)anthracene	56-55-3	$C_{18}H_{12}$	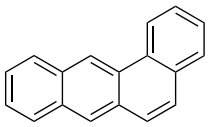	0.01	5.79
Benzo[a]pyrene	50-32-8	$C_{20}H_{12}$	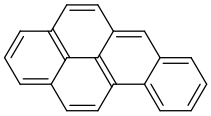	0.01	5.99
Benzo[b]fluoranthene	205-99-2	$C_{20}H_{12}$	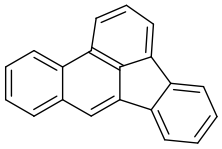	0.02	5.78
Benzo[ghi]perylene	191-24-2	$C_{22}H_{12}$	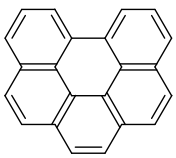	-	6.70

Table A.1. Continued.

Chemical Name	CAS #	Molecular Formula	Molecular Structure	Solubility (mg/L)	LogP
Benzo[k]fluoranthene	207-08-9	$C_{20}H_{12}$	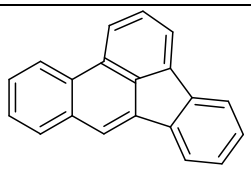	0.01	6.11
Benzothiazole	95-16-9	C_7H_5NS	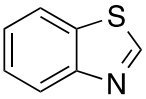	4300	2.01
Benzylamine	100-46-9	C_7H_9N	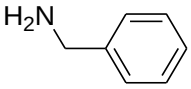	1000000	1.09
Benzyldimethyldodecylammonium	139-07-1	$C_{21}H_{38}ClN$	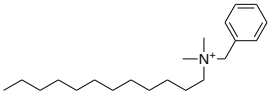	1000000	2.93
Benzyldimethylhexadecylammonium	122-18-9	$C_{25}H_{46}N$	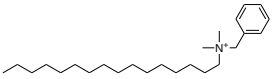	-	4.89
Benzyldimethyltetradecylammonium	5285-67-6	$C_{23}H_{42}N$	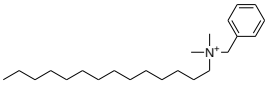	1000	3.91
Benzyltrimethylammonium	14800-24-9	$C_{10}H_{16}N^+$	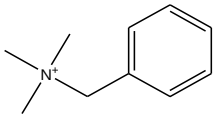	1000000	-2.47
Bifenox	42576-02-3	$C_{14}H_9Cl_2NO_5$	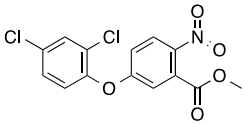	0.40	4.48
Bisphenol-A	80-05-7	$C_{15}H_{16}O_2$	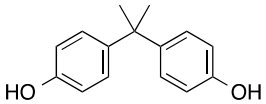	300	3.43
Boisvelone / Iso-Esuper	54464-57-2	$C_{16}H_{26}O$	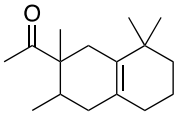	1.08	5.28
Boscalid	188425-85-6	$C_{18}H_{12}Cl_2N_2O$	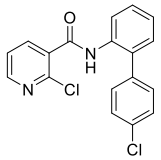	4.6	2.96
Buprofezin	69327-76-0	$C_{16}H_{23}N_3OS$	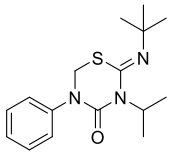	0.9	4.93
Butylmethoxydibenzoylmethane	87075-14-7	$C_{20}H_{22}O_3$	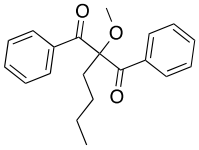	2.20	5.63

Table A.1. Continued.

Chemical Name	CAS #	Molecular Formula	Molecular Structure	Solubility (mg/L)	LogP
Cadusafos	95465-99-9	$C_{10}H_{23}O_2PS_2$	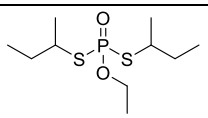	245	3.90
Carbazole	86-74-8	$C_{12}H_9N$	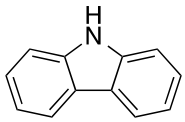	7.61	3.72
Carbendazim	10605-21-7	$C_9H_9N_3O_2$	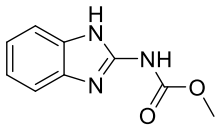	8.00	1.52
Carbofuran	1563-66-2	$C_{12}H_{15}NO_3$	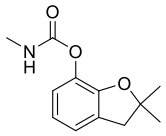	351	2.32
Chloramphenicol	56-75-7	$C_{11}H_{12}Cl_2N_2O_5$	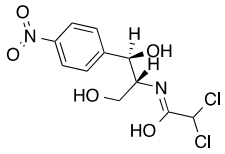	2500	1.14
Chlorfenvinphos	470-90-6	$C_{12}H_{14}Cl_3O_4P$	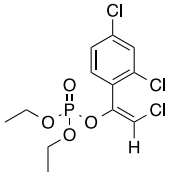	124	3.81
Chloridazon	1698-60-8	$C_{10}H_8ClN_3O$	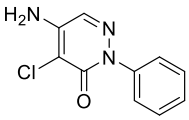	400	1.14
Chlorpyrifos	2921-88-2	$C_9H_{11}Cl_3NO_3PS$	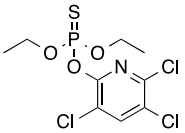	1.12	4.96
Chlorsulfuron	64902-72-3	$C_{12}H_{12}ClN_5O_4S$	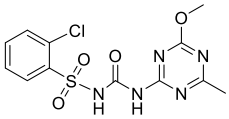	125	-1.34
Ciprofloxacin	85721-33-1	$C_{17}H_{18}FN_3O_3$	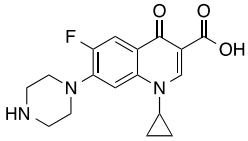	11480	0.28
Clarithromycin	81103-11-9	$C_{38}H_{69}NO_{13}$	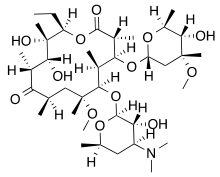	1.69	3.16
Clofentezine	74115-24-5	$C_{14}H_8Cl_2N_4$	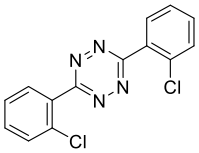	26.5	2.70

Table A.1. Continued.

Chemical Name	CAS #	Molecular Formula	Molecular Structure	Solubility (mg/L)	LogP
Clothianidin	210880-92-5	$C_6H_8ClN_5O_2S$	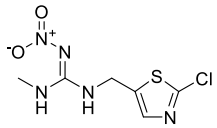	327	0.70
Cybutryne	28159-98-0	$C_{11}H_{19}N_5S$	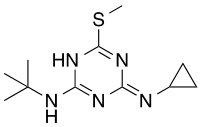	7.52	4.07
Cyclopentadecanolide	106-02-5	$C_{15}H_{28}O_2$	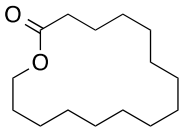	0.15	6.15
Cypermethrin	52315-07-8	$C_{22}H_{19}Cl_2NO_3$	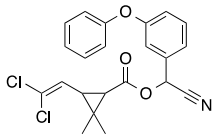	-	6.60
Cyprodinil	121552-61-2	$C_{14}H_{15}N_3$	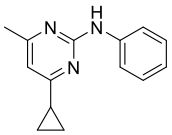	13.00	3.59
Cyromazine	66215-27-8	$C_6H_{10}N_6$	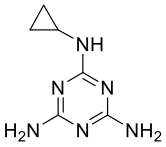	13000	-0.06
Damascone	23726-91-2	$C_{13}H_{20}O$	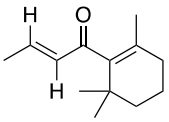	7.99	4.40
Di(2- ethylhexyl)phthalate (DEHP)	117-81-7	$C_{24}H_{38}O_4$	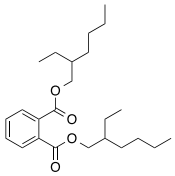	0.27	7.40
Diazinon	333-41-5	$C_{12}H_{21}N_2O_3PS$	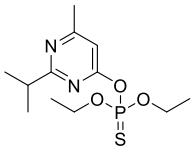	60.00	3.81
Dichlorvos	62-73-7	$C_4H_7Cl_2O_4P$	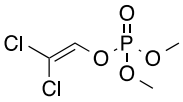	8000	1.43
Dicloxacillin	13412-64-1	$C_{19}H_{17}Cl_2N_3O_5S$	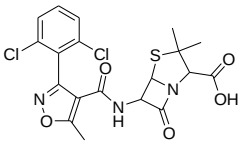	50000	2.91
Diazinon	333-41-5	$C_{12}H_{21}N_2O_3PS$	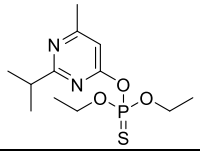	60.00	3.81

Table A.1. Continued.

Chemical Name	CAS #	Molecular Formula	Molecular Structure	Solubility (mg/L)	LogP
Dichlorvos	62-73-7	$C_4H_7Cl_2O_4P$	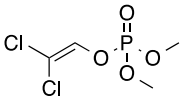	8000	1.43
Dicloxacillin	13412-64-1	$C_{19}H_{17}Cl_2N_3O_5S$	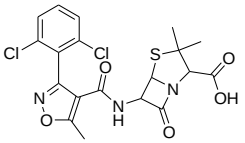	50000	2.91
Dicyclohexylamine	101-83-7	$C_{12}H_{23}N$	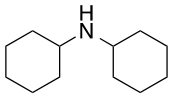	800	3.69
Difenoconazole	119446-68-3	$C_{19}H_{17}Cl_2N_3O_3$	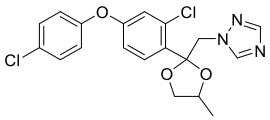	15.00	4.40
Dimethoate	60-51-5	$C_5H_{12}NO_3PS_2$	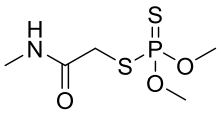	25000	0.78
Dimethomorph	110488-70-5	$C_{21}H_{22}ClNO_4$	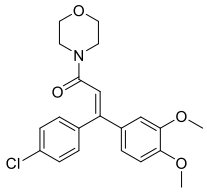	41.80	2.63
Diphenylamine	122-39-4	$C_{12}H_{11}N$	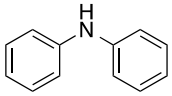	53.00	3.50
Diuron	330-54-1	$C_9H_{10}Cl_2N_2O$	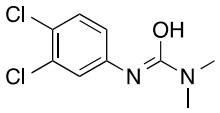	42.00	2.68
Dodecyl Sulfate	151-21-3	$C_{12}H_{25}NaO_4S$	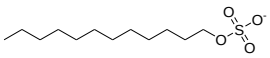	100000	2.42
Doxycycline	564-25-0	$C_{22}H_{24}N_2O_8$	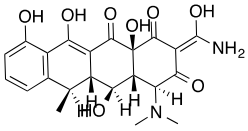	630	-0.02
Drometrizole	2440-22-4	$C_{13}H_{11}N_3O$	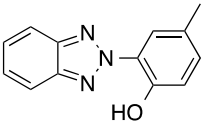	25.59	4.30
Epoxiconazole	106325-08-0	$C_{17}H_{13}ClFN_3O$	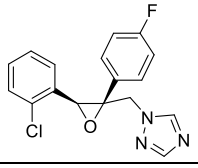	13.04	3.47

Table A.1. Continued.

Chemical Name	CAS #	Molecular Formula	Molecular Structure	Solubility (mg/L)	LogP
Erythromycin	114-07-8	$C_{37}H_{67}NO_{13}$	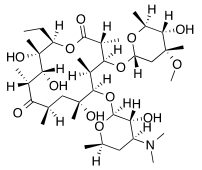	2000	2.70
Ethofumesate	26225-79-6	$C_{13}H_{18}O_5S$	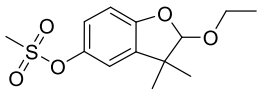	50	2.70
Ethoprophos	13194-48-4	$C_8H_{19}O_2PS_2$	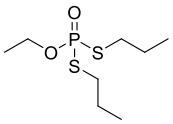	750	3.59
Ethyl paraben	120-47-8	$C_9H_{10}O_3$	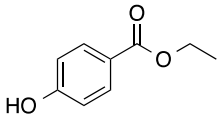	885	2.40
Ethylhexylmethoxycinnamate	5466-77-3	$C_{18}H_{26}O_3$	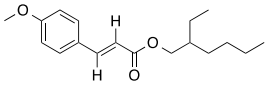	0.20	5.66
Fenamiphos	22224-92-6	$C_{13}H_{22}NO_3PS$	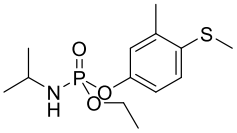	400	3.23
Fenarimol	60168-88-9	$C_{17}H_{12}Cl_2N_2O$	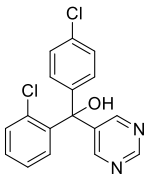	14	3.62
Fenpropimorph	67306-03-0	$C_{20}H_{33}NO$	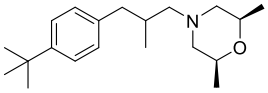	1000	5.50
Fenthion	55-38-9	$C_{10}H_{15}O_3PS_2$	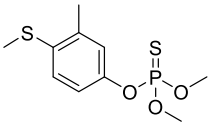	7.5	4.09
Fluopyram	658066-35-4	$C_{16}H_{11}ClF_6N_2O$	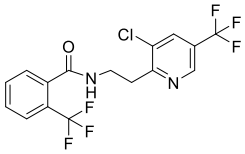	0.61	4.78
Fluoranthene	206-44-0	$C_{16}H_{10}$	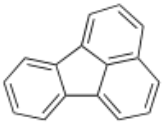	0.26	5.16
Fluquinconazole	136426-54-5	$C_{16}H_8Cl_2FN_5O$	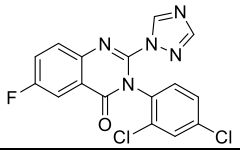	1.00	3.73

Table A.1. Continued.

Chemical Name	CAS #	Molecular Formula	Molecular Structure	Solubility (mg/L)	LogP
Flutolanil	66332-96-5	$C_{17}H_{16}F_3NO_2$	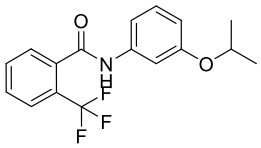	8.01	3.70
Flutriafol	76674-21-0	$C_{16}H_{13}F_2N_3O$	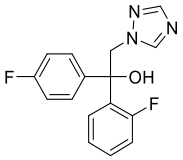	130	2.52
Fosthiazate	98886-44-3	$C_9H_{18}NO_3PS_2$	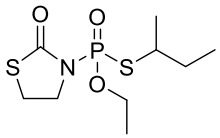	9850	1.68
g-Methylionone	127-51-5	$C_{14}H_{22}O$	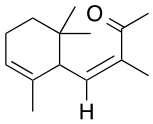	2.98	4.41
Galaxolide	1222-05-5	$C_{18}H_{26}O$	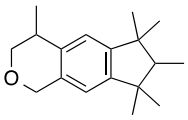	1.75	6.23
Hexa(methoxymethyl)melamine	68002-20-0	$C_{15}H_{30}N_6O_6$	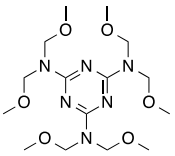	149.30	3.07
Hexachlorobenzene	118-74-1	C_6Cl_6	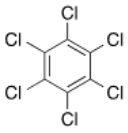	0.01	5.73
Hexaconazole	79983-71-4	$C_{14}H_{17}Cl_2N_3O$	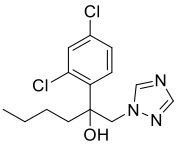	17	3.66
Hexylcinnamaldehyde	101-86-0	$C_{15}H_{20}O$	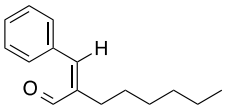	2.75	5.33
Hexythiazox	78587-05-0	$C_{17}H_{21}ClN_2O_2S$	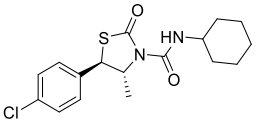	0.5	5.57
Homosalate	118-56-9	$C_{16}H_{22}O_3$	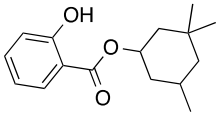	0.42	6.16
Imazalil	35554-44-0	$C_{14}H_{14}Cl_2N_2O$	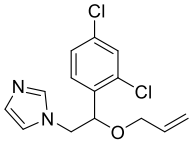	0.18	3.82

Table A.1. Continued.

Chemical Name	CAS #	Molecular Formula	Molecular Structure	Solubility (mg/L)	LogP
Imazamox	114311-32-9	$C_{15}H_{19}N_3O_4$	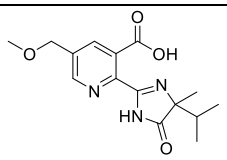	4413	0.73
Imidacloprid	138261-41-3	$C_9H_{10}ClN_5O_2$	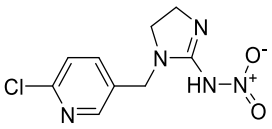	610	0.57
Indeno[1,2,3-cd]pyrene	193-39-5	$C_{22}H_{12}$	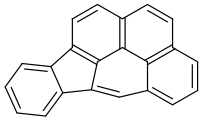	0.03	6.76
Isobutyl paraben	4247-02-3	$C_{11}H_{14}O_3$	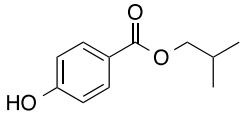	223.70	3.27
Isoproturon	34123-59-6	$C_{12}H_{18}N_2O$	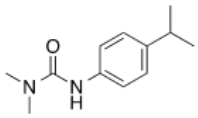	65	2.87
Lenacil	2164-08-1	$C_{13}H_{18}N_2O_2$	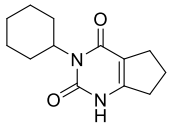	6.00	3.09
Linuron	330-55-2	$C_9H_{10}Cl_2N_2O_2$	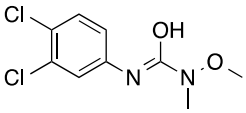	75.00	3.20
Malathion	121-75-5	$C_{10}H_{19}O_6PS_2$	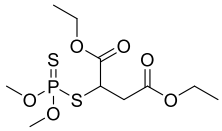	143	2.36
Mandipropamid	374726-62-2	$C_{23}H_{22}ClNO_4$	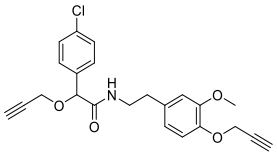	4.2	3.20
Mepiquat chloride	24307-26-4	$C_7H_{16}ClN$		529000	-2.82
Mesotrione	104206-82-8	$C_{14}H_{13}NO_7S$	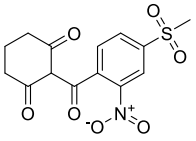	15000	0.90
Metalaxyl	57837-19-1	$C_{15}H_{21}NO_4$	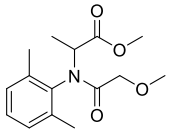	8400	1.65
Methamidophos	10265-92-6	$C_2H_8NO_2PS$	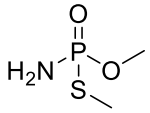	1.01	-0.80

Table A.1. Continued.

Chemical Name	CAS #	Molecular Formula	Molecular Structure	Solubility (mg/L)	LogP
Methidathion	950-37-8	$C_6H_{11}N_2O_4PS_3$	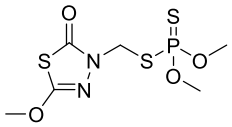	187	2.20
Methomyl	16752-77-5	$C_5H_{10}N_2O_2S$	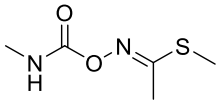	58000	0.60
Methoxyfenozide	10265-92-6	$C_2H_8NO_2PS$	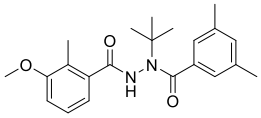	3.3	3.7
Methyl -iso-propylcyclohexenone	6485-40-1	$C_{10}H_{14}O$	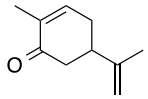	1310	2.27
Methyl Paraben	99-76-3	$C_8H_8O_3$	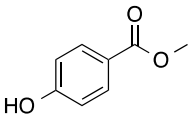	2500	1.86
Methyldihydrojasmonate	24851-98-7	$C_{13}H_{22}O_3$	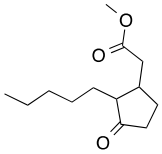	91.72	2.50
Methylsalicylate	119-36-8	$C_8H_8O_3$	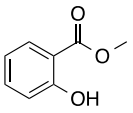	700	2.23
Metolachlor	51218-45-2	$C_{15}H_{22}ClNO_2$	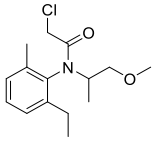	530	3.13
Metrafenone	220899-03-6	$C_{19}H_{21}BrO_5$	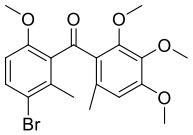	0.23	4.72
Microcystin-LR	101043-37-2	$C_{49}H_{74}N_{10}O_{12}$	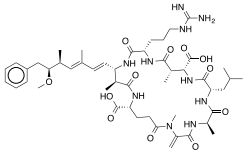	-	-0.56
Microcystin-RR	111755-37-4	$C_{49}H_{75}N_{13}O_{12}$	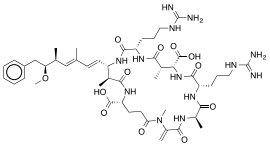	-	-3.96
Microcystin-YR	101064-48-6	$C_{52}H_{72}N_{10}O_{13}$	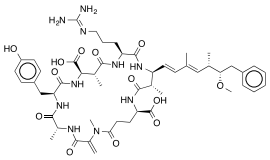	-	-1.85

Table A.1. Continued.

Chemical Name	CAS #	Molecular Formula	Molecular Structure	Solubility (mg/L)	LogP
Molinate	2212-67-1	$C_9H_{17}NOS$	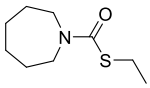	970	3.21
Monocrotophos	6923-22-4	$C_7H_{14}NO_5P$	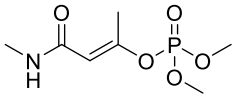	1000000	-0.20
Musk ambrette	83-66-9	$C_{12}H_{16}N_2O_5$	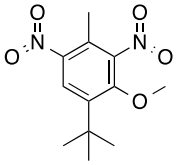	0.79	3.71
Musk ketone	81-14-1	$C_{14}H_{18}N_2O_5$	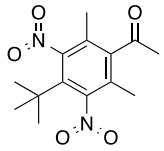	0.46	3.86
Musk xylene	81-15-2	$C_{12}H_{15}N_3O_6$	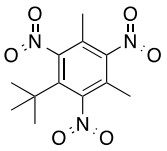	0.15	3.83
Myclobutanil	88671-89-0	$C_{15}H_{17}ClN_4$	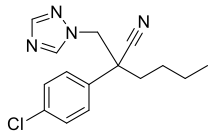	142	2.94
N-Benzyldimethylamine	103-83-3	$C_9H_{13}N$	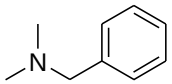	12000	1.98
N-Benzylmethylamine	103-67-3	$C_8H_{11}N$	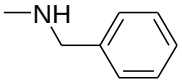	1000000	1.52
N-Ethyl-2-tolysulfonamide	80-39-7	$C_9H_{13}NO_2S$	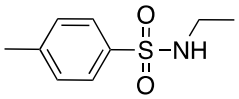	1106	1.96
N-methyl aniline	100-61-8	C_7H_9N	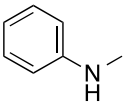	5620	1.66
N-phenyl-napthylamine	90-30-2	$C_{16}H_{13}N$	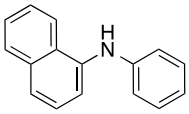	60.00	4.20
N,N-Diethyl-m-toluamide	134-62-3	$C_{12}H_{17}NO$	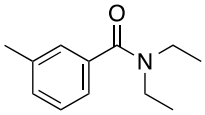	666	2.18
Nonylphenol diethoxylate	20427-84-3	$C_{19}H_{32}O_3$	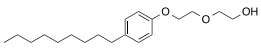	1.05	5.30
Norfloxacin	70458-96-7	$C_{16}H_{18}FN_3O_3$	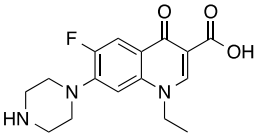	177900	-1.03

Table A.1. Continued.

Chemical Name	CAS #	Molecular Formula	Molecular Structure	Solubility (mg/L)	LogP
Ofloxacin	82419-36-1	$C_{18}H_{20}FN_3O_4$	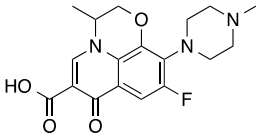	10800	-0.39
Omethoate	1113-02-6	$C_5H_{12}NO_4PS$	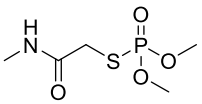	1.01	-0.74
Oxadiazon	19666-30-9	$C_{15}H_{18}Cl_2N_2O_3$	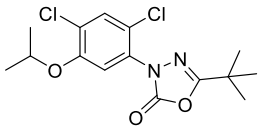	0.70	4.80
Oxadixyl	77732-09-3	$C_{14}H_{18}N_2O_4$	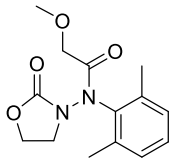	3400	0.80
Oxybenzone	131-57-7	$C_{14}H_{12}O_3$	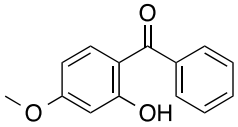	69.00	3.64
Penconazole	66246-88-6	$C_{13}H_{15}Cl2N_3$	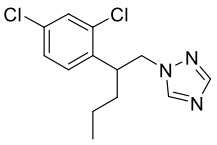	73.00	4.67
Pendimethalin	40487-42-1	$C_{13}H_{19}N_3O_4$	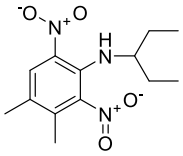	0.33	5.20
Pentachlorobenzene	608-93-5	C_6HCl_5	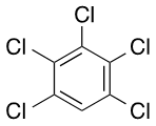	0.83	4.60
Pinoxaden	243973-20-8	$C_{23}H_{32}N_2O_4$	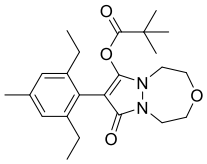	220	3.2
Piperonylbutoxide	51-03-6	$C_{19}H_{30}O_5$	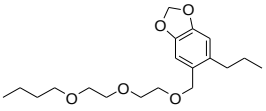	28.90	4.75
Pirimicarb	23103-98-2	$C_{11}H_{18}N_4O_2$	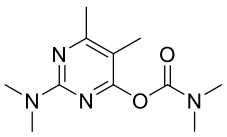	2700	1.70
Polychlorinated biphenyls	1336-36-3	$C_{12}H_4Cl_6$	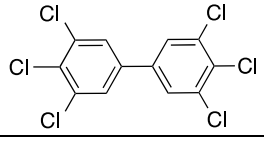	0.00	6.90

Table A.1. Continued.

Chemical Name	CAS #	Molecular Formula	Molecular Structure	Solubility (mg/L)	LogP
Prochloraz	67747-09-5	$C_{15}H_{16}Cl_3N_3O_2$	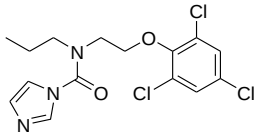	34.00	4.10
Prometryn	7287-19-6	$C_{10}H_{19}N_5S$	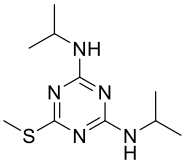	33.00	3.51
Propazine	139-40-2	$C_9H_{16}ClN_5$	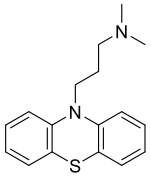	8.60	2.93
Propetamphos	31218-83-4	$C_{10}H_20NO_4PS$	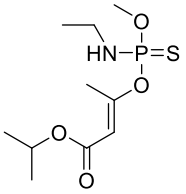	110	3.82
Propiconazole	60207-90-1	$C_{15}H_{17}Cl_2N_3O_2$	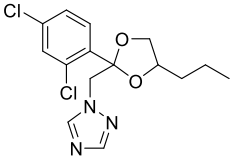	100	3.72
Propyl paraben	94-13-3	$C_{10}H_{12}O_3$	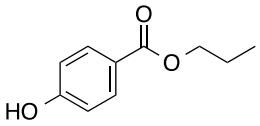	500	3.04
Prothioconazole	178928-70-6	$C_{14}H_{15}Cl_2N_3OS$	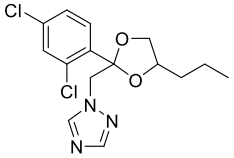	300	3.82
Pyraclostrobin	175013-18-0	$C_{19}H_{18}ClN_3O_4$	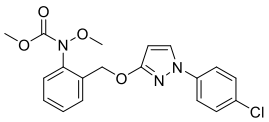	1.90	3.99
Pyridaben	96489-71-3	$C_{19}H_{25}ClN_2OS$	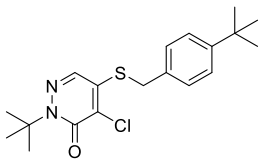	0.01	6.37
Pyrimethanil	53112-28-0	$C_{12}H_{13}N_3$	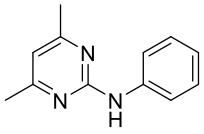	121	2.84
Pyriproxyfen	95737-68-1	$C_{20}H_{19}NO_3$	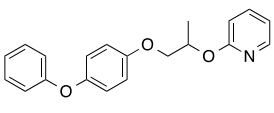	0.68	4.80

Table A.1. Continued.

Chemical Name	CAS #	Molecular Formula	Molecular Structure	Solubility (mg/L)	LogP
Quinalphos	13593-03-8	$C_{12}H_{15}N_2O_3PS$	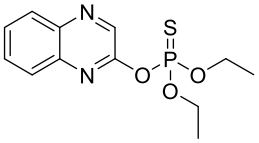	22.00	4.44
Quinoxyfen	124495-18-7	$C_{15}H_8Cl_2FNO$	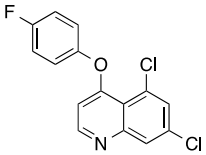	1.15	4.66
Simazine	122-34-9	$C_7H_{12}ClN_5$	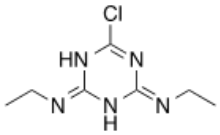	6.20	2.18
Spiroxamine	118134-30-8	$C_{18}H_{35}NO_2$	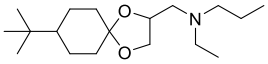	470	5.51
Sulfamethoxazole	723-46-6	$C_{10}H_{11}N_3O_3S$	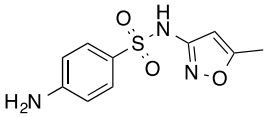	610	0.89
Tebuconazole	107534-96-3	$C_{16}H_{22}ClN_3O$	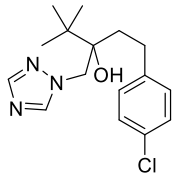	36.00	3.70
Terbuthylazine	5915-41-3	$C_9H_{16}ClN_5$	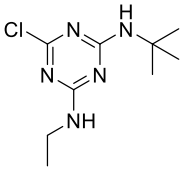	5.00	3.40
Terbutryn	886-50-0	$C_{10}H_{19}N_5S$	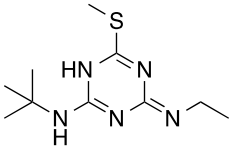	25.00	3.75
Tetraacetylethylenediamine	10543-57-4	$C_{10}H_{16}N_2O_4$	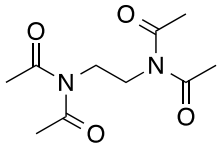	200	-1.61
Tetrabromobisphenol A	79-94-7	$C_{15}H_{12}Br_4O_2$	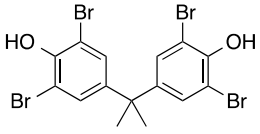	0.24	5.90
Tetracycline	60-54-8	$C_{22}H_{24}N_2O_8$	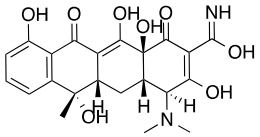	231	-1.30
Thiacloprid	111988-49-9	$C_{10}H_9ClN_4S$	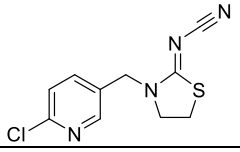	185	1.26

Table A.1. Continued.

Chemical Name	CAS #	Molecular Formula	Molecular Structure	Solubility (mg/L)	LogP
Thiophanate-methyl	23564-05-8	$C_{12}H_{14}N_4O_4S2$	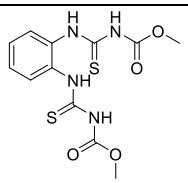	26.60	1.40
Thioridazine	130-61-0	$C_{21}H_{26}N_2S_2$	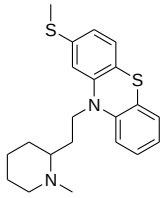	0.14	5.90
Tolfenpyrad	129558-76-5	$C_{21}H_{22}ClN_3O_2$	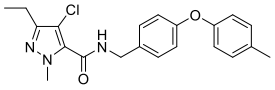	0.36	6.45
Tonalide	1506-02-1	$C_{18}H_{26}O$	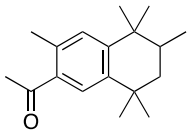	1.25	5.70
Triasulfuron	82097-50-5	$C_{14}H_{16}ClN_5O_5S$	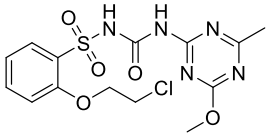	32.00	2.44
Triazophos	24017-47-8	$C_{12}H_{16}N_3O_3PS$	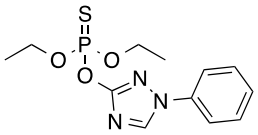	39.00	3.34
Triclosan	3380-34-5	$C_{12}H_7Cl_3O_2$	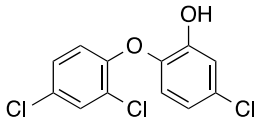	6.05	4.76
Trifloxystrobin	141517-21-7	$C_{20}H_{19}F_3N_2O_4$	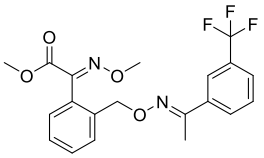	0.61	4.50
Trifluralin	1582-09-8	$C_{13}H_{16}F_3N_3O_4$	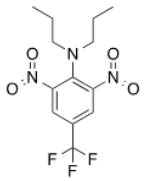	0.18	5.34
Trimethoprim	738-70-5	$C_{14}H_{18}N_4O_3$	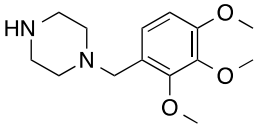	400	0.91
Triphenylphosphineoxide	791-28-6	$C_{18}H_{15}OP$	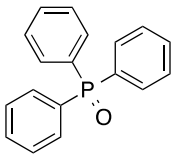	62.76	2.87

Table A.1. Continued.

Chemical Name	CAS #	Molecular Formula	Molecular Structure	Solubility (mg/L)	LogP
Triphenyltin	668-34-8	$C_{18}H_{15}Sn$	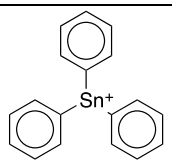	-	4.31
Tris(1-chloro-2-propanyl) phosphate	13674-84-5	$C_9H_{18}Cl_3O_4P$	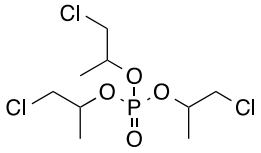	1600	1.53
Tris(2-butoxyethyl) phosphate	78-51-3	$C_{18}H_{39}O_7P$	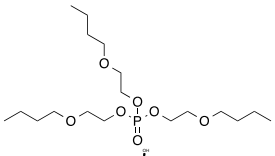	1100	4.30
Vancomycin	1404-93-9	$C_{66}H_{75}Cl_2N_9O_{24}$	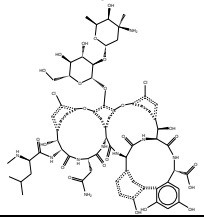	50000	-1.44

Table A.2. MRM transitions and MS/MS parameters.

Compound	Ionization mode	RT (min)	MRM Transitions	DP	EP	CE	CXP
1,2,3-Benzotriazole	ESI (+)	2.87	120 → 65	6	0	29	8
			120 → 92	6	0	23	6
2,4-Dihydroxybenzophenone	ESI (+)	4.56	215 → 136.9	6	0	27	8
			215 → 80.9	6	0	5	6
2-Mercapto-benzothiazole	ESI (+)	3.38	167.9 →135	7	0	35	8
			167.9 → 65	7	0	47	6
2-Methylanthraquinone	ESI (+)	6.29	223 → 152	7	0	4	6
			223 → 65	7	0	47	8
3-Chloroaniline	ESI (+)	2.83	128 → 92.9	5	0	25	8
			128 → 74.9	5	10	43	6
4,4'-Dichlorobenzophenone	ESI (+)	6.67	251 → 139	71	10	27	6
			251 → 110.8	71	10	55	8
4-Aminomethyl-benzenesulfonamide	ESI (+)	0.47	187.1 → 170	46	10	13	8
			187.1 → 106	46	10	25	8
4-Chloroaniline	ESI (+)	2.83	128 → 92.9	56	10	25	8
			128 → 74.9	56	10	43	6
4-Methyl-1H-benzotriazole	ESI (+)	3.09	134 → 76.9	46	10	37	8
			134 → 78.9	46	10	27	6
4-Methylbenzylidenecamphor	ESI (+)	7.1	255.1 → 105	81	10	45	6
			255.1 → 114.9	81	10	89	8
4-Nonylphenol monoethoxylate	ESI (+)	7.96	282.2 → 265	61	10	13	12
			282.2 → 69	61	10	39	6
4-tert-Octylphenol diethoxylate	ESI (+)	7.04	312.2 → 183.1	61	10	17	10
			312.2 → 120.9	61	10	29	8
4-tert-Octylphenol monoethoxylate	ESI (+)	6.99	268.1 → 113	46	10	11	6
			268.1 → 251	46	10	9	12
5,6-Dimethyl-1H-benzotriazole monohydrate	ESI (+)	3.34	148.1 → 76.9	81	10	39	6
			148.1 → 92.9	81	10	27	8
5-Methyl-1H-benzotriazole (5-Tolytriazole)	ESI (+)	3.08	134 → 77	56	10	33	6
			134 → 79	56	10	27	6
8-Hydroxyquinoline	ESI (+)	0.51	146 → 128	61	10	33	6
			146 → 74.9	61	10	57	6
Acetaminophen (Paracetamol)	ESI (+)	2.65	152 → 110	56	10	23	8
			152 → 65	56	10	41	6
Acetamiprid	ESI (+)	2.99	223.1 → 126	76	10	31	11
			223.1 → 99	76	10	55	9
Acetochlor	ESI (+)	5.78	270.2 → 224	46	10	11	15
			270.2 → 148	46	10	29	11
Aclonifen	ESI (+)	6.16	265 → 248	61	10	25	8
			265 → 182.1	61	10	39	12
ADBI (Celestolide)	ESI (+)	7.39	245.2 → 189.1	66	10	19	8
			245.2 → 131	66	10	29	6

Table A.2. Continued.

Compound	Ionization mode	RT (min)	MRM Transitions	DP	EP	CE	CXP
AHDI (Phantolide)	ESI (+)	7.33	245.2 → 175.1	71	10	25	8
			245.2 → 119	71	10	47	6
Alachlor	ESI (+)	5.77	270 → 237.9	21	10	13	10
			270 → 162.1	21	10	25	8
Amoxicillin	ESI (+)	0.51	366.1 → 348.9	16	10	13	6
			366.1 → 113.9	16	10	27	8
ATII (Traseolide)	ESI (+)	7.64	259.1 → 189.1	81	10	21	8
			259.1 → 147.1	81	10	33	6
Atrazine	ESI (+)	4.06	216.1 → 174.1	21	10	25	8
			216.1 → 103.9	21	10	41	8
Atrazine-desethyl	ESI (+)	3.09	188.2 → 146	56	10	25	11
			188.2 → 148	46	10	25	13
Azinphos-methyl	ESI (+)	4.64	318 → 131.9	46	10	19	10
			318 → 76.9	46	10	61	6
Azithromycin	ESI (+)	2.8	749.5 → 591.3	86	10	43	6
			749.5 → 82.8	86	10	89	6
Azoxystrobin	ESI (+)	5.2	404.1 → 372	76	10	21	13
			404.1 → 344.1	76	10	35	25
Bayrepel	ESI (+)	4.14	230 → 174.1	21	10	13	8
			230 → 156	21	10	21	8
Benzaldehyde, (phenylmethylene)hydrazone	ESI (+)	6.39	209 → 106	41	10	25	8
			209 → 76.8	41	10	51	6
Benzenesulfonamide	ESI (+)	2.68	158 → 140.9	41	10	11	10
			158 → 77	41	10	31	6
Benzothiazole	ESI (+)	3.38	136 → 108.9	71	10	33	6
			136 → 64.9	71	10	45	6
Benzylamine	ESI (+)	0.5	108.1 → 90.9	36	10	17	6
			108.1 → 65	36	10	35	8
Benzyldimethyldodecylammonium	ESI (+)	5.75	304.3 → 90.9	11	10	53	8
			304.3 → 212.2	11	10	29	4
Benzyldimethylhexadecylammonium	ESI (+)	6.72	360.4 → 90.9	101	10	71	8
			360.4 → 268.1	101	10	33	12
Benzyldimethyltetradecylammonium	ESI (+)	6.39	332.3 → 90.7	96	10	47	6
			332.3 → 240.1	96	10	31	10
Benzyltrimethylammonium	ESI (+)	0.5	150.1 → 91	66	10	31	6
			150.1 → 64.9	66	10	51	6
Bifenox	ESI (+)	6.59	341.9 → 309.8	26	10	15	14
		6.59	341.9 → 188.9	26	10	33	10
Boisvelone / Iso-Esuper	ESI (+)	7.43	235.2 → 217.2	71	10	19	8
			235.2 → 94.9	71	10	27	6
Boscalid	ESI (+)	5.3	343 → 307	101	10	27	18
			343 → 140	106	10	27	14
Buprofezin	ESI (+)	6.65	305.9 → 201	61	10	11	10

Table A.2. Continued.

Compound	Ionization mode	RT (min)	MRM Transitions	DP	EP	CE	CXP
			305.9 → 115.9	61	10	17	10
Butylmethoxydibenzoylmethane	ESI (+)	7.71	311 → 161.1	91	10	35	8
			311 → 135	91	10	33	6
Cadusafos	ESI (+)	6.62	271.1 → 158.9	66	10	21	13
			271.1 → 214.9	66	10	13	17
Carbazole	ESI (+)	5.29	168 → 167.1	76	10	51	8
			168 → 138.9	76	10	61	8
Carbendazim	ESI (+)	2.73	191.9 → 160	71	10	23	8
			191.9 → 131.9	71	10	39	10
Carbofuran	ESI (+)	3.45	222.1 → 165	76	10	17	15
			222.1 → 123.1	76	10	31	13
Chlorfenvinphos	ESI (+)	6.3	358.9 → 155.1	66	10	19	8
			358.9 → 98.9	66	10	35	8
Chloridazon	ESI (+)	3.02	222 → 92	96	10	35	14
			222 → 104	101	10	31	16
Chlorpyrifos	ESI (+)	7.16	349.9 → 96.8	56	10	55	8
			349.9 → 197.9	56	10	35	6
Chlorsulfuron	ESI (+)	4.17	358 → 141	81	10	23	14
			358 → 167	81	10	25	15
Ciprofloxacin	ESI (+)	2.72	332.2 → 314	76	10	29	12
			332.2 → 230.9	76	10	51	10
Clarithromycin	ESI (+)	3.75	748.4 → 158	46	10	37	10
			748.4 → 82.8	46	10	91	8
Clofentezine	ESI (+)	6.55	302.7 → 137.9	81	10	17	12
			302.7 → 102	81	10	51	10
Clothianidin	ESI (+)	2.93	250 → 169.1	66	10	17	15
			250 → 132	66	10	19	13
Cybutryne	ESI (+)	4.37	254 → 198.1	41	10	25	4
			254 → 68	41	10	57	6
Cypermethrin	ESI (+)	7.56	433 → 191	51	10	21	8
			433 → 415.9	51	10	13	16
Cyprodinil	ESI (+)	5.05	226.1 → 93.1	91	10	49	9
			226.1 → 77	91	10	65	7
Cyromazine	ESI (+)	0.52	167 → 85	66	10	23	8
			167 → 68	66	10	45	6
Damascone	ESI (+)	6.19	193 → 146.8	41	10	15	8
			193 → 137	41	10	17	6
Di(2- ethylhexyl)phthalate (DEHP)	ESI (+)	8.36	391.3 → 120.8	61	10	69	8
			391.3 → 148.9	61	10	35	8
Diazinon	ESI (+)	6.33	305.1 → 169	81	10	31	17
			305.1 → 97	81	10	47	9
Dichlorvos	ESI (+)	3.36	220.9 → 108.9	61	10	25	8
			220.9 → 78.9	61	10	49	6

Table A.2. Continued.

Compound	Ionization mode	RT (min)	MRM Transitions	DP	EP	CE	CXP
Dicloxacillin	ESI (+)	6.62	470.1 → 159.9	71	10	17	12
			470.1 → 310.8	71	10	21	14
Dicyclohexylamine	ESI (+)	2.78	182.2 → 83	61	10	29	6
			182.2 → 100	61	10	27	6
Difenoconazole	ESI (+)	6.65	406 → 251	106	10	37	17
			406 → 188	106	10	37	17
Dimethoate	ESI (+)	2.96	230.1 → 198.9	66	10	15	19
			230.1 → 125	66	10	29	11
Dimethomorph	ESI (+)	5.47	388.1 → 301.1	56	10	31	11
			388.1 → 165.1	56	10	43	17
Diphenylamine	ESI (+)	5.52	170 → 93	71	10	37	8
			170 → 92.4	71	10	27	6
Diuron	ESI (+)	4.22	233 → 71.9	61	10	41	6
			233 → 159.9	61	10	37	8
Doxycycline	ESI (+)	2.91	445.1 → 428	86	10	27	8
			445.1 → 97.9	86	10	61	8
Drometrizole	ESI (+)	6.97	226.1 → 119.9	76	10	25	8
			226.1 → 107	76	10	27	6
Epoxiconazole	ESI (+)	5.89	330.1 → 120.9	81	10	31	13
			330.1 → 101.1	81	10	69	11
Erythromycin	ESI (+)	3.18	734.5 → 158.1	21	10	39	6
			734.5 → 83	21	10	89	8
Ethofumesate	ESI (+)	5.02	304.1 → 121.1	56	10	31	11
			304.1 → 121.1	56	10	31	11
Ethoprophos	ESI (+)	5.82	243 → 131	51	10	29	14
			243 → 97	61	10	41	12
Ethyl paraben	ESI (+)	3.45	167 → 94.9	41	10	23	8
			167 → 120.9	41	10	27	8
Ethylhexylmethoxycinnamate	ESI (+)	7.79	291 → 161	51	10	27	8
			291 → 179	51	10	13	8
Fenamiphos	ESI (+)	6.02	304 → 217	71	10	31	15
			304 → 202	71	10	45	15
Fenarimol	ESI (+)	5.79	331 → 268	76	10	33	23
			331 → 81.1	76	10	49	17
Fenpropimorph	ESI (+)	3.61	304 → 147	76	10	39	14
			304 → 117	91	10	71	14
Fenthion	ESI (+)	6.26	279 → 247.1	76	10	19	21
			279 → 169.1	76	10	25	15
Fluopyram	ESI (+)	5.74	397.1 → 208	86	10	29	17
			397.1 → 173	66	10	25	13
Fluquinconazole	ESI (+)	5.68	376 → 307	86	10	33	20
			376 → 349	81	10	25	22
Flutolanil	ESI (+)	5.44	324 → 262.1	86	10	25	23

Table A.2. Continued.

Compound	Ionization mode	RT (min)	MRM Transitions	DP	EP	CE	CXP
			324 → 282	86	10	19	25
Flutriafol	ESI (+)	4	302 → 123	71	10	39	14
			302 → 109	76	10	43	14
Fosthiazate	ESI (+)	3.79	284 → 228	91	10	15	16
			284 → 104	91	10	27	14
Galaxolide	ESI (+)	7.54	257.1 → 227.1	91	10	41	10
			257.1 → 114.9	91	10	99	8
g-Methylionone	ESI (+)	6.85	207.1 → 111	41	10	17	8
			207.1 → 68.9	41	10	27	6
Hexa(methoxymethyl)melamine	ESI (+)	3.68	391 → 177.1	26	10	39	6
			391 → 283.1	26	10	19	8
Hexaconazole	ESI (+)	6.34	314 → 70	66	10	39	12
			314 → 159	56	10	37	14
Hexylcinnamaldehyde	ESI (+)	7.18	217.1 → 129.1	66	10	25	6
			217.1 → 127.9	66	10	55	10
Hexythiazox	ESI (+)	7.18	353.1 → 228	76	10	23	19
			353.1 → 168	76	10	37	15
Homosalate	ESI (+)	7.98	263 → 139	11	10	15	10
			263 → 121	11	10	37	6
Imazalil	ESI (+)	3.17	297 → 159	56	10	31	14
			297 → 201	51	10	23	15
Imazamox	ESI (+)	3.27	306.2 → 261.1	76	10	31	17
			306.2 → 264.1	76	10	27	19
Imidacloprid	ESI (+)	2.9	256.1 → 175.1	71	10	29	17
			256.1 → 209.1	71	10	21	19
Isoproturon	ESI (+)	4.11	207.1 → 71.9	66	10	37	6
			207.1 → 165.1	66	10	21	8
Lenacil	ESI (+)	4.14	235.1 → 153.1	66	10	19	13
			235.1 → 136.1	66	10	43	11
Linuron	ESI (+)	4.9	249 → 159.9	61	10	27	8
		4.9	249 → 132.9	61	10	47	8
Malathion	ESI (+)	5.41	331.1 → 127	81	10	19	13
			331.1 → 285	81	10	11	11
Mandipropamid	ESI (+)	5.47	412.2 → 328.1	86	10	21	19
			412.2 → 125	86	10	55	11
Mepiquat chloride	ESI (+)	0.5	114 → 58.1	46	10	29	6
			114 → 98.1	46	10	29	10
Mesotrione	ESI (+)	4.26	340 → 228	91	10	23	21
			340 → 104	91	10	41	21
Metalaxyl	ESI (+)	4.14	280.2 → 220.1	56	10	19	19
			280.2 → 160.1	56	10	33	17
Methamidophos	ESI (+)	1.22	142 → 94	36	10	19	17
			142 → 125	36	10	19	9

Table A.2. Continued.

Compound	Ionization mode	RT (min)	MRM Transitions	DP	EP	CE	CXP
Methidathion	ESI (+)	4.41	303 → 145	46	10	15	14
			303 → 85	56	10	27	12
Methomyl	ESI (+)	2.79	163.1 → 88.1	51	10	13	9
			163.1 → 106.1	51	10	13	9
Methoxyfenozide	ESI (+)	5.56	369 → 149	66	10	23	14
			369 → 133	71	10	31	14
Metolachlor	ESI (+)	5.86	284.1 → 252	61	10	23	23
			284.1 → 176.1	61	10	37	15
Metrafenone	ESI (+)	6.5	409.1 → 209.2	71	10	19	19
			409.1 → 227	71	10	23	15
Microcystin-LR	ESI (+)	5.02	995.5 → 135	181	10	111	6
			995.5 → 106.9	181	10	127	6
Microcystin-RR	ESI (+)	3.17	519.8 → 135	96	10	35	6
			519.8 → 102.9	96	10	91	8
Microcystin-YR	ESI (+)	4.61	1045.6 → 135	266	10	115	6
			1045.6 → 106.9	266	10	127	4
Molinate	ESI (+)	5.41	188 → 126	51	10	19	14
			188 → 83	51	10	25	12
Monocrotophos	ESI (+)	2.82	224.2 → 192.9	56	10	13	17
			224.2 → 126.9	56	10	21	11
Myclobutanil	ESI (+)	5.54	289 → 70	66	10	33	12
			289 → 125	51	10	41	14
N,N-Diethyl-m-toluamide	ESI (+)	4.1	192.1 → 118.9	71	10	25	6
			192.1 → 90.9	71	10	43	6
N-Benzyldimethylamine	ESI (+)	0.51	136.1 → 91	41	10	25	6
			136.1 → 65	41	10	47	6
N-Benzylmethylamine	ESI (+)	0.51	122.2 → 90.8	36	10	23	8
			122.2 → 64.9	36	10	41	16
N-Ethyl-2-tolysulfonamide	ESI (+)	3.29	200 → 90.9	46	10	37	8
			200 → 155	46	10	15	8
N-methyl aniline	ESI (+)	0.5	108.1 → 92.9	56	10	23	6
			108.1 → 66	56	10	39	6
Nonylphenol diethoxylate	ESI (+)	7.37	326.2 → 183.1	61	10	15	10
			326.2 → 121	61	10	31	6
Norfloxacin	ESI (+)	2.71	320.2 → 302	71	10	29	12
			320.2 → 231	71	10	55	10
N-phenyl-2-napthylamine	ESI (+)	6.56	220.1 → 143	101	10	37	6
			220.1 → 114.9	101	10	57	4
Ofloxacin	ESI (+)	2.7	362.2 → 318	46	10	27	6
			362.2 → 261	46	10	37	10
Omethoate	ESI (+)	2.66	213.9 → 124.9	51	10	27	10
			213.9 → 182.9	51	10	13	14
Oxadiazon	ESI (+)	7.05	362.1 → 303	56	10	23	19

Table A.2. Continued.

Compound	Ionization mode	RT (min)	MRM Transitions	DP	EP	CE	CXP
			362.1 → 220.1	56	10	35	19
Oxadixyl	ESI (+)	3.21	279.2 → 219	76	10	17	19
			279.2 → 133	76	10	31	13
Oxybenzone	ESI (+)	6.01	229.1 → 151	61	10	27	8
			229.1 → 104.8	61	10	25	12
Penconazole	ESI (+)	6.17	284.2 → 158.9	81	10	37	15
			284.2 → 70.2	81	10	35	7
Pendimethalin	ESI (+)	7.23	282.2 → 211.9	51	10	17	17
			282.2 → 193.9	51	10	25	17
Pinoxaden	ESI (+)	6.5	401.2 → 317.1	81	10	29	27
			401.2 → 57.1	81	10	53	11
Piperonylbutoxide	ESI (+)	6.99	356.2 → 177	16	10	17	8
			356.2 → 118.9	16	10	47	12
Pirimicarb	ESI (+)	2.96	238.7 → 72.1	66	10	33	7
			238.7 → 182.1	66	10	23	17
Prochloraz 1	ESI (+)	5.99	376 → 308	46	10	17	18
		5.99	376 → 266	61	10	23	18
Prometryn	ESI (+)	4.05	242.2 → 158.1	76	10	33	13
			242.2 → 200	81	10	27	15
Propazine	ESI (+)	5.02	229.9 → 145.9	46	10	27	10
			229.9 → 188	46	10	21	10
Propetamphos	ESI (+)	5.55	282.2 → 138	56	8.5	23	14
			282.2 → 156	56	8.5	17	14
Propiconazole	ESI (+)	6.3	342.1 → 159	96	10	43	15
			342.1 → 69.1	96	10	35	7
Prothioconazole	ESI (+)	6.33	344.1 → 326	61	10	17	7
			346.1 → 328.1	61	10	17	7
Pyraclostrobin	ESI (+)	6.45	388 → 194	36	10	19	15
			388 → 163	41	10	29	15
Pyridaben	ESI (+)	7.64	365.1 → 309.1	66	10	19	11
			365.1 → 147.1	66	10	37	13
Pyrimethanil	ESI (+)	3.93	200.2 → 82.1	81	10	37	17
			200.2 → 107.2	81	10	35	11
Pyriproxifen	ESI (+)	7.08	322.1 → 95.9	51	10	23	8
			322.1 → 185.1	51	10	31	8
Pyriproxyfen	ESI (+)	7.11	322.1 → 96	66	10	23	9
			322.1 → 184.9	66	10	33	17
Quinalphos	ESI (+)	6.13	299 → 147	61	10	29	14
			299 → 163	51	10	29	15
Quinoxyfen	ESI (+)	7.07	307.9 → 197	111	10	45	8
			307.9 → 162	111	10	65	8
Simazine	ESI (+)	3.49	202.1 → 103.9	41	10	35	8
			202.1 → 124	41	10	25	8

Table A.2. Continued.

Compound	Ionization mode	RT (min)	MRM Transitions	DP	EP	CE	CXP
Spiroxamine	ESI (+)	3.85	298 → 144	71	10	27	14
			298 → 100	71	10	41	14
Sulfamethoxazole	ESI (+)	2.85	254 → 91.9	46	10	35	6
			254 → 107.8	46	10	35	8
Tebuconazole	ESI (+)	6.17	308.2 → 70.1	91	10	47	7
			308.2 → 125	91	10	53	13
Terbuthylazine	ESI (+)	5.23	230.1 → 174.1	76	7.5	23	12
			230.1 → 104.1	76	7.5	41	12
Terbutryn	ESI (+)	4.09	242 → 186	61	10	27	8
			242 → 68	61	10	63	6
Tetraacetylethylenediamine	ESI (+)	2.85	229.1 → 145.1	36	10	15	8
			229.1 → 85.9	36	10	37	8
Tetracycline	ESI (+)	2.71	445.1 → 409.9	71	10	27	6
			445.1 → 153.9	71	10	35	8
Thiacloprid	ESI (+)	3.06	253.2 → 126	111	12	29	14
			253.2 → 186.1	111	12	19	18
Thiophanate-methyl	ESI (+)	3.34	343 → 151	56	10	15	27
			343 → 192	56	10	25	11
Thioridazine	ESI (+)	3.93	371 → 126.1	66	10	29	6
			371 → 98	66	10	51	8
Tolfenpyrad	ESI (+)	7.03	384.2 → 197.1	131	10	37	15
			384.2 → 91	116	10	37	15
Tonalide	ESI (+)	7.54	259.1 → 175.1	71	10	25	8
			259.1 → 147.1	71	10	37	6
Triasulfuron	ESI (+)	3.36	402 → 167	76	10	25	14
			402 → 141	71	10	29	14
Triazophos	ESI (+)	5.65	314 → 161.9	66	10	27	8
			314 → 119	66	10	51	8
Trifloxystrobin	ESI (+)	6.73	409.1 → 186	61	10	23	19
			409.1 → 205.9	61	10	21	19
Trimethoprim	ESI (+)	2.65	291.1 → 260.9	81	10	35	16
			291.1 → 123	81	10	33	6
Triphenylphosphineoxide	ESI (+)	5.05	279.1 → 201	96	10	37	10
			279.1 → 76.9	96	10	67	6
Triphenyltin	ESI (+)	8.52	351 → 119.8	126	10	73	6
			351 → 196.9	126	10	37	6
Tris(2-butoxyethyl) phosphate	ESI (+)	6.89	399.2 → 299.1	26	10	19	4
			399.2 → 198.8	26	10	23	8
Vancomycin	ESI (+)	0.49	724.7 → 99.9	81	10	73	8
			724.7 → 74	81	10	101	6
17-alpha-Estradiol	ESI(-)	5.47	271 → 144.8	-290	-10	-54	-11
			271 → 142.5	-290	-10	-80	-7
17-alpha-Ethinylestradiol	ESI(-)	5.44	295 → 144.6	-180	-10	-54	-13

Table A.2. Continued.

Compound	Ionization mode	RT (min)	MRM Transitions	DP	EP	CE	CXP
			295 → 142.8	-180	-10	-84	-11
17-beta-Estradiol	ESI(-)	5.39	271.2 → 182.6	-155	-10	-56	-11
			271.2 → 144.7	-155	-10	-58	-17
1-Hydroxyibuprofen	ESI(-)	3.57	220.9 → 158.7	-60	-10	-16	-9
			220.9 → 176.4	-60	-10	-10	-5
2,4,6-Tribromophenol	ESI(-)	6.11	328.5 → 78.8	-45	-10	-64	-7
			328.5 → 80.6	-45	-10	-64	-5
2,4-Dibromophenol	ESI(-)	5.05	250.6 → 80.5	-60	-10	-50	-5
			250.6 → 78.6	-60	-10	-54	-11
2,4-Dinitrophenol	ESI(-)	3.82	183 → 122.6	-5	-10	-26	-3
			183 → 152.4	-5	-10	-24	-15
2-Hydroxyibuprofen	ESI(-)	3.57	221.2 → 132.6	-60	-10	-12	-9
			221.2 → 176.6	-60	-10	-14	-9
4-Nonylphenoxy acetic acid	ESI(-)	7.75	277 → 218.7	-80	-10	-24	-7
			277 → 132.6	-80	-10	-60	-11
Chloramphenicol	ESI(-)	3	320.8 → 151.5	-70	-10	-24	-11
			320.8 → 256.5	-70	-10	-18	-13
Dodecyl sulfate	ESI(-)	9.94	265.2 → 96.6	-85	-10	-38	-3
			265.2 → 79.8	-85	-10	-98	-13
Isobutyl paraben	ESI(-)	5.08	193 → 91.7	-75	-10	-34	-7
			193 → 135.6	-75	-10	-24	-11
Methyl paraben	ESI(-)	3.11	151 → 135.6	-60	-10	-20	-13
			151 → 91.6	-60	-10	-30	-5
Methylsalicylate	ESI(-)	3.11	151.1 → 135.7	-70	-10	-20	-9
			151.1 → 91.6	-70	-10	-28	-13
Propyl paraben	ESI(-)	4.1	179 → 91.7	-60	-10	-36	-9
			179 → 135.7	-60	-10	-22	-11
Tetrabromobisphenol A	ESI(-)	6.9	538.8 → 78.5	-130	-10	-100	-7
			538.8 → 288.5	-130	-10	-50	-1
Triclosan	ESI(-)	6.77	286.7 → 35.1	-55	-10	-28	-5
			286.7 → 218.5	-55	-10	-14	-7
2-(2-Naphthalenyl)benzothiophene	APCI(+)	7.9	261 → 228.1	66	10	40	8
			261 → 260	66	10	40	8
3-Nitrobenzanthrone	APCI(+)	6.56	276 → 202	100	10	44	7
			276 → 230	100	10	33	10
7H-Benzo(de)anthracen-7-one (Benzanthrone)	APCI(+)	6.43	230.8 → 202	40	10	45	14
			230.8 → 150	40	10	89	5
Benzo[a]anthracene	APCI(+)	7.62	228 → 226	160	10	51	10
			228 → 222	160	10	51	10
Tris(1-chloro-2-propanyl) phosphate	APCI(+)	5.36	327.3 → 98.9	6	10	40	8
			327.3 → 80.8	6	10	86	9
Zincpyrithione	APCI(+)	4.02	315.9 → 142	42	10	35	8
			315.9 → 188.9	42	10	35	8

Table A.2. Continued.

Compound	Ionization mode	RT (min)	MRM Transitions	DP	EP	CE	CXP
alpha-Terpineol	APCI(+)	5.4	137.2 → 80.8	10	10	16	6
			137.2 → 136.9	10	10	19	10
Methyldihydrojasmonate	APCI(+)	5.6	227.4 → 209.1	30	10	14	9
			227.4 → 153	30	10	19	7
Methyl -iso-propylcyclohexenone	APCI(+)	4.42	151.4 → 109	38	10	13	6
			151.4 → 123	38	10	17	7
Cyclopentadecanolide	APCI(+)	7.86	241.2 → 223.2	42	10	13	6
			241.2 → 205.3	42	10	15	9
Anthracene	APCI(+)	6.94	178 → 152	152	10	45	8
			178 → 176	152	10	51	8
Fluoranthene	APCI(+)	6.43	202.1 → 200	160	10	55	8
			202.1 → 150	160	10	65	8
Benzo[ghi]perylene	APCI(+)	8.26	276 → 274	281	10	77	42
			276 → 272	281	10	105	14
Indeno[1,2,3-cd]pyrene	APCI(+)	8.27	276 → 274.1	291	10	71	24
			276 → 272.1	291	10	97	26
Benzo[b]fluoranthene	APCI(+)	7.98	252.1 → 250.1	100	10	64	16
			252.1 → 224.1	100	10	85	13
Benzo[k]fluoranthene	APCI(+)	7.98	252.1 → 250.1	172	10	65	15
			252.1 → 224.1	172	10	87	14
Benzo[a]pyrene	APCI(+)	7.97	253.1 → 252.1	80	10	50	16
			253.1 → 250.1	80	10	80	10
Trifluralin	APCI(+)	7.34	336.4 → 232	17	10	25	11
			336.4 → 236	17	10	25	11
1,2,5,6,9,10-Hexabromocyclododecane	APCI(-)	7.83	640.6 → 78.5	-39	-10	-62	-7
			640.6 → 80.7	-39	-10	-44	-5
1,3-Dinitropyrene	APCI(-)	7.11	291.9 → 262	-40	-10	-24	-8
			291.9 → 232.1	-40	-10	-40	-8
1,6-Dinitropyrene	APCI(-)	7.11	291.9 → 261.7	-18	-10	-24	-8
			291.9 → 231.6	-18	-10	-32	-8
1,8-Dinitropyrene	APCI(-)	7.11	291.9 → 261.9	-35	-10	-24	-8
			291.9 → 231.6	-35	-10	-36	-8
2,2',3,3',4,4',5,5',6,6'-Decabromodiphenyl ether	APCI(-)	9.42	894.3 → 79	-55	-10	-108	-10
			894.3 → 81.1	-55	-10	-108	-10
2,2',3,3',4,4',5,5',6-Nonabromodiphenyl ether	APCI(-)	9.29	816.5 → 79	-30	-10	-105	-10
			816.5 → 80.9	-30	-10	-105	-10
2,2',3,4,4',5,5',6-Octabromodiphenyl ether	APCI(-)	9.04	736.5 → 78.6	-61	-10	-99	-10
			736.5 → 80.5	-61	-10	-99	-10
2,2',3,4,4',5',6-Heptabromodiphenyl ether	APCI(-)	8.78	658.5 → 79	-55	-10	-100	-7
			658.5 → 80.9	-55	-10	-100	-7
2,2',4,4',5,5'-Hexabromodiphenyl ether	APCI(-)	8.68	578.6 → 78.9	-60	-10	-110	-7
			578.6 → 81	-60	-10	-110	-7
2,2',4,4',5,6'-Hexabromodiphenyl ether	APCI(-)	8.68	578.6 → 79	-50	-10	-85	-7

Table A.2. Continued.

Compound	Ionization mode	RT (min)	MRM Transitions	DP	EP	CE	CXP
			578.6 → 80.9	-50	-10	-85	-7
2,2',4,4'-Tetrabromodiphenyl ether	APCI(-)	7.98	420.8 → 78.7	-45	-10	-50	-7
			420.8 → 80.6	-45	-10	-50	-7
2,3,3',4,4',5,5',6-Octabromodiphenyl ether	APCI(-)	9.04	736.6 → 78.9	-30	-10	-100	-10
			736.6 → 81	-30	-10	-100	-10
2,4,4'-tribromodiphenylether	APCI(-)	7.68	343 → 78.8	-48	-10	-60	-10
			343 → 80.5	-48	-10	-60	-10
Bisphenol-A	APCI(-)	4.28	226.9 → 211.1	-60	-10	-28	-10
			226.9 → 132.7	-60	-10	-28	-10
Hexachlorobenzene	APCI(-)	8.21	264.8 → 264.4	-15	-10	-14	-13
			264.8 → 35	-15	-10	-47	-8
Musk ambrette	APCI(-)	6.75	252.9 → 45.9	-35	-10	-60	-10
			252.9 → 220.7	-35	-10	-38	-8
Musk ketone	APCI(-)	6.57	264 → 46	-66	-10	-60	-7
			264 → 205.7	-66	-10	-30	-7
Musk xylene	APCI(-)	7.16	266.9 → 46	-33	-10	-52	-12
			266.9 → 175	-33	-10	-35	-7
Pentachlorobenzene	APCI(-)	7.74	230.4 → 194.6	-24	-10	-27	-8
			230.4 → 192.2	-24	-10	-27	-8
Polychlorinated biphenyls	APCI(-)	8.24	340.8 → 340.4	-60	-10	-19	-9
			340.8 → 304.5	-60	-10	-36	-14

APPENDIX B

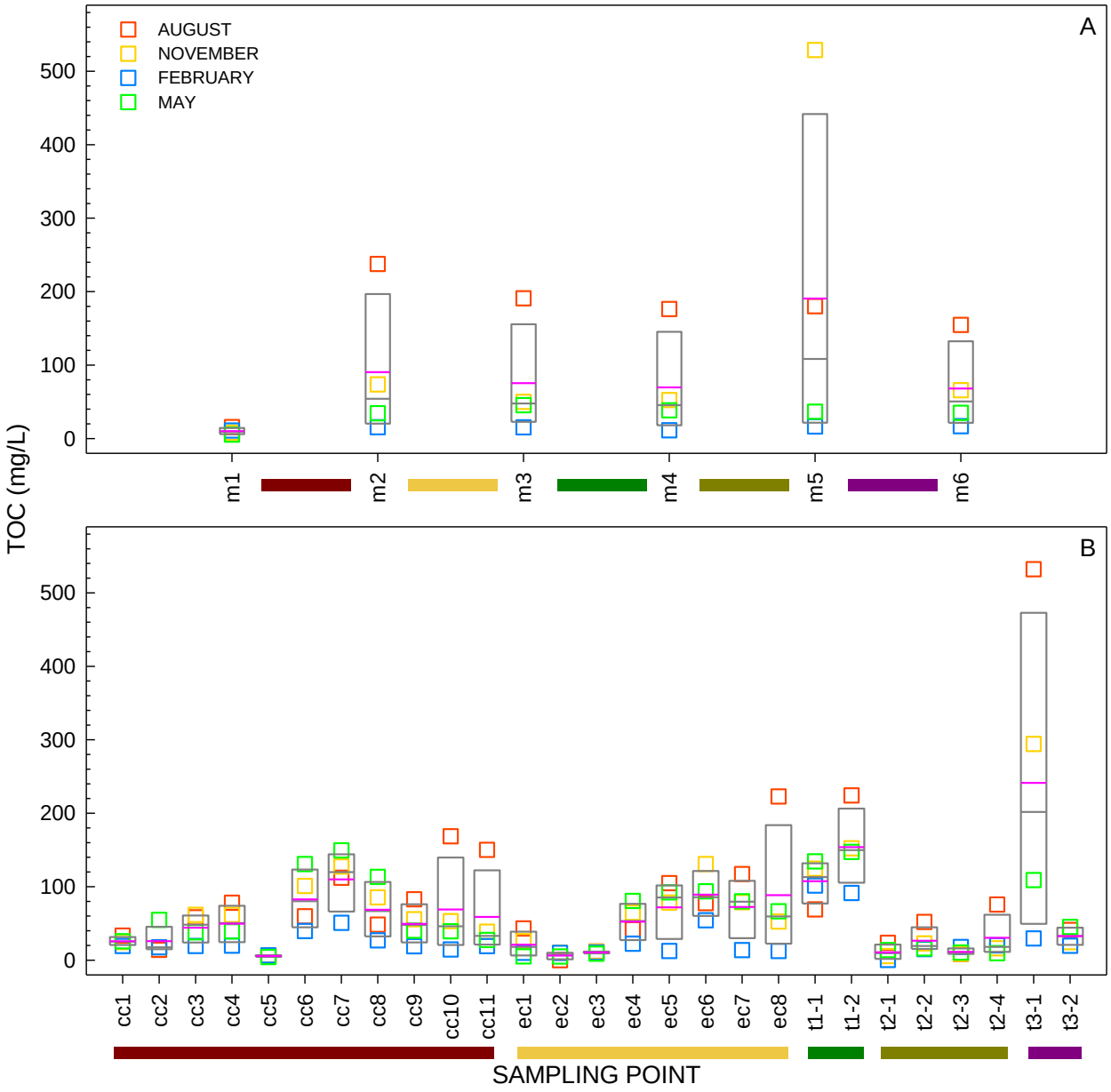

Figure B.1. Seasonal profile of TOC in (A) main stream and (B) tributaries samples taken from ***industrial zone***.

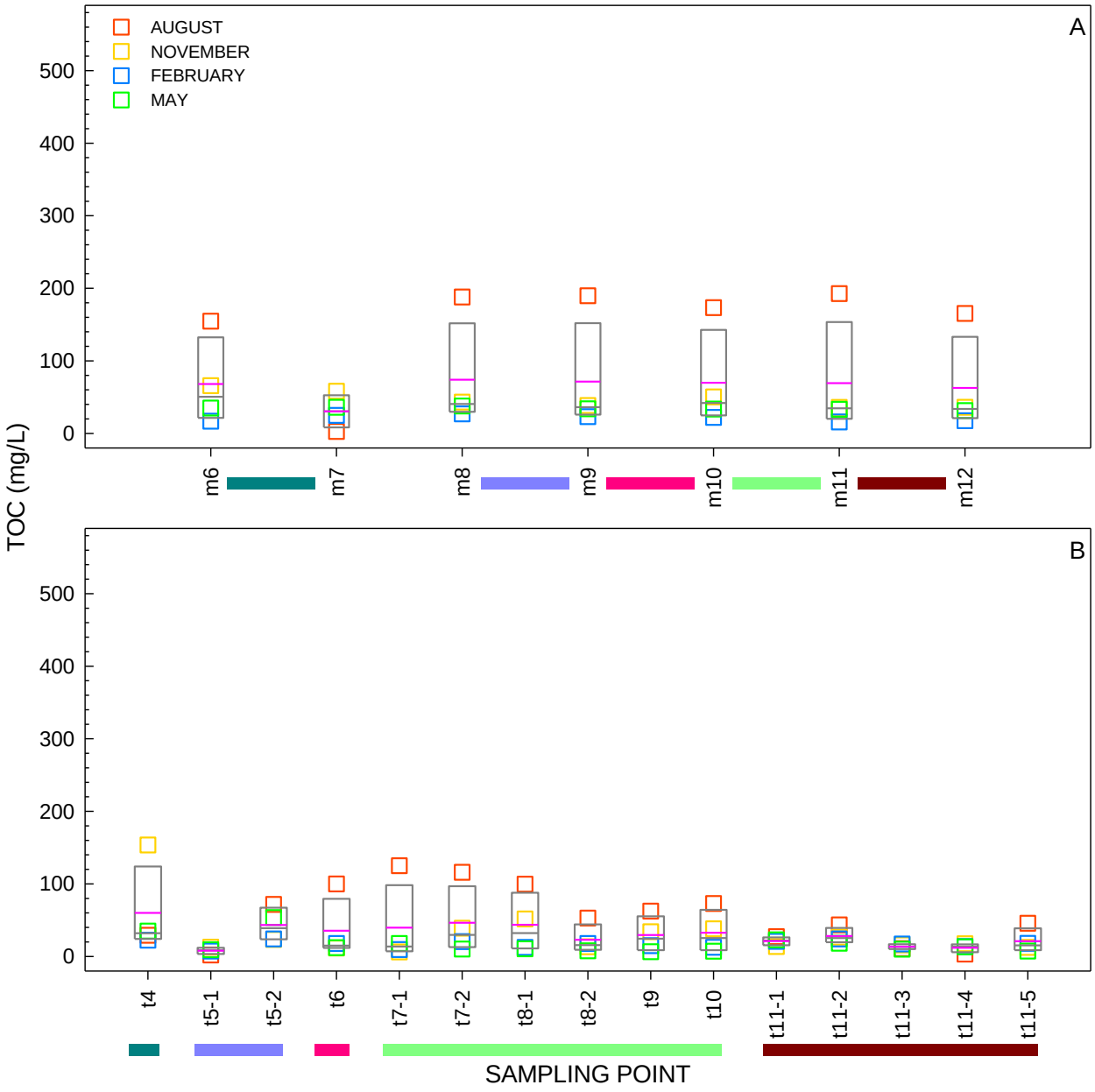

Figure B.2. Seasonal profile of TOC in (A) main stream and (B) tributaries samples taken from ***transition zone***.

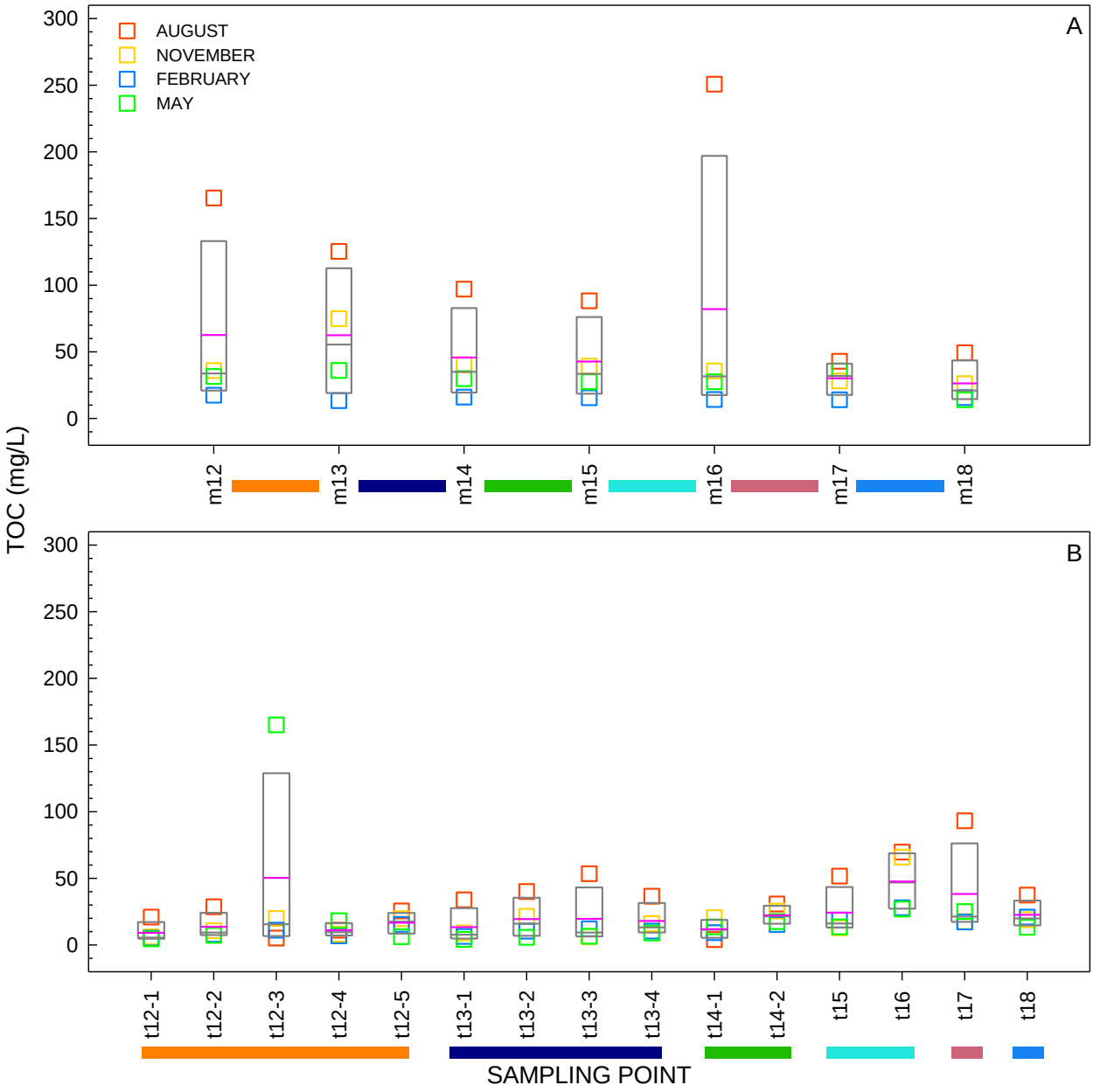

Figure B.3. Seasonal profile of TOC in (A) main stream and (B) tributaries samples taken from ***agricultural zone***.

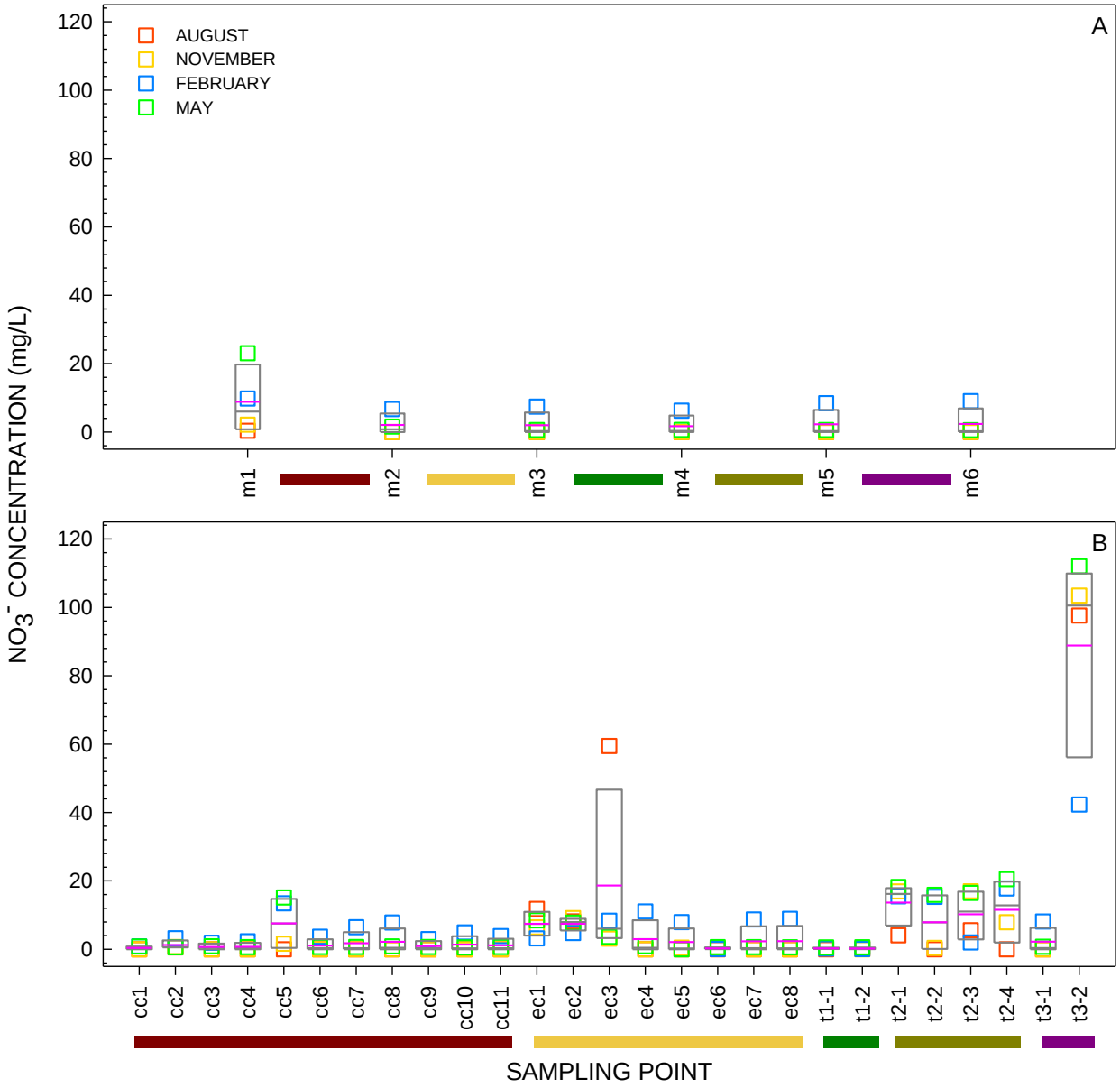

Figure B.7. Seasonal profile of nitrate in (A) main stream and (B) tributaries samples taken from ***industrial zone***.

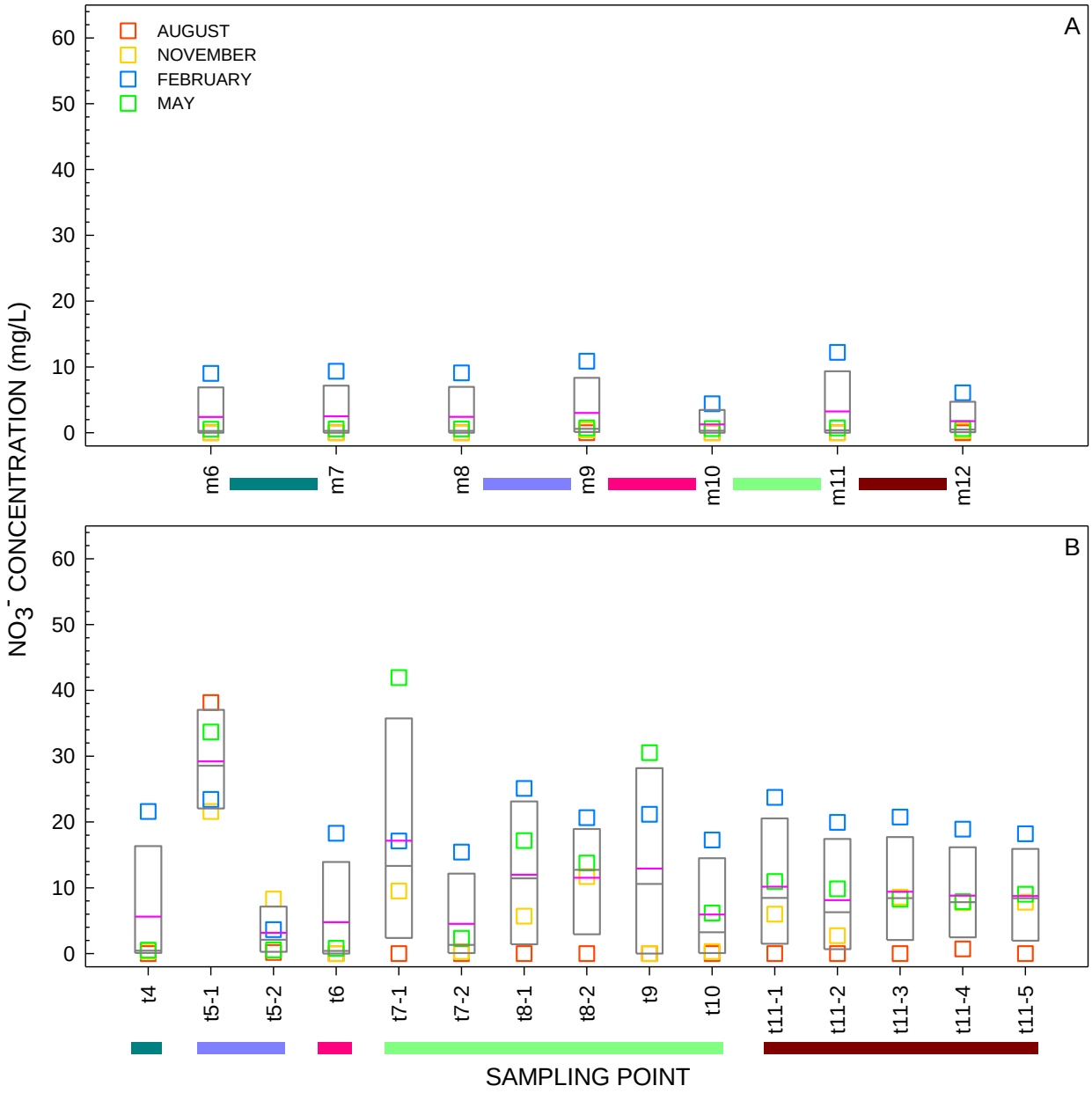

Figure B.8. Seasonal profile of nitrate in (A) main stream and (B) tributaries samples taken from ***transition zone***.

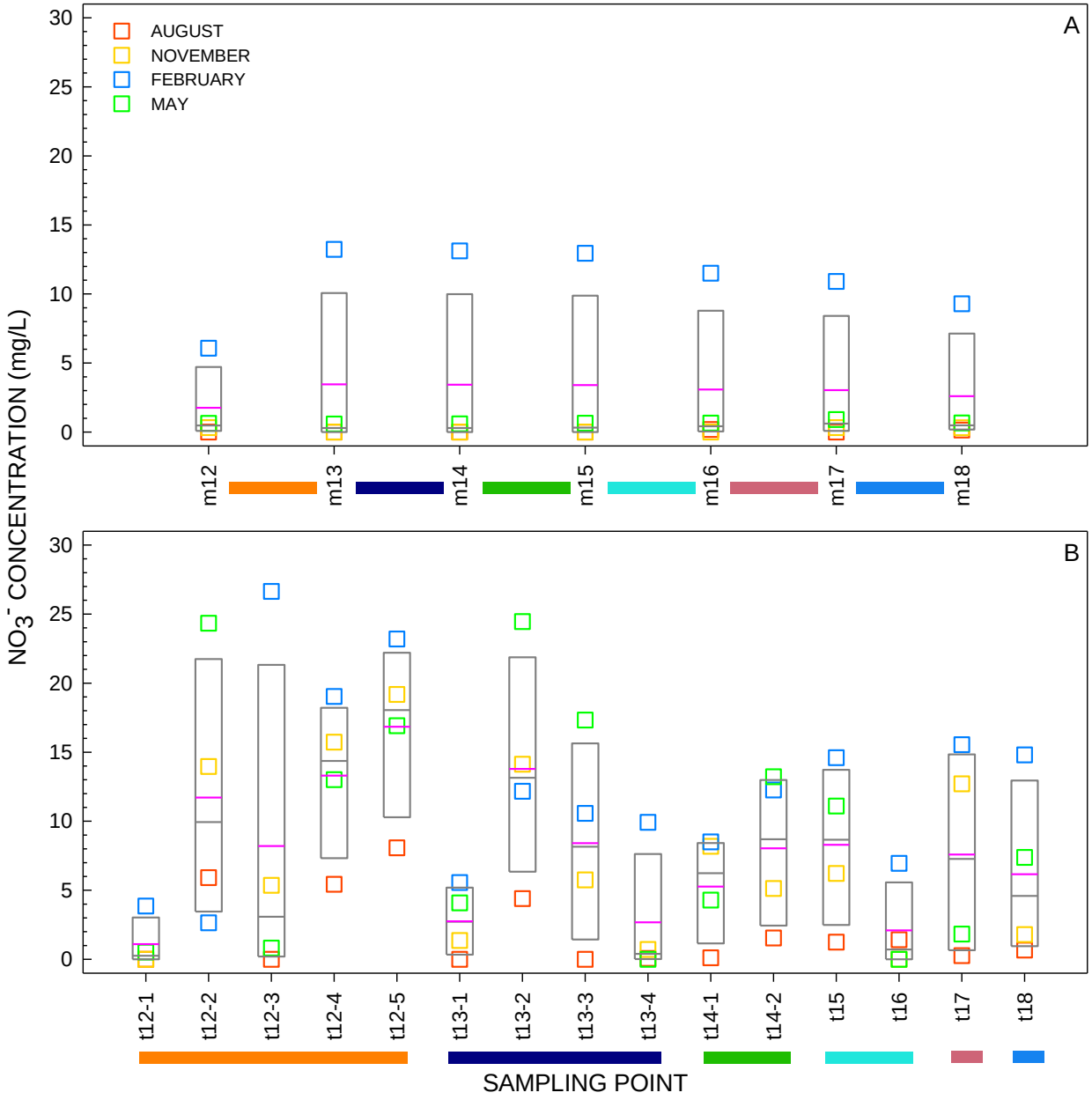

Figure B.9. Seasonal profile of nitrate in (A) main stream and (B) tributaries samples taken from ***agricultural zone***.

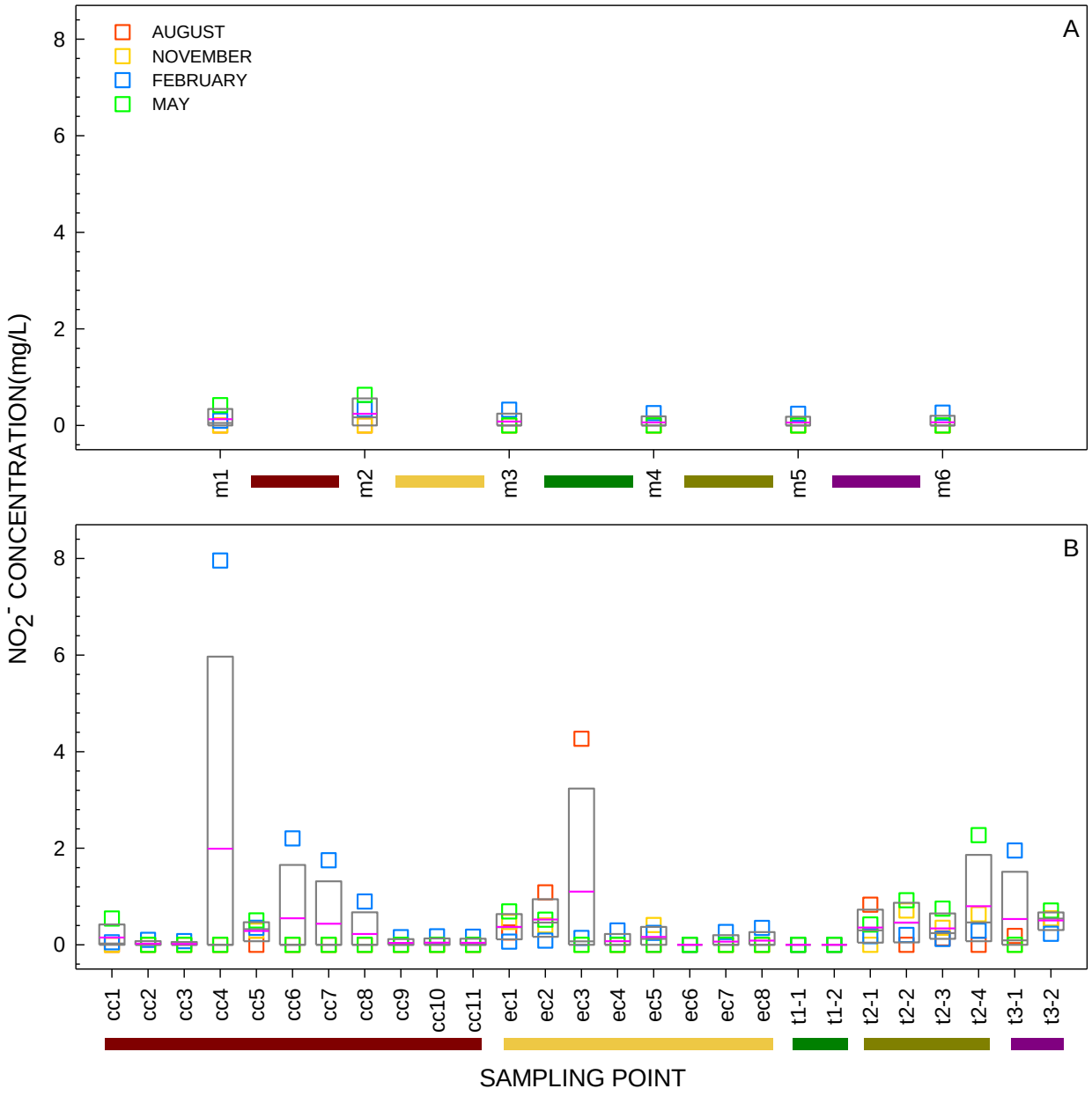

Figure B.10. Seasonal profile of nitrite in (A) main stream and (B) tributaries samples taken from ***industrial zone***.

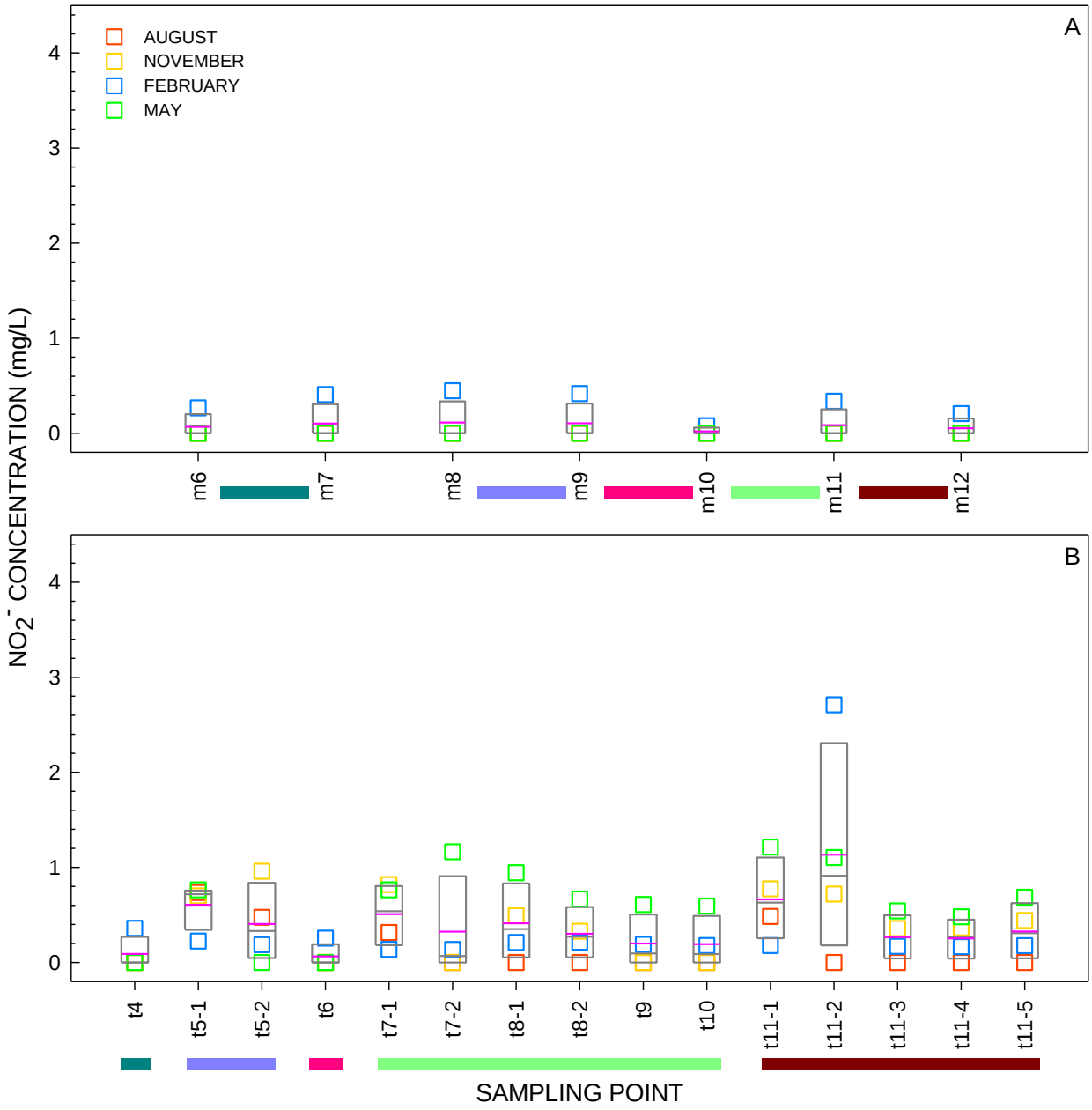

Figure B.11. Seasonal profile of nitrite in (A) main stream and (B) tributaries samples taken from ***transition zone***.

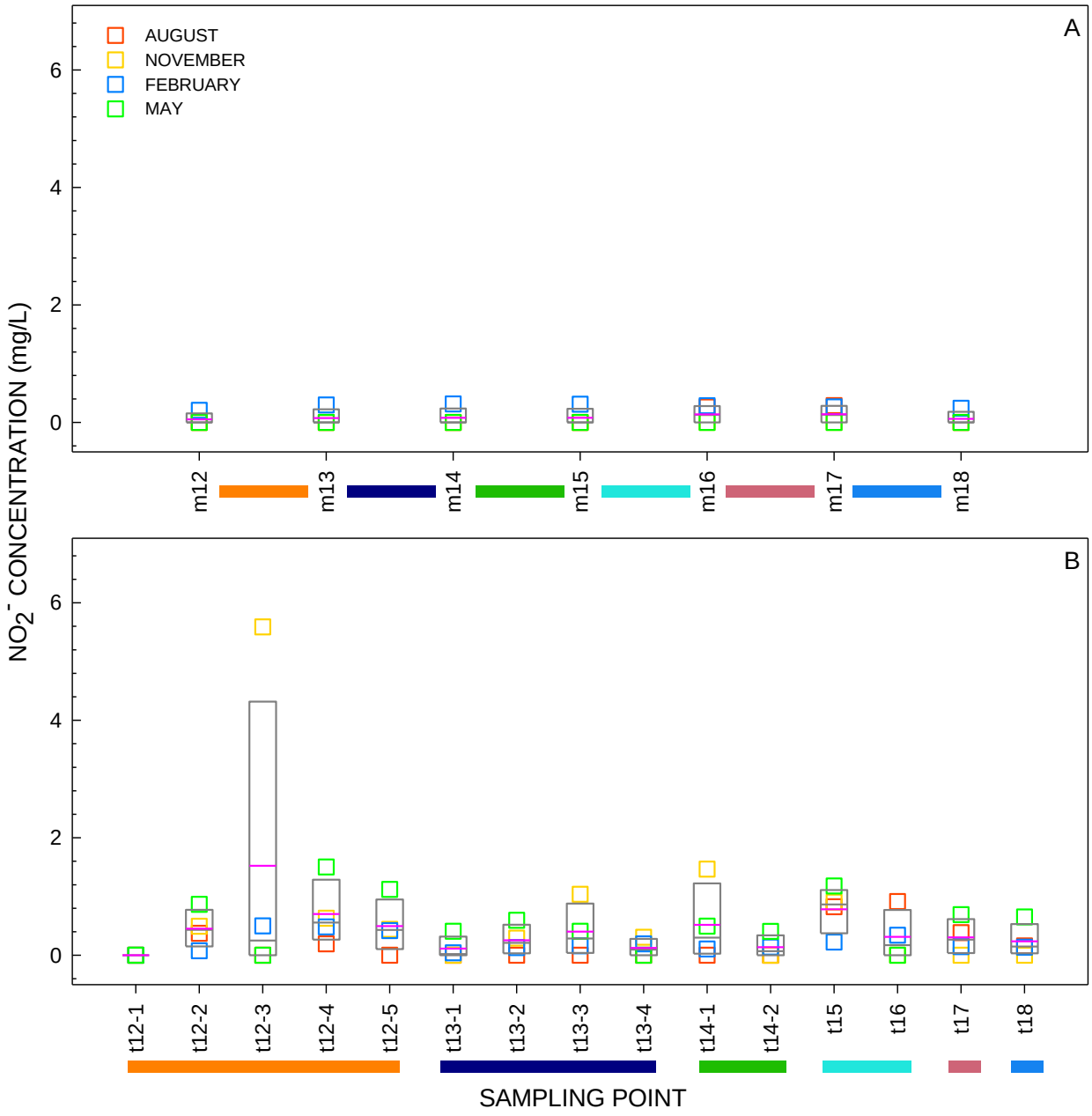

Figure B.12. Seasonal profile of nitrite in (A) main stream and (B) tributaries samples taken from ***agricultural zone***.

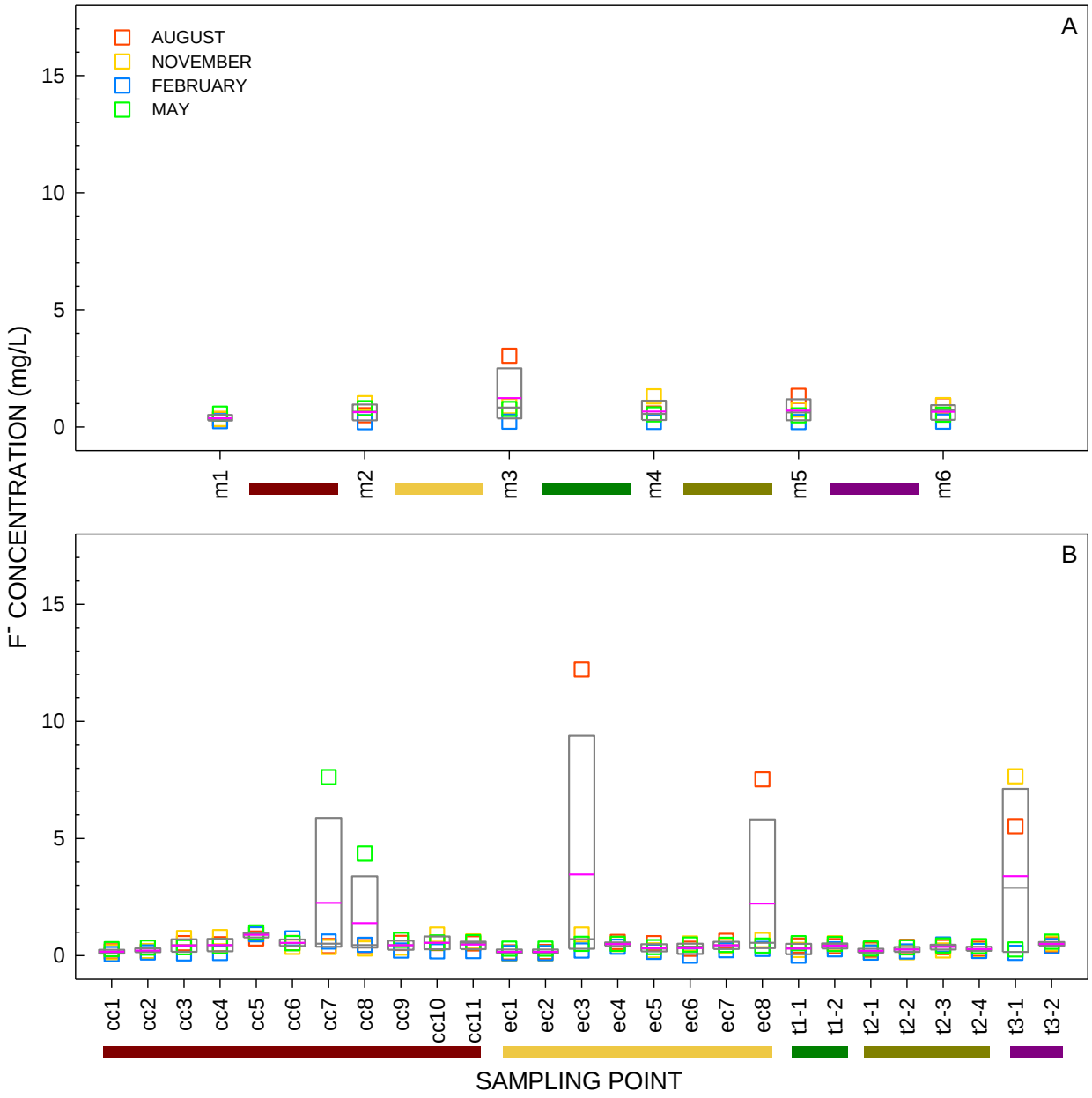

Figure B.16. Seasonal profile of fluoride in (A) main stream and (B) tributaries samples taken from ***industrial zone***.

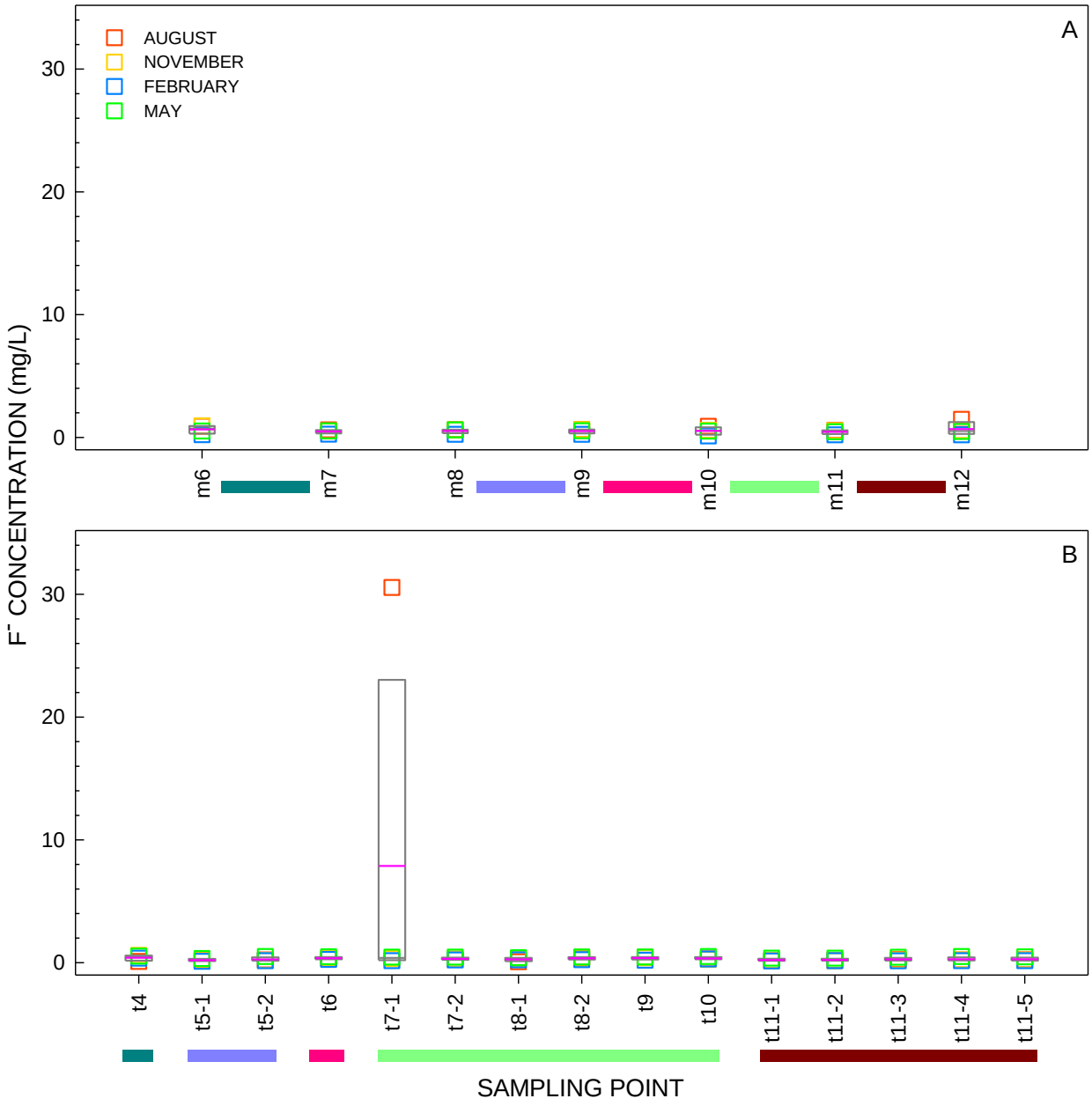

Figure B.17. Seasonal profile of fluoride in (A) main stream and (B) tributaries samples taken from ***transition zone***.

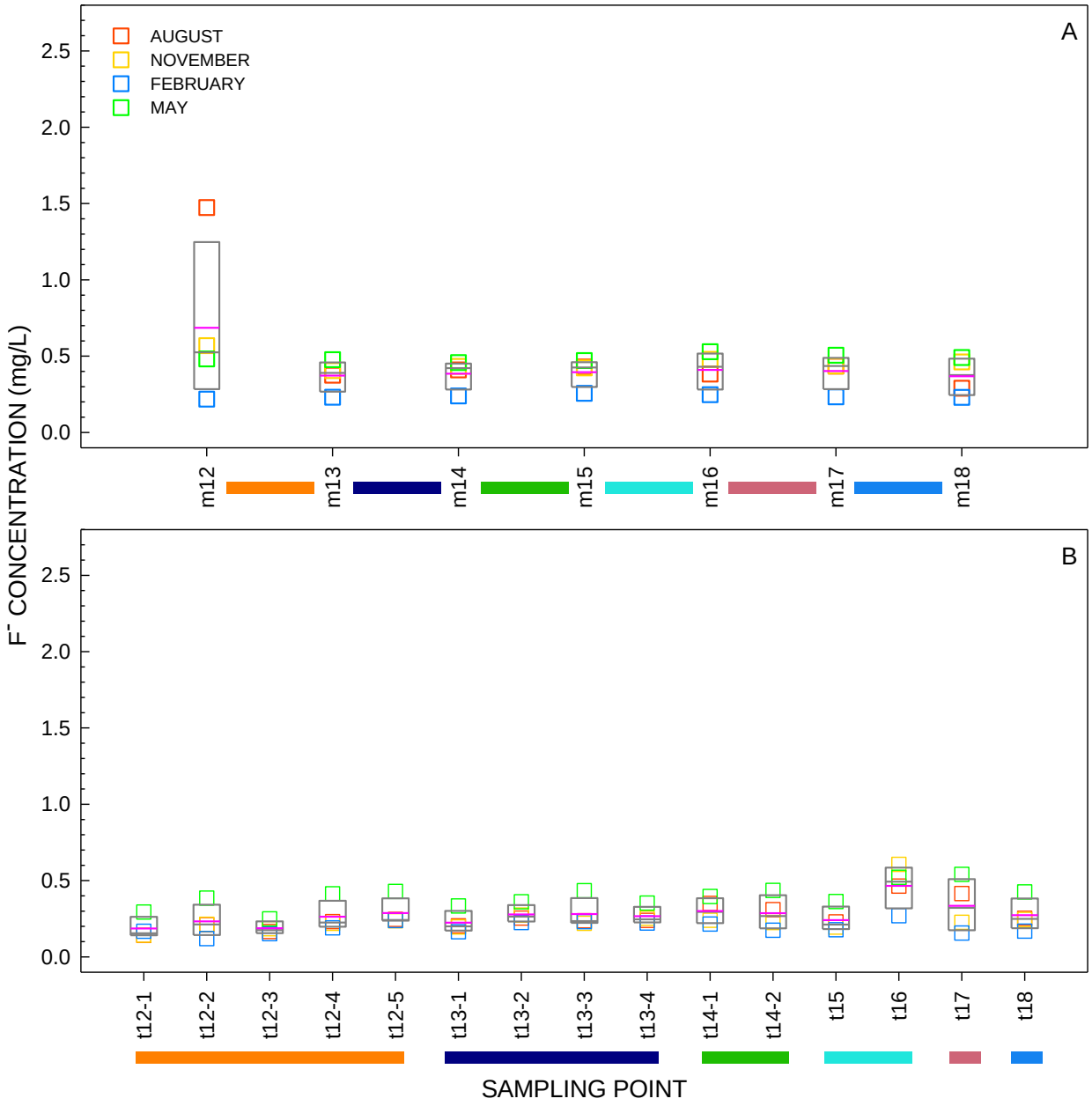

Figure B.18. Seasonal profile of fluoride in (A) main stream and (B) tributaries samples taken from ***agricultural zone***.

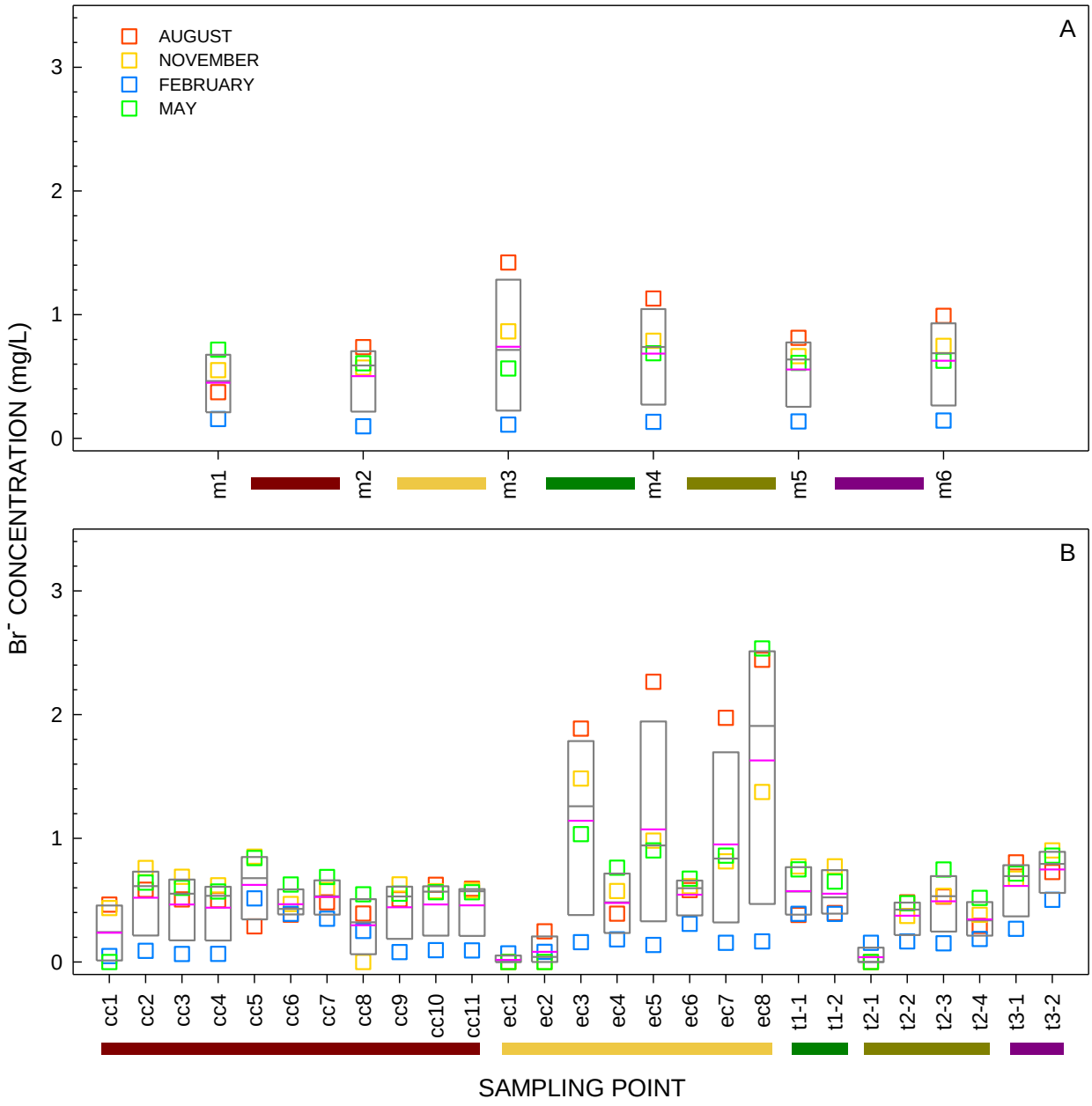

Figure B.19. Seasonal profile of bromide in (A) main stream and (B) tributaries samples taken from ***industrial zone***.

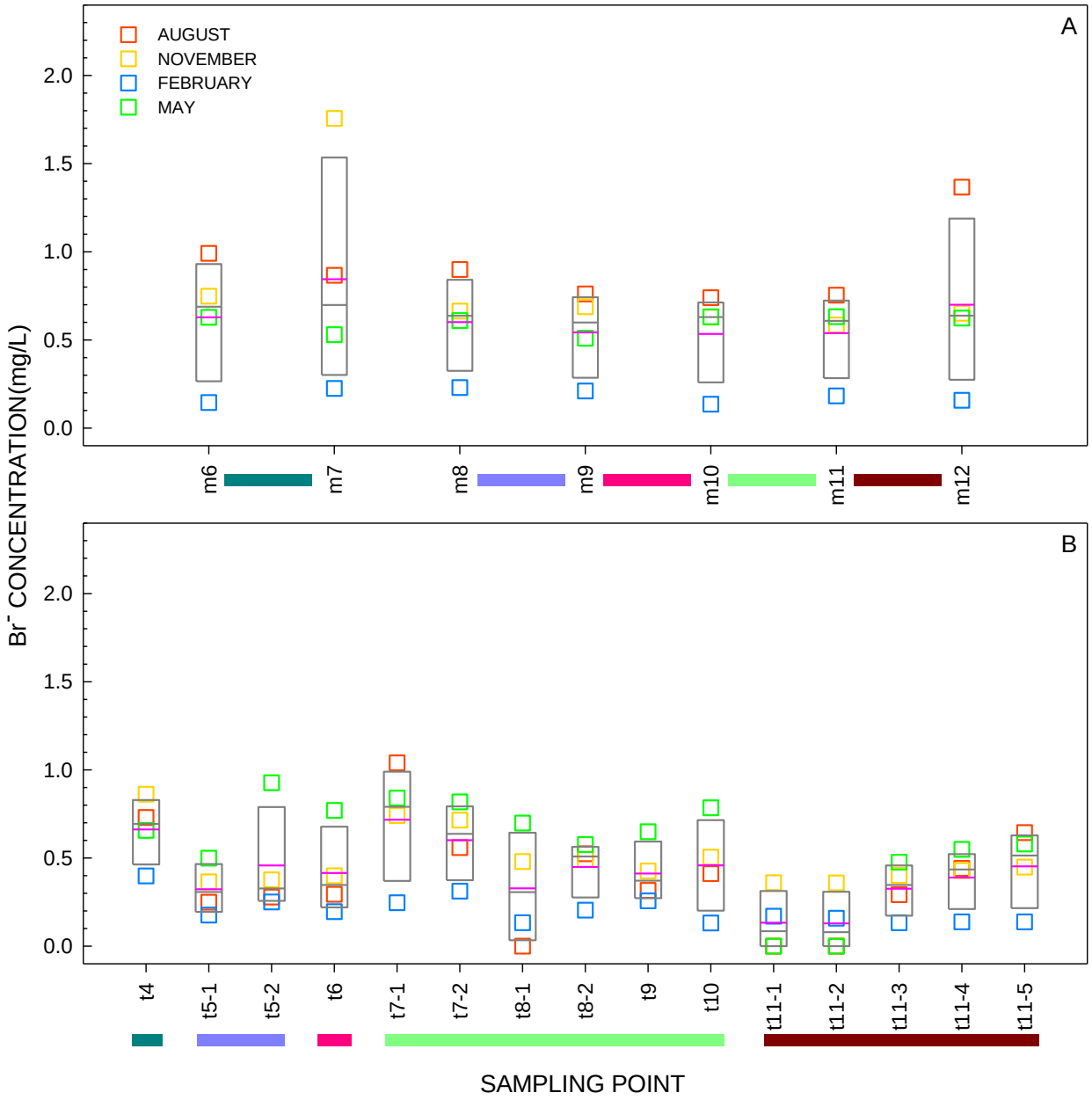

Figure B.20. Seasonal profile of bromide in (A) main stream and (B) tributaries samples taken from ***transition zone***.

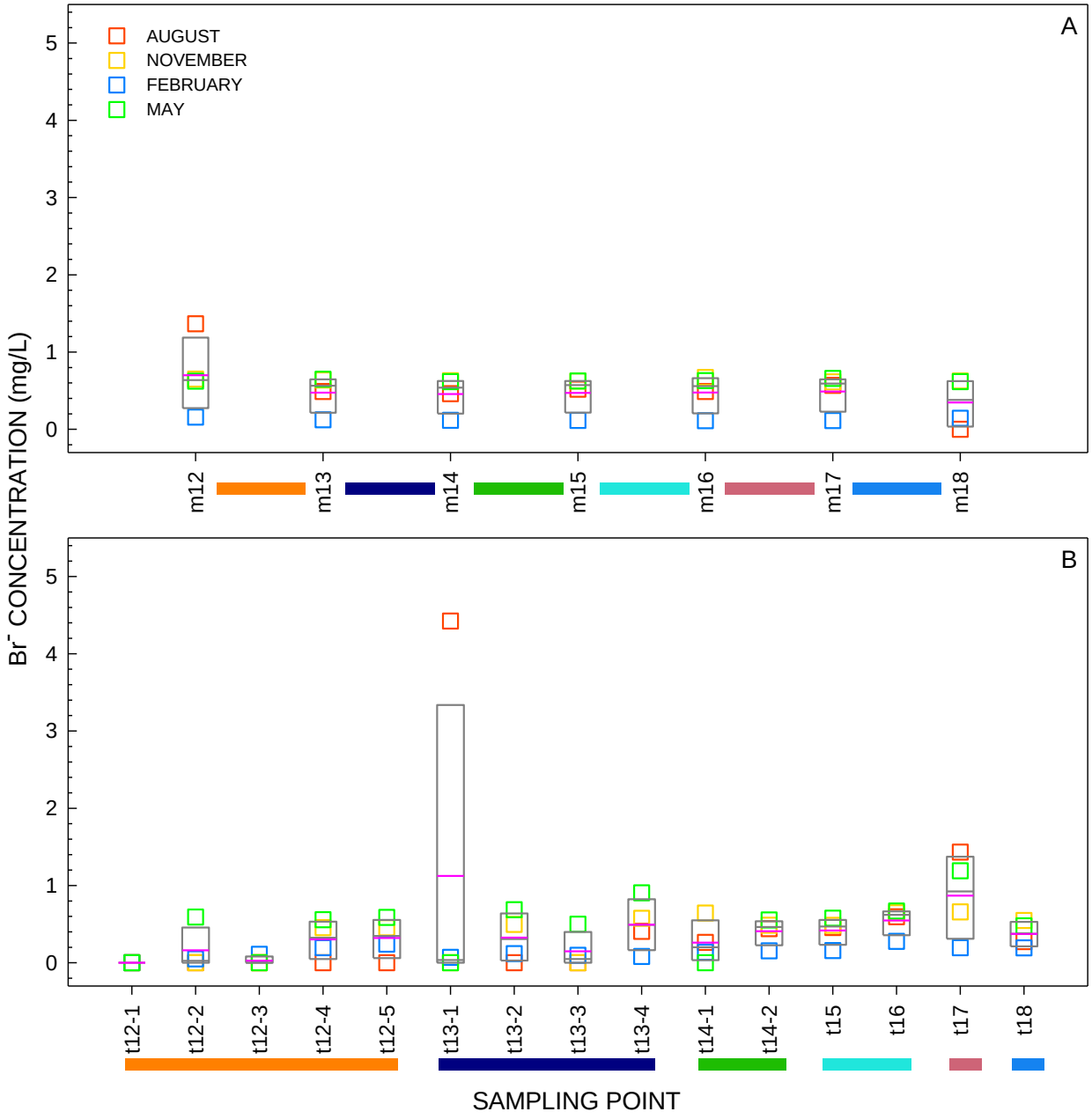

Figure B.21. Seasonal profile of bromide in (A) main stream and (B) tributaries samples taken from ***agricultural zone***.

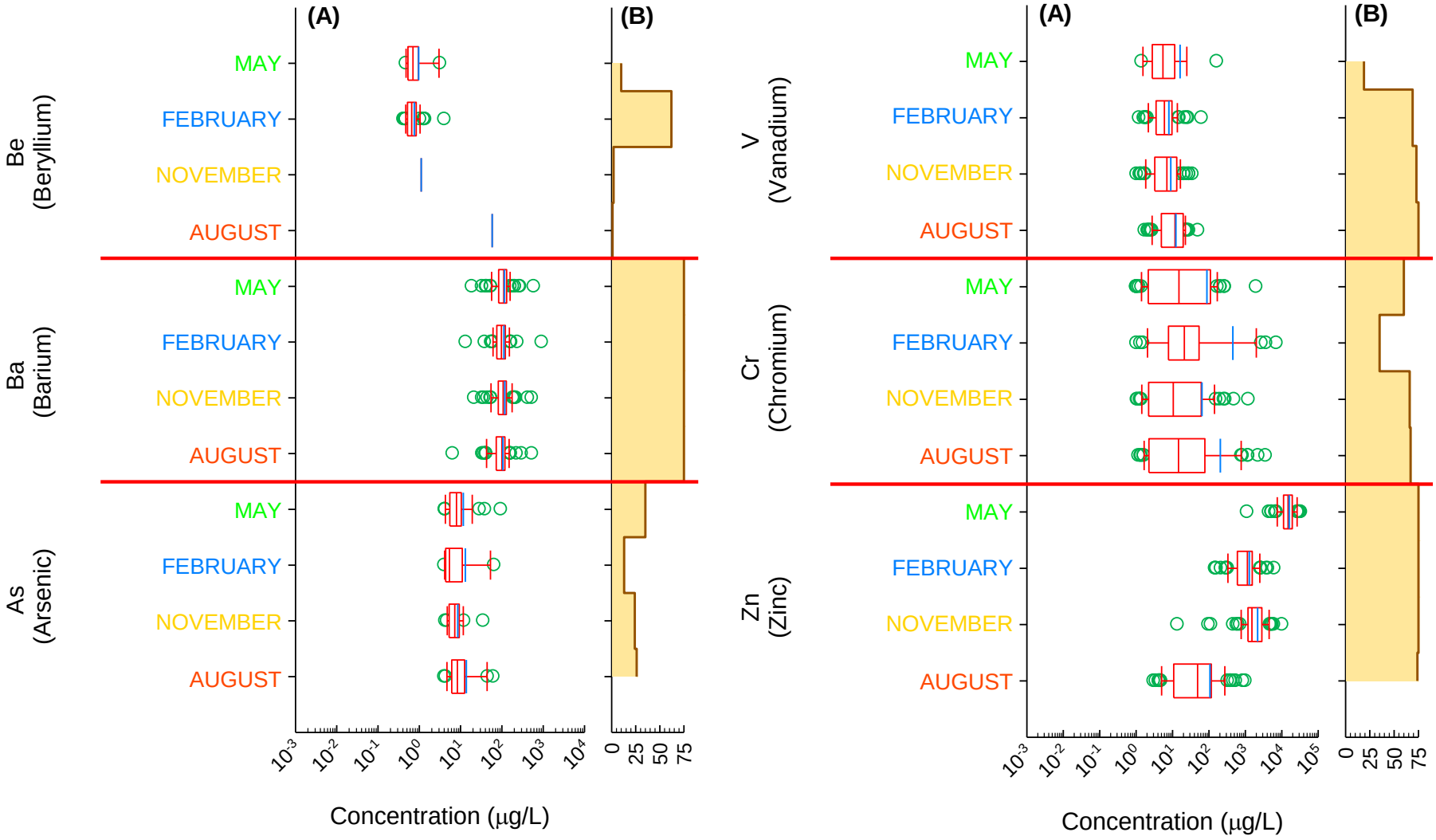

Figure B.22. Seasonal (A) concentration and (B) detection frequency (out of 75) of heavy metals in Ergene River.

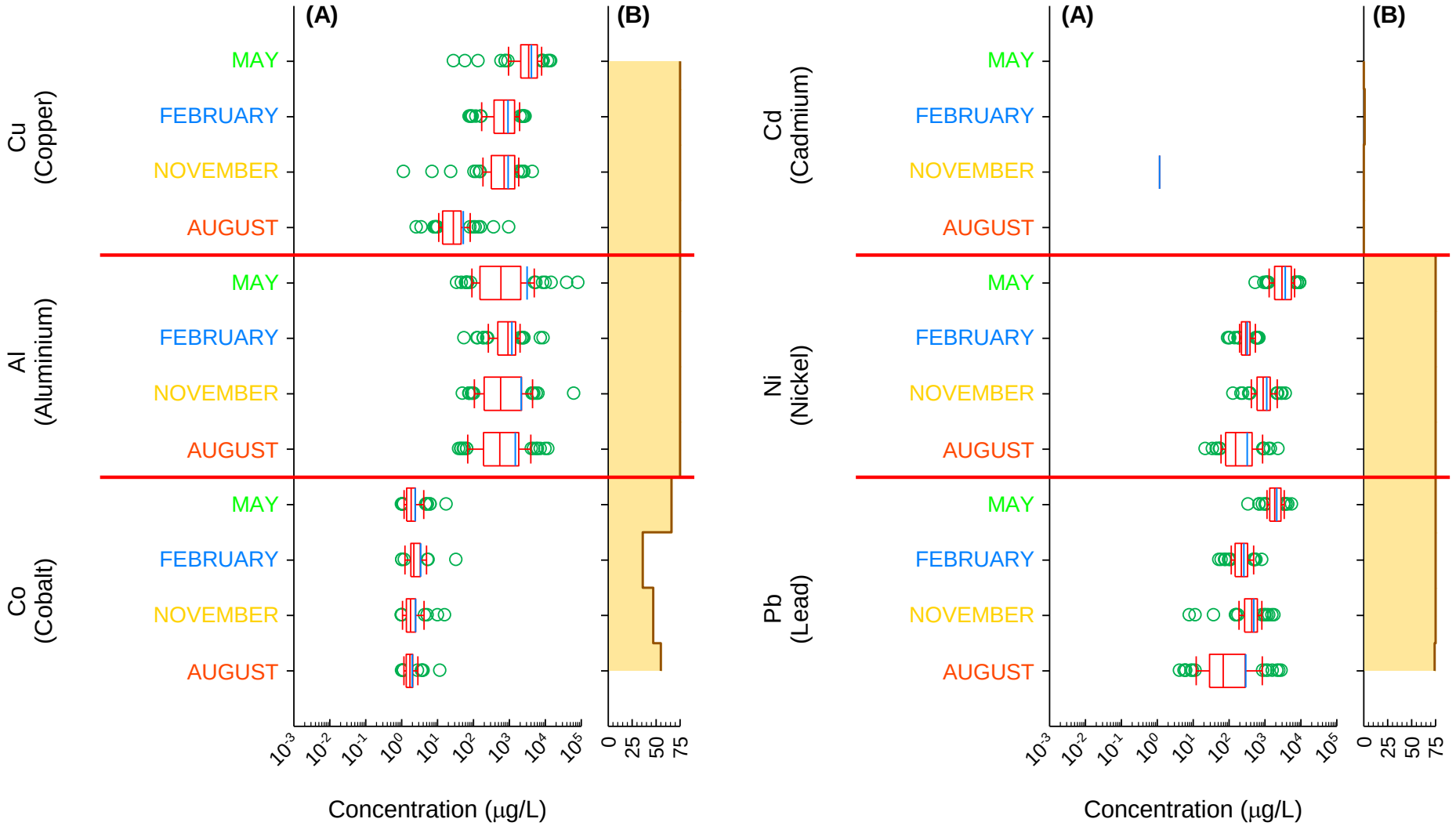

Figure B.22. Continued.

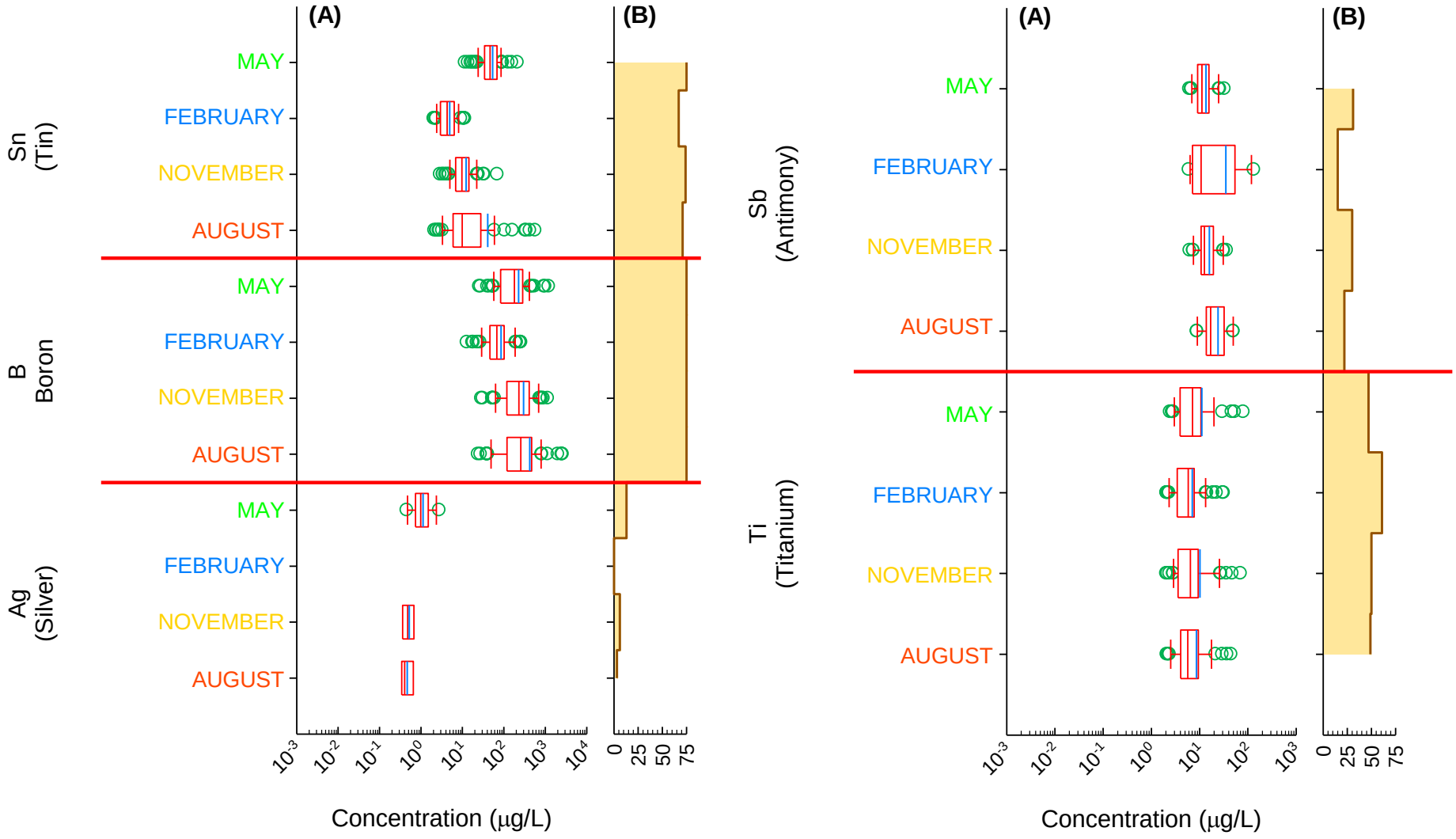

Figure B.22. Continued.

APPENDIX C

Table C.1. LOD and LOQ values of the analytes in this study.

Compound	LOD (ug/L)	LOQ (ug/L)	R^2
1-Hydroxyibuprofen	7.3887	24.6289	0.989
1,2,3-Benzotriazole	0.0831	0.2769	0.998
1,2,5,6,9,10-Hexabromocyclododecane	0.1374	0.4579	0.998
1,3-Dinitropyrene	0.0866	0.2885	0.997
1,6-Dinitropyrene	0.0296	0.0987	0.997
1,8-Dinitropyrene	0.0789	0.2628	0.995
17-alpha-Estradiol	1.5009	5.0031	0.997
17-alpha-Ethinylestradiol	1.8789	6.263	0.994
17-beta-Estradiol	0.8303	2.7675	0.998
2-(2-Naphthalenyl) benzothiophene	0.4447	1.4822	0.993
2,2',3,3',4,4',5,5',6,6'-Decabromodiphenyl ether	0.5829	1.943	0.991
2,2',3,3',4,4',5,5',6-Nonabromodiphenyl ether	0.3983	1.3278	0.999
2,2',3,4,4',5,5',6-Octabromodiphenyl ether	0.1882	0.6273	0.999
2,2',3,4,4',5',6-Heptabromodiphenyl ether	0.1221	0.4071	0.996
2,2',4,4',5,5'-Hexabromodiphenyl ether	0.0418	0.1392	0.998
2,2',4,4',5,6'-Hexabromodiphenyl ether	0.2806	0.9353	0.998
2,2',4,4'-Tetrabromodiphenyl ether	1.0936	3.6455	0.996
2,3,3',4,4',5,5',6-Octabromodiphenyl ether	0.1241	0.4136	0.999
2,4,4'-tribromodiphenylether	1.2483	4.1611	0.998
2,4,6-Tribromophenol	0.1736	0.5785	0.991
2,4-Dibromophenol	0.1393	0.4645	0.991
2,4-Dihydroxybenzophenone	0.0039	0.0129	0.999
2,4-Dinitrophenol	0.6569	2.1897	0.998
2-Hydroxyibuprofen	2.4138	8.0461	0.992
2-Mercapto-benzothiazole	0.0167	0.0556	0.993
2-Methylanthraquinone	0.0184	0.0614	0.999
3-Chloroaniline	0.0229	0.0762	0.998
3-Nitrobenzanthrone	0.3446	1.1488	0.997
4,4'-Dichlorobenzophenone	0.047	0.1568	0.998
4-Aminomethyl-benzenesulfonamide	0.0186	0.0621	0.999
4-Chloroaniline	0.0152	0.0508	0.997
4-Methyl-1H-benzotriazole	0.0145	0.0482	0.999
4-Methylbenzylidenecamphor	0.0682	0.2275	0.999
4-Nonylphenoxy acetic acid	1.7505	5.835	0.984
4-tert-Octylphenol diethoxylate	0.012	0.04	0.997
4-tert-Octylphenol monoethoxylate	1.322	4.4067	0.989
5,6-Dimethyl-1H-benzotriazole	0.0055	0.0182	0.997
5-Methyl-1H-benzotriazole (5-Tolytriazole)	0.0224	0.0747	0.997
7H-Benzo(de)anthracen-7-one (Benzanthrone)	0.0377	0.1257	0.996
8-Hydroxyquinoline	0.013	0.0433	0.999
Acetaminophen (Paracetamol)	0.0455	0.1516	0.998

Table C.1. Continued.

Compound	LOD (ug/L)	LOQ (ug/L)	R^2
Acetamiprid	0.0252	0.0841	0.994
Acetochlor	0.0603	0.2008	0.995
Aclonifen	0.0569	0.1896	0.998
ADBI (Celestolide)	0.0114	0.038	0.998
AHDI (Phantolide)	0.0668	0.2227	0.999
Alachlor	0.0769	0.2563	0.998
alpha-Terpineol	3.1507	10.5022	0.989
Amoxicillin	0.0991	0.3303	0.999
Anthracene	1.5064	5.0213	0.988
ATII (Traseolide)	0.1368	0.4561	0.997
Atrazine	0.0071	0.0237	0.999
Atrazine-desethyl	0.0201	0.0669	0.996
Azinphos-methyl	1.7247	5.7491	0.992
Azithromycin	0.0106	0.0352	0.997
Azoxystrobin	0.0284	0.0947	0.995
Bayrepel	1.3408	4.4693	0.992
Banzaldehyde, (phenylmethylene)hydrazone	0.0146	0.0488	0.998
Benzenesulfonamide	2.0702	6.9006	0.993
Benzo[a]anthracene	0.014	0.0467	0.996
Benzo[a]pyrene	0.0041	0.0138	0.995
Benzo[b]fluoranthene	0.2545	0.8482	0.993
Benzo[ghi]perylene	0.0506	0.1685	0.997
Benzo[k]fluoranthene	0.0017	0.0056	0.995
Benzothiazole	4.0245	13.415	0.987
Benzylamine	0.0201	0.0671	0.999
Benzyldimethyldodecylammonium	0.0059	0.0198	0.999
Benzyldimethylhexadecylammonium	0.0035	0.0116	0.993
Benzyldimethyltetradecylammonium	0.0032	0.0107	0.996
Benzyltrimethylammonium	0.0067	0.0224	1
Bifenox	0.0859	0.2863	0.996
Bisphenol-A	1.1017	3.6723	0.995
Boisvelone / Iso-Esuper	1.6544	5.5145	0.972
Boscalid	0.134	0.4466	0.997
Buprofezin	0.0383	0.1278	0.997
Butylmethoxydibenzoylmethane	0.3144	1.048	0.991
Cadusafos	0.0597	0.1992	0.997
Carbazole	0.0712	0.2375	0.994
Carbendazim	0.0248	0.0828	0.995
Carbofuran	0.0152	0.0506	0.997
Chloramphenicol	0.0542	0.1805	0.997
Chlorfenvinphos	0.034	0.1132	0.999
Chloridazon	0.1374	0.458	0.997
Chlorpyrifos	0.1251	0.417	0.979
Chlorsulfuron	0.0439	0.1462	0.995
Ciprofloxacin	0.3077	1.0258	0.995

Table C.1. Continued.

Compound	LOD (ug/L)	LOQ (ug/L)	R^2
Clarithromycin	0.0037	0.0124	0.999
Clofentezine	0.0438	0.1461	0.977
Clothianidin	0.1358	0.4528	0.994
Cybutryne	0.0008	0.0027	0.998
Cyclopentadecanolide	0.6776	2.2586	0.996
Cypermethrin	0.7397	2.4658	0.999
Cyprodinil	0.0348	0.116	0.993
Cyromazine	0.0347	0.1156	0.844
Damascone	0.0811	0.2702	0.999
Di(2- ethylhexyl)phthalate (DEHP)	2.6823	8.9409	0.991
Diazinon	0.0527	0.1757	0.998
Dichlorvos	0.1708	0.5693	0.998
Dicloxacillin	0.0183	0.0609	0.997
Dicyclohexylamine	0.0129	0.0431	0.998
Difenoconazole	0.0338	0.1127	0.993
Dimethoate	0.0691	0.2303	0.991
Dimethomorph	0.0151	0.0503	0.997
Diphenylamine	0.1253	0.4177	0.993
Diuron	0.0218	0.0726	0.999
Dodecyl sulfate	3.4595	11.5317	0.998
Doxycycline	0.0403	0.1344	0.997
Drometrizole	0.0214	0.0713	0.993
Epoxiconazole	0.0314	0.1047	0.99
Erythromycin	0.0214	0.0713	0.993
Ethofumesate	0.1148	0.3828	0.996
Ethoprophos	0.0822	0.274	0.993
Ethyl paraben	0.1053	0.3511	0.997
Ethylhexylmethoxycinnamate	0.1168	0.3893	0.979
Fenamiphos	0.0489	0.163	0.991
Fenarimol	0.2104	0.7013	0.993
Fenpropimorph	0.0334	0.1114	0.991
Fenthion	0.3377	1.1256	0.99
Fluopyram	0.0095	0.0316	0.998
Fluoranthene	0.0803	0.2675	0.995
Fluquinconazole	0.0809	0.2698	0.986
Flutolanil	0.0476	0.1588	0.989
Flutriafol	0.0683	0.2275	0.993
Fosthiazate	2.7092	9.0306	0.906
Galaxolide	0.0648	0.2161	0.978
g-Methylionone	0.2221	0.7403	0.989
Hexa(methoxymethyl)melamine	4.1916	13.9718	0.953
Hexachlorobenzene	1.5802	5.2675	0.992
Hexaconazole	0.0228	0.076	0.989
Hexylcinnamaldehyde	0.1442	0.4808	0.996
Hexythiazox	0.0314	0.1046	0.998

Table C.1. Continued.

Compound	LOD (ug/L)	LOQ (ug/L)	R^2
Homosalate	5.8768	19.5892	0.981
Imazalil	0.0735	0.2451	0.992
Imazamox	0.0401	0.1338	0.996
Imidacloprid	0.6194	2.0647	0.995
Indeno[1,2,3-cd]pyrene	0.2066	0.6887	0.997
Isobutyl paraben	0.0202	0.0673	0.998
Isoproturon	0.0184	0.0612	0.998
Lenacil	0.0849	0.2829	0.991
Linuron	0.0386	0.1287	0.999
Malathion	0.8947	2.9824	0.985
Mandipropamid	0.0248	0.0827	0.995
Mepiquat chloride	0.0732	0.2439	0.997
Mesotrione	0.0355	0.1184	0.99
Metalaxyl	0.0423	0.141	0.999
Methamidophos	0.2141	0.7135	0.993
Methidathion	0.6959	2.3197	0.985
Methomyl	0.0181	0.0605	0.987
Methoxyfenozide	0.1357	0.4524	0.989
Methyl -iso-propylcyclohexenone	0.0975	0.3252	0.994
Methyl paraben	0.0917	0.3056	0.997
Methyldihydrojasmonate	0.2457	0.819	0.993
Methylsalicylate	0.1137	0.3789	0.998
Metolachlor	0.021	0.07	0.998
Metrafenone	0.0221	0.0735	0.998
Microcystin-LR	1.5059	5.0196	0.984
Microcystin-RR	0.0445	0.1485	0.997
Microcystin-YR	1.7014	5.6714	0.948
Molinate	0.0339	0.1129	0.988
Monocrotophos	0.0174	0.0581	0.998
Musk ambrette	0.191	0.6366	0.996
Musk ketone	0.3823	1.2743	0.995
Musk xylene	0.079	0.2632	0.996
Myclobutanil	0.0038	0.0126	0.987
N,N-Diethyl-m-toluamide	0.0042	0.0139	0.993
N-Benzyldimethylamine	0.0102	0.0341	0.999
N-Benzylmethylamine	0.0371	0.1237	0.988
N-Ethyl-2-tolysulfonamide	0.0243	0.0812	0.994
N-methyl aniline	0.027	0.09	0.996
Nonylphenol diethoxylate	0.0175	0.0582	0.993
Norfloxacin	0.4866	1.622	0.737
N-phenyl-2-napthylamine	0.0051	0.0171	0.995
Ofloxacin	0.0178	0.0593	0.969
Omethoate	0.087	0.2901	0.994
Oxadiazon	0.3647	1.2157	0.992
Oxadixyl	0.0848	0.2828	0.986

Table C.1. Continued.

Compound	LOD (ug/L)	LOQ (ug/L)	R^2
Oxybenzone	0.0059	0.0196	0.997
Penconazole	0.0345	0.1149	0.995
Pendimethalin	0.0186	0.062	0.996
Pentachlorobenzene	0.1066	0.3554	0.995
Pinoxaden	0.0068	0.0225	0.999
Piperonylbutoxide	0.0042	0.0141	0.997
Pirimicarb	0.1223	0.4075	0.992
Polychlorinated biphenyls	1.6739	5.5798	0.998
Prochloraz	0.0027	0.0082	0.984
Prometryn	0.0095	0.0317	0.997
Propazine	0.0087	0.0291	0.996
Propetamphos	0.1644	0.5479	0.994
Propiconazole	0.068	0.2266	0.991
Propyl paraben	0.0357	0.1191	0.998
Prothioconazole	0.1367	0.4558	0.999
Pyraclostrobin	0.0163	0.0542	0.999
Pyridaben	0.0124	0.0412	0.997
Pyrimethanil	0.0679	0.2264	0.998
Pyriproxyfen	0.0067	0.0223	0.999
Quinalphos	0.0382	0.1274	0.995
Quinoxyfen	0.0105	0.0348	0.999
Simazine	0.0066	0.0219	0.999
Spiroxamine	0.0182	0.0607	0.993
Sulfamethoxazole	0.034	0.1133	0.999
Tebuconazole	0.0423	0.141	0.998
Terbuthylazine	0.0178	0.0595	0.996
Terbutryn	0.0038	0.0127	0.999
Tetraacetylethylenediamine	0.4478	1.4926	0.988
Tetrabromobisphenol A	0.1359	0.4531	0.999
Tetracycline	0.0168	0.0561	0.995
Thiacloprid	0.0868	0.2894	0.998
Thiophanate-methyl	0.0212	0.0706	0.994
Thioridazine	0.0042	0.0141	0.997
Tolfenpyrad	0.0209	0.0698	0.998
Tonalide	0.0375	0.1251	0.997
Triasulfuron	0.0496	0.1654	0.998
Triazophos	0.0496	0.1652	0.999
Triclosan	0.4543	1.5144	0.992
Trifloxystrobin	0.0155	0.0517	0.999
Trifluralin	0.0219	0.073	0.994
Trimethoprim	0.0053	0.0177	0.998
Triphenylphosphineoxide	0.1339	0.4464	0.999
Triphenyltin	8.72	29.0665	0.983
Tris(1-chloro-2-propanyl) phosphate	21.737	72.4567	0.942
Tris(2-butoxyethyl) phosphate	0.0256	0.0853	0.999

Table C.1. Continued.

Compound	LOD (ug/L)	LOQ (ug/L)	R^2
Vancomycin	0.0772	0.2573	0.999

APPENDIX D

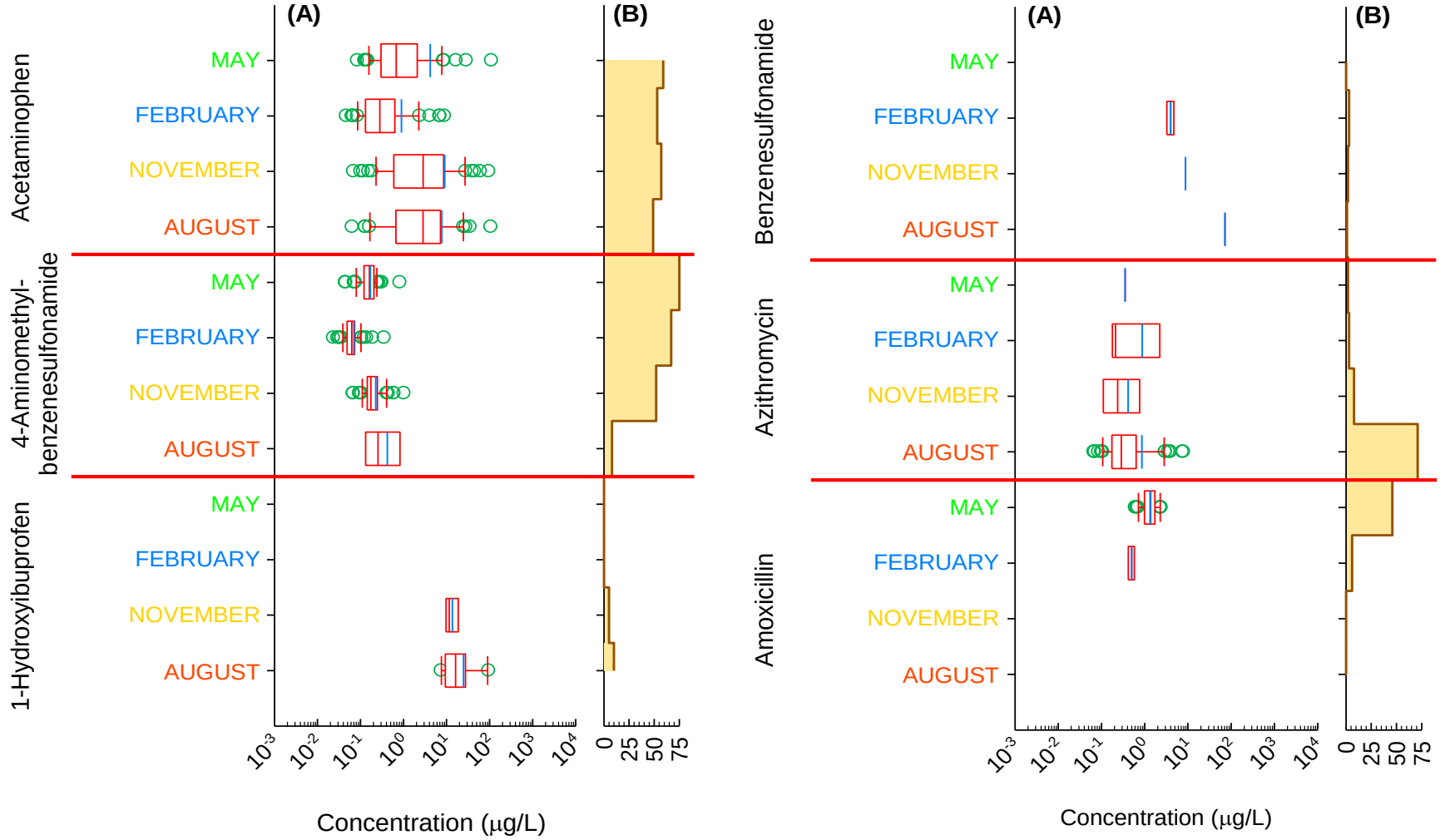

Figure D.1. Seasonal (A) concentration and (B) detection frequency (out of 75) of pharmaceuticals in Ergene River.

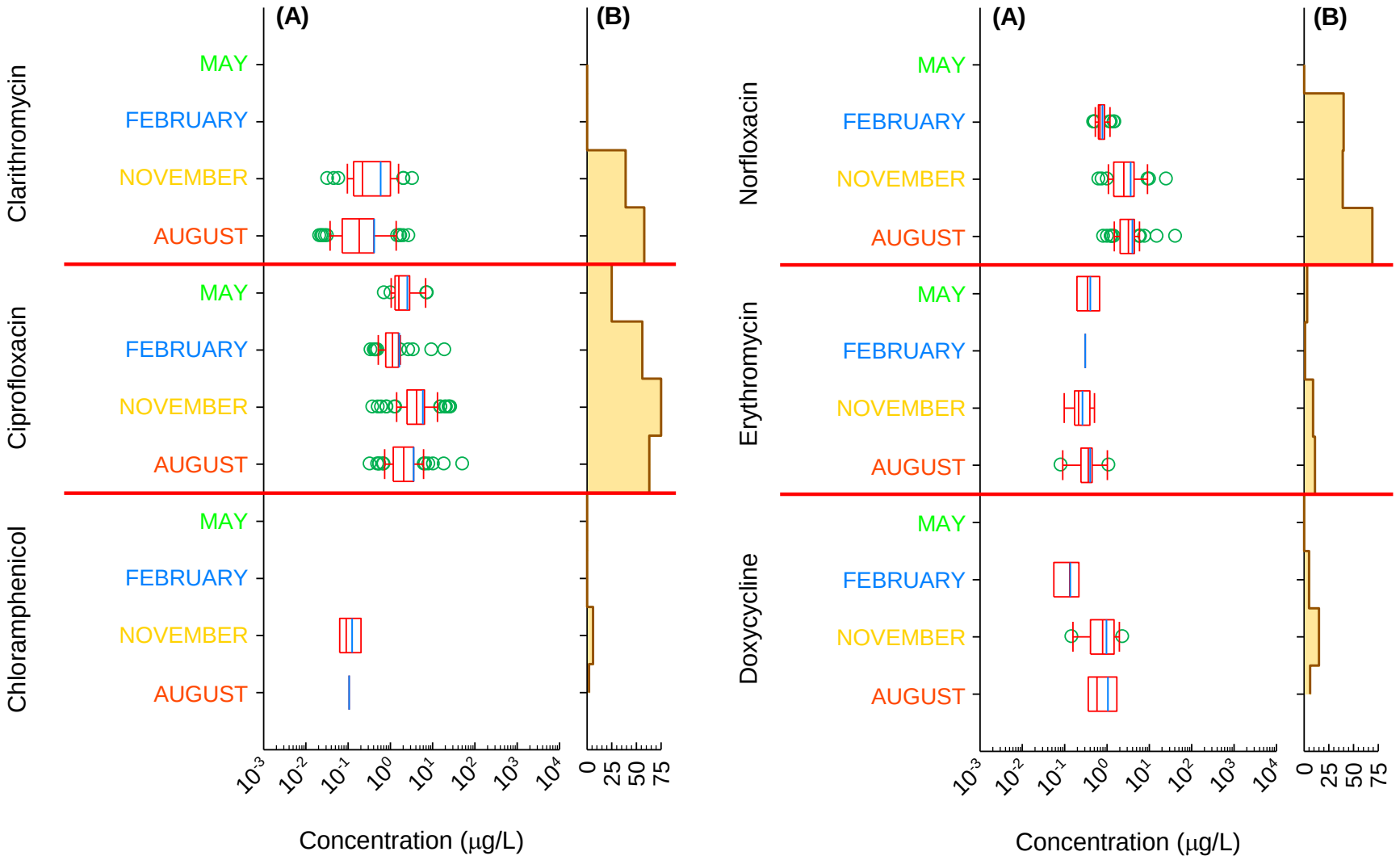

Figure D.1. Continued.

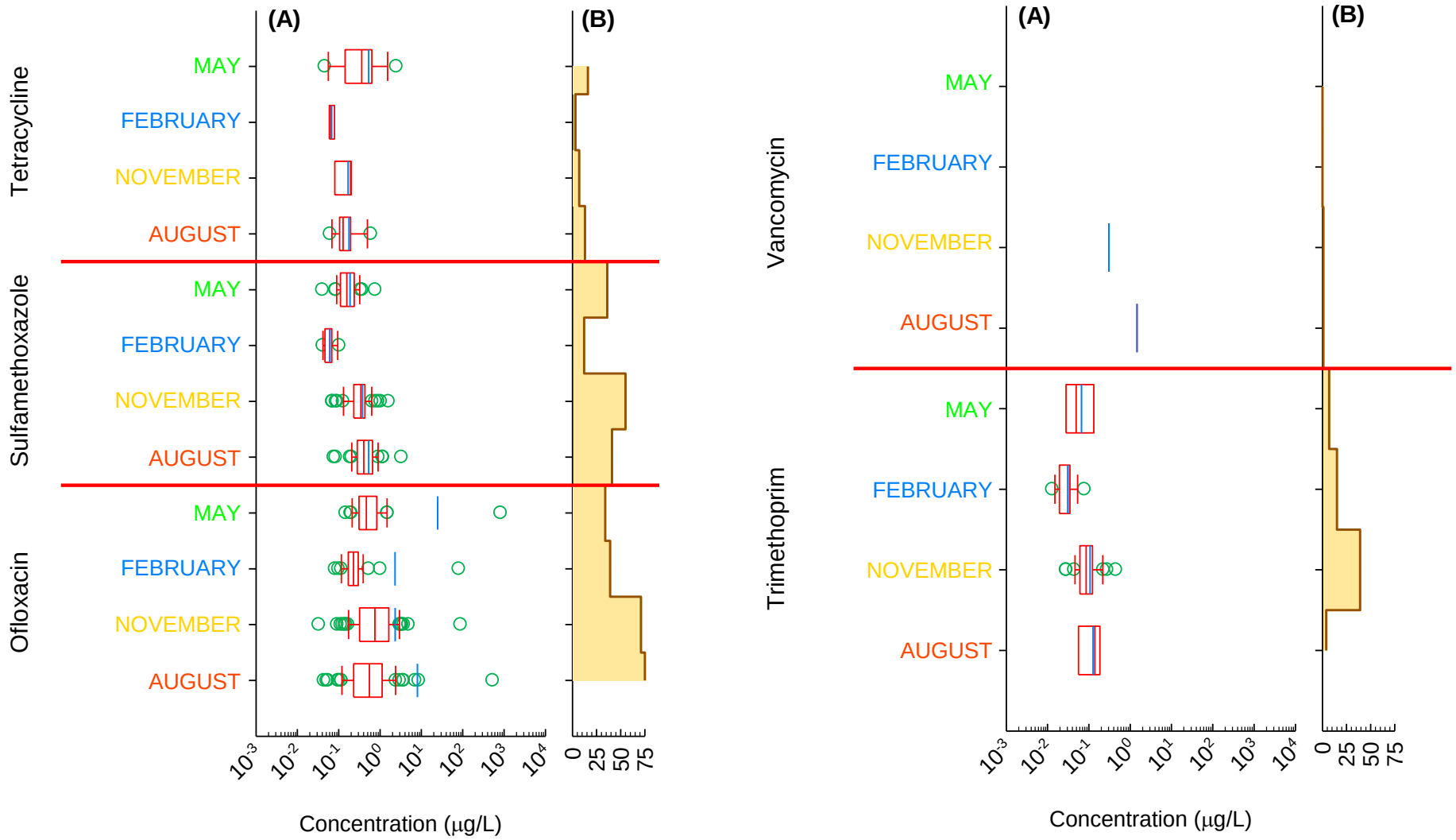

Figure D.1. Continued.

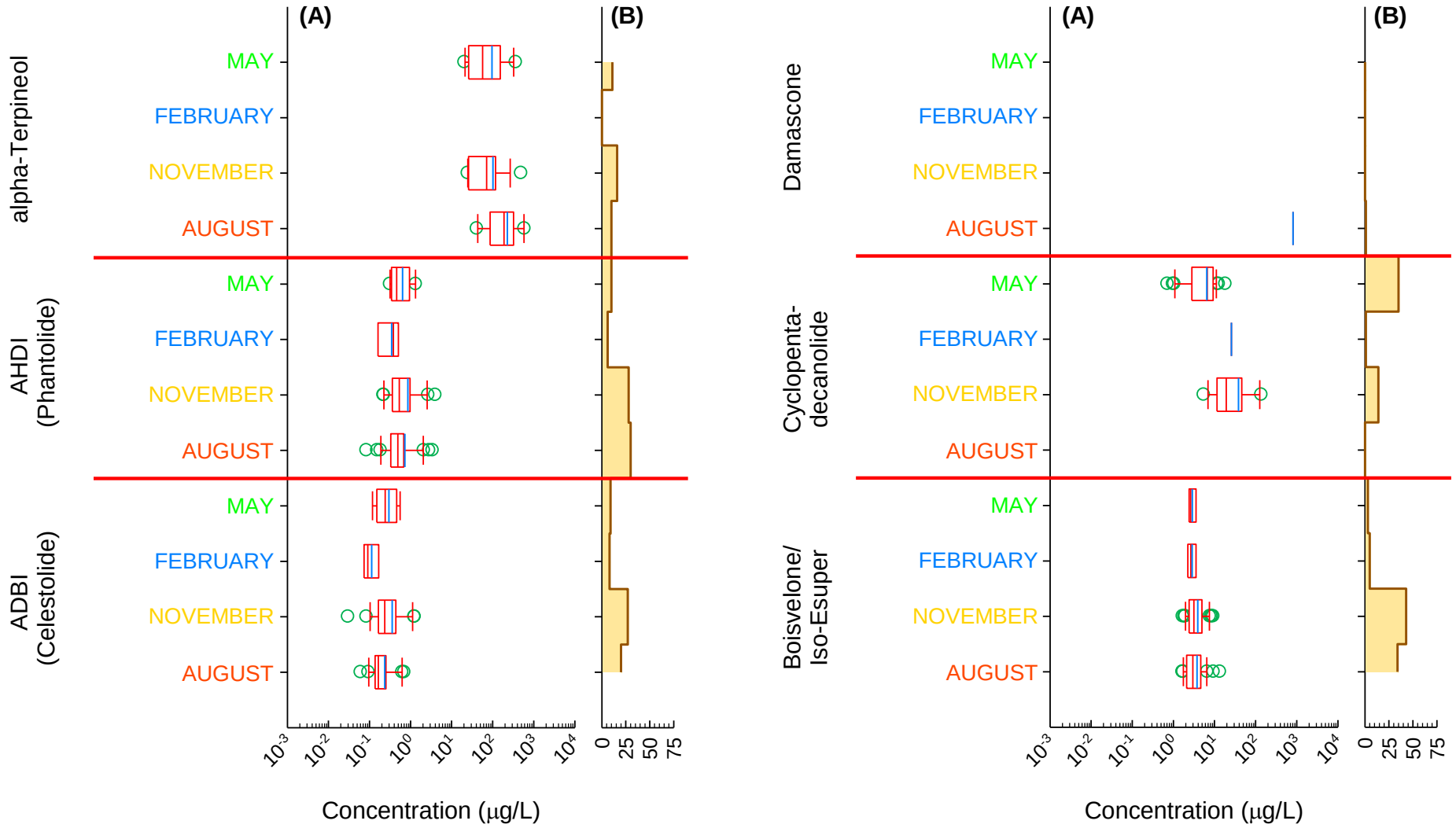

Figure D.2. Seasonal (A) concentration and (B) detection frequency (out of 75) of fragrances and food additives in Ergene River.

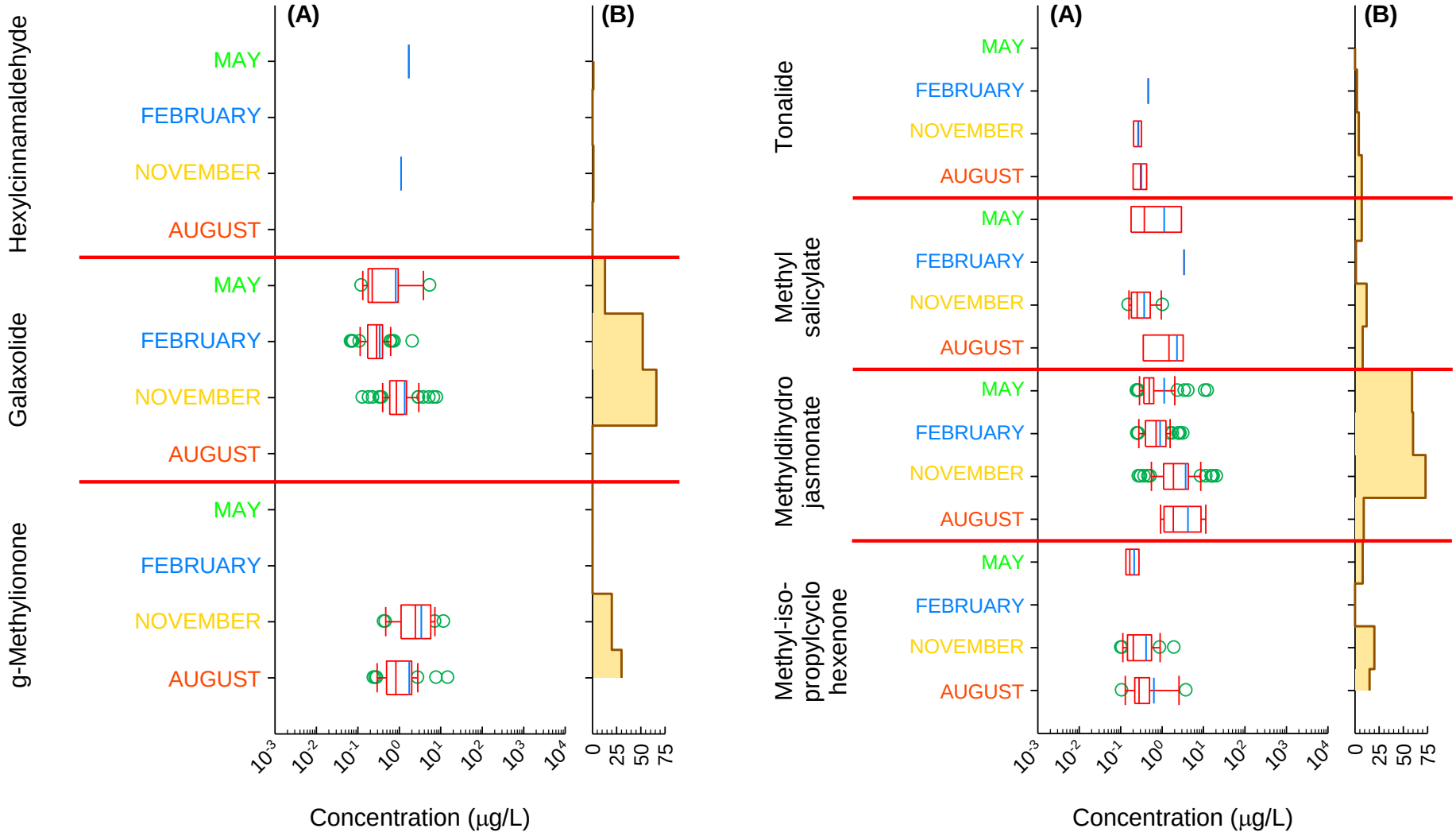

Figure D.2. Continued.

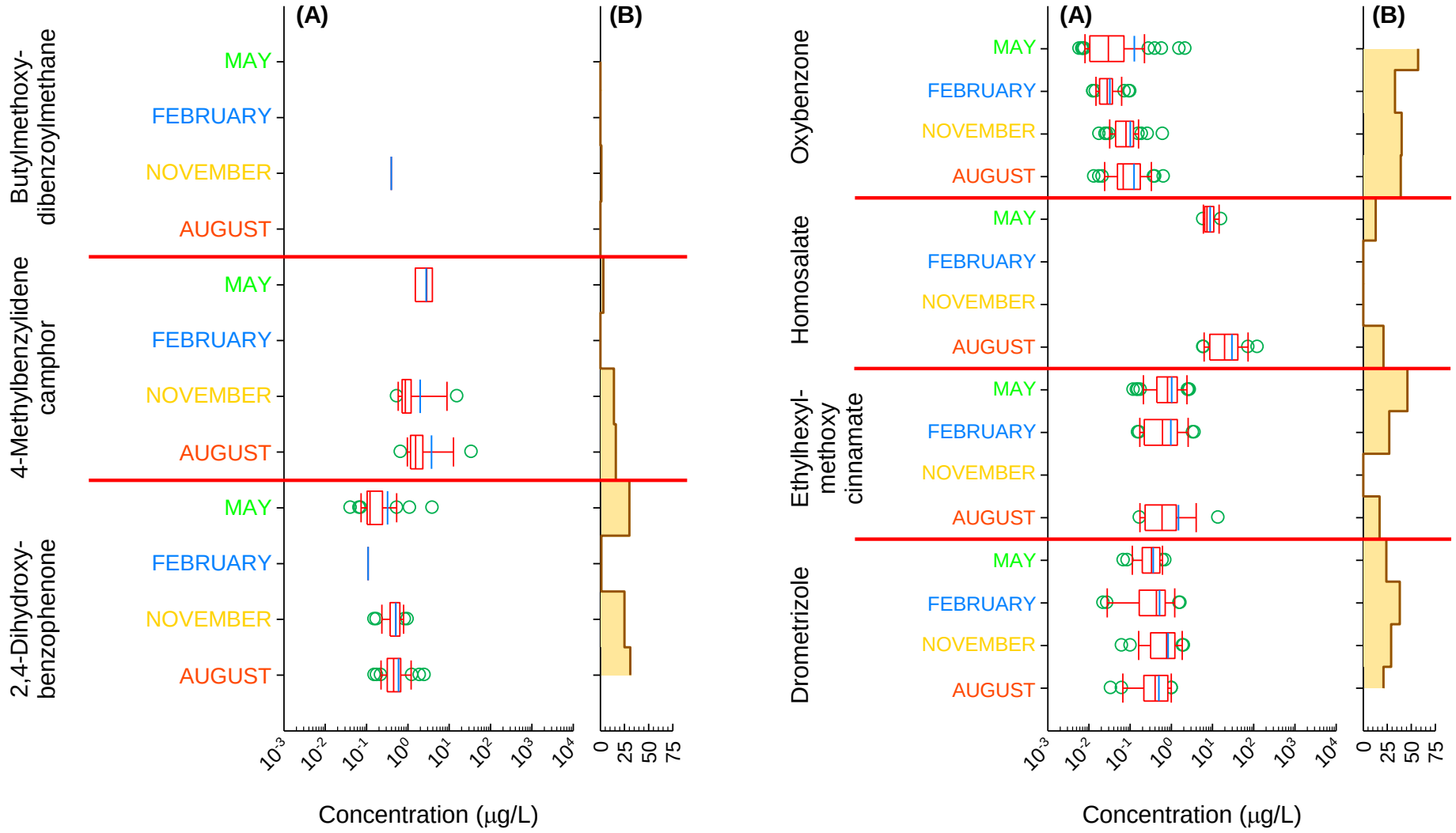

Figure D.3. Seasonal (A) concentration and (B) detection frequency (out of 75) of UV filters (Sunscreening agents) in Ergene River.

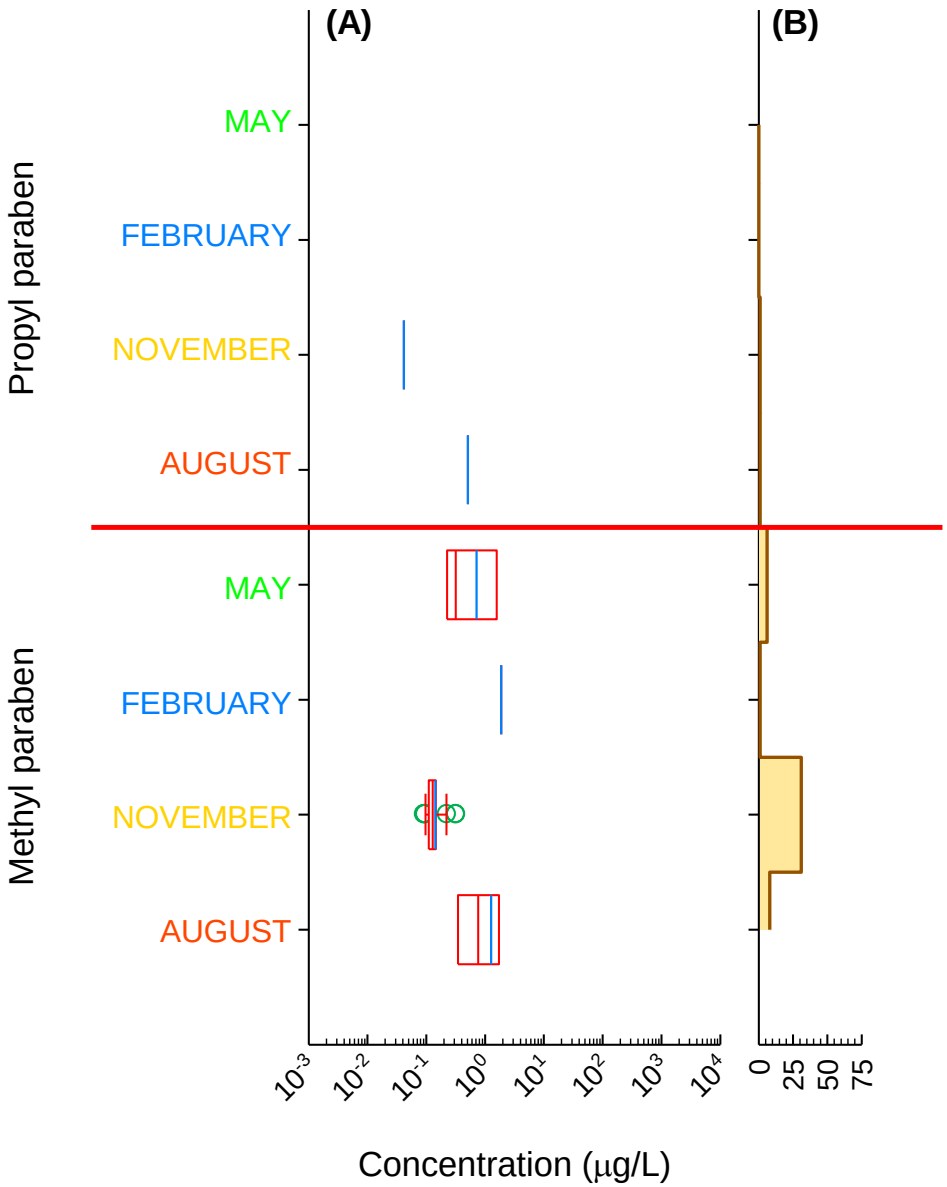

Figure D.4. Seasonal (A) concentration and (B) detection frequency (out of 75) of parabens (Sunscreening agents) in Ergene River.

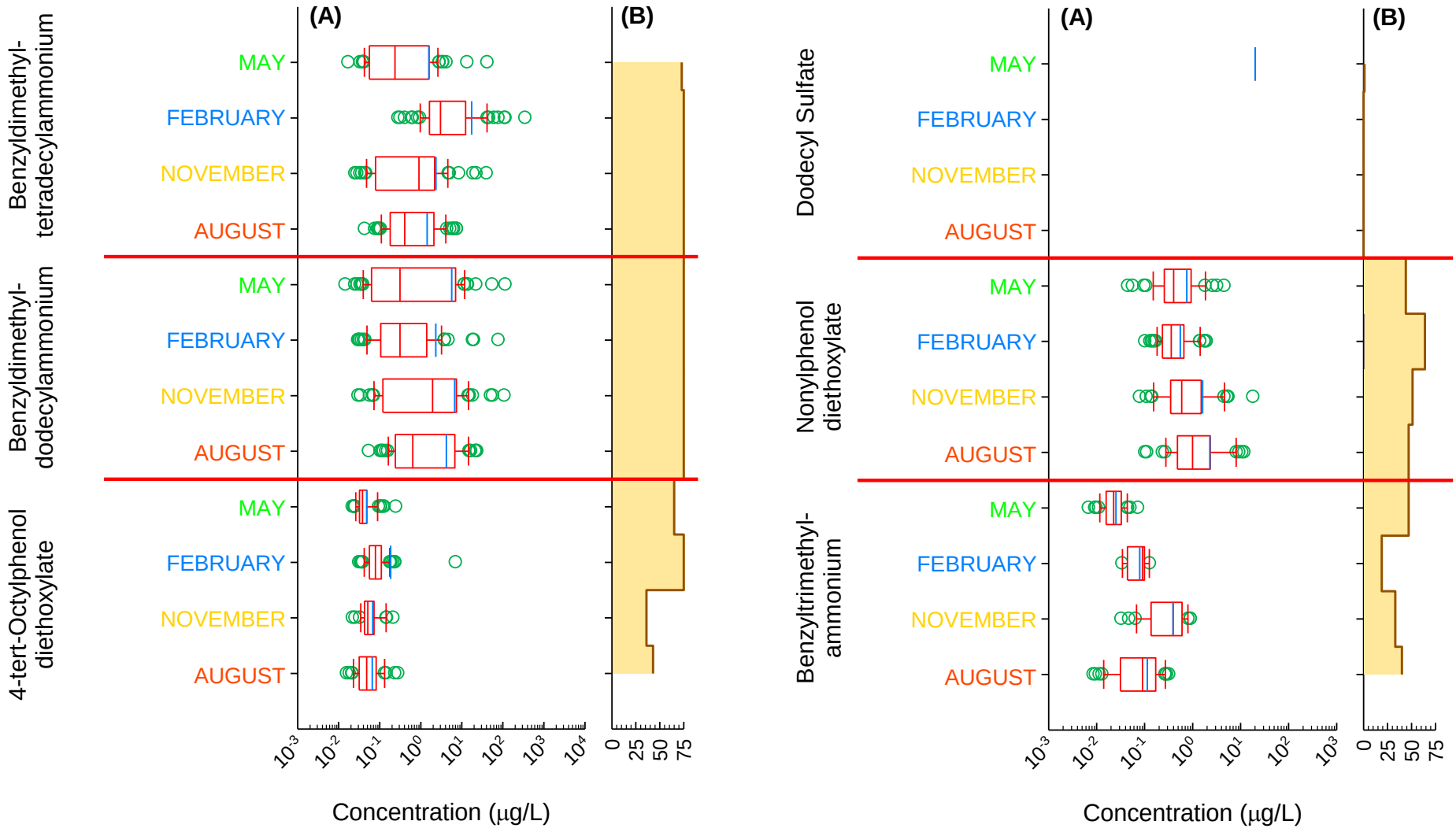

Figure D.5. Seasonal (A) concentration and (B) detection frequency (out of 75) of surfactants in Ergene River.

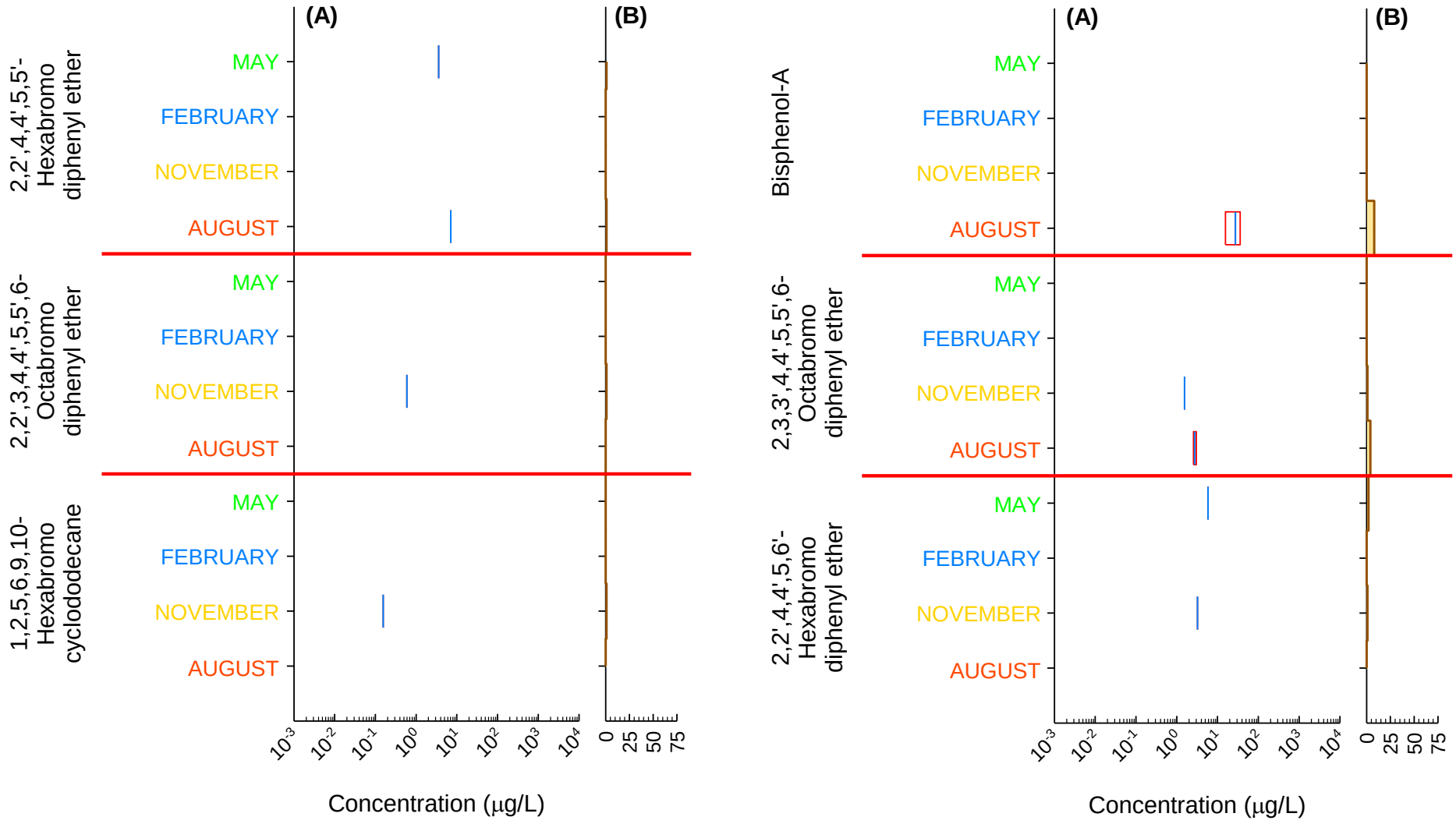

Figure D.6. Seasonal (A) concentration and (B) detection frequency (out of 75) of flame retardants in Ergene River.

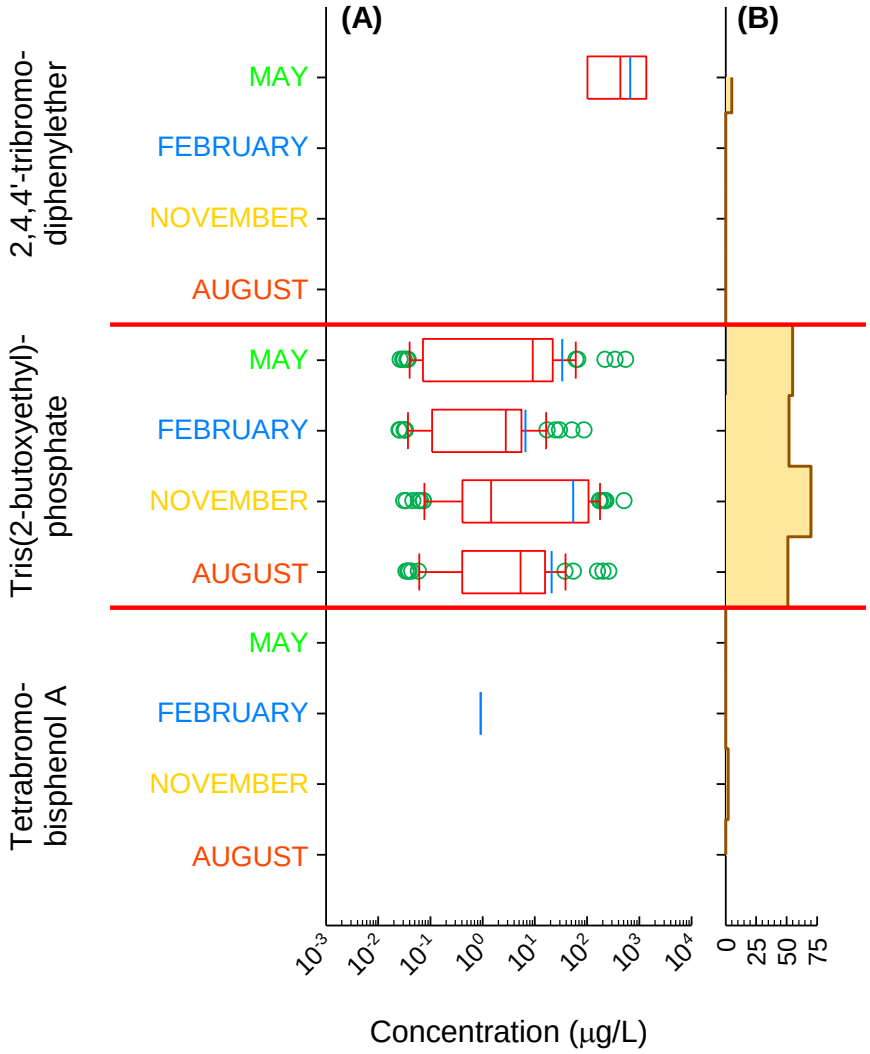

Figure D.6. Continued.

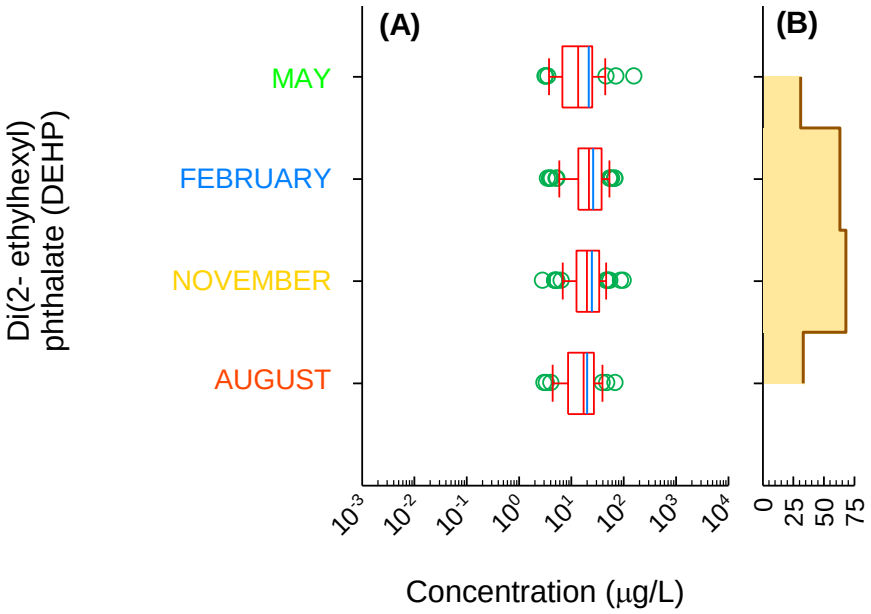

Figure D.7. Seasonal (A) concentration and (B) detection frequency (out of 75) of plasticizers (DEHP) in Ergene River.

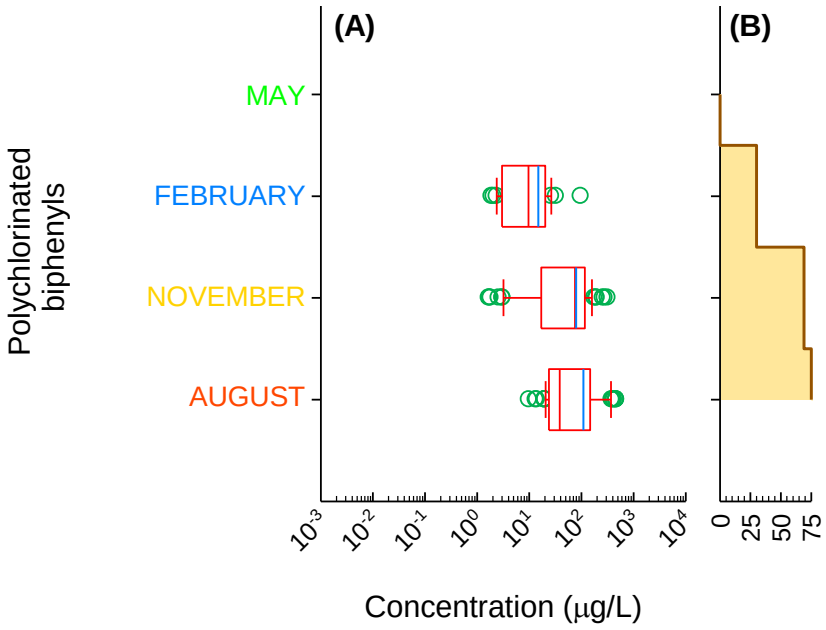

Figure D.8. Seasonal (A) concentration and (B) detection frequency (out of 75) of PCBs in Ergene River.

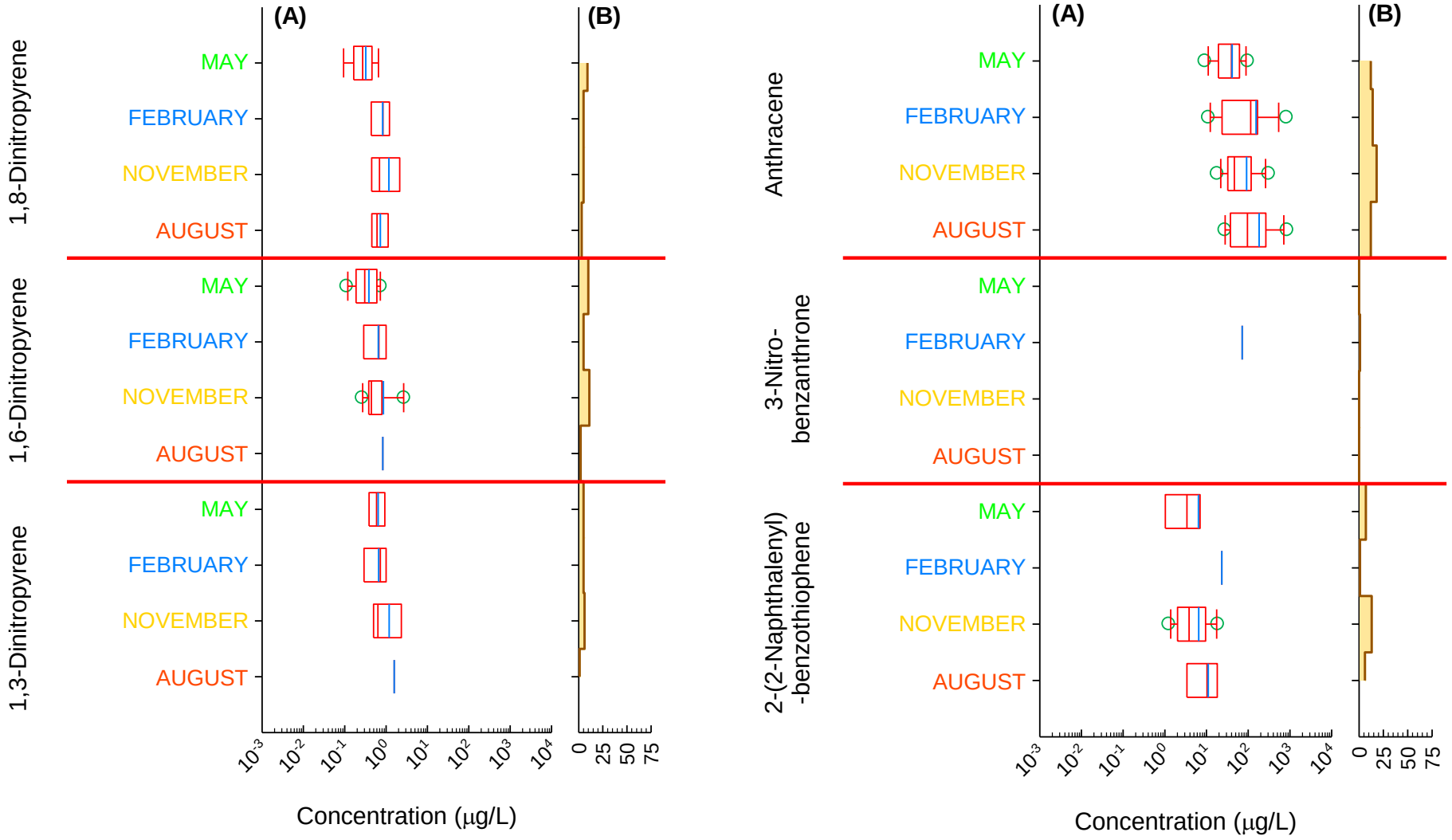

Figure D.9. Seasonal (A) concentration and (B) detection frequency (out of 75) of PAHs in Ergene River.

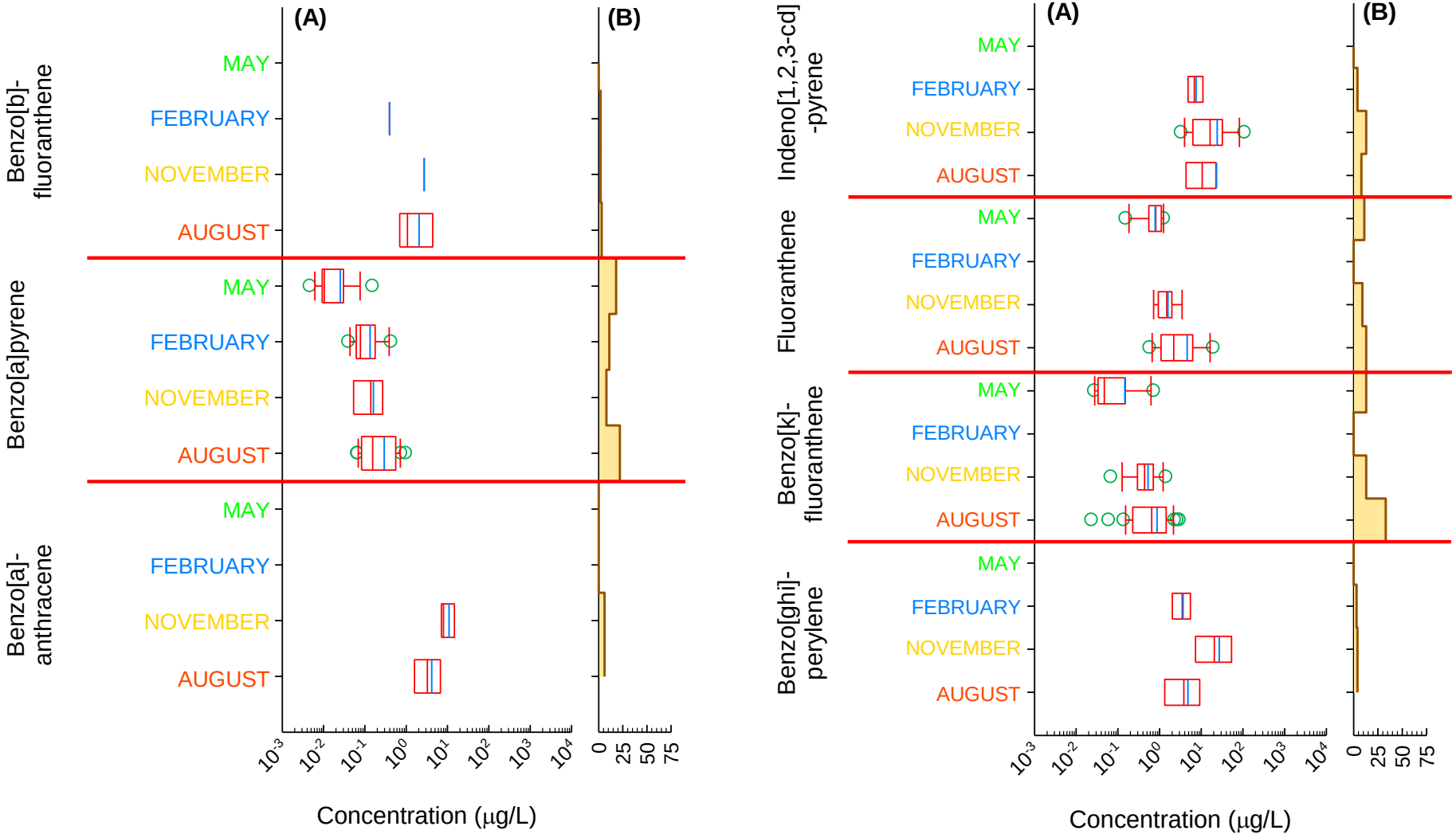

Figure D.9. Continued.

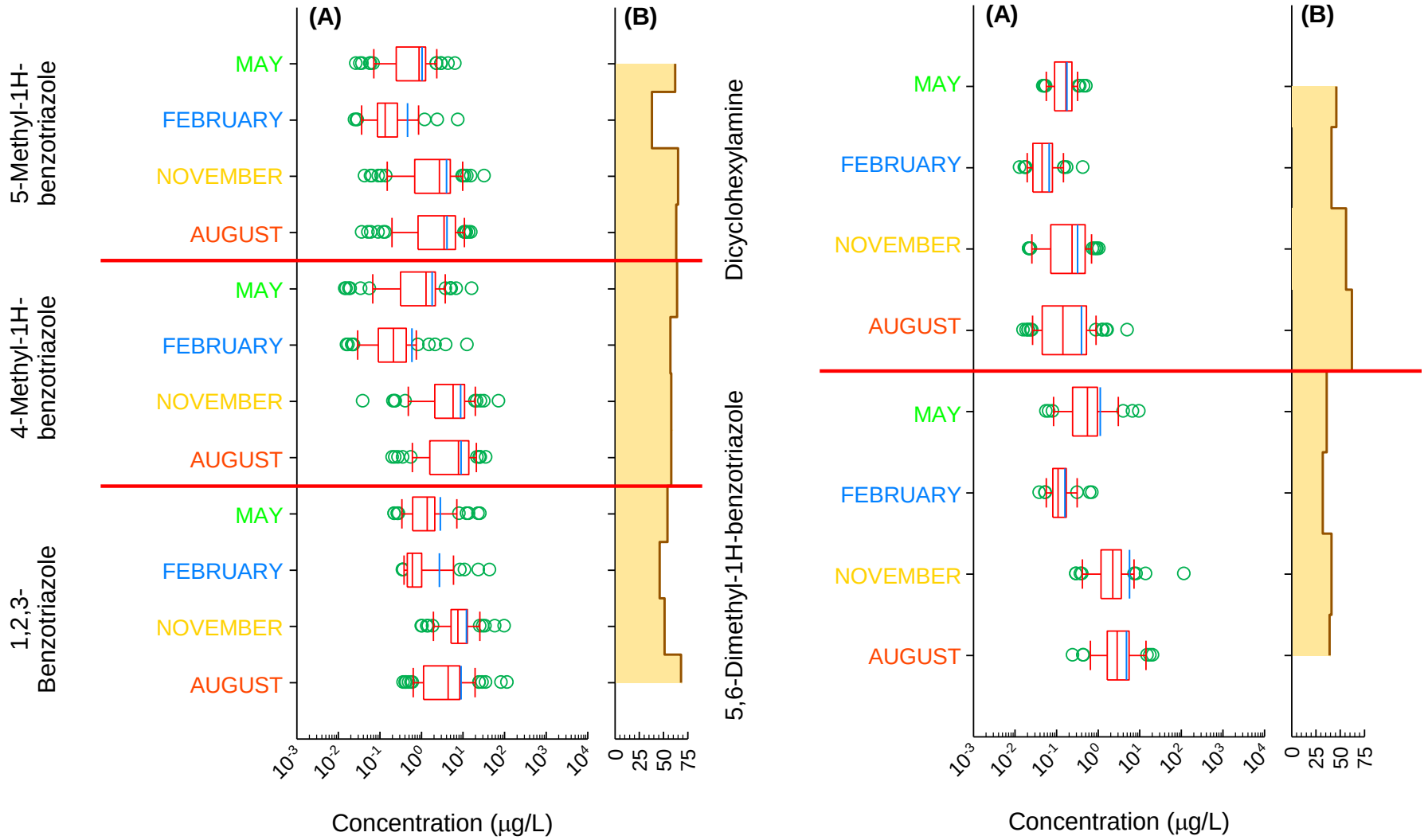

Figure D.10. Seasonal (A) concentration and (B) detection frequency (out of 75) of corrosion inhibitors (benzotriazoles) in Ergene River.

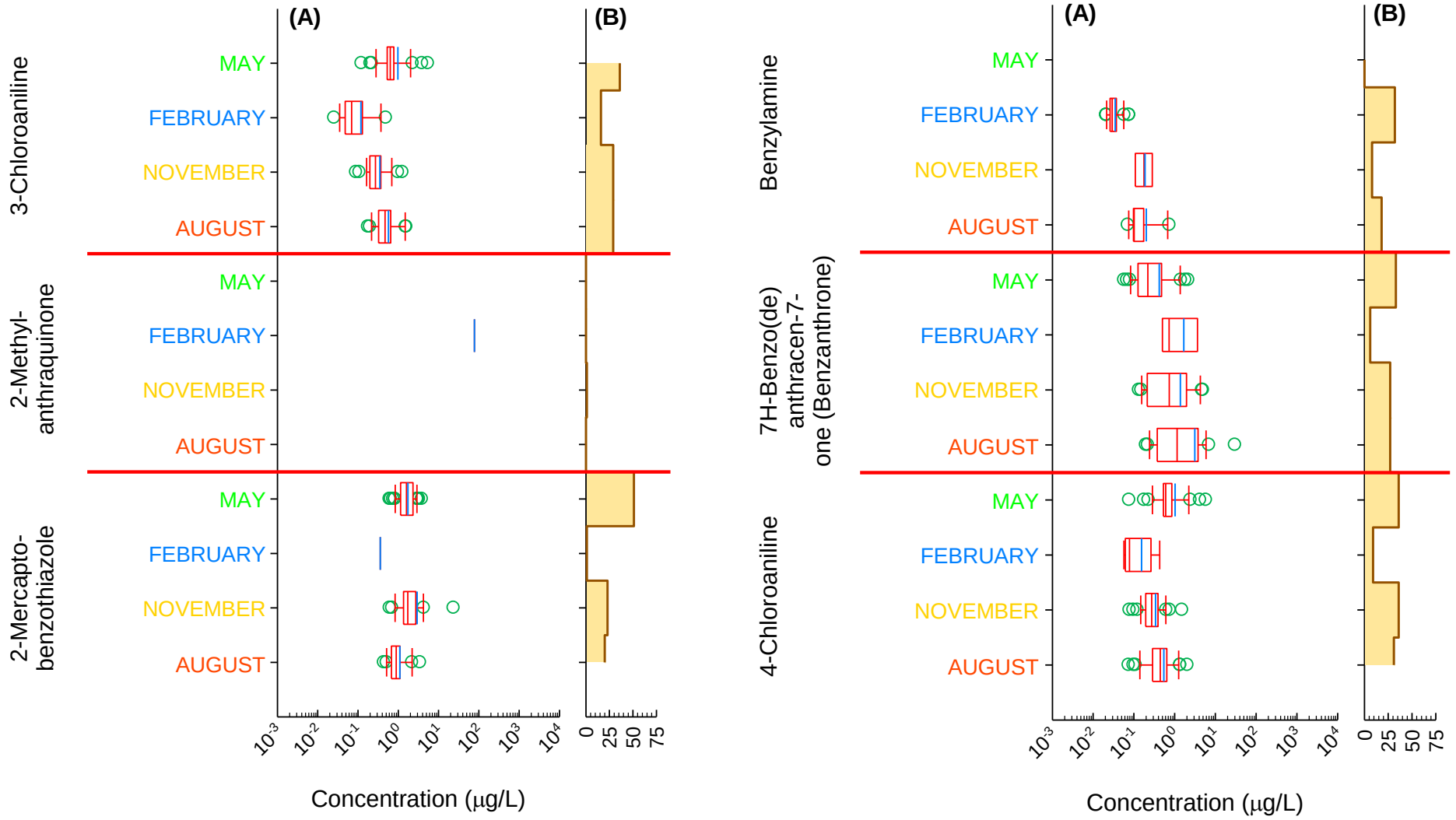

Figure D.11. Seasonal (A) concentration and (B) detection frequency (out of 75) of chemicals used in the manufacturing of other products in Ergene River.

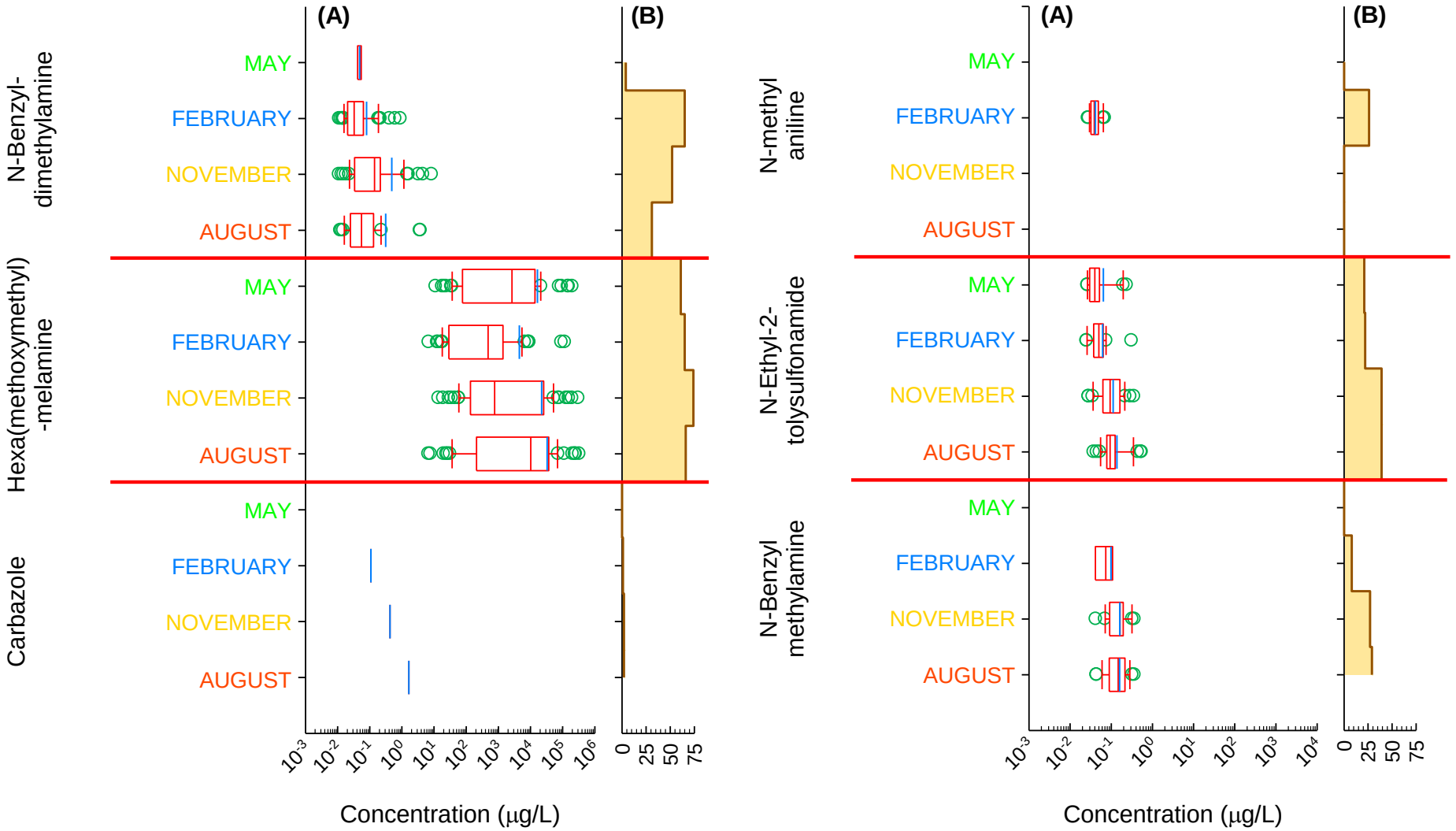

Figure D.11. Continued.

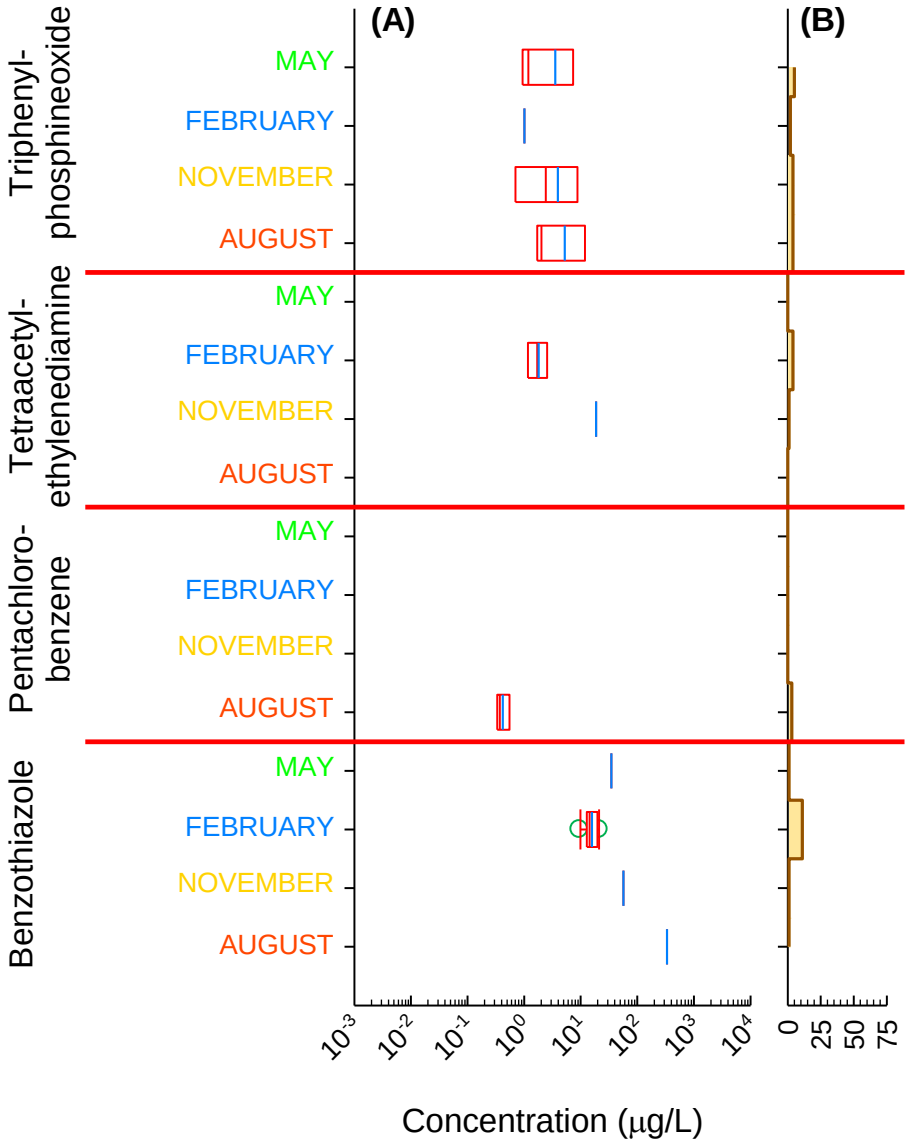

Figure D.11. Continued.

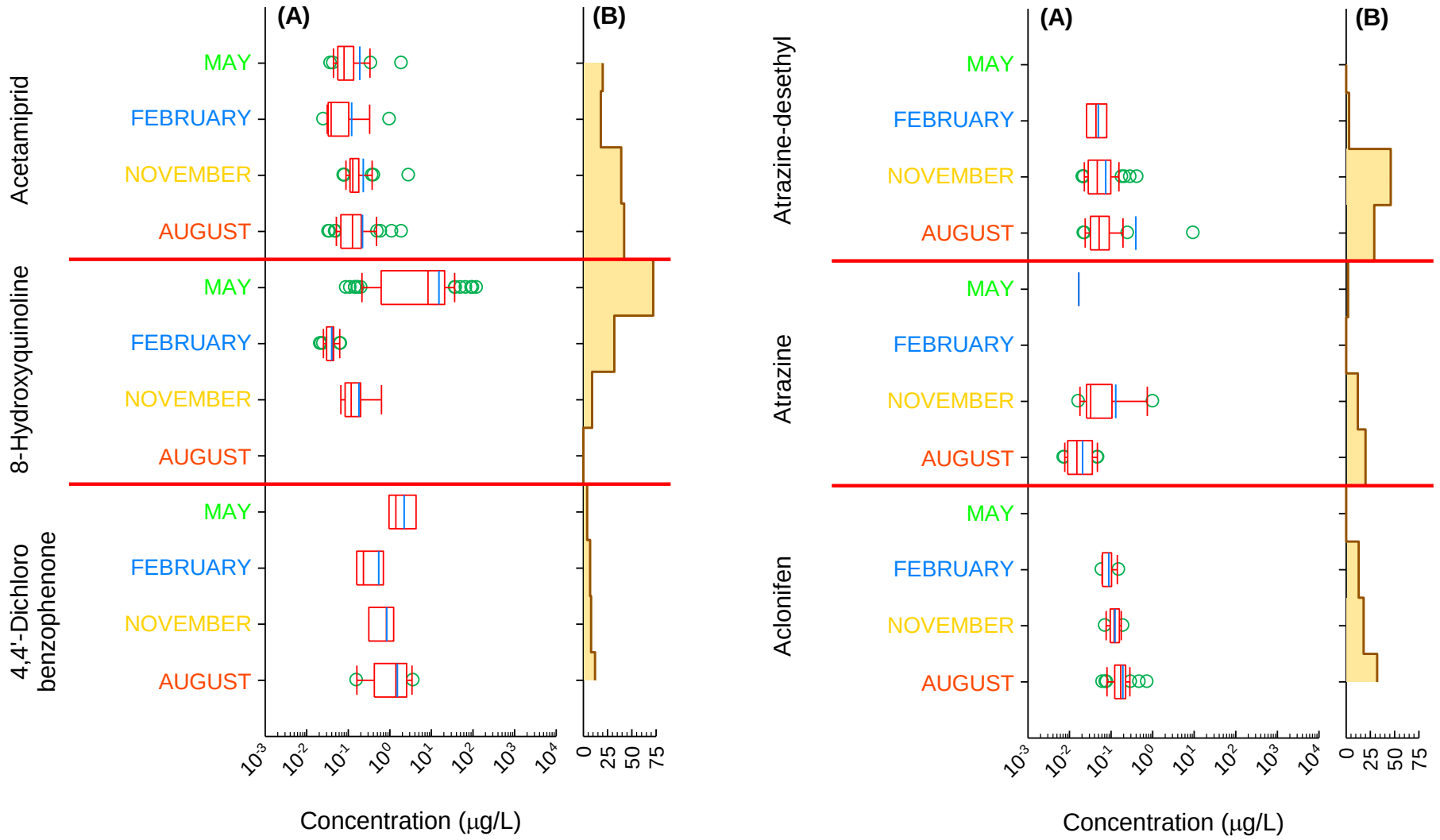

Figure D.12. Seasonal (A) concentration and (B) detection frequency (out of 75) of pesticides in Ergene River.

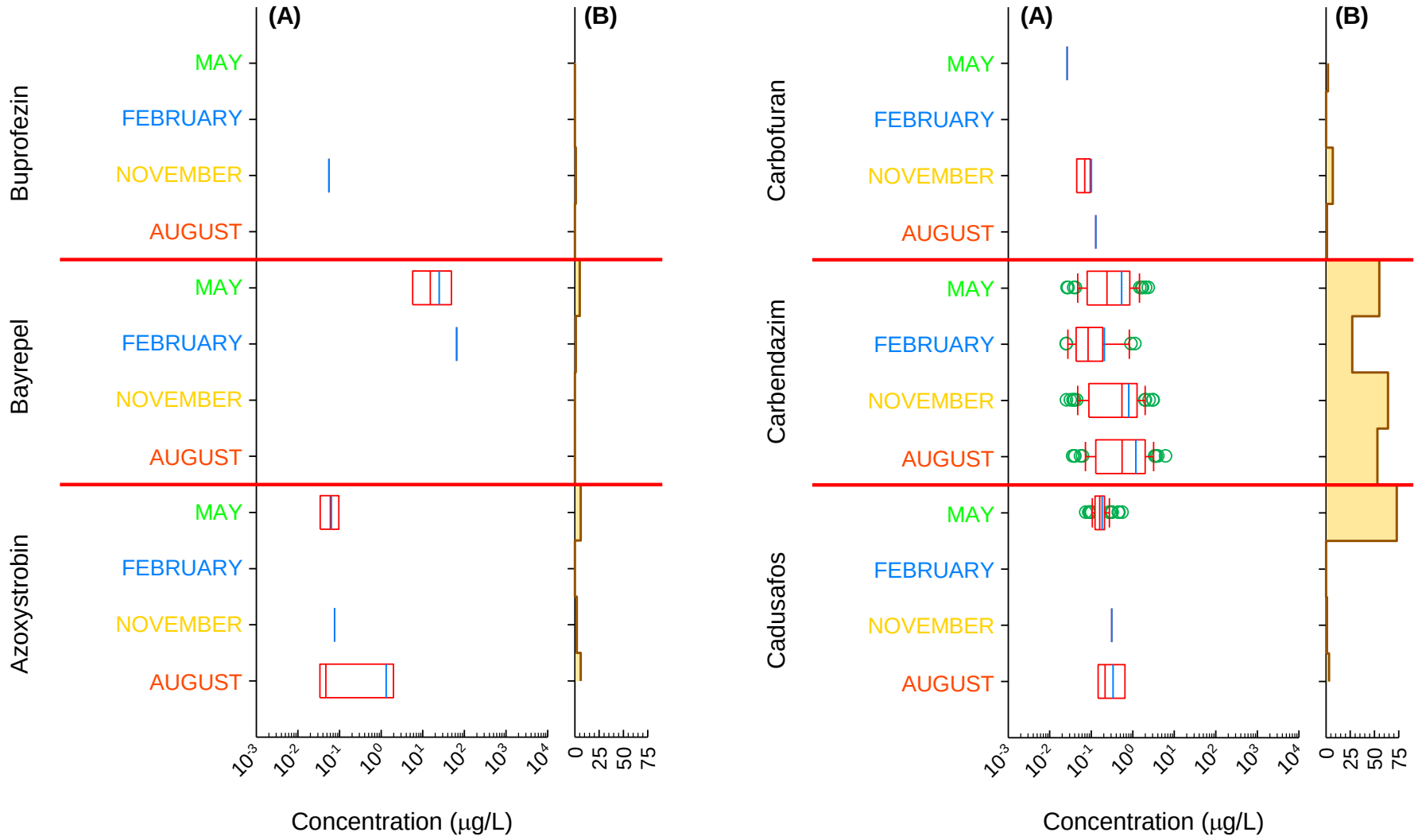

Figure D.12. Continued.

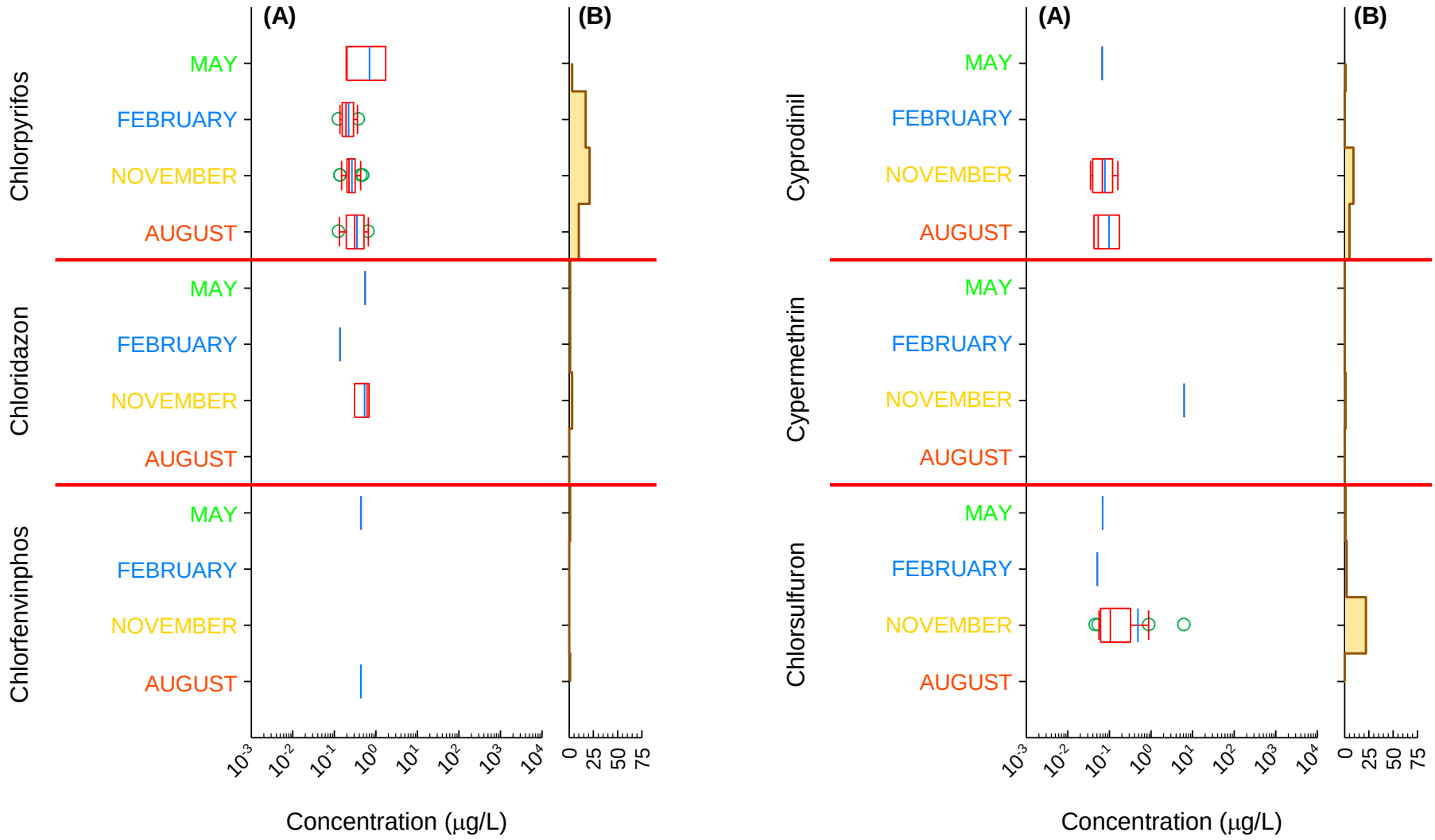

Figure D.12. Continued.

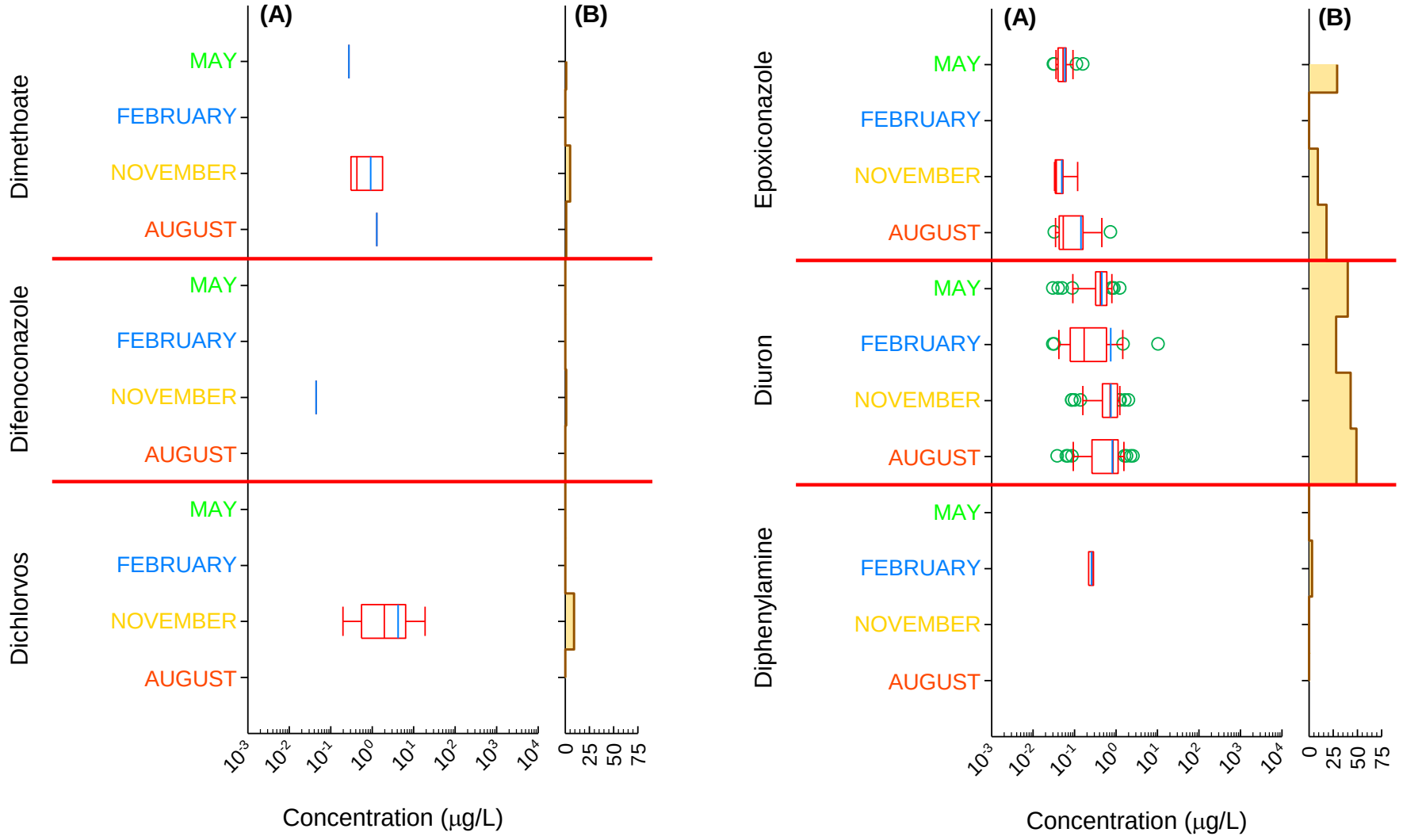

Figure D.12. Continued.

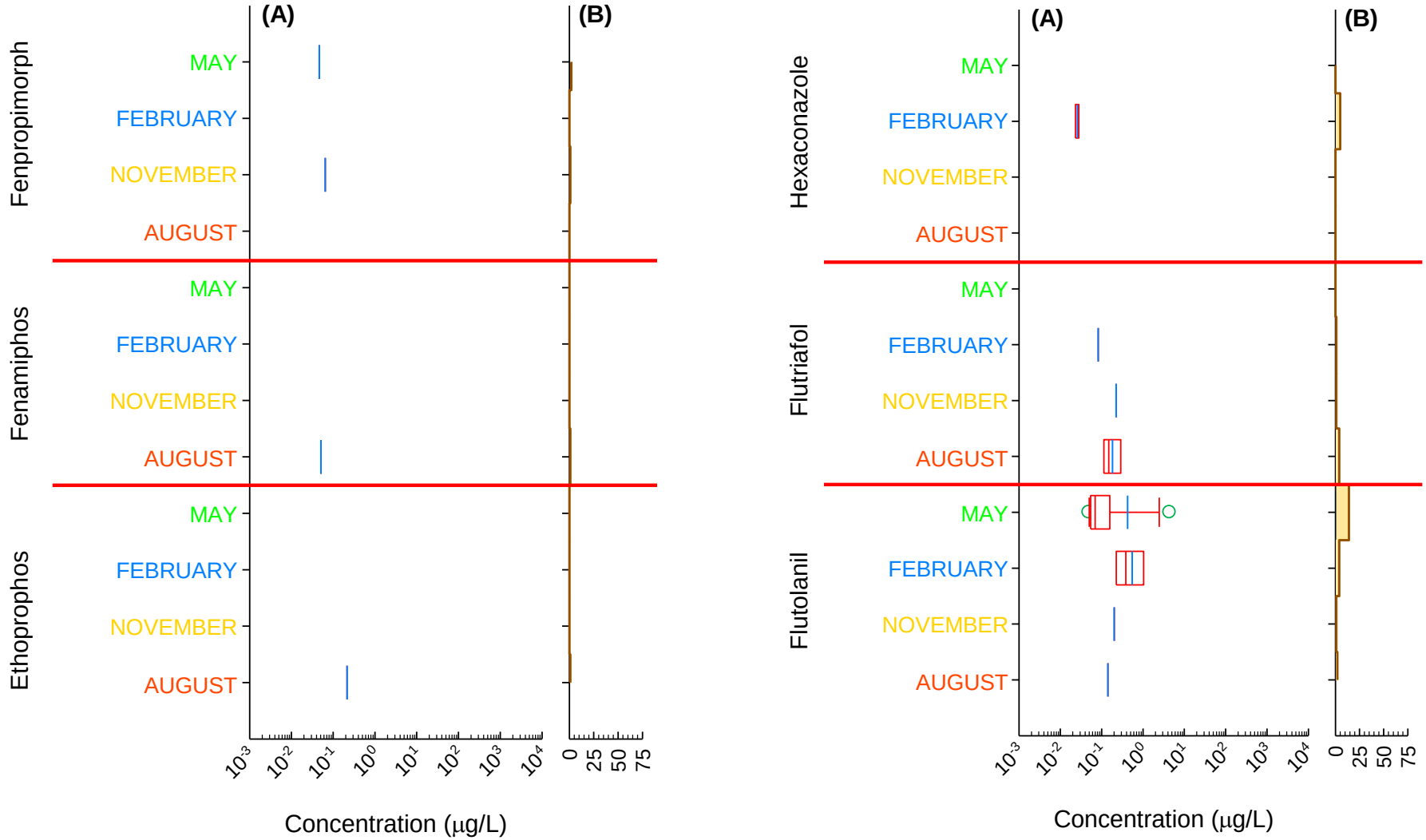

Figure D.12. Continued.

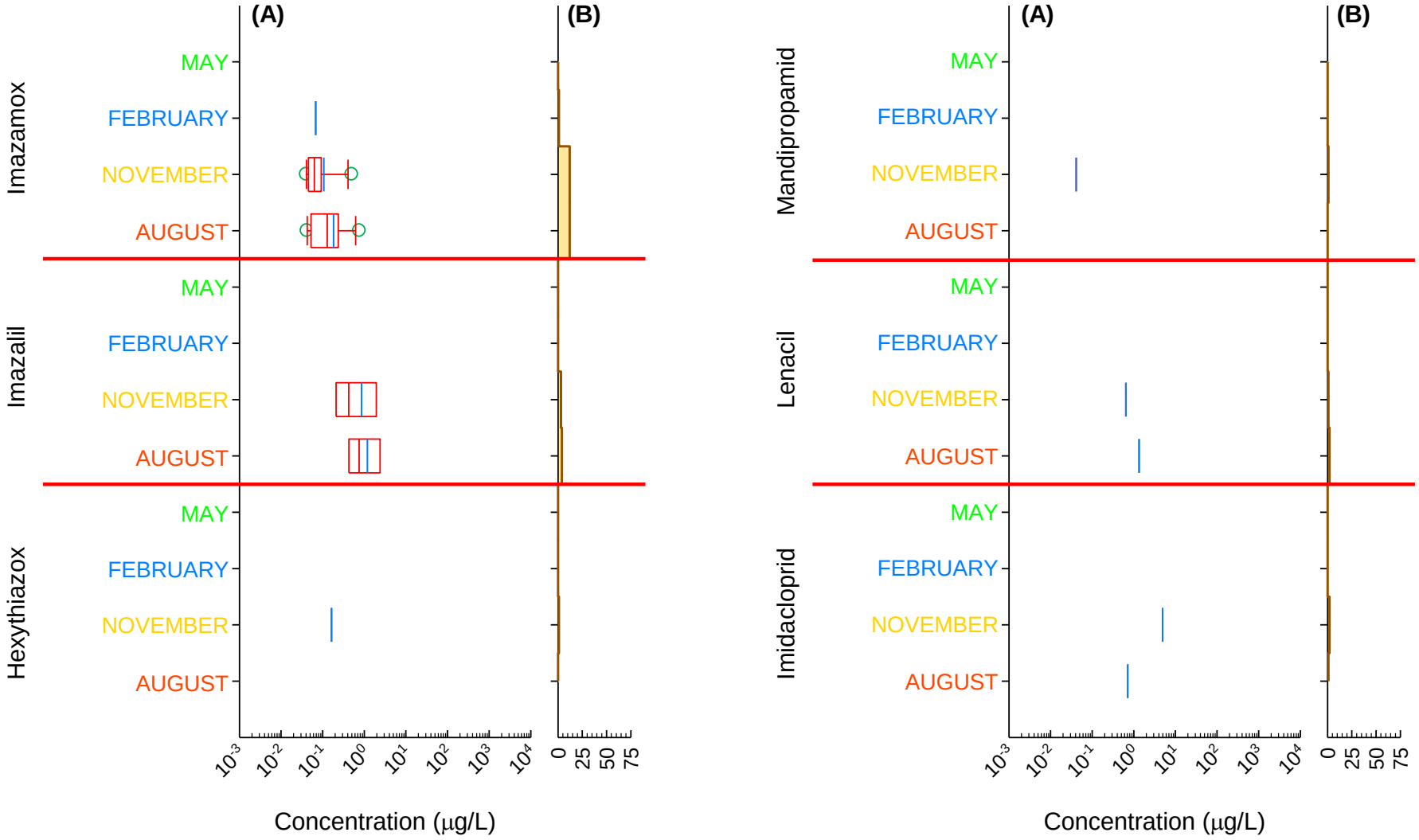

Figure D.12. Continued.

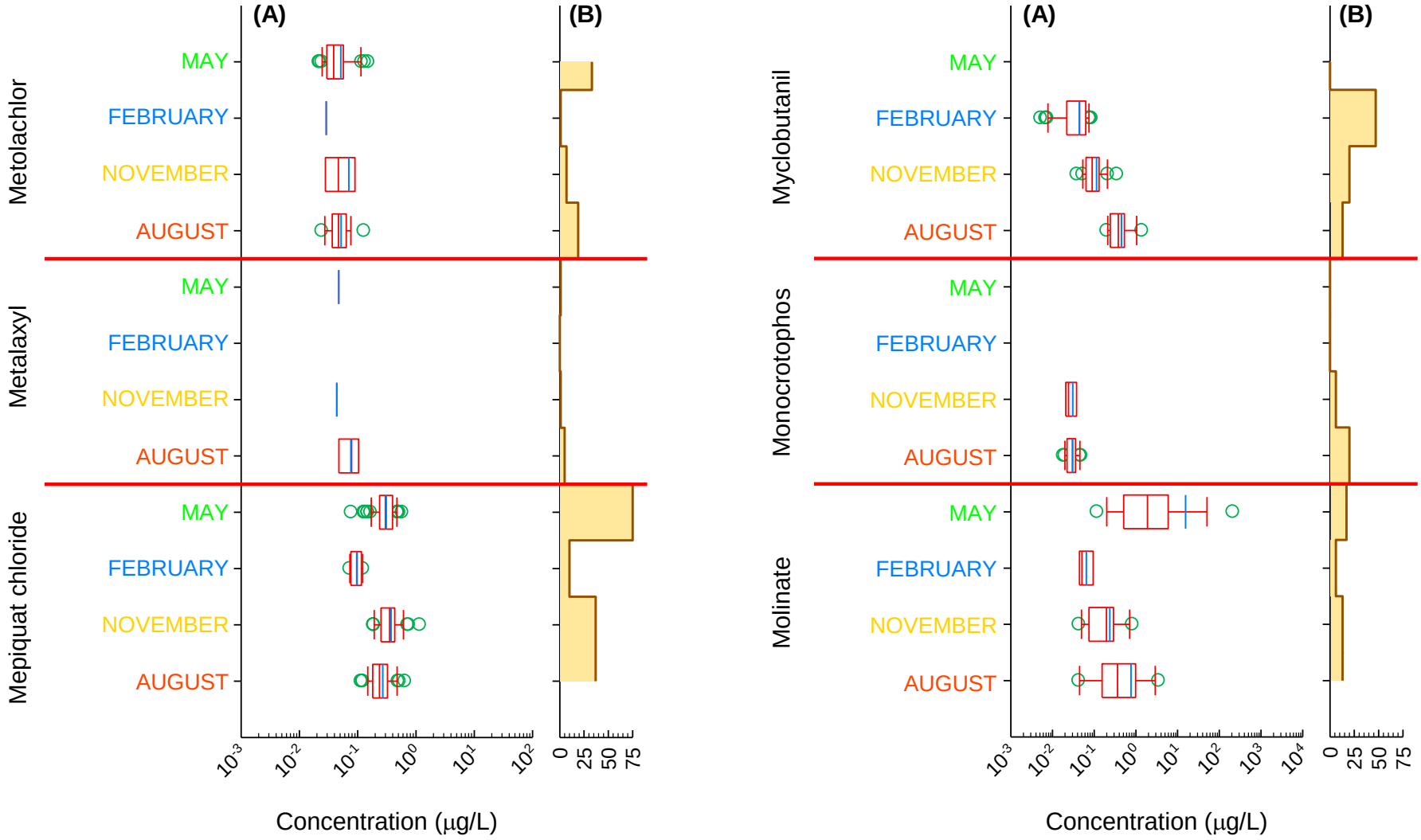

Figure D.12. Continued.

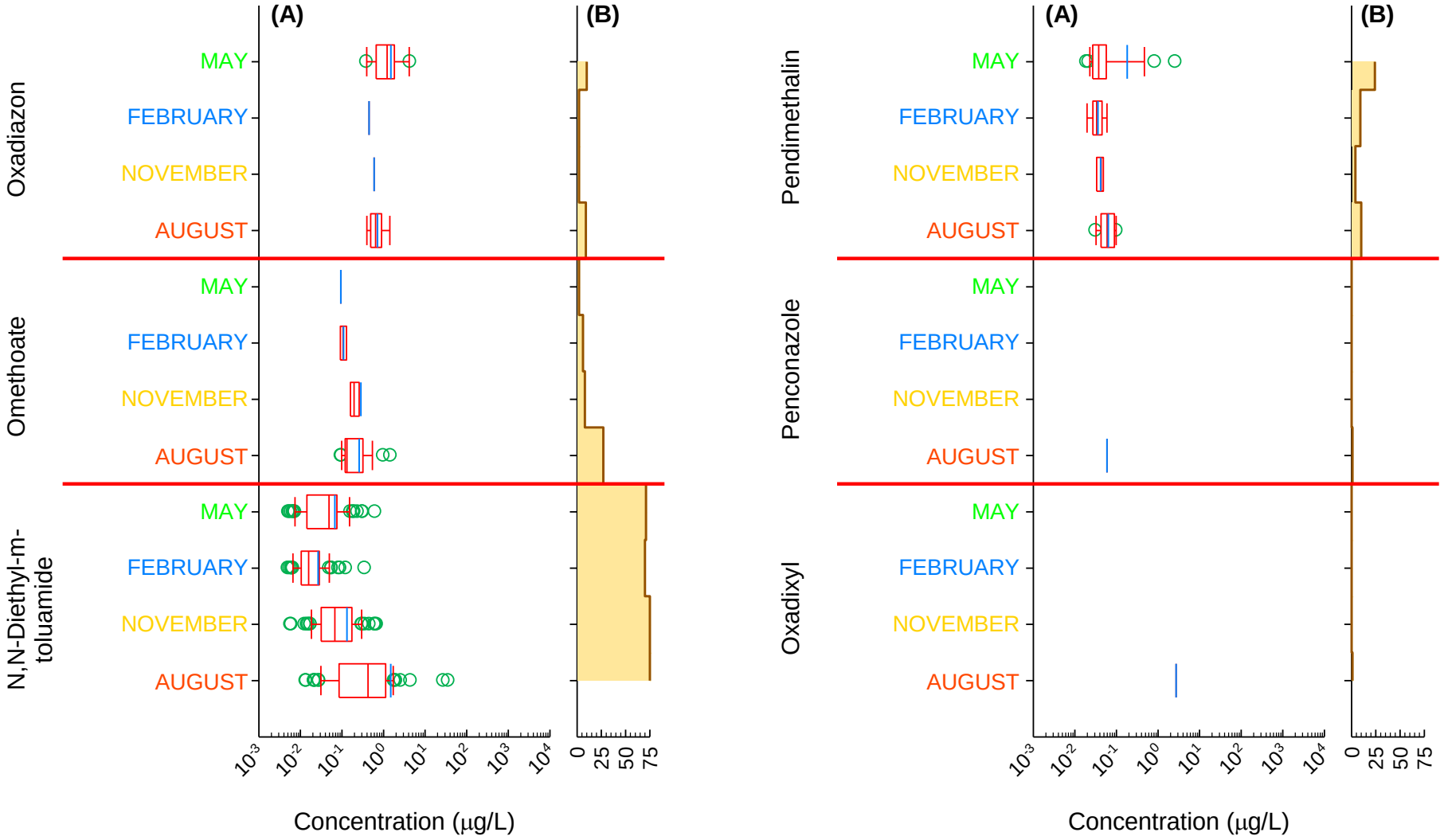

Figure D.12. Continued.

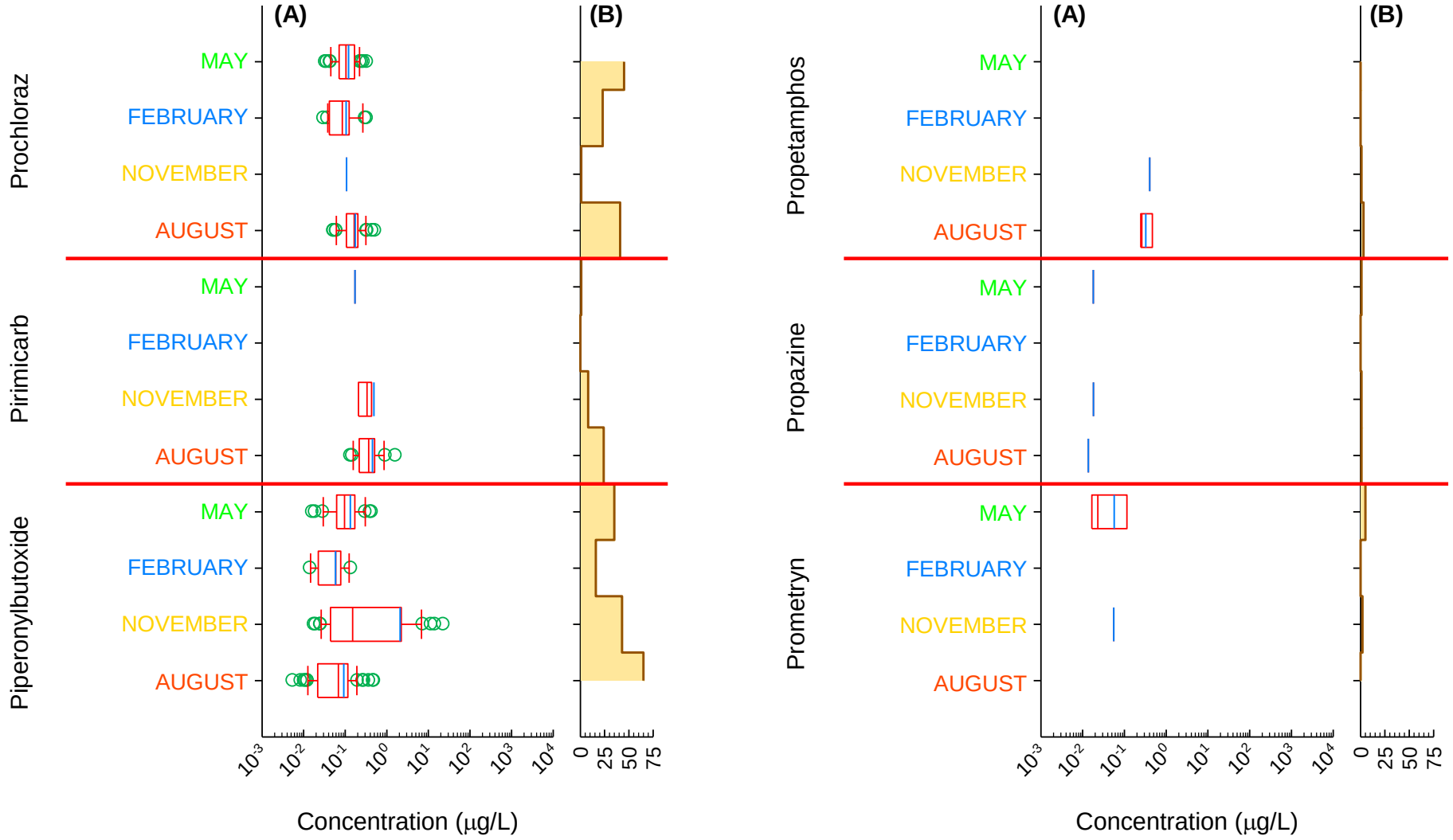

Figure D.12. Continued.

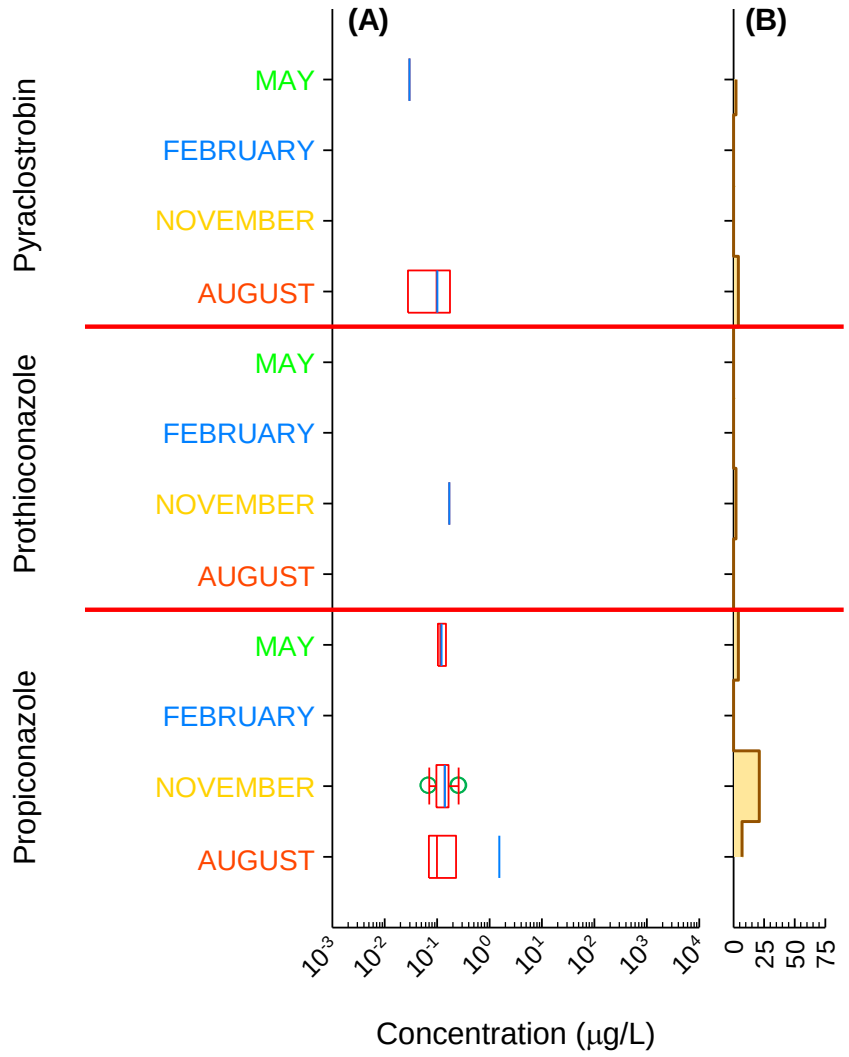

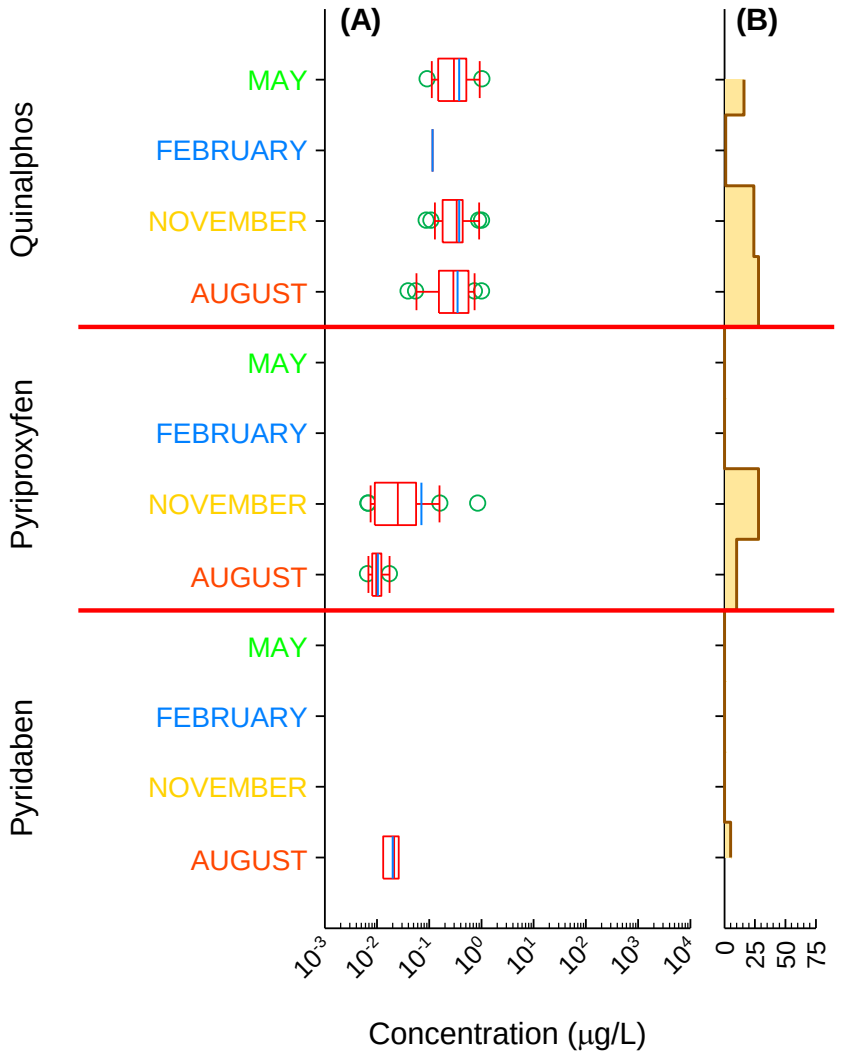

Figure D.12. Continued.

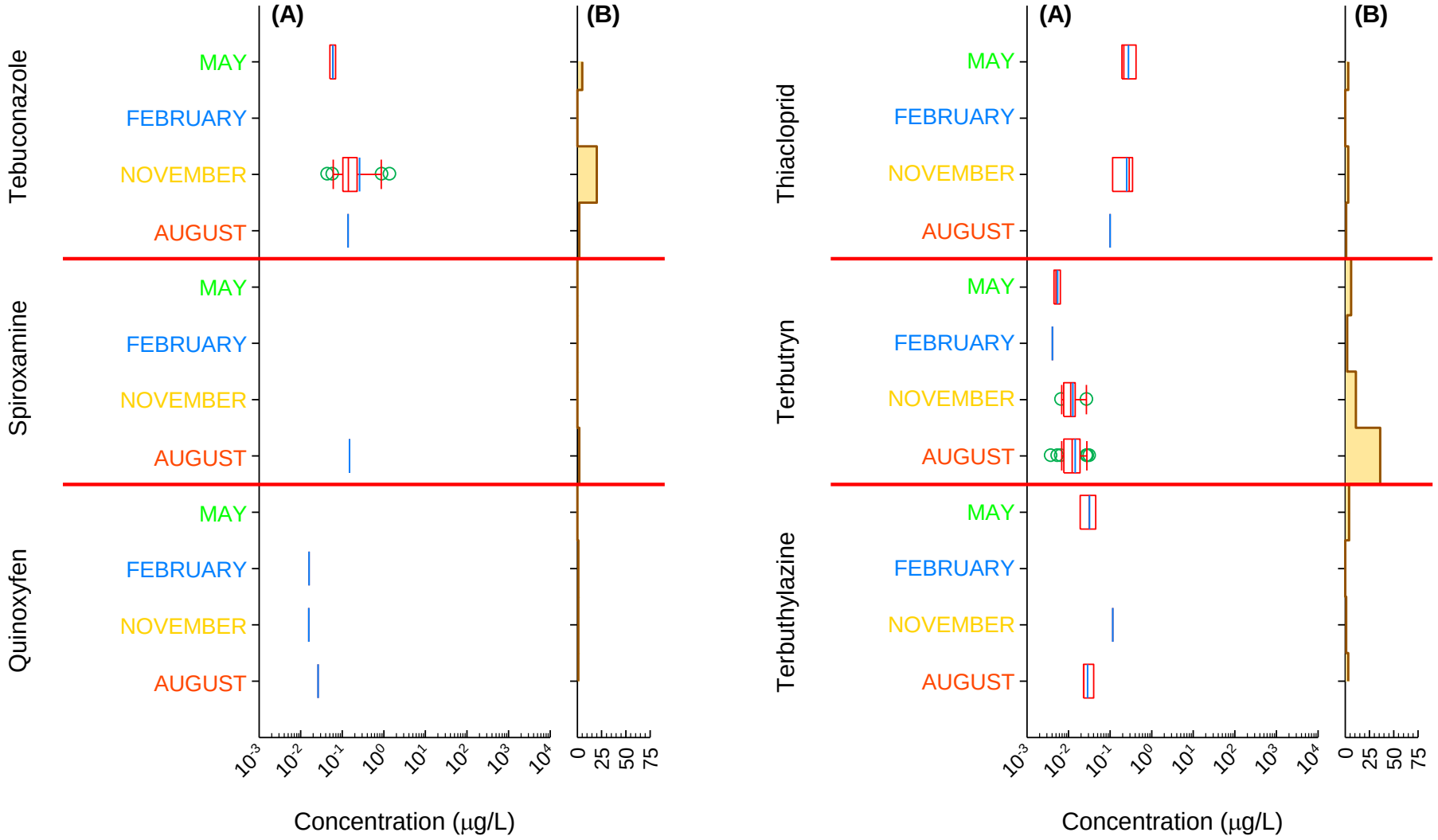

Figure D.12. Continued.

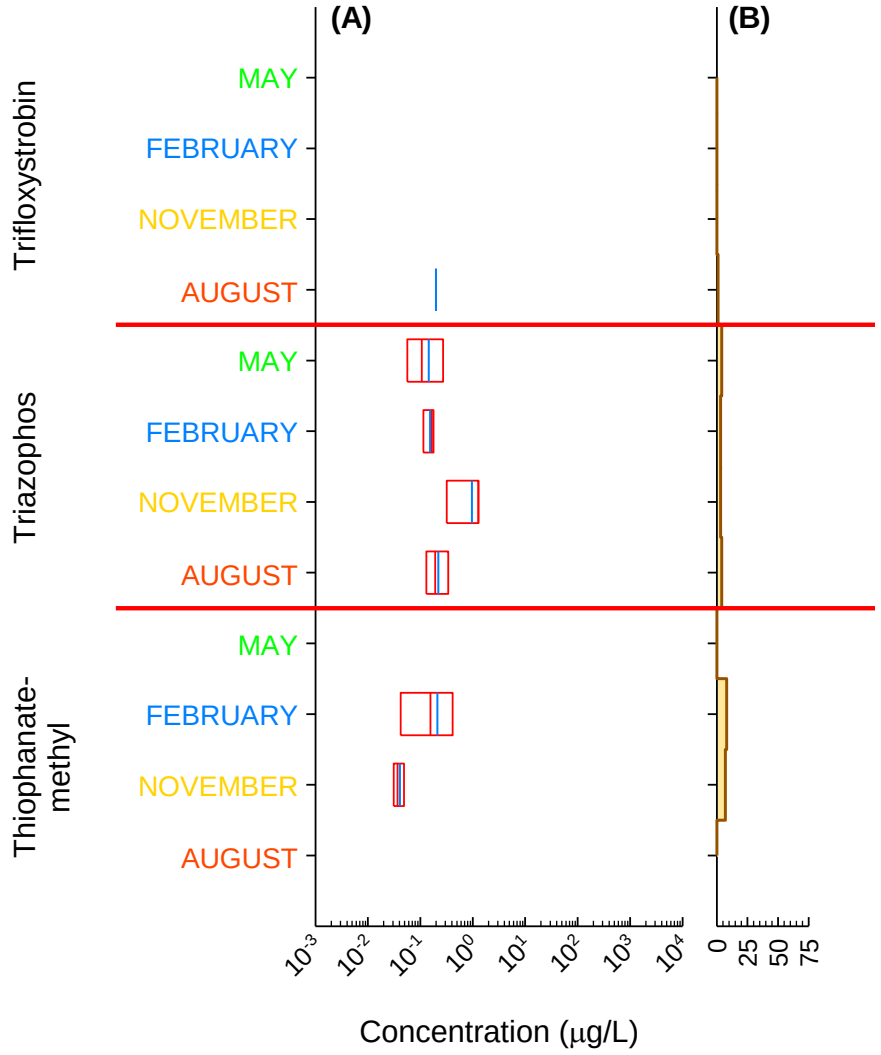

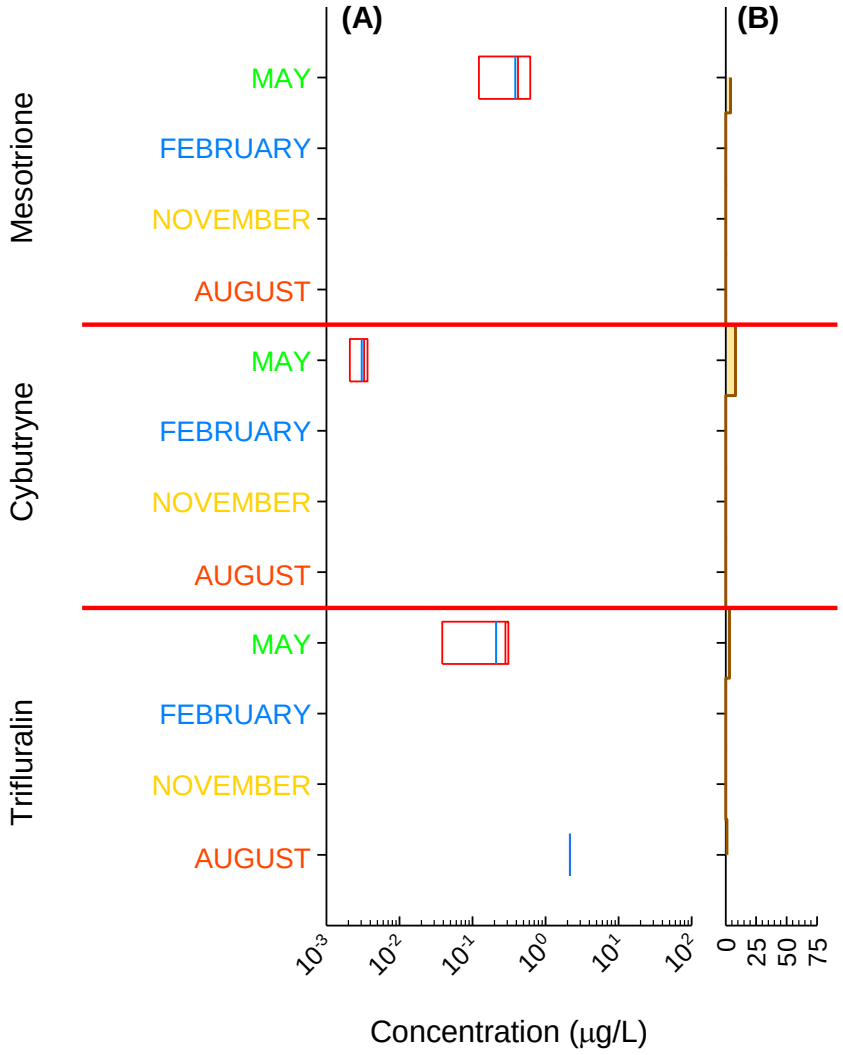

Figure D.12. Continued.

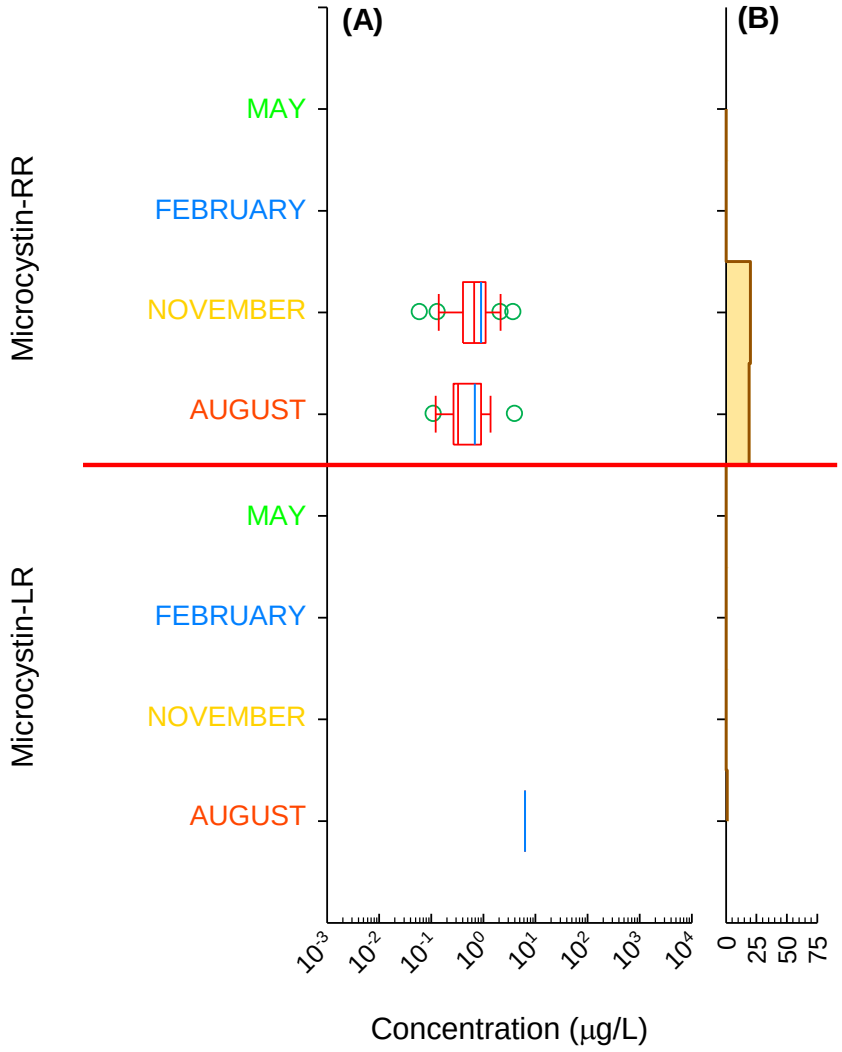

Figure D.13. Seasonal (A) concentration and (B) detection frequency (out of 75) of mirocystins in Ergene River.

APPENDIX E

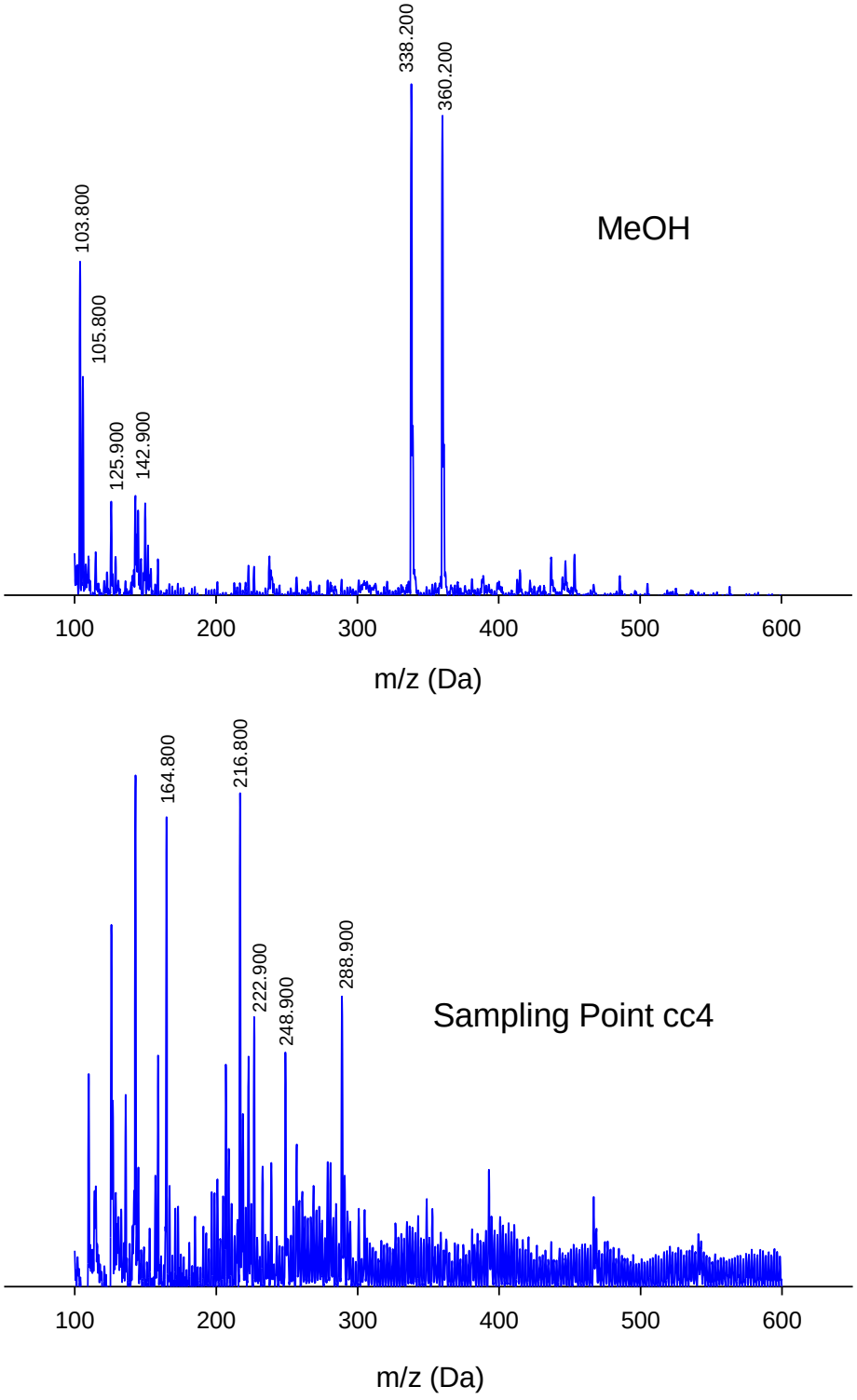

Figure E.1. Q1 screening chromatograms of the blank and selected 13 sampling points in non-targeted analysis.

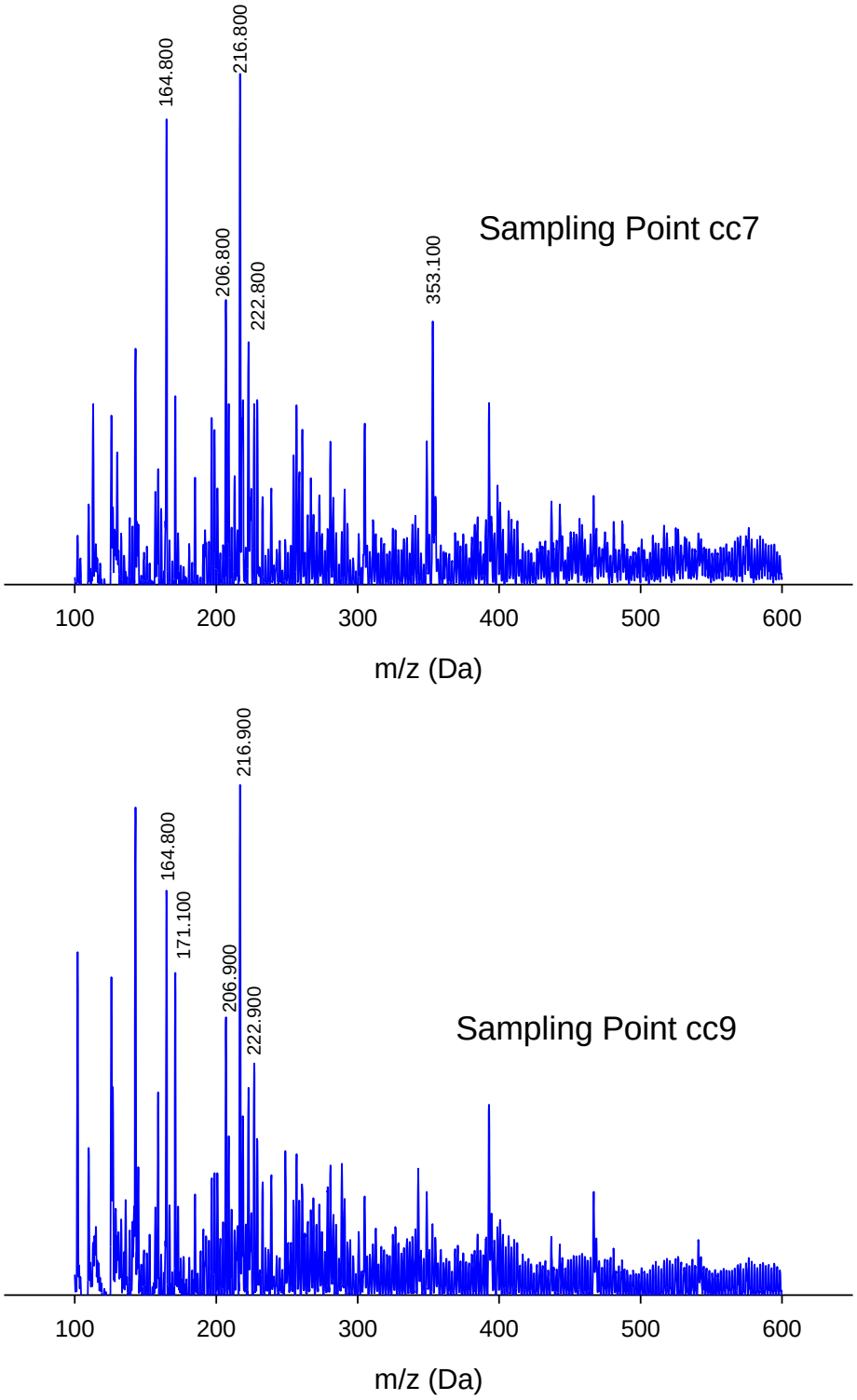

Figure E.1. Continued.

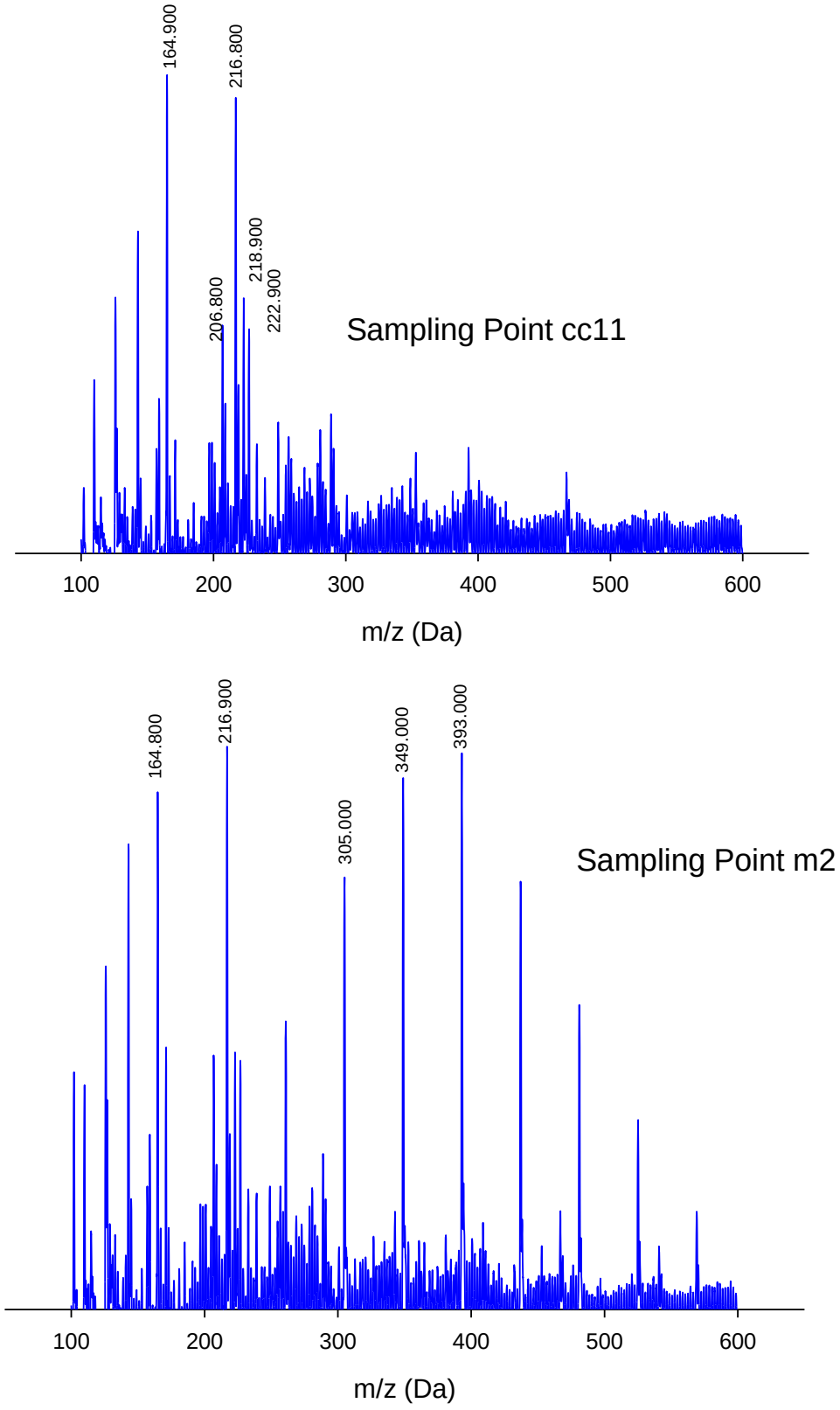

Figure E.1. Continued.

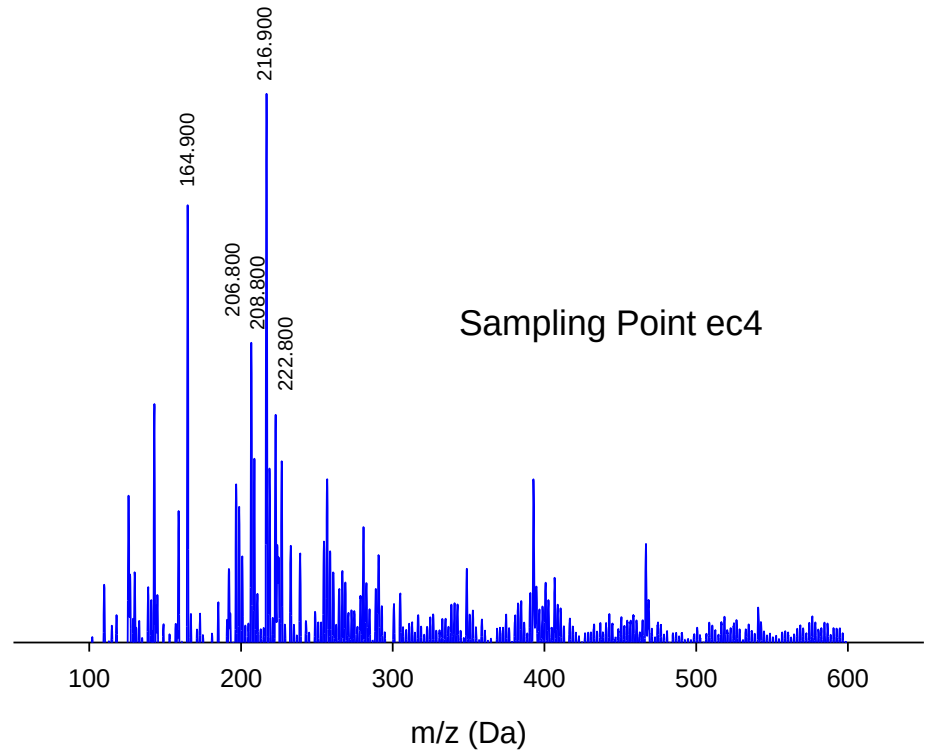

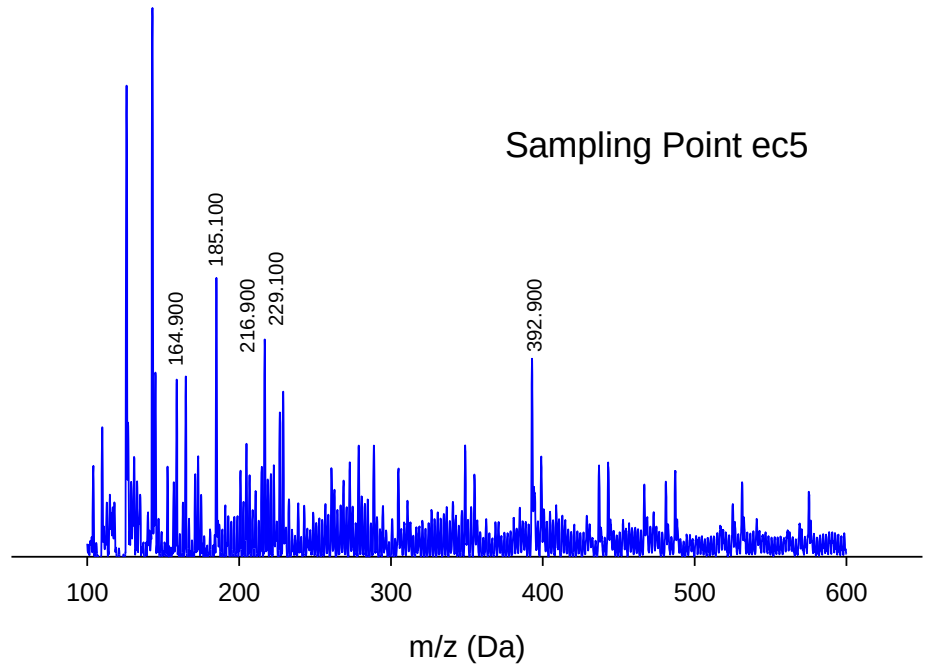

Figure E.1. Continued.

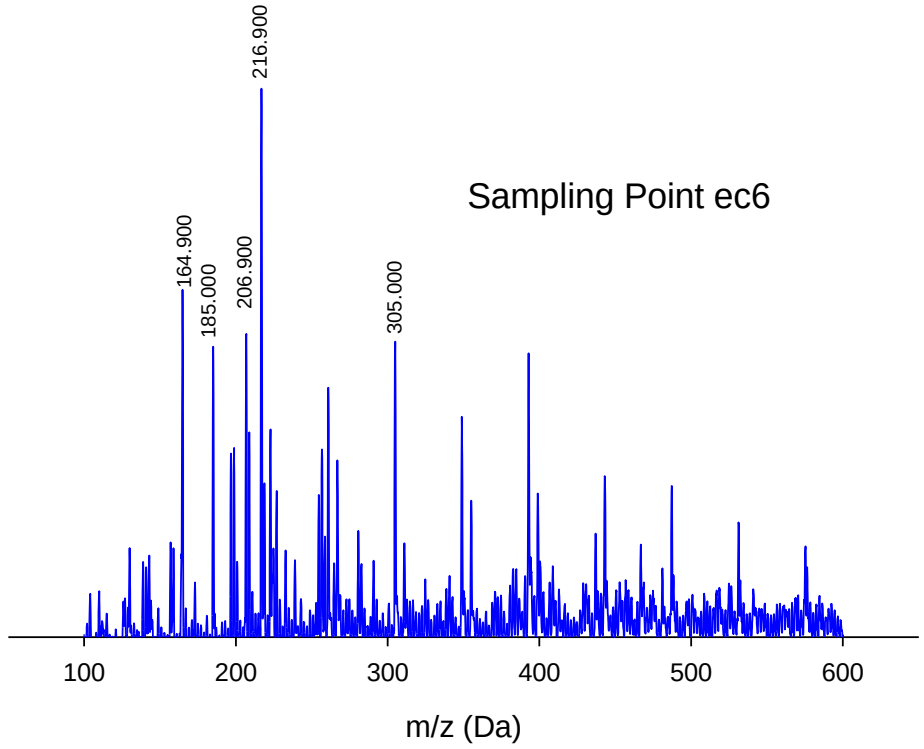

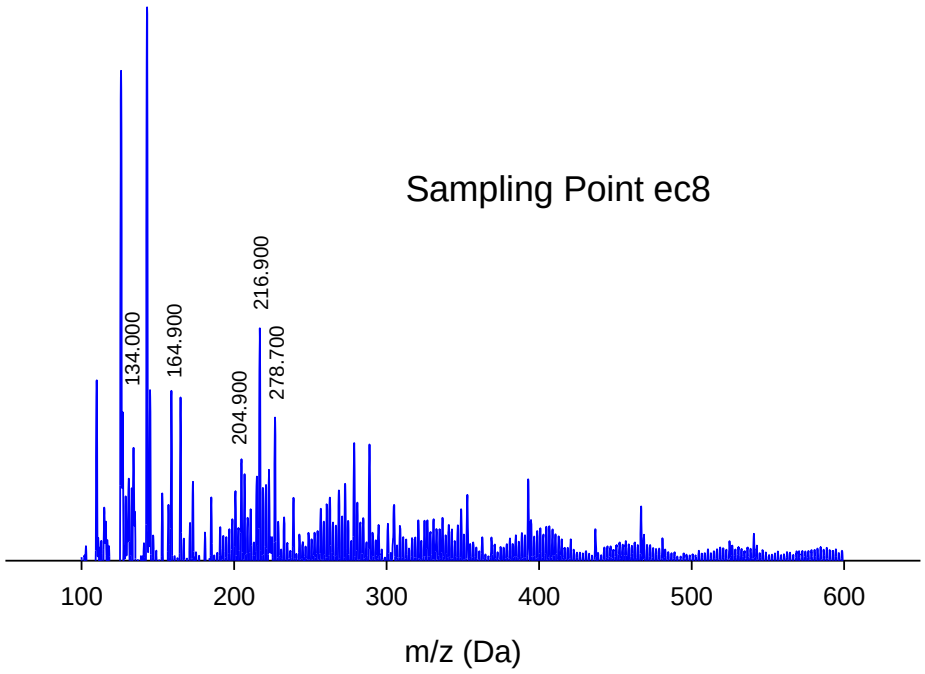

Figure E.1. Continued.

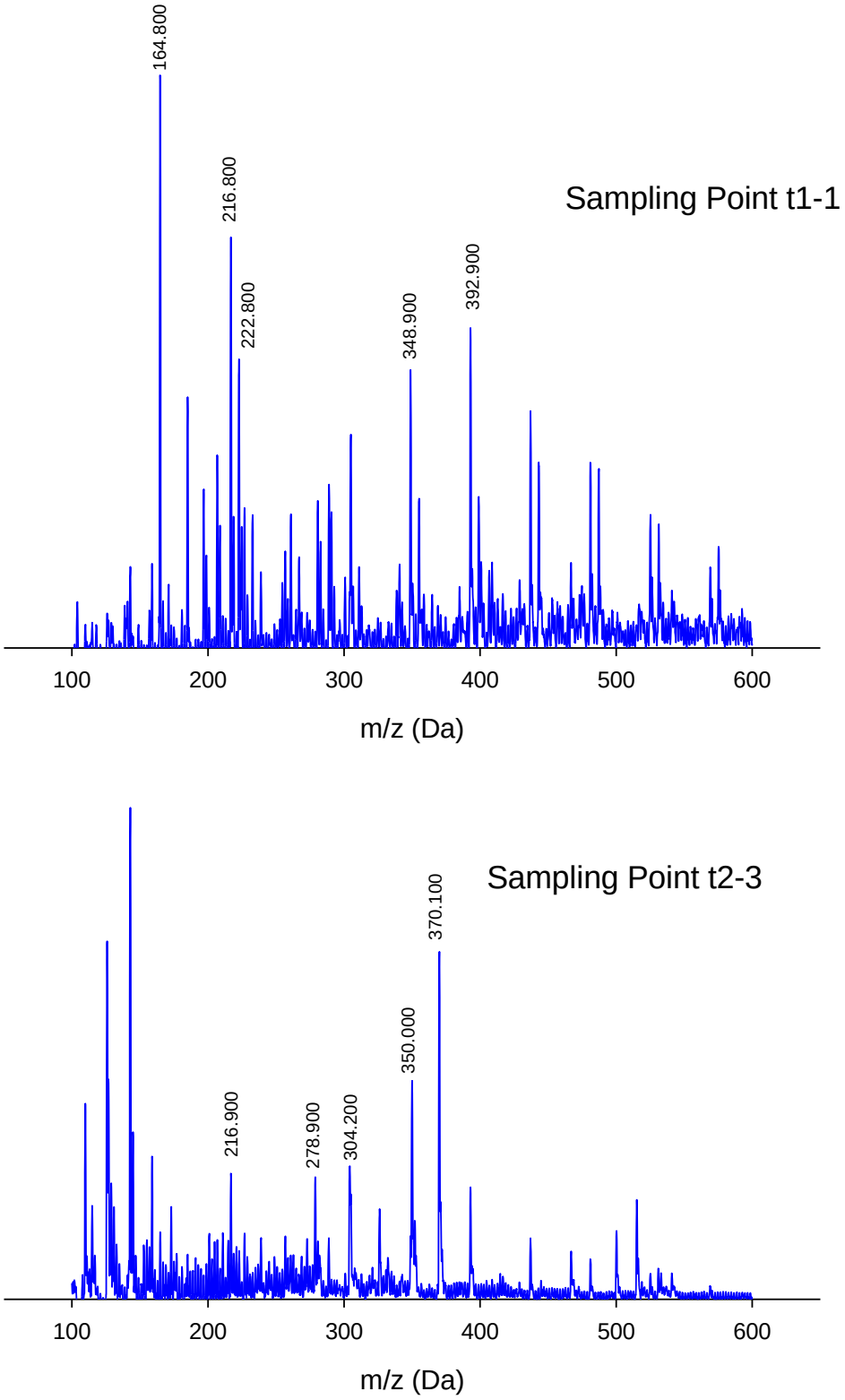

Figure E.1. Continued.

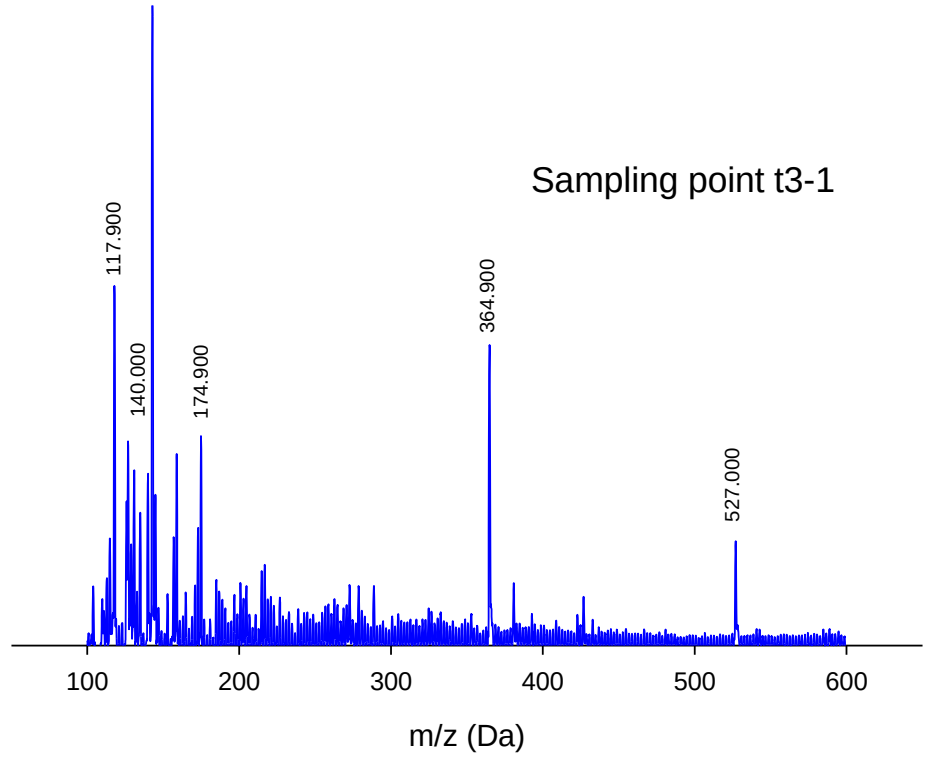

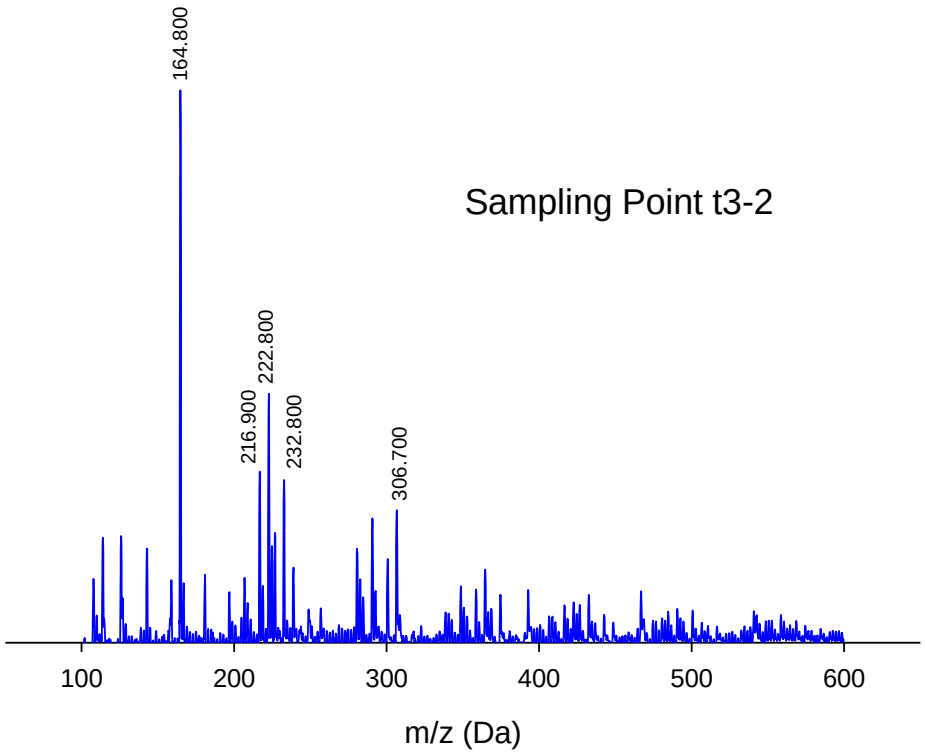

Figure E.1. Continued.

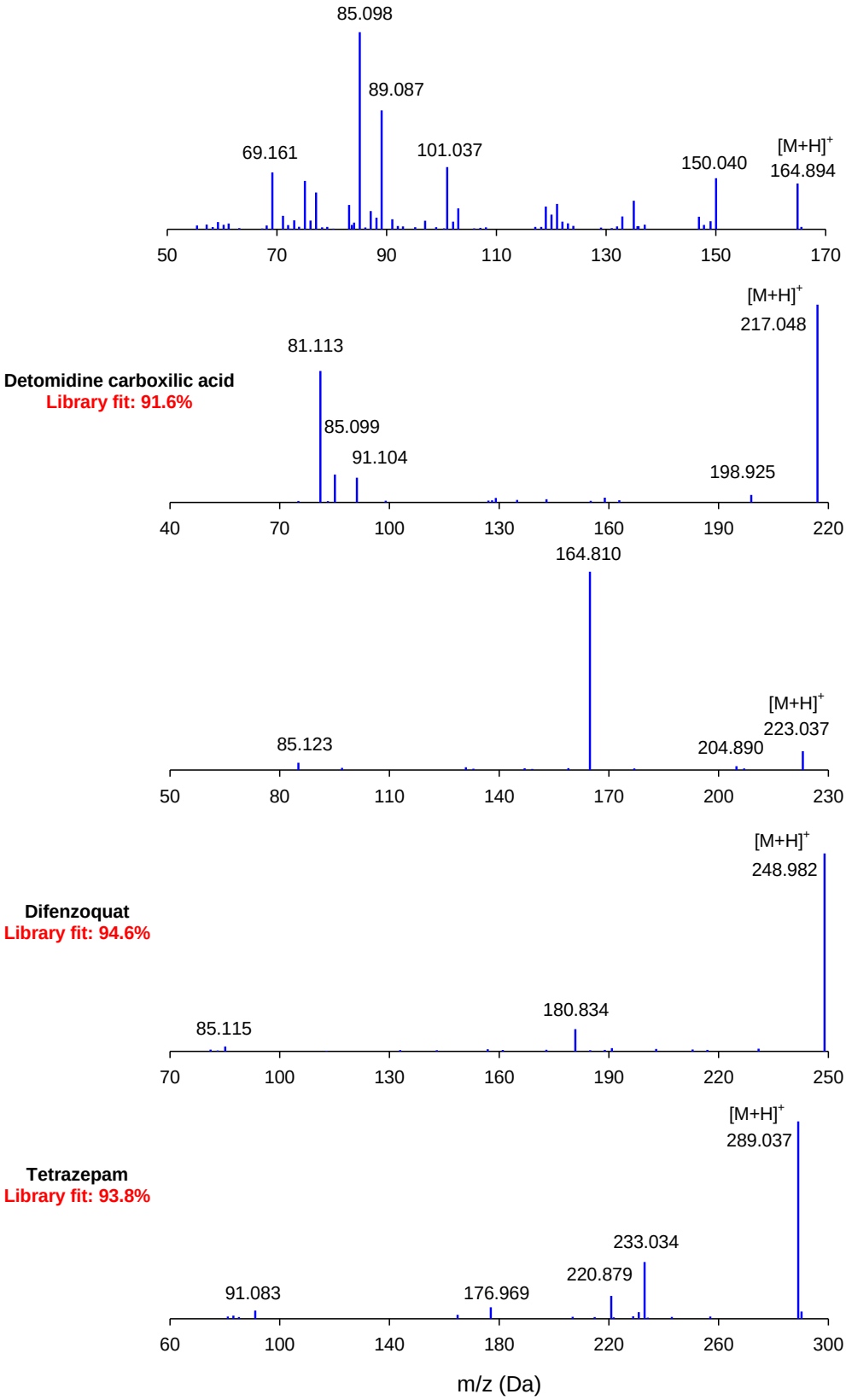

Figure E.2. Extracted product ion results of five most abundant ions in water sample taken from sampling point *cc4*.

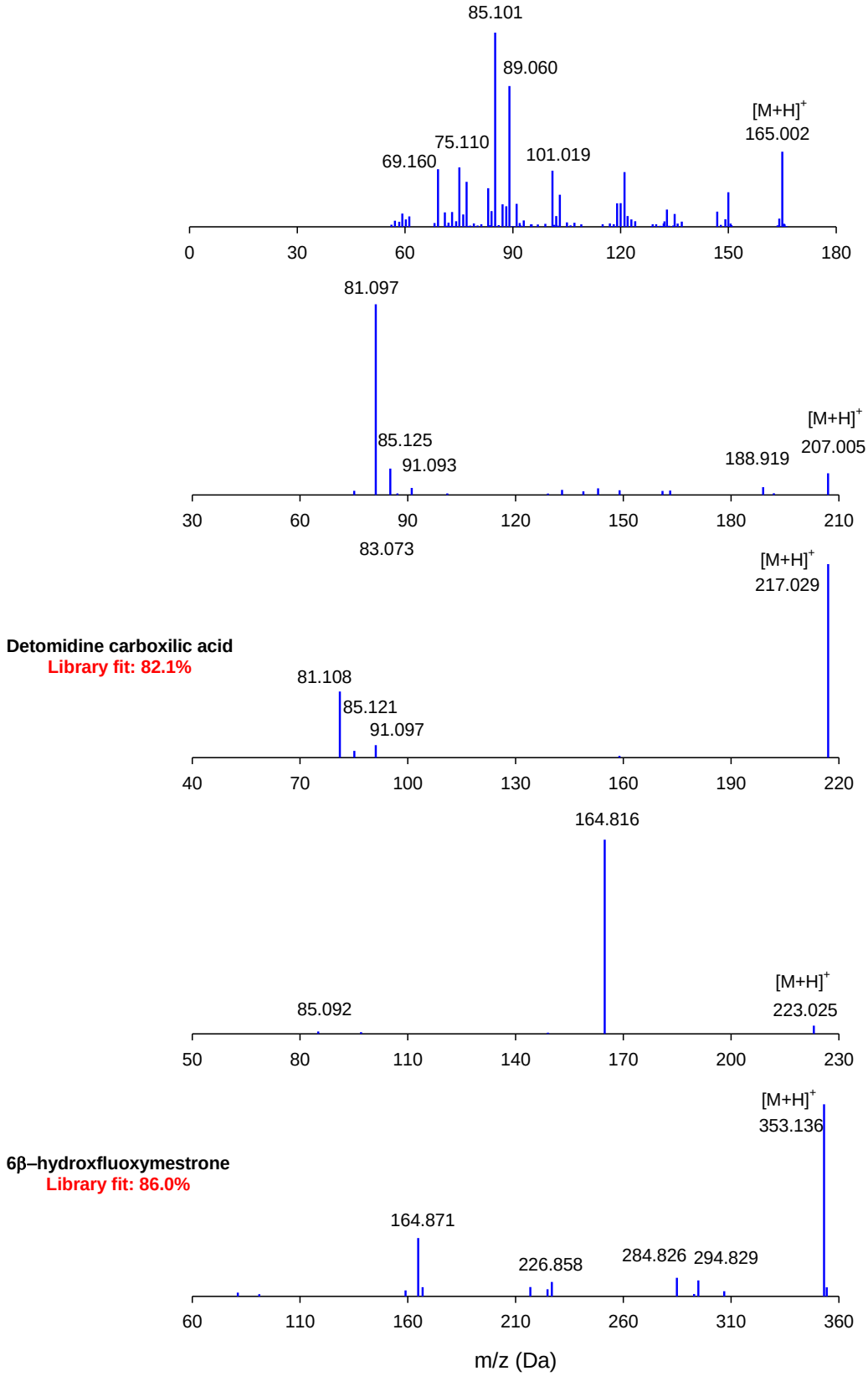

Figure E.3. Extracted product ion results of five most abundant ions in water sample taken from sampling point *cc7*.

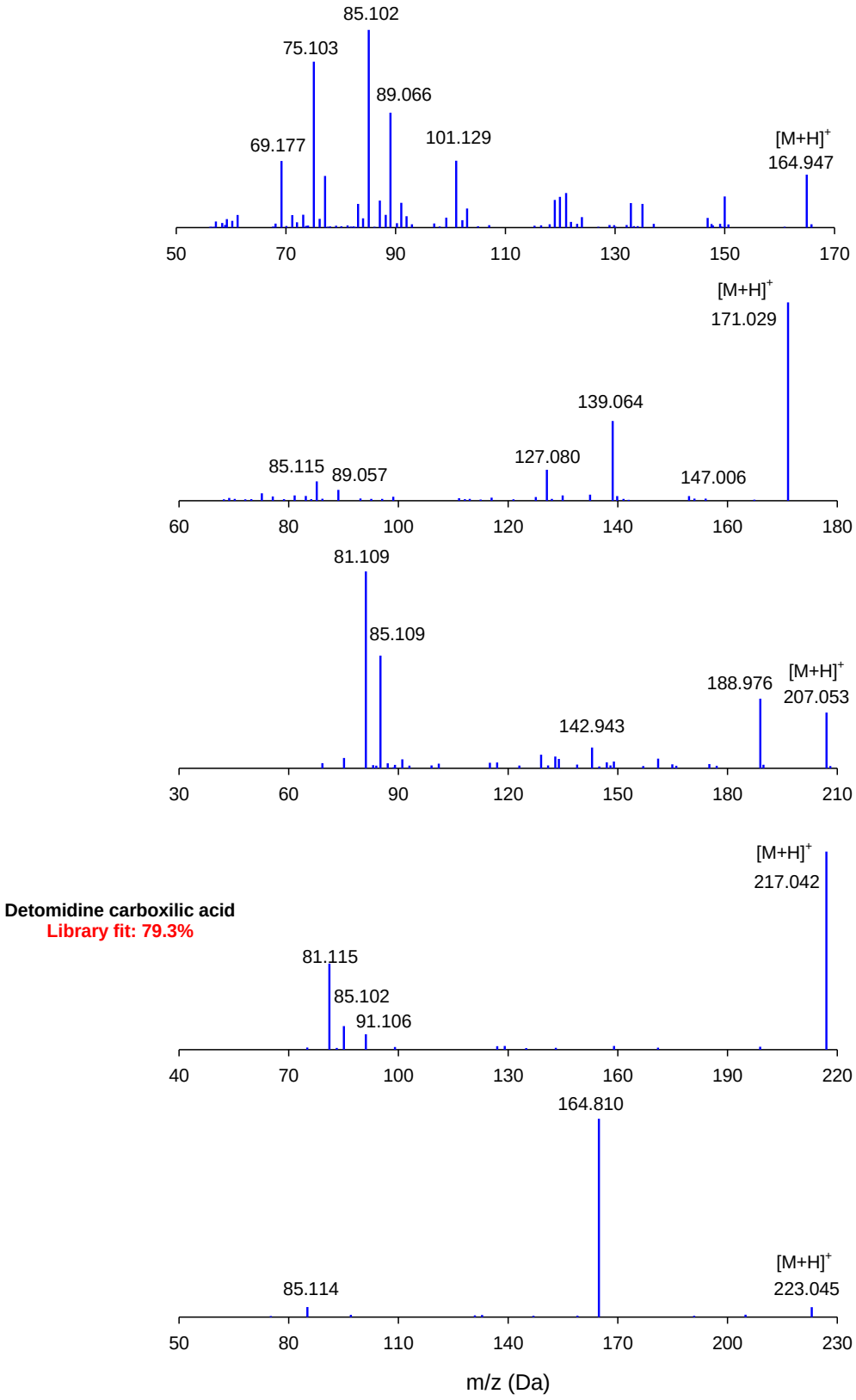

Figure E.4. Extracted product ion results of five most abundant ions in water sample taken from sampling point *cc9*.

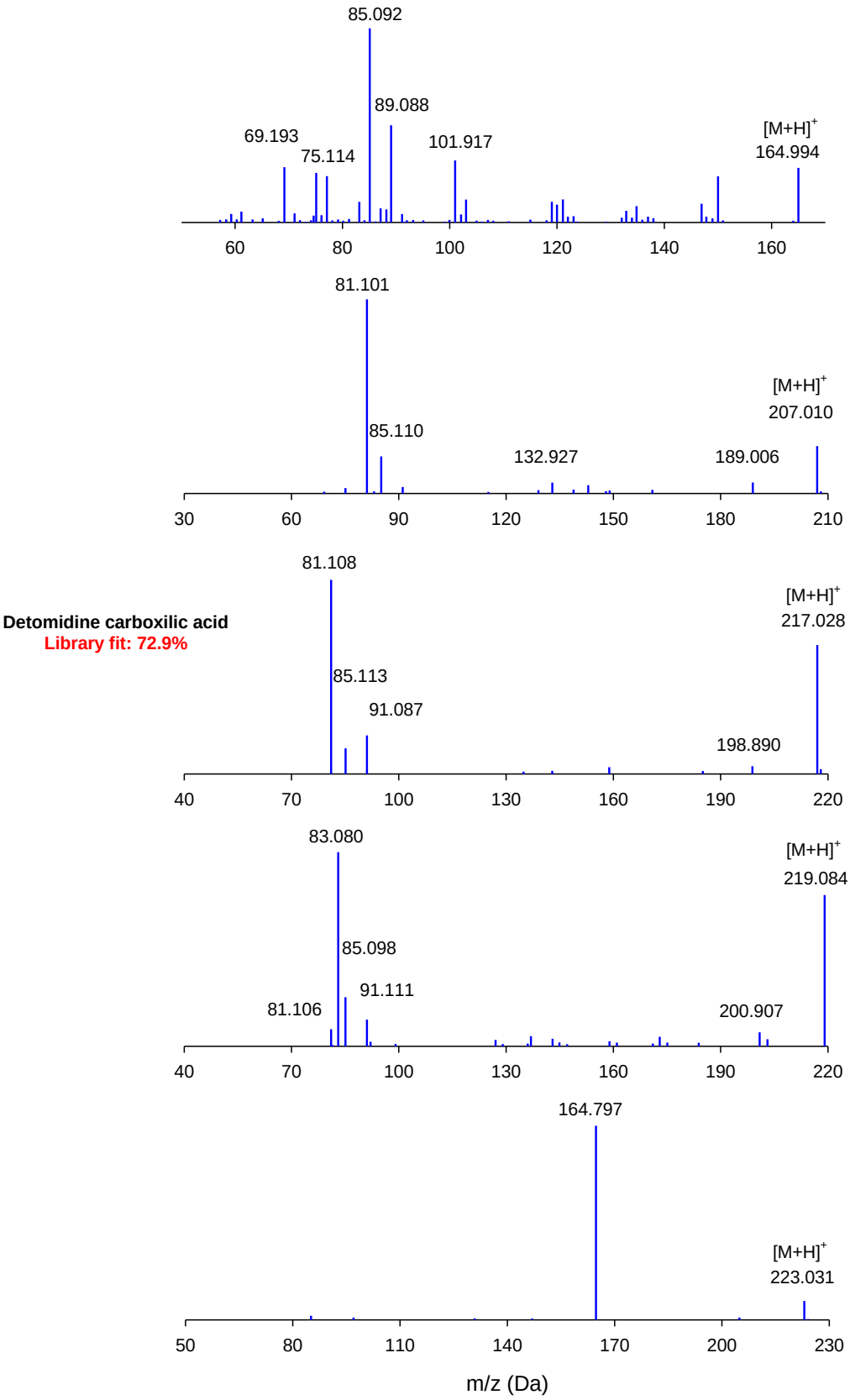

Figure E.5. Extracted product ion results of five most abundant ions in water sample taken from sampling point *cc11*.

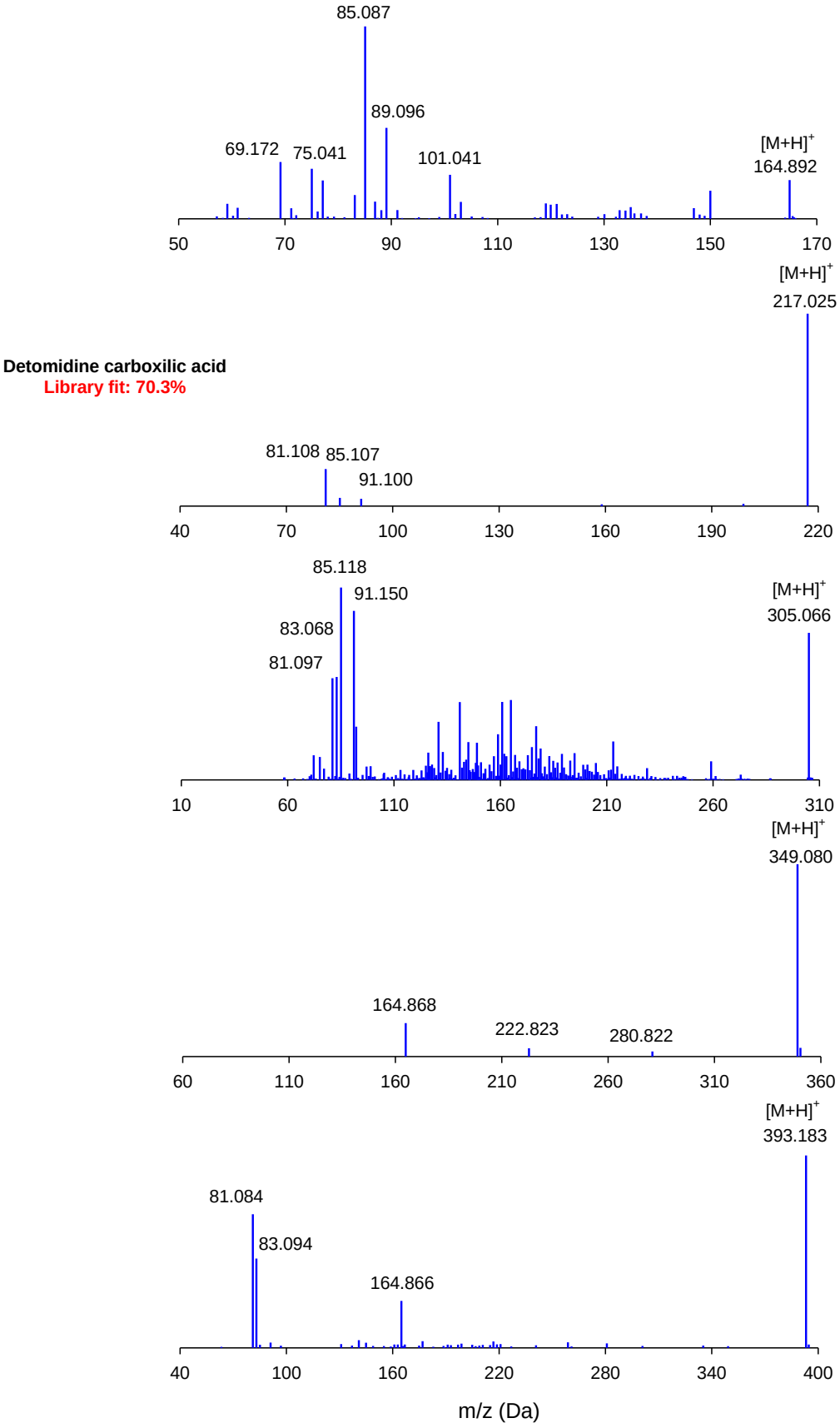

Figure E.6. Extracted product ion results of five most abundant ions in water sample taken from sampling point *m2*.

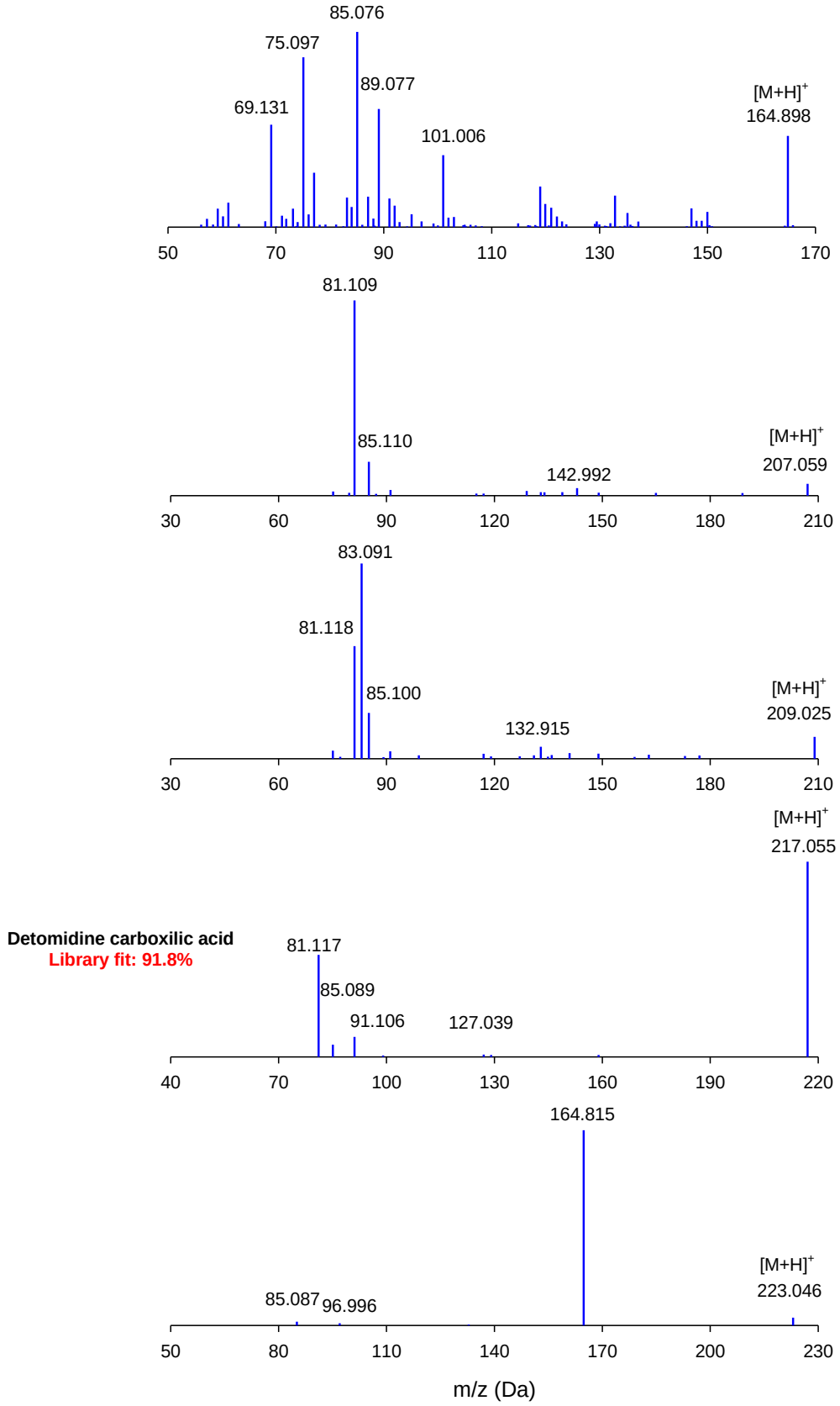

Figure E.7. Extracted product ion results of five most abundant ions in water sample taken from sampling point *ec4*.

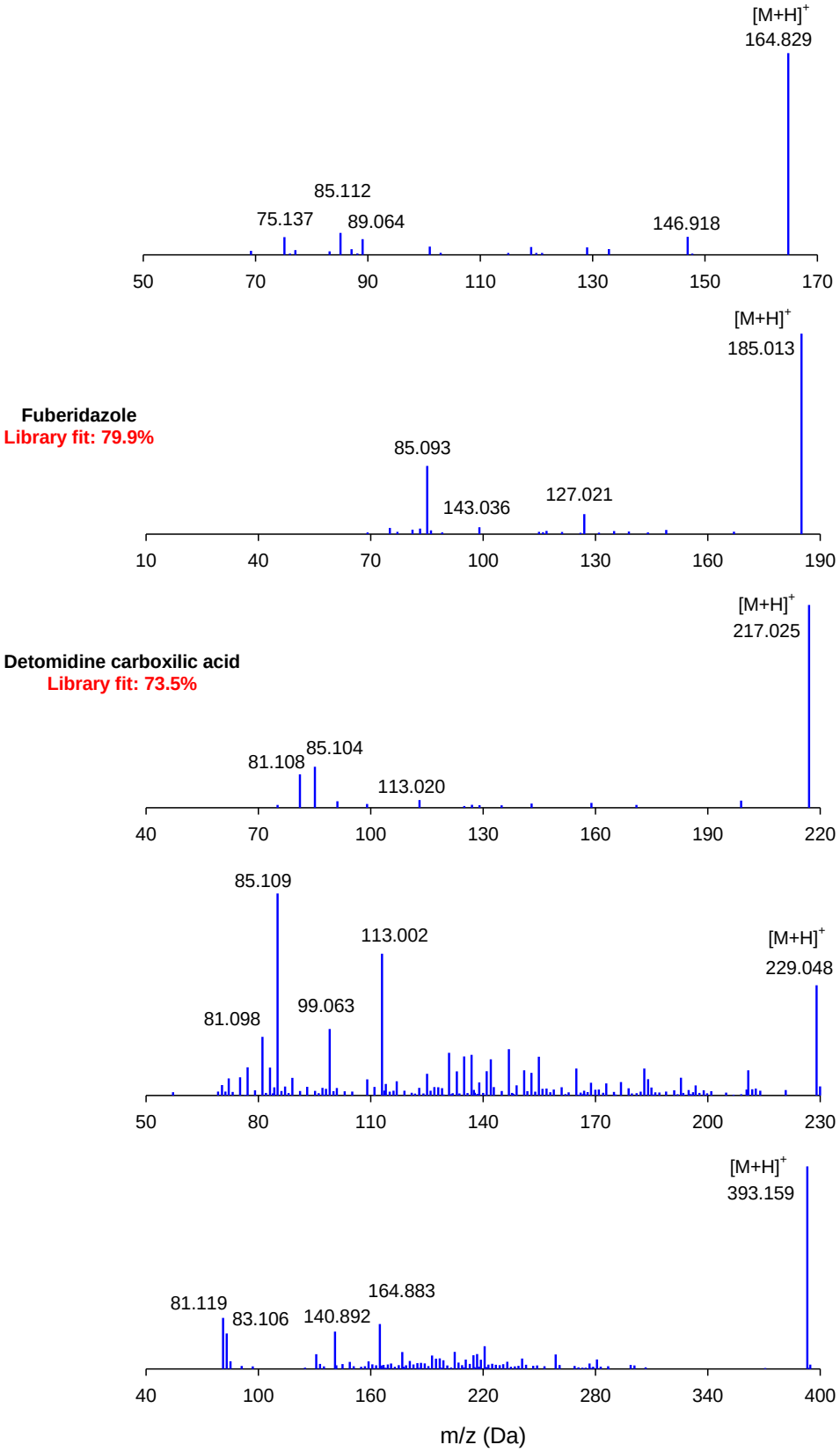

Figure E.8. Extracted product ion results of five most abundant ions in water sample taken from sampling point *ec5*.

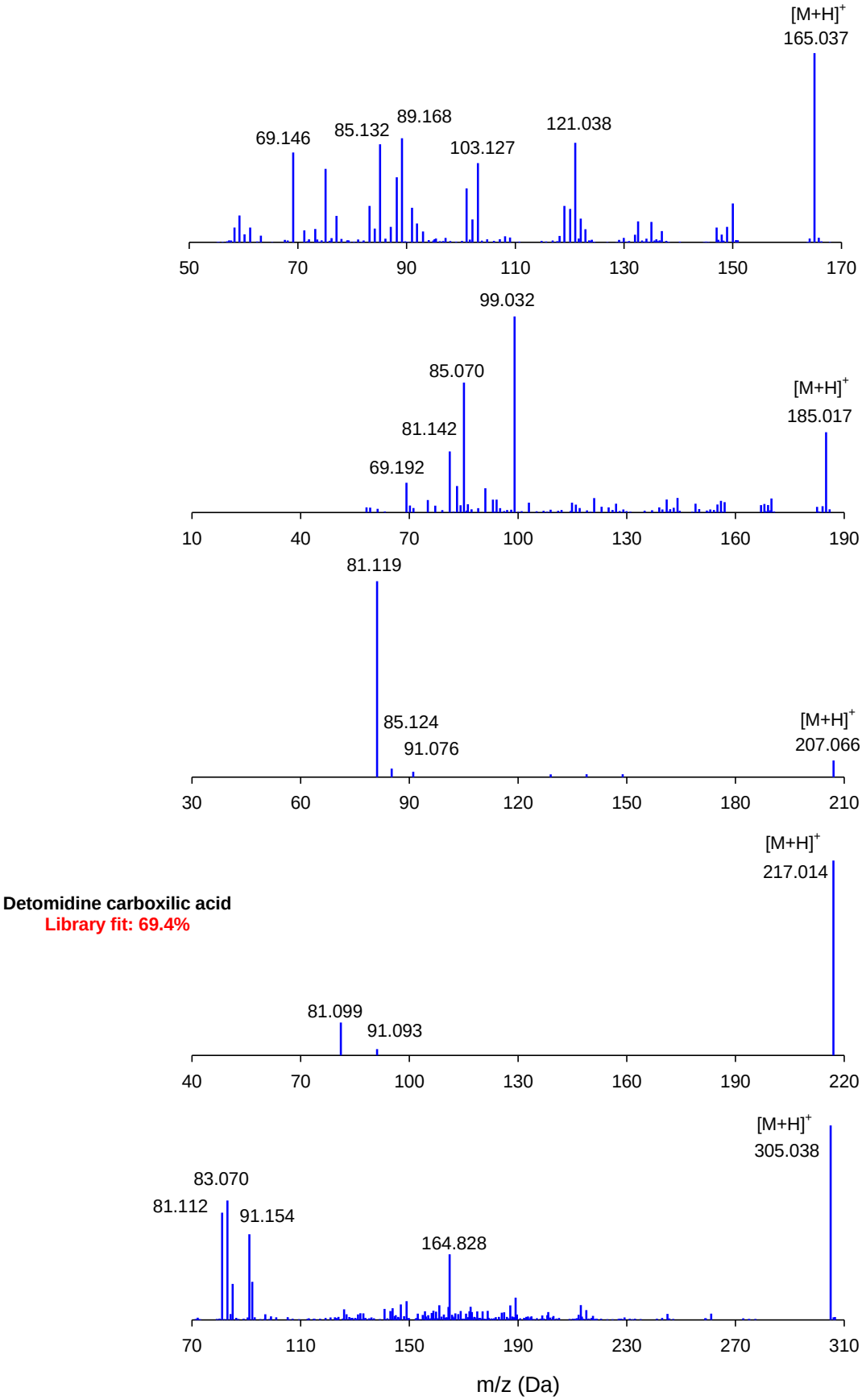

Figure E.9. Extracted product ion results of five most abundant ions in water sample taken from sampling point *ec6*.

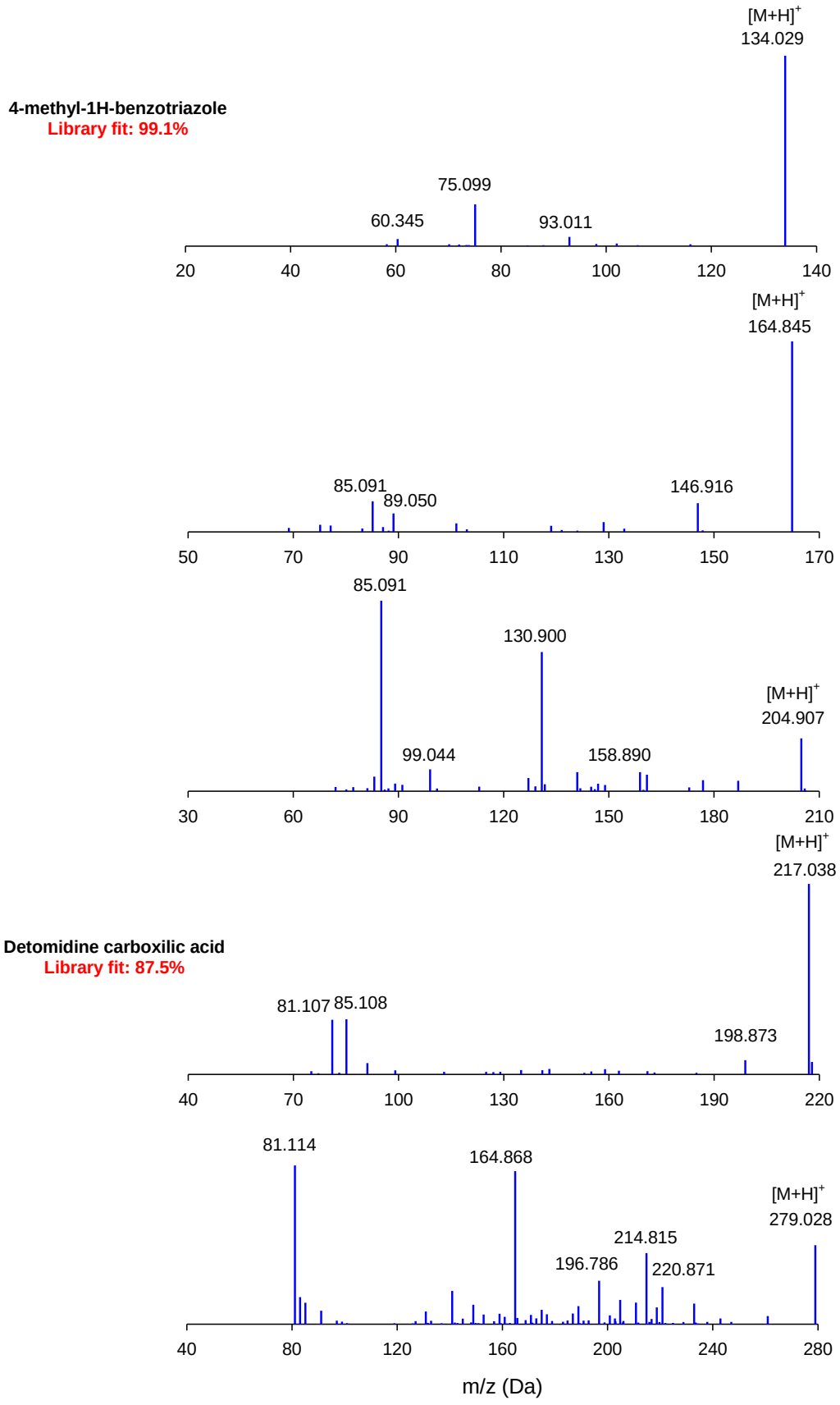

Figure E.10. Extracted product ion results of five most abundant ions in water sample taken from sampling point *ec8*.

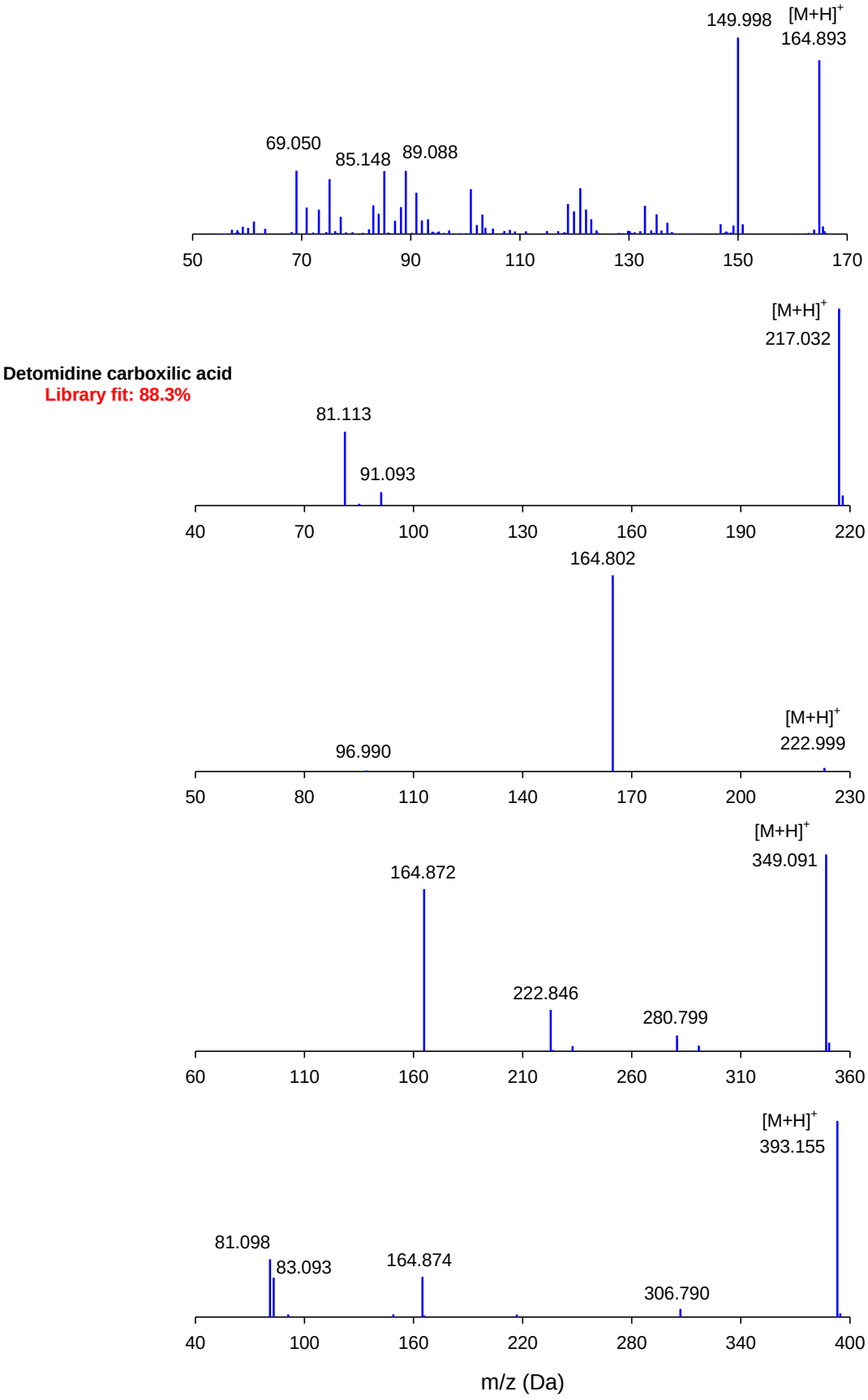

Figure E.11. Extracted product ion results of five most abundant ions in water sample taken from sampling point *t1-1*.

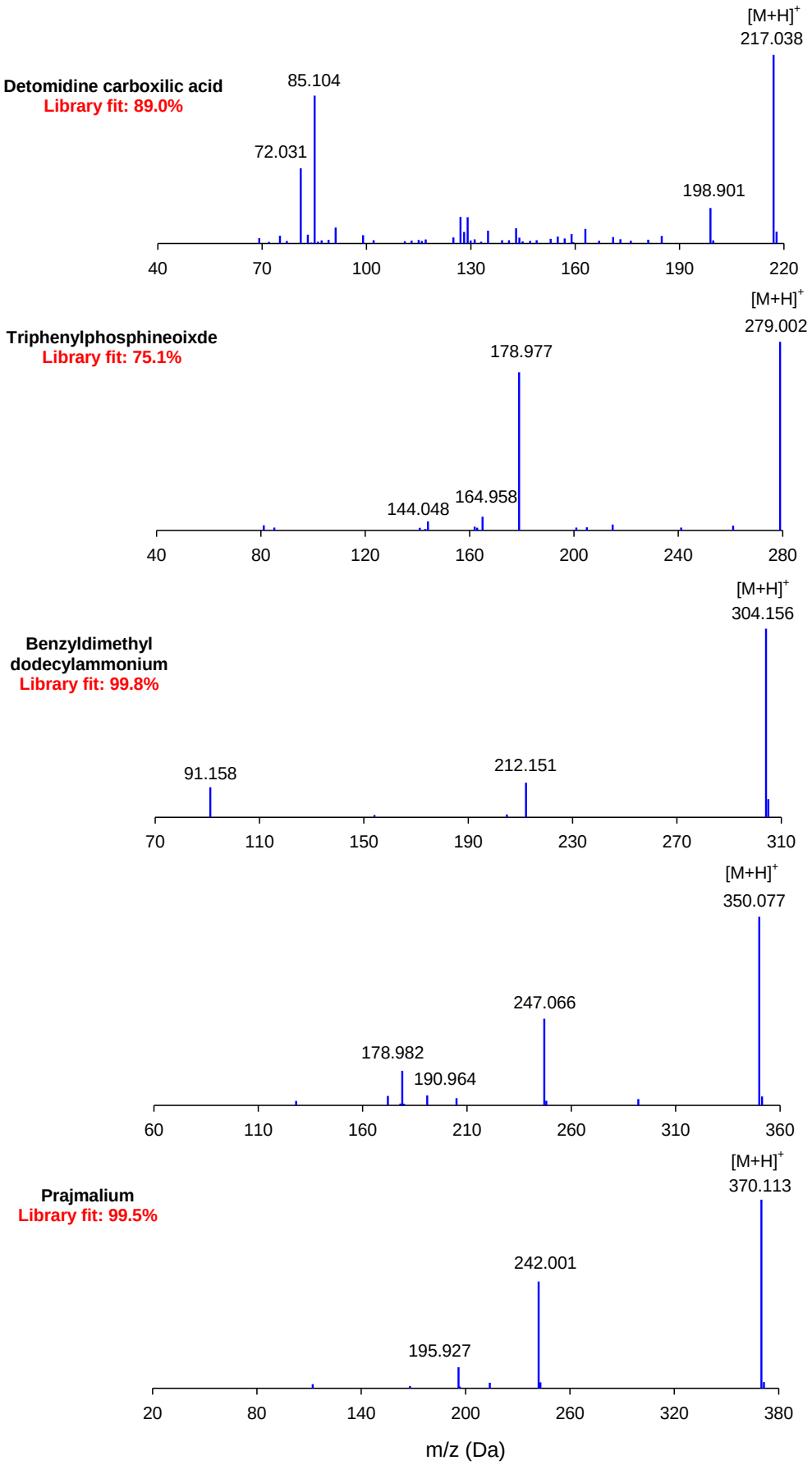

Figure E.12. Extracted product ion results of five most abundant ions in water sample taken from sampling point *t2-3*.

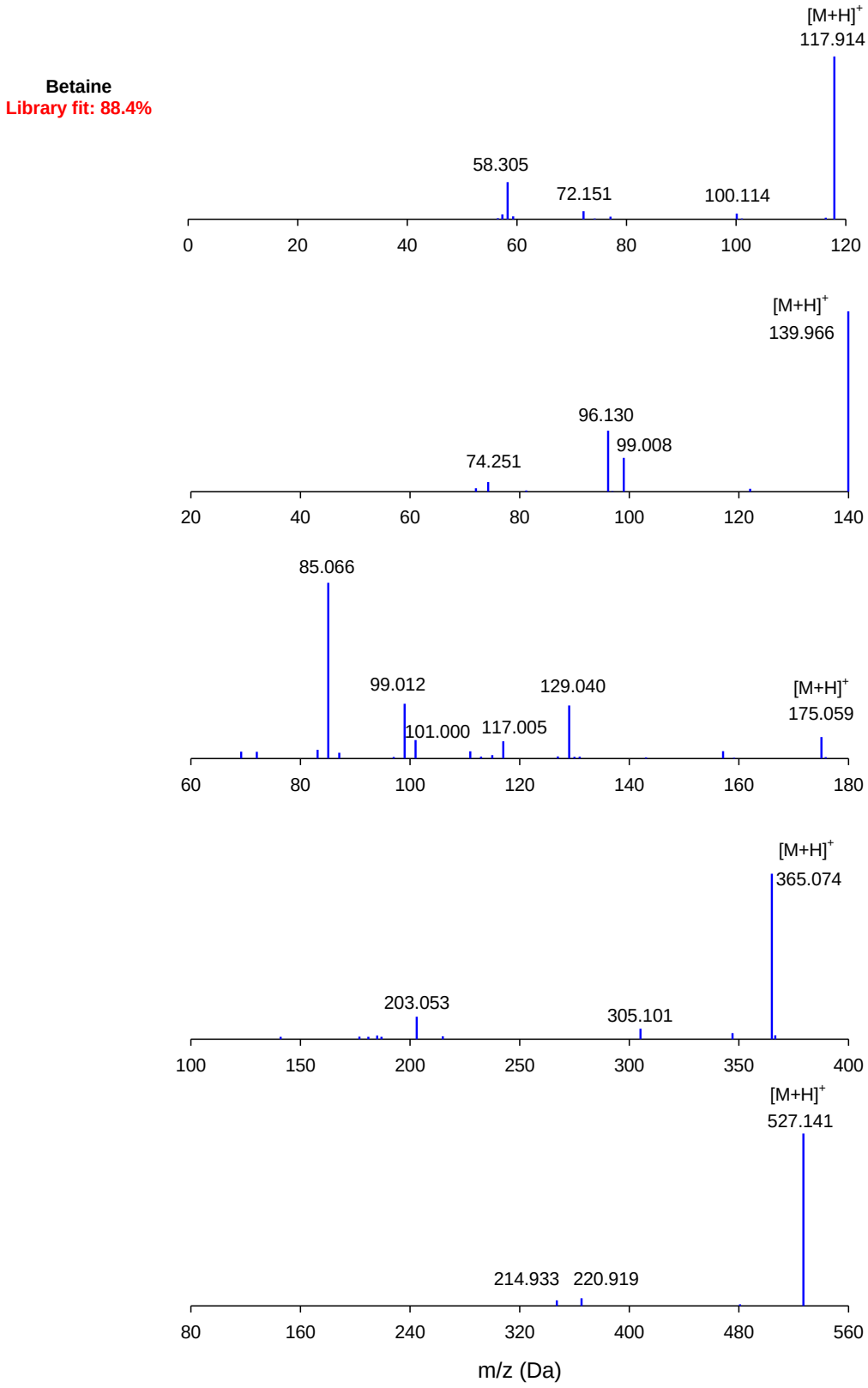

Figure E.13. Extracted product ion results of five most abundant ions in water sample taken from sampling point *t3-1*.

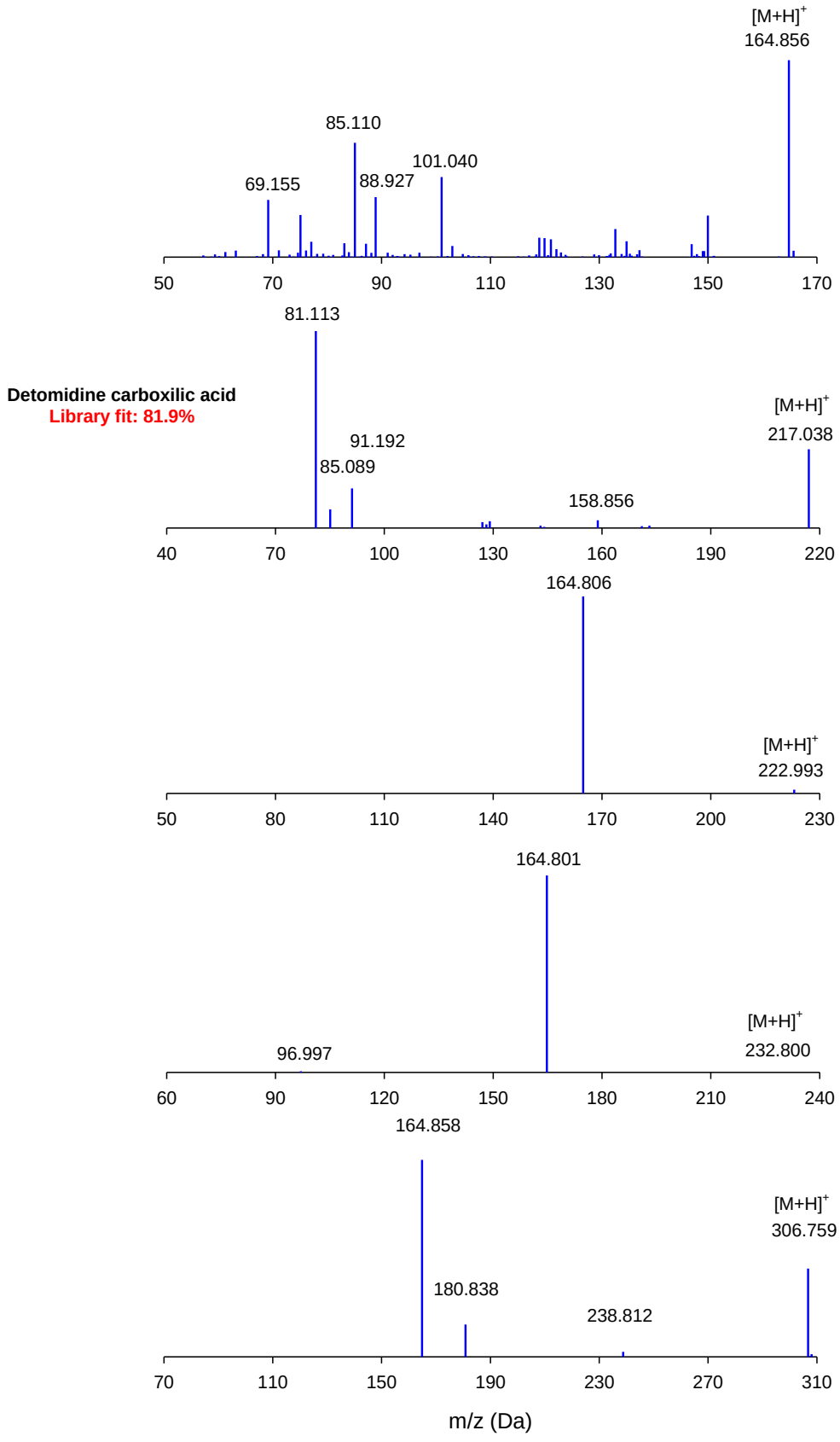

Figure E.14. Extracted product ion results of five most abundant ions in water sample taken from sampling point *t3-2*.